LEABHARLANN CHOLÁISTE NA TRÍONÓIDE, BAILE ÁTHA CLIATH | TRINITY COLLEGE LIBRARY DUBLIN
Ollscoil Átha Cliath | The University of Dublin

Terms and Conditions of Use of Digitised Theses from Trinity College Library Dublin

Copyright statement

All material supplied by Trinity College Library is protected by copyright (under the Copyright and Related Rights Act, 2000 as amended) and other relevant Intellectual Property Rights. By accessing and using a Digitised Thesis from Trinity College Library you acknowledge that all Intellectual Property Rights in any Works supplied are the sole and exclusive property of the copyright and/or other IPR holder. Specific copyright holders may not be explicitly identified. Use of materials from other sources within a thesis should not be construed as a claim over them.

A non-exclusive, non-transferable licence is hereby granted to those using or reproducing, in whole or in part, the material for valid purposes, providing the copyright owners are acknowledged using the normal conventions. Where specific permission to use material is required, this is identified and such permission must be sought from the copyright holder or agency cited.

Liability statement

By using a Digitised Thesis, I accept that Trinity College Dublin bears no legal responsibility for the accuracy, legality or comprehensiveness of materials contained within the thesis, and that Trinity College Dublin accepts no liability for indirect, consequential, or incidental, damages or losses arising from use of the thesis for whatever reason. Information located in a thesis may be subject to specific use constraints, details of which may not be explicitly described. It is the responsibility of potential and actual users to be aware of such constraints and to abide by them. By making use of material from a digitised thesis, you accept these copyright and disclaimer provisions. Where it is brought to the attention of Trinity College Library that there may be a breach of copyright or other restraint, it is the policy to withdraw or take down access to a thesis while the issue is being resolved.

Access Agreement

By using a Digitised Thesis from Trinity College Library you are bound by the following Terms & Conditions. Please read them carefully.

I have read and I understand the following statement: All material supplied via a Digitised Thesis from Trinity College Library is protected by copyright and other intellectual property rights, and duplication or sale of all or part of any of a thesis is not permitted, except that material may be duplicated by you for your research use or for educational purposes in electronic or print form providing the copyright owners are acknowledged using the normal conventions. You must obtain permission for any other use. Electronic or print copies may not be offered, whether for sale or otherwise to anyone. This copy has been supplied on the understanding that it is copyright material and that no quotation from the thesis may be published without proper acknowledgement.

The impact of kynurenine pathway activation in glia on neuronal integrity

Thesis submitted to the University of Dublin, Trinity College

for the degree of Doctor of Philosophy

2017

By

Katherine O'Farrell

School of Pharmacy and Pharmaceutical Sciences
&
Trinity College Institute of Neuroscience,
Trinity College,
Dublin 2.

TRINITY LIBRARY
24 OCT 2017
DUBLIN

Thesis 11441

Declaration

I declare that this thesis is submitted for the degree of Doctor of Philosophy at the University of Dublin, Trinity College and has not been submitted as an exercise for a degree at this or any other university and that it is entirely my own work.

I agree to deposit this thesis in the Universitys open-access institutional repository or allow the library to do so on my behalf, subject to Irish Copyright Legislation and Trinity College Library conditions of use and acknowledgement.

Acknowledgements

First and foremost I would like to thank my supervisor, Prof. Andrew Harkin, for allowing me to carry out my PhD research in his lab. He has been extremely supportive and has provided me with enormous guidance over the past three years for which I am immensely appreciative. Over the last few months, he has devoted a substantial amount of time going through the work outlined in this thesis for which I am truly grateful.

I am incredibly indebted to Prof. Mani Ramaswami and Dr. Joern Huelsmeier for allowing me the use of their fluorescent microscope and helping me out when it all got too technical. I am also extremely grateful to Brian Talbot for all the time and effort he has spent helping me with HPLC. I wish to thank the Institute of Neuroscience and the department of Physiology, in particular, Amir, Ciaran, Kieran, and Alice. I would also like to thank Mark Travers for his patience and flexibility throughout my time at Trinity.

I would like to thank Noreen Boyle for her infinite help throughout my PhD but most importantly for sharing her expertise with me at the beginning. Likewise, I would like to show my appreciation to Eimear Fagan for her work in this area prior to me commencing. I am also grateful to the students that I have had the pleasure of mentoring throughout my PhD including Michelle, Conor, Dervla, Donal, and Patrick, for all their hard work and enthusiasm.

To all of the members of the Andrew Harkin/ Tom Connor lab: Barry, Shane, Justin, Eoin, Eileen, Eimear, Elaine, Alli, Jenny, Chloe, Kelly, Yury and Eoin, thank you for making TCIN such a pleasant place to work. I would also like to thank Hannah and Jen for making the past three years all the more enjoyable. I would specifically like to thank Barry, Elaine, Jen and Alli who helped with proof-reading this thesis.

Finally I would like to thank my parents, Mary and Kieran, and also Libb, Stevie, Ailve, and Keith, and to Barry for their constant love and encouragement without which I would never have completed this PhD.

"The law of morphological progress with increasing functional adaptation is expressed in the neurons by the formation and lengthening of new processes and, consequently, by multiplication and diversification of intercellular connections"

Santiago Ramon y Cajal

Recollections of My Life, 1884

Summary

The kynurenine pathway, which is activated in times of stress and infection has been implicated in the pathophysiology of neurodegenerative and psychiatric disorders. Alterations in neuronal integrity, including neuronal cell death, neuritic atrophy and synapse loss are neurodegenerative features often implicated in the pathophysiology of these disorders. Activation of this tryptophan metabolising pathway results in the production of neuroactive metabolites which have the potential to interfere with normal neuronal functioning, and may contribute to altered neuronal transmission and the emergence of symptoms of these brain disorders. The pathway is compartmentalised within different brain cells as a consequence of preferential expression of specific enzymes. For the most part, microglia contain the neurotoxic arm of this pathway on the basis that they produce the oxidative metabolites 3-hydroxykynurenine, and 3-hydroxyanthranillic acid, alongside the NMDA receptor agonist and oxidative metabolite, quinolinic acid. In contrast, astrocytes are responsible for driving the neuroprotective arm of the pathway with the production of the NMDA receptor antagonist, kynurenic acid.

An *in vitro* cell culture system composed of the BV-2 microglial cell line, alongside primary microglial, astrocytic, mixed glial and neuronal cultures was utilised to investigate the effect of kynurenine pathway activation on neuronal integrity. Quantitative polymerase chain reaction (PCR) and high performance liquid chromatography (HPLC) were implemented for the examination of pathway-related enzyme gene expression and metabolite production respectively. Viability assays were used to assess neurotoxicity, Sholl analysis was employed for the morphological assessment of neurons at days *in vitro* (DIV) 3, while the formation of synapses in neurons at DIV 18-21 was assessed by quantifying the co-localised expression of the pre-synaptic marker, synaptophysin, and post-synaptic marker, post-synaptic density (PSD)-95.

Stimulation of BV-2 microglia with IFNγ (5 ng/ml; 24 hr) increased the mRNA expression of kynurenine pathway enzymes, indoleamine 2, 3-dioxygenase (IDO), kynurenine monooxygenase (KMO) and kynureninase (KYNU), with concomitant increases in the concentrations of tryptophan, and kynurenine pathway metabolites, kynurenine, and 3-hydroxykynurenine in the conditioned media (CM) of these cells. Treatment of neurons (DIV 3) with CM from IFNγ-stimulated BV-2 microglia for 48 hr reduced the viability and neuritic complexity of these cells. Inhibition of IDO, with 1-MT (L) (0.5 mM) or dexamethasone (1 μM) failed to protect against IFNγ CM-induced reductions in viability but rescued the reductions in neuronal complexity. Inhibition of KMO with Ro 61-8084 (1 μM) attenuated both the IFNγ CM-induced reductions in viability and complexity, as did MK-801 (0.1 μM), an NMDA receptor antagonist. The kynurenine pathway metabolites, 3-hydroxkynurneine (0.1 μM), 3-hydroxyanthranillic acid (0.1 μM), and quinolinic acid (1 μM) in combination induced neuronal

atrophy which was mitigated by pre-treatment of neurons with MK-801 (0.1 μM). The use of reactive (IFNγ-stimulated) mixed glial (microglia and astrocytes) cultures was required to achieve an atrophic effect as IFNγ-stimulated microglial CM alone was ineffective in this regard. In this instance, inhibition of IDO with 1-MT (L) (0.5 mM) attenuated these reductions in neuronal complexity. Furthermore, treatment of neurons (DIV 18-21) with IFNγ-stimulated mixed glia CM resulted in synapse loss, which was ameliorated by prior treatment with 1-MT (L). An additional feature of reactive glia is the release of surplus amounts of glutamate into the extracellular milieu. The potential for kynurenic acid to protect against excitotoxic agents including glutamate (500 μM) and glycine (10 μM) or a combination of 3-hydroxykynurenine (0.1 μM) and 3-hydroxyanthranillic acid (0.1 μM) and quinolinic acid (1 μM)-induced neuronal atrophy was also demonstrated.

Following on from this, the ability of activation of the neuroprotective arm of the kynurenine pathway to protect against the atrophy induced by the neurotoxic arm was examined. Initially, the potential of noradrenergic agents to regulate the protective arm of the pathway in primary cortical astrocytes was examined, with noradrenaline (10 μM) increasing the mRNA expression of the rate-limiting enzyme tryptophan 2, 3-dioxygenase (TDO) while reducing the mRNA expression of all other pathway enzymes. In contrast, the β_2-adrenoceptor agonist, formoterol (10 μM), increased the mRNA expression of both TDO and kynurenine aminotransferase (KAT) II. Furthermore, formoterol shifted tryptophan metabolism along the neuroprotective arm of the pathway with reductions in 3-hydroxykynurenine concentrations reported in the CM of formoterol treated astrocytic cultures. The ability of formoterol to protect against the IFNγ-stimulated mixed glial CM-induced atrophy and synapse loss previously observed was subsequently investigated and found to be effective. Inhibition of TDO, with 680C91 (20 μM) failed to attenuate the formoterol-induced neuroprotective effect. This may be as a consequence of additional formoterol-related responses which may elicit protection or indeed TDO inhibition itself may be protective as a result of reduced levels of astrocytic kynurenine available for uptake by microglia and use in the neurotoxic arm of the kynurenine pathway.

Collectively, these findings identify the neurotoxic arm of the kynurenine pathway as an additional, independent mechanism by which reactive microglia can induce neuronal atrophy and synapse loss. Furthermore, the ability to manipulate the neuroprotective arm of this pathway in order to ameliorate this neuronal deterioration was demonstrated. Modulation of this pathway with the clinically relevant β-agonist, formoterol achieved this protective effect, potentially through TDO induction and subsequent release of kynurenic acid.

Table of contents

Declaration i

Acknowledgements ii

Summary iv

Table of contents vi

List of figures xv

List of tables xx

Abbreviations xxi

General introduction 1

Cellular composition of the central nervous system (CNS) 2

1.1.1 Microglia *2*

1.1.1.2 Microglial morphology *3*

1.1.1.3 Microglial activation *3*

1.1.2 Astrocytes *4*

1.1.2.1 Astrocytic morphology *4*

1.1.2.2 Astrocytic activation *4*

1.2 Neurodevelopment 5

1.2.1 Introduction to neurite outgrowth *5*

1.2.2 The stages of neurite outgrowth *7*

1.2.3 Formation of neuritic branches and synapses *9*

1.2.4 Contribution of glia to neurite outgrowth and synaptogenesis *10*

1.2.4.1 The tripartite synapse *10*

1.2.4.2 Microglia; a transient component of the tripartite synapse *11*

1.3 The kynurenine pathway 12

1.3.1 Tryptophan metabolism along the kynurenine pathway *12*

1.3.2 Compartmentalisation of the kynurenine pathway in the CNS *14*

1.3.3 The differential activation and roles of IDO and TDO *14*

1.3.3.1 The role of IDO in kynurenine pathway activation *15*

1.3.3.2 The role of TDO in kynurenine pathway activation *16*

1.3.4 The neuroactive properties of kynurenine pathway metabolites *16*

1.3.4.1 The oxidative metabolites *16*

1.3.4.2 The oxidative and NMDA receptor properties of quinolinic acid *17*

1.3.4.3 The multifaceted nature of kynurenic acid *17*

1.3.5 The kynurenine pathway and neurodegeneration in vitro *18*

1.3.6 A role for the kynurenine pathway in the pathophysiology of neurodegenerative and neuropsychiatric disorders *21*

1.3.7 A role for the kynurenine pathway in neurodevelopment *23*

1.4 The kynurenine pathway; linking neuroinflammation to neurodegeneration 24

1.4.1 A role for IFNγ *25*

1.5 A role for noradrenaline in kynurenine pathway activation 27

1.5.1 Introduction to noradrenergic signalling *27*

1.5.2 The noradrenergic system and the kynurenine pathway *28*

1.5.3 The neuroprotective effects of noradrenaline *29*

1.5.4 The noradrenergic system and neurodegenerative disorders *31*

1.6 Targeting the kynurenine pathway; therapeutic considerations 31

1.6.1 Targeting the rate limiting enzymes of the kynurenine pathway *32*

1.6.2 Targeting the kynurenine pathway downstream of TDO or IDO *33*

1.6.3 Targeting the kynurenine pathway indirectly *33*

1.7 Aims and objectives 36

Materials and Methods 37

2.1 Materials 38

2.1.1 Animals *38*

2.1.2 Cell Culture materials and reagents *38*

2.1.3 General laboratory materials and reagents *39*

2.1.4 General laboratory equipment *39*

2.1.5 Assay kits *40*

2.1.6 Fluorescent immunocytochemistry *40*

2.1.7 HPLC materials and reagents *41*

2.1.8 Molecular materials and reagents *41*

2.1.9 Experimental treatments *41*

2.2 In vitro cell culture 43

2.2.1 Aseptic techniques *43*

2.2.2 Preparation of culture media and experimental treatments *43*

2.2.3 Maintenance of the BV-2 cell line *46*

2.2.4 Preparation of coverslips *47*

2.2.5 Preparation of primary cortical neuronal cultures *47*

2.2.6 Preparation of mixed glial cultures *48*

2.2.7 Preparation of primary astrocytic cultures *49*

2.2.8 Preparation of primary microglial cultures *49*

2.3 Analysis of cell viability 49

2.3.1 The Pierce™ LDH cytotoxicity assay *49*

2.3.2 The Alamar Blue assay 51
2.3.3 CellTiter 96® AQ_{ueous} Non-Radioactive Cell Proliferation assay (MTS assay) 51
2.4 Fluorescent immunocytochemistry 52
2.4.1 General fluorescent immunocytochemistry 52
2.4.2 Sholl analysis 52
2.4.3 Analysis of the co-localisation of synaptic markers in mature neurons 55
2.4.4 Glial immunocytochemistry 57
2.5 Cell preparation for quantitative polymerase chain reaction (PCR) 57
2.5.1 Harvesting cells for mRNA analysis 57
2.5.2 Total RNA extraction 58
2.5.3 RNA equalisation 58
2.5.4 Complementary deoxyribonucleic acid (cDNA) synthesis 59
2.5.5 Quantitative PCR 59
2.5.6 Analysis of the quantitative PCR data 61
2.6 HPLC 61
2.6.1 Detection of kynurenine pathway metabolites by HPLC coupled to UV/fluorescent detection 61
2.7 Statistical analysis 63
Chapter 3 64
3.1 Introduction 65
3.2 Study design 67
3.2.1 Characterisation of the effect of IFNγ on the mRNA expression profile of BV-2 microglia 67
3.2.2 Determination of the concentrations of kynurenine pathway metabolites in the CM of BV-2 microglia following stimulation with IFNγ 67
3.2.3 Characterisation of the effect of CM from IFNγ-stimulated BV-2 microglia on neuronal viability and complexity 68
3.2.4 Effect of kynurenine pathway inhibitors on IFNγ-stimulated BV-2 CM-induced reductions in neuronal viability and complexity 68
3.2.5 Effect of kynurenine pathway metabolites on neuronal viability and complexity 69
3.2.6 Effect of 1400W, or DPI chloride on IFNγ-induced reductions in neuronal viability by BV-2 microglia 70
3.3 Results 73
3.3.1 IFNγ induces kynurenine pathway activation and nitric oxide production in BV-2 microglia. 73
3.3.1.1 Effect of IFNγ on the mRNA expression of kynurenine pathway enzymes and iNOS in BV-2 microglia 73
3.3.1.2 Effect of IFNγ on the concentrations of tryptophan, kynurenine, 3-hydroxykynurenine and the kynurenine/tryptophan ratio in the CM of BV-2 microglia 73

3.3.2 CM from IFNγ-stimulated BV-2 microglia reduces measures of neuronal integrity.....76

3.3.2.1 Effect of CM from IFNγ-stimulated BV-2 microglia on neuronal viability 76

3.3.2.2 Effect of CM from IFNγ-stimulated BV-2 microglia on measures of neuronal complexity 76

3.3.3 Inhibitors of kynurenine pathway activation block IFNγ CM-induced reductions in neuronal viability and complexity. 79

3.3.3.1 Effect of pre-treatment with 1-MT (L), dexamethasone, Ro 61-8048 or MK-801 on IFNγ-stimulated BV-2 CM-induced reductions in neuronal viability.....79

3.3.3.2 Effect of 1-MT (L) on IFNγ-stimulated BV-2 CM-induced reductions in neuronal complexity 79

3.3.3.3 Effect of dexamethasone on IFNγ-stimulated BV-2 microglial-induced reductions in measures of neuronal complexity 80

3.3.3.4 Effect of dexamethasone on IFNγ-induced increases in the mRNA expression of kynurenine pathway enzymes and iNOS in BV-2 microglia.....81

3.3.3.5 Effect of Ro 61-8048 on IFNγ-stimulated BV-2 CM-induced reductions in neuronal complexity 82

3.3.3.6 Effect of MK-801 on IFNγ-stimulated BV-2 CM-induced reductions in neuronal complexity 82

3.3.3.7 Effect of MK-801 on IFNγ-induced increases in the mRNA expression of kynurenine pathway enzymes or iNOS in BV-2 microglia 83

3.3.4 Kynurenine pathway metabolites reduce neuronal complexity.....91

3.3.4.1 Effect of kynurenine pathway metabolites on neuronal complexity.....91

3.3.4.2 Effect of a combination of kynurenine pathway metabolites on neuronal complexity 91

3.3.5 Inhibitors of iNOS and NADPH oxidase block IFNγ-induced reductions in measures of neuronal complexity. 95

3.3.5.1 Effect of 1400W on IFNγ-stimulated BV-2 microglial-induced reductions in measures of neuronal complexity.....95

3.3.5.2 Effect of DPI chloride on IFNγ-stimulated bv-2 microglial-induced reductions in measures of neuronal complexity 96

3.4 Discussion 99

3.4.1 IFNγ activates the kynurenine pathway in BV-2 microglia.....99

3.4.2 CM from IFNγ-stimulated BV-2 microglia reduces neuronal viability and complexity...101

3.4.3 Inhibition of kynurenine pathway activation in BV-2 microglia protects against IFNγ CM-induced reductions in measures of neuronal viability and complexity 102

3.4.4 Inhibition of oxidative and inflammatory processes protects against IFNγ-induced reductions in neuronal complexity 105

3.4.5 Concluding remarks.....106

Chapter 4 107

4.1 Introduction..... 108

4.2 Study design 111

4.2.1 Characterisation of the effect of IFNγ on the mRNA expression profile of kynurenine pathway enzymes in primary cortical cells *111*

4.2.2 Determination of the effect of IFNγ on the concentrations of kynurenine pathway metabolites in the CM of primary cortical cells *111*

4.2.3 Characterisation of the effect of CM from IFNγ-stimulated primary cortical cells on neuronal viability and complexity *111*

4.2.4 Effect of prior treatment with 1-MT (L) on IFNγ CM-induced changes in neuronal complexity *112*

4.2.5 Effect of prior treatment with 1-MT (L) on IFNγ-stimulated primary cortical mixed glial CM-induced changes in the expression of synaptic markers *112*

4.2.6 Effects of kynurenine pathway metabolites on neuronal viability, complexity and the expression of synaptic markers *113*

4.2.7 Effects of glutamate on neuronal viability, complexity and the expression of synaptic markers *113*

4.2.8 Concentration-related effect of kynurenic acid on the glutamate and glycine- or 3-hydroxykynurenine + 3-hydroxyanthranillic acid + quinolinic acid-induced reductions in neuronal complexity and the expression of synaptic markers *114*

4.3 Results 119

4.3.1 Activation of the kynurenine pathway in primary cortical glia and the effect of glia CM on neuronal integrity. *119*

4.3.1.1 Effect of IFNγ on the mRNA expression of kynurenine pathway enzymes in primary cortical microglia *119*

4.3.1.2 Effect of IFNγ on the concentrations of tryptophan, kynurenine, 3-hydroxykynurenine and the kynurenine/tryptophan ratio in the CM of primary microglia *119*

4.3.1.3 Effect of CM from IFNγ-stimulated primary cortical microglia on neuronal viability *119*

4.3.1.4 Effect of CM from IFNγ-stimulated primary cortical microglia on measures of neuronal complexity *119*

4.3.1.5 Effect of IFNγ on the mRNA expression of kynurenine pathway enzymes in primary cortical mixed glia *120*

4.3.1.6 Effect of IFNγ on the concentrations of tryptophan, kynurenine, 3-hydroxykynurenine and the kynurenine/tryptophan ratio in the CM of primary cortical mixed glia *120*

4.3.1.7 Effect of CM from IFNγ-stimulated primary mixed glia on neuronal viability and neuronal complexity *120*

4.3.1.8 Effect of pre-treatment with 1-MT (L) on IFNγ-stimulated mixed glia CM-induced reductions in neuronal complexity *121*

4.3.1.9 Effect of IFNγ on the mRNA expression of kynurenine pathway enzymes in primary cortical astrocytes *122*

4.3.1.10 Effect of IFNγ on the concentrations of tryptophan, kynurenine, 3-hydroxykynurenine and the kynurenine/tryptophan ratio in the CM of primary cortical astrocytes *122*

4.3.1.11 Effect of CM from IFNγ-stimulated primary cortical astrocytes on neuronal viability and measures of neuronal complexity *122*

4.3.1.12 Effect of IFNγ on the mRNA expression of kynurenine pathway enzymes in primary cortical neurons *122*

4.3.1.13 Effect of IFNγ on the concentrations of tryptophan, kynurenine, 3-hydroxykynurenine and the kynurenine/tryptophan ratio in the CM of primary cortical neurons *123*

4.3.2 Examination of the effect of kynurenine pathway metabolites on neuronal integrity ..*138*

4.3.2.1 Concentration-related effects of kynurenine pathway metabolites on the viability of neurons *138*

4.3.2.2 Concentration-related effect of tryptophan on measures of neuronal complexity. *138*

4.3.2.3 Concentration-related effect of kynurenine on measures of neuronal complexity. *138*

4.3.2.4 Concentration-related effect of 3-hydroxykynurenine on measures of neuronal complexity *139*

4.3.2.5 Concentration-related effect of 3-hydroxyanthranillic acid on measures of neuronal complexity *139*

4.3.2.6 Concentration-related effect of quinolinic acid on measures of neuronal complexity. *140*

4.3.2.7 Concentration-related effect of kynurenic acid on measures of neuronal complexity. *140*

4.3.2.8 Effect of combinations of kynurenine pathway metabolites on neuronal viability and complexity *141*

4.3.3 Examination of the effect of kynurenine pathway metabolites on the neuronal integrity of mature neurons *150*

4.3.3.1 Concentration-related effects of kynurenine pathway metabolites on the viability of mature neurons *150*

4.3.3.2 Concentration-related effects of kynurenine pathway metabolites on the expression of synaptic markers in mature neurons *150*

4.3.3.3 Effect of combinations of kynurenine pathway metabolites on the viability of and the expression of synaptic markers in mature neurons *151*

4.3.4 Characterisation of the atrophic effects of glutamate on primary cortical neurons *155*

4.3.4.1 Effect of glutamate and glycine on neuronal viability and complexity *155*

4.3.4.2 Concentration-related effects of glutamate and glycine on the viability of mature neurons *156*

4.3.5 Determination of the ability of kynurenic acid to protect against changes in neuronal integrity induced by the release of soluble factors from reactive microglia *160*

4.3.5.1 Concentration-related effects of kynurenic acid on glutamate and glycine-induced reductions in neuronal complexity *160*

4.3.5.2 Concentration-related effects of kynurenic acid on glutamate and glycine-induced reductions in the expression of synaptic markers *160*

4.3.5.3 Concentration-related effects of kynurenic acid on the 3-hydroxykynurenine + 3-hydroxyanthranillic acid + quinolinic acid combination-induced reductions in neuronal complexity *161*

4.3.5.4 Concentration-related effects of kynurenic acid on the 3-hydroxykynurenine + 3-hydroxyanthranillic acid + quinolinic acid combination-induced reductions in the expression of synaptic markers *162*

4.4 Discussion 167

4.4.1 IFNγ activates the kynurenine pathway in primary cortical cells, of which IFNγ-stimulated mixed glial CM reduces neuronal complexity and synaptogenesis *167*

4.4.2 Kynurenine pathway metabolites alter measures of neuronal integrity *170*

4.4.3 Characterisation of the atrophic effects of glutamate *173*

4.4.4 Kynurenic acid as a potential candidate for attenuating the atrophic effects of glutamate *174*

4.4.5 Conclusion *175*

Chapter 5 177

5.1 Introduction 178

5.2 Study design 180

5.2.1 Effect of noradrenaline on the mRNA expression of kynurenine pathway enzymes in primary cortical astrocytes *180*

5.2.2 Effect of isoproterenol on the mRNA expression of kynurenine pathway enzymes in primary cortical astrocytes *181*

5.2.3 Characterisation of noradrenaline- and formoterol-induced changes in kynurenine pathway enzyme gene expression in primary cortical microglia and neurons *182*

5.2.4 Effect of formoterol on the IFNγ-induced changes in kynurenine pathway enzyme gene expression in primary cortical microglia, astrocytes, neurons and mixed glia *182*

5.2.5 Effect of formoterol on the IFNγ-induced changes in the concentrations of tryptophan and kynurenine pathway metabolites in the CM of primary mixed glia *182*

5.2.6 Effect of formoterol on the IFNγ-stimulated mixed glial CM-induced changes in neuronal complexity and the expression of synaptic markers *183*

5.2.7 Effect of formoterol-stimulated astrocytic CM on 3-hydroxykynurenine + 3-hydroxyanthranillic acid + quinolinic acid-induced reductions in neuronal complexity and expression of synaptic markers *184*

5.3 Results 188

5.3.1 The noradrenergic system modulates the kynurenine pathway in primary cortical astrocytes. *188*

5.3.1.1 Effect of noradrenaline on the mRNA expression of kynurenine pathway enzymes in primary cortical astrocytes *188*

5.3.1.2 Effect of the non-selective α-adrenoceptor antagonist, phentolamine, on the noradrenergic-related changes in kynurenine pathway enzyme mRNA expression in primary cortical astrocytes *188*

5.3.1.3 Effect of a selective α_1-adrenoceptor antagonist, prazosin, and the selective α_2-adrenoceptor antagonist, yohimbine, on the noradrenergic-related changes in kynurenine pathway enzyme mRNA expression in primary cortical astrocytes. *189*

5.3.1.4 Effect of the non-selective β-adrenoceptor antagonist, propranolol, on noradrenergic-related changes in kynurenine pathway enzymes mRNA expression in primary cortical astrocytes. *189*

5.3.2 β-adrenoceptor activation induces the kynurenine pathway in primary cortical astrocytes. *194*

5.3.2.1 Effect of isoproterenol on the mRNA expression of kynurenine pathway enzymes in primary cortical astrocytes *194*

5.3.2.2 Effects of selective β-adrenoceptor antagonists on isoproterenol-related changes in kynurenine pathway enzyme mRNA expression in primary cortical astrocytes *194*

5.3.2.3 Effect of formoterol on the mRNA expression of kynurenine pathway enzymes in primary cortical astrocytes *194*

5.3.2.4 Effect of a non-selective β-adrenoceptor antagonist on formoterol-related changes in kynurenine pathway enzyme mRNA expression in primary cortical astrocytes *195*

5.3.2.5 Effect of a β_2-adrenoceptor antagonist on formoterol-related changes in kynurenine pathway enzyme mRNA expression in primary cortical astrocytes *195*

5.3.2.6 Effect of the cAMP analogue, dbcAMP on the mRNA expression of kynurenine pathway enzymes in primary cortical astrocytes *196*

5.3.2.7 Effect of formoterol on the concentrations of tryptophan, kynurenine, 3-hydroxykynurenine and the tryptophan/kynurenine ratio in the CM of primary astrocytic cultures *196*

5.3.3 Characterisation of the effect of β_2-adrenoceptor stimulation on inflammation associated changes in kynurenine pathway enzyme mRNA expression in primary microglia and neurons *204*

5.3.3.1 Effect of noradrenaline and formoterol on the mRNA expression of kynurenine pathway enzymes in primary cortical microglia *204*

5.3.3.2 Effect of noradrenaline and formoterol on the mRNA expression of kynurenine pathway enzymes in primary cortical neurons *204*

5.3.3.3 Effect of formoterol on IFNγ-induced changes in the mRNA expression of kynurenine pathway enzymes in primary cortical microglia *204*

5.3.3.4 Effect of formoterol on IFNγ-induced changes in the mRNA expression of kynurenine pathway enzymes in primary cortical astrocytes *205*

5.3.3.5 Effect of formoterol on IFNγ-induced changes in the mRNA expression of kynurenine pathway enzymes in primary cortical neurons *205*

5.3.3.6 Effect of formoterol and IFNγ in combination on the mRNA expression of kynurenine pathway enzymes in primary cortical mixed glia *211*

5.3.3.7 Effect of formoterol and IFNγ in combination on the concentrations of tryptophan, kynurenine, 3-hydroxykynurenine and the tryptophan/kynurenine ratio in the CM of primary mixed glial cultures *211*

5.3.3.8 Effect of formoterol on the IFNγ-stimulated mixed glia CM-induced reductions in neurite outgrowth and the expression of synaptic markers *212*

5.3.3.9 Effect of TDO inhibition on the ability of formoterol to protect against the mixed glia IFNγ CM-induced reductions in neurite outgrowth and the expression of synaptic markers *213*

5.3.4 Determination of the ability of the neuroprotective arm of the kynurenine pathway in astrocytes to protect against the neurotoxic, atrophic kynurenine pathway metabolites 219

5.3.4.1 Effect of formoterol-stimulated astrocytic CM on kynurenine pathway metabolite-induced changes in neuronal complexity 219

5.4 Discussion 223

5.4.1 Divergent effects of adrenoceptor subtype stimulation on the activation of the kynurenine pathway in primary cortical astrocytes 223

5.4.2 Characterisation of the effect of mixed glial β_2-adrenoceptor stimulation on inflammation-associated reductions in neuronal complexity and the expression of synaptic markers 225

5.4.3 Conclusion 227

General discussion 229

6.1 Summary of main findings 230

6.2 Activation of the kynurenine pathway in reactive BV-2 microglia induces cytotoxicity and neurite atrophy 231

6.3 Activation of the kynurenine pathway in reactive primary cortical mixed glia induces neuronal atrophy and synapse loss 232

6.4 The impact of kynurenine pathway metabolites on neuronal integrity 235

6.5 A role for the noradrenergic system in regulating the kynurenine pathway in primary cortical glial and neuronal cells 237

6.6 Clinical relevance 242

6.7 Limitations and future directions 243

Appendix xxiv

Publications xxv

Presentations xxv

Supplementary figures xxvi

References xxxi

List of figures

Figure 1.1: The structure of the growth cone 6

Figure 1.2: The stages of neuronal development *in vitro* 8

Figure 1.3: The kynurenine pathway in the periphery and CNS 14

Figure 1.4: The IFNγ signalling cascade 26

Figure 1.5: Adrenoceptor intracellular signalling pathways 27

Figure 1.6: Adrenoceptor signalling system in astrocytes 28

Figure 1.7: Summary diagram of how activation of the kynurenine pathway in glial cells may contribute to alterations in neuronal integrity. 30

Figure 1.8: Drugs that target the kynurenine pathway at discrete stages of tryptophan metabolism 35

Figure 2.1: Fluorescent image of a typical control neuron. 54

Figure 2.2: Quantification of the co-localised expression of synaptic markers, synaptophysin and PSD-95, in mature neurons 56

Figure 2.3: Fluorescent image of glial cultures 57

Figure 3.2.1: Diagram showing the timeline of a typical experiment. 71

Figure 3.3.1.1: Effect of IFNγ on the mRNA expression of kynurenine pathway enzymes and iNOS in BV-2 microglia 74

Figure 3.3.1.2: Effect of IFNγ on the concentrations of tryptophan, kynurenine, 3-hydroxykynurenine and the kynurenine/tryptophan ratio in the CM of BV-2 microglia . 75

Figure 3.3.2.1: Effect of CM from IFNγ-stimulated BV-2 microglia on neuronal viability. 77

Figure 3.3.2.2: Effect of CM from IFNγ-stimulated BV-2 microglia on measures of neuronal complexity 78

Figure 3.3.3.1: Effect of pre-treatment with 1-MT (L), dexamethasone, Ro 61-8048 or MK-801 on IFNγ-stimulated BV-2 CM-induced reductions in neuronal viability 84

Figure 3.3.3.2: Effect of 1-MT (L) on IFNγ-stimulated BV-2 CM-induced reductions in neuronal complexity 85

Figure 3.3.3.3: Effect of dexamethasone on IFNγ-stimulated BV-2 microglial-induced reductions in measures of neuronal complexity 86

Figure 3.3.3.4: Effect of dexamethasone on IFNγ-induced increases in the mRNA expression of kynurenine pathway enzymes and iNOS in BV-2 microglia 87

Figure 3.3.3.5: Effect of Ro 61-8048 on IFNγ-stimulated BV-2 CM-induced reductions in neuronal complexity 88

Figure 3.3.3.6: Effect of MK-801 on IFNγ-induced reductions in measures of neuronal complexity 89

Figure 3.3.3.7: Effect of MK-801 on IFNγ-induced increases in the mRNA expression of kynurenine pathway enzymes or iNOS in BV-2 microglia 90

Figure 3.3.4.1: Effect of kynurenine pathway metabolites on neuronal complexity 93

Figure 3.3.4.2: Effect of a combinations of kynurenine pathway metabolites on neuronal complexity 94

Figure 3.3.5.1: Effect of 1400W on IFNγ-stimulated BV-2 microglial-induced reductions in measures of neuronal complexity 97

Figure 3.3.5.2: Effect of DPI chloride on IFNγ-stimulated BV-2 microglial-induced reductions in measures of neuronal complexity 98

Figure 4.2.1: Diagram showing the timeline of a typical experiment 116

Figure 4.3.1.1: Effect of IFNγ on the mRNA expression of kynurenine pathway enzymes in primary cortical microglia 124

Figure 4.3.1.2: Effect of IFNγ on the concentrations of tryptophan, kynurenine, 3-hydroxykynurenine and the kynurenine/tryptophan ratio in the CM of primary cortical microglia 125

Figure 4.3.1.3: Effect of CM from IFNγ-stimulated primary cortical microglia on neuronal viability 126

Figure 4.3.1.4: Effect of CM from IFNγ-stimulated primary cortical microglia on measures of neuronal complexity 127

Figure 4.3.1.5: Effect of IFNγ on the mRNA expression of kynurenine pathway enzymes in primary mixed glia 128

Figure 4.3.1.6: Effect of IFNγ on the concentrations of tryptophan, kynurenine, 3-hydroxykynurenine and the kynurenine/tryptophan ratio in the CM of primary cortical mixed glia 129

Figure 4.3.1.7: Effect of CM from IFNγ-stimulated primary cortical mixed glia on neuronal viability and neuronal complexity 130

Figure 4.3.1.8: Effect of 1-MT (L) on IFNγ-stimulated mixed glia CM-induced reductions in neuronal complexity 131

Figure 4.3.1.9: Effect of IFNγ on the mRNA expression of kynurenine pathway enzymes in primary cortical astrocytes 132

Figure 4.3.1.10: Effect of IFNγ on the concentrations of tryptophan, kynurenine, 3-hydroxykynurenine and the kynurenine/tryptophan ratio in the CM of primary cortical astrocytes 133

Figure 4.3.1.11: Effect of CM from IFNγ-stimulated primary cortical astrocytes on neuronal viability and measures of neuronal complexity 134

Figure 4.3.1.12: Effect of IFNγ on the mRNA expression of kynurenine pathway enzymes in primary cortical neurons 135

Figure 4.3.1.13: Effect of IFNγ on the concentrations of tryptophan, kynurenine, 3-hydroxykynurenine and the kynurenine/tryptophan ratio in the CM of primary cortical neurons 136

Figure 4.3.1.14: Effect of 1-MT (L) on IFNγ-stimulated mixed glia CM-induced reductions the expression of synaptic markers in mature neurons 137

Figure 4.3.2.1: Concentration-related effects of kynurenine pathway metabolites on the viability of neurons 142

Figure 4.3.2.2: Concentration-related effect of tryptophan on measures of neuronal complexity 143

Figure 4.3.2.3: Concentration-related effect of kynurenine on measures of neuronal complexity 144

Figure 4.3.2.4: Concentration-related effect of 3-hydroxykynurenine on measures of neuronal complexity 145

Figure 4.3.2.5: Concentration-related effect of 3-hydroxyanthranillic acid on measures of neuronal complexity 146

Figure 4.3.2.6: Concentration-related effect of quinolinic acid on measures of neuronal complexity 147

Figure 4.3.2.7: Concentration-related effect of kynurenic acid on measures of neuronal complexity. 148

Figure 4.3.2.8: Effect of combinations of kynurenine pathway metabolites on neuronal viability and complexity 149

Figure 4.3.3.1: Concentration-related effects of kynurenine pathway metabolites on the viability of mature neurons 152

Figure 4.3.3.2: Concentration-related effects of kynurenine pathway metabolites on the expression of synaptic markers in mature neurons 153

Figure 4.3.3.3: Effect of combinations of kynurenine pathway metabolites on the viability of and the expression of synaptic markers in mature neurons 154

Figure 4.3.4.1: Effect of glutamate and glycine on neuronal viability and complexity ... 157

Figure 4.3.4.2: Concentration-related effects of glutamate and glycine on the viability of mature neurons 158

Figure 4.3.4.3: Effects of glutamate and glycine on the expression of synaptic markers in mature neurons 159

Figure 4.3.5.1: Concentration-related effects of kynurenic acid on glutamate and glycine-induced reductions in neuronal complexity 163

Figure 4.3.5.2: Concentration-related effects of kynurenic acid on glutamate and glycine-induced reductions in the expression of synaptic markers 164

Figure 4.3.5.3: Concentration-related effects of kynurenic acid on the 3-hydroxykynurenine + 3-hydroxyanthranillic acid + quinolinic acid combination-induced reductions in neuronal complexity 165

Figure 5.2.1: Diagram showing the timeline of a typical experiment 185

Figure 5.3.1.1 Effect of noradrenaline on the mRNA expression of kynurenine pathway enzymes in primary cortical astrocytes 190

Figure 5.3.1.2: Effect of the non-selective α-adrenoceptor antagonist, phentolamine, on the noradrenergic-related changes in kynurenine pathway enzymes mRNA expression in primary cortical astrocytes 191

Figure 5.3.1.3: Effect of the selective α_1-adrenoceptor antagonist, prazosin, and the selective α_2-adrenoceptor antagonist, yohimbine, on the noradrenergic-related changes in kynurenine pathway enzyme mRNA expression in primary cortical astrocytes 192

Figure 5.3.2.1: Effect of isoproterenol on the mRNA expression of kynurenine pathway enzymes in primary cortical astrocytes 197

Figure 5.3.2.2: Effects of selective β-adrenoceptor antagonists on isoproterenol-related changes in kynurenine pathway enzyme mRNA expression in primary cortical astrocytes 198

Figure 5.3.2.3: Effect of formoterol on the mRNA expression of kynurenine pathway enzymes in primary cortical astrocytes 199

Figure 5.3.2.4: Effect of a non-selective β-adrenoceptor antagonist on the formoterol-related changes in kynurenine pathway enzyme mRNA expression in primary cortical astrocytes 200

Figure 5.3.2.5: Effect of a β2-adrenoceptor antagonist on the formoterol-related changes in kynurenine pathway enzyme mRNA expression in primary cortical astrocytes 201

Figure 5.3.2.6: Effect of the cAMP analogue, dbcAMP on the mRNA expression of kynurenine pathway enzymes in primary cortical astrocytes 202

Figure 5.3.2.7: Effect of formoterol on the concentrations of tryptophan, kynurenine, 3-hydroxykynurenine and the kynurenine/tryptophan ratio in the CM of primary astrocytic cultures 203

Figure 5.3.3.1: Effect of noradrenaline and formoterol on the mRNA expression of kynurenine pathway enzymes in primary cortical microglia 206

Figure 5.3.3.2: Effect of noradrenaline and formoterol on the mRNA expression of kynurenine pathway enzymes in primary cortical neurons 207

Figure 5.3.3.3: Effect of formoterol on IFNγ-induced changes in the mRNA expression of kynurenine pathway enzymes in primary cortical microglia 208

Figure 5.3.3.4: Effect of formoterol on IFNγ-induced changes in the mRNA expression of kynurenine pathway enzymes in primary cortical astrocytes 209

Figure 5.3.3.5: Effect of formoterol on IFNγ-induced changes in the mRNA expression of kynurenine pathway enzymes in primary cortical neurons 210

Figure 5.3.3.6: Effect of formoterol and IFNγ in combination on the mRNA expression of kynurenine pathway enzymes in primary cortical mixed glia 215

Figure 5.3.3.7: Effect of formoterol on the IFNγ-induced changes in the concentrations of tryptophan, kynurenine, 3-hydroxykynurenine and the tryptophan/kynurenine ratio in the CM of primary mixed glial cultures 216

Figure 5.3.3.8: Effect of formoterol of the IFNγ-stimulated mixed glial CM-induced changes in neuronal complexity and the expression of synaptic markers 217

Figure 5.3.3.9: Effect of TDO inhibition on the ability of formoterol to protect against the mixed glia IFNγ CM-induced reductions in neurite outgrowth and the co-localised expression of synaptic markers 218

Figure 5.3.4.1 Effect of formoterol-stimulated astrocytic CM on kynurenine pathway metabolite-induced changes in neuronal complexity 221

Figure 5.3.4.2 Effect of formoterol-stimulated astrocytic CM on kynurenine pathway metabolite-induced changes in the expression of synaptic markers 222

Figure 6.1: Differential effects of adrenoceptor subtypes on KAT II and TDO gene induction 239

Figure 6.2: The combined effect of simultaneous activation of the neurotoxic and neuroprotective arms of the kynurenine pathway on neuronal complexity and the co-localisation of synaptic markers 242

Figure S1: Baseline concentrations of tryptophan, kynurenine, and 3-hydroxykynurenine in cell-free cNBM xxvii

Figure S2: Effect of 1-MT (L) on the basal concentrations of tryptophan, kynurenine, 3-hydroxykynurenine and the kynurenine/tryptophan ratio in the CM of primary cortical mixed glia xxviii

Figure S3: Concentration related effects of formoterol on neuronal viability and complexity xxix

Figure S4: Effect of formoterol on neuronal viability and the expression of synaptic markers in mature neurons xxx

List of tables

Table 1.1 Changes in the levels of kynurenine pathway metabolites in patients suffering from neurological disorders. 22

Table 2.1: List of antibodies used in fluorescent immunocytochemistry 40

Table 2.2: Table of compounds, molecular weights, and solvents 45

Table 2.3: Volumes of the components in the cDNA synthesis master mix 59

Table 2.4: Volumes of the components in the Primer mix 59

Table 2.5: List of FAM-labelled MGB target probes used in PCR 60

Table 3.2.1: Table of compounds and concentrations used 72

Table 4.2.1: Table of compounds and concentrations used 117

Table 5.2.1: Table of compounds and concentrations used 186

Table S1: Average control ΔΔCt values for the gene expression of kynurenine pathway enzymes in BV-2 microglia and primary glia and neurons. xxvi

Abbreviations

ΔΔCT	Cycle difference corrected for endogenous control
1-MT	1-methyltryptophan
3-HAA	3-hydroxyanthranillic acid
3-HK	3-hydroxykynurenine
AC	Adenylate cyclase
ALS	Amylotropic lateral sclerosis
AMPA	α-amino-3-hydroxy-5-methyl-4-isoaxzoleproprionic acid
ANOVA	Analysis of variance
ATP	Adenosine triphosphate
BBB	Blood brain barrier
BDNF	Brain-derived neurotrophic factor
Ca^{2+}	Calcium ion
cAMP	Cyclic adenosine monophosphate
cDMEM	complete DMEM
cDNA	Complimentary DNA
CM	Conditioned media
cNBM	Complete NBM
CNS	Central nervous system
COX	Cyclooxygenase
CREB	cAMP response element-binding protein
cRPMI	Complete RPMI
CT	cycle number
dbcAMP	N^6,2′-O-Dibutyryladenosine 3′,5′-cyclic monophosphate sodium salt
DIV	Days *in vitro*
DMEM	Dulbecco's modified eagle media
DMSO	Dimethyl sulfoxide
DNA	Deoxyribonucleic acid
dNTP	Dinucleotide triphosphates
EAAT	Excitatory amino acid transporter
EtOH	Ethanol
FAM	Fluorescein amidite
FBS	Foetal bovine serum
FRET	Fluorescence resonance energy transfer
GABA	γ-amino butyric acid
GDP	Guanonine diphosphate
GFAP	Glial fibrillary acidic protein
Gly	Glycine
GM-CSF	Granulocyte macrophage colony stimulating factor
GPCR	G protein-coupled receptor
GR	Glucocorticoid receptor
GTP	Guanonine triphosphate
HPA	Hypothalamic pituitary adrenal
HPLC	High performance liquid chromotography
IDO	Indoleamine 2, 3-dioxygenase
IFN	Interferon

IFNγR	interferon gamma receptor
IL	Interleukin
iNOS	Inducible nitric oxide synathase
IP3	Inositol triphosphate
IS	Internal standard
IκB	Inhibitor of NFκB
JAK	Janus-activated kinase
KAT	Kynurenine amino transferase
KMO	Kynurenine monooxygenase
KYNA	Kynurenic acid
KYNU	Kynureninase
L-AAA	L-α aminoadipic acid
LDH	Lactate dehydrogenase
LPS	Lipopolysaccharide
M-CSF	Macrophage colony stimulating factor
MeOH	Methanol
MGB	Minor groove binding
MHC	Major histocompatibility complex
MPP^+	1-methyl-4-phenylpyridinium
MTS assay	CellTiter 96® AQ_{ueous} Non-Radioactive Cell Proliferation assay
NAD^+	Nicotinamide adenine dinucleotide
NADPH	Nicotinamide adenine dinucleotide phosphate
NBM	Neurobasal media
NFQ	Non-fluorescent quencher
NFκB	nuclear factor κ-light-chain-enhancer of activated B cells
NGS	Normal goat serum
NMDA	N-methyl-D-aspartate
NOS	Nitric oxide synthase
PBS	Phosphate buffered saline
PCR	Polymerase chain reaction
PGC-1α	PPARγ co-activator 1α
PKA	Protein kinase A
PLC	Phospholipase C
PMS	Phenazine methosulfate
PPAR	Peroxisome proliferator-activated receptor
PSD	Post-synaptic density
Quin	Quinolinic acid
rDNase	Recombinant deoxyribonuclease
RNA	Ribonucleic acid
Rnase	Ribonuclease
ROI	Region of interest
ROS	Reactive oxygen species
rpm	Rotations per minute
RPMI	Roswell Park Memorial Institute media
RQ	Relative quantity
SAM	Sympathoadrenal medullary
SEM	Standard error of the mean

SOCS	Suppressor of cytokine signalling
STAT	Signal transducer and activator of transcription
TDO	Tryptophan 2, 3-dioxygenase
TGFβ	Transforming growth factor β
UV	Ultraviolet

Chapter 1

General introduction

Cellular composition of the central nervous system (CNS)

The CNS is responsible for the coordination of all bodily functions and as such is an extremely complex and unique organ. The CNS is made up of 10^{12} neurons which allow for communication between different brain regions and also between central and peripheral structures through the transmission of chemical and electrical signals. Glial cells are found in inter-neuronal spaces and provide neuronal support and regulate the homeostasis of the brain through various mechanisms. There are four subtypes of glial cells: microglia, astrocytes, oligodendrocytes and ependymal cells all of which play varying roles in supporting neuronal function and providing neuronal protection (Lodish, 2000).

1.1.1 Microglia

Microglia are the innate immune cells of the brain, with a widespread, non-overlapping distribution and a reduced immune effector cell function under normal circumstances (Banati, 2003). Microglia account for 5-10% of the adult brain population (Czeh et al., 2011), the density of which varies depending on the brain region. Microglia are predominantly found in the grey matter with their highest densities in the hippocampus, substantia nigra and basal ganglia (Lawson et al., 1990).

The exact origin of microglia is still debated, it is thought that functionally different microglia have distinct origins with surveying parenchymal microglia arising from pial macrophages and mesenchymal progenitors which invade the brain in two waves during development via the meninges, choroid plexus and eventually through the blood vessels. However, microglia with a strong ability for antigen presentation are thought to arise from bone-marrow derived myeloid cells (Gate et al., 2010) which can invade both the developing and mature CNS (Monier et al., 2007). During development microglia are proposed to be derived from early embryonic macrophage-like mesodermal precursor cells which migrate to the brain parenchyma where they become resident immune cells (Ginhoux et al., 2013, McGeer and McGeer, 1995).

Activated microglia have a diverse range of functions, depending on their phenotype. During development they are mainly involved in synaptogenesis, synaptic pruning and axon remodelling (Tremblay et al., 2011, Tremblay and Majewska, 2011, Schlegelmilch et al., 2011, Pont-Lezica et al., 2011). In the adult brain microglia have numerous roles in the removal of neurotoxic debris (Glezer et al., 2007), innate immunity (Jack et al., 2005) and the promotion of neuronal survival through the release of trophic and anti-inflammatory molecules (Loane and Byrnes, 2010). They are also involved in repair due to their ability to guide stem cell migration to the site of inflammation or injury (Aarum

et al., 2003) and there is evidence to support their role in promoting neurogenesis (Walton et al., 2006).

1.1.1.2 Microglial morphology

Under normal circumstances in the adult brain microglia exist in a down-regulated or "resting" state, characterised by their ramified morphology which consists of long processes that are constantly motile, allowing microglia to survey their micro-environment and detect changes in homeostatic parameters and identify potential threats (Nimmerjahn et al., 2005). In this state microglia have very low levels of expression of surface markers with minimal release of cytokines and chemokines and no phagocytic function (Aloisi, 2001).

In response to tissue injury or immune stimuli microglia are able to rapidly transform into an activated state, characterised by an amoeboid morphology. This involves the withdrawal of their processes (Fetler and Amigorena, 2005, Nimmerjahn et al., 2005) and the upregulation of certain cell-surface markers such as the phagocytic cell surface marker, major histocompatibility complex (MHC) (Rock et al., 2004). It is now believed that there are more than just three microglial phenotypes as previously outlined by del Rio-Hortega (1939). Activation may stimulate increased expression of cell surface markers involved in the recruitment of peripheral chemotactic cells, it may produce non-phagocytic, but inflammatory-mediating microglia or indeed it could lead to the formation of motile and phagocytic microglia (Kreutzberg, 1996, Sasaki et al., 1993, Streit et al., 1989). It is still unclear whether the different states are induced by specific stimuli and if there are additional multifaceted or transitional states [see, Lynch (2009) for review].

1.1.1.3 Microglial activation

Overall microglia have a beneficial role when activated in a controlled manner for a temporary period. The tight coupling between neuronal activity and microglial functionality provides a means of identifying disease location, development, chronicity and resolution. Following a lesion, extracellular ion concentrations change within milliseconds with microglial activation peaking 2-3 days following this type of tissue damage, and this being maintained in the presence of the pathological stimulus (Banati, 2003).

Over-activation of microglia can be triggered by the persistent presence of environmental toxins or other factors such as neuronal death, which can have detrimental effects as a result of the release of numerous factors leading to neuronal injury (Block et al., 2007b). These factors include cytokines, chemokines, complement factors, and reactive oxygen and nitrogen species (Lynch, 2009). The neuronal damage caused by such toxins can be mediated either by microglia alone, or by synergistic effects whereby the toxins directly affect neurons, but the presence of microglia enhances the

detrimental effects of the toxin. In the lipopolysaccharide (LPS) *in vitro* rat model of neurodegeneration it was shown that LPS is toxic only in the presence of microglia (Gao et al., 2002). While the neurotoxin, 1-methyl-4-phenylpyridinium (MPP+) directly damages cultured rat dopaminergic neurons, it can also activate microglia, enhancing neuronal damage (Gao et al., 2003). In addition, exposure of developing microglia to LPS *in utero* during critical periods results in a potentiated and progressive response to LPS administration in adult mice (Ling et al., 2006). Microglia-mediated toxicity appears to be progressive (Gao et al., 2003), and once over-activated, microglia can be maintained in this state by chronic neuroinflammation.

1.1.2 Astrocytes

Astrocytes are the most abundant and prevalent cells of the CNS, with a diverse range of functions including regulation of the blood brain barrier (BBB), control of ionic concentrations in the extracellular space, scavenging potentially toxic molecules such as glutamate, supplying nutrients to neurons, and also communication through the release of gliotransmitters or calcium (Ca^{2+}) signalling via gap junctions [see, Lee et al. (2013) for review].

1.1.2.1 Astrocytic morphology

Astrocytes are a heterogeneous cell population with variations in their morphology and receptor and protein expression (Matyash and Kettenmann, 2010). During development they are derived from ependymoglia of the neural tube which contributes to their polarization of function with astrocytic endfeet having specialised receptors and metabolic enzyme systems which help to maintain BBB integrity (Abbott et al., 2006). Initially astrocytes were categorised as protoplasmic or fibrous, with protoplasmic astrocytes found in the grey matter exhibiting complex processes, while fibrous astrocytes found in the white matter possess more simple processes with limited branching (Sofroniew and Vinters, 2010). However, over the past decade or so it has been recognised that this division of astrocytes is too simple and now it is believed that there are at least nine different classes of astrocytes spread throughout the brain with the distinct classes not being restricted to any given region but co-existing at various densities (Emsley and Macklis, 2006).

1.1.2.2 Astrocytic activation

In response to alterations in their local environment, astrocytes can rapidly change their morphology and function in order to protect neurons. These so-called reactive astrocytes are capable of producing pro- and anti-inflammatory cytokines, chemokines, neurotrophins, reactive oxygen species (ROS), along with other factors which have the potential to protect neurons, however in times of reactive astrogliosis these factors may elicit further harm to neurons (Farina et al., 2007, Liberto et

al., 2004). Reactive astrogliosis results in a profound change in astrocyctic phenotype. It is a heterogenous state in which the activities of the astrocytes are altered in a stimuli-dependent manner. Although there is a core set of responses that occur following detection of infection, injury, or disease, 50% of altered gene expression is specific to the disease stimuli (Zamanian et al., 2012).

1.2 Neurodevelopment

1.2.1 Introduction to neurite outgrowth

There are numerous different types of neurons, however in general, a neuron contains four distinct morphological regions - dendrites, the cell soma, the axon, and the axon terminals (Lodish, 2000); with the term neurite being designated to any projection from the cell soma, and therefore includes both axons and dendrites (**figure 1.2**). Neurite outgrowth is a sophisticated process that entails initiation of neurite formation, elongation, targeted guidance of neurites and the ultimate formation of synapses. The first stage is driven by protrusion of theneuritic growth cone into the environment (**figure 1.1**). The functionally active synaptic connections allow for effective inter-neuronal communication with an axon transmitting information in the form of an action potential from the cell soma to the pre-synaptic terminals of a neuron. Axons and dendrites differ both morphologically and functionally, with axons extending over large areas with limited branching, while dendrites remain close to the cell body but have elaborate branching allowing for the integration of synaptic information from surrounding cells (Lodish, 2000).

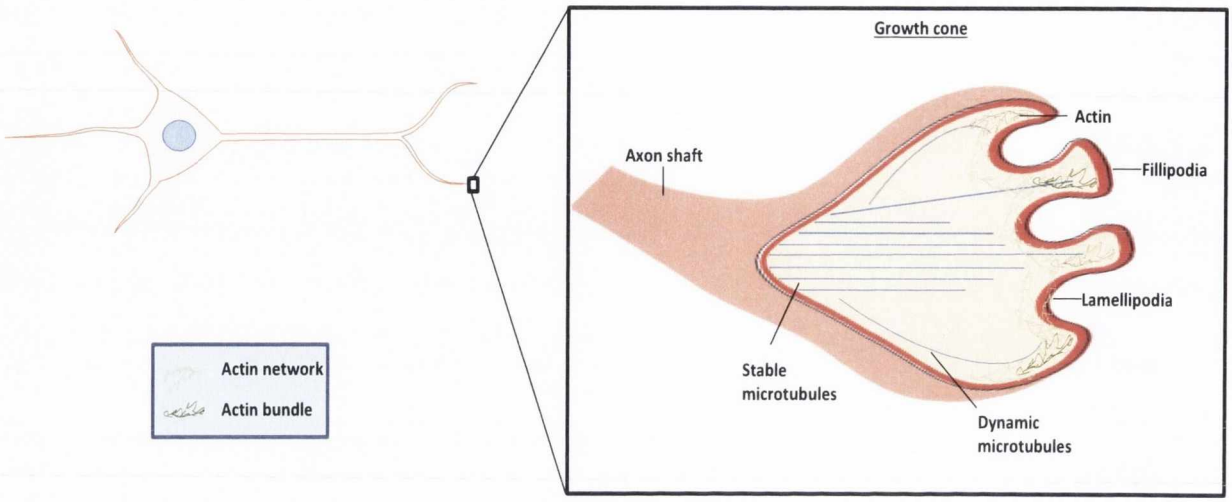

Figure 1.1: The structure of the growth cone

The cytoskeleton of a neurite is composed of three main dynamic proteins complexes; actin filaments, microtubules, and intermediate filaments. In response to either internal or external cues, these protein complexes can modify their assembly to either promote or stunt neurite outgrowth (Flynn, 2013). The growth cone is a sensory-motile specialisation found at the tip of the neurite (Myers et al., 2011). These growth cones are dynamic and are capable of detecting molecular cues in their vicinity allowing them to respond to the environment (Dent and Gertler, 2003). The growth cone engages its cytoskeleton to allow it to advance in a particular direction (Goldberg and Burmeister, 1986). The leading edge of the growth cone is made up of dynamic filipodia which contain bundles of actin filaments, with membrane containing branched actin filament networks, referred to as lamellipodia, connecting each filipodium. Within the growth cone there are three distinct domains, the peripheral domain which contains the filipodia, the central domain which contains a stable bundle of microtubules which stems from the axonal shaft, and the transition domain which is found between the peripheral and central domains and contains actomyosin contractile structures perpendicularly orientated to the actin filament bundles of the filipodia. Movement of the growth cone is driven by the interplay between two processes known as actin filament treadmilling and actin filament retrograde flow. Actin filament treadmilling consists of polymerisation of actin at the end closest to the leading edge and depolymerisation of the filament at the opposite end maintaining a stable filament length. Actin filament retrograde flow refers to movement of the filament from the leading edge towards the centre of the growth cone providing the growth cone with the potential to initiate movement while it is in an immotile state [see, Lowery and Van Vactor (2009) for review].

1.2.2 The stages of neurite outgrowth

Neurite outgrowth can be divided into three distinct stages, the first being protrusion which involves the extension of the actin filament containing filipodia into the environment; engorgement, where microtubules from the central domain expand into the peripheral domain bringing with them essential outgrowth machinery; and consolidation where the axon shaft reassembles using growth cone residues [see, Dent and Gertler (2003) for review].

Receptors are present on the surface of the growth cones and at the tips of the filipodia which bind to ligands in the extracellular matrix (O'Donnell et al., 2009). These receptors allow for the formation of connections with the environment or they can trigger intracellular biochemical signalling. Receptor binding in the growth cone can influence outgrowth either positively or negatively, with locally produced graded signals in the growth cone allowing for axon turning (Myers et al., 2011).

Regulatory molecules in the extracellular matrix are produced by both neurons and glia (Venstrom and Reichardt, 1993). Growth cone extension requires continuous exocytosis and endocytosis which are SNARE-dependent and clathrin-dependent/independent respectively (Tojima et al., 2011). The development of hippocampal neurons *in vitro* has been described in five stages (**figure 1.2**) (Dotti et al., 1988). Axonal outgrowth occurs prior to that of dendrites. A neurite intended to become an axon displays increased actin mobility and instability allowing the microtubules to extend (Luo, 2002). Dendritic outgrowth occurs either after axonal outgrowth or following the formation of the first synapses. This process is more progressive and stable during which neurons lose the ability to further elongate the axon (Scott and Luo, 2001). Both axons and dendrites respond in a similar manner to growth and guidance cues (Goldberg, 2003).

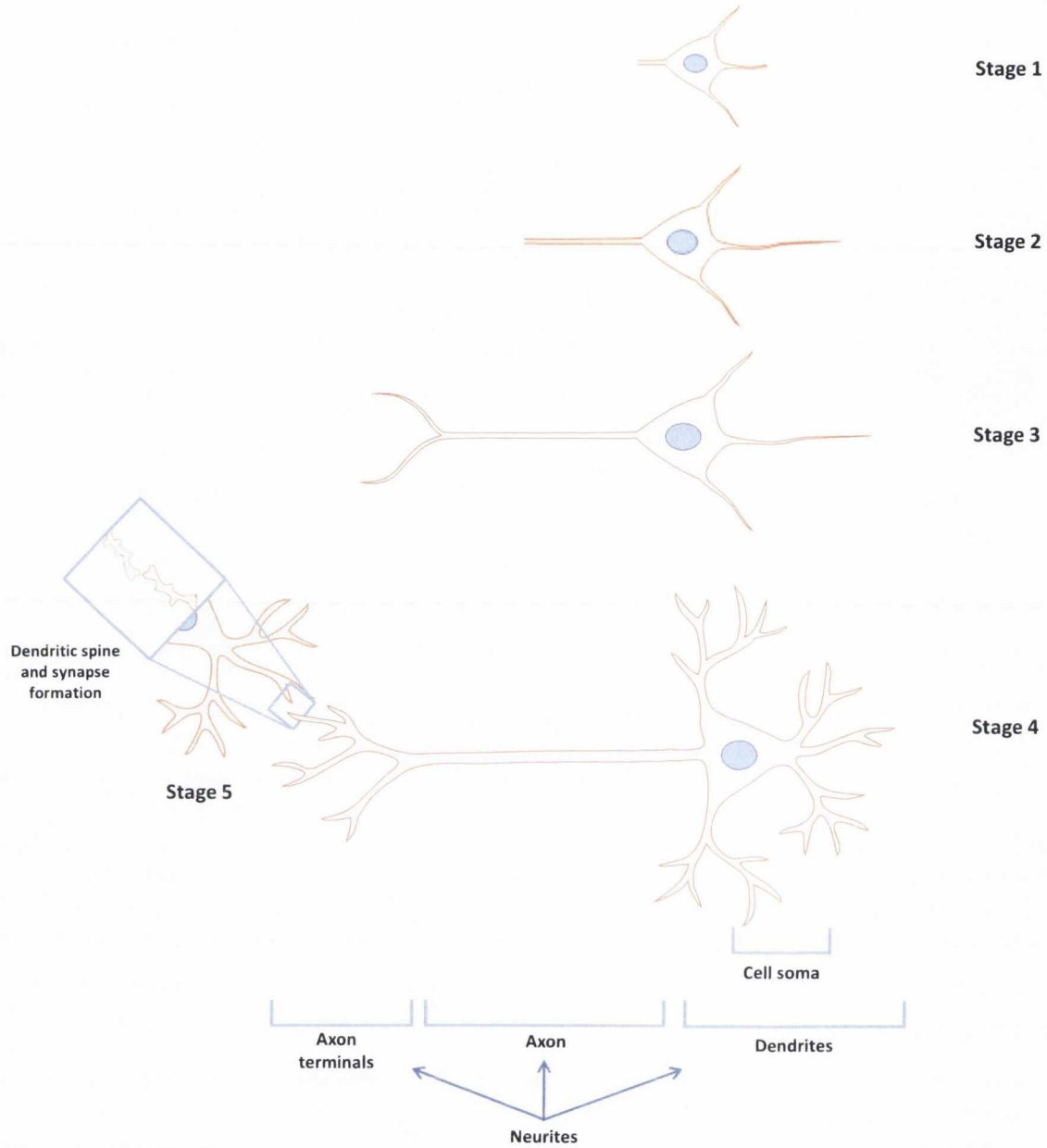

Figure 1.2: The stages of neuronal development *in vitro*

Following plating, neurons extend their intracellular filipodia and lamellipodial, marking stage 1 of development. Stage 2 involves the extension of immature neurites which occurs at days *in vitro* (DIV) 1-2. Stage 3, neurite polarisation, begins at DIV 3-4 with a single neurite destined to become an axon extending rapidly, while all other neurites become dendrites. Stage 4 occurs between 3-15 DIV, with all neurites extending and the initiation of branching. At 15-25 DIV stage 5 occurs which involves the formation of dendritic spines and synaptogenesis. Neurites including the axon and dendrites stem from the cell soma which contains the nucleus. The axon terminals are found at the end of the axon and are involved in neurotransmitter release. Primary neurites stem directly from the cell soma, while neuritic branches are offshoots from the primary neurite with growth cones located at the tips of neurites.

1.2.3 Formation of neuritic branches and synapses

Neuritic branches can be produced when an active growth cone encounters an inhibitory signal causing it to terminate its advancement. This interruption in outgrowth can result in the growth cone splitting and the progression of the daughter growth cones occurring at different rates resulting in independent branches. Another mechanism which may lead to the development of a neuritic branch is when collections of actin filaments known as actin filament patches form along the axon shaft resulting in the formation of a filipodium which must become stabilised by the invasion of microtubules to prevent it re-integrating with the axon shaft allowing it to eventually develop into a new neuritic branch. This type of neuritic branching is referred to as interstitial branching and is the predominant mechanism of branching [see, Gallo (2011) for review]. When this occurs along an axon, an axon collateral forms which elongates until it reaches its target at which point the growth cone develops into the pre-synaptic terminal. With regard to dendritic branching, rapid extension and retraction of filipodia and branches along dendrites enable the development of intrinsic dendritic trees. Dendritic spines are the primary sites of synaptic contact in the brain and develop in a similar manner to branches. In contrast however, they primarily contain actin filaments as opposed to microtubules, enabling rapid formation and degradation (Luo, 2002).

Synapse formation and stabilisation is a dynamic process requiring bi-directional communication from pre- and post-synaptic elements. Synaptogenesis refers to synapse formation, maturation, stabilisation and potentially elimination. Upon reaching target dendritic arbors or the cell soma, both axonal and dendritic filipodia enable synapse formation. Pre-synaptic differentiation occurs within 1-2 hr following initial contact both *in vitro* and *in vivo* (Cohen-Cory, 2002), with the emergence of varicosities containing synaptic vesicles, alongside the active recycling of vesicles (Ahmari et al., 2000, Friedman et al., 2000). In cultured hippocampal neurons, pre-synaptic differentiation occurs prior to post-synaptic differentiation (Okabe et al., 2001), while both occur simultaneously in cultured cortical neurons (Friedman et al., 2000), with the major component of the post-synaptic specialisation being the scaffolding protein, post-synaptic density-95 (PSD-95). Upon formation of a synaptic contact, stabilisation of the pre-synaptic specialisation occurs via trafficking of protein complexes, such as synaptic vesicles and synaptophysin-containing packets (Goldberg, 2003). The accumulation of synaptic proteins such as synaptophysin or PSD-95 in the pre- or post-synaptic synapses forms pre- or post-synaptic 'puncta' - a cluster of synaptic proteins representing a stable synapse. Synapse remodelling is believed to coincide with morphological maturation of neurites. During development, an excess of synapses are formed, with elimination of obsolete synapses – 'synaptic pruning'; representing a critical process in synaptic circuit maturation (Cohen-Cory, 2002).

1.2.4 Contribution of glia to neurite outgrowth and synaptogenesis

It is now well accepted that glia are essential in the formation and maintenance of neuronal synapses (Murai and Van Meyel, 2007, Chen and Swanson, 2003). Astrocytes in particular are associated with promoting neurite outgrowth and synaptogenesis, with their extended processes enveloping neuronal cell somas, neurites and synapses, while their end-feet contact central capillaries. This intimate association with neurons alongside their constitutive release of trophic factors aids neuronal survival and proliferation (Chen and Swanson, 2003). Indeed, there is a temporal correlation between synapse formation and the development of astrocytes in the rodent brain (Pfrieger and Barres, 1996). Initially glia are involved in assisting neurons in finding target neurons by promoting outgrowth and providing guidance (Johnson et al., 2007). Interestingly, glia appear to be primarily involved in the formation of glutamatergic synapses, while inhibitory γ-aminobutyric acid (GABA)-ergic synapses form prior to glial differentiation (Huang and Scheiffele, 2008, Ben-Ari, 2002). Studies carried out in culture have demonstrated that the presence of glia is not essential for the formation of neuronal synapses, however in their absence some neurons fail to form or form far less synaptic connections (Ullian et al., 2001). The turn-over of synaptic connections is particularly high, and is believed to prompt the deleterious cascade in neurodegenerative disease (Knobloch and Mansuy, 2008).

In contrast, microglial proliferation occurs prior to synapse formation (Dalmau et al., 1998), however their effect on neurite outgrowth and synaptogenesis has been proposed to be primarily deleterious, with the release of microglial-associated factors such as inflammatory cytokines, nitric oxide, and glutamate inducing-neuronal atrophy and synapse loss (O'Neill et al., 2016, Doucet et al., 2015, Munch et al., 2003).

1.2.4.1 The tripartite synapse

As a consequence of the intimate association of astrocytes and neuronal synapses the concept of the 'tripartite synapse' has emerged, implicating astrocytes as an integral component of synaptic connections (Araque et al., 1999). Astrocytes are capable of communicating with neurons via Ca^{2+}-dependent glutamate release. Glutamate is the main excitatory neurotransmitter in the brain which acts at a range of ionotropic and metabotropic receptors. Of these receptors, N-methyl-D-aspartate (NMDA), α-amino-3-hydroxy-5-methyl-4-isoxazole propionate (AMPA) and kainite receptors are ionotropic, and consist of four subunits surrounding an ion channel. NMDA receptors are made up of a combination of NR_1 or NR_2 subunits, while AMPA and kainate receptors consist of a combination of $GluR_{1\text{-}7}$ and $KA_{1,2}$ (Rang and Dale, 2012).

Astrocytic-mediated release of glutamate causes an increase in the intracellular levels of Ca^{2+} in neurons *in vitro* (Verkhratsky and Kettenmann, 1996, Parpura et al., 1994), with electrophysiology studies demonstrating astrocyte-induced neuronal depolarisation via both NMDA- and non-NMDA-dependent mechanisms (Verkhratsky and Kettenmann, 1996). Extracellular levels of glutamate are typically in the micromolar range, however these concentrations can increase 100-fold resulting in excitotoxicity (Gras et al., 2012). Astrocytes are important in maintaining a homeostatic concentration of synaptic glutamate, by re-uptake via the excitatory amino acid transporter (EAAT) 1 or 2 followed by the conversion of glutamate to glutamine by glutamine synthetase (Dantzer and Walker, 2014a). Glutamine can be released from astrocytes and taken up by neurons as a glutamate precursor, giving rise to the 'glutamate shunt'. Intracellular elevations of astrocytic glutamate downregulates the expression of EAAT1 ensuring that the synapse is not overly depleted of glutamate (Takaki et al., 2012). The biphasic effects of glutamate on neuronal complexity have been demonstrated *in vitro* by Doucet et al. (2015), who show a positive effect on neurite length and branching with treatment with 100 μM glutamate, while 500 μM glutamate has no beneficial effect. Indeed, in the presence of the NMDA receptor co-agonist, glycine, 500 μM glutamate reduced neurite length and branching, while 100 μM glutamate has no effect. This atrophic effect was demonstrated to be NMDA receptor-mediate, as opposed to through activation of other glutamaergic receptors.

1.2.4.2 Microglia; a transient component of the tripartite synapse

Due to the motile nature of microglia, their presence at specific synapses is not necessarily constant, however when they are in close proximity, their interaction with neurons influences dendritic spine and synapse formation (Lim et al., 2013b, Tremblay and Majewska, 2011). Reactive microglia represent another source of synaptic glutamate, as a consequence of their uptake of extracellular glutamine which they convert to glutamate (Takeuchi et al., 2006). Reactive microglia release large amounts of glutamate into the extracellular milieu (Piani et al., 1992) via connexion hemichannels of gap junctions which form *in vitro* in response to inflammatory agents, in the presence of clusters of microglial (Eugenin et al., 2001). An additional and more prominent mechanism of glutamate release from microglia occurs via a transporter system known as system x_c^-. Activation of this system occurs under oxidative or inflammatory circumstances to aid in maintaining the redox balance through the influx of cysteine in exchange for glutamate, and subsequent production of the antioxidant glutathione (Conrad and Sato, 2012).

Both microglia and astrocytes are capable of influencing neuronal integrity through either direct cell-cell interactions, or through the release of factors which subsequently promote or discourage outgrowth and synapse formation. Commonly identified permissive cues include growth factors,

neurotrophins, glutamate and cytokines (Day et al., 2014, Doucet et al., 2013, Lim et al., 2013b, Citri and Malenka, 2007), while atrophy can occur through NMDA receptor over-activation, in addition to the increased presence of ROS, nitric oxide or pro-inflammatory cytokines (O'Neill et al., 2016, Scheiblich and Bicker, 2016, Munnamalai and Suter, 2009, Mattson, 2008). Another potential, unexplored mechanism that may be implicated in neurite atrophy and synapse loss, is disrupted kynurenine pathway activation. The kynurenine pathway is a tryptophan metabolism pathway that is induced in times of stress or immune activation, resulting in the production of a range of metabolites which have neuromodulatory properties of which NMDA receptor activation and ROS generation are implicated (**figure 1.3**). Dysregulation of this pathway has been identified in multiple CNS disorders ranging from psychiatric disorders to neurodegenerative diseases (Bohar et al., 2015, Karakuła-juchnowicz et al., 2015, Reus et al., 2015). The potential for this pathway to attenuate neuronal outgrowth has been demonstrated though interaction of the metabolite quinolinic acid with the phosphorylating system associated with cytoskeletal proteins (Pierozan et al., 2015, Pierozan et al., 2010). Moreover, metabolites upstream of quinolinic acid are capable of generating ROS which have the potential to alter neuronal structures through the oxidation of lipids, proteins and DNA (Munnamalai and Suter, 2009)

1.3 The kynurenine pathway

1.3.1 Tryptophan metabolism along the kynurenine pathway

The kynurenine pathway is the main pathway by which the essential amino acid tryptophan is metabolised. Tryptophan circulates in the blood, with 70-90% of it being bound to albumin (Fernstrom, 1984). Upon reaching central capillaries, it can cross the BBB via the large amino acid active transporter (Fernstrom, 1984), where albumin is stripped off releasing free tryptophan into the brain (Yewiler et al., 1977). Once in the brain tryptophan is taken up by glial cells by an unknown mechanism and catabolised down the kynurenine pathway, ultimately leading to the production of nicotinamide adenine dinucleotide (NAD^+). Continuous generation of NAD^+ is essential to cell survival (Ying, 2006). For one, it is of utmost importance in the generation of energy (Berger et al., 1986), as well as being involved in the regulation of intracellular Ca^{2+} and gene expression (Sauve et al., 2006, Berger et al., 2004).

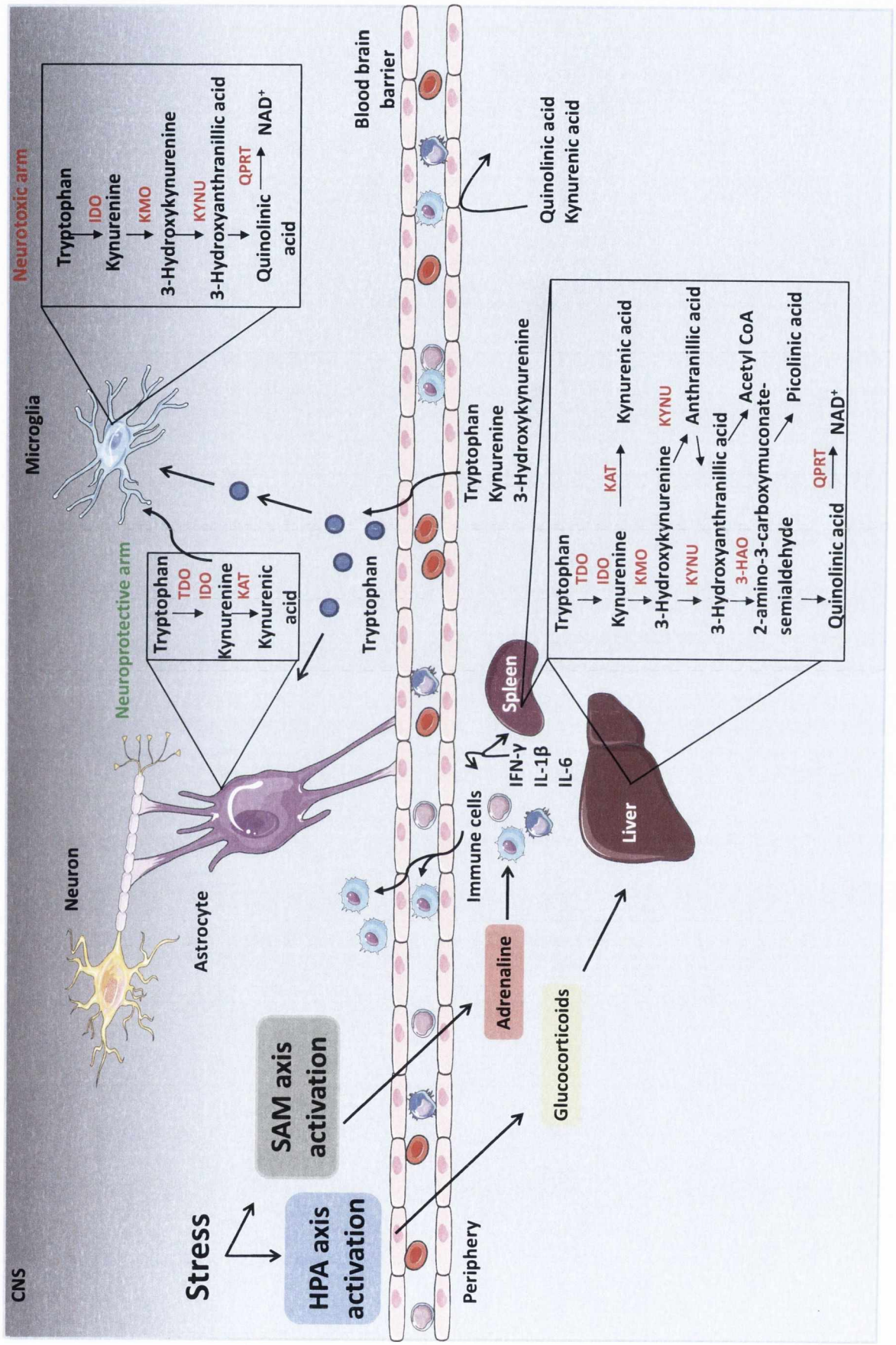
CNS
Stress
HPA axis activation
SAM axis activation
Periphery
Glucocorticoids
Adrenaline
Immune cells
IFN-γ
IL-1β
IL-6
Spleen
Liver
Blood brain barrier
Neuron
Astrocyte
Microglia
Neuroprotective arm
Neurotoxic arm
Tryptophan
TDO
IDO
Kynurenine
KAT
Kynurenic acid
KMO
3-Hydroxykynurenine
KYNU
3-Hydroxyanthranillic acid
QPRT
Quinolinic acid
NAD+
Tryptophan
Kynurenine
3-Hydroxykynurenine
Quinolinic acid
Kynurenic acid
Anthranillic acid
3-HAO
Acetyl CoA
2-amino-3-carboxymuconate-semialdehyde
Picolinic acid

Figure 1.3: The kynurenine pathway in the periphery and CNS
The initial conversion of tryptophan to kynurenine requires induction of either of the rate limiting enzymes, tryptophan 2, 3-dioxygenase (TDO) or indoleamine 2, 3-dioxygenase (IDO). Induction of IDO by the stress response can be achieved through sympathoadrenal medullary (SAM) system-associated adrenergic action at β-adrenoceptors on immune cells resulting in the release of pro-inflammatory cytokines including interleukin (IL)-1β, IL-6 and interferon (IFN)γ (Elenkov et al., 2000) which are capable of inducing IDO. Stress-induced activation of the hypothalamic pituitary adrenal (HPA) axis results in the release of glucocorticoids from the adrenals which can lead to the induction of TDO upon activation of intracellular glucocorticoid receptors (GR). TDO/IDO subsequently metabolises tryptophan to kynurenine, which is then converted to either kynurenic acid by kynurenine aminotransferase (KAT) or 3-hydroxykynurenine by kynurenine monooxygenase (KMO). 3-hydroxykynurenine is further metabolised to either anthranillic acid or 3-hydroxyanthranillic acid by kynureninase (KYNU), which gives rise to acetyl CoA, or it can be metabolised to the unstable intermediate, 2-amino-3-carboxymuconate by 3-hydroxyanthranillic acid 3, 4-dioxygenase (3-HAAO). This metabolite is further enzymatically converted to picolinic acid, or non-enzymatically transformed to quinolinic acid, the precursor for NAD^+ (Lugo-Huitron et al., 2013, Vecsei et al., 2013). Within the CNS the kynurenine pathway is differentially compartmentalised within astrocytes and microglia in the brain. Tryptophan uptake and metabolism in astrocytes leads to the production of kynurenic acid which is reported to have neuroprotective actions in the CNS. Metabolism of tryptophan in microglia gives rise to the metabolites with reactive oxidative properties including 3-hydroxykynurenine and 3-hydroxyanthranillic acid and quinolinic acid (Guillemin et al., 2001, Guillemin et al., 2003).

1.3.2 Compartmentalisation of the kynurenine pathway in the CNS

Following metabolism of tryptophan to kynurenine, the kynurenine pathway branches giving rise to a neurotoxic arm and a neuroprotective arm. The cell type in which kynurenine is produced determines the arm along which kynurenine is metabolised due to the intracellular enzymatic profile. It has been shown that microglia preferentially express the enzymes KMO and KYNU which are necessary for activation of the neurotoxic arm (Guillemin et al., 2003), while astrocytes preferentially express KAT which drives the neuroprotective arm of the kynurenine pathway (Guillemin et al., 2001) (**figure 1.3**).

1.3.3 The differential activation and roles of IDO and TDO

Both TDO and IDO have evolved to have similar functions, differing primarily in substrate specificity and tissue and cellular localisation. Most species contain both tryptophan-metabolising enzymes, with gene duplications resulting in certain species having several homologs of these enzymes (Ball et al., 2014). IDO is a monomeric enzyme with a broader substrate specificity than TDO. IDO and TDO have a sequence identity of only 10%, while the recently discovered tryptophan-catabolising enzyme IDO-2 which is encoded by a gene adjacent to that of IDO, shares 43% sequence identity and

structural similarities with IDO (Forouhar et al., 2007). IDO is expressed extra-hepatically in intestinal, lung, placental and brain tissue (Stone, 1993) with high expression of IDO found in the spleen as a consequence of the accumulation of IDO-expressing immune cells, including dendritic cells and peripheral blood mononuclear cells (Jones et al., 2015, Bronte and Pittet, 2013, Hwu et al., 2000).

1.3.3.1 The role of IDO in kynurenine pathway activation

Induction of IDO is pivotal in the immune response. IDO activation is associated with the anti-parasitic, anti-fungal, anti-viral, and anti-bacterial activities of polymorphonuclear immune cells (Kwidzinski and Bechmann, 2007, Bozza et al., 2005). These effects are achieved through tryptophan depletion and the production of kynurenine, 3-hydroxykynurenine, and 3-hydroxyanthranillic acid in pathogens, which are anti-proliferative and increase the apoptotic susceptibility of the cells in which they are produced. Moreover, activation of IDO results in immunosuppression and can lead to immune tolerance (Kwidzinski and Bechmann, 2007) if the aforementioned mechanisms occur in T lymphocytes (Fallarino et al., 2002). The kynurenine pathway metabolites also shift the T cell response towards the development of regulatory T cells. This occurs as a consequence of a positive feedback cycle which exists between dendritic cells and regulatory T cells, in so much as IDO induction in dendritic cells drives the development of $CD4^+$ T cells towards the regulatory T cell phenotype, which further induces IDO in dendritic cells (Hill et al., 2007). In addition, 3-hydroxyanthranillic acid triggers the production of transforming growth factor β (TGFβ) which further promotes the development of regulatory T cells, alongside suppressing the development of Th_1 cells (Munn, 2011).

In the CNS, IDO is expressed in neurons, macrophages, microglia and astrocytes, but not oligodendrocytes (Lim et al., 2010). Neurons express both IDO and IDO-2 which exhibit a reciprocal relationship with TDO expression, in that induction of IDO results in decreased expression of TDO (Guillemin et al., 2007). IDO-2 is present in different tissues to that of IDO, such as the epididymis, liver and kidneys (Fukunaga et al., 2012, Ball et al., 2007) indicating that it is not functionally redundant. However, the neurological and immune effects of IDO-2 are not fully elucidated and its function in human cells is unknown (Fatokun et al., 2013, Vecsei et al., 2013). Moreover, IDO-2 appears to be much less enzymatically active than IDO as indicated by its lower substrate binding affinity and lower turnover rates (Pantouris et al., 2014).

Activation of the sympathoadrenal medullary (SAM) axis following stress leads to the release of noradrenaline from sympathetic nerve endings and adrenaline from the adrenal medulla. Catecholamines can in turn lead to IDO induction through the activation of beta-adrenergic receptors expressed on natural killer cells, T cells, B cells and monocytes (Maisel et al., 1989) which results in the expression and release of pro-inflammatory cytokines, specifically IFNγ, IL-1β and IL-6, which are

capable of inducing IDO (Elenkov et al., 2000). Inflammation is also capable of activating the downstream kynurenine pathway enzyme KMO (Connor et al., 2008), which is a flavin adenine dinucleotide dependent monooxygenase enzyme (Alberati-Giani et al., 1997), located in the outer mitochondrial membrane (Erickson et al., 1992). KMO is expressed peripherally in the kidney and liver as well as in the brain where it is primarily found in microglia (Guillemin et al., 2005b), with low expression of it in neurons (Guillemin et al., 2007).

1.3.3.2 The role of TDO in kynurenine pathway activation

TDO is a homotetrameric enzyme with its expression primarily restricted to the liver in the periphery (Stone, 1993), while it is present in both astrocytes and neurons in the brain (Miller et al., 2004). In fact, there are now three variants of the *tdo* gene which have been identified in adult mice referred to as *tdo* variant 1, *tdo* variant 2, and the classic gene, *tdo* full-form (Kanai et al., 2009). Under normal circumstances, TDO activity is regulated by tryptophan availability with its activity being relatively stable (Myint and Kim, 2014). Regulation of TDO expression occurs chiefly through GR-mediated induction. Consequently, stress-related changes in the expression of TDO are primarily influenced by activation of the HPA axis through the action of glucocorticoids.

Considering the nature of factors which influence the expression of TDO, the relevance for TDO induction in times of stress is unclear. It is believed that induction of TDO is a protective mechanism against the unfavourable effects of excess tryptophan which are mediated through the production of indoles, and are capable of disrupting the membrane potential (Kim et al., 2013a). In addition, it may be that induction of hepatic TDO in times of stress is important for driving the synthesis of NAD^+. This would further enable energy production for use in other immune reactions, while induction of central TDO provides astrocytes with the substrate for the production of kynurenic acid which in turn may have important neuromodulatory actions in response to stress.

1.3.4 The neuroactive properties of kynurenine pathway metabolites

1.3.4.1 The oxidative metabolites

3-hydroxykynurenine and 3-hydroxyanthranillic acid are kynurenine pathway metabolites which contribute to the generation of free radicals (Forrest et al., 2004), leading to lipid peroxidation and oxidative stress. This is achieved directly through the generation of ROS such as hydrogen peroxide from these metabolites (Okuda et al., 1996). Moreover, 3-hydroxykynurenine, 3-hydroxyanthranillic acid and anthranillic acid can inhibit complexes I, II and IV, I and II, and I-III in the electron transport chain respectively (Schuck et al., 2007). This inhibition may lead to impaired mitochondrial function

contributing further to oxidative stress within cells (Maes et al., 2011). Activation of oxidative and nitrosative pathways, and impairments in mitochondrial function are widely reported to be involved in the pathology of neurodegenerative and neuropsychiatric disorders (Muller, 2013, Federico et al., 2012, Maes, 2011, Glass et al., 2010).

1.3.4.2 The oxidative and NMDA receptor properties of quinolinic acid

Quinolinic acid is a weak but specific competitive agonist at the NMDA receptor containing NR_{2A} and NR_{2B} subunits (Guillemin, 2012). The concentrations of quinolinic acid in the human brain are usually less than 100 nM but these can increase drastically in inflamed tissues (Guillemin et al., 2005a, Guidetti and Schwarcz, 2003, Guillemin and Brew, 2002). In addition to it being directly able to generate ROS (Behan et al., 1999), quinolinic acid can also indirectly drive free radical formation through the activation of the NMDA receptor resulting in increased levels of intracellular Ca^{2+}. This can occur through the downstream conversion of xanthine dehydrogenase into xanthine oxidase - an enzyme responsible for the production of ROS, and also through stimulation of nitric oxide synthase (NOS) (Forrest et al., 2004). Moreover, quinolinic acid stimulates the release of glutamate from neurons (Tavares et al., 2002) and inhibits the uptake of glutamate by astrocytes, enhancing its synaptic availability which in turn may over-activate the NMDA receptor (Tavares et al., 2002). Furthermore, quinolinic acid impairs post-synaptic elements, causes neuronal degeneration (Kerr et al., 1998), and destabilizes the cytoskeleton (Pierozan et al., 2010). In addition, quinolinic acid triggers pro-inflammatory responses and apoptosis of neurons and astrocytes (Braidy et al., 2009a), as well as disrupting the BBB (St'astny et al., 1999). Further effects of quinolinic acid-induced cytotoxicity have been discussed elsewhere [see, Lugo-Huitron et al. (2013) for review].

1.3.4.3 The multifaceted nature of kynurenic acid

Kynurenic acid is found in the human cortex at concentrations of 150 pmol/g wet weight (Moroni et al., 1988). It is produced from kynurenine by the KAT enzymes of which there are 4, KAT I, II, III, IV, all of which are involved to varying degrees in the conversion of kynurenine to kynurenic acid (see also **figure 1.3**) (Agudelo et al., 2014, Zinger et al., 2011). Within the brain, KAT II is mostly responsible for the production of kynurenic acid (75%) (Zinger et al., 2011). KAT II-mediated conversion is the primary source for kynurenic acid production in the brain due to the inability of kynurenic acid to cross the BBB (Fukui et al., 1991). Kynurenic acid is often referred to as a neuroprotective kynurenine pathway metabolite on account of antagonistic properties at the NMDA receptor (Stone, 1993), which may serve to counteract quinolinic acid-related toxicity (Perkins and Stone, 1982). Specifically kynurenic acid is an antagonist at the glycine recognition and co-agonist site of the NMDA receptor complex (Birch et al., 1988b). Consequently, the ratio of quinolinic acid to kynurenic acid is used as an index to gauge for NMDA receptor-related activation and neurotoxicity (Saito et al., 1993). At

higher concentrations, kynurenic acid has the capacity to antagonise the NMDA receptor at the glutamate binding site (Birch et al., 1988a), thus kynurenic acid has the potential to interfere with glutamatergic signalling. In addition to its NMDA receptor antagonistic properties, kynurenic acid also blocks other glutamate receptors including kainate and AMPA receptors (Birch et al., 1988a). It is also a non-competitive inhibitor at the α7-nicotinic receptor (Hilmas et al., 2001), an important component of the cholinergic anti-inflammatory pathway that inhibits cytokine activities and glutamate release (Gallowitsch-Puerta and Tracey, 2005, Marchi et al., 2002).

In addition, kynurenic acid can act on NMDA auto-receptors on pre-synaptic neurons inhibiting glutamate release - an effect which is not seen with other NMDA or α7-nicotinic receptor antagonists in rodents both *in vivo* and *in vitro* (Luccini et al., 2007, Carpenedo et al., 2001). The actions of kynurenic acid at the α7-nicotinic receptor and the glycine binding site of the NMDA receptor occur at more physiologically relevant concentrations (Szalardy et al., 2012, Prescott et al., 2006), while its antagonism at the AMPA receptor or at the NMDA binding site of the NMDA receptor occurs at higher concentrations (Szalardy et al., 2012).

Despite its reputation as a neuroprotective metabolite, kynurenic acid has been found to be a full agonist at the orphan receptor, g-protein coupled receptor 35 (GPR35) in rodents (Wang et al., 2006). Activation of this receptor results in $G_{\alpha 13}$ and $G_{i/o}$ signalling leading to mobilisation of intracellular Ca^{2+} and the disruption of synaptic currents (Divorty et al., 2015, Jenkins et al., 2011, Wang et al., 2006). The degree of potency of kynurenic acid at GPR35 is species-specific, with it being more potent at rat, in comparison with human, GPR35 (Wang et al., 2006). Considering that GPR35 is not widely distributed in the brain (Wang et al., 2006), it is more likely that kynurenic acid exerts its action via this receptor in the periphery, primarily in the gastrointestinal tract or immune cells, where GPR35 is predominantly expressed (Wang et al., 2006). Furthermore, the plasma concentration of kynurenic acid required to activate GPR35 is not reached under normal circumstances in humans, suggesting that kynurenic acid-driven GPR35 activation may only be relevant in the presence of disease salient stimuli (Divorty et al., 2015). In spite of the potential of kynurenic acid to perturb neuronal signalling through GPR35 activation, further studies are required in order to determine whether this receptor may influence the neuroactive properties of kynurenic acid.

1.3.5 The kynurenine pathway and neurodegeneration in vitro

Kynurenine pathway metabolites have the potential to influence neuronal transmission by affecting neuronal integrity via reducing viability, neuritic complexity, or synapse formation. The number, length and complexity of dendrites is widely believed to underlie neuronal interaction and network

integration corresponding to key aspects of brain function such as cognitive function (Ferrante et al., 2013). As such, *in vitro* experiments which assess the impact of kynurenine pathway metabolites on neuronal integrity are of interest. Furthermore, the use of glial cultures enables the manipulation of kynurenine pathway activation in discrete glial cell populations. Examination of the effect of activation of the different arms of the kynurenine pathway on neuronal integrity can be achieved through the use of isolated astrocytic or microglial cultures. This *in vitro* system generates an exploratory platform allowing the identification of the presence of and the contribution that each arm of the pathway has in modulating neuronal complexity and synapse formation. Examining both these features of neuronal morphology imparts information relative to neurodevelopmental processes and the preservation of neurons in the adult brain respectively. Furthermore, alterations in these parameters of neuronal integrity can often be ameliorated, and precede cell death (Kim et al., 2002). Surprisingly, this *in vitro* culture set up is yet to be taken advantage of, with current research focusing primarily on the direct application of kynurenine pathway metabolites onto neurons with a focus on neuronal viability, an often irreversible neurodegenerative event.

3-hydroxykynurenine, and to a lesser extent 3-hydroxyanthranillic acid, at concentrations ranging from 1-100 μM were reported to be toxic to rat striatal neurons where toxicity was prevented by treatment with the xanthine oxidase inhibitor, allopurinol (Okuda et al., 1996). Furthermore, the same group reported that other kynurenine pathway metabolites tested including quinolinic acid over a similar range of micromolar concentrations did not affect the viability of these cultured striatal neurons (Okuda et al., 1998). In another report, 3-hydroxykynurenine was capable of inducing cell death in both undifferentiated and differentiated SH-SY5Y and SK-N-SH neuroblastoma cells (Wszelaki and Melzig, 2011). 3-hydroxykynurenine, 3-hydroxyanthranillic acid and quinolinic acid, but not kynurenic acid have been reported to affect the viability of human neuronal cells, with lactate dehydrogenase (LDH) release from cells indicative of neuronal cell death at concentrations greater than 0.5 μM (Braidy et al., 2009b). In a further report, the quinolinic acid-induced reduction in neuronal viability was prevented by the pre-treatment with the NMDA receptor antagonist, MK-801 or the inducible nitric oxide (iNOS) inhibitor, L-NAME (Braidy et al., 2009a).

Pierozan et al. (2015) have reported that quinolinic acid, at concentrations between 10-100 μM with exposure times ranging from 24 to 72 hr, failed to affect the viability of primary rat astrocytes or neurons. Some metabolites are likely to contribute to neuronal cell death to a greater degree than others and this may have implications with regard to underlying mechanisms associated with the influence of the kynurenine pathway in neurodegenerative disorders. Exposure of primary striatal neurons to quinolinic acid at 10, 25 and 100 μM has been reported to result in hyperphosphorylation of neurofilament subunits which is believed to be mediated by NMDA receptor-driven increases in

intracellular Ca^{2+}. In addition, this group demonstrated that these same concentrations of quinolinic acid reduced neurite length. It was proposed that quinolinic acid-induced neuronal injury interferes with the physiological roles of the axonal cytoskeleton in mediating neuronal outgrowth (Pierozan et al., 2015). This same group had previously reported similar results in striatal cortical slices from young rats after an infusion with quinolinic acid into the brain, where the hyperphosphorylation of neurofilaments was prevented by the NMDA receptor antagonist, MK801, or the NOS inhibitor, L-NAME (Pierozan et al., 2010).

Variations in the literature regarding the effects that kynurenine pathway metabolites have on neuronal complexity may be as a consequence of variations between experimental parameters. These may include differences in the treatment duration and concentration, including the varied protocols used for the preparation of primary cultures and also the specific type of neuron utilised in the respective experiments. In particular the age at which the neuronal cultures are treated may greatly influence the outcomes and cellular resilience or lack thereof to exposure to the various metabolites. Verstraelen et al. (2014) have recently described the maturation of primary murine hippocampal neurons and illustrated the changes in morphological and electrophysiological properties that occur with respect to the age of the cells in culture. In addition, they showed that the balance between kynurenic acid and quinolinic acid was critical to the maintenance of the activity of hippocampal neuronal networks, with either quinolinic acid or kynurenic acid alone disturbing the synchronous burst firing of these networks, while consecutive addition of the NMDA receptor modulators allowed for normal network activity.

Macrophages of the murine cell line, BAC1.2F5 stimulated with IFNγ release nitric oxide alongside 3-hydroxykynurenine and quinolinic acid into the culture media. These effects may be blocked by treatment with the IDO inhibitor, norharmane (Chiarugi et al., 2000). Circulating or infiltrating macrophages act as a peripheral source of kynurenine pathway metabolites (**figure 1.3**). Circulating metabolites may in turn gain access to the brain which provides a putative link between systemic immune activation and inflammation influencing neuronal transmission. It is now well recognised that bidirectional communication occurs between the CNS and the immune system. This is achieved through cytokines accessing the brain directly via circumventricular organs, being transported across the BBB by their respective active transporters, or by infiltrating immune cells. In addition cytokines can act via the vagus nerve to alter neurotransmission in the brain. Abnormalities in the peripheral immune system and the resulting neuroinflammation are well accepted as having a role in neurological disorders [see, Najjar et al. (2013), Haroon et al. (2012), Glass et al. (2010) for review]. As such, direct activation of the kynurenine pathway centrally, through locally produced or infiltrating cytokines may therefore impact upon neuronal transmission through the aforementioned

neuroactive mechanisms of the kynurenine pathway metabolites. Additionally, activation of the kynurenine pathway peripherally may influence neuronal transmission following certain kynurenine pathway metabolites gaining access to the brain (**figure 1.3**). Thus, kynurenine pathway-mediated alterations in neuronal transmission and integrity may be one such mechanism by which inflammation or stress could contribute to the development of symptoms of neuropsychiatric and degenerative disorders.

1.3.6 A role for the kynurenine pathway in the pathophysiology of neurodegenerative and neuropsychiatric disorders

The kynurenine pathway is appreciated as having an important part to play in the development of multiple neurodegenerative disorders including Parkinson's disease, Alzheimer's disease, Huntington's disease, amylotroic lateral sclerosis (ALS), multiple sclerosis and stroke (Bohar et al., 2015, Maddison and Giorgini, 2015, Cuartero et al., 2014, Tan et al., 2012, Anderson and Rodriguez, 2011, Lim et al., 2010). A role for IDO-related activation of the kynurenine pathway in the pathophysiology of neurological disease and psychiatric disorders has been examined extensively over the past decade (Myint and Kim, 2014, Schwarcz et al., 2012, Maes et al., 2011, Myint and Kim, 2003). The extent to which TDO-related activation of the kynurenine pathway is involved is yet to be fully investigated and understood [see, O'Farrell and Harkin (2015) for review]. Metabolite-based evidence for disrupted kynurenine pathway activation in CNS disorders is summarised in **table 1.1** below.

Table 1.1 Changes in the levels of kynurenine pathway metabolites in patients suffering from neurological disorders.

Metabolites written with a green/ red type face indicates increases/ decreases in levels respectively.

CNS disorder	Altered levels of metabolites	Regions investigated	Reference
Parkinson's disease	3-hydroxykynurenine Kynurenic acid	Frontal cortex Putamen Substantia nigra	(Ogawa et al., 1992)
Alzheimer's disease	Kynurenine 3-hydroxykynurenine Tryptophan Kynurenic acid	Serum	(Schwarz et al., 2013, Hartai et al., 2007)
Huntington's disease	3-hydroxykynurenine Quinolinic acid	Cortex Neostriatum	(Guidetti et al., 2004)
ALS	Kynurenine Quinolinic acid	Serum Cerebrospinal fluid	(Chen et al., 2010)
Multiple sclerosis	Kynurenic acid- relapse Kynurenic acid- remission	Cerebrospinal fluid	(Rejdak et al., 2007, Rejdak et al., 2002)
Stroke	Kynurenine Anthranillic acid Kynurenic acid Tryptophan	Serum	(Darlington et al., 2007)
Depression	Kynurenine 3-hydroxykynurenine Quinolinic acid Kynurenic acid Kynurenic acid	Cerebrospinal fluid Plasma	(Raison et al., 2010, Myint et al., 2007)
Schizophrenia	3-hydroxykynurenine Kynurenic acid Tryptophan Kynurenic acid	Cerebrospinal fluid Plasma	(Schwieler et al., 2015, Myint et al., 2011, Kim et al., 2009)
Anxiety disorders	Kynurenine	Plasma	(Maes et al., 2002)

1.3.7 A role for the kynurenine pathway in neurodevelopment

It is well established that genetic pre-disposition and altered brain development in early life are factors which can increase a person's vulnerability to the emergence of psychiatric symptoms in later life. The kynurenine pathway may play a role in mediating the effects of genetic or early life adversity factors on this vulnerability. Development of the brain can be influenced by early life adversity including exposure to infectious agents, activation of the immune system and exposure to stress. A number of studies have been carried out to date which assess a role for the kynurenine pathway in driving developmental processes (Khalil et al., 2014b, Pisar et al., 2014, Forrest et al., 2013b). These studies suggest that activation of the kynurenine pathway as a consequence of prenatal stress and inflammation may have the potential to contribute to alterations in the development of the nervous system. Preclinical models, such as poor maternal care, demonstrate that early life adversity has the potential to alter brain development [see, Lucassen et al. (2013), McEwen (2008) for review].

In early life, tryptophan is an important factor involved in the development of regions of the brain associated with psychiatric disorders. This may be due to the fact that it is the precursor for serotonin which has been shown to exert effects in the development of target tissues [see, Lauder (1990) for review] alongside altering the gene expression of brain derived neurotrophic factor (BDNF) (Vaidya et al., 1997). The identification of fluctuations in the expression of TDO mRNA and its variants in both the developing and adult brain suggests that TDO is important in the regulation of the development of specific brain regions such as the hippocampus and cerebellum (Kanai et al., 2010). Thus, disruptions in TDO expression may be responsible for subsequent behavioural changes, such as the emergence of anxiety-related behaviour in adult life (Funakoshi et al., 2011). Tryptophan restriction in rats during an early postnatal stage was shown to result in reduced levels of serotonin in the brain alongside reduced dendritic arborisation, spine density and cell proliferation in the dentate gyrus of the hippocampus. These rats also displayed anxiety-like and depressive-like behaviour, however this study failed to examine a role for kynurenine pathway activation in mediating these morphological and behavioural changes (Zhang et al., 2006).

Kynurenine pathway activation has been implicated in normal brain development (Pisar et al., 2014, Pershing et al., 2016, Forrest et al., 2013a, Forrest et al., 2013b). Prenatal inhibition of the kynurenine pathway downstream of TDO/IDO, using the KMO inhibitor, Ro 61-8048 results in rapid changes in protein expression. For instance, the levels of NMDA receptor subunits $GluN_{2A}$ and $GluN_{2B}$ were decreased and increased respectively in the brains of embryos 5 hr post KMO inhibition. In 21 day old offspring, there was increased neurogenesis, neuronal excitability and paired-pulse firing, alongside increased long term potentiation and protein expression of $GluN_{2A}$, $GluN_{2B}$ and PSD-95. These changes highlight that inhibition of activation of the neurotoxic arm of the kynurenine

pathway prenatally affects the neuronal development of adult offspring differently to those observed at weaning [postnatal day 21]. (Forrest et al., 2013a, Forrest et al., 2013b). In addition, prenatal administration of Ro 61-8048, which by way of inhibiting KMO, increased the levels of kynurenine and kynurenic acid in the brain of embryos (Forrest et al., 2013a), altered dendritic parameters in the hippocampus such as increased radial intersections at various distances from the cell body (Pisar et al., 2014). It is proposed that such changes may be as a consequence of altered NMDA receptor expression at the various stages of development (Forrest et al., 2013b). Another study which involved the administration of kynurenine to cultured murine astrocytes has been shown to induce the expression of nerve growth factor (NGF), which the authors propose may be a mechanism by which circulating tryptophan and kynurenine may exert trophic support (Dong-Ryul et al., 1997)

Furthermore, clinical studies suggest that early life adversity and subsequent neurodevelopmental abnormalities and alterations in the stress response, such as HPA axis hyperactivity can persist during adulthood [see, Faravelli et al. (2012) for review]. Reductions in the levels of GR expression were found in the post mortem brains of patients with major depression, bipolar disorder and schizophrenia, indicating altered GR functioning (Webster et al., 2002). Similarly, findings reviewed by Holtzman et al. (2013) show that schizophrenic patients exhibit a hyperactive HPA axis as well as dexamethasone non suppression in the dexamethasone suppression test. This re-programming of the HPA axis and associated blunted GR signalling in immune cells, is believed to be an important link between prenatal stress and risk of psychosis in later life (Koenig et al., 2002). How these early life stress-related physiological changes affect kynurenine pathway activation both peripherally and centrally in the long term is yet to be examined, with interesting findings having emerged over the past decade on a role for kynurenine pathway activation in psychiatric and neurodegenerative disorders.

1.4 The kynurenine pathway; linking neuroinflammation to neurodegeneration

Neuroinflammation is a normal beneficial defence mechanism coordinated by both microglia and astrocytes in order to protect the CNS against infection, injury or disease. Under normal circumstances it is resolved on its own, however when the presence of an insult persists, this inflammatory response may become imbalanced leading to chronic neuroinflammation. As previously discussed, early life neuroinflammation is capable of contributing to altered neurodevelopment with chronic neuroinflammation being associated with many neurodegenerative diseases and several psychiatric disorders [see, O'Farrell and Harkin (2015) for review]. This chronic neuroinflammation can be achieved through lack of resolution following infection or injury, or

blunted GR anti-inflammatory signalling as a consequence of over-activation of the HPA or SAM stress axes (Connor and Leonard, 1998).

Glial-induced inflammation is believed to be an amplifier of neurodegenerative pathologies, with common inflammatory pathways being activated across several of these diseases perturbing the protective effect of glia toward a pathogenic effect. Lack of resolution of this inflammatory response may indeed be a contributing factor to the neurotoxicity that occurs in these diseases (Glass et al., 2010). Glia-induced neurotoxicity can be achieved through various different mechanisms, of which excitotoxicity and concurrently oxidative stress are the primary instigators.

Excitotoxicity involves the influx of Ca^{2+} and is primarily driven by increased levels of synaptic glutamate which stimulates NMDA, AMPA and metabotropic receptors. Initial stimulation of AMPA receptors opens voltage-gated Ca^{2+} channels and removes the magnesium block from NMDA receptors allowing NMDA receptor-related Ca^{2+} influx. Activation of the metabotropic receptors stimulates the release of Ca^{2+} from intracellular stores. Overload of intracellular Ca^{2+} stores such as in the mitochondria can disrupt normal mitochondrial functioning leading to reduced adenosine triphosphate (ATP) production and subsequently reduced functioning of Ca^{2+} efflux pumps. Overall increased levels of intracellular Ca^{2+} affect neuronal functioning via activation of proteases and lipases resulting in membrane damage, alongside activation of NOS and arachidonic acid release, which increases the presence of free radicals leading to lipid, protein and DNA damage (Rang and Dale, 2012).

Oxidative stress can occur independently to excitotoxicity, often in response to glial-associated inflammatory cytokines which can activate NOS, or nicotinamide adenine dinucleotide phosphate (NADPH) oxidase, both of which generate ROS (Yang et al., 2007, Kaur et al., 2004). ROS are oxygen-derived molecules-including superoxide, peroxyl and hydroxide, which are either oxidizing agents or are readily converted into radicals such as hydrogen peroxide. These radicals are capable of interfering with proteins, lipids and DNA often causing irreversible damage or destroying their target molecule (Bedard and Krause, 2007).

1.4.1 A role for IFNγ

IFNγ is the most potent inducer of IDO gene expression (Yasui et al., 1986) and is also capable of inducing the neurotoxic enzymes KMO and KYNU (Connor et al., 2008). In addition to being a commonly used microglial activator, IFNγ is the preferred stimulus for studying kynurenine pathway activation (Lim et al., 2013a, Chen et al., 2011, Pallotta et al., 2011, Smith et al., 1998, Thomas et al.,

1994). IFNγ is a type II IFN and is a key regulator of the immune system. It is distinct from type 1 IFNs as it is induced exclusively in T-lymphocytes and natural killer cells as a result of immune activation and inflammation as opposed to viral infection (Bach et al., 1997). IFNγ utilises the janus activating kinase-signal transducer and activator of transcription (JAK-STAT) signalling pathway to induce the expression of immune effector genes (Hu and Ivashkiv, 2009) with it signalling predominantly via STAT1 (Stark, 2007) (**figure 1.4**).

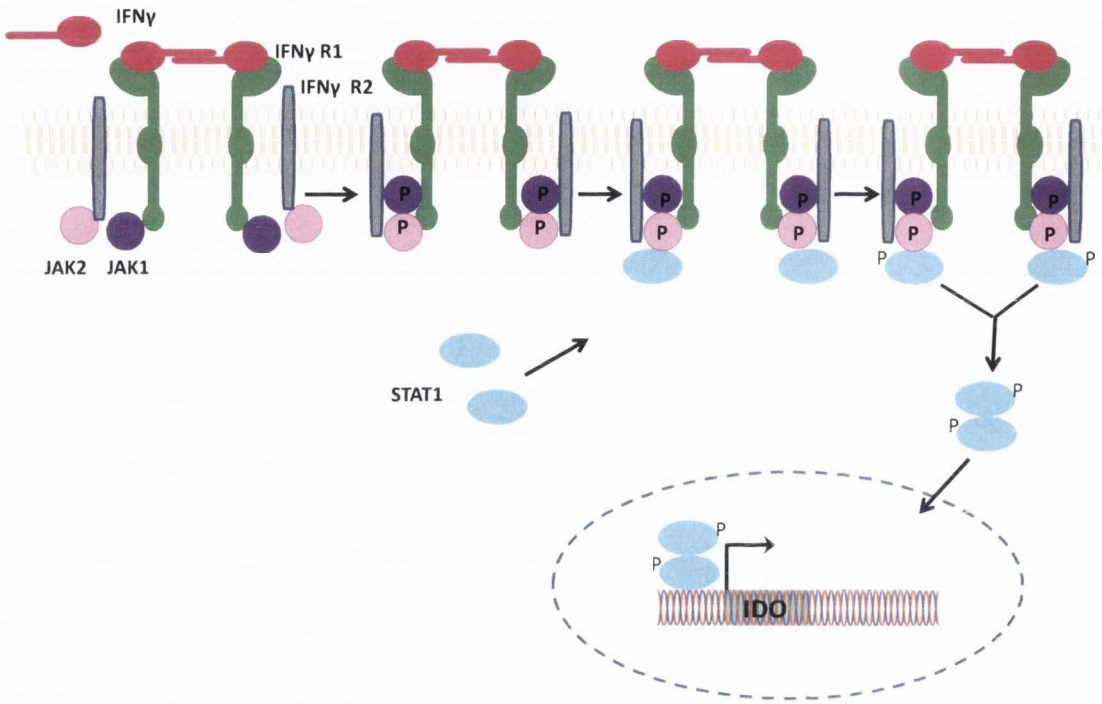

Figure 1.4: The IFNγ signalling cascade
IFNγ binds as a homodimer to the IFNγ receptor (IFNγR) 1 subunit which makes up the ligand binding domain, and this ligation triggers association with another IFNγR1 subunit. IFNγR1 is associated via intracellular domains with an IFNγR2 subunit which is the signalling domain of the receptor complex (Marsters et al., 1995). IFNγR1 is constitutively expressed at a moderate level in the cell membranes of most cells, while IFNγR2 is constitutively expressed at low levels with this expression being inducible by external stimuli, including IFNγ itself, providing a control mechanism for IFNγ responsiveness in cells (Bach et al., 1997). Both IFNγR1 and IFNγR2 are of the class 2 cytokine receptor family in which the intracellular domain lacks intrinsic kinase and phosphatase activity. Consequently, JAK1 and JAK2 are constitutively bound to the intracellular domains of IFNγR1 and IFNγR2 respectively and ligand binding results in transactivation of the JAKs and phosphorylation on their kinase domains, leading to the phosphorylation of IFNγR1 in two places allowing for the recruitment of latent cytosolic STAT1 via its SH2 domain (Igarashi et al., 1994). Phosphorylated STAT1 then translocates to the nucleus and binds as a dimer to gamma activating sequences in DNA to induce STAT1 target genes such as suppressor of cytokine signalling (SOCS) 1 (Hu and Ivashkiv, 2009) and IDO. The dimer then dissociates from the DNA and is dephosphorylated by phosphatases (Mao et al., 2005) allowing for its return to the cytosol for subsequent use as a substrate in future rounds of activation and inactivation.

1.5 A role for noradrenaline in kynurenine pathway activation

1.5.1 Introduction to noradrenergic signalling

Noradrenaline is a catecholaminergic neurotransmitter synthesized from the non-essential amino acid, tyrosine. Receptors for noradrenaline are known as adrenoceptors of which there are two types, α and β, that are further divided into subtypes α_1, α_2, β_1, β_2, β_3. These receptors, present peripherally and centrally on both neurons and glia, are metabotropic G-protein coupled receptors (GPCRs), composed of an extracellular region (N terminal), a seven transmembrane α-helical domains, and intracellular region (C terminal) (Ahles and Engelhardt, 2014, Rang and Dale, 2012). Activation of adrenoceptors results in dissociation of the α subunit of the G-protein from the receptor and initiation of intracellular signalling pathways. Additionally, the βγ subunit of the G-protein is activated and can stimulate alternative signalling pathways (Rang and Dale, 2012) (**figure 1.5**).

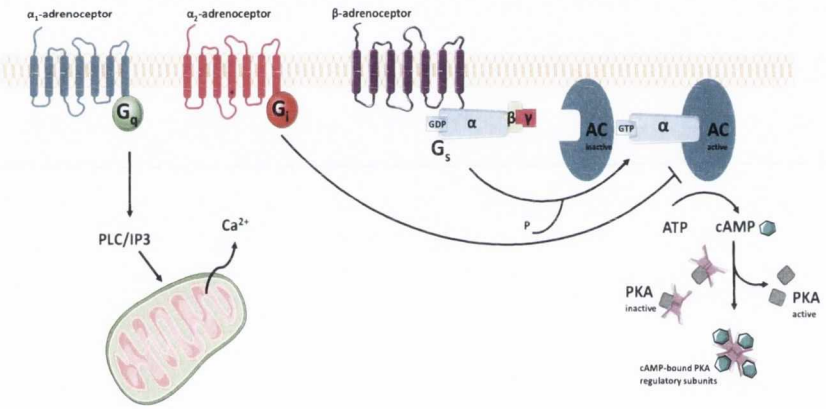

Figure 1.5: Adrenoceptor intracellular signalling pathways
Noradrenaline binds to α- and β-adrenoceptors, all of which are GPCRs. α_1-adrenoceptors are divided into α_{1a}, α_{1b}, α_{1d}, all of which are coupled to G_q, the activation of which initiates phospholipase C (PLC) signalling which increases inositol triphosphate (IP3) levels and subsequently stimulates the release of Ca^{2+} from intracellular stores such as the endoplasmic reticulum or mitochondria. α_2-adrenoceptors are further divided into α_{2a}, α_{2b}, α_{2c}, all of which are coupled to G_i. The activation of this inhibits adenylate cyclase and subsequently reduces cAMP levels and protein kinase A (PKA) activation. Within the CNS, the α_2-adrenoceptor functions as an auto-receptor, preventing the release of noradrenaline from the pre-synaptic terminal (Rang and Dale, 2012). All β-adrenoceptor subtypes are coupled to G_s proteins, the activation of which leads to phosphorylation [(guanosine diphosphate (GDP) to guanosine triphosphate (GTP)] and dissociation of the α subunit of the G protein. Upon interaction with the α subunit, adenylate cyclase (AC) becomes activated, allowing for the synthesis of cAMP from ATP, which is capable of activating the downstream enzyme PKA by binding to the regulatory subunits which maintain it in an inactive state (Rang and Dale, 2012). PKA activation is associated with downstream signalling pathways such as cAMP response element binding protein (CREB) activation which plays an important role in neurodevelopment and plasticity, the dysfunction of which is often implicated in disease (Lonze and Ginty, 2002).

1.5.2 The noradrenergic system and the kynurenine pathway

The noradrenergic system has been proposed as a mechanism where by the neuroprotective arm of the kynurenine pathway may be activated *in vitro* (Luchowska et al., 2009, Luchowska et al., 2008, Kocki et al., 2003b). The concentrations of kynurenic acid in the rat brain have been demonstrated to be regulated by β-adrenoceptor stimulation in a cAMP- and PKA-dependent manner (Luchowska et al., 2009). Luchowska et al. (2009) showed that stimulation of either rat cortical slices or rat mixed glial cultures with either β-adrenoceptor agonists or cAMP analogues resulted in increased kynurenic acid which was blocked by the PKA inhibitor, KT5720. Similarly, the β-adrenoceptor agonist formoterol, and the cAMP analogues, pCPT-cAMP and 8-Br-cAMP, resulted in increased KAT activity in mixed glial cultures (**figure 1.7**). Other mechanisms for induction of central kynurenic are unclear, however glutamate flux may provide another mechanism of control. For instance, it has been demonstrated that sulphur-containing acidic amino acids, which exert neuroexcitatory actions similar to those of glutamate, reduced kynurenic acid production and inhibited KAT I and II activity in the brains of Wistar rats, as assessed by HPLC and enzyme activity assays respectively (Kocki et al., 2003a). The effect of both α- and β-adrenoceptor agonists on glutamate release in rat cerebellar slices has demonstrated a negative and positive effect respectively (Dolphin, 1982), suggesting an indirect method by which noradrenaline may modulate kynurenic acid synthesis (**figure 1.6**).

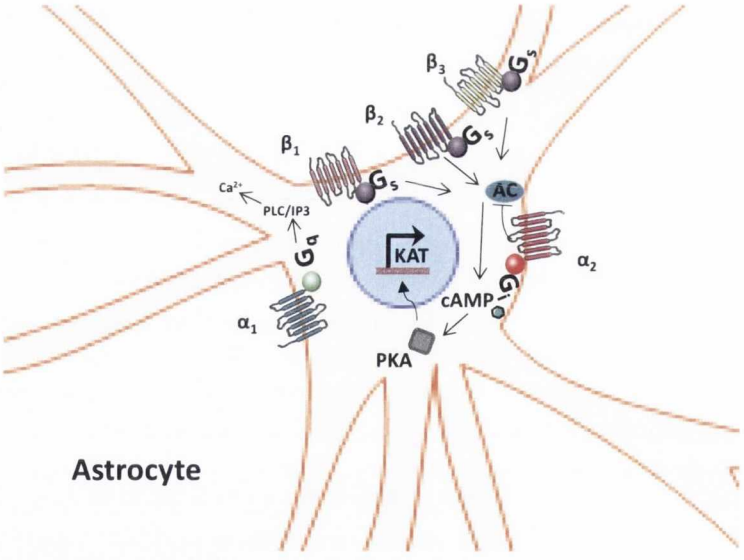

Figure 1.6: Adrenoceptor signalling system in astrocytes
Activation of the α_1-adrenoceptor leads to increased levels of PLC, IP3, and subsequently increased release of Ca^{2+} from intracellular stores. Activation of α_2-adrenoceptor inhibits adenylate cyclase (AC) activity, while activation of $\beta_{1,\ 2,\ 3}$-adrenoceptors stimulated this activity resulting in increased levels of cAMP and subsequently PKA activation which is proposed to influence KAT gene expression.

1.5.3 The neuroprotective effects of noradrenaline

Within the CNS, astrocytes are one of the primary targets of noradrenaergic neurons (Cohen et al., 1997), with the β_2-adrenoceptor being the dominant adrenoceptor expressed by these cells (Mantyh et al., 1995). Noradrenergic stimulation of the astrocytic β_2-adrenoceptor and subsequent downstream cAMP synthesis and PKA activation can result in interaction with a range of transcription factors including CREB (Lonze and Ginty, 2002), peroxisome proliferator-activated receptor (PPAR)γ (Klotz et al., 2003) and NFκB (Junker et al., 2002). The anti-inflammatory effects of noradrenaline are achieved through its inhibitory action on NFκB, preventing the induction of pro-inflammatory cytokines. *In vivo* the β-adrenoceptor agonist, clenbuterol, has been shown to suppress LPS-induced expression of inflammatory cytokines and other inflammatory factors in the rat cortex (McNamee et al., 2010a).

Noradrenaline both directly and indirectly, through its action on astrocytes, has demonstrated its ability to increase neurite outgrowth and complexity. These effects were mimicked by both β_2-adrenoceptor agonists, clenbuterol and salmeterol, but not by the β_1-adrenoceptor agonist xamoterol. The noradrenaline stimulated-astrocytic conditioned media (CM) effect on neurite outgrowth and complexity was related to the induction of growth factors including NGF, fibroblast growth factor 2 (FGF2), glial cell-derived neurotrophic factor (GDNF) as well as IL-6 (Day et al., 2014) in response to noradrenaline. Furthermore both clenbuterol and salmeterol blocked glutamate-induced toxicity in rat hippocampal neurons, the effect of which was blocked by non-selective β-adrenoceptor antagonist, propranolol, and the selective β_2-adrenoceptor antagonist, ICI 118, 551 (Junker et al., 2002). Similarly, noradrenaline protected against the neurotoxicity of primary cortical neurons observed with CM from LPS-stimulated mixed glia (McNamee et al., 2010b)

In vivo the neuroprotective efficacy of noradrenergic agents have been investigated. Stimulation of the β_2-adrenoceptor with clenbuterol in a mouse model of focal cerebral ischemia was neuroprotective, with co-treatment with clenbuterol and the β_1-adrenoceptor agonist, metoprolol, reducing the infarct size more so than treatment with clenbuterol alone (Junker et al., 2002). Similarly, clenbuterol attenuated kainic acid-induced cell death, reduced the pro-inflammatory profile, and increased the gene expression of trophic factors following kainic acid-induced seizures and hippocampal neurodegeneration in rats. This was proposed to be mediated through astrocytic β-adrenoceptor stimulation (Gleeson et al., 2010).

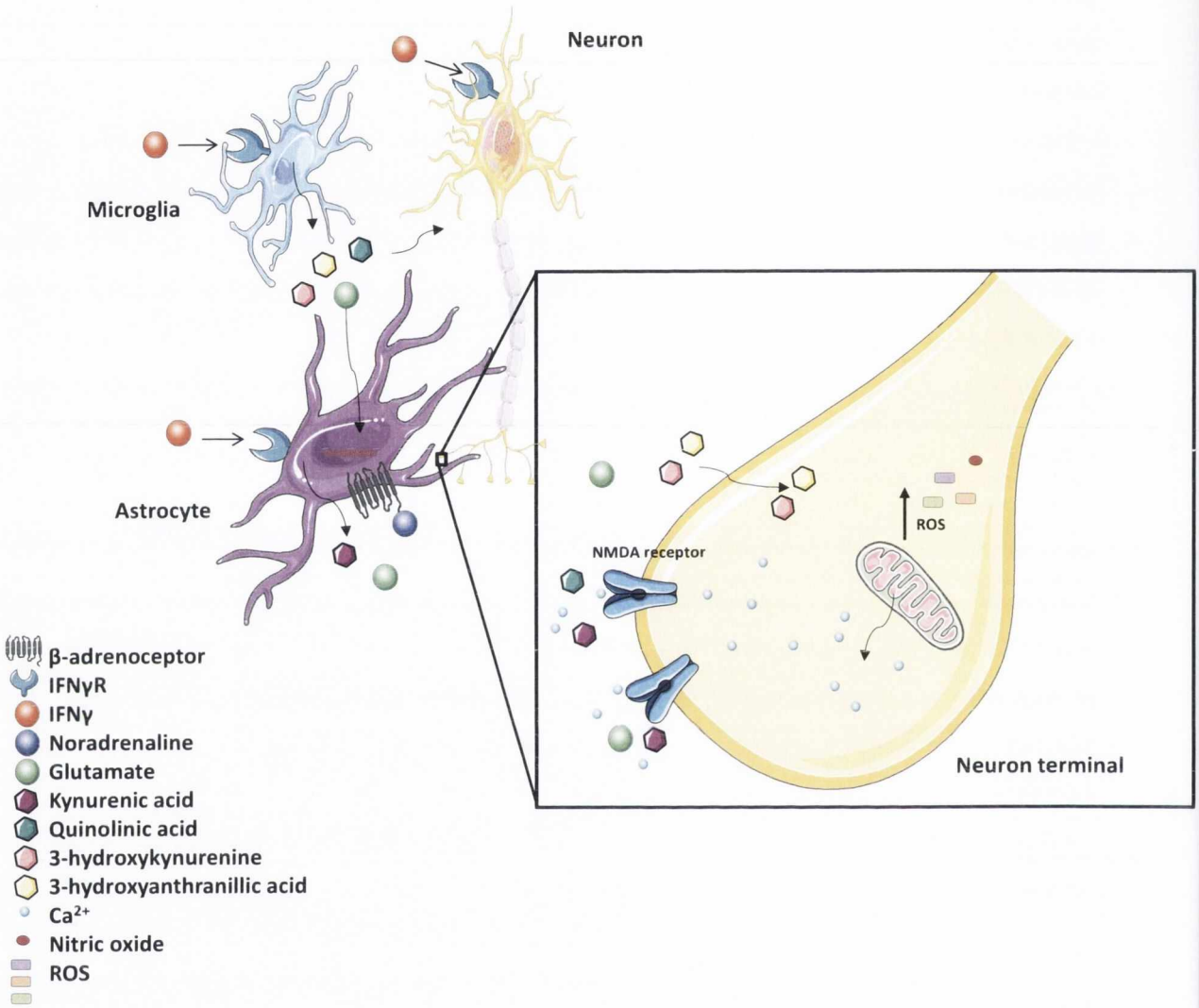

Figure 1.7: Summary diagram of how activation of the kynurenine pathway in glial cells may contribute to alterations in neuronal integrity.

IFNγ stimulation of microglia results in activation of the neurotoxic arm of the kynurenine pathway and the release of 3-hydroxykynurenine, 3-hydroxyanthranillic acid, quinolinic acid and glutamate resulting in NMDA receptor over-activation and oxidative stress. IFNγ stimulation of astrocytes leads to partial kynurenine pathway activation through induction of IDO but not KAT II and the release of glutamate while additional noradrenergic stimulation of the astrocytic β-adrenoceptor results in kynurenine pathway induction and release of the NMDA receptor antagonist, kynurenic acid.

1.5.4 The noradrenergic system and neurodegenerative disorders

Defective noradrenergic signalling, primarily as a consequence of cell loss in the locus coeruleus - a subcortical region of the brain - has been associated with a range of neurodegenerative disorders including Alzheimer's disease and Parkinson's disease (Marien et al., 2004). Neurodegeneration is associated with a variety of genetic and environmental risk factors, the most prominent of these being ageing with a 25-50% decrease in noradrenaline concentrations occurring between the fourth to ninth decades of life (Hendrie, 1998, Kilbourn et al., 1998, Mann, 1983). Compensatory mechanisms within the brain can result in neurodegeneration having no obvious physiological deficits, however, the noradrenergic projections from the locus coeruleus are proposed to be integral to the regulation of these compensatory mechanisms. The noradrenergic system is involved in regulating emotional behaviour, arousal, attention, behavioural and physiological response to stress, balance, and neuroplasticity (Hertz et al., 2004). Consequently, substantial noradrenergic cell loss in this subcortical region results in the emergence of neurological deficits which cannot be superseded by compensatory mechanisms (Marien et al., 2004).

In a study carried out by Zarow et al. (2003) on both Alzheimer's and Parkinson's disease patients, the most extensive neurodegeneration was reported in the locus coeruleus as opposed to the nucleus basalis or substantia nigra to which the prominent clinical features of these diseases are associated. There is estimated to be between 45,000-60,000 noradrenergic neurons in the locus coeruleus of a young adult human brain (Baker et al., 1989, German et al., 1988) and approximately 1600 in the rat brain (Swanson, 1976). These neurons project extensively throughout the brain and form either conventional synapses, or chiefly varicosities which result in extra-synaptic release of noradrenaline which can diffuse enabling stimulation of adrenoceptors on glia and more distant neurons or blood vessels by a process called volume transmission (Aoki, 1992, Beaudet and Descarries, 1978).

1.6 Targeting the kynurenine pathway; therapeutic considerations

Considering the multi-step metabolism of tryptophan along the kynurenine pathway, in addition to the branching of this pathway resulting in the production of neuroprotective or neurotoxic metabolites, there are multiple points where the pathway can be interrupted and modified. At present the competitive IDO inhibitor 1-MT is in clinical trials for the treatment of cancer (http://clinicaltrials.gov/show/NCT01191216), while KMO and KAT II inhibitors are under investigation for the treatment of neurodegenerative and cognitive disorders respectively (**figure 1.8**) [see, Bohar et al. (2015), Dounay et al. (2015a), Maddison and Giorgini (2015), Amaral et al. (2013)

for review]. So far, TDO, IDO, KMO and KAT II exhibit the greatest potential as targets for drug development based on evidence emerging from both preclinical models and clinical studies which implicate a role for kynurenine pathway activation in CNS disorders.

1.6.1 Targeting the rate limiting enzymes of the kynurenine pathway

Allopurinol is now a widely accepted inhibitor of TDO, and renders enzymatic inhibition by way of preventing TDO from conjugating with its cofactor, heme (Welch and Badawy, 1980, Green et al., 1976). It is a purine analogue commonly used for treating gout due to its action as a xanthine oxidase inhibitor (Pacher et al., 2006). In addition, it has been repeatedly demonstrated that in the presence of stress, allopurinol is capable of reducing hepatic TDO activity (Green et al., 1976, Curzon and Green, 1969). The recently discovered TDO inhibitors, 680C91 and LM10 (Dolusic et al., 2011, Madge et al., 1996, Salter et al., 1995), show high selectivity for TDO over IDO (Pilotte et al., 2012), with LM10 showing chemotherapeutic efficacy in a pre-clinical tumour model in mice (Pilotte et al., 2012). It is suggested that simultaneous inhibition of both TDO and IDO may be a complementary approach rather than serving as conflicting pathways in cancer therapy (Pilotte et al., 2012). This combined approach could also be therapeutically relevant with regards to use in neuropsychiatric and degenerative disorders. Considering that these disorders are linked with stress and exhibit an underlying inflammatory phenotype [see, Glass et al. (2010), Esch et al. (2002) for review], this multi-inhibitory approach may be efficacious as it would target both IDO- and TDO-driven kynurenine pathway activation. As a consequence of IDOs role in dampening down the immune response, in this instance an anti-inflammatory may be required to account for the lack of immunosuppression that may occur.

1-MT exists as either a dextro (D) or levo (L) enantiomer, with some *in vivo* and *in vitro* studies suggesting they have divergent actions. *In vitro* enzyme and cellular assays have demonstrated that the L enantiomer is a more potent inhibitor of IDO (Qian et al., 2009, Lob et al., 2008), while *in vivo* studies have reported that the D enantiomer evokes a more effective anti-tumour response (Hou et al., 2007). The inconsistent findings are believed to be associated with the fact that the D enantiomer may have more off-target effects, and also that it is a more potent inhibitor of IDO-2 than IDO (Lob et al., 2008). Other IDO inhibitors such as, imadizole, imadizothiazole, and triazole are extensively reviewed by Rohrig et al. (2015), and the apparent inconsistencies which occur with 1-MT also seem to appear with other current compounds. Considering that IDO is more so implicated in kynurenine pathway activation than IDO-2, research has been done involving the design of compounds such as, NLG919 which exhibits increased potency and ligand efficacy for IDO over IDO-2, in order to provide

more selective experimental tools as well as potential novel therapeutic compounds [see, Dounay et al. (2015a) for review].

1.6.2 Targeting the kynurenine pathway downstream of TDO or IDO

The first published KMO inhibitor, *m*-NBA, as well as other inhibitors including UPF648 and Ro 61-8048 result in increased concentrations of kynurenic acid and decreased concentrations of 3-hydroxykynurenine when administered to rodents (Forrest et al., 2013a, Pellicciari et al., 2003). JM6, originally believed to be a pro-drug of Ro 61-8048 has been studied extensively and shows therapeutic potential in animal models of Huntington's and Alzheimer's disease [see, Bohar et al. (2015), Dounay et al. (2015a), Amaral et al. (2013) for review]. To this end, the need for a BBB permeable KMO inhibitor has not been met. The development of such an agent would increase the potential for the development of this clinically relevant therapeutic target.

The transaminase class of KAT enzymes have become a target as a potential therapeutic intervention point in modulating the kynurenine pathway. Various KAT II inhibitors have been developed, including S-ESBA which showed selectivity for rat KAT II over KMO or KYNU, however it failed to inhibit the human orthologue (Rossi et al., 2010). A more promising inhibitor developed by Pfizer, PF-04859989, is irreversible and shows high selectivity for KAT II, the main driver of kynurenic acid in the brain, over KAT I, III or IV isoforms in addition to it being capable of penetrating the BBB (Dounay et al., 2012). PF-04859989, will be a useful tool in deciphering the exact role that kynurenic acid plays in various neurological disorders in terms of investigating under what circumstances, or what concentrations, it promotes a toxic disposition on account of reducing the known protective function of kynurenic acid.

1.6.3 Targeting the kynurenine pathway indirectly

Considering that the neurotoxic enzymes IDO and KMO are induced by inflammatory stimuli both *in vivo* and *in vitro* (Connor et al., 2008) it is important to consider anti-inflammatory strategies as a method for manipulating kynurenine pathway activation. A study involving patients suffering from treatment-resistant depression who received three infusions of the TNFα antagonist, infliximab indicated that this strategy, although not effective in all circumstances, may improve depressive symptoms in patients with higher baseline inflammatory biomarkers (Raison et al., 2013). Furthermore, the non-steroidal anti-inflammatory, diclofenac, which non-selectively inhibits cyclooxygenase (COX)-1 and -2, increased the levels of rat brain kynurenic acid following systemic

administration. Similarly, indomethacin, which exhibits a slight preference for COX-1 over COX-2, increased rat brain kynurenic acid. By contrast, the COX-2 selective inhibitors parecoxib and meloxicam reduced the levels of central kynurenic acid (Schwieler et al., 2005). Furthermore, β-adrenoceptor mediated anti-inflammatory effects may provide a novel mechanism of modulating the kynurenine pathway. The β_2-adrenoceptor agonist, clenbuterol was shown to have anti-inflammatory actions in rats following subcutaneous administration of kainic acid. Clenbuterol prevented the kainic acid-induced increases in inflammatory cytokines, IDO and KMO in the hippocampus of these rats (Gleeson et al., 2010). Moreover, various other β-agonists including noradrenaline, formoterol, and xamoterol, have been shown to increase kynurenic acid production both *in vitro* and *ex vivo* in mixed glial cells and rat brain cortical slices respectively (Luchowska et al., 2009). Overall, modulation of the kynurenine pathway could be achieved through the use of various anti-inflammatory agents depending on the dysregulation of the pathway [see Muller (2013), for review]. COX-2 selective inhibitors may be a beneficial adjunctive treatment in schizophrenia. A study by Muller et al. (2010) involved patients exhibiting their first manifestation of schizophrenia demonstrated celecoxib as an effective adjunctive treatment to amisulpiride. This study showed that patients receiving both treatments had a more effective outcome in the positive and negative symptom scale and the clinical impression scale.

At present, there is scope for the development of compounds targeting other kynurenine pathway enzymes, such as KYNU, for which selective inhibitors do not already exist. In addition, there is potential for modification of existing compounds in terms of BBB permeability and increased efficacy and selectivity. Considering the extent to which the kynurenine pathway and its downstream metabolites have been implicated in neurological disease, development of efficacious drugs which modulate this pathway may be widely applicable and potentially beneficial clinically.

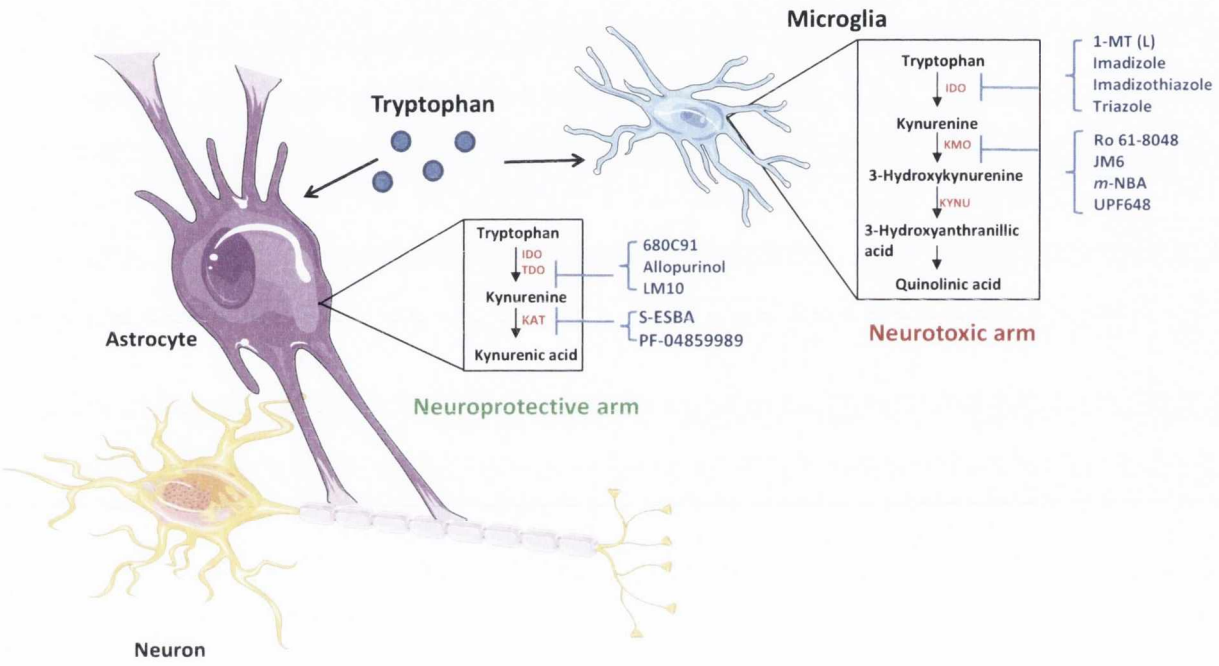

Figure 1.8: Drugs that target the kynurenine pathway at discrete stages of tryptophan metabolism
The rate limiting step of this pathway can be inhibited by the use of IDO inhibitors- 1-MT (L), imadizole, imadizothiazole or triazole; or TDO inhibitors- 680C91, allopurinol, LM10. Downstream enzyme KMO can be inhibited by Ro 61-8048, JM6 *m*-NBA, or UPF648, while KAT activity can be attenuated by S-ESBA or PF-04859989.

1.7 Aims and objectives

The main focus of this thesis is to determine the extent to which the kynurenine pathway is present in glial and neuronal cells and thus determine the role of kynurenine pathway activation in altering measures of neuronal integrity including neuronal viability, complexity and synaptic formation (co-localisation of pre- and post-synaptic markers).

The specific aims were as follows:

1) To elucidate the role of the kynurenine pathway in facilitating the deleterious effects of inflammatory-activated microglia on neuronal viability and complexity by use of the BV-2 microglial cell line. Moreover, we aim to determine whether pharmacological modulators of kynurenine pathway activation represent a mechanism for rescuing inflammatory-driven microglial-associated deficits in neuronal viability and complexity.
2) To characterise the kynurenine pathway in rat primary cortical microglia, astrocytes, mixed glia (astrocytic and microglial co-cultures) and neurons, and examine the effect of pathway activation in discrete glial populations on neuronal integrity. Furthermore, we aim to identify the effect of direct application of kynurenine pathway metabolites and the interactive effects of combinations of metabolites on neuronal integrity.
3) To establish a role for noradrenaline in regulating the kynurenine pathway in rat primary cortical astrocytes, microglia, mixed glia and neuronal cells, and to further assess the potential for β-adrenoceptor stimulation as a protective strategy against reactive glial-associated reductions in neuronal integrity.

Chapter 2

Materials and Methods

2.1 Materials

2.1.1 Animals

Wistar rats (male/female)	Comparative Medicine, TCD

2.1.2 Cell Culture materials and reagents

24-well plates	Sarstedt, Ireland
Absolute Ethanol	Hazmat, TCD
B-27 Supplement	Gibco, UK
Biocidal ZF™	WAK-Chemie Medical, Germany
BV-2 Microglia	Centro Biotecnologie Avanzate, Genova, Italy
Cell culture flasks (T75 cm^2)	Corning, Ireland
Cell scrapers	Sarstedt, Ireland
Cell strainers (40 µm)	BD Falcon, UK
Coverslips (glass, 13 mM)	VWR Scientfic, Ireland
Cryovials	Sigma Aldrich, UK
Dimethyl sulfoxide	Sigma Aldrich, UK
Dulbecco's modified Eagle medium: F12	Labtech Int., UK
Dulbecco's phosphate buffered saline (10X)	Sigma Aldrich, UK
Filter units (0.22 µm), sterile	Millipore, Ireland
Foetal Bovine Serum- heat inactivated	Invitrogen, UK
Fungizone	Invitrogen Life Technologies, UK
Glutamax	Gibco, UK
Granulocyte macrophage colony-stimulating factor	R&D Systems, UK
Haemocytometer	VWR Int., Ireland
Macrophage colony-stimulating factor	R&D Systems, UK
Mycoplasma-OFF	Minerva Biolabs, Germany
Neurobasal A medium	Invitrogen, UK
Penicillin-streptomycin	Invitrogen, UK
Petri dish	Sarstedt, Ireland
Poly-D-lysine hydrobromide	Sigma Aldrich, UK
Resazurin sodium salt ($C_{12}H_6NNaO_4$)	Sigma Aldrich, UK

Roswell Park Memorial Institute medium	Invitrogen, UK
Scalpel (disposable)	Swann-Morton, UK
Serological pipette (10, 25 ml)	Sarstedt, Ireland
Syringes (20 ml)	BD Medical Supplies, Ireland
Syringe filters (0.2 µm)	Pall Corporation, USA
Transfer pipettes (sterile; 3 ml)	Sarstedt, Ireland
Trypan Blue (0.4%)	Sigma Aldrich, UK
Trypsin-EDTA solution (0.25%)	Sigma Aldrich, UK
Virkon	Antec Int., USA

2.1.3 General laboratory materials and reagents

96-well plates	Sarstedt, Ireland
β-mercaptoethanol	Sigma Aldrich, Ireland
Bovine serum albumin	Sigma Aldrich, Ireland
Falcon tubes (15 ml, 50 ml)	Sarstedt, Ireland
Laboratory tissue rolls	VWR Int., Ireland
Microscope slides 76 mm x 26 mm	Thermo Fisher Scientific, Ireland
Microtubes (0.5 ml, 1.5 ml, 2 ml)	Sarstedt, Ireland
Methanol (MeOH)	VWR Int., Ireland
Parafilm	Thermo Fisher Scientific, Ireland
Pipettes (manual and automated)	Gilson Inc.
Pipette tips (20 µl, 200 µl, 1000 µl)	Sarstedt, Ireland
Syringe (1 ml)	BD Medical Supplies, Ireland
Transfer pipettes (3 ml)	Sarstedt, Ireland
Triton X-100	Sigma Aldrich, UK

2.1.4 General laboratory equipment

Autoclave	Sanyo, Ireland
Biosafety cabinet	ADS Laminaire, France
Centrifuge: Legend RT+	Sorvall, Ireland
Gyro rocker	Stuart, Ireland
Haemocytometer	VWR Int., Ireland
Incubator (Innova CO-48)	New Brunswick, Ireland

Microscope: CKX41	Olympus, UK
Microscope: Axio Imager Z1	Carl Zeiss, UK
Microtitre plate reader Elx800	Biotek, Germany
Nanodrop® ND1000 Spectrophotometer	Thermo Fisher Scientific, Ireland
pH meter	Mettler-Toledo, Ireland
Vortex	Ika, Ireland

2.1.5 Assay kits

CellTiter 96® AQ_{ueous} Non-Radioactive Cell Proliferation assay (MTS)	Promega
Pierce™ LDH cytotoxicity assay	Thermo Fisher Scientific, Ireland

2.1.6 Fluorescent immunocytochemistry

Table 2.1: List of antibodies used in fluorescent immunocytochemistry

Name	*Host species*	*Company*	*Dilution*
Primary antibodies:			
β-III tubulin	Mouse	Promega, Ireland	1:1000
CD11b	Mouse	Millipore, Ireland	1:1000
GFAP	Rabbit	Dako, Ireland	1:1000
PSD-95	Mouse	Fischer Scientific	1:500
Synaptophysin	Rabbit	Thermo Scientific	1:500
Secondary antibodies:			
Alexa Fluor 488 anti-mouse	Goat	Invitrogen, Ireland	1:2000
Alexa Fluor 594 anti-rabbit	Goat	Invitrogen, Ireland	1:1000
Alexa Fluor 647 anti-rabbit	Goat	Invitrogen, Ireland	1:2000

Normal goat serum (NGS)	Sigma Aldrich, UK
Vectashield mounting medium with DAPI	Vector Laboratories, UK

2.1.7 HPLC materials and reagents

Acetonitrile	Sigma Aldrich, UK
Glacial Acetic Acid	Thermo Fisher Scientific, Ireland
Glass Inserts	Thermo Fischer Scientific, Ireland
Glass screw top vials	VWR Int., Ireland
Glass vials	VWR Int., Ireland
Methanol (HPLC grade)	Thermo Fisher Scientific, Ireland
N-methy-5-hydroxytryptophan	Sigma Aldrich, UK
Nylon filter (0.45 µm)	Thermo Fischer Scientific, Ireland
Perchloric Acid	Thermo Fisher Scientific, Ireland
Water (HPLC Grade)	Pharmacy Dept., Trinity College Dublin
Zinc Acetate	Sigma Aldrich, UK

2.1.8 Molecular materials and reagents

Biosphere filter tips (10, 20, 200, 1000 µl)	Sparks Labs supplies Ltd., Ireland
Molecular grade ethanol	Sigma Aldrich, UK
High capacity cDNA archive kit	Applied Biosystems, UK
Microamp 96-well reaction plate	Applied Biosystems, UK
Nucleospin* RNA II Isolation kit	Macherney-Nagel, Germany
Optical adhesive covers	Applied Biosystems, UK
PCR minitubes	Sarstedt, Ireland
RNase-free microtubes (1.5 ml)	Ambicon Inc., USA
RNaseZap* wipes	Ambicon Inc., USA
TaqMan* Gene Expression Assays	Applied Biosystems, UK
TaqMan* Universal PCR Master Mix	Applied Biosystems, UK

2.1.9 Experimental treatments

1400W	Calbiochem, Germany
1-Methyl tryptophan (L)	Sigma Aldrich, UK
3-Hydroxyanthranillic acid	Sigma Aldrich, UK
3-Hydroxykynurenine	Sigma Aldrich, UK
680C91	Sigma Aldrich, UK
Atenolol	Sigma Aldrich, UK

Dexamethasone	Sigma Aldrich, UK
DPI Chloride	Sigma Aldrich, UK
Formoterol hydrochloride	Tocris Bioscience, UK
Glutamate	Sigma Aldrich, UK
Glycine	Sigma Aldrich, UK
ICI 118, 551 hydrochloride	Sigma Aldrich, UK
Isoprenaline hydrochloride	Sigma Aldrich, UK
Kynurenic acid	Sigma Aldrich, UK
Kynurenine	Sigma Aldrich, UK
(+)-MK-801 hydrogen maleate (MK-801)	Tocris Bioscience, UK
N^6, 2′-O-Dibutyryladenosine 3′, 5′-cyclic -monophosphate sodium salt (dbcAMP)	Sigma Aldrich, UK
Norepinephrine bitartrate salt monohydrate	Sigma Aldrich, UK
Phentolamine methanesulfonate salt	Sigma Aldrich, UK
Prazosin hydrochloride	Sigma Aldrich, UK
Propranolol hydrochloride	Sigma Aldrich, UK
Quinolinic acid	Sigma Aldrich, UK
Recombinant mouse cytokines; IFNγ	Biolegend, UK
Recombinant rat cytokines; IFNγ	Biolegend, UK
Ro 61-8048	Tocris Bioscience, UK
L-Tryptophan	Sigma Aldrich, UK
Yohimbine hydrochloride	Sigma Aldrich, UK

2.2 In vitro cell culture

2.2.1 Aseptic techniques

Aseptic techniques were employed throughout all cell culture work, including the preparation of cell culture reagents. Such aseptic techniques were utilised to ensure a sterile environment was maintained and that all surface areas, equipment and compounds which came in contact with cultures were free from fungal, bacterial and viral infections which could otherwise alter normal cellular function. Aseptic techniques included the use of sterile disposable plastics, and sterilisation of glassware, plastics and H_2O by autoclaving at 121°C for 25 min. Dissection kit instruments were sterilised by baking for a minimum of 2 hr at 200°C. All cell culture work was carried out in a laminar flow hood (ADS Laminaire, France). This allows only filtered air to come into contact with cells, thus preventing contamination with airborne pathogens. The interior of the hood was wiped down with 70% ethanol (EtOH) before and after use. The hood surface was also exposed to ultraviolet (UV) light for 15-30 min after use. Any items taken into the flow hood were lightly sprayed with 70% EtOH to prevent introduction of any pathogens to the hood work area. Disposable latex gloves were worn and sprayed with EtOH before use. Gloves were changed regularly during cell culture work. Cells were maintained in an incubator at 37°C in a 5% CO_2 humidified atmosphere (Thermo Steri Cycle CO_2 Incubator Hepa Class 100). Both the incubator and laminar flow hood were regularly cleaned with Biocidal ZF to maintain a sterile environment.

2.2.2 Preparation of culture media and experimental treatments

For BV-2 microglia: Roswell Park Memorial Institute medium (RPMI) 1640 containing 10% foetal bovine serum (FBS), 1% penicillin-streptomycin and fungizone (0.25 µg/ml) (complete RPMI) was used for maintenance of BV-2 microglia. In short, 50 ml of FBS, 5 ml of penicillin-streptomycin and 500 µl of fungizone were filter-sterilised using a 0.2 µm syringe filter and added to a 500 ml bottle of RPMI, producing complete RPMI (cRPMI).

For primary mixed glial cultures: Dulbecco's Modified Eagle's Medium (DMEM) containing 10% foetal bovine serum (FBS), 1% penicillin-streptomycin and fungizone (0.25 µg/ml) was used for maintenance of primary mixed glial cultures. Supplements added to DMEM as described above, producing complete DMEM (cDMEM).

For primary microglial cultures: DMEM containing 10% foetal bovine serum (FBS), 1% penicillin-streptomycin and fungizone (0.25 µg/ml) supplemented with GM-CSF and M-CSF was used for maintenance of primary mixed glial cultures. Supplements added to DMEM as described above,

producing cDMEM. GM-CSF (100 ng/ml) and M-CSF (100 ng/ml) were added to the primary microglial cultures on day 2 to give a final concentration of 10 ng/ml of each.

For primary astrocytic cultures: DMEM containing 10% foetal bovine serum (FBS), 1% penicillin-streptomycin and fungizone (0.25µg/ml) was used for maintenance of primary mixed glial cultures. Supplements added to DMEM as described above, producing complete cDMEM.

For primary neuronal cultures: Neurobasal media (NBM) containing 1% penicillin-streptomycin, fungizone (0.25 µg/ml) and 1% glutamax was used for maintenance of primary neuronal cultures. In short, 5 ml of penicillin-streptomycin, 500 µl of fungizone and 5 ml of glutamax, were filter-sterilised using a 0.2 µm syringe filter and added to a 500 ml bottle of NBM. NBM was supplemented with 1% B-27 producing complete NBM (cNBM).

Phosphate buffered saline (PBS): 10X PBS was diluted to 1X PBS by adding 5 ml 10X PBS to 45 ml dH_2O.

Preparation of compounds for treating cultures: Following preparation, stock solutions were filter-sterilised using a 0.2 µm syringe filter. All stock solutions aliquots were frozen at -20/-80°C for future use, except for quinolinic acid which was prepared freshly prior to use. Recombinant cytokines were frozen at the recommended temperature of -80°C. Stock solutions were diluted to working concentrations in the appropriate heated media prior to cell treatment. The molecular weight and appropriate solvent can be found in **table 2.2**.

Table 2.2: Table of compounds, molecular weights, and solvents

Compound name	Molecular weight (g/mol)	Dissolved in
1400W	250.2	cNBM
1-Methyl tryptophan (L)	218.25	cNBM
3-Hydroxyanthranillic acid	153.14	cNBM
3-Hydroxykynurenine	224.21	cNBM
680C91	238.26	Dimethyl sulfoxide (DMSO)
Atenolol	266.34	cNBM
dbcAMP	491.37	cNBM
Dexamethasone	392.46	cNBM
DPI chloride	314.55	DMSO
Formoterol	420.47	DMSO
Glutamate	147.13	cNBM
Glycine	75.07	cNBM
ICI 118, 551	313.86	cNBM
Isoproterenol	247.72	cNBM
Kynurenic acid	189.97	cNBM
Kynurenine	208.21	cNBM
MK-801	327.27	cRPMI
Noradrenaline	337.38	cNBM
Recombinant rat/mouse IFNγ	N/A	0.1% bovine serum albumin in 1x PBS
Phentolamine	377.46	cNBM
Prazosin	419.86	MeOH
Propranolol	295.8	cNBM
Quinolinic acid	167.12	DMSO
Ro 61-8048	421.45	DMSO
Tryptophan	204.23	cNBM
Yohimbine	390.90	cNBM

2.2.3 Maintenance of the BV-2 cell line

BV-2 cells are a murine microglial cell line which were immortalised after infection with a v-raf/v-myc recombinant retrovirus. These BV-2 cells express the nuclear v-myc and the cytoplasmic v-raf oncogene products as well as the env gp70 antigen on the cell surface. These cells, which grow in semi-adherent culture, express characteristics and similar functionality to that of cultured microglial cells and as such they were used in these studies as a suitable model of activated microglia (Bocchini et al., 1992). BV-2 cells were maintained in T75 cm^2 flasks at 37°C in a 5% CO_2 humidified atmosphere in cRPMI. The media was changed every 3–4 days and cells were passaged when 90% confluent using a scraper for cell detachment. Prior to experiments, cells were plated onto 24-well plates at a density of $1x10^6$ cells per well. Cells were allowed to adapt for 24 hours prior to any experimental procedures. All cells used in experiments were between passage numbers 5 and 25.

Resuscitation: A cryovial containing frozen down BV-2 microglia was removed from liquid nitrogen storage and thawed in the incubator as rapidly as possible to prevent the formation of intracellular ice crystals. Once defrosted, the cells were added to a new falcon tube in the laminar flow hood and 10 ml pre-warmed cRPMI was slowly added to the cells to dilute out the DMSO. The cell suspension was then centrifuged at 2,000 rotations per minute (rpm) for 5 min at 21°C. The supernatant was removed and the cells were resuspended in 1 ml cRPMI. Cells were counted using the trypan blue exclusion method. Viable cells with intact cellular membranes have the ability to exclude trypan blue dye whereas dead cells do not. The cell suspension was diluted 1:100 in trypan blue and a plastic haemocytometer was used to count the cells under a light microscope (Olympus CKX41). The number of cells per ml was determined using the formula: cell count x dilution factor x 10^4 BV-2 cells were seeded onto a T75 cm^2 flask at 1 x 10^6 cells/ml, with 1 ml of cells being seeded per flask and left to adhere for 2 hr before flooding with 9 ml pre-warmed cRPMI.

Conservation: BV-2 microglia were incubated at 37°C in a 5% CO_2 humidified atmosphere in cRPMI. Media was changed bi-weekly. When the BV-2 microglia became confluent they were split using a cell scraper. The cells were collected, spun at 2,000 rpm for 5 min at 21°C, the supernatant was removed and cells were resuspended in 1 ml. The cells were counted using trypan blue and a haemocytometer and then reseeded on T75 cm^2 flasks at $1x10^6$ cells/ml as previously described. For experimental manipulations, BV-2 microglia were plated at 1 x 10^6 cells/well in 24-well plates 24 hr prior to any treatments to allow them to adapt, only cells between passage numbers 5-25 were used for experiments.

Cryopreservation: BV-2 microglia were scraped off T75 cm^2 flasks, spun at 2,000 rpm for 5 min at 21°C, the supernatant was removed and cells were resuspended in 1 ml cRPMI. The cells were counted using trypan blue and a haemocytometer. The cells were spun down again and diluted in a

freezing solution of RPMI supplemented with 40% FBS and 10% DMSO to a concentration of $5x10^6$ cells/ml. The cryovials were frozen overnight in a Nalgene Mr. Frosty freezing container at -80°C. After 24 hr, cryovials were quickly transferred to liquid nitrogen (Taylor-Wharton HC35) for long-term storage.

2.2.4 Preparation of coverslips

Glass coverslips (13 mm) were placed in each of the wells of a 24-well plate and were exposed to UV light for 60 min. Poly-$_D$-lysine (25 mg) was reconstituted in autoclaved ddH_2O and vortexed thoroughly to produce a stock solution of 0.04 µg/ml. This solution was sterilised using a 0.2 µm syringe filter and frozen in 5 ml aliquots at -20°C. Poly-D-lysine was added to autoclaved ddH_2O to yield a final concentration of 40 µg/ml. The surfaces of glass coverslips were covered with poly-D-lysine solution (75 µl) and the plates were incubated at 37°C for 45 min. Following this, poly-D-lysine was aspirated and stored at 4°C for reuse up to 3 times. Coverslips were washed twice with sterile ddH_2O and left to dry prior to use.

2.2.5 Preparation of primary cortical neuronal cultures

Cultures of primary cortical neuronal cells were prepared as previously described (Day et al., 2014, McNamee et al., 2010) from postnatal day 1 neonate Wistar rat pups under sterile conditions in a laminar flow hood. Pups were decapitated using a large, sharp scissor. The skin was cut along the midline using a smaller scissors and pulled back to reveal the skull. The skull was cut along the midline ensuring no pressure was placed on the brain. A curved forceps was used to carefully remove the brain from the skull and was subsequently placed in a sterile petri dish. A straight forceps was used to remove the surrounding meninges, and obvious blood vessels. Cortical tissue from both hemispheres was removed from the rest of the brain and was placed in a drop of pre-warmed cNBM to prevent it from drying out. The cortical tissue was cross chopped and placed in 5 ml trypsin-EDTA for 2 min. Following this, 5 ml cDMEM containing 10% FBS was added to inactivate the trypsin and this solution was triturated quickly and then spun at 2,000 rpm for 3 min at 21°C. The supernatant was removed and the pellet of cells was resuspended in 5 ml DMEM and triturated to a homogenous suspension. This suspension was then passed through a cell strainer with a 40 µm filter into a new sterile falcon tube. This was then spun at 2,000 rpm for 3 min at 21°C. The supernatant was removed and the pellet was resuspended in 1 ml complete cNBM. Cells were counted using the trypan blue exclusion method. The cell suspension was diluted 1:100 in trypan blue and a plastic

haemocytometer was used to count the cells under a light microscope (Olympus CKX41). The cell suspension was diluted to 3 x 10^5 cells/well using cNBM. 100 µl of cell suspension was added onto each coverslip of a 24-well plate and left to incubate at 37°C for 2 hr to allow adherence of neurons to the coverslips before flooding with 200 µl of warm cNBM. Neurons were left to grow for 3 days before treatment with the exception of neurons used for the analysis of synaptic markers which were left for 18-21 days before treatment. In this instance, 100 µl of fresh pre-warmed cNBM was added to each well weekly. Neuronal purity was ensured by staining for astrocytic marker glial fibrillary acidic protein (GFAP) and the microglial marker mouse cluster of differentiation molecule 11b/c (CD11b).

2.2.6 Preparation of mixed glial cultures

Cultures of primary cortical mixed glial cells were prepared as previously described (McNamee et al., 2010) from postnatal day 2-3 neonate Wistar rat pups under sterile conditions in a laminar flow hood. These cultures were prepared in a manner that consisted of approximately 70% astrocytes and 30% microglia (Day et al., 2014). Cortical tissue from both hemispheres was removed from the rest of the brain as previously described and was placed in a drop of pre-warmed cDMEM to prevent it from drying out. The meninges and blood vessels were removed. The cortical tissue was cross chopped and placed in 6 ml cDMEM and left to incubate for 20 min. Following this, the mixture was triturated to a homogeneous suspension and then subsequently passed through a 40 µM cell strainer into a 50 ml falcon tube and spun at 2,000 rpm for 3 min at 21°C. The supernatant was removed and the pellet was resuspended in 1 ml cDMEM for counting using the trypan blue exclusion method. The cell suspension was diluted to 5 x 10^6 cells/ml using cDMEM and 5 ml of this solution was then added to each T75 cm^2 flasks. The flasks were then left to incubate for 2 hr and were then flooded with 5 ml DMEM. The media was replaced every 3-4 days and the cells were plated when 90% confluent, which occurred between days 8-12. Prior to plating, the media was removed from the T75 cm^2 flasks, 3 ml fresh pre-warmed cDMEM was added, and the cells were scraped and the cell suspension was collected and spun at 2,000 rpm for 5 min at 21°C. The supernatant was discarded and the pellet of cells was resuspended in 1 ml cDMEM. Mixed glial cells were counted as previously described and plated at 1 x 10^6 cells/well. 100 µl of cell suspension was added to each well of a 24-well plate and left to incubate for 2 hr to allow adherence of cells before flooding with 200 µl cDMEM. Mixed glia were left for a minimum of 24 hr before treating.

2.2.7 Preparation of primary astrocytic cultures

Primary astrocytic cultures were prepared as previously described (Day et al., 2014). Initially, primary mixed glial cultures were prepared as described above. Once 90% confluent, the mixed glia were split by placing the T75 cm^2 flasks in an orbital cell shaker at 200 rpm for 2 hr at room temperature to remove microglia from the astrocytic monolayer. Flasks were vigorously tapped 10 times to encourage the separation of microglial cells. The cell suspension was removed and the remaining astrocytes were collected and plated in 24-well plates as described above.

2.2.8 Preparation of primary microglial cultures

Primary microglial cultures were prepared as previously described (Day et al., 2014). Initially, primary mixed glial cultures were prepared as described above. At 1 DIV, granulocyte macrophage-colony stimulating factor (GM-CSF, 10 ng/ml) and macrophage-colony stimulating factor (M-CSF, 10 ng/ml) were added to each flask to promote microglial proliferation. Both GM-CSF and M-CSF were added every 3-4 days when the media was changed. The cells were split as described above. The cell suspension was collected and spun at 2,000 rpm for 5 min at 21°C and plated in 24-well plates as described above.

2.3 Analysis of cell viability

2.3.1 The Pierce™ LDH cytotoxicity assay

The Pierce™ lactate dehydrogenase (LDH) cytotoxicity assay is a reliable colorimetric method used for quantifying cellular cytotoxicity. LDH is a cytosolic enzyme, which upon cell membrane damage is released into the culture media. This extracellular LDH can subsequently be quantified by a coupled enzymatic reaction in which LDH catalyses the conversion of lactate to pyruvate via NAD^+ reduction to NADH. Diaphorase utilises this NADH to reduce the tetrazolium salt to a red formazan product which can be measured spectrophotometrically. The level of formazan in the culture media is directly proportional to the amount of LDH which was released from the damaged cell, and thus is indicative of cytotoxicity. Reagents were made up as per the manufacturer's instructions. In brief, one vial of assay buffer was added to 11.4 ml substrate mix. Following inversion this reaction mixture was protected from light and kept at -20°C until required. Plates were prepared as normal with the inclusion of additional wells to account for a triplicate of spontaneous LDH controls and maximum LDH controls. Upon treatment with the compound of interest, the additional controls were

simultaneously prepared. For the spontaneous LDH controls 200 µl ultrapure H_2O was added, and for the maximum LDH controls nothing was added. Following incubation for the desired treatment time, 10 µl lysis buffer was added to the maximum LDH control set of triplicate wells which was mixed by gently tapping. The plate was left to incubate for 45 min. Following incubation, 50 µl of each sample medium was transferred to a 96-well plate in duplicate wells. 50 µl of reaction mixture was added to each well and mixed well using a multi-channel pipette. The plate was left at room temperature for 30 min protected from light. 50 µl Stop Solution was added to each sample well and was mixed by gently tapping. Any bubbles were broken with a syringe needle to avoid interference with the reading by the spectrophotometer. The absorbance was then read at 490 nm and 680 nm. To determine the LDH activity the 680 nm absorbance value was subtracted from the 480 nm absorbance value before calculating the % cytotoxicity with the following equation;

$$\% \text{ Cytotoxicity} = \frac{\text{Compound-treated LDH activity} - \text{Spontaneous LDH activity}}{\text{Maximum LDH activity} - \text{Spontaneous LDH activity}} \times 100$$

2.3.2 The Alamar Blue assay

The Alamar Blue assay is a colorimetric metabolic assay used to assess the ability of living cells to convert resazurin ($C_{12}H_6NNaO_4$) dye into the fluorescent end product resorufin. Viable cells are capable of reducing resazurin into resorufin via mitochondrial enzymes. As such the more viable cells present the greater the colour change. A 440 µM solution of Alamar Blue was made by dissolving 25 mg resazurin in 226.21 ml dH_2O. Following neuronal treatment, media was removed and 200 µl of Alamar Blue (1:10 dilution in media) was added to each well, as well as to empty wells to provide a blank. Plates were incubated for 1-4 hr at 37°C in a humidified, 5% CO_2 atmosphere. Following a colour change, aliquots of supernatants (75 µl) were transferred in duplicate to a 96-well flat-bottomed plate. Absorbance was read at 600 nm using a microtitre plate reader. The following equation was used for analysis, where Am= average absorbance of blank wells, Ac= average absorbance of Control wells and As= average absorbance of particular sample, % viability= ((Am – As)/ (Am – Ac))*100.

2.3.3 CellTiter 96® AQ_{ueous} Non-Radioactive Cell Proliferation assay (MTS assay)

The CellTiter 96® AQ_{ueous} Non-Radioactive Cell Proliferation assay is a colorimetric assay used for determining the number of viable cells in proliferation or chemosensitivity assays. The CellTiter 96® is composed of solutions of a novel tetrazolium [3-(4, 5-dimethylthiazol-2-yl)-5-(3-carboxymethoxyphenyl)-2-(4-sulfophenyl)-2H-tetrazolium, inner salt; MTS] and an electron coupling reagent (phenazine methosulfate; PMS). MTS is reduced by cells into a soluble formazan product that is soluble in tissue culture medium. The conversion of MTS into aqueous formazan is accomplished by dehydrogenase enzymes found in metabolically active cells. The quantity of formazan product as measured by the absorbance at 490 nm is directly proportional to the number of living cells in culture. MTS/PMS solution was thawed. Media was removed from all wells of the 24-well plate. 100 µl of pre-warmed media was added to each well and 20 µl of thawed MTS/PMS was pipetted into each well. Plates were incubated for 1-4 hr at 37°C in a humidified, 5% CO_2 atmosphere. Following a colour change, aliquots of supernatants (50 µl) were transferred in duplicate to a 96-well flat-bottomed plate. Absorbance was read at 490 nm using a microtitre plate reader. The following equation was used for analysis, where Am = average absorbance of blank wells, Ac = average absorbance of control wells and As = average absorbance of particular sample, % viability = ((Am – As)/ (Am – Ac))*100.

2.4 Fluorescent immunocytochemistry

2.4.1 General fluorescent immunocytochemistry

Fluorescent immunocytochemistry was performed on primary cortical neurons grown on glass coverslips in 24-well plates. Following treatment, the supernatant was aspirated from each well and the cells were quickly washed in 1X PBS. Cells were then fixed by adding 300 µl ice cold methanol to each well and leaving at -20°C for 20 minutes. The methanol was then removed and the coverslips were washed 3 times with 1X PBS, leaving the plates on a platform rocker (Stuart Scientific 3D Gyratory Rocker) between washes. After 3 x 5 min washes with 1X PBS, non-specific interactions were blocked by adding 300 µl normal goat serum (NGS) to each well and were left on a rocker at room temperature. The NGS was subsequently discarded. The cells were washed with 1X PBS before adding the primary antibody which was left overnight at 4°C. After 3 x 5 min washes with 1X PBS, the secondary antibody was added for 2 hr at room temperature in the dark on a rocker. After 3 x 5 min washes with 1X PBS, dH_2O was added to each well. One drop of Vectashield fluorescent mounting media with DAPI was placed on a slide (1-1.2 mm). The coverslip was lifted from the plate using a forceps and inverted onto a drop of Vectashield fluorescent mounting medium which contained the nuclear marker DAPI. Excess Vectashield was removed from the slide with tissue paper. The edges of the coverslip were sealed using nail varnish and the slides allowed to dry in a light-protected environment before storage in the dark at 4°C.

2.4.2 Sholl analysis

Neurons were fixed and blocked with 4% NGS for 2 hr. Neurons were stained with the primary antibody which was raised against mouse β-III tubulin (1:1000 in 1X PBS) and subsequently the secondary antibody, Alexa Fluor goat anti-mouse 488 (1:2000 in 1X PBS).

Sholl analysis was used to quantify and compare various parameters of neuronal complexity following the various treatments. Sholl analysis is a widely used method for quantifying and graphically representing neurite morphology. This simplified version (Fast Sholl) was adapted from Sholl (1953) and Gutierrez and Davies (2007). Matlab was used to carry out Sholl analysis on all neuronal images. This involved identifying the number of primary neurites, the neurite length, the number of neuritic branches as well as the Sholl profile (**figure 2.1**). All images were taken using an epifluorescent microscope with a 200X magnification and images were captured using an AxioImager Z1 epifluorescent microscope, a Zeiss AxioCam HR camera and AxioVision 4.8.2 software (Carl Zeiss MicroImaging). A minimum of 5 images were taken of each coverslip provided the coverslip looked

globally healthy. All neuronal images were randomly selected with the neuron of choice being representative of the surrounding neurons. For a neuron to qualify for imaging it must be isolated and have a defined nucleus with the longest neurite being longer than the nucleus.

Sholl analysis involves the overlay of 25 concentric rings with regular radial increments of 10 µm onto the neuron, with the number of neurites intersecting each ring being counted (**figure 2.1 B**). Neurites are measured using the following equation: $x_i = x_{i-1} + b_i - t_i$, where x_i is the number of neurites for the "ith" segment, b_i is the number of branches occurring in the "ith" segment and t_i the number of terminations in that segment. This equation was implemented into the Matlab (2012b) programming software to allow for a semi-automated procedure.

Primary neurites were classified as those arising directly from the cell soma and branches were classified as where a neurite divided in two for at least 5 µm. Neuritic length represents the total number of estimated intersections per cell, linearly proportional to the metric length of the neuritic arbour, while the Sholl profile illustrates the number of intersections relative to their distance from the cell soma (**figure 2.1C**).

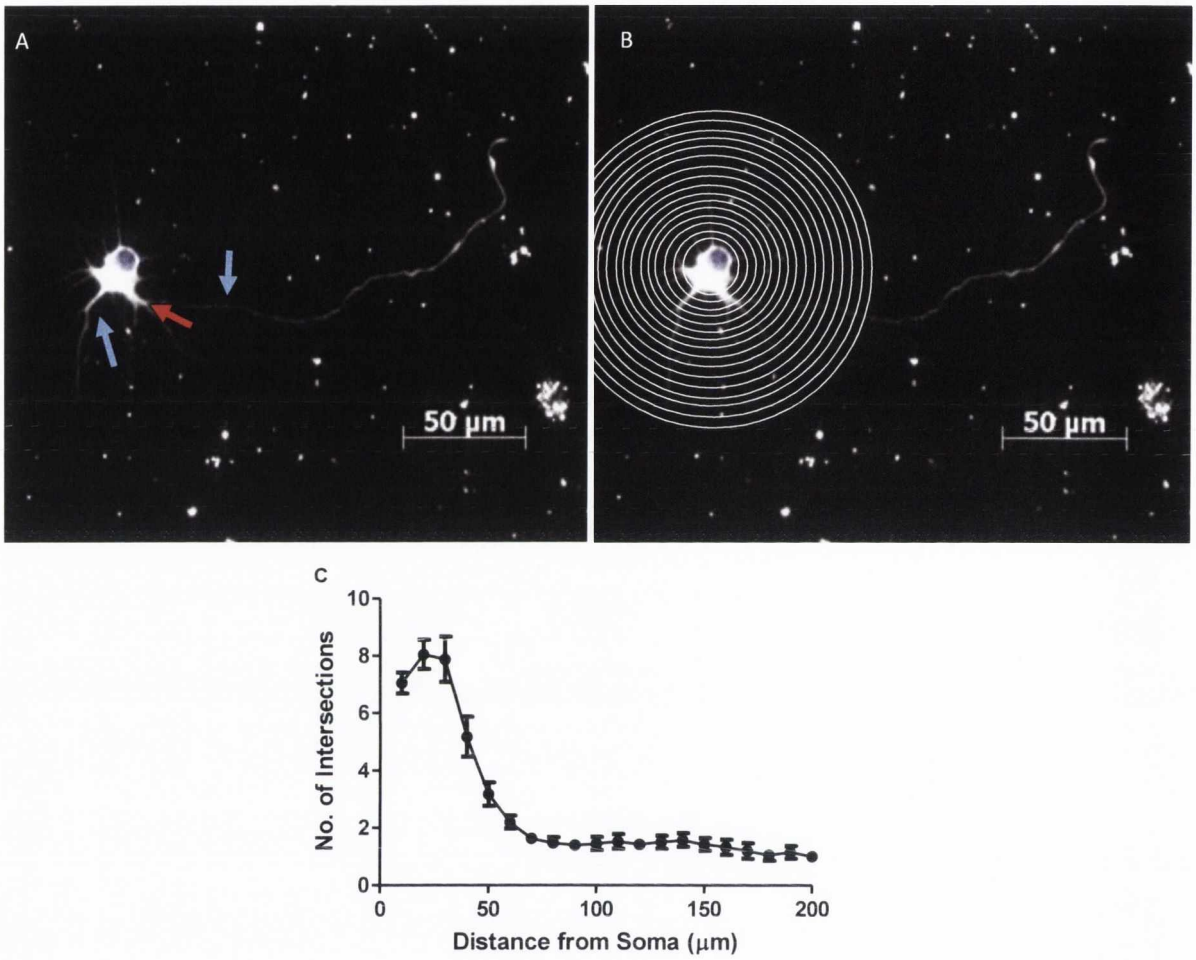

Figure 2.1: Fluorescent image of a typical control neuron.
(A) The blue arrows indicate the primary neurites while the red arrow indicates an intersection from which a neuritic branch arises. (B) The nucleus is stained blue with DAPI, while the projections and cell soma are stained with β-III tubulin and appear white with overlaying Sholl analysis concentric rings which are 10 µm apart and radiate out from the cell soma. (C) A scatter plot of the number of intersections at specific distances from the cell soma for control neurons, demonstrating a Sholl profile (n= 8).

2.4.3 Analysis of the co-localisation of synaptic markers in mature neurons

For these studies, neurons (DIV 18-21) were treated and then fixed as described above. The cells were permeabilised and blocked in 50% NGS + 0.2% triton-X-100 for 30 min at room temperature. The blocking buffer was then removed, cells were washed with 1X PBS and 200 µl of primary antibody cocktail raised against rabbit synaptophysin (1:500 in 1X PBS) and mouse PSD-95 (1:500 in 1X PBS) was added to each well and left overnight at 4°C. After 3 x 5 min washes with 1X PBS the cells were stained with 200 µl of the secondary antibody cocktail which consisted of Alexa Fluor goat anti-rabbit 546 and Alexa Fluor goat anti-mouse 488 (1:1000 in 1X PBS) in a light-protected environment for 2 hr at room temperature. The glass coverslips were then removed and mounted onto glass slides as described above.

The synaptogenesis procedure was adapted from Ippolito and Eroglu (2010b). For this procedure, mature neurons were immunostained with the pre-synaptic marker, synaptophysin, and the post-synaptic marker, PSD-95 as described above. Synaptophysin and PSD-95-stained neuronal coverslips were visualised at 400X magnification, images were captured using an AxioImager Z1 epifluorescent microscope, a Zeiss AxioCam HR camera and AxioVision 4.8.2 software. Coverslips included in this analysis displayed neurons with a healthy network phenotype throughout the entire coverslip. The optimum exposure intensity was determined using a control coverslip and was maintained for all other coverslips. This exposure intensity was the same for both the synaptophysin and PSD-95 channels. 3-4 individual images were captured from each coverslip and 6 coverslips per experimental condition were typically collected for analysis. Where possible, groups were blinded. In this assay, synapses were defined as 'puncta', or points of co-localisation between the signals generated by pre-synaptic synaptophysin and post-synaptic PSD-95. The number of co-localisations were quantified using a plugin 'Puncta Analyser' for use in ImageJ analysis software platform. This procedure was adapted from Ippolito and Eroglu, using the ImageJ analysis programme (NIH) and the Puncta Analyzer plug-in written by Barry Wark (Ippolito and Eroglu, 2010a). For image analysis, individual images were opened in ImageJ and a region of interest (ROI) was selected which was typically one-cell diameter radially around the soma of interest. The Puncta Analyser was then used to adjust the thresholds of the red channel (synaptophysin expression) and green channel (PSD-95 expression) so that the intensity corresponded to discrete individual puncta. Minimum puncta size was set at a value of 4 for each experiment. The threshold value was standardised for each based on a value established for a control-treated neuron in order to maintain a consistent approach for comparison between groups.

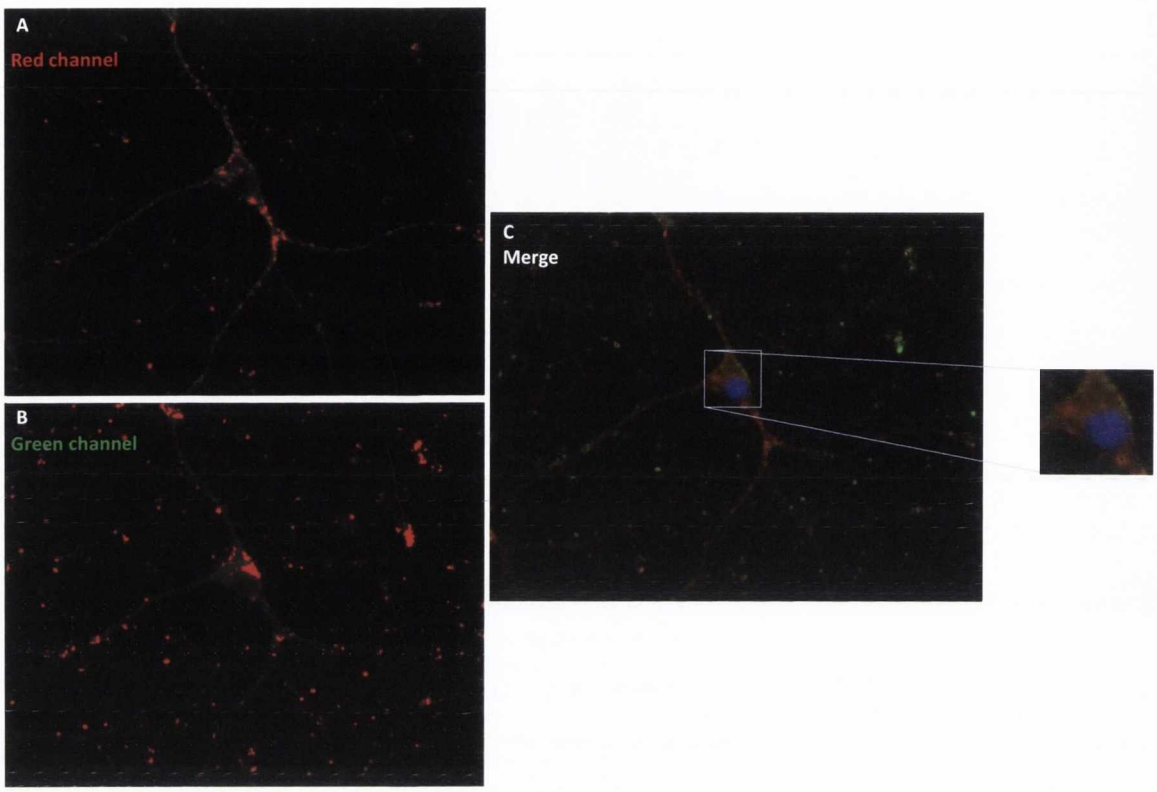

Figure 2.2: Quantification of the co-localised expression of synaptic markers, synaptophysin and PSD-95, in mature neurons

Primary cortical neurons (DIV 18-21) were treated for 24 hr before fixation. Neurons were stained with the pre-synaptic marker, synaptophysin (A), and the post-synaptic marker, PSD-95 (B). (C) Merged image showing synaptophysin, PSD-95, and the nuclear marker, DAPI (blue). Quantification of the co-localised expression of synaptic markers was achieved using ImageJ software where co-localisation of synaptophysin and PSD-95 was indicative of a synapse. Individual synaptic co-localised puncta are displayed as black dots in the inset image.

2.4.4 Glial immunocytochemistry

Isolated microglia, astrocytes and mixed glia were fixed in 4% NGS for 2 hr and were subsequently washed with 1X PBS and stained with 200 µl primary antibody cocktail raised against rabbit GFAP (1:1000 in 1X PBS) and (1:1000 in 1X PBS) overnight at 4°C. After 3 x 5 min washes with 1X PBS the cells were stained with 200 µl of the secondary antibody cocktail which consisted of Alexa Fluor goat anti-rabbit 546 and Alexa Fluor goat anti-mouse 488 (1:2000 in 1X PBS) in a light-protected environment for 2 hr at room temperature. The glass coverslips were then removed and mounted onto glass slides as described above.

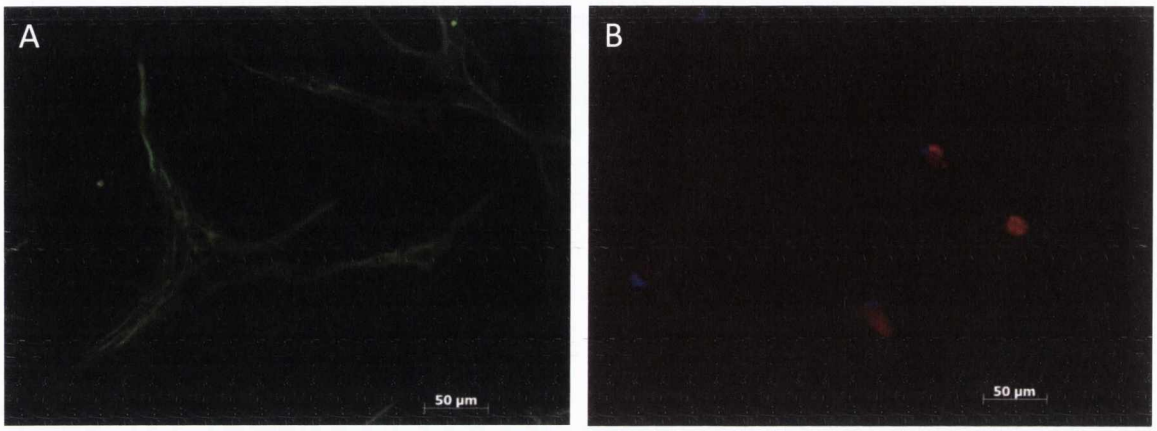

Figure 2.3: Fluorescent image of glial cultures
Images show representative cultures of (A) purified primary astrocytes stained with anti-GFAP (green) and (B) purified primary microglia stained with anti-CD11b (red) and DAPI (blue).

2.5 Cell preparation for quantitative polymerase chain reaction (PCR)

2.5.1 Harvesting cells for mRNA analysis

Before carrying out ribonucleic acid (RNA) extraction all the surfaces involved in the procedure were wiped down with RNase Zap wipes (Ambion, UK) to prevent RNA breakdown during the extraction, and therefore prevent reduction in the RNA yield. Following treatment, supernatants were aspirated from wells and cells were lysed by adding 100 µl RA1 lysis buffer supplemented with 1% β-mercaptoethanol to each well. Cells were scraped from the base of the wells using a 1000 µl filtered pipette tip and the lysate was transferred to a 2 ml RNase-free microtube. Pipette tips were changed between treatment groups in order to prevent cross-contamination. Cell lysates were harvested and stored at -80˚C for subsequent RNA extraction.

2.5.2 Total RNA extraction

RNA extraction was carried out using NucleoSpin® RNA II kits (Macherey-Nagel) following the procedure outlined in the user's manual. The lysate was filtered using a NucleoSpin® Filter Column and centrifuged (APOLLO) for 1 min at 13,000 rpm. The NucleoSpin® Filter Column was then removed and 350 µl of 70% EtOH was added to the filtered lysate to adjust RNA binding conditions. The mixture was pipetted up and down a few times to ensure mixing of EtOH and the lysate and to disaggregate any precipitate. The lysate-EtOH mixture was then loaded into a NucleoSpin® RNA II Column and centrifuged for 30 sec at 13,000 rpm. The silica membrane was desalted using 350 µl of Membrane Desalting Buffer (MDB) and centrifuged for 1min at 13,000 rpm. This step makes the recombinant deoxyribonuclease (rDNase) digest more effectively. 95 µl of the rDNase reaction mixture (10 µl reconstituted rDNase and 90 µl Reaction Buffer for rDNase) was added onto the centre of the silica membrane of the NucleoSpin® RNA II Column and was then incubated for 15 min at room temperature. Following incubation the silica membrane was washed using 200 µl of Buffer RA2 and centrifuged for 30 sec at 13,000 rpm. The column was then changed to a new 2 ml collection tube and washed two more times using 600 µl RA3 and centrifuging for 30 sec at 13,000 rpm and then using 250 µl RA3 and centrifuging for 2 min at 13,000 rpm. Using a new collection tube the pure RNA was eluted in 40 µl Ribonuclease (RNase)-free water by centrifuging for 1 min at 13,000 rpm. These RNA samples were either equalised or stored at -80˚C until required.

2.5.3 RNA equalisation

The RNA extraction samples as prepared above were defrosted slowly on ice if they had been stored at -80˚C. These samples were kept on ice throughout the RNA equalisation procedure. In this case Nanodrop® ND_1000 (Nano Drop Technologies, Thermo Fisher Scientific) was the spectrophotometer used to quantify total RNA concentrations in each sample. The Nanodrop was connected to a laptop computer and it was initialised with 1 µl of RNase-free water. Another 1 µl of RNase-free water was used to blank the Nanodrop. 1 µl of each RNA sample was added sequentially to the pedestal and its absorbance was measured. Two readings as ng/ml were obtained for each 1 µl sample to provide an average. Following each sample the pedestal was wiped with absorbent paper and the sample to be analysed was quickly vortexed (Genie 2, Scientific Industries). The protein contamination of each sample was determined using $A_{260/280}$. After the concentrations for all samples had been calculated, they were all equalised to the lowest concentration using RNase free water.

2.5.4 Complementary deoxyribonucleic acid (cDNA) synthesis

A master mix solution was prepared (**table 2.3**). The RNA samples were vortexed and then 5 µl was added to 5 µl of master mix solution in mini-tubes. These mini-tubes were then briefly vortexed and centrifuged and placed in a thermocycler (Peltier Thermal Cycler- 200) and set to the "Abirt" programme which ran at 25˚C for 10 min, 37˚C for 120 min and 85˚C for 5 min. The samples were then stored at -20˚C until required.

Table 2.3: Volumes of the components in the cDNA synthesis master mix

Reverse Transcriptase Master Mix	**Volume for 1 sample (µl)**
10x Reverse transcription buffer	1
25x deoxyribonucleotide triphosphates (dNTPs)	0.4
10x Random primers	1
Multiscribe reverse transcriptase	0.5
Nuclease free water (H_2O)	2.1
Total Volume	**5**

2.5.5 Quantitative PCR

The cDNA samples which were prepared as described previously were defrosted on ice along with β-actin and the primers of interest. Upon first use, the cDNA was diluted 1 in 5 with RNase-free water. When the components were defrosted 4 µl of each cDNA sample were added to an individual well in a PCR plate. The primers were made up using FAST Taqman, the primer of interest and β-actin as the endogenous control (**table 2.4**). They were vortexed and 6 µl was added to each well making up a final concentration of 10 µl in each well. The plate was then covered and sealed using an optically clear plastic cover and pulse centrifuged for 30 sec.

Table 2.4: Volumes of the components in the Primer mix

Primer Mix	**Volume for 1 sample (µl)**
FAST Taqman	5
Primer of interest	0.5
β-actin	0.5
Total Volume	**6**

The plate was put in the quantitative PCR thermocycler (Applied Biosystems) and Step One software was used. The Comparative CT method and fast run were chosen and the target gene expression was assessed using a TaqMan gene expression assay (**table 2.5**), which comprises specific target primers and fluorescein amidite (FAM)-labelled minor groove binding (MGB) target probes (Applied Biosystems). The gene expression of the endogenous control β-actin was measured using specific primers and a VIC-labelled MGB probe.

Table 2.5: List of FAM-labelled MGB target probes used in PCR

Gene Symbol	**Gene Name**	**Taqman Gene Expression Assay ID**
Aadat	KAT II	mM00496169_m1 Rn00567882_m1
Actb	β-actin	4352341E Rn00667869_m1
IDO1	Indoleamine 2,3-dioxygenase	mM00492586_m1 Rn01482210_m1
KMO	Kynurenine monooxygenase	mM00505511_m1 Rn00665313_m1
Kynase	Kynureninase	mM00551012_m1 Rn00588108_m1
NOS2	Inducible nitric oxide synthase	mM00440502_m1
TDO 2	Tryptophan 2, 3-dioxygenase	mM00451266_m1 Rn00574499_m1

Quantitative PCR consisted of several different steps. The first step involved a temperature setting of 50°C for 2 min, followed by 95°C for 20 sec. This next step was repeated 40 times and involved a temperature setting of 95°C for 1 sec followed by 60°C for 20 sec, these were the denaturing, and annealing and extension phase temperatures respectively. The labelled MGB target probe binds to the cDNA as the temperature falls from 95°C to 60°C prior to the target primer binding as it has a higher melting point than the primer. The probe consists of a reporter dye (FAM/VIC) and a non-fluorescent quencher (NFQ) dye which prevents the reporter dye from fluorescing by fluorescence resonance energy transfer (FRET) technology (Applied Biosystems). Once the primers anneal at 60°C and the extension phase occurs via Taq polymerase activity the reporter dye can fluoresce due to the displacement of the NFQ by Taq polymerase. Taq polymerase activity causes the FRET between the reporter dye (FAM/VIC) and the quencher dye to be broken allowing a fluorescent signal to be generated for each new copy of cDNA.

2.5.6 Analysis of the quantitative PCR data

The gene expression of all the quantitative PCR was assessed using the ΔΔCT method (Applied Biosystems RQ software). This ΔΔCT method compares the gene expression of the samples with the controls, which enables a fold difference to be determined between samples of different treatments. To obtain this fold change the cycle number (CT) difference between samples must be calculated. This was done by subtracting the CT of the endogenous control (β-actin) from the CT of the target gene for each sample. This is referred to as ΔCT and accounts for any differences in cDNA quantity. The ΔΔCT (cycle difference corrected for endogenous control) was then calculated by subtracting the ΔCT of a control sample from itself and from all the other samples. ΔΔCT can be changed into a fold difference which can then be used to calculate the related change in expression. The data obtained from quantitative PCR was exported into an Excel file (Microsoft Excel 2013). The average of the relative quantity (RQ) values was calculated for the control group and then all other RQ values were divided by this average to obtain the fold change relative to the control. These fold change values were then visualised using GraphPad Prism 5.

2.6 HPLC

2.6.1 Detection of kynurenine pathway metabolites by HPLC coupled to UV/fluorescent detection

Instrumentation

HPLC analysis was conducted with an automated HPLC system (Shimadzu ADVP module). 20 µl of sample was injected into a reverse phase analytical column (Kinetex Core Shell Technology, Phenomenex UK) with specific area of 100 mm x 4.6 mm and particle size of 2.6 µm and fitted with a guard column (Lichrosorb RP18, specific surface area 30 x 4 mm, Phenomenex). Two detectors were connected in series; a PDA-UV detector (SPD-M10A VP, Shimadzu) and a fluorescent detector (RF-10A XL, Shimadzu). The PDA-UV detector was calibrated to analyse a UV spectrum from 240 nm to 370 nm while integrating at 250 nm. The fluorescence wavelengths were set to 254 nm excitation and 404 nm emission. The flow rate was 0.8 ml/min (LC-10AT pump, Shimadzu) and the acquisition time was 18 min. CLASS-VP software (Shimadzu) was used for chromatographic control, data collection and processing. The signal to noise ratio was taken as 3 to 1 as a limit of detection. Peak heights compared with internal and external standards allowed for the quantification of the concentrations of the kynurenine pathway metabolites in the samples.

Reagents

The mobile phase consisted of 50 nM glacial acetic acid, 100 mM zinc acetate and 3% acetonitrile dissolved in HPLC grade H_2O. The pH was adjusted to 4.9, using 5 M NaOH. HPLC standards [N-methyl-5-hydroxy-tryptamine [Internal standard (IS)], L-tryptophan, L-kynurenine, 3-hydroxykynurenine, 3-hydroxyanthranillic acid, quinolinic acid and kynurenic acid] were obtained from Sigma Aldrich. Standard solutions of 10 mg/10 ml were prepared by dissolving the standards in 10 ml of HPLC mobile phase and stored refrigerated in glass volumetric flasks. A 10 ml standard mix containing 200 ng/20 µl of each standard was prepared as well as 10 ml solutions of each individual standard at 200 ng/20 µl.

Retention Times and resolvability

A 150 µl aliquot of each 200 ng/20 µl standard was pipetted into an individual 0.2 ml conical insert and transferred into a 2 ml vial. Analysis was carried out by HPLC as described in the mobile phase in order to determine the retention times of each standard.

Cell culture CM preparation for HPLC Analysis

150 µl CM was harvested from cells and was added to 150 µl of homogenisation buffer (mobile phase containing 6% perchloric acid and 1% IS at 200 ng/20 µl) and the samples were subsequently vortexed thoroughly. The samples were then centrifuged at 14,000 *g*-force for 20 min at 4˚C. The supernatants were transferred to new 1.5 ml eppendorfs. Each supernatant was filtered using a 4 mm diameter, 0.45 µm pore size, syringe filters and analysed immediately by injection into an automated HPLC system coupled with UV and fluorescent detection in an injection volume of 20 µl. The flow rate was 0.8 ml/min with a run time of 18 min. For each HPLC system, a mobile phase was injected intermittently and a standard mix was injected every six samples in order to recalibrate the system and track divergences in the retention times during sample runs. The auto-samplers were pre-programmed to self-rinse with HPLC grade methanol between each sample injection. Peak heights obtained from the chromatographs were used to calculate nanograms of metabolite per millilitre of CM.

2.7 Statistical analysis

Statistical tests including Student's *t*-test, or a one-, or two-, or three-way analysis of variance (ANOVA) were used where relevant as indicated in the experimental sections where significance was found, the data was subjected to either Newman-Keuls, Dunnett's or Bonferroni *post hoc* tests as appropriate. Data was expressed as mean ± standard error of the mean (SEM) and data was considered significant when $P<0.05$.

Chapter 3

Inhibition of the kynurenine pathway protects against reactive microglial-associated reductions in the integrity of primary cortical neurons

3.1 Introduction

The role of altered kynurenine pathway activation is now recognised as being a contributing factor in several neurological disorders including Alzheimer's disease, Parkinson's disease, ALS, major depression, and schizophrenia (O'Farrell and Harkin, 2015). These various disorders exhibit an underlying neuroinflammatory phenotype which may potentially result in the activation of the kynurenine pathway. IFNγ, a pro-inflammatory cytokine, is the most potent inducer of the kynurenine pathway rate limiting enzyme, IDO (Pemberton et al., 1997). At a particular point in the kynurenine pathway, a division occurs giving rise to what are commonly referred to as a neurotoxic arm and a neuroprotective arm. Within the CNS, the different arms of the kynurenine pathway are compartmentalised, with the neurotoxic arm being present in microglia (Guillemin et al., 2003), while the neuroprotective arm is restricted to astrocytes (Guillemin et al., 2001). Both microglia and astrocytes possess IDO which catalyses the conversion of tryptophan to kynurenine, however unlike astrocytes, microglia preferentially express the neurotoxic enzymes, KMO and KYNU, which lead to the production of the free radical producing metabolites, 3-hydroxykynurenine and 3-hydroxyanthranillic acid respectively and subsequently the production of the NMDA receptor agonist quinolinic acid (Guillemin et al., 2003, Guillemin et al., 2001). As such, microglial activation as a consequence of inflammation, may lead to altered neuronal integrity and transmission due to excessive production of neurotoxic kynurenine pathway metabolites.

IFNγ, in addition to being the principal activator of the kynurenine pathway, also drives an assortment of other responses in microglial cells, including enhanced production of nitric oxide (Dello Russo et al., 2004), superoxide (Colton and Gilbert, 1987), alongside the induction of various chemokines, cytokines, and MHC molecules (Rock et al., 2005). Currently, increased nitric oxide production and NMDA receptor activation are the primary mechanisms thought to mediate cytokine-induced neurotoxicity. Furthermore, it is believed that cytokines directly induce neuronal cell death through their synergistic action with other cytokines on neurons, or indirectly through interaction with local glial cells, with the subsequent release of soluble glial-associated factors inducing neurotoxicity (Chao et al., 1995). At present it is proposed that *in vitro*, individual cytokines primarily exert their neurotoxic effect through the induction of iNOS with the subsequent release of nitric oxide from microglia. The release of this resultant nitric oxide can trigger astrocytic release of glutamate and subsequently excitotoxicity of neurons (Bal-Price et al., 2002). Superoxide may also be generated as a result of NMDA receptor driven excitotoxicity and activation of NADPH oxidase in reactive microglia. Superoxide reacts with nitric oxide to produce peroxynitrite which in turn causes mitochondrial damage and cell death (Brown and Bal-Price, 2003).

Overall the aim of the study outlined in this chapter is to examine the effect of CM from IFNγ-stimulated microglia on neuronal integrity. Moreover, this investigation aims to determine a role for kynurenine pathway activation in driving IFNγ-stimulated microglial-induced changes in neuronal integrity.

IFNγ-mediated activation of the kynurenine pathway in microglia is assessed by quantification of pathway-related gene expression and quantification of pathway-related metabolites in microglial cells and CM respectively. Subsequently, the effect of the microglial CM on neuronal viability and complexity, including the number of neuritic branches, neurite length, the number of primary neurites, and the number of branches in relation to varying distances from the cell soma/ body, were examined. A role for the pathway was further substantiated by direct assessment of pathway metabolites on neuronal complexity. Additionally, a role for related oxidative processes implicated in microglial responses was also investigated.

An *in vitro* cell culture system, with use of an immortalised murine microglial cell line (BV-2), was employed in these experiments to ensure the purity of microglial cells and allowed for the identification of mediators responsible for reactive BV-2 microglial-induced changes in neuronal viability and complexity.

3.2 Study design

3.2.1 Characterisation of the effect of IFNγ on the mRNA expression profile of BV-2 microglia

BV-2 microglia were treated with IFNγ (5 ng/ml) for 24 hr. Cells were harvested for RNA extraction followed by quantitative PCR to measure mRNA expression of kynurenine pathway enzymes, including the rate limiting enzymes, IDO and TDO, and the downstream enzymes, KMO, KYNU and KAT II/Aadat, in addition to the inflammatory microglial marker iNOS. It has been shown that microglia preferentially express the enzymes KMO and KYNU which are necessary for activation of the aforementioned neurotoxic arm of the pathway (Guillemin et al., 2003), while astrocytes preferentially express KAT which drives the neuroprotective arm of the kynurenine pathway (Guillemin et al., 2001). Of the four isoforms of the KAT enzyme, KAT II is responsible for 75% of brain kynurenic acid production (Zinger et al., 2011), thus KAT II expression was measured in this experiment. The concentration of IFNγ used was based on prior research carried out in our laboratory which resulted in no effect on the viability of BV-2 or neuronal cells at this concentration as determined by the MTS assay.

3.2.2 Determination of the concentrations of kynurenine pathway metabolites in the CM of BV-2 microglia following stimulation with IFNγ

BV-2 microglia were pre-treated with the IDO inhibitor, 1-MT (L) (0.5 mM; 30 min), followed by stimulation with IFNγ (5 ng/ml) for 24 hr. CM was harvested for HPLC analysis of tryptophan and the kynurenine pathway metabolites kynurenine and 3-hydroxykynurenine.

1-methyl tryptophan (1-MT) is a competitive inhibitor of IDO and exists as either a dextro (D) or levo (L) enantiomer with some *in vivo* and *in vitro* studies suggesting they have divergent actions. *In vitro* enzyme and cellular assays have demonstrated that the L enantiomer is a more potent inhibitor of IDO (Qian et al., 2009, Lob et al., 2008), while *in vivo* studies have reported that the D enantiomer evokes a more effective anti-tumour response through IDO inhibition (Hou et al., 2007). The inconsistent findings are believed to be associated with the fact that the D enantiomer may have more off-target effects, and also that it is a more potent inhibitor of IDO-2 than IDO (Lob et al., 2008).

3.2.3 Characterisation of the effect of CM from IFNγ-stimulated BV-2 microglia on neuronal viability and complexity

BV-2 microglia were treated with IFNγ (5 ng/ml) for 24 hr. The resultant CM was collected, sterile-filtered and placed on primary cortical neurons (DIV 3) - after removal of cNBM - for 48 hr. Neuronal viability was assessed using the LDH cytotoxicity assay, the alamarBlue® cell proliferation assay, and the CellTiter 96® AQ_{ueous} Non-Radioactive Cell Proliferation (MTS) assay – widely used colorimetric assays, of which the former quantifies the % cytotoxicity, whereas the latter two quantify the % viability relative to the control. Fixation and fluorescent immunocytochemistry were performed on neurons for Sholl analysis as previously described.

In addition to the CM studies, neurons were treated directly with IFNγ to assess whether IFNγ affected either neuronal viability or complexity. For this experiment, primary cortical neurons (DIV 3) were treated with IFNγ (5 ng/ml) for 48 hr. Neuronal viability was assessed using the LDH cytotoxicity assay, the alamarBlue® cell proliferation assay, and the MTS assay. Fixation and fluorescent immunocytochemistry were performed on neurons for Sholl analysis.

3.2.4 Effect of kynurenine pathway inhibitors on IFNγ-stimulated BV-2 CM-induced reductions in neuronal viability and complexity

To further investigate a role for kynurenine pathway activation in altering neuronal viability and complexity, inhibitors of IDO and KMO were utilised to assess if the deleterious effects of CM obtained from IFNγ-stimulated BV-2 microglial CM could be dissipated when the activity/induction of these enzymes are inhibited. BV-2 microglia were pre-treated with either 1-MT (L) (0.5 mM; 30 min), dexamethasone (1 μM; 2 hr), Ro 61-8048 (1 μM; 30 min), a KMO inhibitor, or MK-801 (0.1 μM; 30 min), an NMDA receptor antagonist and inhibitor of quinolinic acid action at the receptor, followed by stimulation with IFNγ (5 ng/ml) for 24 hr. The resultant CM from these cells was collected, sterile-filtered and placed on primary cortical neurons (DIV 3) for 48 hr. Neuronal viability was assessed using the LDH cytotoxicity assay. Fixation and fluorescent immunocytochemistry were performed on neurons for Sholl analysis. In addition, BV-2 microglia were harvested for mRNA extraction and quantitative PCR analysis, to determine if dexamethasone or MK-801 were acting to influence the expression of kynurenine pathway enzymes and/or iNOS.

Dexamethasone is a synthetic glucocorticoid that dampens down the inflammatory response by inhibition of the inflammatory transcription factor, nuclear factor κ-light-chain-enhancer of activated B-cells (NFκB) (Ardite et al., 1998). As such it was used in this experiment as an inhibitor of IDO gene induction as opposed to inhibiting enzyme activity as is the case with 1-MT (L). Ro 61-8048 is a widely

used KMO inhibitor and has been shown to increase the central levels of kynurenic acid in rodents without altering 3-hydroxykynurenine or quinolinic acid levels, indicating that it cannot cross the blood brain barrier limiting potential clinical efficacy (Zwilling et al., 2011). However it has been demonstrated that in the presence of strong immune stimulation, Ro 61-8048 is capable of reducing the levels of quinolinic acid in the blood and brain of mice (Chiarugi and Moroni, 1999). MK-801 is a potent, non-competitive antagonist of the NMDA receptor, and is highly selective for this receptor over other glutamatergic receptors (Wong et al., 1986). Other selective non-competitive antagonists of the NMDA receptor including phenylcyclidine and ketamine displace MK-801 from its binding site, indicating that MK-801 binds within the ion channel of the NMDA receptor as opposed to the agonist binding site (Wong et al., 1986). The action of MK-801 is intensified by the presence of excitatory amino acids and glycine (Foster and Wong, 1987, Wong et al., 1986) giving rise to the notion that MK-801 is an agonist- or use-dependent antagonist.

3.2.5 Effect of kynurenine pathway metabolites on neuronal viability and complexity

Primary cortical neurons (DIV 3) were treated with the kynurenine pathway metabolites 3-hydroxykynureine (0.1 μM), 3-hydroxyanthranillic acid (0.1 μM), or quinolinic acid (1 μM) for 48 hr. Fixation and fluorescent immunocytochemistry were performed on neurons for Sholl analysis.

Primary cortical neurons (DIV 3) were treated with a combination of kynurenine pathway metabolites consisting of 3-hydroxykynureine (0.1 μM) + 3-hydroxyanthranillic acid (0.1 μM) + quinolinic acid (1 μM) for 48 hr. Fixation and fluorescent immunocytochemistry were performed on neurons for Sholl analysis.

Primary cortical neurons (DIV 3) were pre-treated with MK-801 (0.1 μM; 30 min) followed by a combination of metabolites consisting of 3-hydroxykynureine (0.1 μM) + 3-hydroxyanthranillic acid (0.1 μM) + quinolinic acid (1 μM) for 48 hr. Fixation and fluorescent immunocytochemistry were performed on neurons for Sholl analysis.

3.2.6 Effect of 1400W, or DPI chloride on IFNγ-induced reductions in neuronal viability by BV-2 microglia

Considering the diverse nature of responses that can be elicited by IFNγ stimulation, oxidative and inflammatory pathways were assessed to determine if attenuation of other IFNγ driven cascades might also prevent IFNγ CM-induced decreases in neuronal viability and complexity. Accordingly, BV-2 microglia were pre-treated with the iNOS inhibitor, 1400W (25 μM; 30 min), or the NADPH oxidase inhibitor, DPI chloride (0.001 μM; 30 min), followed by stimulation with IFNγ (5 ng/ml) for 24 hr. CM from these cells was collected, sterile-filtered and placed on primary cortical neurons (DIV 3). Fixation and fluorescent immunocytochemistry were performed on neurons for Sholl analysis.

1400W is an irreversible/slowly reversible selective inhibitor of iNOS and is effective both *in vitro* and *in vivo* (Garvey et al. 1997). NADPH oxidases are enzymes responsible for the production of reactive oxygen and nitrogen species by way of transferring electrons across a membrane to either oxygen or nitrogen. These oxidants can interact with a variety of molecules including lipids, proteins, and DNA whereby they can destroy or alter the function of their targets (Bedard and Krause, 2007).

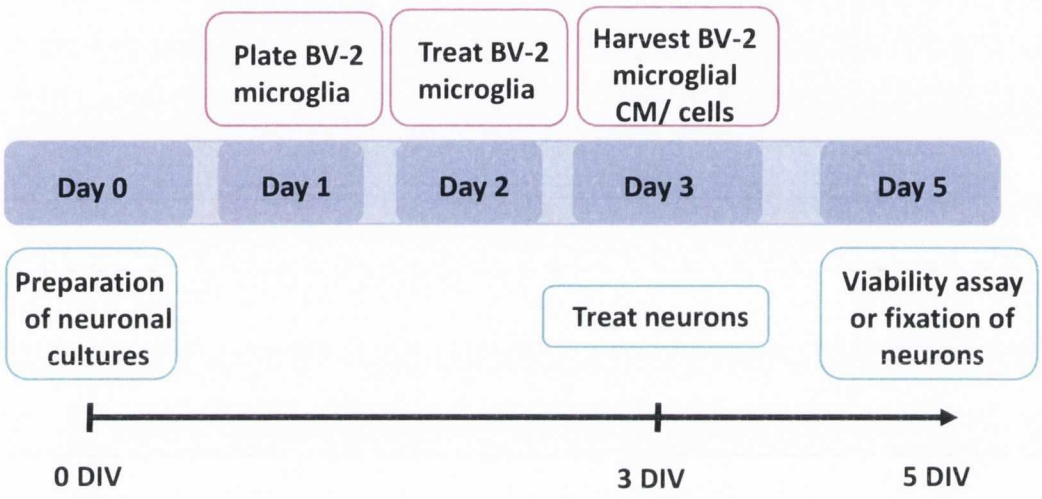

Figure 3.2.1: Diagram showing the timeline of a typical experiment.
BV-2 microglia are plated for a minimum of 24 hr prior to treatment. BV-2 microglia are treated with IFNγ for 24 hr (+/- pre-treatment, 1-MT (L), dexamethasone, Ro 61-8048, MK-801, 1400W, or DPI chloride) after which their CM and/or cells are harvested. Neuronal cells are cultured and grown for 3 days upon which they are subsequently treated for 48 hr with CM or kynurenine pathway metabolites (+/- pre-treatment with MK-801). On day 5 neurons are either assessed for neuronal viability, or fixed to allow for assessment of neuronal complexity by Sholl analysis.

Table 3.2.1: Table of compounds and concentrations used

To ensure maximal inhibition, all inhibitors, unless otherwise stated, were incubated on cells for 30 min before any other stimulation with IFNγ. Concentrations of drugs used were based on those from the literature indicated in the reference column of the table below.

Compound name	***Final concentration***	***Reference***
1400W	25 μM	(Garvey et al., 1997)
1-Methyl-tryptophan (L)	0.5 mM	(Lob et al., 2008)
3-Hydroxyanthranillic acid	0.1 μM	(Braidy et al., 2009b)
3-Hydroxykynurenine	0.1 μM	(Braidy et al., 2009b)
Dexamethasone	1 μM	(Pariante et al., 1997)
DPI chloride	0.001 μM	(Qian et al., 2007)
MK-801	0.1 μM	(Freeman and Goldberg, 1994)
Quinolinic acid	1 μM	(Braidy et al., 2009b)
Recombinant mouse IFNγ	5 ng/ml	Previous studies using either BV-2 cells or primary neurons showed at this concentration, induction of the kynurenine pathway enzymes in BV-2 cells, and had no effect on the viability of either cell type.
Ro 61-8048	1 μM	Dose based on IC_{50}= 37 nM

3.3 Results

3.3.1 IFNγ induces kynurenine pathway activation and nitric oxide production in BV-2 microglia.

3.3.1.1 Effect of IFNγ on the mRNA expression of kynurenine pathway enzymes and iNOS in BV-2 microglia

Stimulation of BV-2 microglia with IFNγ lead to an increase in the mRNA expression of **IDO** ($t= 9.714$, $P<0.001$, d.f.= 21) (a), **KMO** ($t= 27.26$, $P<0.001$, d.f.= 20) (c), **KYNU** ($t= 16.51$, $P<0.001$. d.f.= 21) (d), and **iNOS** ($t= 9.275$, $P<0.001$, d.f.= 21) (f) compared with control, while having no effect on the mRNA expression of **TDO** ($t= 0.4327$, $P= 0.6694$, d.f.= 22) (b), or **KAT II** ($t= 0.01984$, $P= 0.9844$, d.f.= 22) (e) (**figure 3.3.1.1**).

3.3.1.2 Effect of IFNγ on the concentrations of tryptophan, kynurenine, 3-hydroxykynurenine and the kynurenine/tryptophan ratio in the CM of BV-2 microglia

Two-way ANOVA of the concentration of **tryptophan** in BV-2 CM showed an effect of 1-MT (L) [$F_{(1, 46)} = 72.836$, $P<0.0001$], IFNγ [$F_{(1, 46)} = 22.4$, $P<0.0001$], but no interaction [$F_{(1, 46)} = 0.234$, $P= 0.631$]. *Post hoc* analysis revealed increases in the concentration of tryptophan following treatment with 1-MT (L) ($P<0.001$) or IFNγ ($P<0.01$) compared to control (a).

Two-way ANOVA of the concentration of **kynurenine** in BV-2 CM showed an effect of 1-MT (L) [$F_{(1, 47)} = 11.16$, $P= 0.02$], IFNγ [$F_{(1, 47)} = 19.635$, $P<0.0001$], but no interaction [$F_{(1, 47)} = 0.205$, $P= 0.653$]. *Post hoc* analysis revealed increases in the concentration of kynurenine following treatment with IFNγ ($P<0.01$) compared to control (b).

Two-way ANOVA of the concentration of **3-hydroxykynurenine** in BV-2 CM showed an effect of 1-MT (L) [$F_{(1, 45)} = 52.502$, $P<0.0001$], IFNγ [$F_{(1, 45)} = 65.284$, $P<0.0001$], but no interaction [$F_{(1, 45)} = 0.975$, $P= 0.975$]. *Post hoc* analysis revealed increases in the concentration of 3-hydroxykynurenine following treatment with 1-MT (L) ($P<0.001$) or IFNγ ($P<0.001$) compared to control. Pre-treatment with 1-MT (L) prevented these IFNγ-induced reductions ($P<0.001$) (c).

Two-way ANOVA of the **kynurenine over tryptophan ratio** in BV-2 CM showed an effect of 1-MT (L) [$F_{(1, 47)} = 90.399$, $P<0.001$], but no effect of IFNγ [$F_{(1, 47)} = 0.057$, $P= 0.812$], or an interaction [$F_{(1, 47}= 0.078$, $P= 0.781$]. *Post hoc* analysis revealed reductions in the kynurenine over tryptophan ratio following treatment with 1-MT (L) ($P<0.001$) compared to control (d) (**figure 3.3.1.2**).

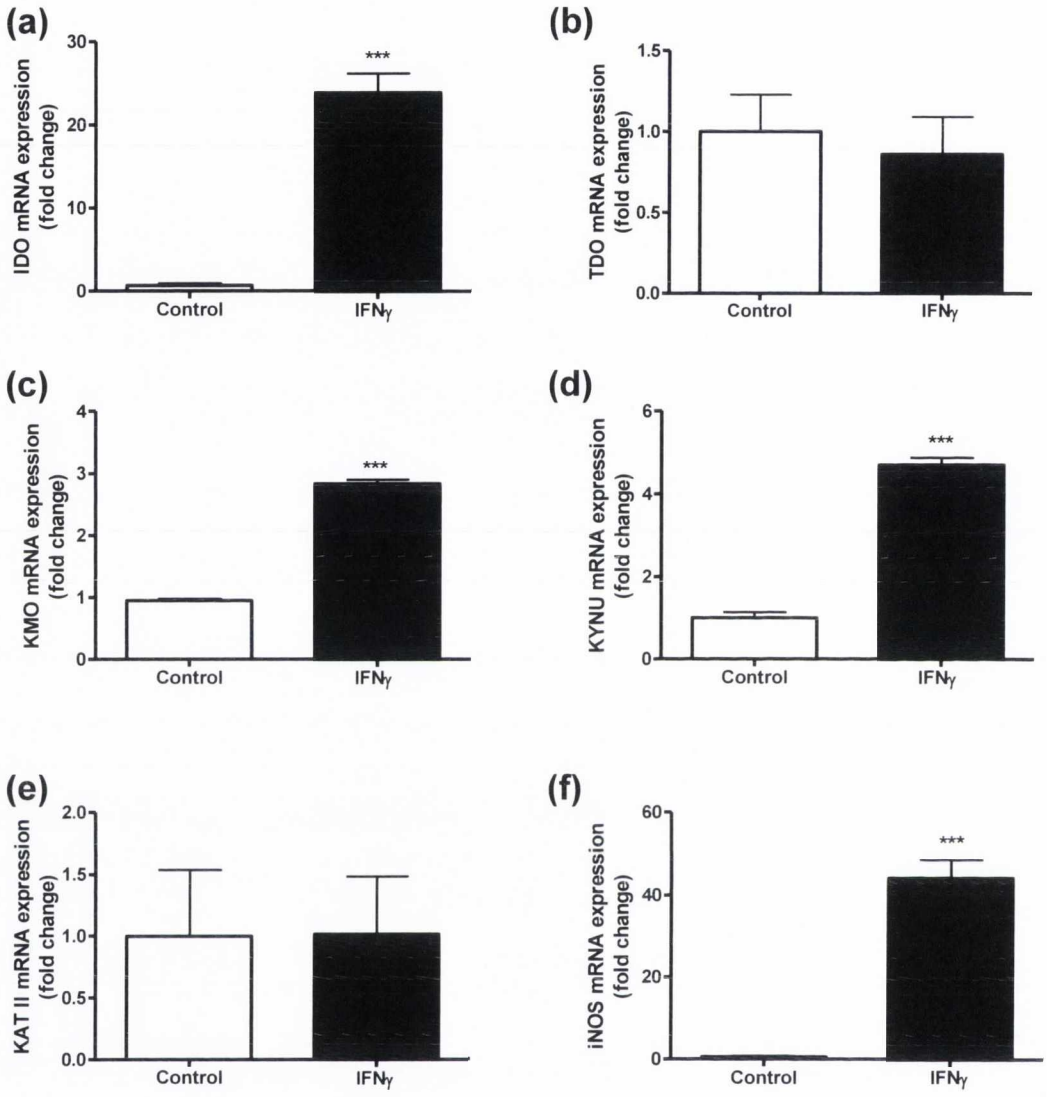

Figure 3.3.1.1: Effect of IFNγ on the mRNA expression of kynurenine pathway enzymes and iNOS in BV-2 microglia

BV-2 microglia were stimulated with IFNγ (5 ng/ml) for 24 hr. Cells were harvested for mRNA extraction followed by quantitative PCR to analyse the mRNA expression of (a) IDO, (b) TDO, (c) KMO, (d) KYNU, (e) KAT II and (f) iNOS. Data expressed as mean ± SEM (n= 11-12). ***P<0.001 vs. control (Student's *t*-test).

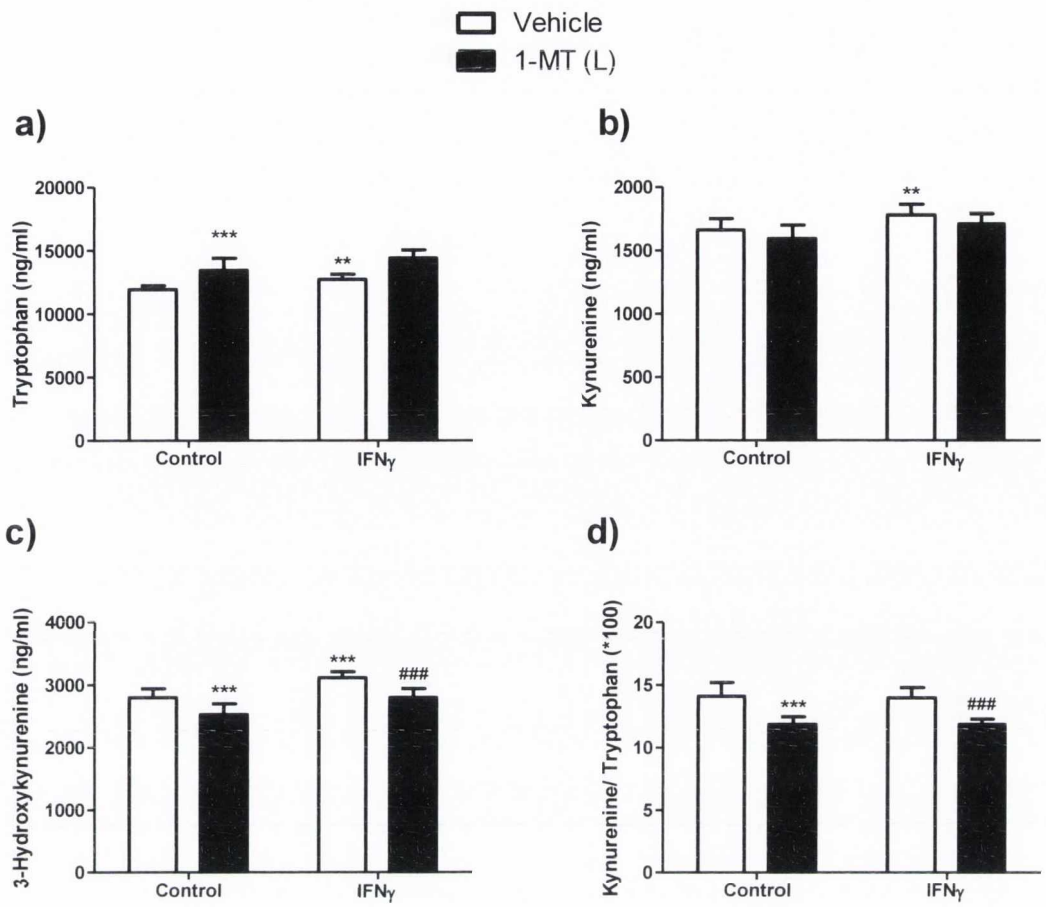

Figure 3.3.1.2: Effect of IFNγ on the concentrations of tryptophan, kynurenine, 3-hydroxykynurenine and the kynurenine/tryptophan ratio in the CM of BV-2 microglia

BV-2 microglia were pre-treated with 1-MT (L) (0.5 mM; 30 min) followed by stimulation with IFNγ (5 ng/ml) for 24 hr. CM was harvested for analysis of the concentrations of (a) tryptophan, (b) kynurenine, (c) 3-hydroxykynurenine, (d) kynurenine over tryptophan ratio. Data expressed as mean ± SEM (n= 11-12, from 2 independent experiments). **P<0.01, ***P<0.001 vs. control, ###P<0.001, vs. IFNγ (Two-way ANOVA followed by Newman-Keuls *post hoc* test).

3.3.2 CM from IFNγ-stimulated BV-2 microglia reduces measures of neuronal integrity.

3.3.2.1 Effect of CM from IFNγ-stimulated BV-2 microglia on neuronal viability

CM from IFNγ-stimulated BV-2 microglia increased the **% cytotoxicity** ($t = 6.212$, $P<0.0001$, d.f. = 10) (a; *Left hand side*). Direct treatment with IFNγ reduced the **% cytotoxicity** ($t = 3.825$, $P = 0.0041$, d.f. = 9) compared to control CM (a; *Right hand side*).

CM from IFNγ-stimulated BV-2 microglia reduced **neuronal viability** ($t = 2.121$, $P = 0.0454$, d.f. = 21) (b; *Left hand side*). Direct treatment with IFNγ had no effect on **neuronal viability** ($t = 0.1534$, $P = 0.8803$, d.f. = 14) (b; *Right hand side*).

CM from IFNγ-stimulated BV-2 microglia reduced **neuronal viability** ($t = 6.278$, $P<0.0001$, d.f. = 14) (c; *Left hand side*). Direct treatment with IFNγ had no effect on **neuronal viability** ($t = 1.290$, $P = 0.2213$, d.f. = 12) (c; *Right hand side*) (**figure 3.3.2.1**).

3.3.2.2 Effect of CM from IFNγ-stimulated BV-2 microglia on measures of neuronal complexity

Left hand side:

CM from IFNγ-stimulated BV-2 microglia reduced the number of **neuritic branches** ($t = 2.043$, $P = 0.042$, d.f. = 64) (a), **neurite length** ($t = 3.209$, $P = 0.021$, d.f. = 64) (b), and the number of **primary neurites** ($t = 2.36$, $P = 0.0213$, d.f. = 64) (c).

Two-way repeated measures ANOVA of the number of **neuritic branches at specific distances from the neuronal cell soma** showed an effect of IFNγ CM [$F_{(1, 1600)} = 10.3$, $P = 0.002$], an effect of distance [$F_{(25, 1600)} = 514.5$, $P<0.0001$] and an interaction [$F_{(25, 1600)} = 3.903$, $P<0.0001$]. *Post hoc* analysis revealed reductions in the number of branches at 10, 20 and 30 μm from the cell soma following treatment with IFNγ CM ($P<0.001$) (d) (**figure 3.3.2.2**).

Right hand side:

IFNγ had no effect on the number of **neuritic branches** ($t=0.2737$, $P = 0.7856$, d.f. = 45) (a), **neurite length** ($t=0.6309$, $P = 0.5313$, d.f. = 45) (b), or the number of **primary neurites** ($t = 0.701$, $P = 0.4869$, d.f. = 45) (c).

A two-way repeated measures ANOVA of the number of **neuritic branches at specific distances from the neuronal cell soma** showed no effect of IFNγ [$F_{(1, 1025)} = 0.2009$, $P = 0.9975$], an effect of distance [$F_{(25, 1025)} = 351.5$, $P<0.0001$] but no interaction [$F_{(25, 1025)} = 0.3837$, $P = 0.6563$] (e) (**figure 3.3.2.2**).

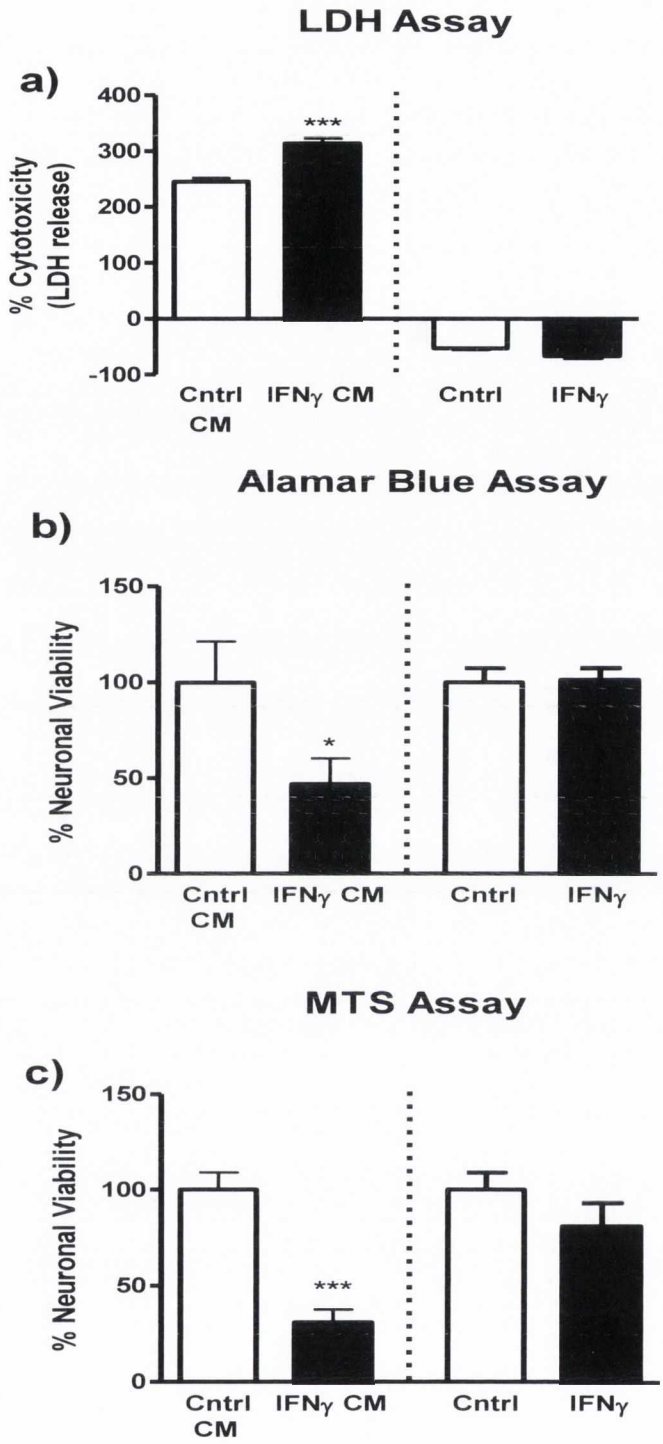

Figure 3.3.2.1: Effect of CM from IFNγ-stimulated BV-2 microglia on neuronal viability
CM from BV-2 microglia treated with IFNγ (5 ng/ml; 24 hr) (left) or IFNγ (5 ng/ml) was applied directly (right) to primary cortical neurons (DIV 3) for 48 hr. Neuronal viability were assessed using the LDH cytotoxicity assay (a), the alamarBlue® cell proliferation assay (b) and the MTS assay (c). Data are expressed as mean ± SEM (n= 6-12 wells from 2 independent experiments). *P<0.05, **P<0.01, ***P<0.001, vs. respective control (Student *t*-test).

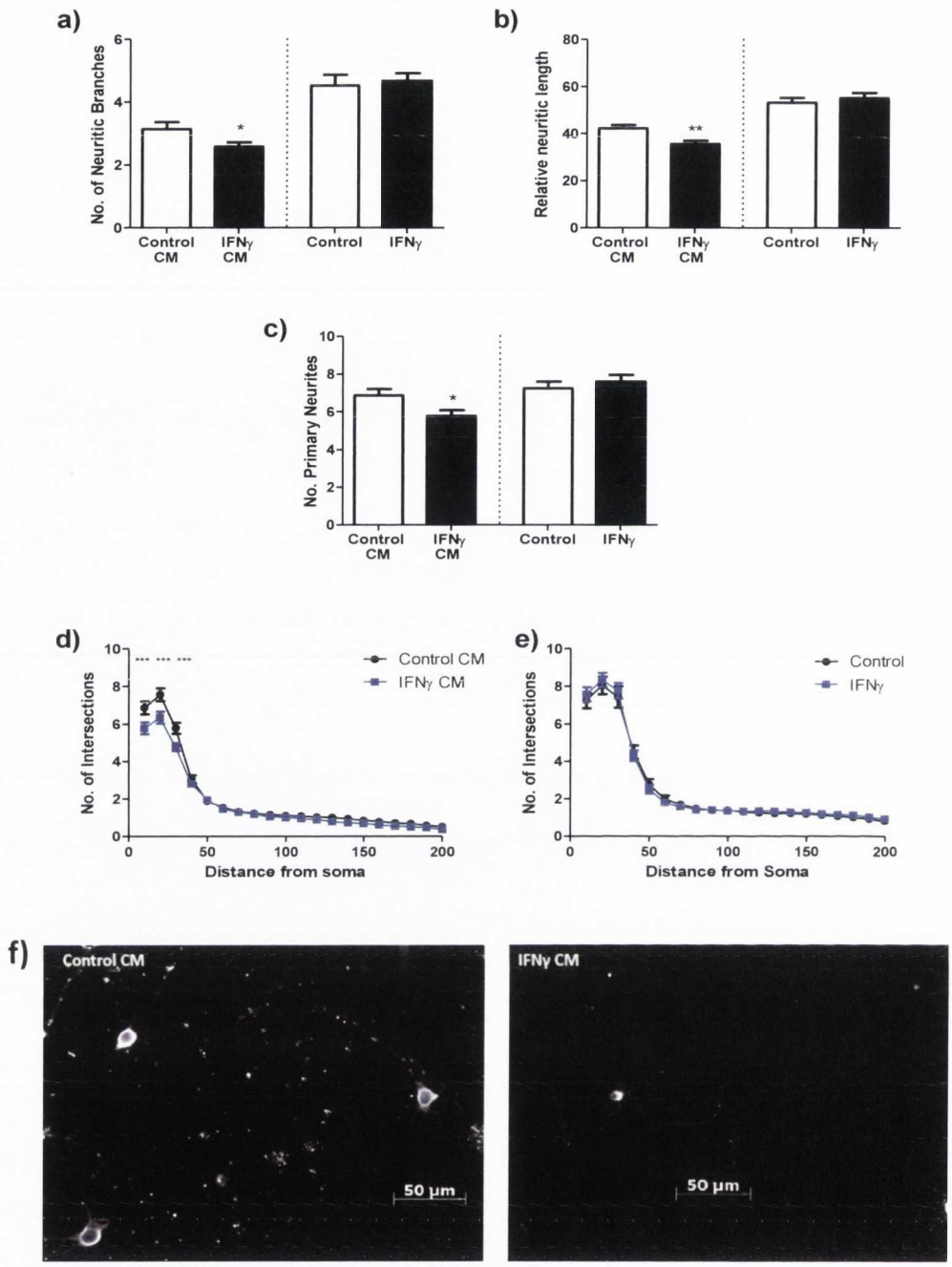

Figure 3.3.2.2: Effect of CM from IFNγ-stimulated BV-2 microglia on measures of neuronal complexity

CM from BV-2 microglia treated with IFNγ (5 ng/ml; 24 hr) or IFNγ (5 ng/ml) was placed on primary cortical neurons (DIV 3) for 48 hr. Sholl analysis was performed on neurons to examine (a) the number of neuritic branches, (b) neurite length, (c) the number of primary neurites, and (d, e) the number of branches at various distances from the cell soma. Representative images of neurons identified using the neuronal structural marker β-III tubulin (white) and the nuclear stain DAPI (blue) with fluorescent microscopy (f). Data expressed as mean ± SEM (n= 23-34 coverslips from 3-4 independent experiments). *P<0.05, **P<0.01, ***P<0.001, vs. respective control [Student's *t*-test (a-c), two-way repeated measures ANOVA followed by Bonferroni *post hoc* test (d, e)].

3.3.3 Inhibitors of kynurenine pathway activation block IFNγ CM-induced reductions in neuronal viability and complexity.

3.3.3.1 Effect of pre-treatment with 1-MT (L), dexamethasone, Ro 61-8048 or MK-801 on IFNγ-stimulated BV-2 CM-induced reductions in neuronal viability

Two-way ANOVA of the **% cytotoxicity** showed an effect of IFNγ CM [$F_{(1, 23)} = 49.602$, $P<0.0001$], no effect of 1-MT (L) CM [$F_{(1, 23)} = 3.792$, $P= 0.066$], and no interaction [$F_{(1, 23)} = 0.556$, $P= 0.464$]. *Post hoc* analysis revealed increases in the % cytotoxicity following treatment with IFNγ CM ($P<0.001$) compared to control CM (a).

Two-way ANOVA of the **% cytotoxicity** showed an effect of dexamethasone CM [$F_{(1, 61)} = 19.956$, $P<0.0001$], IFNγ CM [$F_{(1, 61)} = 44.274$, $P<0.0001$], but no interaction [$F_{(1, 61)} = 2.619$, $P= 0.111$]. *Post hoc* analysis revealed increases in the % cytotoxicity following treatment with dexamethasone CM ($P<0.05$) or IFNγ CM ($P<0.01$) compared to control CM (b).

Two-way ANOVA of the **% cytotoxicity** showed an effect of Ro 61-8048 CM [$F_{(1, 23)} = 42.802$, $P<0.0001$], IFNγ CM [$F_{(1, 23)} = 65.152$, $P<0.0001$], but no interaction [$F_{(1, 23)} = 1.283$, $P= 0.271$]. *Post hoc* analysis revealed increases in the % cytotoxicity with IFNγ CM ($P<0.001$) compared to control CM. Pre-treatment with Ro 61-8048 prevented the IFNγ CM-induced increases in the % cytotoxicity ($P<0.001$) (c).

Two-way ANOVA of the **% cytotoxicity** showed an effect of MK-801 CM [$F_{(1, 23)} = 10.719$, $P= 0.004$], IFNγ CM [$F_{(1, 23)} = 38.776$, $P<0.0001$], and an interaction [$F_{(1, 23)} = 4.488$, $P= 0.047$]. *Post hoc* analysis revealed increases in the % cytotoxicity with IFNγ CM ($P<0.001$) compared to control CM. Pre-treatment with MK-801 prevented the IFNγ CM-induced increases in the % cytotoxicity ($P<0.01$) (d) (**figure 3.3.3.1**).

3.3.3.2 Effect of 1-MT (L) on IFNγ-stimulated BV-2 CM-induced reductions in neuronal complexity

Two-way ANOVA of the number of **neuritic branches** showed an effect of IFNγ CM [$F_{(1, 102)} = 6.529$, $P= 0.012$], no effect of 1-MT (L) CM [$F_{(1, 102)} = 0.84$, $P= 0.361$], and no interaction [$F_{(1, 102)} = 2.492$, $P= 0.118$]. *Post hoc* analysis revealed reductions in the number of neuritic branches following treatment with IFNγ CM ($P<0.05$) compared to control CM. Pre-treatment with 1-MT (L) prevented the IFNγ CM-induced reductions ($P<0.05$) (a).

Two-way ANOVA of **neurite length** showed an effect of IFNγ CM [$F_{(1, 102)} = 12.146$, $P= 0.001$], no effect of 1-MT (L) CM [$F_{(1, 102)} = 2.362$, $P= 0.127$], and an interaction [$F_{(1, 102)} = 6.678$, $P= 0.011$]. *Post hoc* analysis revealed reductions in neurite length following treatment with IFNγ CM ($P<0.01$)

compared to control CM. Pre-treatment with 1-MT (L) prevented the IFNγ CM-induced reductions ($P<0.001$) (b).

Two-way ANOVA of the number of **primary neurites** showed an effect of IFNγ CM [$F_{(1, 102)} = 17.621$, $P<0.0001$], no effect of 1-MT (L) CM [$F_{(1, 102)} = 3.062$, $P= 0.083$], and no interaction [$F_{(1, 102)} = 2.772$, $P= 0.099$]. *Post hoc* analysis revealed reductions in the number of primary neurites following treatment with IFNγ CM ($P<0.01$) compared to control CM. Pre-treatment with 1-MT (L) prevented the IFNγ CM-induced reductions ($P<0.001$) (c).

Three-way repeated measures ANOVA of the number of **neuritic branches at specific distances from the neuronal cell soma** showed an effect of distance ($F_{(25, 2575)}= 4.595$, $P<0.0001$), of IFNγ CM x distance ($F_{(25, 2575)}= 0.496$, $P= 0.009$), but no effect of 1-MT (L) CM ($F_{(1, 103)}= 0.425$, $P= 0.516$), IFNγ CM ($F_{(1, 103)}= 0.595$, $P= 0.424$), 1-MT (L) x IFNγ CM ($F_{(1, 103)}= 0.635$, $P= 0.428$), 1-MT (L) CM x distance ($F_{(25, 2575)}= 0.804$, $P= 0.229$), 1-MT (L) x IFNγ CM x distance ($F_{(25, 2575)}= 0.462$, $P= 0.99$). *Post hoc* analysis revealed reductions following treatment with IFNγ CM ($P<0.001$) in the number of branches at 10, 20, 30 μm from the cell soma compared with control CM. Pre-treatment with 1-MT (L) prevented the IFNγ CM-induced reductions at 10, 20, and 30 μm ($P<0.001$) (d) (**figure 3.3.3.2**).

3.3.3.3 Effect of dexamethasone on IFNγ-stimulated BV-2 microglial-induced reductions in measures of neuronal complexity

Two-way ANOVA of the number of **neuritic branches** showed an effect of dexamethasone CM [$F_{(1, 110)} = 4.273$, $P= 0.041$], IFNγ CM [$F_{(1, 110)} = 9.851$, $P= 0.002$], but no interaction [$F_{(1, 110)} = 0.288$, $P= 0.593$]. *Post hoc* analysis revealed reductions in the number of neuritic branches following treatment with IFNγ CM ($P<0.01$) compared to control CM. Pre-treatment with dexamethasone prevented the IFNγ CM-induced reductions ($P<0.01$) (a).

Two-way ANOVA of **neurite length** showed an effect of dexamethasone CM [$F_{(1, 110)} = 4.007$, $P= 0.048$], IFNγ CM [$F_{(1, 110)} = 13.643$, $P<0.0001$], and an interaction [$F_{(1, 110)} = 4.99$, $P= 0.028$]. *Post hoc* analysis revealed reductions in neurite length following treatment with IFNγ CM ($P<0.01$) compared to control CM. Pre-treatment with dexamethasone prevented the IFNγ CM-induced reductions ($P<0.001$) (b).

Two-way ANOVA of the number of **primary neurites** showed an effect of dexamethasone CM [$F_{(1, 110)} = 4.658$, $P= 0.033$], of IFNγ CM [$F_{(1, 110)} = 16.367$, $P<0.0001$], but no interaction [$F_{(1, 110)} = 1.567$, $P= 0.212$]. *Post hoc* analysis revealed reductions in the number of primary neurites following treatment with IFNγ CM ($P<0.01$) compared to control CM. Pre-treatment with dexamethasone prevented the IFNγ CM-induced reductions ($P<0.01$) (c).

Three-way repeated measures ANOVA of the number of **neuritic branches at specific distances from the neuronal cell soma** showed an effect of distance ($F_{(25, 2700)}$= 5.235, P<0.0001), dexamethasone CM ($F_{(1, 108)}$= 0.491, P= 0.004), IFNγ CM ($F_{(1, 108)}$= 0.409, P= 0.006), dexamethasone x IFNγ CM ($F_{(1, 108)}$= 0.406, P= 0.006), but no effect of dexamethasone CM x distance ($F_{(25, 2700)}$= 0.916, P= 0.583), IFNγ CM x distance ($F_{(25, 2700)}$= 0.525, P= 0.975), or dexamethasone x IFNγ CM x distance ($F_{(25, 2700)}$= 0.551, P= 0.965). *Post hoc* analysis revealed reductions in the number of branches at 10, 20, 30 μm from the cell soma following treatment with IFNγ CM (P<0.001) compared to control CM. Pre-treatment with dexamethasone prevented the IFNγ CM-induced reductions at 10, 20, and 30 μm from the cell soma (P<0.001) (d) (**figure 3.3.3.3**).

3.3.3.4 Effect of dexamethasone on IFNγ-induced increases in the mRNA expression of kynurenine pathway enzymes and iNOS in BV-2 microglia

Two-way ANOVA of **IDO** mRNA expression showed an effect of IFNγ [$F_{(1, 18)}$ = 8.984, P= 0.009], no effect of dexamethasone [$F_{(1, 18)}$ = 3.722, P= 0.073], and an interaction [$F_{(1, 18)}$ = 5.603, P= 0.032]. *Post hoc* analysis revealed increases in the mRNA expression of IDO following treatment with IFNγ (P<0.01) compared to control. Pre-treatment with dexamethasone prevented the IFNγ CM-induced increases (P<0.05) (a).

Two-way ANOVA of **KMO** mRNA expression showed an effect of dexamethasone [$F_{(1, 17)}$ = 233.826, P<0.0001], of IFNγ [$F_{(1, 17)}$ = 291.674, P<0.0001], and an interaction [$F_{(1, 17)}$ = 81.37, P<0.0001]. *Post hoc* analysis revealed increases in KMO mRNA expression following treatment with IFNγ (P<0.001) compared to control. Pre-treatment with dexamethasone prevented the IFNγ CM-induced increases (P<0.001) (b).

Two-way ANOVA of **KYNU** mRNA expression showed an effect of IFNγ [$F_{(1, 17)}$ = 6.558, P= 0.023], no effect of dexamethasone [$F_{(1, 17)}$ = 4.349, P= 0.056], and no interaction [$F_{(1, 17)}$ = 2.206, P= 0.16]. *Post hoc* analysis revealed increases in KYNU mRNA expression following treatment with IFNγ (P<0.01) compared to control. Pre-treatment with dexamethasone prevented the IFNγ CM-induced increases (P<0.05) (c).

Two-way ANOVA of **iNOS** mRNA expression showed an effect of dexamethasone [$F_{(1, 17)}$ = 41.208, P<0.0001], IFNγ [$F_{(1, 17)}$ = 71.672, P<0.0001], and an interaction [$F_{(1, 17)}$ = 37.729, P<0.0001]. *Post hoc* analysis revealed increases in iNOS mRNA expression following treatment with IFNγ (P<0.001) compared to control. Pre-treatment with dexamethasone prevented the IFNγ CM-induced increases (P<0.001) (d) (**figure 3.3.3.4**).

3.3.3.5 Effect of Ro 61-8048 on IFNγ-stimulated BV-2 CM-induced reductions in neuronal complexity

Two-way ANOVA of the number of **neuritic branches** showed an effect of IFNγ CM [$F_{(1, 105)} = 8.245$ P= 0.005], no effect of Ro 61-8048 CM [$F_{(1, 105)} = 0.36$, P= 0.55], and no interaction [$F_{(1, 105)} = 0.372$, P= 0.543]. *Post hoc* analysis revealed reductions in the number of neuritic branches following treatment with IFNγ (P<0.05) compared to control CM (a).

Two-way ANOVA of **neurite length** showed an effect of Ro 61-8048 CM [$F_{(1, 105)} = 10.653$, P= 0.002], IFNγ CM [$F_{(1, 105)} = 6.719$ P= 0.01], and no interaction [$F_{(1, 105)} = 3.091$, P= 0.082]. *Post hoc* analysis revealed reductions in neurite length following treatment with IFNγ CM (P<0.001) compared to control CM. Pre-treatment with Ro 61-8048 prevented the IFNγ CM-induced reductions (P<0.001) (b).

Two-way ANOVA of the number of **primary neurites** showed an effect of Ro 61-8048 CM [$F_{(1, 105)} = 13.729$, P<0.0001], IFNγ CM [$F_{(1, 105)} = 2.472$ P= 0.009], and no interaction [$F_{(1, 105)} = 3.274$, P= 0.073]. *Post hoc* analysis revealed reductions in the number of primary neurites following treatment with IFNγ CM (P<0.01) compared with control CM. Pre-treatment with Ro 61-8048 prevented the IFNγ CM-induced reductions (P<0.01) (c).

Three-way repeated measures ANOVA of the number of **neuritic branches at specific distances from the neuronal cell soma** showed an effect of distance ($F_{(25, 2650)} = 4.47$, P<0.0001), but no effect of Ro 61-8048 CM ($F_{(1, 106)} = 0.452$, P= 0.503), IFNγ CM ($F_{(1, 106)} = 0.662$, P= 0.418), Ro 618048 x IFNγ CM ($F_{(1, 106)} = 0.659$, P= 0.419), Ro 61-8048 CM x distance ($F_{(25, 2650)} = 0.841$, P= 0.69), IFNγ CM x distance ($F_{(25, 2650)} = 0.468$, P= 0.989), Ro 61-8048 x IFNγ CM x distance ($F_{(25, 2650)} = 0.56$, P= 0.961). *Post hoc* analysis revealed reductions following treatment with IFNγ CM (P<0.001) in the number of branches at 10, 20 and 30 μm from the cell soma compared to control CM. Pre-treatment with Ro 61-8048 prevented the IFNγ CM-induced reductions at 20 and 30 μM from the cell soma (P<0.001) (d) (**figure 3.3.3.5**).

3.3.3.6 Effect of MK-801 on IFNγ-stimulated BV-2 CM-induced reductions in neuronal complexity

Two-way ANOVA of the number of **neuritic branches** showed an effect of MK-801 CM [$F_{(1, 101)} = 6.401$, P= 0.013], IFNγ CM [$F_{(1, 101)} = 4.223$, P= 0.042], and no interaction [$F_{(1, 101)} = 2.006$, P= 0.16]. *Post* hoc analysis revealed reductions in the number of neuritic branches following treatment with IFNγ CM (P<0.01) compared to control CM. Pre-treatment with MK-801 prevented the IFNγ CM-induced reductions (P<0.05) (a).

Two-way ANOVA of **neurite length** showed an effect of MK-801 CM [$F_{(1, 101)} = 20.291$, P<0.0001], but no effect of IFNγ CM [$F_{(1, 101)} = 3.608$, P= 0.06], and no interaction [$F_{(1, 101)} = 1.415$, P= 0.237]. *Post hoc*

analysis revealed reductions in neurite length following treatment with IFNγ CM ($P<0.05$) compared to control CM. Pre-treatment with MK-801 prevented the IFNγ CM-induced reductions ($P<0.001$) (b).

Two-way ANOVA of the number of **primary neurites** showed an effect of MK-801 CM [$F_{(1, 101)} = 14.803$, $P<0.0001$], IFNγ CM [$F_{(1, 101)} = 4.18$, $P= 0.044$], and no interaction [$F_{(1, 101)} = 0.091$, $P= 0.764$]. *Post hoc* analysis revealed reductions in the number of primary neurite following treatment with IFNγ CM ($P<0.05$) compared to control CM. Pre-treatment with MK-801 prevented the IFNγ CM-induced reductions ($P<0.01$) (c).

Three-way repeated measures ANOVA of the number of **neuritic branches at specific distances from the neuronal cell soma** showed an effect of distance ($F_{(25, 2275)}= 2.921$, $P<0.0001$), MK-801 CM ($F_{(1, 91)}= 0.301$, $P= 0.003$), IFNγ CM ($F_{(1, 91)}= 0.544$, $P= 0.006$), MK-801 x IFNγ CM ($F_{(1, 91)}= 0.52$, $P= 0.006$), but no effect of MK-801 CM x distance ($F_{(25, 2275)}= 0.664$, $P= 0.895$), IFNγ CM x distance ($F_{(25, 2275)}= 0.372$, $P= 0.998$), MK-801 x IFNγ CM x distance ($F_{(25, 2275)}= 0.448$, $P= 0.992$). *Post hoc* analysis revealed reductions in the number of branches at 10, 20, 30 μm from the cell soma following treatment with IFNγ CM ($P<0.01$) compared to control CM. Pre-treatment with MK-801 prevented thee IFNγ CM-induced reductions ($P<0.001$) (d) (**figure 3.3.3.6**).

3.3.3.7 Effect of MK-801 on IFNγ-induced increases in the mRNA expression of kynurenine pathway enzymes or iNOS in BV-2 microglia

Two-way ANOVA of **IDO** mRNA expression showed an effect of IFNγ [$F_{(1, 16)} = 17.381$, $P= 0.001$], no effect of MK-801 [$F_{(1, 16)} = 2.5641$, $P= 0.133$], and no interaction [$F_{(1, 16)} = 0.088$, $P= 0.722$]. *Post hoc* analysis revealed increases in the mRNA expression of IDO following treatment with IFNγ ($P<0.05$) compared to control (a).

Two-way ANOVA of **KMO** mRNA expression showed an effect of IFNγ [$F_{(1, 17)} = 254.635$, $P<0.0001$], no effect of MK-801 [$F_{(1, 17)} = 0.000$, $P= 0.996$], and no interaction [$F_{(1, 17)} = 0.000$, $P= 0.989$]. *Post hoc* analysis revealed increases in the mRNA expression of KMO following treatment with IFNγ ($P<0.001$) compared to control (b).

Two-way ANOVA of **KYNU** mRNA expression showed an effect of IFNγ [$F_{(1, 16)} = 30.786$, $P<0.0001$], no effect of MK-801 [$F_{(1, 16)} = 0.05$, $P= 0.826$], and no interaction [$F_{(1, 16)} = 0.097$, $P= 0.761$]. *Post hoc* analysis revealed increases in the mRNA expression of KYNU ($P<0.001$) compared to control (c).

Two-way ANOVA of **iNOS** mRNA expression showed an effect of IFNγ [$F_{(1, 17)} = 162.3$, $P<0.0001$], no effect of MK-801 [$F_{(1, 17)} = 0.446$, $P= 0.515$], and no interaction [$F_{(1, 17)} = 0.348$, $P= 0.565$]. *Post hoc* analysis revealed increases the mRNA expression of iNOS following treatment with IFNγ ($P<0.001$) compared to control (d) (**figure 3.3.3.7**).

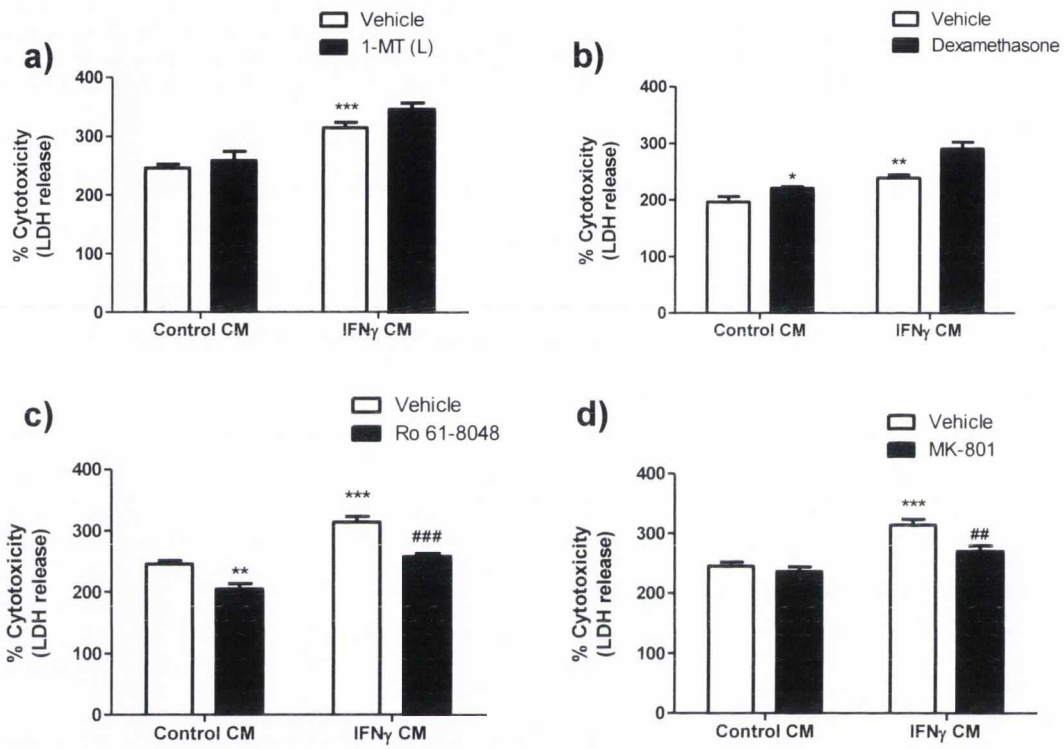

Figure 3.3.3.1: Effect of pre-treatment with 1-MT (L), dexamethasone, Ro 61-8048 or MK-801 on IFNγ-stimulated BV-2 CM-induced reductions in neuronal viability

CM from BV-2 microglia pre-treated with either vehicle, 1-MT (L) (0.5 mM; 30 min), dexamethasone (1 μM; 2 hr), Ro 61-8048 (1 μM; 30 min) or MK-801 (0.1 μM; 30 min) followed by stimulation with IFNγ (5 ng/ml; 24 hr) was placed on primary cortical neurons (DIV 3) for 48 hr. Neuronal viability was assessed using the LDH cytotoxicity assay (a-d). *P<0.05, **P<0.01, ***P<0.0001, vs. control CM, ##P<0.01, ###P<0.001, vs. IFNγ CM. Data are expressed as mean ± SEM (n= 8 wells). (Two-way ANOVA followed by Newman-Keuls *post hoc* test).

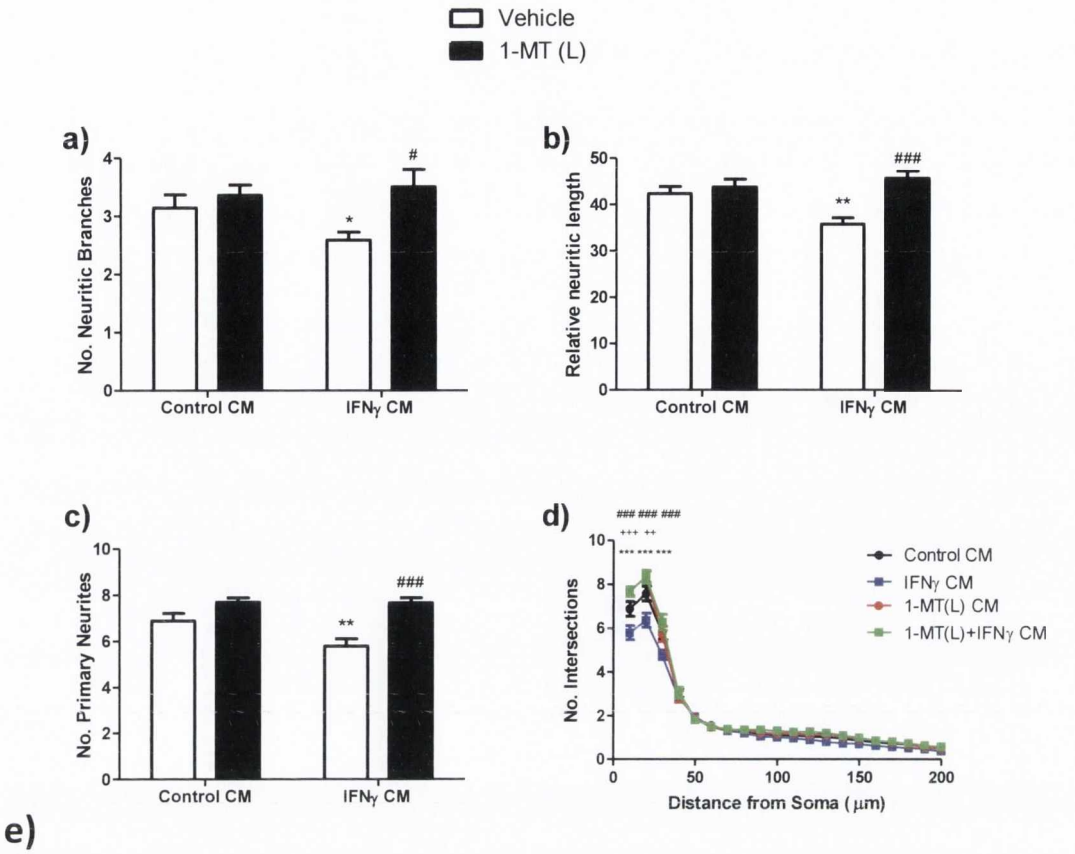

Figure 3.3.3.2: Effect of 1-MT (L) on IFNγ-stimulated BV-2 CM-induced reductions in neuronal complexity

CM from BV-2 microglia pre-treated with either vehicle or 1-MT (L) (0.5 mM; 30 min) followed by stimulation with IFNγ (5 ng/ml; 24 hr) was placed on primary cortical neurons (DIV 3) for 48 hr. Sholl analysis was performed on neurons to examine the number of neuritic branches (a), neurite length (b), the number of primary neurites (c) or the number of branches at specific distances from the soma (d). Representative images of neurons identified using the neuronal structural marker β-III tubulin (white) and the nuclear stain DAPI (blue) with fluorescent microscopy (e). Data are expressed as mean ± SEM (n= 18-34 coverslips from 4 independent experiments). *P<0.05, **P<0.01, ***P<0.001 vs. control CM, ##P<0.01, ###P<0.001, vs. IFNγ CM [Two-way ANOVA followed by Newman-Keuls *post hoc* test (a-c)]; Sholl profile, ***P<0.001, IFNγ CM vs. control CM, ++P<0.01, +++P<0.001, 1-MT (L) CM vs. control CM, ###P<0.001, 1-MT (L) +IFNγ CM vs. IFNγ CM [Three-way repeated measures ANOVA followed by Bonferroni *post hoc* test (d)].

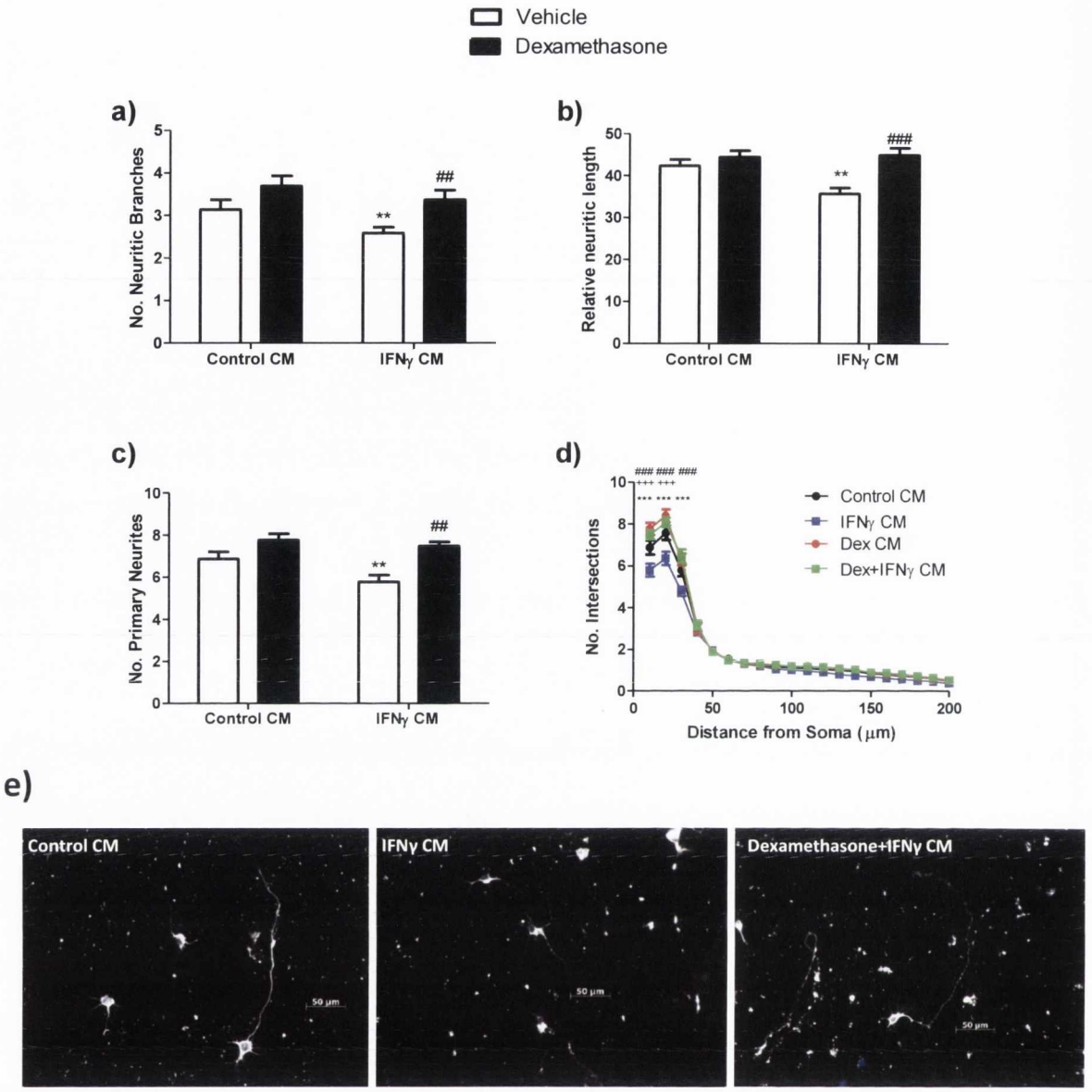

Figure 3.3.3.3: Effect of dexamethasone on IFNγ-stimulated BV-2 microglial-induced reductions in measures of neuronal complexity

CM from BV-2 microglia pre-treated with either vehicle or dexamethasone (1 μM; 2 hr) followed by stimulation with IFNγ (5 ng/ml; 24 hr) was placed on primary cortical neurons (DIV 3) for 48 hr. Sholl analysis was performed on neurons to examine the number of neuritic branches (a), neurite length (b), the number of primary neurites (c) or the number of branches at specific distances from the soma. Representative images of neurons identified using the neuronal structural marker β-III tubulin (white) and the nuclear stain DAPI (blue) with fluorescent microscopy (e). Data expressed as mean ± SEM (n= 21-34 coverslips from 4 independent experiments). **P<0.01, vs. control CM, ##P<0.01, ###P<0.001, vs. IFNγ CM. [Two-way ANOVA followed by Newman-Keuls *post hoc* test (a-c)]; Sholl profile, ***P<0.001, IFNγ CM vs. control, +++P<0.001, Dex CM vs. control CM, ###P<0.001, Dex + IFNγ CM vs. IFNγ CM [Three-way repeated measures ANOVA followed by Bonferroni *post hoc* test (d)].

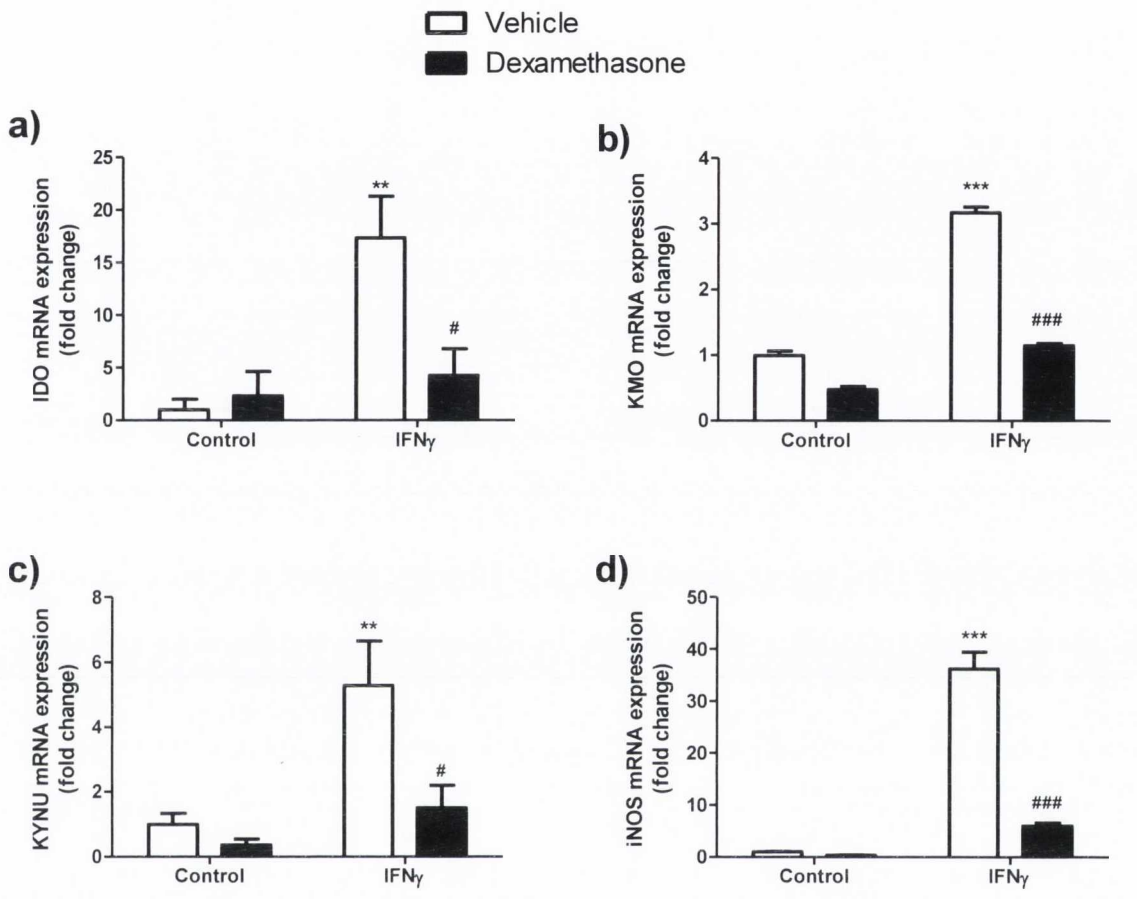

Figure 3.3.3.4: Effect of dexamethasone on IFNγ-induced increases in the mRNA expression of kynurenine pathway enzymes and iNOS in BV-2 microglia

BV-2 microglia were pre-treated with either vehicle or dexamethasone (1 μM; 2 hr) followed by stimulation with IFNγ (5 ng/ml) for 24 hr. Cells were harvested for mRNA extraction followed by quantitative PCR to analyse the expression of (a) IDO, (b) KMO, (c) KYNU and (d) iNOS. Data expressed as mean ± SEM (n= 3-6). **P<0.01, ***P<0.001 vs. control, #P<0.05, ###P<0.001 vs. IFNγ (Two-way ANOVA followed by Newman-Keuls *post hoc* test).

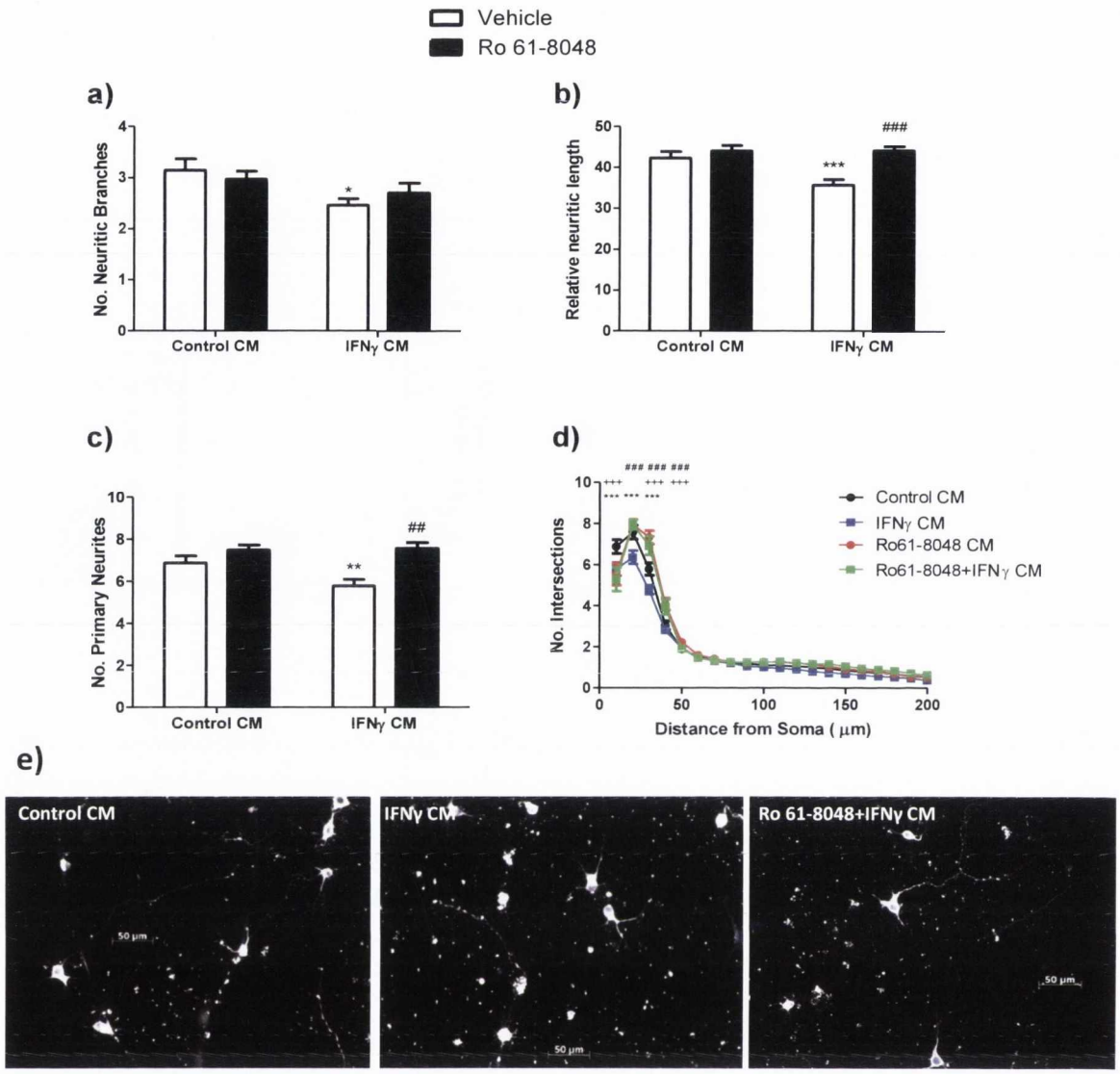

Figure 3.3.3.5: Effect of Ro 61-8048 on IFNγ-stimulated BV-2 CM-induced reductions in neuronal complexity

CM from BV-2 microglia pre-treated with either vehicle or Ro 61-8048 (1 μM; 30 min) followed by stimulation with IFNγ (5 ng/ml; 24 hr) was placed on primary cortical neurons (DIV 3) for 48 hr. Sholl analysis was performed on neurons to examine the number of neuritic branches (a), neurite length (b), the number of primary neurites (c) or the number of branches at specific distances from the soma (d). Representative images of neurons identified using the neuronal structural marker β-III tubulin (white) and the nuclear stain DAPI (blue) with fluorescent microscopy (e). Data expressed as mean ± SEM (n= 21-34 coverslips from 4 independent experiments). *P<0.05, **P<0.01, ***P<0.001, vs. control CM, ##P<0.01, ###P<0.001 vs. IFNγ CM. [Two-way ANOVA followed by Newman-Keuls *post hoc* test (a-c)]; Sholl profile, ***P<0.001, IFNγ CM vs. control CM, +++P<0.001, Ro 61-8048 CM vs. control CM, ###P<0.001, Ro 61-8048+IFNγ CM vs. IFNγ CM [Three-way repeated measures ANOVA followed by Bonferroni *post hoc* test (d)].

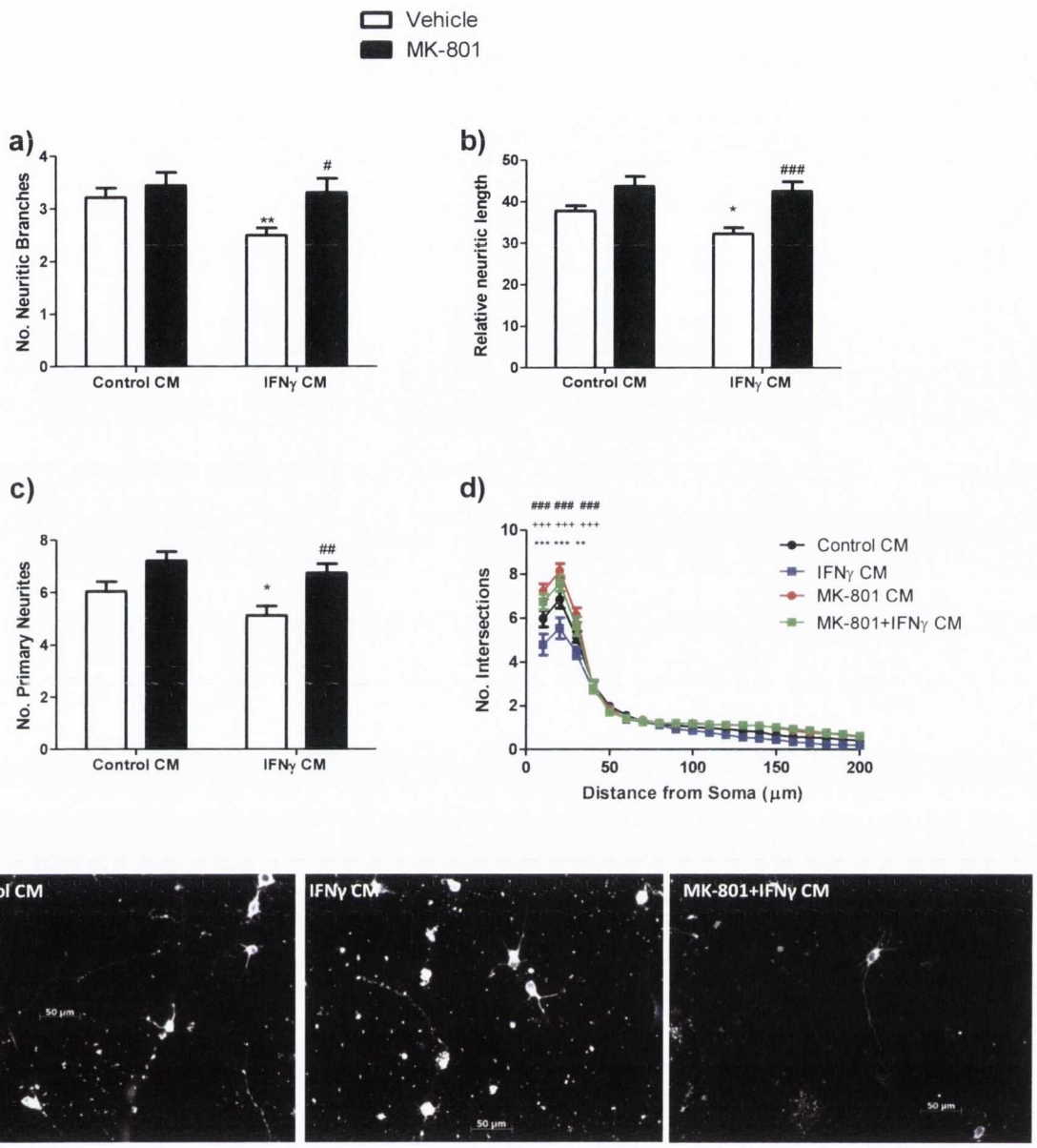

Figure 3.3.3.6: Effect of MK-801 on IFNγ-induced reductions in measures of neuronal complexity
CM from BV-2 microglia pre-treated with either vehicle or MK-801 (0.1 μM; 30 min) followed by stimulation with IFNγ (5 ng/ml; 24 hr) was placed on primary cortical neurons (DIV 3) for 48 hr. Sholl analysis was performed on neurons to examine the number of neuritic branches (a), neurite length (b), the number of primary neurites (c) or the number of branches at specific distances from the soma (d). Representative images of neurons identified using the neuronal structural marker β-III tubulin (white) and the nuclear stain DAPI (blue) with fluorescent microscopy (e). Data expressed as mean ± SEM (n= 20-34 coverslips from 4 independent experiments). *P<0.05, **P<0.01, vs. control CM, #P<0.05, ##P<0.01, ###P<0.001, vs IFNγ CM. [Two-way ANOVA followed by Newman-Keuls *post hoc* test (a-c)]; Sholl profile, **P<0.01, ***P<0.001, IFNγ CM vs. control CM, +++P<0.001, MK-801 CM vs. control CM, ###P<0.001, MK-801+IFNγ CM vs. IFNγ CM [Three-way repeated measures ANOVA followed by Bonferroni *post hoc* test (d)].

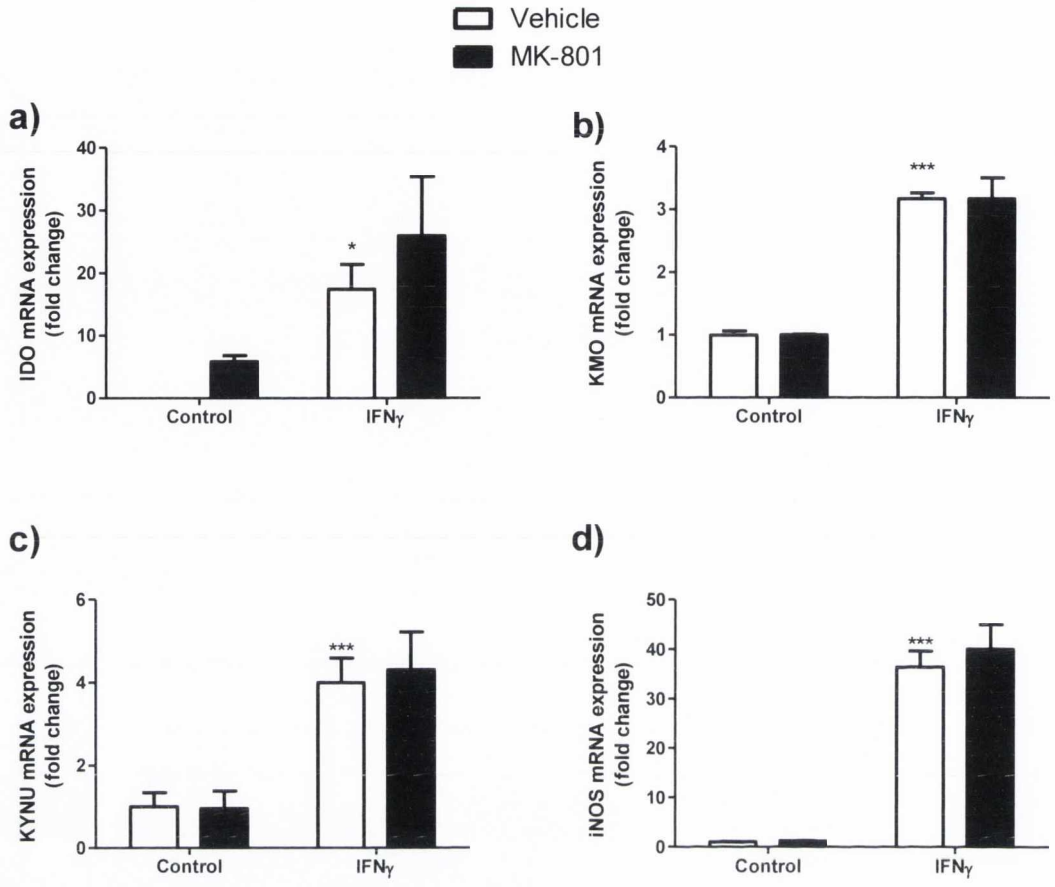

Figure 3.3.3.7: Effect of MK-801 on IFNγ-induced increases in the mRNA expression of kynurenine pathway enzymes or iNOS in BV-2 microglia

BV-2 microglia were pre-treated with either vehicle or MK-801 (0.1 μM; 30 min) followed by stimulation with IFNγ (5 ng/ml) for 24 hr. Cells were harvested for mRNA extraction followed by quantitative PCR to analyse the expression of (a) IDO, (b) KMO, (c) KYNU and (d) iNOS. Data expressed as mean ± SEM (n= 3-6). *P<0.05, ***P<0.001 vs. control (Two-way ANOVA followed by Newman-Keuls *post hoc* test).

3.3.4 Kynurenine pathway metabolites reduce neuronal complexity

3.3.4.1 Effect of kynurenine pathway metabolites on neuronal complexity

One-way ANOVA of the number of **neuritic branches** [$F_{(3, 91)} = 2.554$, P= 0.0605] (a), **neurite length** [$F_{(3, 91)} = 1.139$, P= 0.3379] (b), or the number of **primary neurites** [$F_{(3, 91)} = 0.7105$, P= 0.5483] (c) showed no effect of treatment.

Two-way ANOVA of the number of **neuritic branches at specific distances from the neuronal cell soma** showed an effect of distance [$F_{(25, 2200)} = 1037$, P<0.0001], no effect of treatment [$F_{(3, 2200)} = 1.139$, P= 0.3379], and no interaction [$F_{(75, 2200)} = 1.013$, P= 0.4476] (d) (**figure 3.3.4.1**).

3.3.4.2 Effect of a combination of kynurenine pathway metabolites on neuronal complexity

Two-way ANOVA of the number of **neuritic branches** showed an effect of the 3-hydroxykynurenine + 3-hydroxyanthrnaillic acid + quinolinic acid combination [$F_{(1, 85)} = 5.883$, P= 0.017], no effect of MK-801 [$F_{(1, 85)} = 0.564$, P= 0.327], and no interaction [$F_{(1, 85)} = 1.863$, P= 0.176]. *Post hoc* analysis revealed reductions in the number of neuritic branches following treatment with the 3-hydroxykynurenine + 3-hydroxyanthrnaillic acid + quinolinic acid combination (P<0.01) compared to control (a).

Two-way ANOVA of **neurite length** showed an effect of MK-801 [$F_{(1, 85)} = 9.973$, P= 0.002], the 3-hydroxykynurenine + 3-hydroxyanthrnaillic acid + quinolinic acid combination [$F_{(1, 85)} = 17.159$, P<0.0001], and an interaction [$F_{(1, 85)} = 8.23$, P= 0.005]. *Post hoc* analysis revealed reductions in neurite length following treatment with the 3-hydroxykynurenine + 3-hydroxyanthrnaillic acid + quinolinic acid combination (P<0.001) compared to control. Pre-treatment with MK-801 prevented the 3-hydroxykynurenine + 3-hydroxyanthrnaillic acid + quinolinic acid combination-induced reductions (P<0.001) (b).

Two-way ANOVA of the number of **primary neurites** showed an effect of MK-801 [$F_{(1, 85)} = 11.933$, P= 0.001], the 3-hydroxykynurenine + 3-hydroxyanthrnaillic acid + quinolinic acid combination [$F_{(1, 85)} = 5.102$, P= 0.027], but no interaction [$F_{(1, 85)} = 0.701$, P= 0.405]. *Post hoc* analysis revealed reductions in the number of primary neurites following treatment with the 3-hydroxykynurenine + 3-hydroxyanthrnaillic acid + quinolinic acid combination (P<0.01) compared to control. Pre-treatment with MK-801 prevented the 3-hydroxykynurenine + 3-hydroxyanthrnaillic acid + quinolinic acid combination-induced reductions (P<0.01) (c).

Three-way repeated measures ANOVA of the number of **neuritic branches at specific distances from the neuronal cell soma** showed an effect of distance ($F_{(25, 2075)} = 2.861$, P<0.0001), but no effect of MK-801 CM ($F_{(1, 83)} = 0.606$, P= 0.439), 3-hydroxykynurenine + 3-hydroxyanthrnaillic acid + quinolinic

acid ($F_{(1, 83)}$= 0.937, P= 0.336), MK-801 x 3-hydroxykynurenine + 3-hydroxyanthrnaillic acid + quinolinic acid ($F_{(1, 83)}$= 0.874, P= 0.353), MK-801 x distance ($F_{(25, 2075)}$= 0.743, P= 0.817), 3-hydroxykynurenine + 3-hydroxyanthrnaillic acid + quinolinic acid x distance ($F_{(25, 2075)}$= 0.693, P= 0.869), MK-801 x 3-hydroxykynurenine + 3-hydroxyanthrnaillic acid + quinolinic acid x distance ($F_{(25, 2075)}$= 0.713, P= 0.849) on the number of neuritic branches at specific distances from the cell soma. *Post hoc* analysis revealed reductions in the number of branches at 10, 20 and 30 µm from the cell soma following treatment with 3-hydroxykynurenine + 3-hydroxyanthrnaillic acid + quinolinic acid ($P<0.05$) compared to control. Pre-treatment with MK-801 prevented the 3-hydroxykynurenine + 3-hydroxyanthrnaillic acid + quinolinic acid-induced reductions at 10 and 20 µM from the cell soma ($P<0.001$) (d) (**figure 3.3.4.2**).

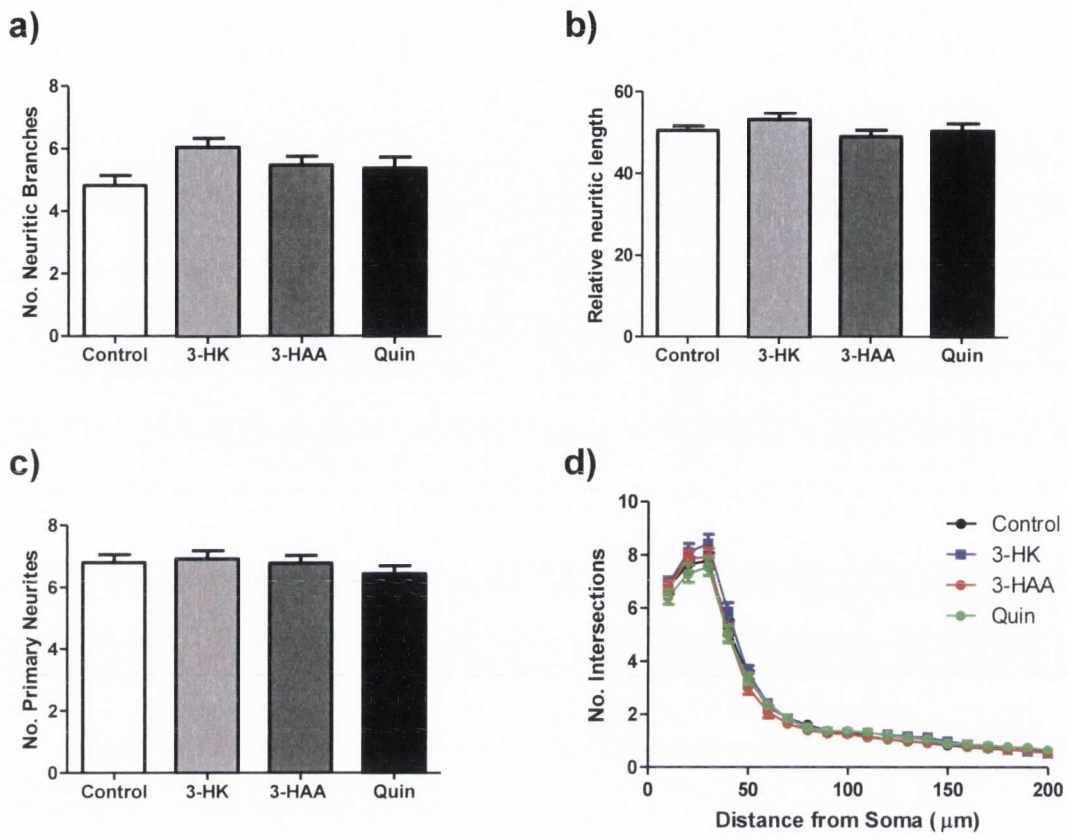

Figure 3.3.4.1: Effect of kynurenine pathway metabolites on neuronal complexity
Primary cortical neurons (DIV 3) were treated with 3-hydroxykynurenine (3-HK; 0.1 μM), 3-hydroxyanthranillic acid (3-HAA; 0.1 μM) or quinolinic acid (Quin; 1 μM) for 48 hr. Sholl analysis was performed on neurons to examine the number of neuritic branches (a), neurite length (b), the number of primary neurites (c) or the number of branches at specific distances from the soma (d). Data expressed as mean ± SEM (n= 22-24 coverslips from 3 independent experiments) [One-way ANOVA (a-c), two-way repeated measures ANOVA (d)].

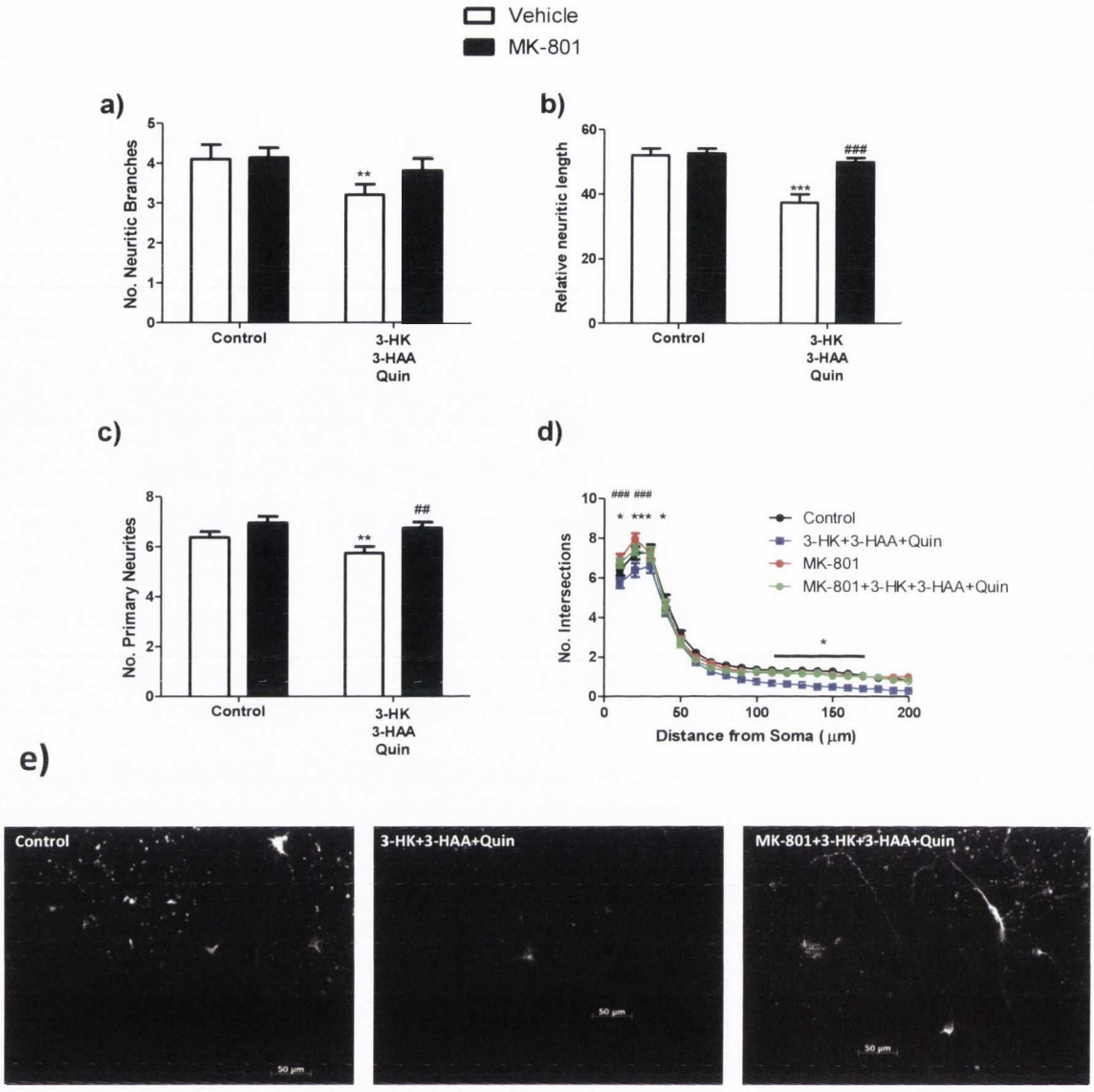

Figure 3.3.4.2: Effect of a combinations of kynurenine pathway metabolites on neuronal complexity

Primary cortical neurons (DIV 3) were pre-treated with ether vehicle or MK-801 (0.1 μM; 30 min) followed by treatment with a combination of 3-hydroxykynurenine (3-HK; 0.1 μM), 3-hydroxyanthranillic acid (3-HAA; 0.1 μM) and quinolinic acid (Quin; 1 μM) for 48 hr. Sholl analysis was performed on neurons to examine the number of neuritic branches (a), neurite length (b), the number of primary neurites (c) or the number of branches at specific distances from the soma (d). Representative images of neurons identified using the neuronal structural marker β-III tubulin (white) and the nuclear stain DAPI (blue) with fluorescent microscopy (e). Data expressed as mean ± SEM (n= 19-24 coverslips from 3 independent experiments). **P<0.01, ***P<0.001 vs, control, ##P<0.01, ###P<0.001, vs 3-HK+3-HAA+Quin [Two-way ANOVA followed by Newman-Keuls *post hoc* test (a-c)]; Sholl profile, *P<0.05, ***P<0.001, 3-HK+3-HAA+Quin vs. control, ###P<0.001, MK-801+3-HK+3-HAA+Quin CM vs. 3-HK+3-HAA+Quin [Three-way repeated measures ANOVA followed by Bonferroni *post hoc* test (d)].

3.3.5 Inhibitors of iNOS and NADPH oxidase block IFNγ-induced reductions in measures of neuronal complexity.

3.3.5.1 Effect of 1400W on IFNγ-stimulated BV-2 microglial-induced reductions in measures of neuronal complexity

Two-way ANOVA of the number of **neuritic branches** showed an effect of IFNγ CM [$F_{(1, 100)} = 10.537$, P= 0.002], no effect of 1400W CM [$F_{(1, 100)} = 0.465$, P= 0.497], and no interaction [$F_{(1, 100)} = 2.955$, P= 0.089]. *Post hoc* analysis revealed reductions in the number of neuritic branches following treatment with IFNγ CM (P<0.05) compared to control CM. Pre-treatment with 1400W prevented the IFNγ CM-induced reductions (P<0.01) (a).

Two-way ANOVA of **neurite length** showed an effect of 1400W CM [$F_{(1, 100)} = 9.403$, P= 0.003], IFNγ CM [$F_{(1, 100)} = 4.902$, P= 0.029], but no interaction [$F_{(1, 100)} = 1.438$, P= 0.233]. *Post hoc* analysis revealed reductions in neurite length following treatment with IFNγ CM (P<0.01) compared to control CM. Pre-treatment with 1400W prevented the IFNγ CM-induced reductions (P<0.001) (b).

Two-way ANOVA of the number of **primary neurites** showed an effect of IFNγ CM [$F_{(1, 100)} = 10.292$, P= 0.002], no effect of 1400W CM [$F_{(1, 100)} = 2.811$, P= 0.097], and no interaction [$F_{(1, 100)} = 1.878$, P= 0.174]. *Post hoc* analysis revealed reductions in the number of primary neurites following treatment with IFNγ CM (P<0.05) compared to control CM. Pre-treatment with 1400W prevented the IFNγ CM-induced reductions (P<0.01) (c).

Three-way repeated measures ANOVA of the number of **neuritic branches at specific distances from the neuronal cell soma** showed an effect of distance ($F_{(25, 2250)} = 772.961$, P<0.0001), 1400W CM ($F_{(1, 90)} = 5.898$, P= 0.017), IFNγ CM ($F_{(1, 90)} = 7.891$, P= 0.006), 1400W CM x distance ($F_{(25, 2250)} = 9.164$, P<0.0001), 1400W x IFNγ CM x distance ($F_{(25, 2250)} = 2.336$, P<0.0001) but no effect of 1400W x IFNγ CM ($F_{(1, 90)} = 0.465$, P= 0.497), or IFNγ CM x distance ($F_{(25, 2250)} = 0.536$, P= 0.971). *Post hoc* analysis revealed reductions in the number of branches at 10, 20, 30 μm from the cell soma following treatment with IFNγ CM (P<0.001) compared to control CM. Pre-treatment with 1400W prevented the IFNγ CM-induced reductions at 10, 20, and 30 μm from the cell soma (P<0.001) (d) (**figure 3.3.5.1**).

3.3.5.2 Effect of DPI chloride on IFNγ-stimulated bv-2 microglial-induced reductions in measures of neuronal complexity

Two-way ANOVA of the number of **neuritic branches** showed an effect of DPI chloride CM [$F_{(1, 113)} = 41.515$, $P<0.0001$], no effect of IFNγ CM [$F_{(1, 113)} = 1.951$, $P= 0.165$], and no interaction [$F_{(1, 113)} = 2.207$ $P= 0.14$]. *Post hoc* analysis revealed reductions in the number of neuritic branches following treatment with IFNγ CM ($P<0.05$) compared to control CM. Pre-treatment with DPI chloride prevented the IFNγ CM-induced reductions ($P<0.001$) (a).

Two-way ANOVA of **neurite length** showed an effect of DPI chloride CM [$F_{(1, 113)} = 12.011$, $P= 0.001$], IFNγ CM [$F_{(1, 113)} = 4.545$, $P= 0.035$], and an interaction [$F_{(1, 113)} = 6.094$, $P= 0.015$]. *Post hoc* analysis revealed reductions in neurite length following treatment with IFNγ CM ($P<0.01$) compared to control. Pre-treatment with DPI chloride prevented the IFNγ CM-induced reductions ($P<0.001$) (b).

Two-way ANOVA of the number of **primary neurites** showed an effect of DPI chloride CM [$F_{(1, 113)} = 12.786$, $P= 0.001$], IFNγ CM [$F_{(1, 113)} = 6.311$, $P= 0.013$], but no interaction [$F_{(1, 113)} = 1.000$, $P= 0.319$]. *Post hoc* analysis revealed reductions in the number of primary neurites following treatment with IFNγ CM ($P<0.05$) compared to control CM. Pre-treatment with DPI chloride prevented the IFNγ CM-induced reductions ($P<0.01$) (c).

Three-way repeated measures ANOVA of the number of **neuritic branches at specific distances from the neuronal cell soma** showed an effect of distance ($F_{(25, 2775)}= 5.547$, $P<0.0001$), but no effect of DPI chloride CM ($F_{(1, 111)}= 0.527$, $P= 0.469$), IFNγ CM ($F_{(1, 111)}= 0.734$, $P= 0.393$), DPI chloride x IFNγ CM ($F_{(1, 111)}= 0.748$, $P= 0.389$), DPI chloride CM x distance ($F_{(25, 2775)}= 0.978$, $P= 0.494$), IFNγ CM x distance ($F_{(25, 2775)}= 0.595$, $P= 0.944$), or DPI chloride x IFNγ CM x distance ($F_{(25, 2775)}= 0.567$, $P= 0.958$). *Post hoc* analysis revealed reductions in the number of branches at 10, 20, 30 μm from the cell soma following treatment with IFNγ CM ($P<0.001$) compared to control CM. Pre-treatment with DPI chloride prevented the IFNγ CM-induced reductions at 10, 20, and 30 μm from the cell soma ($P<0.001$) (d) (**figure 3.3.5.2**).

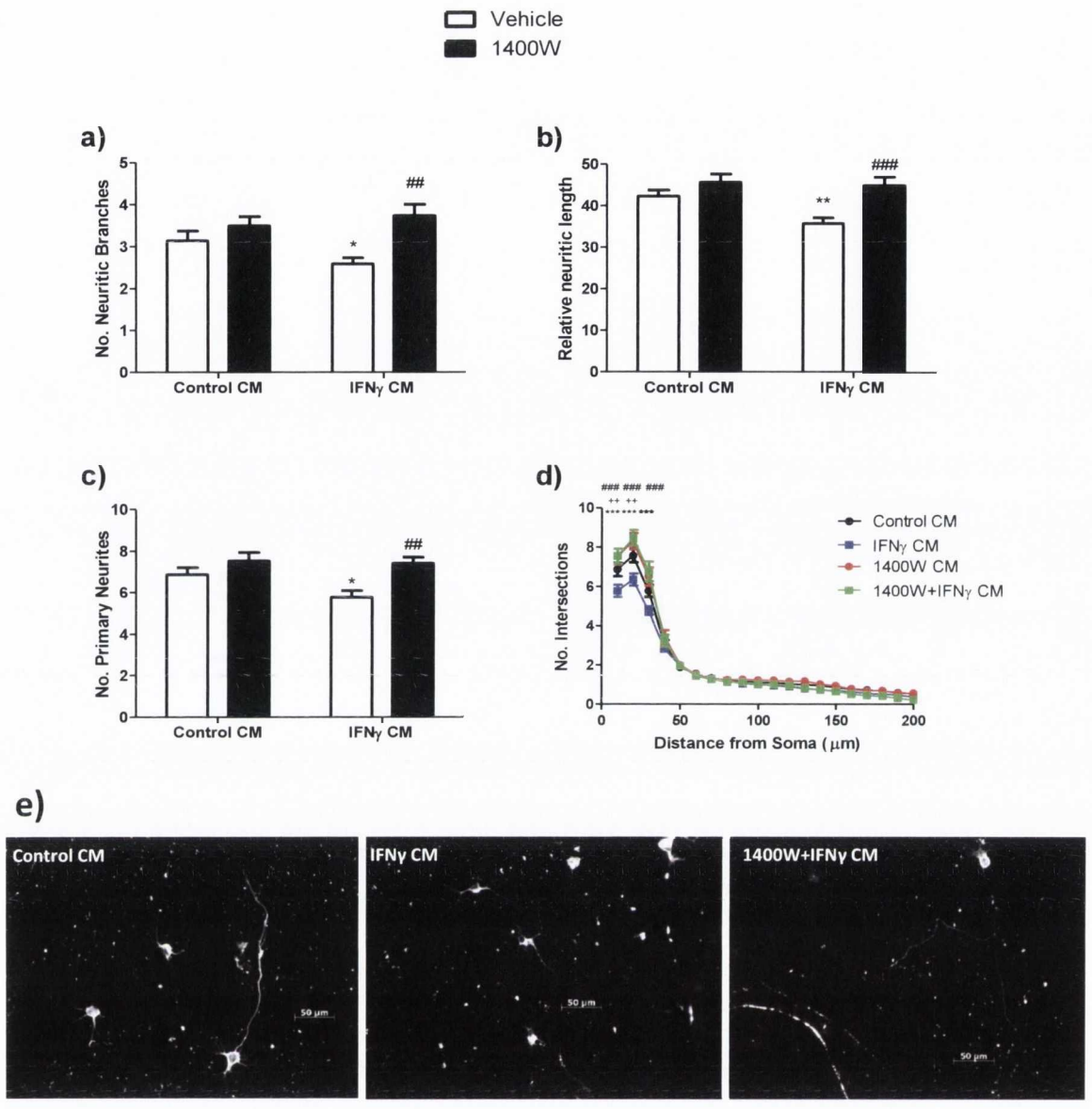

Figure 3.3.5.1: Effect of 1400W on IFNγ-stimulated BV-2 microglial-induced reductions in measures of neuronal complexity

CM from BV-2 microglia pre-treated with either vehicle or 1400W (25 μM; 30 min) followed by stimulation with IFNγ (5 ng/ml; 24 hr) was placed on primary cortical neurons (DIV 3) for 48 hr. Sholl analysis was performed on neurons to examine the number of neuritic branches (a), neurite length (b), the number of primary neurites (c) or the number of branches at specific distances from the soma. Representative images of neurons identified using the neuronal structural marker β-III tubulin (white) and the nuclear stain DAPI (blue) with fluorescent microscopy (e). Data expressed as mean ± SEM (n= 23-35 coverslips from 4 independent experiments). *P<0.05, **P<0.01, vs. control CM, ##P<0.01, ###P<0.001, vs. IFNγ CM. [Two-way ANOVA followed by Newman-Keuls *post hoc* test (a-c)]; Sholl profile, ***P<0.001, IFNγ CM vs. control CM, ++P<0.01, 1400W CM vs. control CM, ###P<0.001, 1400W+IFNγ CM vs. IFNγ CM [Three-way repeated measures ANOVA followed by Bonferroni *post hoc* test (d)].

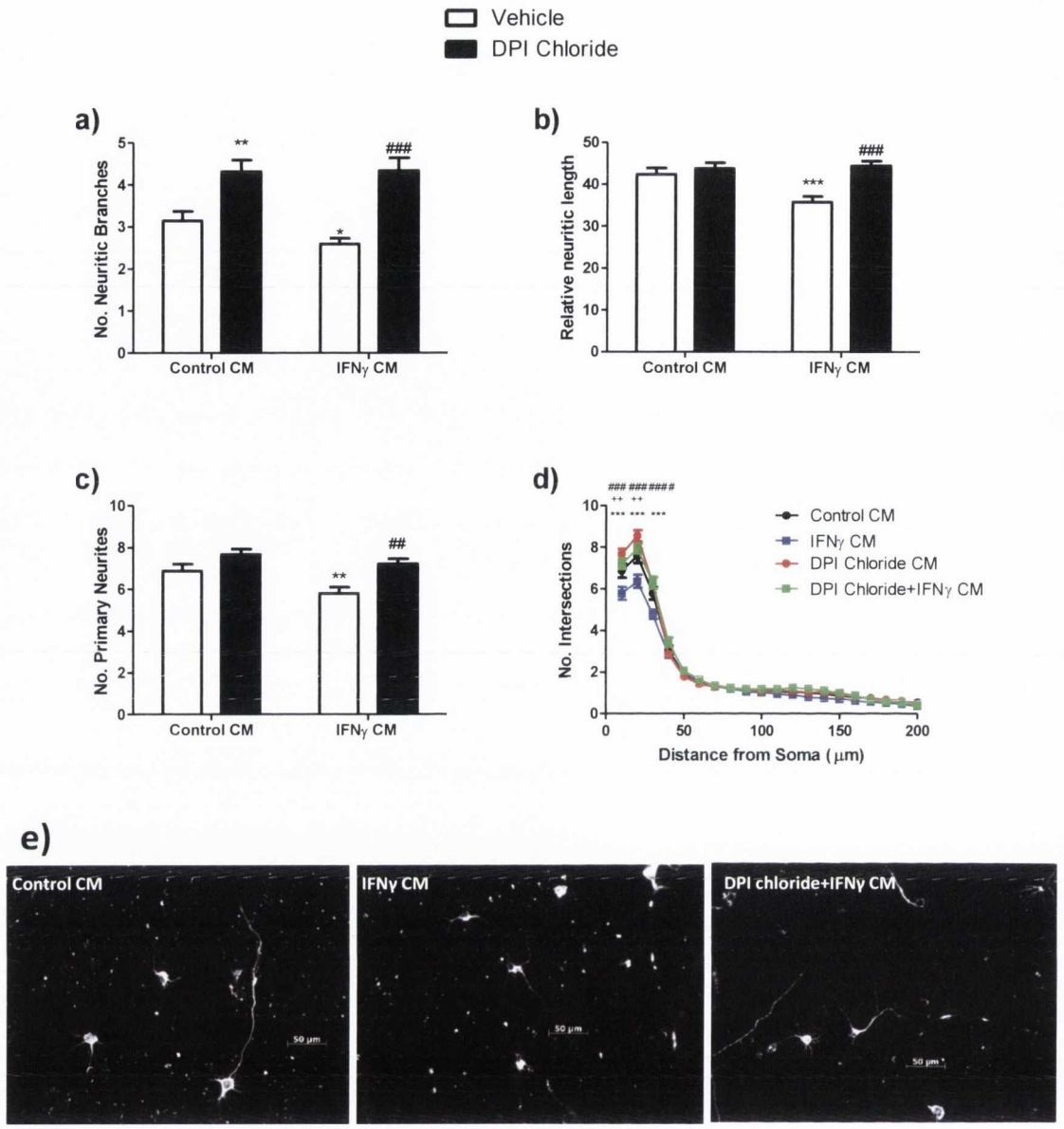

Figure 3.3.5.2: Effect of DPI chloride on IFNγ-stimulated BV-2 microglial-induced reductions in measures of neuronal complexity

CM from BV-2 microglia pre-treated with either vehicle or DPI chloride (0.001 μM; 30 min) followed by stimulation with IFNγ (5 ng/ml; 24 hr) was placed on primary cortical neurons (DIV 3) for 48 hr. Sholl analysis was performed on neurons to examine the number of neuritic branches (a), neurite length (b), the number of primary neurites (c) or the number of branches at specific distances from the soma. Representative images of neurons identified using the neuronal structural marker β-III tubulin (white) and the nuclear stain DAPI (blue) with fluorescent microscopy (e). Data expressed as mean ± SEM (n= 24-34 coverslips from4 independent experiments). *P<0.05, **P<0.01 ***P<0.001, vs. control CM, ##P<0.01, ###P<0.001 vs. IFNγ CM. [Two-way ANOVA followed by Newman-Keuls *post hoc* test (a-c)]; Sholl profile, ***P<0.001, IFNγ CM vs. control CM, ++P<0.01, DPI chloride CM vs. control CM, #P<0.05, ###P<0.001, DPI chloride +IFNγ CM vs. IFNγ CM [Three-way repeated measures ANOVA followed by Bonferroni *post hoc* test (d)].

3.4 Discussion

Initial findings from these studies demonstrate that stimulation of BV-2 microglia with IFNγ (5 ng/ml) for 24 hr activates the kynurenine pathway in this microglial cell line. In tandem with an induction of the rate limiting enzyme, IDO, and the downstream pathway enzymes, KMO and KYNU, there were increases in the concentrations of tryptophan, kynurenine and 3-hydroxykynurenine in the CM of these cells. Treatment of BV-2 cells with the IDO inhibitor 1-MT (L) was found to reverse the IFNγ-induced changes in metabolite concentrations in the CM. CM from the IFNγ-stimulated BV-2 microglia over a 48 hr period of exposure increased cytotoxicity and suppressed all measures of neurite outgrowth and complexity of primary cortical neurons (DIV 3). Prior treatment of BV-2 microglia with 1-MT (L) protected against the IFNγ CM-induced reductions in neurite outgrowth and complexity, but not cytotoxicity. Similarly, the anti-inflammatory agent, dexamethasone, which suppressed the IFNγ-induced gene expression of IDO, KMO, and KYNU, failed to protect against the IFNγ CM-induced increases in cytotoxicity but was successful in attenuating reductions in complexity. Additionally, prior treatment with either the KMO inhibitor, Ro 61-8048, or NMDA receptor antagonist, MK-801, afforded protection against both IFNγ CM-induced increases in cytotoxicity and reductions in neurite outgrowth and complexity. Overall, these data support a role for a novel mechanism, kynurenine pathway activation, by which stimulated microglia impair neuronal viability and complexity, the manipulation of which may pave the way for effective and innovative therapeutic approaches to neurodegenerative disorders where microglial activation is implicated.

In support of a role for kynurenine pathway activation and associated metabolites, direct application of 3-hydroxykynurenine, 3-hydroxyanthranillic acid and quinolinic acid in combination suppressed neurite outgrowth and complexity. These effects were not apparent when the metabolites were applied in isolation indicating a synergistic action of the combination. Moreover, changes in neuronal complexity were attenuated by pre-treatment with MK-801 indicating an important role for the NMDA receptor in mediating these actions.

3.4.1 IFNγ activates the kynurenine pathway in BV-2 microglia

At present most of the *in vitro* studies published in this area involve the use of mixed glial cultures of which the proportion of astrocytes to microglia is usually in favour of astrocytes [60-70%; (Hansson, 1984)] with common microglia isolation protocols only yielding approximately 10% of microglia from a mixed glial culture (Giulian and Baker, 1986). As such, BV-2 microglia, a murine microglial cell line which have similar morphological and functional characteristics when compared with those of

primary microglia (Bocchini et al. 1992) were utilised to characterise the kynurenine pathway in purified microglia in response to an inflammatory stimulus.

As IFNγ is a potent inducer of both the gene expression and enzyme activity of IDO (Yasui et al. 1986), it was chosen as the inflammatory stimulus for these experiments. The concentration of IFNγ was based on previous work done in our own laboratory demonstrating that at this concentration, IFNγ has no effect on the viability of either primary cortical neurons (DIV 3) or BV-2 microglia. Although Mizuno et al. (2008) suggest that IFNγ directly induces neuronal toxicity in primary neuronal cultures; no changes in viability were reported using the MTS assay. This study also used a significantly higher dose, 100 ng/ml IFNγ compared with our low concentration (5 ng/ml) of IFNγ.

IFNγ induces the expression of IDO along with the neurotoxic kynurenine pathway enzymes KMO and KYNU. In addition to this, there was no induction of the astrocyte-specific TDO or the neuroprotective kynurenine pathway enzyme KAT II. These findings are also supported by studies carried out with human foetal microglia and macrophages, as-well as murine microglia and macrophages, and BV-2 microglia, which demonstrated that IFNγ induced increases in the mRNA expression of IDO, KMO and KYNU (Chen et al., 2011, Guillemin et al., 2005b, Alberati-Giani et al., 1996). Coupled with this increase in the expression of the kynurenine pathway neurotoxic enzymes, was the induction of the inflammatory marker iNOS, indicative of microglial activation. iNOS catalyses the conversion of L-arginine to nitric oxide, which when present at high levels becomes cytotoxic (for review see Aktan 2004). IFNγ is a known inducer of iNOS in both BV-2 microglia and primary microglia (Sheng et al. 2011) and as such it was unsurprising to find its mRNA expression upregulated.

Following on from this, the concentrations of tryptophan and the kynurenine pathway metabolites kynurenine and 3-hydroxykynureine in the CM of BV-2 microglia were determined and found to be increased in response to IFNγ. It is of interest to note that high concentrations of tryptophan, kynurenine and 3-hydroxykynurneine were identified in the cell-free media (see supplementary **figure S1**), which susbquently contribute to a large proportion of the levels found in the CM. Nevertheless, in spite of the high baseline levels of tryptophan and pathway metabolites in this media, increases in concentrations were observed in response to IFNγ, however the values obtained may not truly reflect those of which are produced by the BV-2 microglia. Similarly, another study determined increased concentrations of kynurenine in both human and macaque macrophages following stimulation with IFNγ (100 IU/ml) for 24 hr (Lim et al., 2013a). In spite of the previously described enzyme profile of these cells, the kynurenine/tryptophan ratio – a commonly used indicatior of kynurenine pathway activation – failed to show any change in response to IFNγ treatment. This is as a consequence of IFNγ increasing the concentrations of tryptophan in addition to kynurenine which is contradictory to the literature. This may be associated with increased release

of trypophan from reactive microglia which, under normal physiological conditions would be taken up by surrounding neurons and astrocytes. Nevertheless, the ability of 1-MT (L) to attenuate these changes was demonstrated, with 1-MT (L) being found to increase the concentrations of tryptophan which may be as a consequence of baseline activity of IDO and also the ability of 1-MT (L) to inhibit the tryptophan transport system L (Kudo and Boyd, 2001). In contrast, 1-MT (L) attenuated the IFNγ-induced increases in the concentrations of 3-hydroxykynurenine in the BV-2 CM, and the increased kynurenine over tryptophan ratio indicating inhibition of pathway activation.

3.4.2 CM from IFNγ-stimulated BV-2 microglia reduces neuronal viability and complexity

Microglial-mediated neurotoxicity is well established and discussed in the literature [see Block et al. (2007b), for review]. Specifically, BV-2 microglia-mediated neurotoxicity has now also been established. Hornik et al. (2016), demonstrated that pheochromocytoma (PC12) cells, a cell line of neuronal origin, were phagocytosed when co-incubated with LPS treated BV-2 microglia. Additionally, LPS-stimulated BV-2 microglia exacerbated oxygen glucose deprivation-induced cell death of mouse organotypic hippocampal slices (Girard et al., 2013). Furthermore, Chen et al. (2011), reported that exposure of the murine motor neuron cell line, NSC-34 to CM from IFNγ-stimulated BV-2 microglia, increased cytotoxicity after 48 hr, as measured by LDH release. In the current investigation, we aimed to extend these findings by measuring not only viability, but also neurite outgrowth and complexity with a novel focus on a role for kynurenine pathway activation in mediating microglial-associated neurotoxicity and atrophy.

In all cases direct treatment of primary cortical neurons with IFNγ had no effect on the cytotoxicity, viability or neurite outgrowth and complexity of primary cortical neurons. As such, considering that the CM from IFNγ-stimulated BV-2 microglia was found to increase cytotoxicity, reduce neuronal viability and all measures of neuronal outgrowth and complexity, such effects are likely due to the production and release of unknown factors from the BV-2 microglia into the media in which they are cultured. Indeed, Kim et al. (2007) characterised the secretome – i.e. the CM, from BV-2 microglia that were co-stimulated with LPS and IFNγ. Similar to our findings, this group demonstrated that this CM was neurotoxic when placed on primary cortical mouse neurons, which they suggested was mediated by cathepsin D released by activated microglia (Kim et al., 2007). It is important to note that even unstimulated BV-2 microglial CM-induced neuronal cytotoxicity which is not reflected by the Alamar Blue or MTS viability assays. As a consequence of the latter two assays being normalised to the control, the true effect on neuronal viability may be masked.

3.4.3 Inhibition of kynurenine pathway activation in BV-2 microglia protects against IFNγ CM-induced reductions in measures of neuronal viability and complexity

In order to further elucidate the potential role for microglial-associated kynurenine pathway activation in driving the aforementioned IFNγ CM-induced reductions in neuronal integrity, a series of experiments were carried out which employed pharmacological agents. As previously discussed, activation of the kynurenine pathway gives rise to neuroactive metabolites, of which 3-hydroxykynurenine, 3-hydroxyanthranillic acid, and quinolinic acid are produced by the neurotoxic arm preferentially expressed in microglia. The rate-limiting step of this pathway was targeted by two independent mechanisms, inhibition of IDO enzyme activity with 1-MT (L) or inhibition of IDO gene induction with dexamethasone, both of which prevent the conversion of tryptophan to kynurenine. Downstream of IDO, the KMO enzyme was targeted due to its specific involvement in the microglial neurotoxic arm of the pathway, with inhibition of KMO with Ro 61-8048 preventing the conversion of kynurenine to 3-hydroxykynurenine. Finally, the ultimate effect of quinolinic acid - released from microglia as a consequence of kynurenine pathway activation - at the NMDA receptor on neuronal viability and complexity was assessed through the use of the NMDA receptor antagonist, MK-801. Manipulation of the kynurenine pathway using enzyme inhibitors has exhibited neuroprotection in *in vitro* models of various neurological disorders including cerebral ischemia and Huntington's disease (Stone et al., 2012). Similarly, Chen et al. (2011) demonstrated that 1-MT (L) was capable of protecting against the IFNγ-stimulated BV-2 CM-induced increases in cytotoxicity of NSC-34 cells used as an *in vitro* model of ALS.

Contrary to this, 1-MT (L) was not capable of protecting against the IFNγ CM-induced increases in cytotoxicity, however it did protect against reductions in neurite length, the number of primary neurites, and branching at 10, 20 and 30 μm from the cell soma. This lack of protection against increased cytotoxicity may be as consequence of IDOs other roles in microglia. Physiologically, IDO is capable of dampening down inflammatory responses through tryptophan depletion in immune cells. Thus, inhibition of IDO in an inflammatory setting may exacerbate microglial activation, enhancing the production of other neurotoxic mediators. Indeed, dexamethasone which blocks the induction of IDO failed to protect against the IFNγ CM-induced increases in cytotoxicity, while exhibiting a protective effect against IFNγ CM-induced atrophy. Dexamethasone is a synthetic glucocorticoid exhibiting potent anti-inflammatory properties. It has been shown to partially inhibit microglial activation, and decrease cytokine and nitric oxide production (Castano et al., 2002, Kurkowska-Jastrzebska et al., 1999). Further to this, it has been demonstrated that treatment with dexamethasone can attenuate the toxicity of hippocampal neurons which have been treated with CM from LPS-activated macrophages (Flavin et al., 1997). In this instance, dexamethasone was successful in preventing the IFNγ CM-induced reductions in neurite length, the number of primary

neurites, alongside branching at 10, 20 and 30 μm from the cell soma. This protection may be as a consequence of dexamethasones ability to reduce the IFNγ driven increases in the mRNA expression of the downstream neurotoxic kynurenine pathway enzymes, KMO and KYNU as well as iNOS or through its inhibitory action on NFκB. However the role of NFκB in regulating outgrowth appears complex and context-dependent, with its influence on outgrowth being dependent on the mechanism by which it is activated (Gutierrez et al. 2008).

Contrary to this, Ro 61-8048 proved more effective than either 1-MT (L) or dexamethasone, in that it attenuated both IFNγ CM-induced increases in cytotoxicity, and reductions in the number of primary neurites and branching at 20 and 30 μm from the cell soma. As such, targeting downstream of IDO might be a more effective and discreet way of blocking kynurenine pathway activation.

Aside from its oxidative properties, quinolinic acid primarily functions as an excitotoxin through its NMDA receptor agonistic action alongside its ability to potentiate the toxicity of other excitatory neurotransmitters, such as glutamate (Schurr & Rigor 1993). Quinolinic acid is present in the CNS at nanomolar concentrations, however in the presence of an inflammatory stimulus these levels can drastically increase from less than 100 nM to between 500-1200 nM (Chen & Guillemin 2009) at which, these concentrations have been found to increase the cytotoxicity of human primary neurons (Braidy et al., 2009b). *In vitro* experiments with human microglia, monocyte-derived macrophages and astrocytes suggest that activated macrophages produce much higher concentrations of quinolinic acid than microglia when stimulated with LPS and IFNγ. However, within the brain parenchyma microglia may be the prominent cell type responsible for the production of quinolinic acid (Espey et al., 1997). In this instance, MK-801 protected against the IFNγ CM-induced reductions in the number of neuritic branches, neurite length and branching at 10, 20 and 30 μm from the cell soma. This MK-801-mediated protection was deemed to be NMDA receptor-associated as MK-801 had no effect on the IFNγ driven increases in the mRNA expression of the kynurenine pathway enzymes IDO, KMO and KYNU or iNOS.

It is of interest to note that inhibition of KMO, and blockade of the NMDA receptor were more successful than 1-MT (L) in terms of attenuating activated microglia-associated reductions in neuronal integrity. This illustrates that targeting downstream of IDO, specifically using KMO or NMDA receptor-related compounds, despite being more discreet, is also more effective in terms of protecting against kynurenine pathway-induced reductions in neuronal viability, outgrowth and complexity.

In parallel to the aforementioned kynurenine pathway inhibitor studies, neurons were treated directly with the kynurenine pathway metabolites, 3-hydroxykynurenine, 3-hydroxyanthranillic acid and quinolinic acid. Much work has been done examining the effect of these metabolites on

neuronal viability for instance, Chen et al. (2011) demonstrated that MK-801 is capable of blocking the quinolinic acid (2 μM)-induced increases in cytotoxicity after a 48 hr incubation. Similarly, Braidy et al. (2009a), prevented quinolinic acid (550 nM)-induced increases in cytotoxicity in human astrocytes by additional treatment with MK-801 (1 μM). Additionally, it has previously been shown *in vitro* that 3-hydroxykynurenine and 3-hydroxyanthranillic acid induce neurotoxicity at much lower concentrations than quinolinic acid (Okuda et al. 1998). A role for these metabolites in driving atrophy is for the most part less understood, thus examining neuronal outgrowth and complexity was the primary focus in this instance. Treatment of neurons with individual pathway metabolites alone, and in combination, was examined to further characterise the effect of these metabolites on neuronal complexity. These studies demonstrated that at concentrations that had no effect alone on neurite outgrowth and complexity, in combination they cause atrophy. Furthermore, pre-treatment with MK-801 afforded protection against these reductions in both viability and complexity. This is consistent with the literature which implicates quinolinic acid as the chief driver of kynurenine pathway neurotoxicity (Stone 1993), with quinolinic acid-induced cytoskeletal disruption depicted as an initial event in quinolinic acid-induced toxicity, and this subsequently being prevented by MK-801 administration (Pierozan et al. 2014). Contrary to this, *in vivo* experiments have shown that the anti-oxidant, N-acetyl-L-cysteine, and not MK-801, attenuates 3-HK-induced neurotoxicity in rat striatum, suggesting that 3-HK exerts its neurotoxic effects via generation of free radicals as opposed to via NMDA receptor stimulation (Nakagami et al., 1996). However, MK-801 has also been shown to protect against oxidative stress in rodent models of acute lung injury or focal epilepsy (da Cunha et al., 2011, Kucukkaya et al., 1998). As such, MK-801 attenuates the synergistic action of these metabolites through its effect on both the NMDA receptor and through reducing oxidative stress.

3.4.4 Inhibition of oxidative and inflammatory processes protects against IFNγ-induced reductions in neuronal complexity

It is known that IFNγ triggers an array of physiological changes in activated microglia, with the current view on microglial-mediated toxicity in the literature pointing towards nitric oxide and free radical generation as the neurotoxic molecules, along with cytokines such as TNF-α (Block et al., 2007b, Sawada et al., 1989). Considering this, studies were done to assess whether inhibition of oxidative or inflammatory pathways could provide alternative protection against IFNγ CM-induced reductions in neuronal integrity. Recalling that iNOS expression was increased in IFNγ-stimulated BV-2 microglia, its role in driving the reductions in outgrowth was also examined.

Nitric oxide which is an important signalling molecule in the brain (Garthwaite 2010) has been shown to play an extensive role in neuronal growth and synaptogenesis during development (Downen, 1999). Furthermore, partial chronic inhibition of NOS causes reductions in neurite growth (Cooke et al. 2013). In contrast the data presented here indicates that nitric oxide is at least in part contributing to reductions in neurite outgrowth, which may be due to the high levels of nitric oxide produced in response to IFNγ at which it can become neurotoxic (Wei et al. 2000). The studies outlined here demonstrate that inhibition of the enzyme iNOS protected against the IFNγ CM-induced reductions in neurite length, the number of primary neurites alongside branching at 10, 20 and 30 μm from the cell soma.

Moreover, NADPH oxidase is a common source of microglial-mediated oxidative stress and is required for the production of neurotoxic pro-inflammatory factors (Block and Hong, 2005). It is suggested that this enzyme mediates neurotoxicity through either the production of extracellular ROS, or via the production of intracellular ROS which facilitate increased pro-inflammatory cytokine production both of which are toxic to neurons. In this instance, inhibition of NADPH oxidase attenuated the IFNγ CM-induced reductions in neurite length, the number of primary neurites, alongside branching at 10, 20 and 30 μm from the cell soma. DPI chloride itself showed a neurotrophic capacity, increasing the number of neuritic branches, and branching at 10 and 20 μm from the cell soma. Likewise, it has been demonstrated in the literature that accumulation of ROS by neuronal NADPH oxidase in response to TNFα causes reductions in neurite outgrowth, with these reductions being attenuated by blunting ROS production (Barth et al. 2012).

3.4.5 Concluding remarks

Overall, these data support the hypothesis that targeting the kynurenine pathway in an inflammatory environment is protective against both neurotoxicity and atrophy. A noteworthy finding is the divergent effects of IDO inhibition on rescuing IFNγ CM-induced cytotoxicity and atrophy, with pathway intervention downstream of this enzyme appearing to demonstrate greater efficacy. Remarkably, inhibiting the production of both kynurenine pathway metabolites and nitric oxide has the same beneficial effect in terms of protecting against reductions in neuronal complexity. It is of interest to note that the kynurenine pathway and NOS pathways are linked, with nitric oxide capable of inhibiting IDO (Thomas et al. 1994), while the downstream kynurenine pathway metabolite, 3-hydroxyanthranillic acid has been shown to inhibit NOS activity and interfere with the expression of NOS mRNA in a murine macrophage cell line (Sekkaï et al. 1997). Examination of the interplay between these two systems is beyond the scope of these studies; however the fact that blockade of either has a redundant effect on neurite outgrowth is compelling. Alternative to iNOS inhibition, kynurenine pathway inhibition appears a more attractive target for impeding neurodegenerative processes due to the beneficial effects associated with controlled levels of nitric oxide including but not limited to its role in learning and memory, nociception, and the immune response (Garthwaite and Boulton, 1995). Limitations to this work include the assessment of neurite outgrowth and complexity in the presence of a backdrop of toxicity which vehicle-treated BV-2 microglial CM exhibits, alongside the inability to detect the complete repertoire of kynurenine pathway metabolites such as 3-hydroxyanthranillic acid or quinolinic acid.

Chapter 4

An investigation into the impact of kynurenine pathway activation in reactive primary glia on the integrity of primary cortical neurons

4.1 Introduction

The kynurenine pathway, which is activated in times of stress and infection, has been implicated in the pathophysiology of multiple CNS disorders ranging from psychiatric disorders to neurodegenerative diseases (Bohar et al., 2015, Karakuła-juchnowicz et al., 2015, Reus et al., 2015). Activation of this tryptophan metabolising pathway results in the production of neuroactive metabolites which have the potential to influence neuronal transmission. Within the CNS the kynurenine pathway is physically segregated in different cells of the brain. This compartmentalisation occurs as a consequence of different cells showing preferential expression of the various enzymes responsible for tryptophan metabolism down this pathway. In humans, microglia, astrocytes and neurons express both rate limiting enzymes, IDO and TDO as well as the downstream enzymes KYNU and 3-HAAO. Differential expression occurs with KAT II and KMO with the former being expressed in both microglia and astrocytes while the latter is preferentially expressed in microglia and neurons (Guillemin et al., 2007, Guillemin et al., 2001, Espey et al., 1997). Consequently, it is proposed that astrocytes are responsible for the generation of the neuroprotective metabolite, kynurenic acid, an NMDA receptor antagonist. Whereas microglia are accountable for the generation of the neurotoxic metabolites, 3-hydroxykynurenine, 3-hydroxyanthranillic acid, and quinolinic acid, all of which display oxidative properties with the latter being an NMDA receptor agonist. Considering that both glial cell types express the inflammatory-driven rate limiting enzyme IDO, neuroinflammation has the potential to activate each arm albeit to varying extents as a consequence of KAT II mRNA expression remaining unchanged in the presence of LPS (Connor et al., 2008).

The concept of kynurenine pathway compartmentalisation although definitive, requires further investigation to verify that it is as clear-cut as the literature proposes. Although much work has been done characterising the existence of the two arms of the pathway in different brain cell types, this work primarily involves the use of primate cells or rodent cell lines (Lim et al., 2013a, Chen et al., 2011, Guillemin et al., 2007, Lim et al., 2007, Guillemin et al., 2005b, Guillemin et al., 2001, Espey et al., 1997). The pathway has been established *in vivo* in rodents via identification of pathway-related enzymes and metabolites (Gibney et al., 2013, O'Connor et al., 2009, Connor et al., 2008), however, little is known about the compartmentalisation of this pathway in primary rat brain cells. The extent to which each brain cell type contributes to central levels of these metabolites is of importance to allow for discrete pathway manipulation. Preferentially targeting one arm would be potentially beneficial by way of counterbalancing shifts in pathway activation which occur in multiple neurological disorders [see, O'Farrell and Harkin (2015) for review].

Kynurenine pathway metabolites have the potential to influence neuronal transmission by affecting neuronal integrity via reducing viability, neuritic complexity, or plasticity. The number, length and

complexity of dendrites is widely believed to underlie neuronal interaction and network integration corresponding to key aspects of brain function such as cognitive function (Ferrante et al., 2013). As such, *in vitro* experiments which assess the impact of kynurenine pathway metabolites on neuronal viability and complexity are of interest. Its likely contribution to underlying mechanisms associated with CNS disorders indicates that regulation of the kynurenine pathway is of critical importance and may serve as an important target for the future development of treatments for a range of CNS-related illnesses.

Findings from chapter 3 demonstrated IFNγ-mediated kynurenine pathway activation in the BV-2 microglial cell line, with CM from these cells reducing both neuronal viability and complexity. Inhibition of the pathway by prior treatment with either an IDO or KMO inhibitor attenuated the IFNγ-stimulated BV-2 CM-induced reductions in complexity. Furthermore, blockade of the NMDA receptor with MK-801 prevented these reductions highlighting kynurenine pathway activation as a novel mechanism implicated in driving reactive microglial-associated reductions in neuronal viability and complexity.

The potential for BV-2 cells to accurately represent primary microglia remains undecided (Butovsky et al., 2014, Henn et al., 2009, Horvath et al., 2008). BV-2 cells have been shown to respond similarly to primary microglia in response to LPS with a 90% overlap in gene expression, however this up-regulation is substantially inferior to that seen with mouse primary microglia (Henn et al., 2009). Additionally, BV-2 responses have been found to be inconsistent in the presence of LPS compared to those of rat primary microglia with regard to inflammatory cytokine release, IBA1 expression, and the concentration at which the microglial inhibitor, minocycline, was effective at blocking migration (Horvath et al., 2008). Consequently this group deem BV-2 cells to be an inadequate model for assessing inflammatory-driven primary microglial responses.

Having determined the potential for the involvement of kynurenine pathway activation in mediating neurotoxicity and atrophy in chapter 3 we propose to replicate the findings in primary microglia. We aim to examine neuronal complexity and subsequently synaptogenesis in the absence of reduced viability to more clearly target atrophic processes which precede cell death (Knight and Verkhratsky, 2010). In the current investigation, the extent to which the kynurenine pathway is activated in distinct primary glial cells in an inflammatory setting is assessed. Mixed glial cultures, consisting of astrocytes (70%) and microglia (30%) (McNamee et al., 2010b) along with purified astrocytic or microglial cultures were utilised to delineate the two arms of the kynurenine pathway. As such, the investigation aims to identify the effect that activation of either arm of the pathway separately or in combination has on neuronal integrity. IFNγ driven activation of the kynurenine pathway is assessed by quantification of pathway-related gene expression and quantification of pathway-related metabolites in the glial cells and CM respectively. This investigation aims to examine the effect that

glial-associated kynurenine pathway activation has on neuronal integrity by way of assessing neuronal viability and complexity, including the number of neuritic branches, neurite length, the number of primary neurites and the number of branches in relation to varying distances from the cell soma/ body. An additional parameter of neuronal integrity that is explored in this study is the formation of synapses in mature neurons as an indicative measure of functionality at a later point in neuronal development. The direct effect of kynurenine pathway metabolites on these measures of neuronal integrity (viability, complexity, synaptogenesis) were examined in parallel to provide a comprehensive understanding of the extent to which kynurenine pathway activation alters neuronal integrity.

A supplementary aim was to provide further insight into the detrimental effects of glutamate on neuronal complexity (Doucet et al., 2015) with examination of its effect on the viability of and formation of synapses in mature neurons. Reactive microglia release large amounts of glutamate into the extracellular milieu (Piani et al., 1992) via connexion hemichannels of gap junctions (Eugenin et al., 2001) or more regularly by the system x_c^- glutamate antiporter. Activation of this system under inflammatory circumstances aids in maintaining the redox balance through the influx of cysteine in exchange for glutamate, and subsequent production of the antioxidant glutathione (Conrad and Sato, 2012). In a mixed glial setting inflammatory-activated microglia and subsequent release of glutamate may contribute to excitotoxicity in conjunction with quinolinic acid, which may be exacerbated by the inflammation-induced downregulation of the astrocytic EAAT resulting in failure of astrocytes to remove extracellular glutamate (Takaki et al., 2012). As a consequence of system x_c^- being induced by both inflammation and oxidative stress, it is proposed that in the context of IDO activation, system x_c^- converts oxidative stress into excitotoxic stress through the release of glutamate from microglia (Dantzer and Walker, 2014a). The recommended strategy for ameliorating this excitotoxicity is by enhancing the brain-to-blood efflux of glutamate through accelerated degradation of circulating glutamate via administration of oxaloacetate which activates glutamic oxaloacetic transaminase which metabolises glutamate in to 2-ketoglutarate (Dantzer and Walker, 2014a). The ability of this technique to afford neuroprotection has been demonstrated in models of ischemic stroke, traumatic brain injury and epilepsy (Leibowitz et al., 2012). However, as a consequence of the potential side effects - systemic toxicity and pharmacokinetic properties of glutamate scavengers (Zhumadilov et al., 2015) - this chapter investigates the potential of the neuroprotective kynurenine pathway as an alternative mechanism for attenuating glutamate-induced neurotoxicity. The ability of kynurenic acid to ameliorate glutamate-induced neuronal atrophy and synapse loss through direct application of kynurenic acid in the presence of glutamate is assessed.

4.2 Study design

4.2.1 Characterisation of the effect of IFNγ on the mRNA expression profile of kynurenine pathway enzymes in primary cortical cells

Primary cortical microglia (DIV 12-13), mixed glia (DIV 12-13), astrocytes (DIV 12-13) and neurons (DIV 3) were treated with IFNγ (10 ng/ml) for 6 hr. Cells were harvested for RNA extraction followed by quantitative PCR to measure mRNA expression of kynurenine pathway enzymes, including the rate limiting enzymes, IDO and TDO, and the downstream enzymes, KMO, KYNU and KAT II/Aadat. The concentration and time point were adjusted from previous studies in chapter 3 due to a lack of induction of kynurenine pathway enzymes following stimulation of primary cortical microglia with IFNγ 5 ng/ml for 24 hr. As such, a dose of 10 ng/ml IFNγ was utilised with mRNA expression examined following a 6 hr incubation period. This time point is based on previous gene expression assessments in rat primary glia carried out by our laboratory (Day et al., 2014).

4.2.2 Determination of the effect of IFNγ on the concentrations of kynurenine pathway metabolites in the CM of primary cortical cells

Primary cortical microglia (DIV 12-13), mixed glial (DIV 12-13), astrocytes (DIV 12-13) and neurons (DIV 3) were treated with IFNγ (10 ng/ml) for 24 hr. CM was harvested for HPLC analysis for the determination of tryptophan and the kynurenine pathway metabolites, kynurenine and 3-hydroxykynurenine.

4.2.3 Characterisation of the effect of CM from IFNγ-stimulated primary cortical cells on neuronal viability and complexity

Primary cortical microglia (DIV 12-13) were treated with IFNγ (10 ng/ml) for 24 hr. The resultant CM was collected, sterile-filtered and placed on primary cortical neurons (DIV 3) for 24 hr or 48 hr. Neuronal viability was assessed using the alamarBlue® cell proliferation assay to quantify the % viability. Fixation and fluorescent immunocytochemistry were performed on neurons for Sholl analysis as previously described.

Primary cortical mixed glia (DIV 12-13) and astrocytes (DIV 12-13) were treated with IFNγ (10 ng/ml) for 24 hr. The resultant CM was collected, sterile-filtered and placed on primary cortical neurons (DIV 3) for 24 hr. Neuronal viability was assessed using the alamarBlue® cell proliferation assay to quantify

the % viability. Fixation and fluorescent immunocytochemistry were performed on neurons for Sholl analysis.

In addition to the CM studies, primary cortical neurons (DIV 3) were treated directly with IFNγ to assess whether IFNγ affected either neuronal viability or complexity. Primary cortical neurons (DIV 3) were treated with IFNγ (10 ng/ml) for 24 hr. Neuronal viability was assessed using the alamarBlue® cell proliferation assay. Fixation and fluorescent immunocytochemistry were performed on neurons for Sholl analysis.

4.2.4 Effect of prior treatment with 1-MT (L) on IFNγ CM-induced changes in neuronal complexity

To further investigate a role for kynurenine pathway activation in altering neuronal complexity, an inhibitor of IDO, 1-MT (L), was used to assess if the effects of CM from IFNγ-stimulated mixed glia could be dissipated. In this instance the concentration of 1-MT (L) chosen inhibited kynurenine pathway activation in unstimulated mixed glia (see supplementary **figure S2**).

Primary cortical mixed glia (DIV 12-13) were pre-treated with 1-MT (L) (0.5 mM; 30 min) followed by stimulation with IFNγ (10 ng/ml) for 24 hr. The resultant CM from these cells was collected, sterile-filtered and placed on primary cortical neurons (DIV 3) for 24 hr. Fixation and fluorescent immunocytochemistry were performed on neurons for Sholl analysis.

4.2.5 Effect of prior treatment with 1-MT (L) on IFNγ-stimulated primary cortical mixed glial CM-induced changes in the expression of synaptic markers

Primary cortical mixed glia (DIV 12-13) were treated with IFNγ (10 ng/ml) for 24 hr. The resultant CM was collected, sterile-filtered and placed on primary cortical neurons (DIV 18-21) for 24 hr. Neuronal viability was assessed using the alamarBlue® cell proliferation assay. Fixation and fluorescent immunocytochemistry were performed on neurons for analysis of the expression of synaptic markers, synaptophysin and PSD-95, as a measure of synaptogenesis.

In addition to the CM studies, primary cortical neurons (DIV 18-21) were treated directly with IFNγ to assess whether IFNγ affected either neuronal viability or synaptogenesis. Primary cortical neurons (DIV 18-21) were treated with IFNγ (10 ng/ml) for 24 hr. Neuronal viability was assessed using the alamarBlue® cell proliferation assay. Fixation and fluorescent immunocytochemistry were performed on neurons for the analysis of the expression of synaptic markers, synaptophysin and PSD-95.

Primary cortical mixed glia (DIV 12-13) were pre-treated with 1-MT (L) (0.5 mM; 30 min) followed by stimulation with IFNγ (10 ng/ml) for 24 hr. The resultant CM was collected, sterile-filtered and placed on primary cortical neurons (DIV 18-21) for 24 hr. Fixation and fluorescent immunocytochemistry were performed on neurons for analysis of the expression of synaptic markers, synaptophysin and PSD-95.

4.2.6 Effects of kynurenine pathway metabolites on neuronal viability, complexity and the expression of synaptic markers

In comparison to chapter 3 where the effect of 3-hyrdroxykynurenine, 3-hydroxyanthranillic acid, and quinolinic acid on neuronal complexity were examined following a 48 hr incubation period, in this chapter the incubation period is 24 hr, thus the effects of these metabolites are re-examined.

Primary cortical neurons (DIV 3/ 18-21) were treated with tryptophan (1, 10, 25, 100 μM), and the kynurenine pathway metabolites kynurenine (1, 10 μM), 3-hydroxykynureine (0.01, 0.03, 0.1 μM), 3-hydroxyanthranillic acid (0.01, 0.03, 0.1 μM), quinolinic acid (0.03, 0.1, 1, 10, 25, 100 μM) or kynurenic acid (0.003, 0.01, 0.03, 0.1, 1, 10 μM) for 24 hr. Neuronal viability was assessed using the alamarBlue® cell proliferation assay. Fixation and fluorescent immunocytochemistry were performed on neurons for Sholl analysis or analysis of the synaptic markers, synaptophysin and PSD-95.

Primary cortical neurons (DIV 3/ 18-21) were treated with combinations of kynurenine pathway metabolites consisting of 3-hydroxykynureine (0.03 μM), 3-hydroxyanthranillic acid (0.03 μM), and quinolinic acid (0.1 μM) for 24 hr. Neuronal viability was assessed using the alamarBlue® cell proliferation assay. Fixation and fluorescent immunocytochemistry were performed on neurons for Sholl analysis or analysis of the synaptic markers, synaptophysin and PSD-95.

4.2.7 Effects of glutamate on neuronal viability, complexity and the expression of synaptic markers

It has previously been reported by our laboratory that activation of the NMDA receptor is responsible for glutamate-induced neuronal atrophy (Doucet et al., 2015). Considering that reactive microglia release glutamate in addition to quinolinic acid, the ability of kynurenic acid to protect against these reductions was examined. Glycine was added as a consequence of it being a co-agonist at the NMDA receptor (Dingledine et al., 1999), with glutamate-induced neurite atrophy only occurring in the presence of glycine (Doucet et al., 2015). Concentrations of both glutamate and glycine were based on the previous work carried out by our laboratory whereby glutamate 500 μM and glycine 10 μM in combination reduced neurite length and neuronal complexity (Doucet et al., 2015).

Primary cortical neurons (DIV 3) were treated with either glutamate (500 μM), glycine (10 μM) or a combination of glutamate (500 μM) and glycine (10 μM) for 24 hr. Neuronal viability was assessed using the alamarBlue® cell proliferation assay. Fixation and fluorescent immunocytochemistry were performed on neurons for Sholl analysis.

Primary cortical neurons (DIV 18-21) were treated with either glycine (1, 10 μM), glutamate (0.1, 1, 10, 50, 100, 500 μM) or a combination of glutamate and glycine for 24 hr. Neuronal viability was assessed using the alamarBlue® cell proliferation assay. Due to the increased sensitivity of these mature neurons to glutamate a greater range of doses was required to establish a subthreshold concentration.

Primary cortical neurons (DIV 18-21) were treated with either glycine (1 μM), or a combination of glutamate (50 μM) and glycine (1 μM) for 24 hr. Fixation and fluorescent immunocytochemistry were performed on neurons for analysis of the synaptic markers, synaptophysin and PSD-95. A reduced dose of 50 μM was required in order to examine the effect of glutamate on the expression of synaptic markers in the absence of effects on neuronal viability.

4.2.8 Concentration-related effect of kynurenic acid on the glutamate and glycine- or 3-hydroxykynurenine + 3-hydroxyanthranillic acid + quinolinic acid-induced reductions in neuronal complexity and the expression of synaptic markers

Primary cortical neurons (DIV 3) were treated with a combination of glutamate (500 μM) and glycine (10 μM) with or without the addition of kynurenic acid (0.03, 0.1, 1, 10 μM) for 24 hr. Fixation and fluorescent immunocytochemistry were performed on neurons for Sholl analysis.

Primary cortical neurons (DIV 18-21) were treated with glutamate (50 μM) with or without the addition of kynurenic acid (0.03, 0.1 μM) for 24 hr. Fixation and fluorescent immunocytochemistry were performed on neurons for analysis of the synaptic markers, synaptophysin and PSD-95. On the basis that glutamate alone reduced the expression of synaptic markers to the same extent as a combination of both glutamate and glycine, the addition of glycine was not warranted in this investigation.

Primary cortical neurons (DIV 3) were treated with a combination of 3-hydroxykynureine (0.03 μM), 3-hydroxyanthranillic acid (0.03 μM), and quinolinic acid (0.1 μM), with or without the addition of kynurenic acid (0.03, 0.1, 1 μM) for 24 hr. Fixation and fluorescent immunocytochemistry were performed on neurons for Sholl analysis.

Primary cortical neurons (DIV 18-21) were treated with a combination of 3-hydroxykynureine (0.03 μM), 3-hydroxyanthranillic acid (0.03 μM), and quinolinic acid (0.1 μM), with or without the addition of kynurenic acid (0.03, 0.1 μM) for 24 hr. Fixation and fluorescent immunocytochemistry were performed on neurons for analysis of the synaptic markers, synaptophysin and PSD-95.

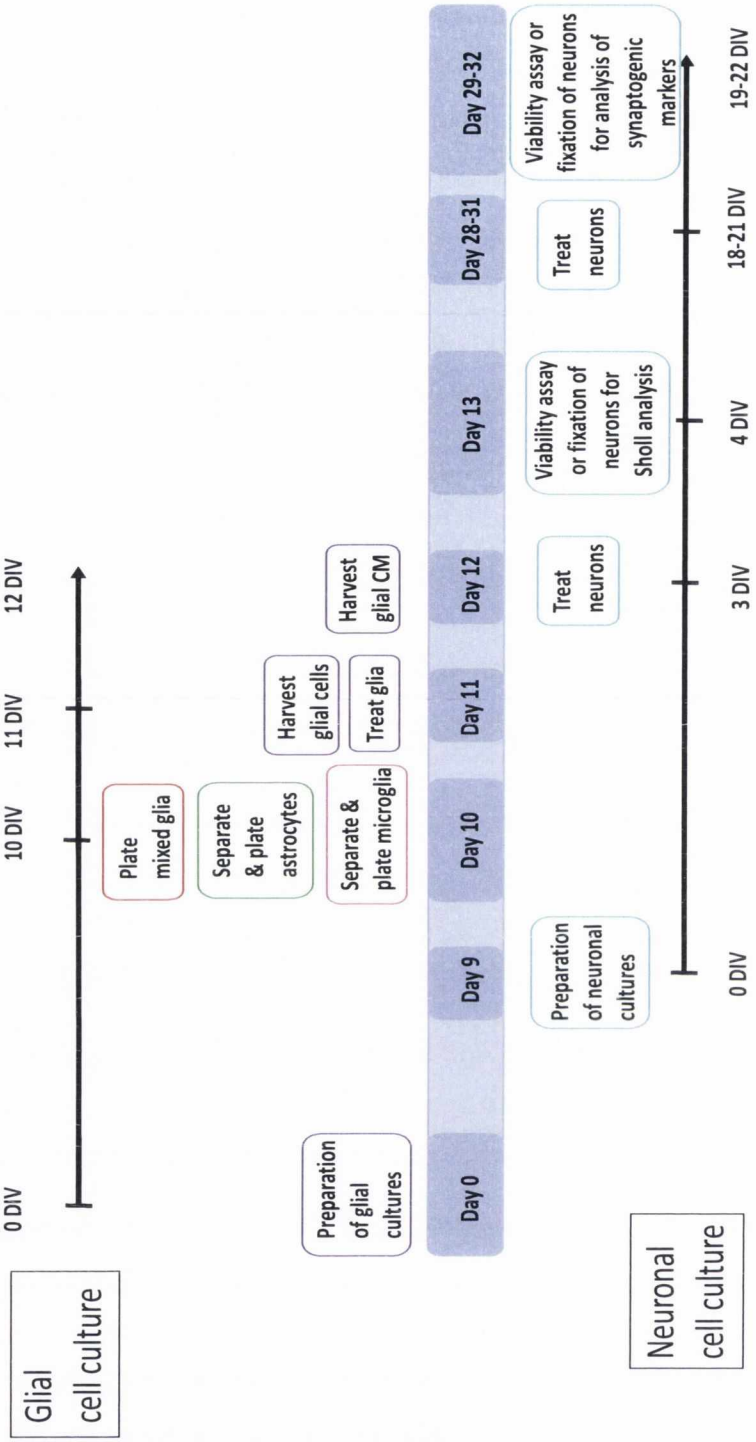

Figure 4.2.1: Diagram showing the timeline of a typical experiment

Glial cells are cultured and grown for 10-12 days upon which they are plated for a minimum of 24 hr prior to treatment with IFNγ [+/- pre-treatment with 1-MT (L)]. Neuronal cells are cultured and grown for 3 days upon which they are subsequently treated for 24 hr with CM or kynurenine pathway metabolites. On day 13 one set of neurons are assessed for neuronal viability or they are fixed to allow for assessment of neuronal complexity by Sholl analysis. On day 29-32 the other set of neurons are either assessed for neuronal viability, or they are fixed to allow for assessment of the expression of synaptic markers by Image J analysis.

Table 4.2.1: Table of compounds and concentrations used

To ensure maximal inhibition, 1-MT (L) was incubated on cells for 30 min before additional stimulation with IFNγ. Concentrations of agents used were chosen based on those reported in the literature indicated in the reference column of the table below.

Compound name	***Final concentration***	***In vitro experimental details***	***Reference***
1-MT (L)	0.5 mM	0.5 mM 1-MT (L) reversed the IFNγ-induced changes in tryptophan and kynurenine pathway metabolites in BV-2 CM. Reduced the kynurenine over tryptophan ratio in unstimulated mixed glial cells	Concentration based on previous work carried out in chapter 3 and supplementary data.
3-Hydroxyanthranillic acid	0.01, 0.03, 0.1 µM	No effect on the viability of human primary neurons	(Braidy et al., 2009b)
3-Hydroxykynurenine	0.01, 0.03, 0.1 µM	No effect on the viability of human primary neurons	(Braidy et al., 2009b)
Glutamate	0.1, 1, 10, 50, 100, 500 µM	100 µM reduces dendrite growth of primary mouse neurons while having no effect on the viability	(Monnerie et al., 2003)
Glycine	1, 10 µM	10 µM enhances the atrophic properties of glutamate on rat primary cortical neurons	(Doucet et al., 2015)
Kynurenic acid	0.003, 0.01, 0.1, 1, 10 µM	No effect on the viability of human primary neurons	(Braidy et al., 2009b)
Kynurenine	1, 10 µM	Reduced the viability of human primary neurons	(Braidy et al., 2009b)
Quinolinic acid	0.1, 1, 10, 25, 100 µM	Concentrations ranging from a subthreshold to concentrations which reduce the viability of human neurons	(Braidy et al., 2009b)

Recombinant rat IFNγ	10 ng/ml	At this concentration, IFNγ activated primary microglia as determined by measuring TNFα mRNA expression and protein release.	Concentration based on previous studies carried out in our laboratory
Tryptophan	1, 10, 25, 100 µM	No effect on the viability of human primary neurons	(Braidy et al., 2009b)

4.3 Results

4.3.1 Activation of the kynurenine pathway in primary cortical glia and the effect of glia CM on neuronal integrity.

4.3.1.1 Effect of IFNγ on the mRNA expression of kynurenine pathway enzymes in primary cortical microglia

Stimulation of primary microglia with IFNγ increased the mRNA expression of **IDO** (t= 4.043, P= 0.0023, d.f.= 10) (a) and **KYNU** (t= 3.146, P= 0.0104. d.f.= 10) (d), decreased the mRNA expression of **KAT II** (t= 2.84, P= 0.0194, d.f.= 9) (e), and had no effect on the mRNA expression of **TDO** (t= 1.096, P= 0.2987, d.f.= 10) (b) or **KMO** (t= 1.497, P= 0.1727, d.f.= 8) (c) (**figure 4.3.1.1**).

4.3.1.2 Effect of IFNγ on the concentrations of tryptophan, kynurenine, 3-hydroxykynurenine and the kynurenine/tryptophan ratio in the CM of primary microglia

Stimulation of primary microglia with IFNγ increased the concentration of **tryptophan** (t= 2.212, P= 0.0377, d.f. = 22) (a), **kynurenine** (t= 2.799, P= 0.0105, d.f. = 22) (b), but not **3-hydroxykynurenine** (t= 2.728, P= 0.7875, d.f. = 22) (c) or the **kynurenine over tryptophan ratio** (t= 1.342, P= 0.1934, d.f. = 22) in the CM of primary microglia (**figure 4.3.1.2**).

4.3.1.3 Effect of CM from IFNγ-stimulated primary cortical microglia on neuronal viability

CM from IFNγ-stimulated primary microglia had no effect on **neuronal viability** at 24 hr (t= 2.010, P= 0.0568, d.f. = 22) (a) or 48 hr (t= 0.5872, P= 0.5633, d.f. = 21) (b) (**figure 4.3.1.3**).

4.3.1.4 Effect of CM from IFNγ-stimulated primary cortical microglia on measures of neuronal complexity

CM from IFNγ-stimulated primary microglia had no effect on the number of **neuritic branches** at 24 hr (t= 0.6062, P= 0.5479, d.f.= 39) (a) or 48 hr (t= 0.2526, P= 0.8019, d.f.= 40) (b), **neurite length** at 24 hr (t= 1.103, P= 0.2766, d.f.= 39) (c) or 48 hr (t= 0.9508, P= 0.3474, d.f.= 40) (d), or the number of **primary neurites** at 24 hr (t= 1.34, P= 0.1881, d.f.= 39) (e) or 48 hr (t= 1.479, P= 1.469, d.f.= 40) (f).

Two-way repeated measures ANOVA of the number of **neuritic branches at specific distances from the neuronal cell soma** at 24 hr showed an effect of distance [$F_{(25, 975)}$ = 636.9, P<0.0001], but no effect of IFNγ CM [$F_{(1, 975)}$ = 1.218, P= 0.2766], or an interaction [$F_{(25, 975)}$ = 0.543, P= 0.9677] (g).

Two-way repeated measures ANOVA of the number of **neuritic branches at specific distances from the neuronal cell soma** at 48 hr showed an effect of distance [$F_{(25, 1000)} = 0.9041$, $P<0.0001$], but no effect of IFNγ CM [$F_{(1, 1000)} = 6.266$, $P= 0.3474$], or an interaction [$F_{(25, 1000)} = 531.3$, $P= 0.5294$] (h) (**figure 4.3.1.4**).

4.3.1.5 Effect of IFNγ on the mRNA expression of kynurenine pathway enzymes in primary cortical mixed glia

Stimulation of primary mixed glia with IFNγ increased the mRNA expression of **IDO** (t= 8.034, P<0.0001, d.f.= 10) (a), decreased the mRNA expression of **KAT II** (t= 3.131, P= 0.0107, d.f.= 10), but had no effect on the mRNA expression of **TDO** (t= 1.352, P= 0.2093, d.f.= 9) (b), **KMO** (t= 0.9726, P= 0.3537, d.f.= 10) (c), or **KYNU** (t= 1.752, P= 0.1103. d.f.= 10) (d) (**figure 4.3.1.5**).

4.3.1.6 Effect of IFNγ on the concentrations of tryptophan, kynurenine, 3-hydroxykynurenine and the kynurenine/tryptophan ratio in the CM of primary cortical mixed glia

Stimulation of primary mixed glia with IFNγ decreased the concentration of **tryptophan** (t= 3.138, P= 0.0048, d.f.= 22) (a), **kynurenine** (t= 4.08, P= 0.0005, d.f.= 22) (b), but had no effect on **3-hydroxykynurenine** (t= 0.2423, P= 0.8108, d.f.= 22) (c) or the **kynurenine over tryptophan ratio** (t= 0.187, P= 0.8534, d.f.= 22) in the CM of primary mixed glia (**figure 4.3.1.6**).

4.3.1.7 Effect of CM from IFNγ-stimulated primary mixed glia on neuronal viability and neuronal complexity

CM from IFNγ-stimulated primary mixed glia had no effect on **neuronal viability** (t=1.677, P= 0.1158, d.f. = 14) (a; *LHS*). Direct treatment with IFNγ had no effect on **neuronal viability** (t=6.121, P= 0.5503, d.f. = 14) (a; *RHS*).

CM from IFNγ-stimulated mixed glia reduced the number of **neuritic branches** (t= 4.187, P= 0.0002, d.f. = 33) (b; *LHS*), **neurite length** (t= 6.423, P<0.0001, d.f. = 33) (c; *LHS*) and the number of **primary neurites** (t= 3.734, P= 0.0007, d.f. = 33) (d; *LHS*).

Two-way repeated measures ANOVA of the number of **neuritic branches at specific distances from the neuronal cell soma** showed an effect of distance [$F_{(25, 825)} = 335.4$, $P<0.0001$], IFNγ CM [$F_{(1, 825)} = 22.15$, $P<0.0001$], and an interaction [$F_{(25, 825)} = 2.189$, $P= 0.0007$]. *Post hoc* analysis revealed reductions following treatment with IFNγ CM in the number of branches at 10, 20, 30, 40 μm ($P<0.0001$) and 50 μm ($P<0.05$) from the cell soma compared to control CM (e).

IFNγ had no effect on the number of **neuritic branches** (t= 0.2737, P= 0.7856, d.f. = 45) (b; *RHS*), **neurite length** (t= 0.6309, P= 0.5313, d.f. = 45) (c; *RHS*), or the number of **primary neurites** (t= 0.7010, P= 0.4869, d.f. = 45) (d; *RHS*).

Two-way repeated measures ANOVA of the number of **neuritic branches at specific distances from the neuronal cell soma** showed an effect of distance [$F_{(25, 1025)} = 351.5$, P<0.0001], no effect of IFNγ [$F_{(1, 1025)} = 0.2009$, P= 0.6563], or an interaction [$F_{(25, 1025)} = 0.3837$, P= 0.9975] (f) (**figure 4.3.1.7**).

4.3.1.8 Effect of pre-treatment with 1-MT (L) on IFNγ-stimulated mixed glia CM-induced reductions in neuronal complexity

Two-way ANOVA of the number of **neuritic branches** showed an effect of IFNγ CM [$F_{(1, 66)} = 8.644$, P= 0.005], no effect of 1-MT (L) CM [$F_{(1, 66)} = 1.82$, P= 0.182], and an interaction [$F_{(1, 66)} = 4.22$, P= 0.044]. *Post hoc* analysis revealed reductions in the number of neuritic branches following treatment with IFNγ CM (P<0.01) compared to control CM. Pre-treatment with 1-MT (L) prevented IFNγ CM-induced reductions (P<0.05) (a).

Two-way ANOVA of **neurite length** showed an effect of 1-MT (L) CM [$F_{(1, 66)} = 9.909$, P= 0.003], IFNγ CM [$F_{(1, 66)} = 9.12$, P= 0.003], and an interaction [$F_{(1, 66)} = 19.661$, P= 0.004]. *Post hoc* analysis revealed reductions in neurite length following treatment with IFNγ CM (P<0.001) compared to control CM. Pre-treatment with 1-MT (L) prevented IFNγ CM-induced reductions (P<0.001) (b).

Two-way ANOVA of the number of **primary neurites** showed an effect of IFNγ CM [$F_{(1, 66)} = 6.929$, P= 0.011], no effect of 1-MT (L) CM [$F_{(1, 66)} = 3.629$, P= 0.061], and an interaction [$F_{(1, 66)} = 7.273$, P= 0.009]. *Post hoc* analysis revealed reductions in the number of primary neurites following treatment with IFNγ CM (P<0.01) compared to control CM. Pre-treatment with 1-MT (L) prevented IFNγ CM-induced reductions (P<0.01) (c).

Three-way repeated measures ANOVA of the number of **neuritic branches at specific distances from the neuronal cell soma** showed an effect of distance ($F_{(25, 1625)}= 750.83$, P<0.0001), IFNγ CM ($F_{(1, 65)}=$ 15.74, P<0.0001), IFNγ CM x distance ($F_{(25, 1625)}= 2.672$, P<0.0001), 1-MT (L) x IFNγ CM ($F_{(1, 65)}= 8.386$, P= 0.005), but no effect of 1-MT (L) CM ($F_{(1, 65)}= 1.411$, P= 0.239), 1-MT (L) CM x distance ($F_{(25, 1625)}=$ 0.111, P= 1.000), 1-MT (L) CM x IFNγ CM x distance ($F_{(25, 1625)}= 0.194$, P= 0.997). *Post hoc* analysis revealed reductions following treatment with IFNγ CM in the number of branches at 10, 20, 30 40, (P<0.001) and 50 μm (P<0.05) from the cell soma compared to control CM. Pre-treatment 1-MT (L) prevented IFNγ CM-induced reductions at 10, 20 30, 40 (P<0.001) and 50 μm (P<0.01) (d) (**figure 4.3.1.8**).

4.3.1.9 Effect of IFNγ on the mRNA expression of kynurenine pathway enzymes in primary cortical astrocytes

Stimulation of primary astrocytes with IFNγ increased the mRNA expression of **IDO** (t= 2.225, P= 0.0503, d.f.= 10) (a), **KMO** (t= 3.371, P= 0.0082, d.f.= 9) (c), reduced the mRNA expression of **TDO** (t= 4.495, P= 0.0015, d.f.= 9) (b), and **KYNU** (t= 3.906, P= 0.0036. d.f.= 9) (d), and had no effect on the mRNA expression of **KAT II** (t= 1.148, P= 0.2889, d.f.= 7) (e) (**figure 4.3.1.9**).

4.3.1.10 Effect of IFNγ on the concentrations of tryptophan, kynurenine, 3-hydroxykynurenine and the kynurenine/tryptophan ratio in the CM of primary cortical astrocytes

Stimulation of primary astrocytes with IFNγ had no effect on the concentration of **tryptophan** (t= 1.273, P= 0.2237, d.f. = 14) (a), **kynurenine** (t= 0.5093, P= 0.6185, d.f. = 14) (b), **3-hydroxykynurenine** (t= 0.3632, P= 0.7219, d.f. = 14) (c) or the **kynurenine over tryptophan ratio** (t= 1.137, P= 0.2748, d.f. = 14) in the CM of primary astrocytes (**figure 4.3.1.10**).

4.3.1.11 Effect of CM from IFNγ-stimulated primary cortical astrocytes on neuronal viability and measures of neuronal complexity

CM from IFNγ-stimulated primary cortical astrocytes increased **neuronal viability** (t= 2.681, P= 0.0179, d.f. = 14) (a).

CM from IFNγ-stimulated primary astrocytes had no effect on the number of **neuritic branches** (t= 0.9575, P= 0.3457, d.f. = 31) (b), **neurite length** (t= 0.05434, P= 0.9570, d.f. = 31) (c), or the number of **primary neurites** (t= 0.2705, P= 0.7886, d.f. = 31) (d).

Two-way repeated measures ANOVA of the number of **neuritic branches at specific distances from the neuronal cell soma** showed an effect of distance [$F_{(25, 775)} = 447.1$, $P<0.0001$], no effect of IFNγ CM [$F_{(1, 775)} = 0.002953$, P= 0.957], or an interaction [$F_{(25, 775)} = 0.7240$, P= 0.8357] (e) (**figure 4.3.1.11**).

4.3.1.12 Effect of IFNγ on the mRNA expression of kynurenine pathway enzymes in primary cortical neurons

Stimulation of primary cortical neurons with IFNγ increased the mRNA expression of **IDO** (t= 2.339, P= 0.0441, d.f.= 9) (a) while having no effect on the mRNA expression of **TDO** (t= 0.6431, P= 0.5362, d.f.= 9) (b), **KMO** (t= 1.424, P= 0.1882, d.f.= 9) (c), **KYNU** (t= 2.114, P= 0.0607, d.f.= 9) (d), or **KAT II** (t= 1.269, P= 0.2363, d.f.= 9) (e) (**figure 4.3.1.12**).

4.3.1.13 Effect of IFNγ on the concentrations of tryptophan, kynurenine, 3-hydroxykynurenine and the kynurenine/tryptophan ratio in the CM of primary cortical neurons

Stimulation of primary cortical neurons with IFNγ had no effect on the concentration of **tryptophan** (t= 08494, P= 0.4099 d.f. = 14) (a), **kynurenine** (t= 1.266, P= 0.2263, d.f. = 14) (b), **3-hydroxykynurenine** (t= 1.512, P= 0.1527, d.f. = 14) (c) or the **kynurenine over tryptophan ratio** (t= 0.5936, P= 0.5622, d.f. = 14) in the CM of primary neurons (**figure 4.3.1.13**).

4.3.1.14 Effect of pre-treatment with 1-MT (L) on IFNγ-stimulated mixed glia CM-induced reductions in the expression of synaptic markers in mature neurons

CM from IFNγ-stimulated primary mixed glia had no effect on **neuronal viability** of mature neurons (t=0.9406, P= 0.3581, d.f. = 20) (b; *LHS*). Direct treatment with IFNγ had no effect on **neuronal viability** of mature neurons (t=1.668, P= 0.1160, d.f. = 15) (b; *RHS*).

CM from IFNγ-stimulated primary mixed glia reduced the **co-localised expression of synaptic markers** (t= 6.568, P<0.0001, d.f. = 101) (b; *LHS*). Direct treatment with IFNγ had no effect on the **co-localised expression of synaptic markers** (t= 0.4141, P= 0.9671, d.f. = 96) (b; *RHS*). CM from IFNγ-stimulated primary mixed glia had no effect on the number of **synaptophysin puncta** (t= 0.02711, P= 0.978, d.f. = 101) (c; *LHS*). Direct treatment with IFNγ had no effect on the number of **synaptophysin puncta** (t= 0.004945, P= 0.9961, d.f. = 96) (c; *RHS*). CM from IFNγ-stimulated primary mixed glia reduced the number of **PSD-95 puncta** (t= 3.778, P= 0.0003, d.f. = 96) (d; *LHS*). Direct treatment with IFNγ had no effect on the number of **PSD-95 puncta** (t= 0.3027, P= 0.7628, d.f. = 96) (d; *RHS*).

Two-way ANOVA of the **co-localised expression of synaptic markers** showed an effect of IFNγ CM [$F_{(1, 171)} = 6.121$, P= 0.014], an interaction [$F_{(1, 171)} = 8.732$, P= 0.004], and no effect of 1-MT (L) CM [$F_{(1, 171)} = 1.811$, P= 0.18]. *Post hoc* analysis revealed reductions in the expression of co-localised synaptic markers following treatment with IFNγ CM (P<0.001) compared to control CM. Pre-treatment with 1-MT (L) prevented IFNγ CM-induced reductions (P<0.01) (e).

Two-way ANOVA of the number of **synaptophysin puncta** showed no effect of 1-MT (L) CM [$F_{(1, 170)} = 0.494$, P= 0.483], IFNγ CM [$F_{(1, 170)} = 1.681$, P= 0.1997], or an interaction [$F_{(1, 170)} = 1.254$, P= 0.264] (f).

Two-way ANOVA of the number of **PSD-95 puncta** showed an effect of IFNγ CM [$F_{(1, 171)} = 30.282$, P<0.0001], no effect of 1-MT (L) CM [$F_{(1, 171)} = 2.79$, P= 0.097], and no interaction [$F_{(1, 171)} = 0.531$, P= 0.467]. *Post hoc* analysis revealed reductions in the number of PSD-95 puncta following treatment with IFNγ CM (P<0.05) compared to control CM. Pre-treatment with 1-MT (L) prevented IFNγ CM-induced reductions (P<0.001) (g) (**figure 4.3.1.14**).

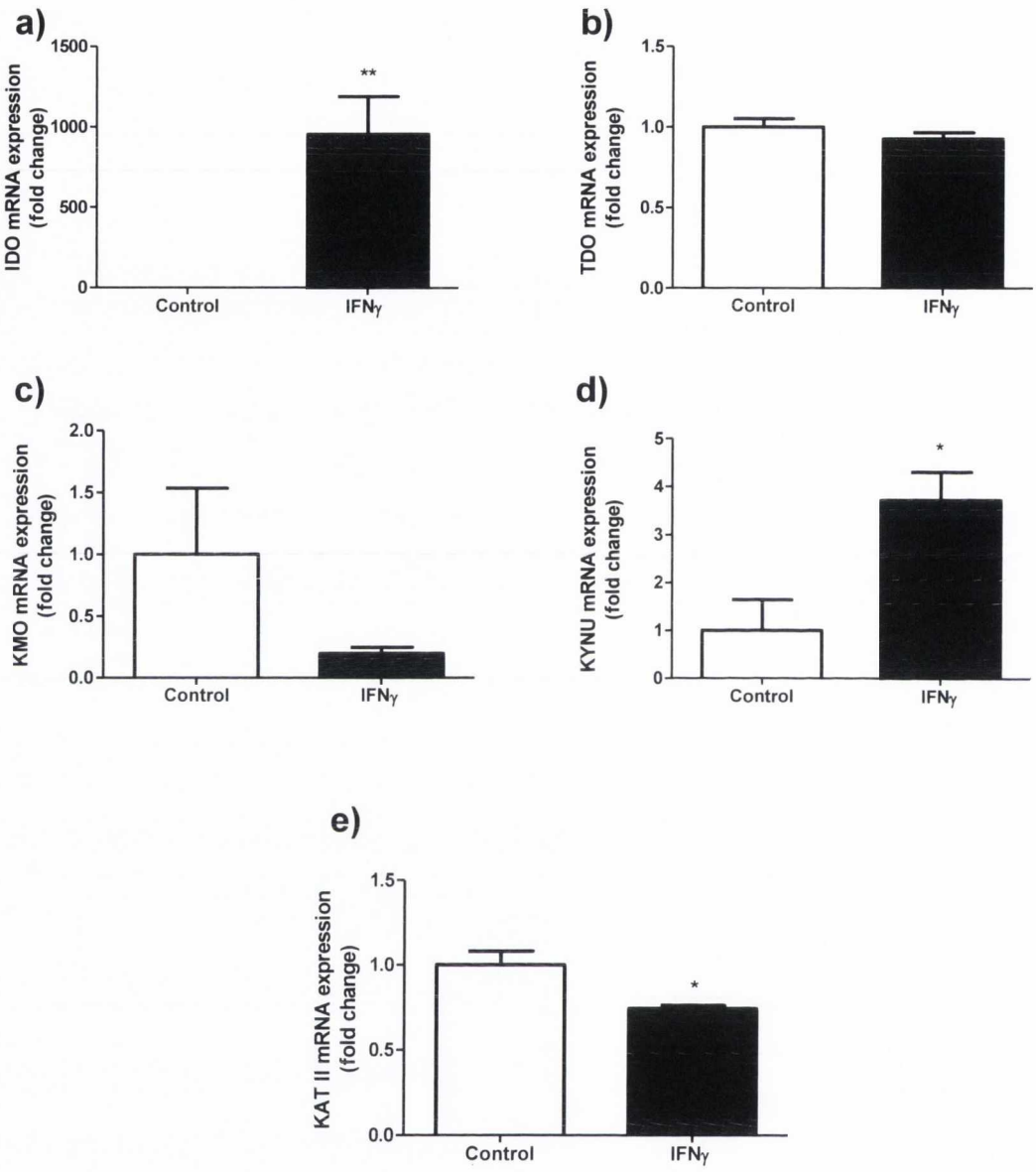

Figure 4.3.1.1: Effect of IFNγ on the mRNA expression of kynurenine pathway enzymes in primary cortical microglia

Primary cortical microglia (DIV 12-13) were stimulated with IFNγ (10 ng/ml) for 6 hr. Cells were harvested for mRNA extraction followed by quantitative PCR analysis of the expression of (a) IDO, (b) TDO, (c) KMO, (d) KYNU, and (e) KAT II. Data expressed as mean ± SEM (n= 5-6). *P<0.05, **P<0.01 vs. control (Student's *t*-test).

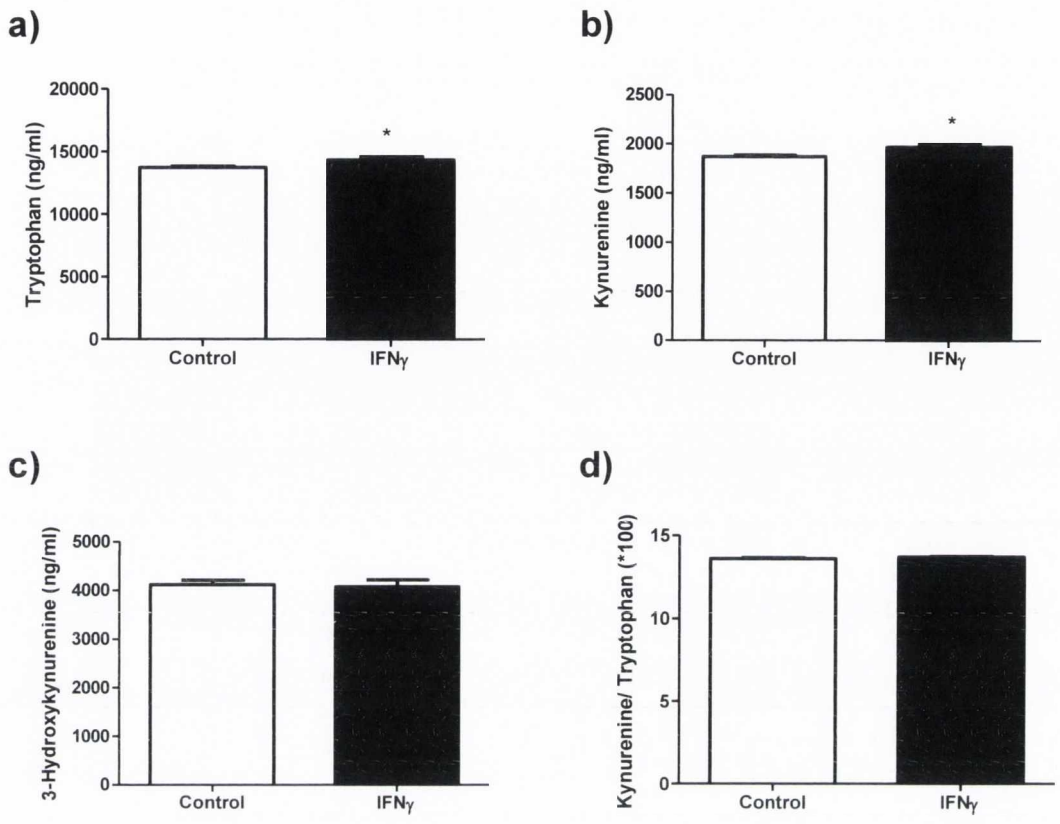

Figure 4.3.1.2: Effect of IFNγ on the concentrations of tryptophan, kynurenine, 3-hydroxykynurenine and the kynurenine/tryptophan ratio in the CM of primary cortical microglia
Primary cortical microglia (DIV 12-13) were stimulated with IFNγ (10 ng/ml) for 24 hr. CM was harvested for analysis of the concentrations of (a) tryptophan, (b) kynurenine, (c) 3-hydroxykynurenine, and (d) the kynurenine over tryptophan ratio. Data expressed as mean ± SEM (n= 12, from 2 independent experiments). *P<0.05, vs. control (Student's *t*-test).

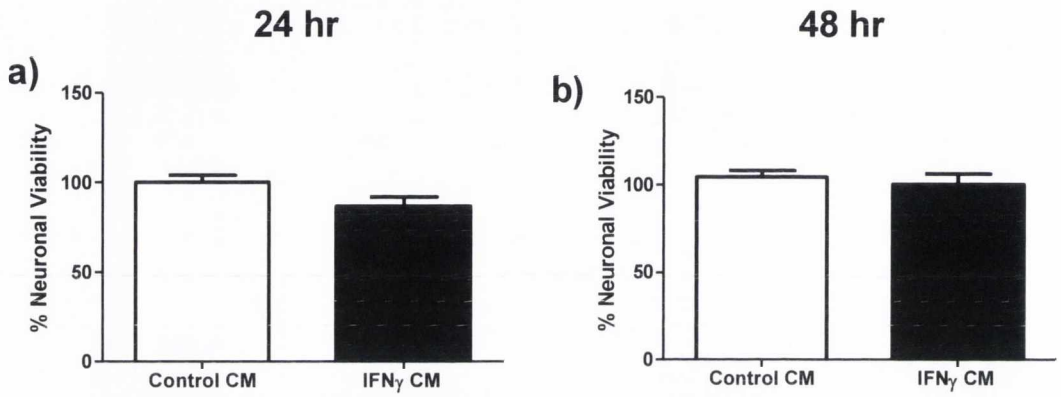

Figure 4.3.1.3: Effect of CM from IFNγ-stimulated primary cortical microglia on neuronal viability
CM from primary cortical microglia (DIV 12-13) treated with IFNγ (10 ng/ml; 24 hr) was placed on primary cortical neurons (DIV 3) for 24 (a) or 48 hr (b). Neuronal viability was assessed using the alamarBlue® cell proliferation assay. Data are expressed as mean ± SEM (n= 11-12 wells from 2 independent experiments) (Student's *t*-test).

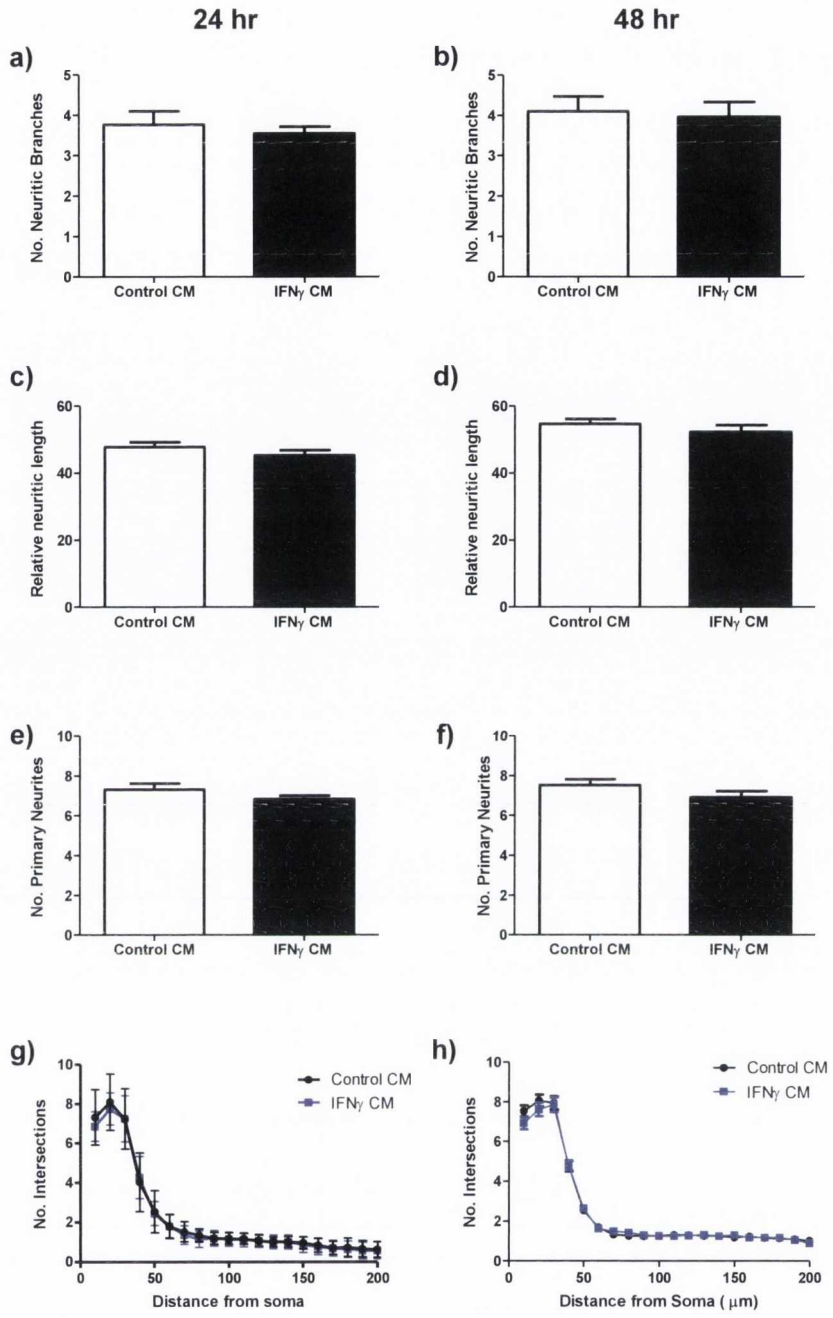

Figure 4.3.1.4: Effect of CM from IFNγ-stimulated primary cortical microglia on measures of neuronal complexity

CM from primary cortical microglia (DIV 12-13) treated with IFNγ (10 ng/ml; 24 hr) was placed on primary cortical neurons (DIV 3) for 24 or 48 hr. Sholl analysis was performed on neurons to examine (a, b) the number of neuritic branches, (c, d) neurite length, (e, f) the number of primary neurites, and (g, h) the number of branches at varying distances from the cell soma. Data expressed as mean ± SEM (n= 19-22 coverslips from 3 independent experiments) [Student's *t*-test (a-f), two-way repeated measures ANOVA (g, h)].

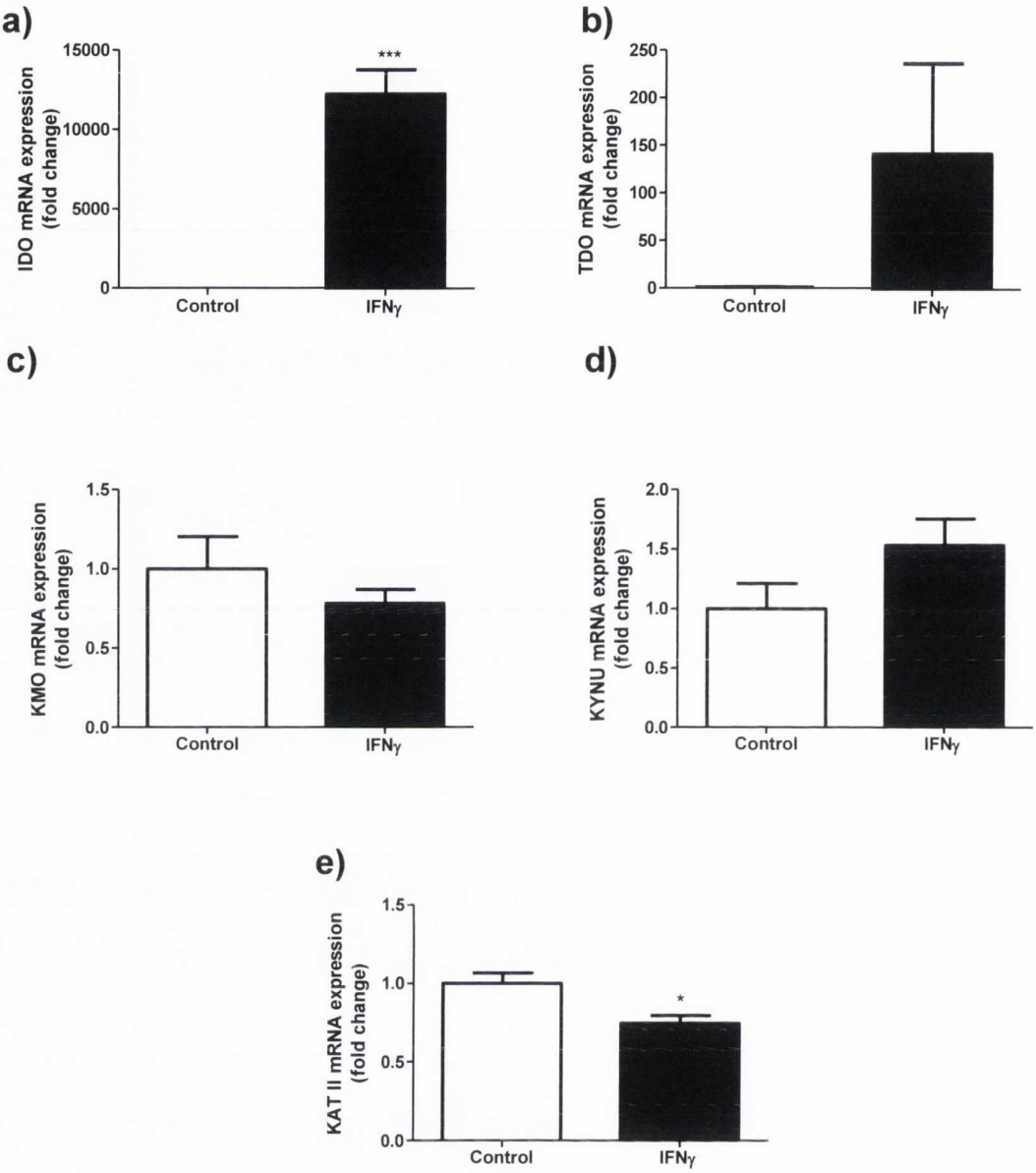

Figure 4.3.1.5: Effect of IFNγ on the mRNA expression of kynurenine pathway enzymes in primary mixed glia

Primary cortical mixed glia (DIV 12-13) were stimulated with IFNγ (10 ng/ml) for 6 hr. Cells were harvested for mRNA extraction followed by quantitative PCR analysis of the expression of (a) IDO, (b) TDO, (c) KMO, (d) KYNU, and (e) KAT II. Data expressed as mean ± SEM (n= 5-6). *P<0.05, ***P<0.001 vs. control (Student's *t*-test).

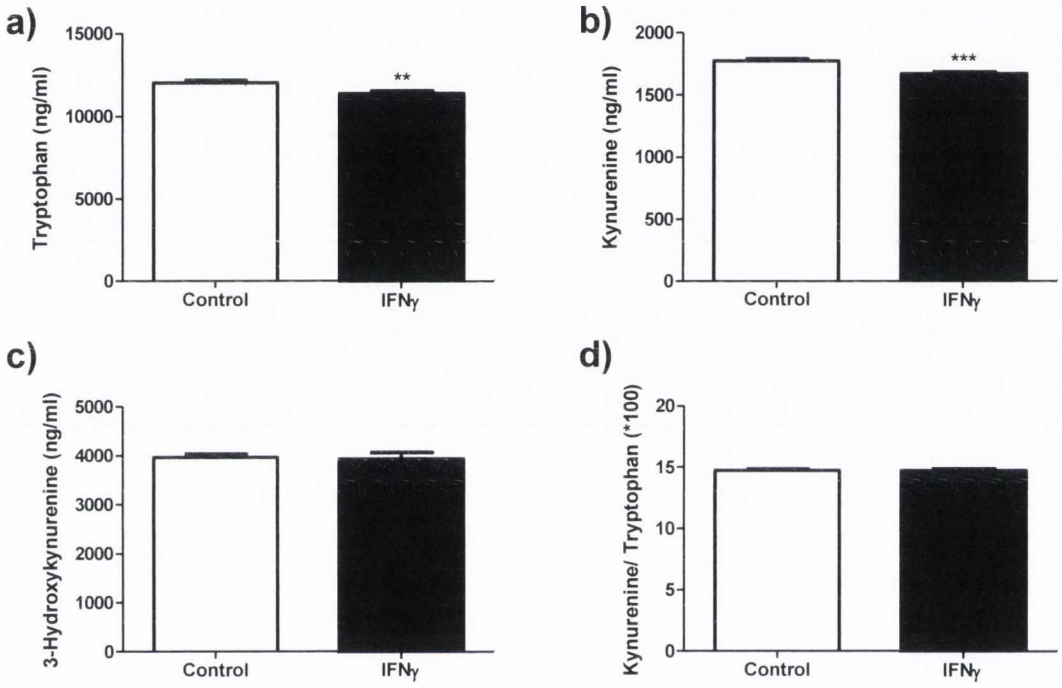

Figure 4.3.1.6: Effect of IFNγ on the concentrations of tryptophan, kynurenine, 3-hydroxykynurenine and the kynurenine/tryptophan ratio in the CM of primary cortical mixed glia
Primary cortical mixed glia (DIV 12-13) were stimulated with IFNγ (10 ng/ml) for 24 hr. CM was harvested for analysis of the concentrations of (a) tryptophan, (b) kynurenine, (c) 3-hydroxykynurenine, and (d) the kynurenine over tryptophan ratio. Data expressed as mean ± SEM (n= 12, from 2 independent experiments). **P<0.01, ***P<0.001, vs. control (Student's *t*-test).

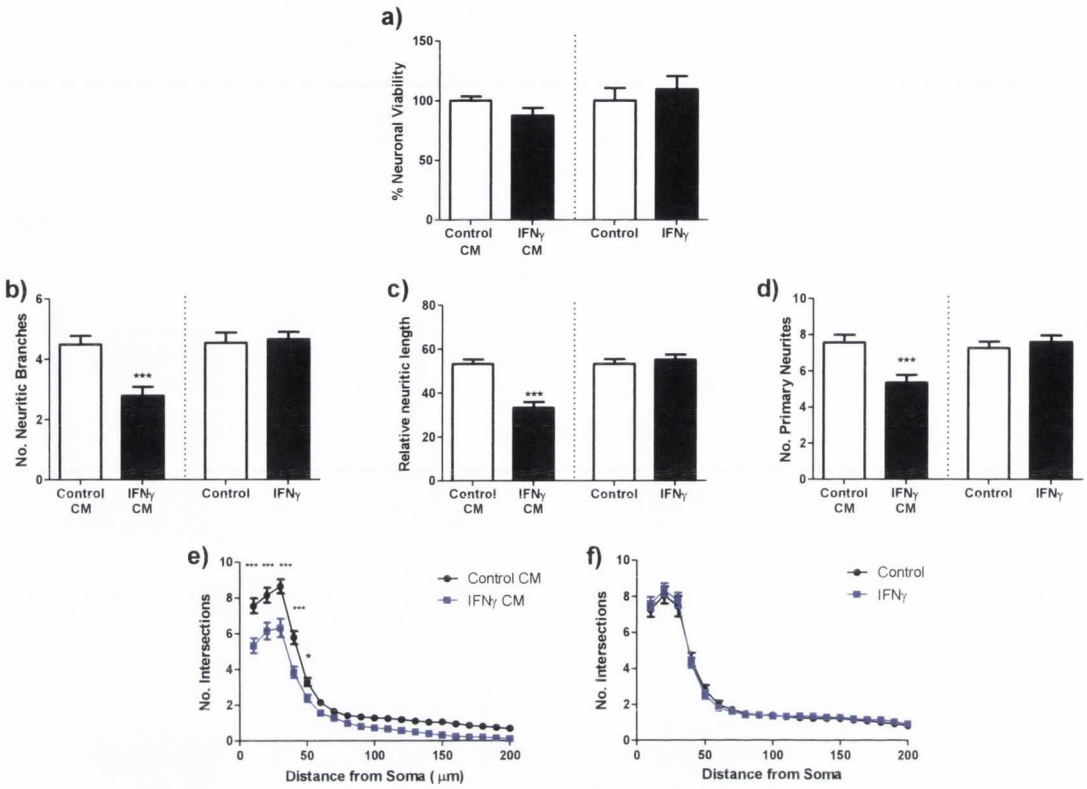

Figure 4.3.1.7: Effect of CM from IFNγ-stimulated primary cortical mixed glia on neuronal viability and neuronal complexity

CM from primary cortical mixed glia (DIV 12-13) treated with IFNγ (10 ng/ml; 24 hr) (left) or IFNγ (10 ng/ml) was applied directly to primary cortical neurons (DIV 3) for 24 hr (right). Neuronal viability was assessed using the alamarBlue® cell proliferation assay (a). Data are expressed as mean ± SEM (n= 11-12 wells from 2 independent experiments). Sholl analysis was performed on neurons to examine (b) the number of neuritic branches, (c) neurite length, (d) the number of primary neurites, and (e, f) the number of branches at varying distances from the cell soma. Data expressed as mean ± SEM (n= 17-24 coverslips from 3 independent experiments). *P<0.05, ***P<0.001, vs. respective control [Student's *t*-test (a-d), two-way repeated measures ANOVA followed by Bonferroni *post hoc* test (e, f)].

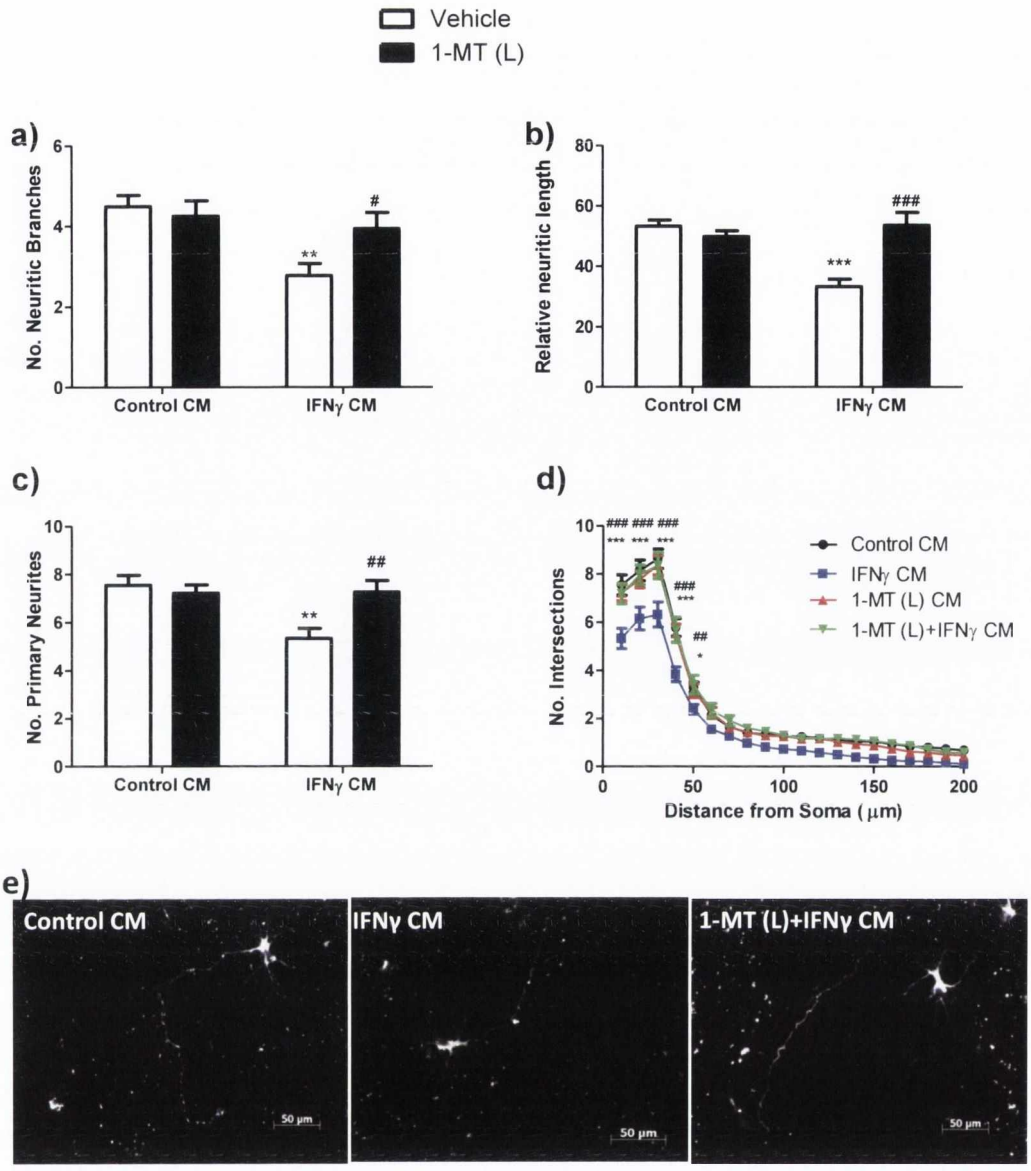

Figure 4.3.1.8: Effect of 1-MT (L) on IFNγ-stimulated mixed glia CM-induced reductions in neuronal complexity

CM from primary cortical mixed glia (DIV 12-13) pre-treated with either vehicle or 1-MT (L) (0.5 mM; 30 min) followed by stimulation with IFNγ (10 ng/ml; 24 hr) was placed on primary cortical neurons (DIV 3) for 24 hr. Sholl analysis was performed on neurons to examine (a) the number of neuritic branches, (b) neurite length, (c) the number of primary neurites, and (d) the number of branches at varying distances from the cell soma. Representative images of neurons identified using the neuronal structural marker β-III tubulin (white) and the nuclear stain DAPI (blue) with fluorescent microscopy (e). Data expressed as mean ± SEM (n= 17-18 coverslips from 3 independent experiments). *P<0.05, **P<0.01, ***P<0.001, vs. control CM, #P<0.05, ##P<0.01, ###P<0.001, vs. IFNγ CM [Two-way ANOVA followed by Newman Keuls *post hoc* test (a-c), three-way repeated measures ANOVA followed by Bonferroni *post hoc* test (d)].

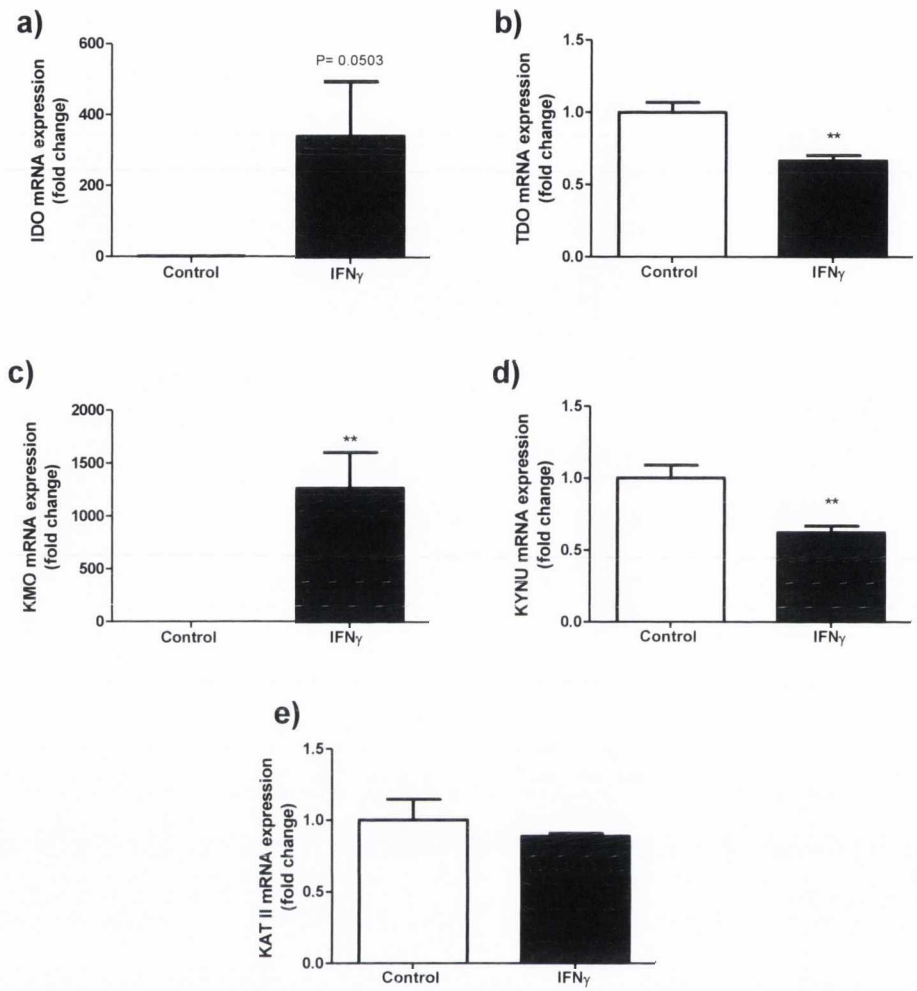

Figure 4.3.1.9: Effect of IFNγ on the mRNA expression of kynurenine pathway enzymes in primary cortical astrocytes

Primary cortical astrocytes (DIV 12-13) were stimulated with IFNγ (10 ng/ml) for 6 hr. Cells were harvested for mRNA extraction followed by quantitative PCR analysis of the expression of (a) IDO, (b) TDO, (c) KMO, (d) KYNU, and (e) KAT II. Data expressed as mean ± SEM (n= 3-6). **P<0.01 vs. control (Student's *t*-test).

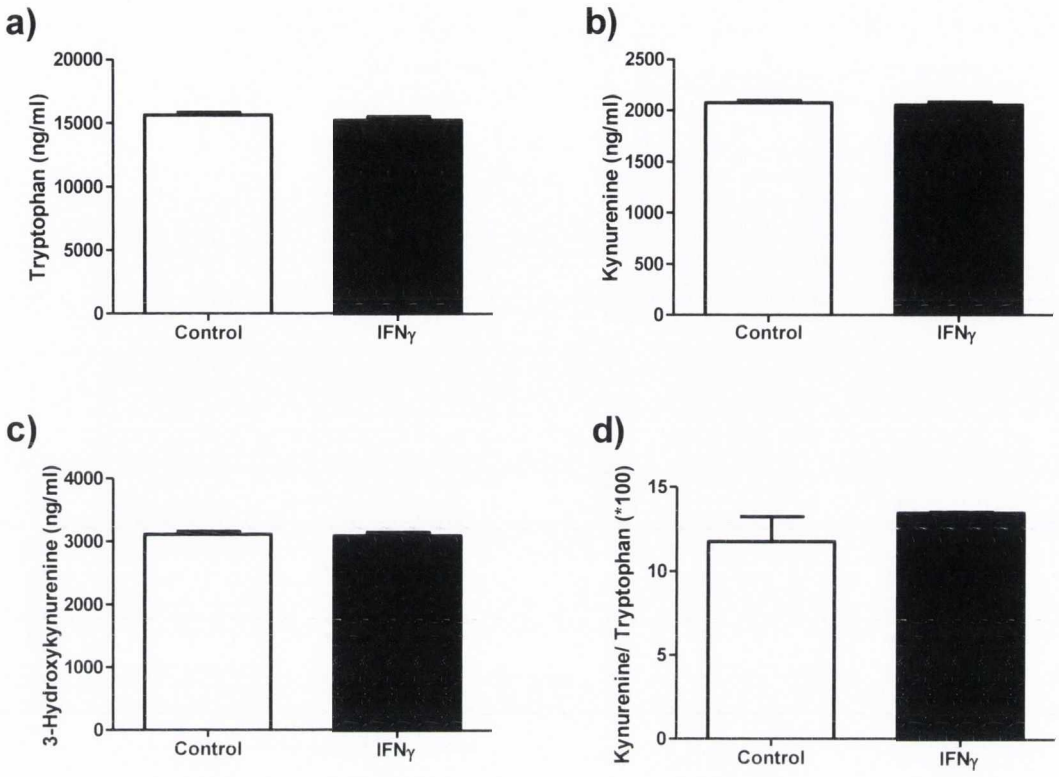

Figure 4.3.1.10: Effect of IFNγ on the concentrations of tryptophan, kynurenine, 3-hydroxykynurenine and the kynurenine/tryptophan ratio in the CM of primary cortical astrocytes
Primary cortical astrocytes (DIV 12-13) were stimulated with IFNγ (10 ng/ml) for 24 hr. CM was harvested for analysis of the concentrations of (a) tryptophan, (b) kynurenine, (c) 3-hydroxykynurenine, and (d) the kynurenine over tryptophan ratio. Data expressed as mean ± SEM (n= 12, from 2 independent experiments) (Student's *t*-test).

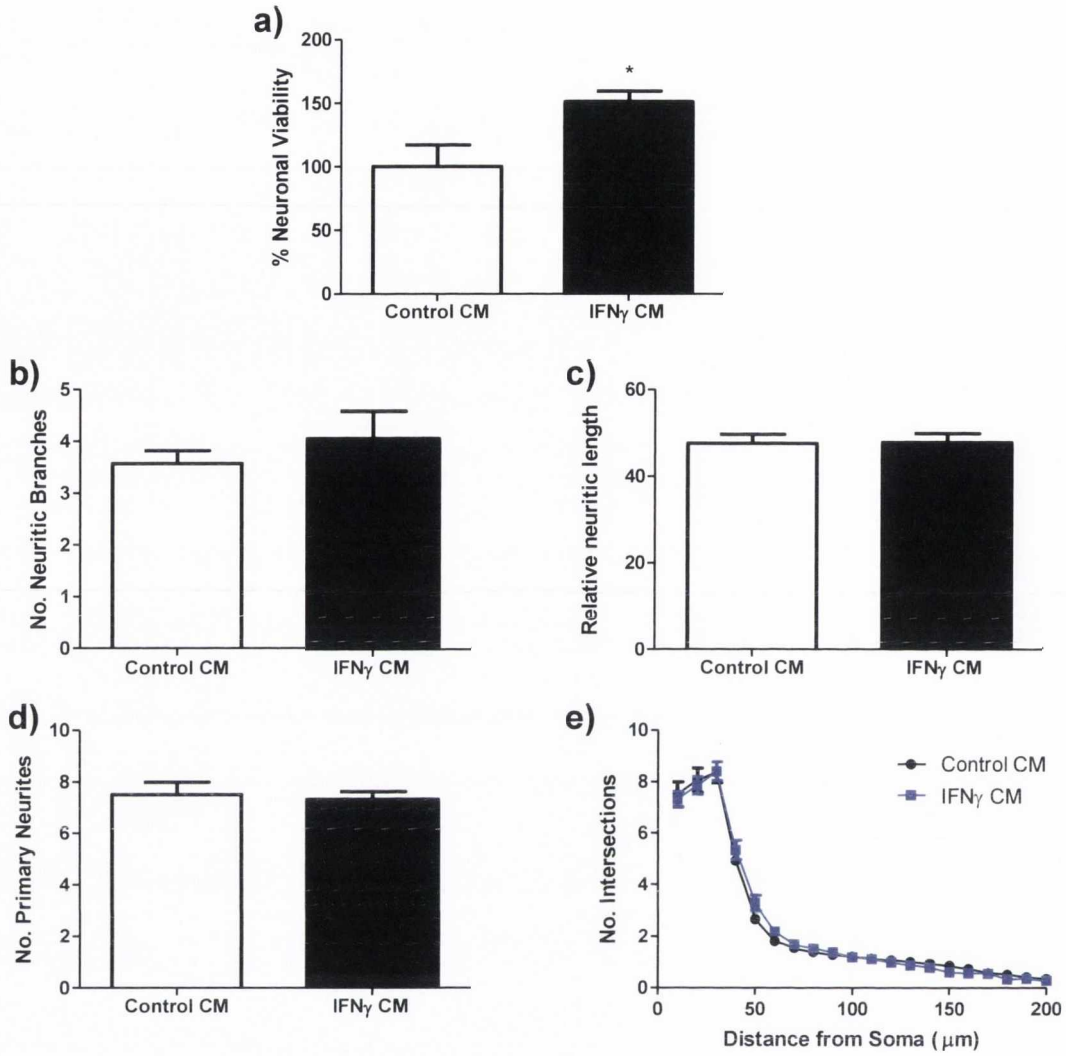

Figure 4.3.1.11: Effect of CM from IFNγ-stimulated primary cortical astrocytes on neuronal viability and measures of neuronal complexity

CM from primary cortical astrocytes (DIV 12-13) treated with IFNγ (10 ng/ml; 24 hr) was placed on primary cortical neurons (DIV 3) for 24 hr. Neuronal viability was assessed using the alamarBlue® cell proliferation assay (a). Data are expressed as mean ± SEM (n= 8 wells from 2 independent experiments). Sholl analysis was performed on neurons to examine (b) the number of neuritic branches, (c) neurite length, (d) the number of primary neurites, and (e) the number of branches at varying distances from the cell soma. Data expressed as mean ± SEM (n= 13-20 coverslips from 2 independent experiments) [Student's *t*-test (a-d), two-way repeated measures ANOVA followed by Bonferroni *post hoc* test (e)].

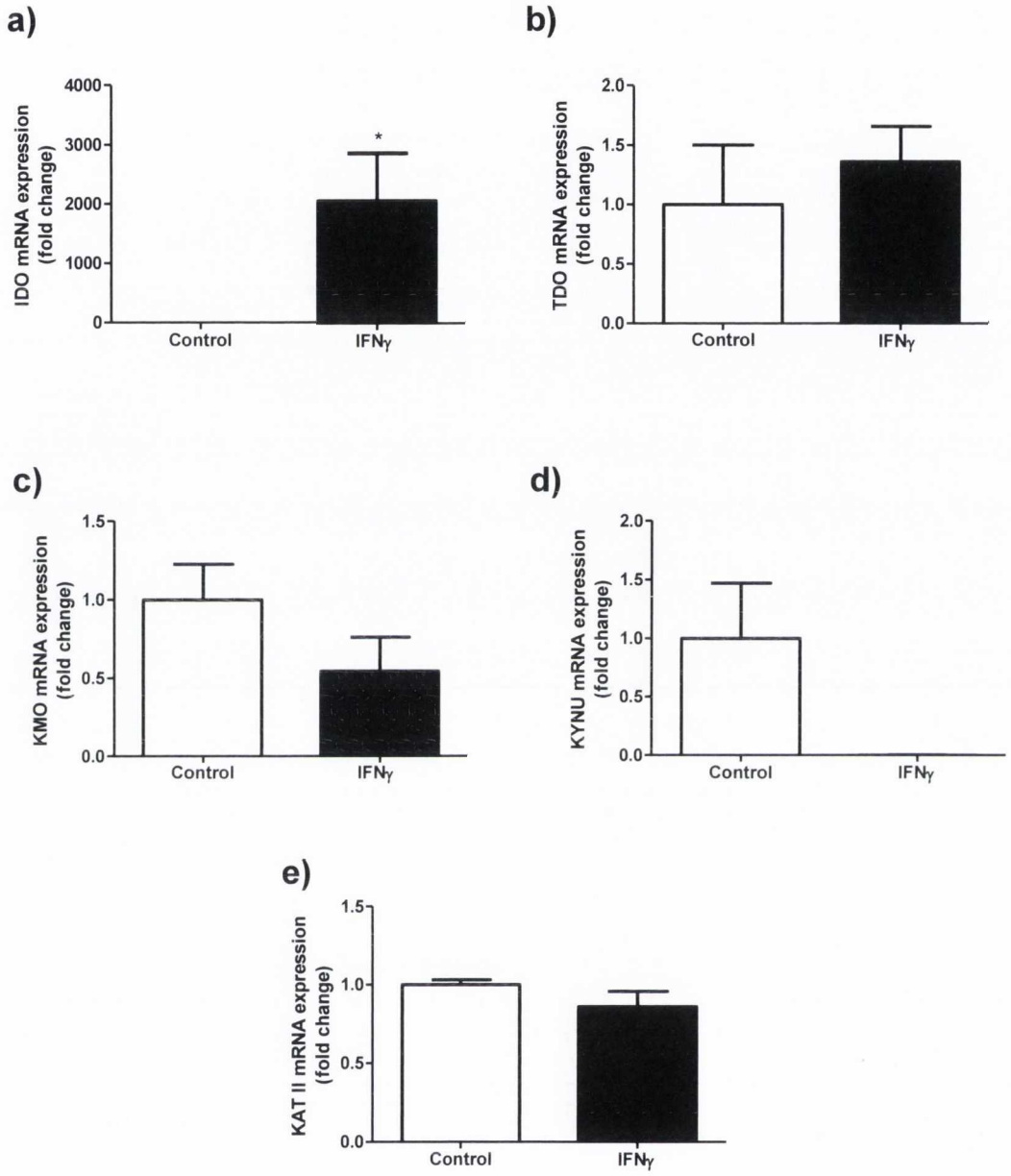

Figure 4.3.1.12: Effect of IFNγ on the mRNA expression of kynurenine pathway enzymes in primary cortical neurons

Primary cortical neurons (DIV 3) were stimulated with IFNγ (10 ng/ml) for 6 hr. Cells were harvested for mRNA extraction followed by quantitative PCR analysis of the expression of (a) IDO, (b) TDO, (c) KMO, (d) KYNU, and (e) KAT II. Data expressed as mean ± SEM (n= 5-6). *P<0.05 vs. control (Student's *t*-test).

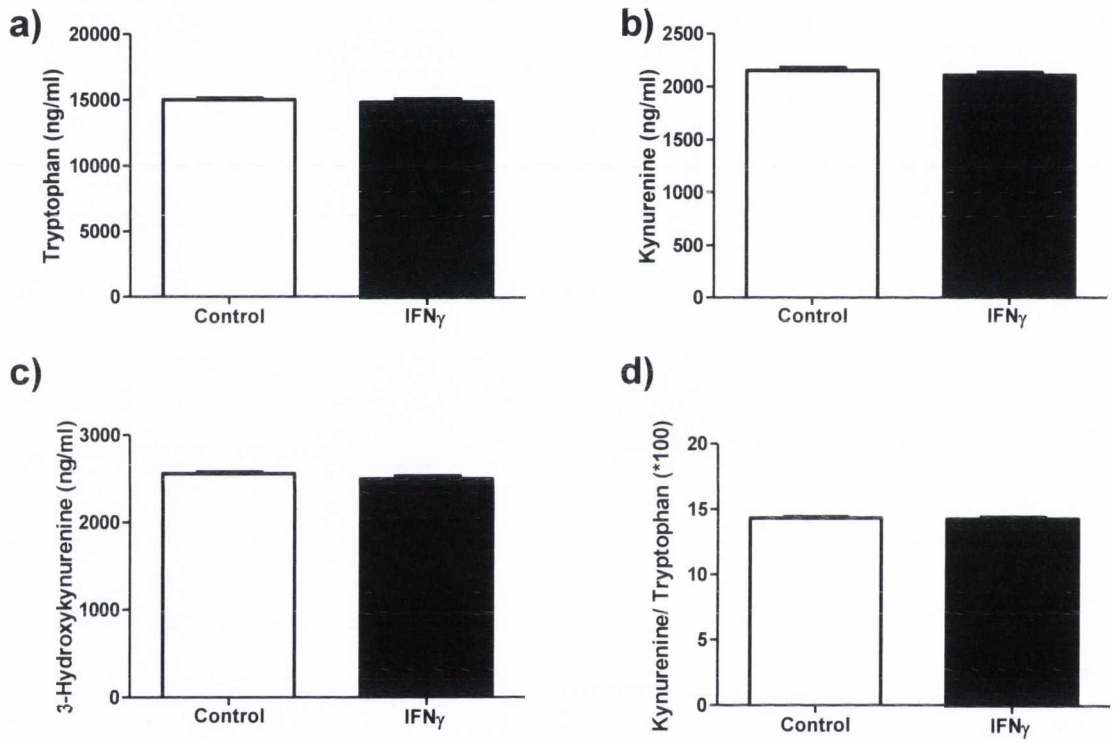

Figure 4.3.1.13: Effect of IFNγ on the concentrations of tryptophan, kynurenine, 3-hydroxykynurenine and the kynurenine/tryptophan ratio in the CM of primary cortical neurons
Primary cortical neurons (DIV 3) were stimulated with IFNγ (10 ng/ml) for 24 hr. CM was harvested for analysis of the concentrations of (a) tryptophan, (b) kynurenine, (c) 3-hydroxykynurenine, and (d) the kynurenine over tryptophan ratio. Data expressed as mean ± SEM (n= 12, from 2 independent experiments) (Student's *t*-test).

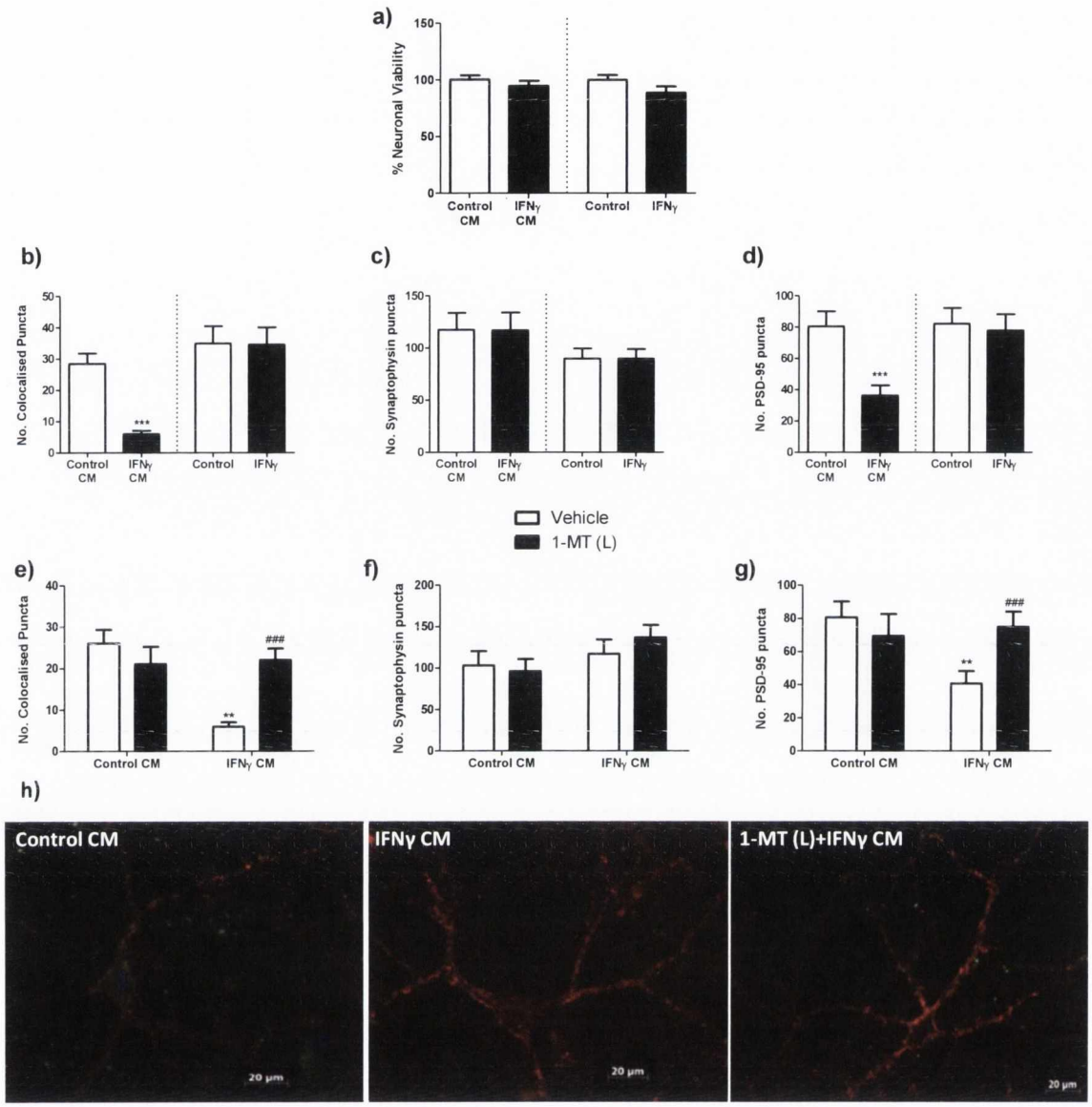

Figure 4.3.1.14: Effect of 1-MT (L) on IFNγ-stimulated mixed glia CM-induced reductions the expression of synaptic markers in mature neurons

IFNγ (10 ng/ml) or CM from primary mixed glia (DIV 12-13) pre-treated with either vehicle or 1-MT (L) (0.5 mM; 30 min) followed by stimulation with IFNγ (10 ng/ml; 24 hr) was placed on primary cortical neurons (DIV 18-21) for 24 hr. Neuronal viability of one set of neurons was assessed using the alamarBlue® cell proliferation assay (a). Data expressed as mean ± SEM (n= 8-11 wells from 2 independent experiments) (Student's *t* test). Another set of neurons were examined to determine the co-localised expression of pre- and post-synaptic markers synaptophysin and PSD-95 (b, e), and the number of synaptophysin puncta (c, f), and PSD-95 puncta (d, g) in isolation using ImageJ software. Representative images of neuron stained with the anti-synaptophysin antibody (red), the anti-PSD-95 antibody (green) and the nuclear stain DAPI (blue) with fluorescent microscopy (h). Data expressed as mean ± SEM (n= 37-53 neurons from 3 independent experiments). **P<0.01, ***P<0.01, vs. control CM, ###P<0.001, vs. IFNγ CM [Student's *t* test (a-d) or two-way ANOVA followed by Newman Keuls *post hoc* test (e, f, g)].

4.3.2 Examination of the effect of kynurenine pathway metabolites on neuronal integrity

4.3.2.1 Concentration-related effects of kynurenine pathway metabolites on the viability of neurons

One-way ANOVA of **neuronal viability** showed an effect of kynurenic acid [$F_{(6, 111)}$= 4.381, P= 0.0005] (f), but not of tryptophan [$F_{(4, 60)}$= 5.016, P= 0.7346] (a), kynurenine [$F_{(2, 36)}$= 1.86, P= 0.1712] (b), 3-hydroxykynurenine [$F_{(3, 45)}$= 0.8460, P= 0.4765] (c), 3-hydroxyanthranillic acid [$F_{(3, 47)}$= 0.819, P= 0.4904] (d) or quinolinic acid [$F_{(5, 64)}$= 1.757, P= 0.1358] (e). *Post hoc* analysis revealed increases in neuronal viability following treatment with kynurenic acid 0.03 μM (P<0.01) compared to control (**figure 4.3.2.1**).

4.3.2.2 Concentration-related effect of tryptophan on measures of neuronal complexity

One-way ANOVA of the number of **neuritic branches** [$F_{(4, 117)}$ = 0.6842, P= 0.6044] (a), **neurite length** [$F_{(4, 117)}$ = 1.551, P= 0.1923] (b), or the number of **primary neurites** [$F_{(4, 117)}$ = 0.3327, P=0.8555] (c) showed no effect of tryptophan.

Two-way repeated measures ANOVA of the number of **neuritic branches at specific distances from the neuronal cell soma** showed an effect of distance [$F_{(25, 2825)}$ = 1311, P<0.0001], no effect of tryptophan [$F_{(4, 2825)}$ = 1.55, P= 0.1925], and no interaction [$F_{(100, 2825)}$ = 0.5758, P= 0.9998] (d) (**figure 4.3.2.2**).

4.3.2.3 Concentration-related effect of kynurenine on measures of neuronal complexity.

One-way ANOVA of the number of **neuritic branches** [$F_{(27, 69)}$ = 0.9087, P= 0.4079] (a), **neurite length** [$F_{(27, 69)}$ = 1.906, P= 0.1566] (b), or the number of **primary neurites** [$F_{(27, 69)}$ = 0.8868, P= 0.4167] (c) showed no effect of kynurenine.

Two-way repeated measures ANOVA of the number of **neuritic branches at specific distances from the neuronal cell soma** showed an effect of distance [$F_{(25, 1675)}$ = 962.5, P<0.0001], no effect of kynurenine [$F_{(2, 1675)}$ = 1.906, P= 0.1566], and no interaction [$F_{(50, 1675)}$ = 0.7176, P= 0.9316] (d) (**figure 4.3.2.3**).

4.3.2.4 Concentration-related effect of 3-hydroxykynurenine on measures of neuronal complexity

One-way ANOVA of the number of **neuritic branches** showed no effect of 3-hydroxykynurenine [$F_{(3, 84)} = 0.9441$, $P= 0.4223$] (a).

One-way ANOVA of **neurite length** showed an effect of 3-hydroxykynurenine [$F_{(3, 84)} = 3.096$, $P= 0.0314$]. *Post hoc* analysis revealed reductions in neurite length following treatment with 3-hydroxykynurenine 0.1 μM ($P<0.05$) compared to control (b).

One-way ANOVA of the number of **primary neurites** showed an effect of 3-hydroxykynurenine [$F_{(3, 84)} = 2.888$, $P= 0.0407$]. *Post hoc* analysis revealed reductions in the number of primary neurites following treatment with 3-hydroxykynurenine 0.1 μM ($P<0.05$) compared to control (c).

Two-way repeated measures ANOVA of the number of **neuritic branches at specific distances from the neuronal cell soma** showed an effect of distance [$F_{(25, 2025)} = 1069$, $P<0.0001$], no effect of 3-hydroxykynurenine [$F_{(3, 2025)} = 1.744$, $P= 0.1586$], or an interaction [$F_{(75, 2025)} = 0.613$, $P= 0.9963$] (d) (**figure 4.3.2.4**).

4.3.2.5 Concentration-related effect of 3-hydroxyanthranillic acid on measures of neuronal complexity

One-way ANOVA of the number of **neuritic branches** showed no effect of 3-hydroxyanthranillic acid [$F_{(3, 81)} = 0.549$, $P= 0.6503$] (a).

One-way ANOVA of **neurite length** showed an effect of 3-hydroxyanthranillic acid [$F_{(3, 81)} = 8.061$, $P<0.0001$]. *Post hoc* analysis revealed reductions in neurite length following treatment with 3-hydroxyanthranillic acid 0.01 μM ($P<0.05$) and 0.1 μM ($P<0.01$) compared to control (b).

One-way ANOVA of the number of **primary neurites** showed an effect of 3-hydroxyanththranillic acid [$F_{(3, 81)} = 2.843$, $P= 0.0431$]. *Post hoc* analysis revealed reductions in the number of primary neurites following treatment with 3-hydroxyanthranillic acid 0.1 μM ($P<0.05$) compared to control.

Two-way repeated measures ANOVA of the number of **neuritic branches at specific distances from the neuronal cell soma** showed an effect of distance [$F_{(25, 1950)} = 980.6$, $P<0.0001$], an effect of 3-hydroxyanthranillic acid [$F_{(3, 1950)} = 3.335$, $P= 0.0236$], but no interaction [$F_{(75, 1950)} = 1.073$, $P= 0.3166$]. *Post hoc* analysis revealed reductions in the number of branches at 10 μm and 20 μm from the soma following treatment with 3-hydroxyanthranillic acid (0.1 μM) ($P<0.001$) and at 20 μm from the soma following treatment with 3-hydroxyanthranillic acid 0.01 ($P<0.01$) and 0.03 μM ($P<0.05$) compared to control (d) (**figure 4.3.2.5**).

4.3.2.6 Concentration-related effect of quinolinic acid on measures of neuronal complexity.

One-way ANOVA of the number of **neuritic branches** showed an effect of quinolinic acid [$F_{(5, 138)}$ = 2.293, P= 0.0491]. *Post hoc* analysis revealed reductions in the number pf neuritic branches following treatment with quinolinic acid 1 μM (P<0.05) compared to control (a).

One-way ANOVA of **neurite length** showed an effect of quinolinic acid [$F_{(5, 138)}$ = 8.142, P<0.0001] (b). *Post hoc* analysis revealed reductions in neurite length following treatment with quinolinic acid 1 μM (P<0.01), 10 μM (P<0.05), 25μM (P<0.001) and 100 μM (P<0.001) compared to control (b).

One-way ANOVA of the number of **primary neurites** showed an effect of quinolinic acid [$F_{(5, 138)}$ = 4.517, P= 0.0008]. *Post hoc* analysis revealed reductions in the number of primary neurites following treatment with quinolinic acid 1 μM (P<0.001), 25 μM (P<0.05), and 100 μM (P<0.05) (c).

Two-way repeated measures ANOVA of the number of **neuritic branches at specific distances from the neuronal cell soma** showed an effect of distance [$F_{(25, 3225)}$ = 1504, P<0.0001], quinolinic acid ($F_{(5, 3225)}$ = 6.286, P<0.0001), and an interaction [$F_{(125, 3225)}$ = 1.274, P= 0.0233]. *Post hoc* analysis revealed reductions in the number of branches at 10 and 20 μm from the soma following treatment with quinolinic acid 0.1 μM (P<0.05), 1 μM (P<0.01), and 100 μM (P<0.05), at 30 μm from the soma following treatment with quinolinic acid 25 μM (P<0.01) and 100 μM (P<0.05), and at 40 μm from the soma following treatment with quinolinic acid 1 μM (P<0.05) compared to control (d) (**figure 4.3.2.6**).

4.3.2.7 Concentration-related effect of kynurenic acid on measures of neuronal complexity.

Left-hand side:

One-way ANOVA of the number **neuritic branches** [$F_{(3, 72)}$ = 0.08675, P= 0.9671] (a), **neurite length** [$F_{(3, 75)}$ = 1.434, P= 0.24] (b), or the number of **primary neurites** [$F_{(3, 73)}$ = 1.947, P= 0.1299] (c) showed no effect of kynurenic acid.

Two-way repeated measures ANOVA of the number of **neuritic branches at specific distances from the neuronal cell soma** showed an effect of distance [$F_{(25, 1800)}$ = 931.9, P<0.0001], no effect of kynurenic acid [$F_{(3, 1800)}$ = 1.434, P= 0.24], and no interaction [$F_{(75, 1800)}$ = 1.023 P= 0.4243] (d).

Right-hand side:

One-way ANOVA of the number of **neuritic branches** showed no effect of kynurenic acid [$F_{(3, 86)}$ = 2.621, P= 0.0561] (a).

One-way ANOVA of **neurite length** showed an effect of kynurenic acid [$F_{(3, 86)}$ = 5.996, P= 0.0009]. *Post hoc* analysis revealed reductions in neurite length following treatment with kynurenic acid 0.1 μM (P<0.01), 1 μM (P<0.01) and 10 μM (P<0.01) compared to control (b).

One-way ANOVA of the number of **primary neurites** showed an effect of kynurenic acid [$F_{(3, 86)}$ = 7.668, P= 0.0001]. *Post hoc* analysis revealed reductions in the number of primary neurites following treatment with kynurenic acid at 0.1 µM (P<0.001), 1 µM (P<0.001) and 10 µM (P<0.05) compared to control (c).

Two-way repeated measures ANOVA of the number of **neuritic branches at specific distances from the neuronal cell soma** showed an effect of distance [$F_{(25, 2225)}$ = 1177, P<0.0001], kynurenic acid [$F_{(3, 2225)}$ = 5.281, P= 0.0021], and an interaction [$F_{(75, 2225)}$ = 2.576, P<0.0001]. *Post hoc* analysis revealed reductions in the number of branches at 10 and 20 µm from the soma following treatment with kynurenic acid 0.1 µM (P<0.001), 1 µM (P<0.001) and 10 µM (P<0.05) compared to control (d) (**figure 4.3.2.7**).

4.3.2.8 Effect of combinations of kynurenine pathway metabolites on neuronal viability and complexity

One-way ANOVA of **neuronal viability** showed no effect of treatment [$F_{(4, 100)}$ = 1.19, P= 0.3202] (a).

One-way ANOVA of the number of **neuritic branches** showed no effect of treatment [$F_{(4, 107)}$ = 0.589, P= 0.6713] (b).

One-way ANOVA of **neurite length** showed an effect of treatment [$F_{(4, 107)}$ = 8.203, P<0.0001]. *Post hoc* analysis revealed reductions in neurite length following treatment with the combination of 3-hydroxykynurenine + 3-hydroxyanthranillic acid + quinolinic acid (P<0.001) compared to control (c).

One-way ANOVA of the number of **primary neurites** showed an effect of treatment [$F_{(4, 107)}$ = 4.041, P= 0.0044]. *Post hoc* analysis revealed reductions in the number of primary neurites following treatment with the combination of 3-hydroxykynurenine + 3-hydroxyanthranillic acid + quinolinic acid (P<0.05) compared to control. The combination of 3-hydroxykynurenine + 3-hydroxyanthranillic acid also caused reductions in the number of primary neurites (P<0.05) compared to control (d).

Two-way repeated measures ANOVA of the number of **neuritic branches at specific distances from the neuronal cell soma** showed an effect of distance [$F_{(25, 2575)}$ = 1564, P<0.0001], treatment [$F_{(4, 2575)}$ = 8.203, P<0.0001], and an interaction [$F_{(100, 2575)}$ = 1.717, P<0.0001]. *Post hoc* analysis revealed reductions in the number of branches at 10 µm (P<0.01) and 20 µm (P<0.05) from the soma following treatment with 3-hydroxykynurenine + 3-hydroxyanthranillic acid compared to control. Furthermore, *post hoc* analysis revealed reductions in branching at 10 µm (P<0.05), 30 µm, 40 µm (P<0.001) and 50 µM (P<0.05) from the soma following treatment with 3-hydroxykynurenine + 3-hydroxyanthranillic acid and quinolinic acid compared to control (e) (**figure 4.3.2.8**).

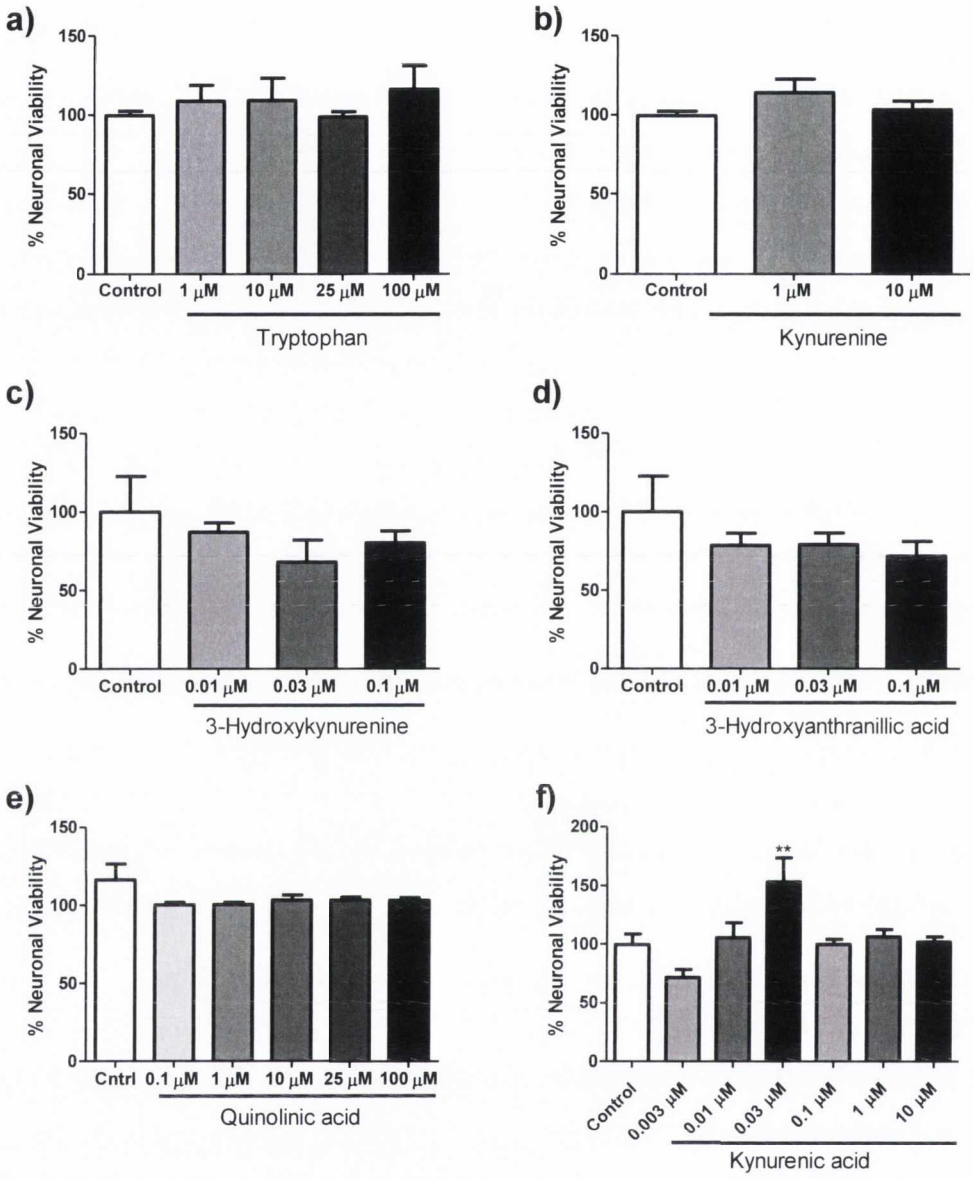

Figure 4.3.2.1: Concentration-related effects of kynurenine pathway metabolites on the viability of neurons

Primary cortical neurons (DIV 3) were treated with varying concentrations of tryptophan (1-100 μM) (a), kynurenine (1, 10 μM) (b), 3-hydroxykynurenine (0.01-0.1 μM) (c), 3-hydroxyanthranillic acid (0.01-0.1 μM) (d), quinolinic acid (e) and kynurenic acid (0.003-10 μM) (f) for 24 hr. Neuronal proliferation was assessed using the alamarBlue® cell proliferation assay. Data expressed as mean ± SEM (n= 10-30 wells from 2-4 independent experiments). **P<0.01, vs. control (One-way ANOVA followed by Dunnett's *post hoc* test).

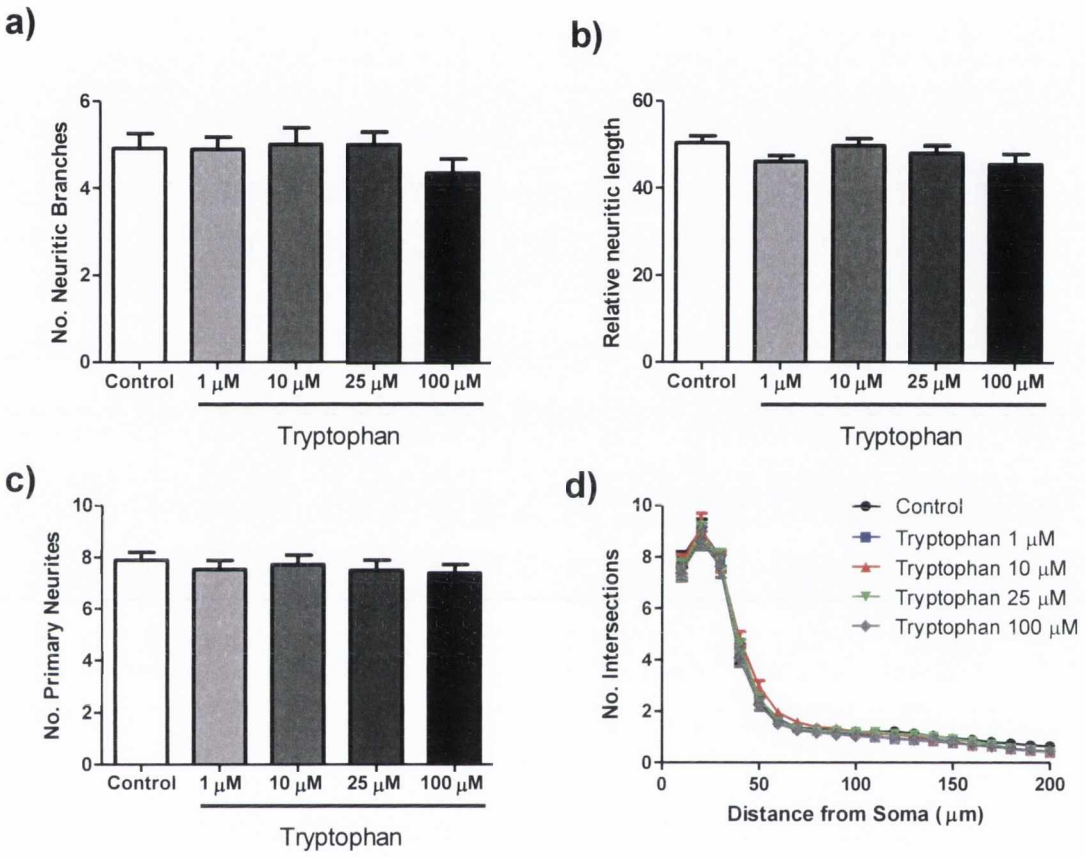

Figure 4.3.2.2: Concentration-related effect of tryptophan on measures of neuronal complexity
Primary cortical neurons (DIV 3) were treated with tryptophan (1, 25, 10, 100 μM; 24 hr). Sholl analysis was performed on neurons to examine (a) the number of neuritic branches, (b) neurite length, (c) the number of primary neurites or (d) the number of branches at varying distances from the soma. Data expressed as mean ± SEM (n= 23-24 coverslips from 3 independent experiments) [One-way ANOVA (a-c), two-way repeated measures ANOVA (d)].

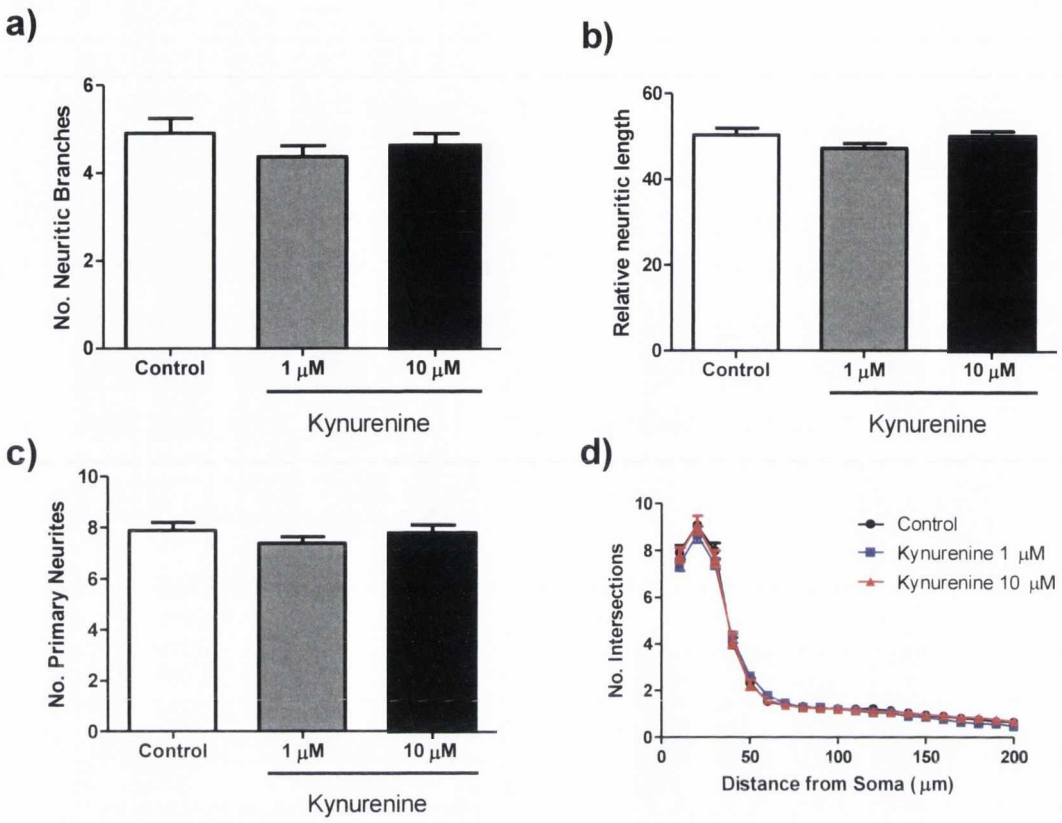

Figure 4.3.2.3: Concentration-related effect of kynurenine on measures of neuronal complexity
Primary cortical neurons (DIV 3) were treated with kynurenine (1, 10 μM; 24 hr). Sholl analysis was performed on neurons to examine (a) the number of neuritic branches, (b) neurite length, (c) the number of primary neurites or (d) the number of branches at varying distances from the soma. Data expressed as mean ± SEM (n= 22-24 coverslips from 3 independent experiments) [One-way ANOVA (a-c), two-way repeated measures ANOVA (d)].

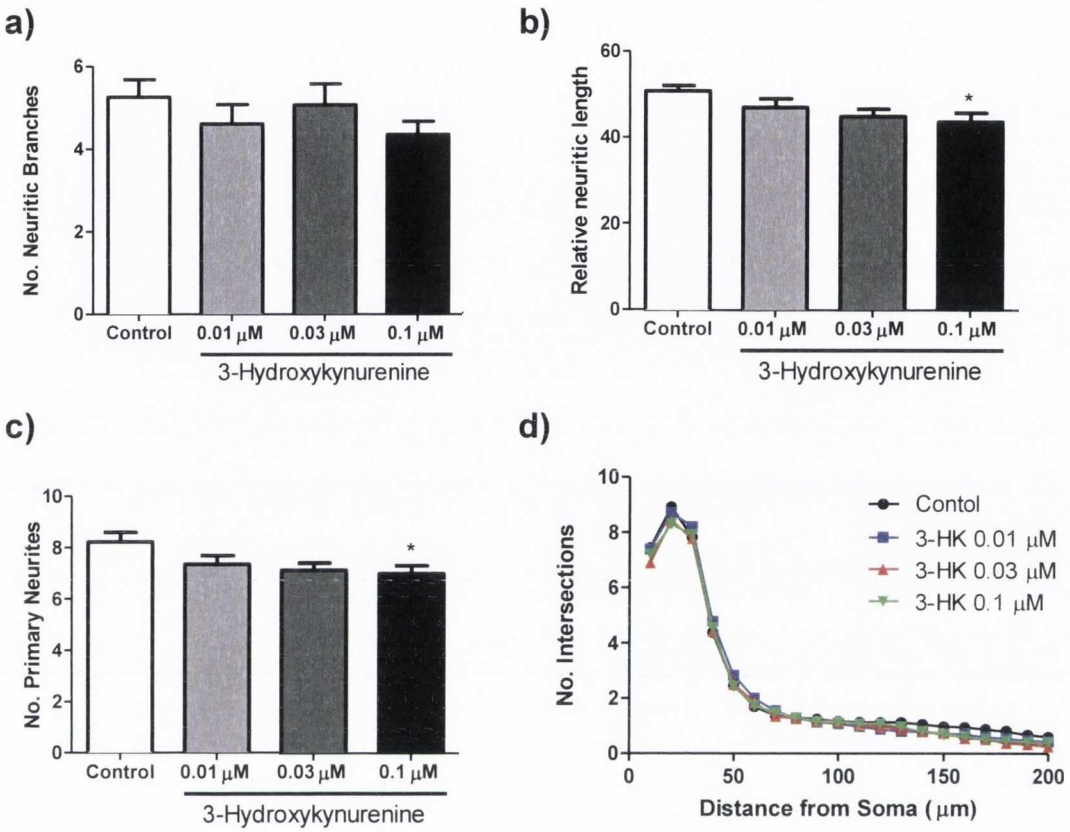

Figure 4.3.2.4: Concentration-related effect of 3-hydroxykynurenine on measures of neuronal complexity

Primary cortical neurons (DIV 3) were treated with 3-hydroxykynurenine (3-HK) (0.01, 0.03, 0.1 μM; 24 hr). Sholl analysis was performed on neurons to examine (a) the number of neuritic branches, (b) neurite length, (c) the number of primary neurites or (d) the number of branches at varying distances from the soma. Data expressed as mean ± SEM (n= 19-22 coverslips from 3 independent experiments). *P<0.05, vs. control [One-way ANOVA followed by Dunnett's *post hoc* test (a-c), two-way repeated measures ANOVA (d)].

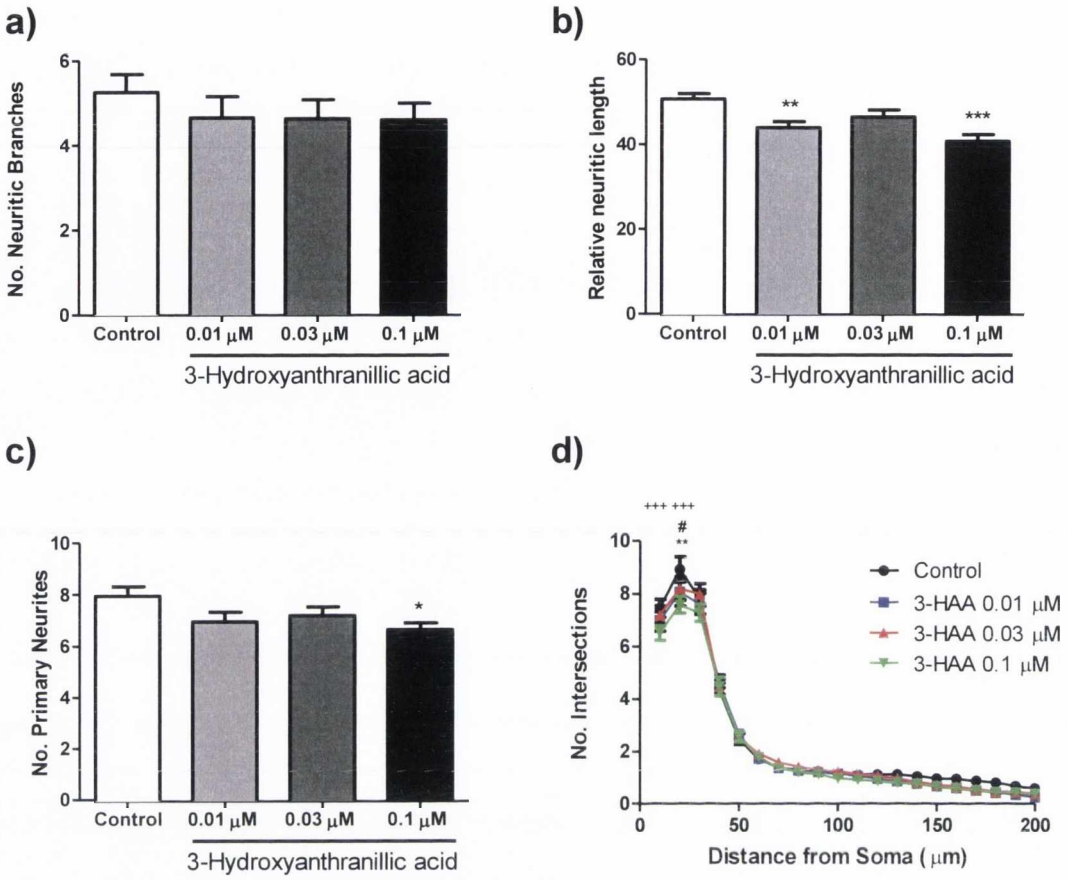

Figure 4.3.2.5: Concentration-related effect of 3-hydroxyanthranillic acid on measures of neuronal complexity

Primary cortical neurons (DIV 3) with treated with 3-hydroxyanthranillic acid (3-HAA) (0.01, 0.03, 0.1 μM; 24 hr). Sholl analysis was performed on neurons to examine (a) the number of neuritic branches, (b) neurite length, (c) the number of primary neurites or (d) the number of branches at varying distances from the soma. Data expressed as mean ± SEM (n= 17-20 coverslips from 3 independent experiments). *P<0.05, ***P<0.001 vs. control [One-way ANOVA followed by Dunnett's *post hoc* test (a-c)]; Sholl profile, **P<0.01, 3-HAA (0.01 μM) vs. control, #P<0.05, 3-HAA (0.03 μM) vs. control, +++P<0.001, 3-HAA (0.1 μM) vs control [Two-way repeated measures ANOVA followed by Bonferroni *post hoc* test (d)].

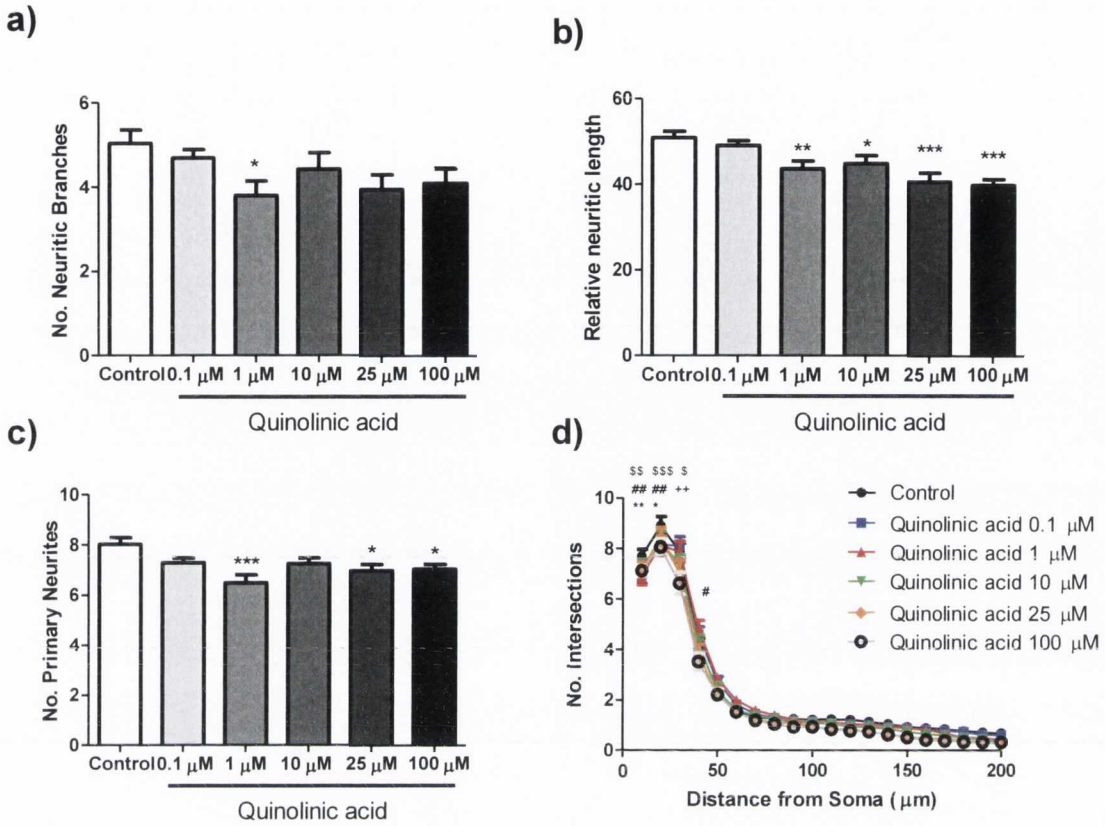

Figure 4.3.2.6: Concentration-related effect of quinolinic acid on measures of neuronal complexity
Primary cortical neurons (DIV 3) were treated with quinolinic acid (0.1, 1, 10, 25, 100 μM; 24 hr). Sholl analysis was performed on neurons to examine (a) the number of neuritic branches, (b) neurite length, (c) the number of primary neurites or (d) the number of branches at varying distances from the soma. Data expressed as mean ± SEM (n= 18-28 coverslips from 4 independent experiments). *P<0.05, **P<0.01, ***P<0.001, vs. control [One-way ANOVA followed by Dunnett's *post hoc* test (a-c)]; Sholl profile, *P<0.05, **P<0.01 quinolinic acid (0.1 μM) vs. control, #P<0.05, ##P<0.01, quinolinic acid (1 μM) vs. control, ++P<0.01, quinolinic acid (25μM) vs. control, $P<0.05, $$P<0.01, $$$P<0.001, quinolinic acid (100 μM) vs. control [Two-way repeated measures ANOVA followed by Bonferroni *post hoc* test (d)].

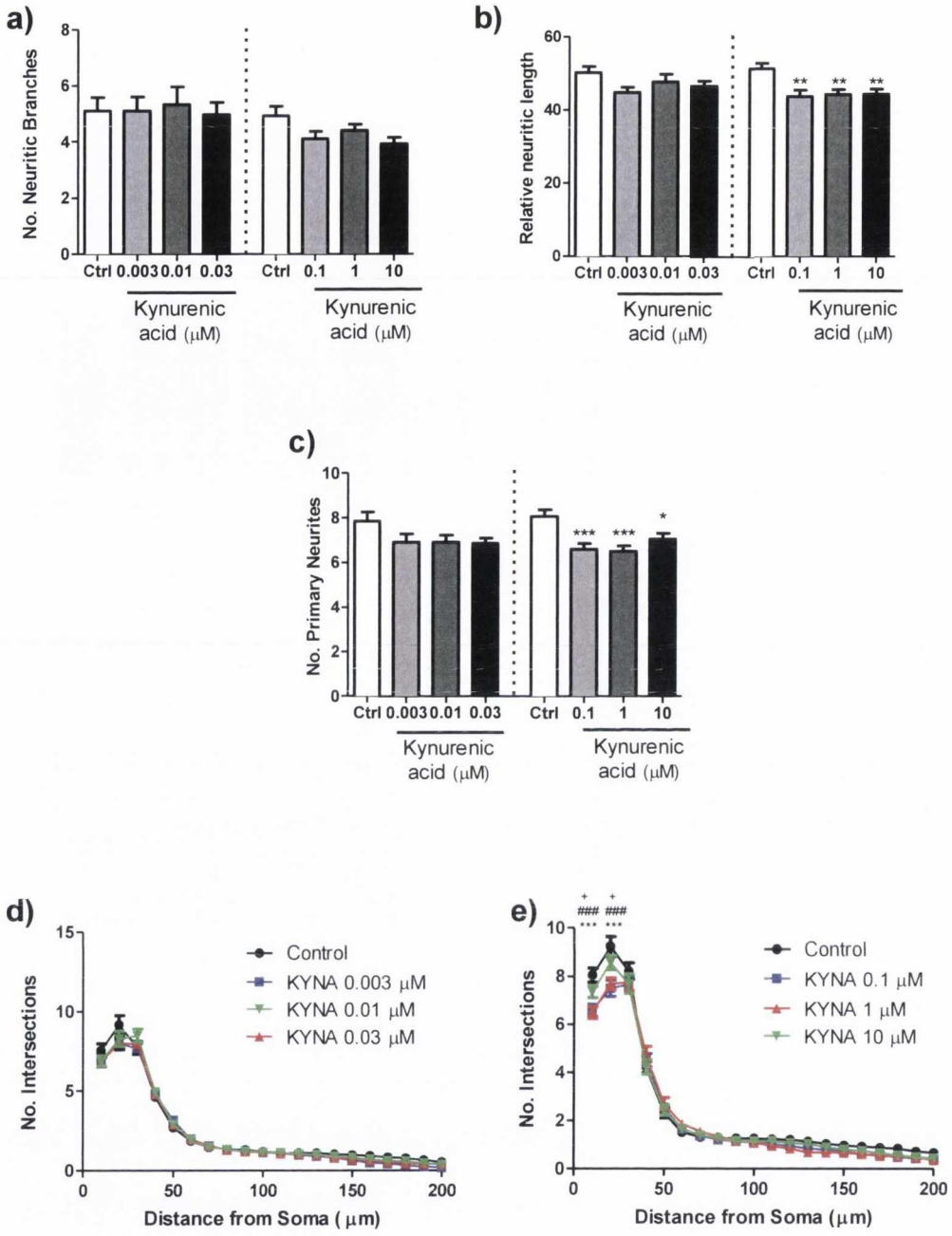

Figure 4.3.2.7: Concentration-related effect of kynurenic acid on measures of neuronal complexity. Primary cortical neurons (DIV 3) were treated with kynurenic acid (KYNA) (0.003, 0.01, 0.03, 0.1, 1, 10μM; 24 hr). Sholl analysis was performed on neurons to examine (a) the number of neuritic branches, (b) neurite length, (c) the number of primary neurites or (d) the number of branches at varying distances from the soma. Data expressed as mean ± SEM (n= 14-24 coverslips from 3 independent experiments). *P<0.05, **P<0.01, ***P<0.001, vs. control [One-way ANOVA followed by Dunnett's *post hoc* test (a-c)]. Sholl profile, ***P<0.001, kynurenic acid 0.1 μM vs. control, ###P<0.001, kynurenic acid 1 μM vs. control, +P<0.05, kynurenic acid 10 μM vs. control [Two-way repeated measures ANOVA followed by Bonferroni *post hoc* test (d-e)].

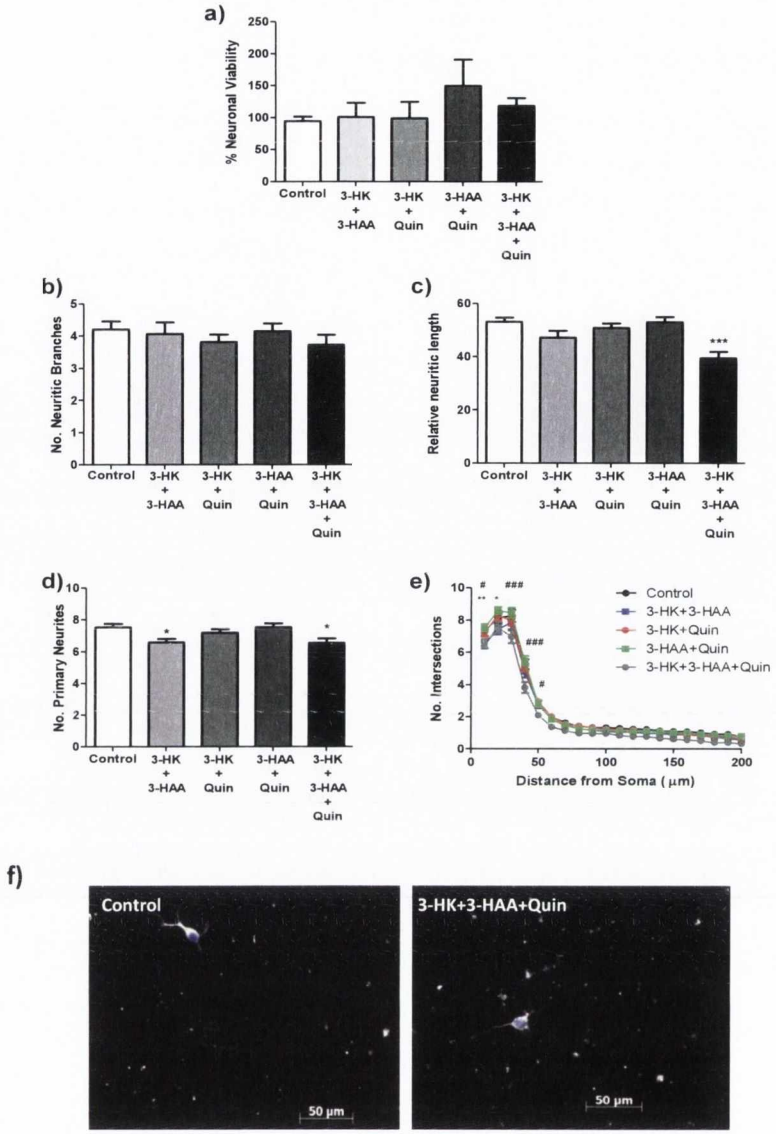

Figure 4.3.2.8: Effect of combinations of kynurenine pathway metabolites on neuronal viability and complexity

Primary cortical neurons (DIV 3) were treated with different combinations of 3-hydroxykynurenine (0.03 μM), 3-hydroxyanthranillic acid (0.03 μM) and quinolinic acid (0.1 μM) for 24 hr. Neuronal viability was assessed and the alamarBlue® cell proliferation assay (a). Data are expressed as mean ± SEM (n= 15-31 wells from 3 independent experiments). Sholl analysis was performed on neurons to examine (a) the number of neuritic branches, (b) neurite length, (c) the number of primary neurites or (d) the number of branches at varying distances from the soma. Representative images of neurons identified using the neuronal structural marker β-III tubulin (white) and the nuclear stain DAPI (blue) with fluorescent microscopy (e). Data expressed as mean ± SEM (n= 19-23 coverslips from 3 independent experiments). *P<0.05, ***P<0.001, vs. control [One-way ANOVA followed by Dunnett's *post hoc* test (a-d)]; Sholl profile, *P<0.05, **P<0.01, 3-HK+3-HAA vs. control, #P<0.05, ###P<0.001, 3-HK+3-HAA+Quin vs. control [Two-way repeated measures ANOVA followed by Bonferroni *post hoc* test (e)].

4.3.3 Examination of the effect of kynurenine pathway metabolites on the neuronal integrity of mature neurons

4.3.3.1 Concentration-related effects of kynurenine pathway metabolites on the viability of mature neurons

One-way ANOVA of **neuronal viability** showed no effect of tryptophan [$F_{(4, 89)}$= 0.7522, P= 0.5593] (a), 3-hydroxykynurenine [$F_{(3, 42)}$= 0.4152, P= 0.7431] (c), 3-hydroxyanthranillic acid [$F_{(3, 47)}$= 0.06952, P= 0.9759] (d), or quinolinic acid [$F_{(3, 45)}$= 1.733, P= 0.167] (e), but an effect of kynurenine [$F_{(2, 53}$= 5.03, P= 0.0101] (b), and kynurenic acid [$F_{(5, 115)}$= 3.576, P= 0.005]. *Post hoc* analysis revealed reductions in neuronal viability following treatment with kynurenine 1 μM (P<0.01) compared to control, while treatment with kynurenic acid caused no change in neuronal viability compared to the control (**figure 4.3.3.1**).

4.3.3.2 Concentration-related effects of kynurenine pathway metabolites on the expression of synaptic markers in mature neurons

One-way ANOVA of the **co-localised expression of synaptic markers** showed an effect of 3-hydroxykynurenine [$F_{(3, 280)}$= 3.391, P= 0.0185] (a), 3-hydroxyanthranillic acid [$F_{(3, 301)}$= 2.638, P= 0.0498] (d), kynurenic acid [$F_{(3, 266)}$= 3.834, P= 0.0103] (j), but not of quinolinic acid [$F_{(3, 263)}$= 1.215, P= 0.05] (g). *Post hoc* analysis revealed reductions in the co-localised expression of synaptic markers following treatment with 3-hydroxyanthranillic acid (0.01, 0.1 μM) (P<0.05) compared to control.

One-way ANOVA of the number of **synaptophysin puncta** showed an effect of 3-hydroxykynurenine [$F_{(3, 280)}$ = 2.971, P= 0.0322] (b), 3-hydroxyanthranillic acid [$F_{(3, 301)}$ = 3.179, P= 0.0244] (e), kynurenic acid [$F_{(3, 266)}$ = 0.3834, P= 0.0103] (k), but not of quinolinic acid [$F_{(3, 260)}$ = 1.215, P= 0.3049] (h). *Post hoc* analysis revealed reductions in the number of synaptophysin puncta following treatment with 3-hydroxykynurenine (0.03, 0.1 μM) (P<0.05), 3-hydroxyanthranillic acid (0.01 μM) (P<0.05) and kynurenic acid (0.01, 0.03, 0.1 μM) (P<0.05) compared to control.

One-way ANOVA of the number of **PSD-95 puncta** showed an effect of quinolinic acid [$F_{(3, 263)}$= 2.733, P= 0.0442] (i), but not of 3-hydroxykynurenine [$F_{(3, 280)}$= 1.44, P= 2.313] (c), 3-hydroxyanthranillic acid [$F_{(3, 301)}$= 1.402, P= 0.2442] (f), or kynurenic acid [$F_{(3, 266)}$= 0.2051, P= 0.8928] (l). *Post hoc* analysis revealed no changes in the expression of PSD-95 compared to control (**figure 4.3.3.2**).

4.3.3.3 Effect of combinations of kynurenine pathway metabolites on the viability of and the expression of synaptic markers in mature neurons

One-way ANOVA of neuronal **viability** showed no effect of treatment [$F_{(4, 56)} = 0.5581$, $P= 0.694$].

One-way ANOVA of the **co-localised expression of synaptic markers** showed an effect of treatment [$F_{(4, 264)} = 11.86$, $P<0.0001$]. *Post hoc* analysis revealed reductions in the co-localised expression of synaptic markers following treatment with 3-hydroxykynurenine + 3-hydroxyanthranillic acid ($P<0.001$), 3-hydroxykynurenine + quinolinic acid ($P<0.001$), 3-hydroxyanthranillic acid + quinolinic acid ($P<0.001$), 3-hydroxykynurenine + 3-hydroxyanthranillic acid + quinolinic acid ($P<0.05$) compared to control (b).

One-way ANOVA of the number of **synaptophysin puncta** showed no effect of treatment [$F_{(4, 266)} = 1.205$, $P= 0.3091$] (c).

One-way ANOVA of the number of **PSD-95 puncta** showed an effect of treatment [$F_{(4, 265)} = 16.29$, $P<0.0001$]. *Post hoc* analysis revealed reductions in the expression of PSD-95 following treatment with 3-hydroxykynurenine + 3-hydroxyanthranillic acid ($P<0.001$), 3-hydroxykynurenine + quinolinic acid ($P<0.001$), 3-hydroxyanthranillic acid + quinolinic acid ($P<0.001$), 3-hydroxykynurenine + 3-hydroxyanthranillic acid + quinolinic acid ($P<0.001$) compared to control (d) (**figure 4.3.3.3**).

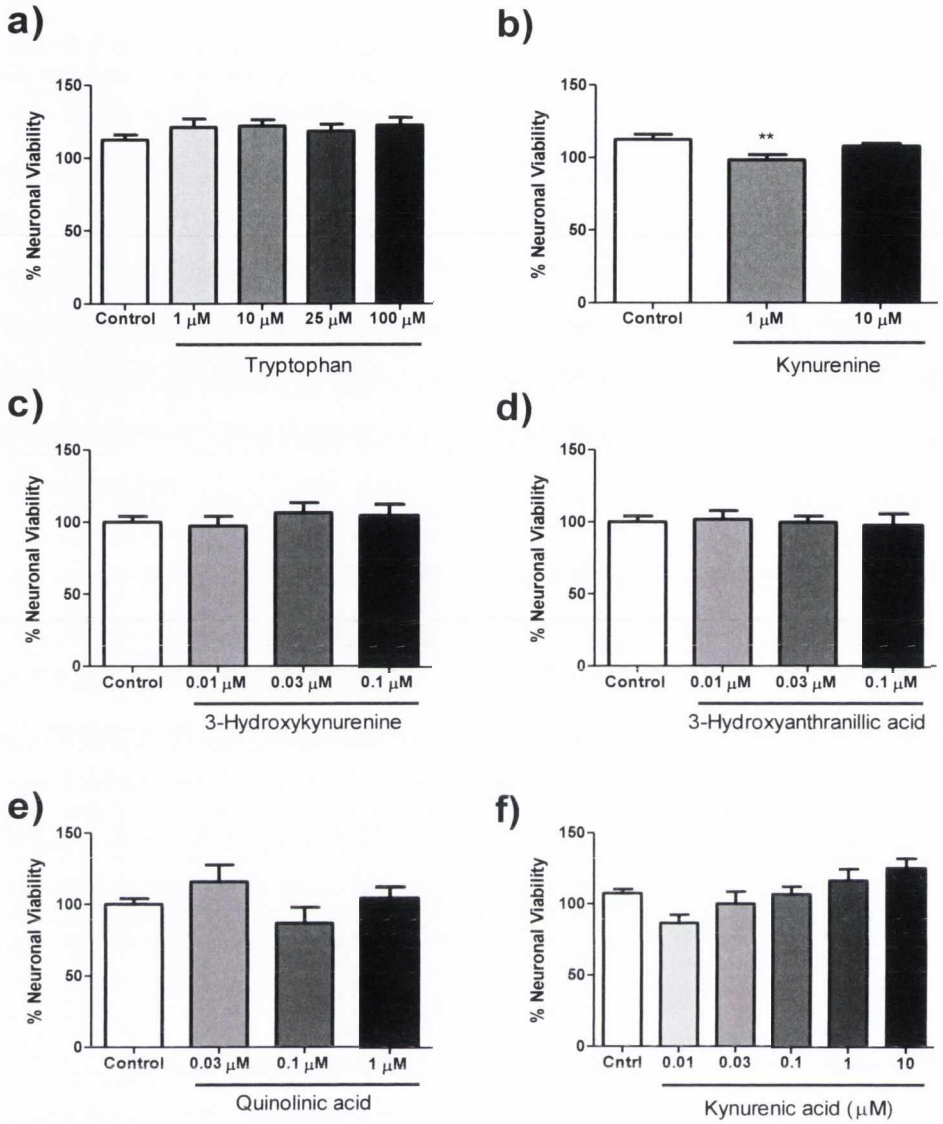

Figure 4.3.3.1: Concentration-related effects of kynurenine pathway metabolites on the viability of mature neurons

Primary cortical neurons (DIV 18-21) were treated with varying concentrations of tryptophan (1-100 μM) (a), kynurenine (1, 10 μM) (b), 3-hydroxykynurenine (0.01-0.1 μM) (c), 3-hydroxyanthranillic acid (0.01-0.1 μM) (d), quinolinic acid (e) or kynurenic acid (0.03-10 μM) (f) for 24 hr. Neuronal viability was assessed using the alamarBlue® cell proliferation assay. Data expressed as mean ± SEM (n= 10-30 wells from 2-3 independent experiments). **P<0.01, vs. control (One-way ANOVA followed by Dunnett's *post hoc* test).

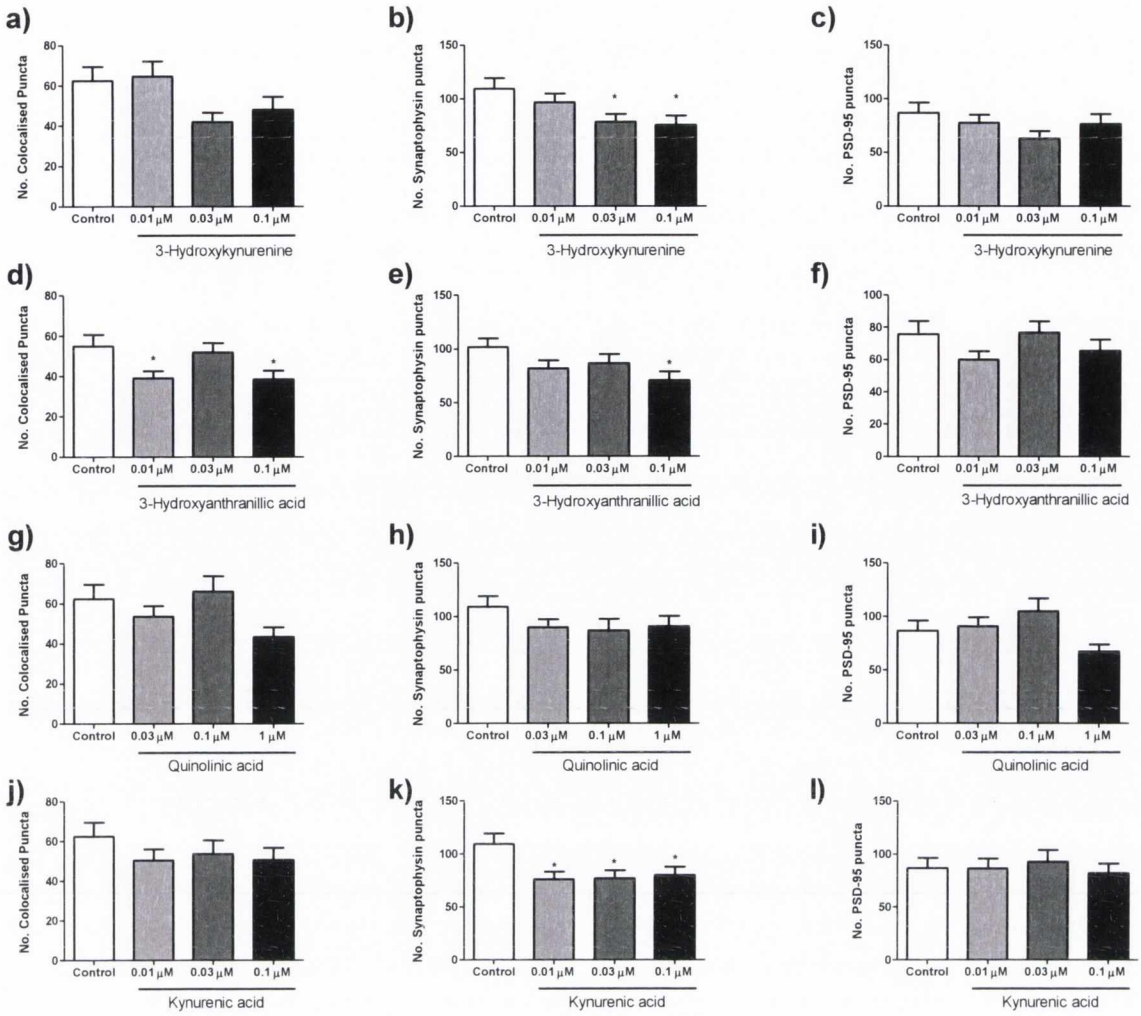

Figure 4.3.3.2: Concentration-related effects of kynurenine pathway metabolites on the expression of synaptic markers in mature neurons

Primary cortical neurons (DIV 18-21) were treated with varying concentrations of 3-hydroxykynurenine (0.01-0.1 μM) (a-c), 3-hydroxyanthranillic acid (0.01-0.1 μM) (d-f), quinolinic acid (0.03-1 μM) (g-i) or kynurenic acid (0.01-0.1 μM) (j-l) for 24 hr. The neurons were examined to determine the co-localised expression of pre- and post-synaptic markers synaptophysin and PSD-95 (a, d, g, j), alongside the number of synaptophysin puncta (b, e, h, k), and PSD-95 puncta (c, f, i, l) in isolation using ImageJ software. Data expressed as mean ± SEM (n= 45-95 neurons from 3 independent experiments). *P<0.05, vs. control (One-way ANOVA followed by Dunnett's *post hoc* test).

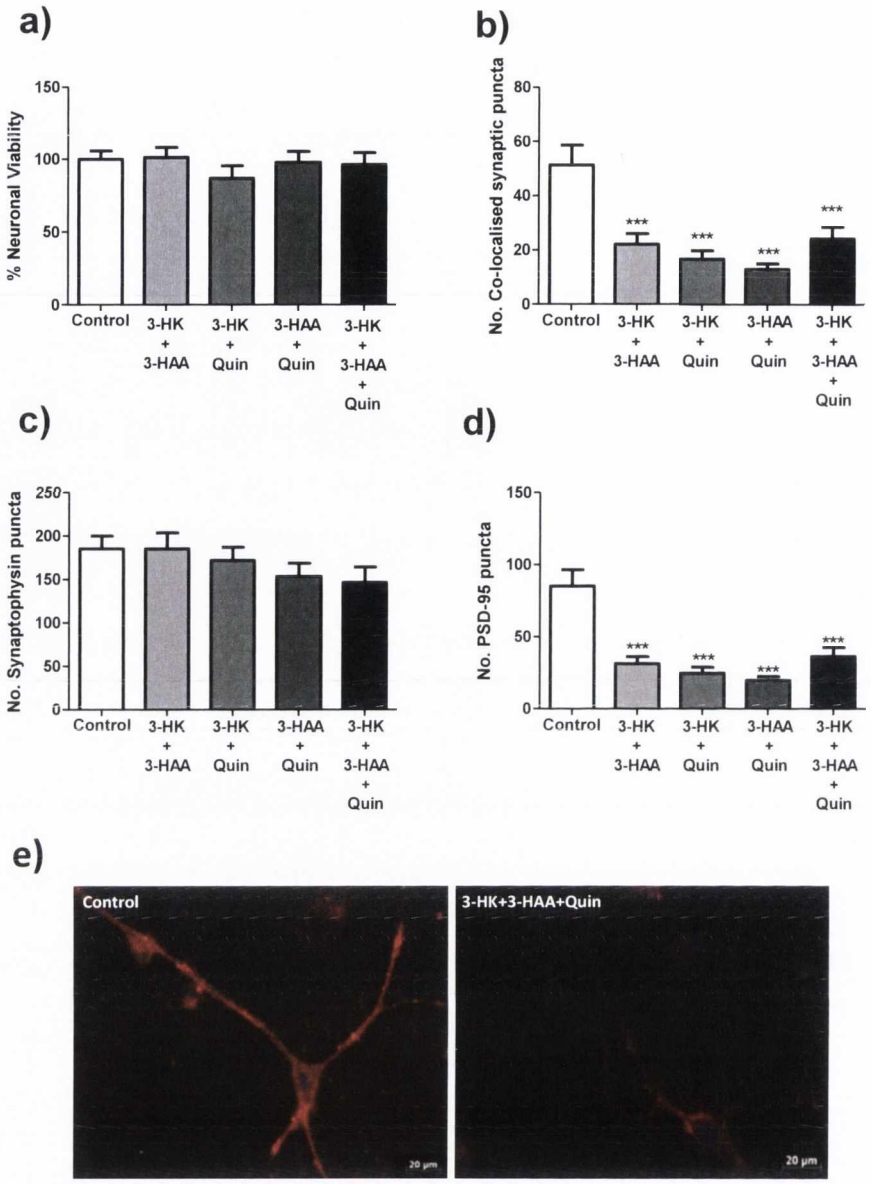

Figure 4.3.3.3: Effect of combinations of kynurenine pathway metabolites on the viability of and the expression of synaptic markers in mature neurons

Primary cortical neurons (DIV 18-21) were treated with different combinations of 3-hydroxykynurenine (0.03 µM), 3-hydroxyanthranillic acid (0.03 µM) and quinolinic acid (0.1 µM) for 24 hr. Neuronal viability was assessed and the alamarBlue® cell proliferation assay (a). The neurons were examined to determine (b) the co-localised expression of pre- and post-synaptic markers synaptophysin and PSD-95, (c) the number of synaptophysin puncta, and (d) the number of PSD-95 puncta in isolation using ImageJ software. Representative images of neuron stained with the anti-synaptophysin antibody (red), the anti-PSD-95 antibody (green) and the nuclear stain DAPI (blue) with fluorescent microscopy (h). Data are expressed as mean ± SEM (n= 51-56 neurons from 3 independent experiments. ***P<0.001, vs. control (One-way ANOVA followed by Dunnett's *post hoc* test).

4.3.4 Characterisation of the atrophic effects of glutamate on primary cortical neurons

It has previously been reported by our laboratory that activation of the NMDA receptor is responsible for glutamate-induced neuronal atrophy (Doucet et al., 2015). Considering that reactive microglial-released glutamate acts through the same mechanism as quinolinic acid, its potential role in driving IFNγ-stimulated mixed glial CM-induced atrophy and synapse loss was of interest. Glycine was added as a consequence of it being a co-agonist at the NMDA receptor (Dingledine et al., 1999), with glutamate-induced neurite atrophy only occurring in the presence of glycine (Doucet et al., 2015). Concentrations of both glutamate and glycine were based on the previous work carried out by our laboratory whereby glutamate 500 µM and glycine 10 µM in combination reduced neurite length and neuronal complexity (Doucet et al., 2015). With the aim of examining neuronal complexity and synaptogenesis in the absence of reduced viability, the effects of various concentrations of glutamate and glycine were investigated due to the increased sensitivity of mature neurons to both of these agents. Where glutamate alone is sufficient to induce atrophy, co-treatment with glycine is not required.

4.3.4.1 Effect of glutamate and glycine on neuronal viability and complexity

Two-way ANOVA of **neuronal viability** showed no effect of glycine [$F_{(1, 92)} = 1.394$, $P= 0.249$], glutamate [$F_{(1, 92)} = 0.063$, $P= 0.802$], and no interaction [$F_{(1, 92)} = 0.557$, $P= 0.458$] (a).

Treatment of neurons with glutamate + glycine reduced the number of **neuritic branches** ($t= 3.264$, $P= 0.002$, d.f. = 51) (b), **neurite length** ($t= 5.52$, $P<0.0001$, d.f. = 51) (c), and the number of **primary neurites** ($t= 3.557$, $P= 0.008$, d.f. = 51) compared to control (d).

A two-way repeated measures ANOVA of the number of **neuritic branches at specific distances from the neuronal cell soma** showed an effect of distance [$F_{(25, 1275)} = 702.9$, $P<0.0001$], glutamate + glycine [$F_{(1, 1275)} = 30.47$, $P<0.0001$], and no interaction [$F_{(25, 1275)} = 1.168$, $P= 0.2583$]. *Post hoc* analysis revealed reductions in the number of branches at 10, 20 30, 140, 150, 160 and 170 µm from the cell soma following treatment with glutamate + glycine ($P<0.05$) compared to control (e) (**figure 4.3.4.1**).

4.3.4.2 Concentration-related effects of glutamate and glycine on the viability of mature neurons

One-way ANOVA of neuronal viability showed an effect of treatment [$F_{(5, 95)} = 8.910$, $P<0.0001$]. *Post hoc* analysis revealed reductions in neuronal viability following treatment with glutamate 100 μM + glycine 10 μM and glutamate 500 μM + glycine 10 μM ($P<0.001$), compared to control (a).

One-way ANOVA of neuronal viability showed an effect of treatment [$F_{(3, 32)} = 3.557$, $P= 0.0263$]. *Post hoc* analysis revealed reductions in neuronal viability following treatment with glutamate 500 μM + glycine 1 μM ($P<0.001$) compared to control (b).

One-way ANOVA of neuronal viability showed an effect of treatment [$F_{(5, 56)} = 4.181$, $P= 0.0025$]. *Post hoc* analysis revealed reductions in neuronal viability following treatment with glutamate 0.1/ 1/ 10/ 50 μM + glycine 10 μM ($P<0.05$) compared to control (c).

One-way ANOVA of neuronal viability showed no effect of treatment [$F_{(5, 54)} = 0.9114$, $P= 0.4814$] (d) (**figure 4.3.4.2**).

4.3.4.3 Effects of glutamate and glycine on the expression of synaptic markers in mature neurons

Two-way ANOVA of the **co-localised expression of synaptic markers** showed no effect of glycine 1 μM [$F_{(1, 182)} = 1.092$, $P= 0.297$], an effect of glutamate 50 μM [$F_{(1, 182)} =29.335$, $P<0.0001$], and no interaction [$F_{(1, 182)} = 2.219$, $P= 0.138$]. *Post hoc* analysis revealed reductions in the co-localised expression of synaptic markers following treatment with glutamate 50 μM ($P<0.001$) and glutamate 50 μM + glycine 1 μM ($P<0.001$) compared to control (a).

Two-way ANOVA of the number of **synaptophysin puncta** showed no effect of glycine 1 μM [$F_{(1, 182)} = 2.645$, $P= 0.106$], an effect of glutamate 50 μM [$F_{(1, 182)} =5.204$, $P= 0.024$], and no interaction [$F_{(1, 182)} = 0.156$, $P= 0.694$]. *Post hoc* analysis revealed reductions in the expression of synaptophysin following treatment with and glutamate 50 μM + glycine 1 μM ($P<0.05$) compared to control (b).

Two-way ANOVA of the number of **PSD-95 puncta** showed no effect of glycine 1 μM [$F_{(1, 182)} = 2.249$, $P= 0.135$], an effect of glutamate 50 μM [$F_{(1, 182)} = 31.586$, $P<0.0001$], and an interaction [$F_{(1, 182)} = 3.896$ $P= 0.05$]. *Post hoc* analysis revealed reductions in the expression of PSD-95 following treatment with and glutamate 50 μM ($P<0.001$), and glutamate 50 μM + glycine 1 μM ($P<0.001$) compared to control (c) (**figure 4.3.4.3**).

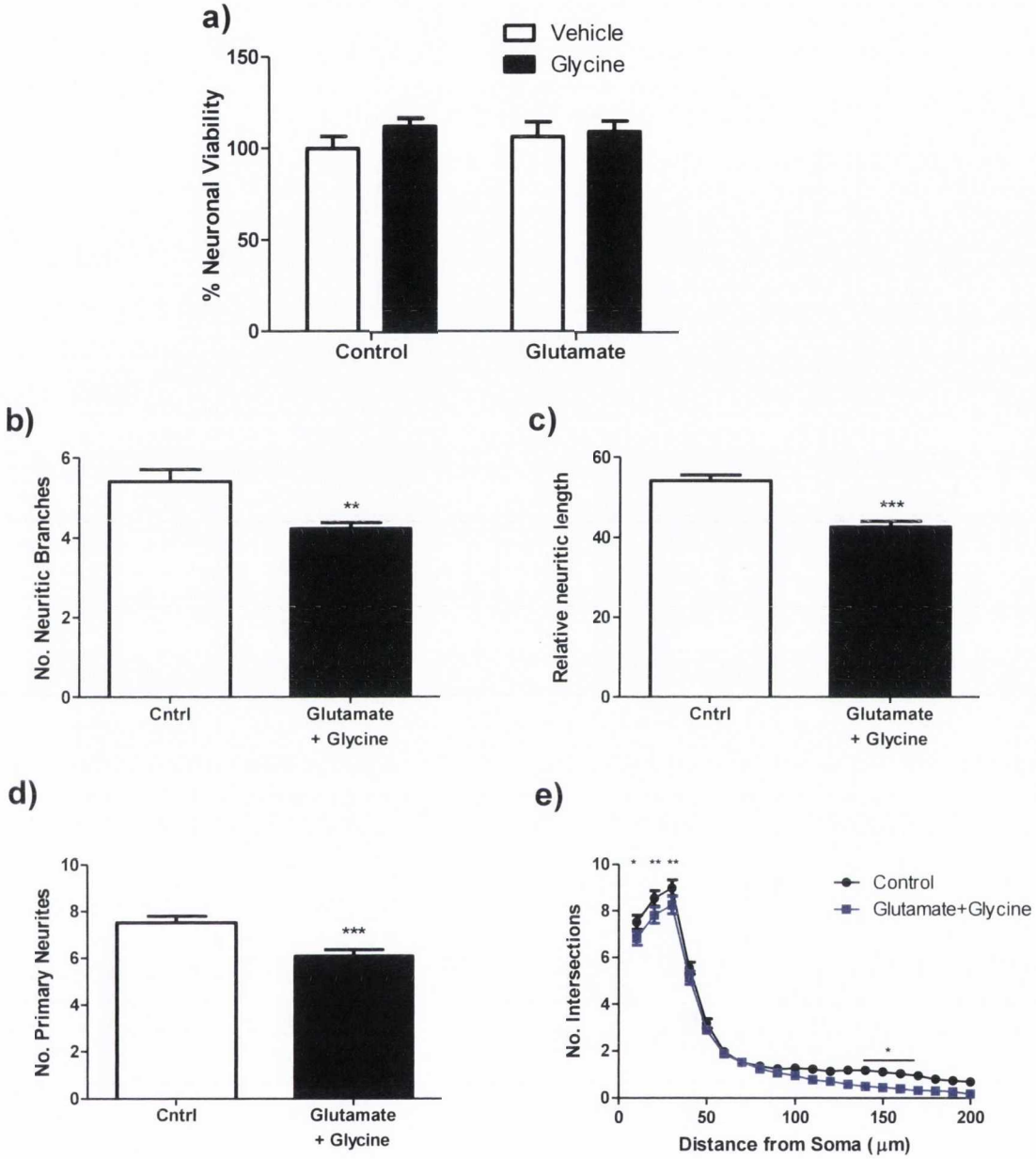

Figure 4.3.4.1: Effect of glutamate and glycine on neuronal viability and complexity
Primary cortical neurons (DIV 3) were treated with glutamate (500 μM) and/or glycine (10 μM) for 24 hr. Neuronal viability was assessed using the alamarBlue® cell proliferation assay (a). Sholl analysis was performed on neurons to examine (b) the number of neuritic branches, (c) neurite length, (d) the number of primary neurites, or (e) the number of branches at specific distances from the soma. Data expressed as mean ± SEM (n= 11-29 wells/coverslips from 2-3 independent experiments). *P<0.05, **P<0.01, ***P<0.001, vs. control [Two-way ANOVA (a), Student's *t* test (b-d), two-way repeated measures ANOVA followed by Bonferroni *post hoc* test (e)].

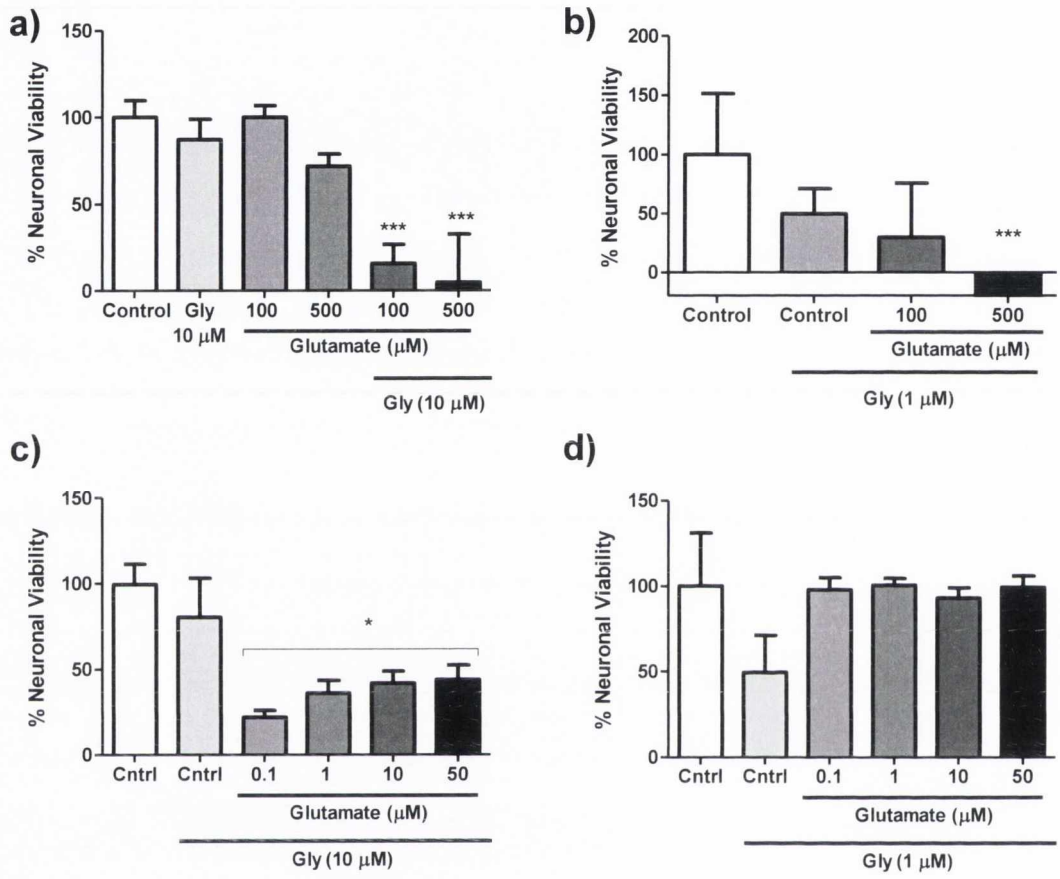

Figure 4.3.4.2: Concentration-related effects of glutamate and glycine on the viability of mature neurons

Primary cortical neurons (DIV 18-21) were treated with glutamate (0.1, 1, 10, 50, 100, 500 μM) and/or glycine (1, 10 μM) for 24 hr. Neuronal viability was assessed using the alamarBlue® cell proliferation assay (a-d). Data expressed as mean ± SEM (n= 4-14 wells from 1-2 independent experiments). *P<0.05, ***P<0.001, vs. control (One-way ANOVA followed by Newman-Keuls *post hoc*).

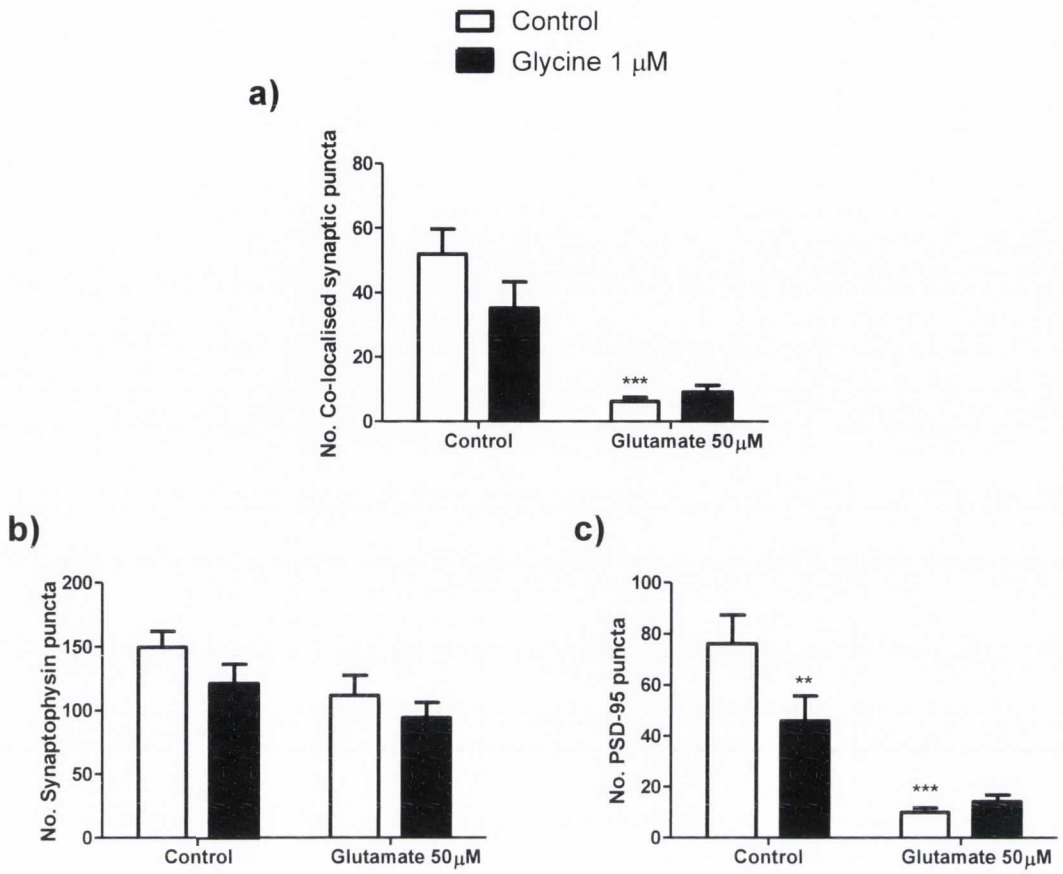

Figure 4.3.4.3: Effects of glutamate and glycine on the expression of synaptic markers in mature neurons

Primary cortical neurons (DIV 18-21) were treated with glutamate (50 μM) and/or glycine (1 μM) for 24 hr. The neurons were examined to determine (a) the co-localised expression of pre- and post-synaptic markers synaptophysin and PSD-95, alongside (b) the number of synaptophysin puncta, and (c) the number of PSD-95 puncta in isolation using ImageJ software. Data expressed as mean ± SEM (n= 36-52 neurons from 3 independent experiments). **P<0.01, ***P<0.001, vs. control (Two-way ANOVA followed by Newman-Keuls *post hoc* test).

4.3.5 Determination of the ability of kynurenic acid to protect against changes in neuronal integrity induced by the release of soluble factors from reactive microglia

4.3.5.1 Concentration-related effects of kynurenic acid on glutamate and glycine-induced reductions in neuronal complexity

One-way ANOVA of the number of **neuritic branches** showed an effect of treatment [$F_{(5, 125)} = 2.87$, P= 0.0175]. *Post hoc* analysis revealed reductions in the number of neuritic branches following treatment with glutamate + glycine (P<0.05) compared to control. Kynurenic acid (1, 10 μM) prevented glutamate + glycine-induced reductions (P<0.05) (a).

One-way ANOVA of **neurite length** showed an effect of treatment [$F_{(5, 124)} = 8.825$, P<0.0001]. *Post hoc* analysis revealed reductions in the neurite length following treatment with glutamate + glycine (P<0.001) compared to control. Kynurenic acid (0.03, 0.1, 1, 10 μM) prevented glutamate + glycine-induced reductions (P<0.05) (b).

One-way ANOVA of the number of **primary neurites** showed an effect of treatment [$F_{(5, 124)} = 3.711$, P= 0.0037]. *Post hoc* analysis revealed reductions in the number of primary neurites following treatment with glutamate + glycine (P<0.01) compared to control. Kynurenic acid (0.03, 1 μM) prevented glutamate + glycine-induced reductions (P<0.05) (c).

Two-way repeated measures ANOVA of the number of **neuritic branches at specific distances from the neuronal cell soma** showed an effect of distance [$F_{(25, 2850)} = 1519$, P<0.0001], treatment [$F_{(5, 2850)} = 7.068$, P<0.0001], and an interaction [$F_{(125, 2850)} = 1.326$, P= 0.0102]. *Post hoc* analysis revealed reductions in the number of branches at 10, 20 30, 130, 140, 150, 160, and 170 μm from the cell soma with glutamate + glycine (P<0.05) compared to control. Kynurenic acid (0.03 μM) prevented reductions at 160, 180 and 200 μm from the cell soma (P<0.05), and kynurenic acid (1 μM) prevented reductions at 20 μm (P<0.001) and 30 μm (P<0.05) from the cell soma (d) (**figure 4.3.5.1**).

4.3.5.2 Concentration-related effects of kynurenic acid on glutamate and glycine-induced reductions in the expression of synaptic markers

One-way ANOVA of the **co-localised expression of synaptic markers** showed an effect of treatment [$F_{(3, 200)} = 4.427$, P= 0.049]. *Post hoc* analysis revealed reductions in the co-localised expression of synaptic markers following treatment with glutamate (P<0.01) compared to control (a).

One-way ANOVA of the number of **synaptophysin puncta** showed an effect of treatment [$F_{(3, 204)} = 7.175$, P= 0.0001]. *Post hoc* analysis revealed reductions in the number of synaptophysin puncta following treatment with glutamate (P<0.001) compared to control (b).

One-way ANOVA of the number of **PSD-95 puncta** showed no effect of treatment [$F_{(3, 171)} = 1.002$, P= 0.393] (c) (**figure 4.3.5.2**).

4.3.5.3 Concentration-related effects of kynurenic acid on the 3-hydroxykynurenine + 3-hydroxyanthranillic acid + quinolinic acid combination-induced reductions in neuronal complexity

One-way ANOVA of the number of **neuritic branches** showed an effect of treatment [$F_{(4, 67)} = 4.238$, P= 0.0041]. *Post hoc* analysis revealed reductions in the number of neuritic branches following treatment with the 3-hydroxykynurenine + 3-hydroxyanthranillic acid + quinolinic acid combination (P<0.05) compared to control. Kynurenic acid (0.03, 0.01, 1 μM) prevented 3-hydroxykynurenine + 3-hydroxyanthranillic acid + quinolinic acid-induced reductions (P<0.05) (a).

One-way ANOVA of **neurite length** showed an effect of treatment [$F_{(4, 67)} = 16.52$, P<0.0001]. *Post hoc* analysis revealed reductions in neurite length following treatment with the 3-hydroxykynurenine + 3-hydroxyanthranillic acid + quinolinic acid combination (P<0.001) compared to control. Kynurenic acid (003/0.01/ 1 μM) prevented 3-hydroxykynurenine + 3-hydroxyanthranillic acid + quinolinic acid-induced reductions (P<0.001) (b).

One-way ANOVA of the number of **primary neurites** showed an effect of treatment [$F_{(4, 67)} = 5.781$, P= 0.0005]. *Post hoc* analysis revealed reductions in the number of primary neurites following treatment with the 3-hydroxykynurenine + 3-hydroxyanthranillic acid + quinolinic acid combination (P<0.05) compared to control. Kynurenic acid (0.01, 1 μM) prevented 3-hydroxykynurenine + 3-hydroxyanthranillic acid + quinolinic acid-induced reductions (P<0.05) (c).

Two-way repeated measures ANOVA of the number of **neuritic branches at specific distances from the neuronal cell soma** showed an effect of distance [$F_{(25, 1575)} = 992.1$, P<0.0001], treatment [$F_{(4, 1575)} = 5.623$, P<0.0001], and an interaction [$F_{(100, 1575)} = 3.191$, P<0.0001]. *Post hoc* analysis revealed reductions in the number of branches at 10, 20 30 and 40 μm from the cell soma following treatment with the 3-hydroxykynurenine + 3-hydroxyanthranillic acid + quinolinic acid combination (P<0.001) compared to control. Kynurenic acid (0.03 μM) (P<0.05), (0.1 μM) (P<0.01), (1 μM) (P0.001) prevented reductions at 10, 20, 30 and 40 μm from the cell soma (d) (**figure 4.3.5.3**).

4.3.5.4 Concentration-related effects of kynurenic acid on the 3-hydroxykynurenine + 3-hydroxyanthranillic acid + quinolinic acid combination-induced reductions in the expression of synaptic markers

One-way ANOVA of the **co-localised expression of synaptic markers** showed an effect of treatment [$F_{(3, 198)} = 4.1$, $P = 0.0075$]. *Post hoc* analysis revealed reductions in the co-localised expression of synaptic markers following treatment with the 3-hydroxykynurenine + 3-hydroxyanthranillic acid + quinolinic acid combination ($P<0.05$) compared to control (a).

One-way ANOVA of the number of **synaptophysin puncta** showed an effect of treatment [$F_{(3, 198)} = 2.957$, $P = 0.0336$]. *Post hoc* analysis revealed reductions in the number of synaptophysin puncta following treatment with the kynurenic acid (0.03 μM) + 3-hydroxykynurenine + 3-hydroxyanthranillic acid + quinolinic acid combination ($P<0.05$) compared to control (b).

One-way ANOVA of the number of **PSD-95 puncta** showed an effect of treatment [$F_{(3, 198)} = 3.182$, $P = 0.0251$]. *Post hoc* analysis revealed reductions in the number of PSD-95 puncta following treatment with the kynurenic acid (0.03 μM) + 3-hydroxykynurenine + 3-hydroxyanthranillic acid + quinolinic acid combination ($P<0.05$) compared to control (c) (**figure 4.3.5.4**).

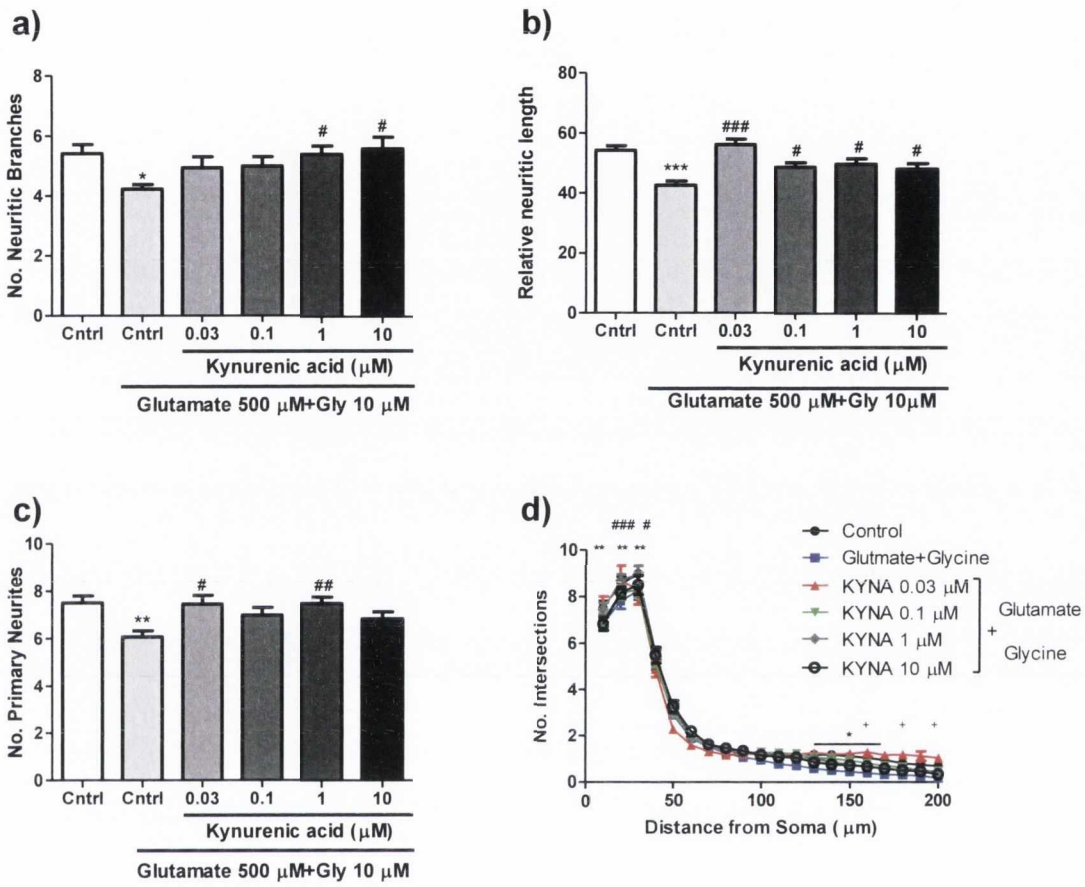

Figure 4.3.5.1: Concentration-related effects of kynurenic acid on glutamate and glycine-induced reductions in neuronal complexity

Primary cortical neurons (DIV 3) were treated with kynurenic acid (KYNA; 0.03, 0.1, 1, 10 μM) and/or glutamate (500 μM) + glycine (10 μM) for 24 hr. Sholl analysis was performed on neurons to examine (a) the number of neuritic branches, (b) neurite length, (c) the number of primary neurites or (d) the number of branches at specific distances from the soma. Data expressed as mean ± SEM (n= 14-29 coverslips from 2-3 independent experiments). *P<0.05, **P<0.01, ***P<0.001, vs. control, #P<0.05, ##P<0.01, ###P<0.001, vs. glutamate+glycine [One-way ANOVA followed by Newman Keuls *post hoc* test (a-c)]; Sholl profile, *P<0.05, **P<0.01, glutamate+glycine vs. control, +P<0.05, KYNA 0.03 μM vs. glutamate+glycine, #P<0.05, ###P<0.001, KYNA 1 μM vs. glutamate+glycine [Two-way repeated measures ANOVA followed by Bonferroni post hoc test (d)].

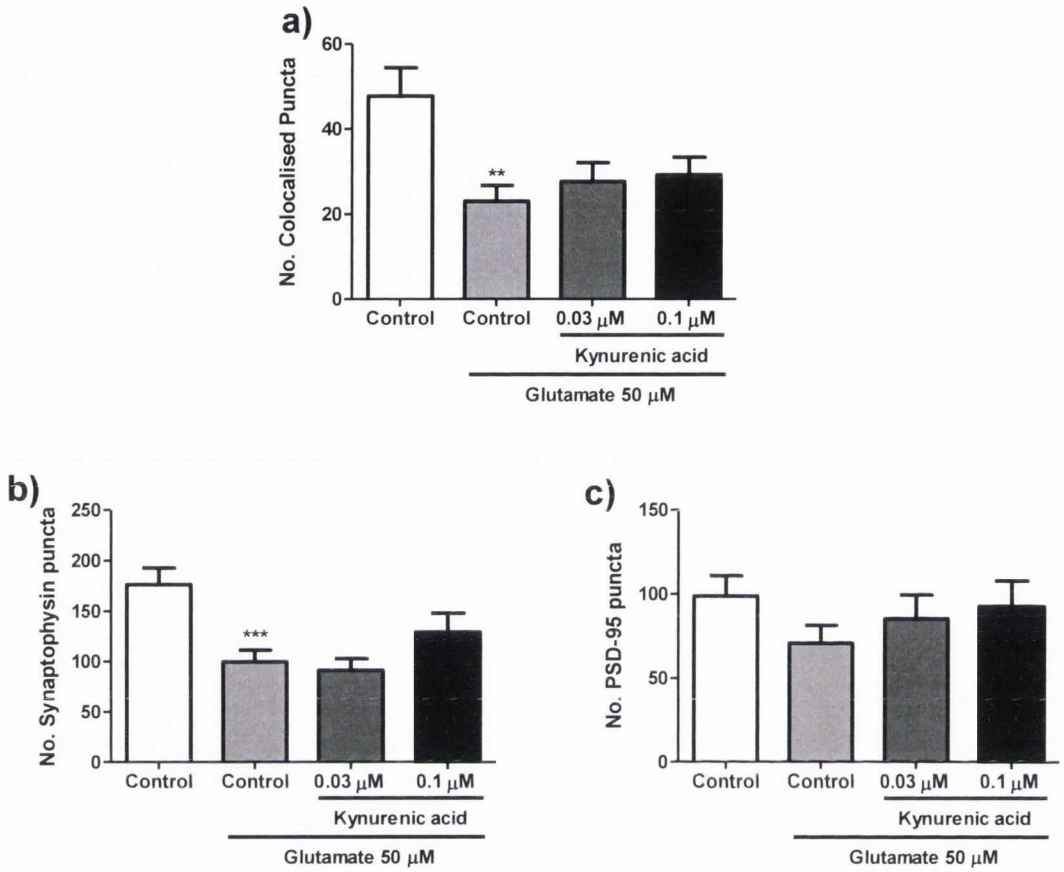

Figure 4.3.5.2: Concentration-related effects of kynurenic acid on glutamate and glycine-induced reductions in the expression of synaptic markers

Primary cortical neurons (DIV 18-21) were treated with kynurenic acid (0.03 or 0.1 μM) and/or glutamate (50 μM) for 24 hr. The neurons were examined to determine (a) the co-localised expression of pre- and post-synaptic markers synaptophysin and PSD-95, (b) the number of synaptophysin puncta, and (c) the number of PSD-95 puncta in isolation using ImageJ software. Data expressed as mean ± SEM (n= 33-78 neurons from 3-4 independent experiments). **P<0.01, ***P<0.001, vs. control (One-way ANOVA followed by Newman Keuls *post hoc* test).

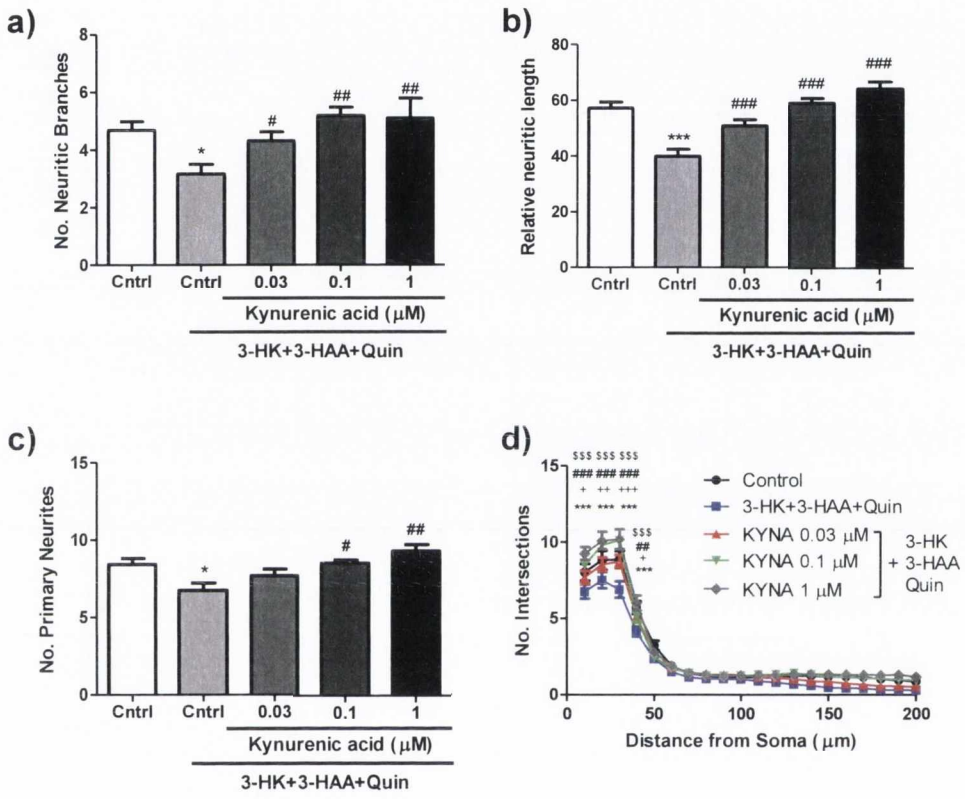

Figure 4.3.5.3: Concentration-related effects of kynurenic acid on the 3-hydroxykynurenine + 3-hydroxyanthranillic acid + quinolinic acid combination-induced reductions in neuronal complexity
Primary cortical neurons (DIV 3) were treated with kynurenic acid (KYNA; 0.03, 0.1, 1 μM) and/or the 3-hydroxykynurenine (3-HK; 0.03 μM) + 3-hydroxyanthranillic acid (3-HAA; 0.03 μM) + quinolinic acid (Quin; 0.1μM) combination for 24 hr. Sholl analysis was performed on neurons to examine (a) the number of neuritic branches, (b) neurite length, (c) the number of primary neurites, or (d) the number of branches at specific distances from the soma (d). Data expressed as mean ± SEM (n= 12-16 coverslips from 2 independent experiments). *P<0.05, ***P<0.001, vs. control, #P<0.05, ##P<0.01, ###P<0.001, vs. 3-HK+3-HAA+Quin [One-way ANOVA followed by Newman Keuls *post hoc* test (a-c)]; Sholl profile, ***P<0.001, 3-HK+3-HAA+Quin, +P<0.05, ++P<0.01, +++P<0.001, KYNA 0.03 μM vs. 3-HK+3-HAA+Quin, ##P<0.01, ###P<0.001, KYNA 0.1 μM vs. 3-HK+3-HAA+Quin, $$$P<0.001, KYNA 1 μM vs. 3-HK+3-HAA+Quin [Two-way repeated measures ANOVA followed by Bonferroni post hoc test (d)].

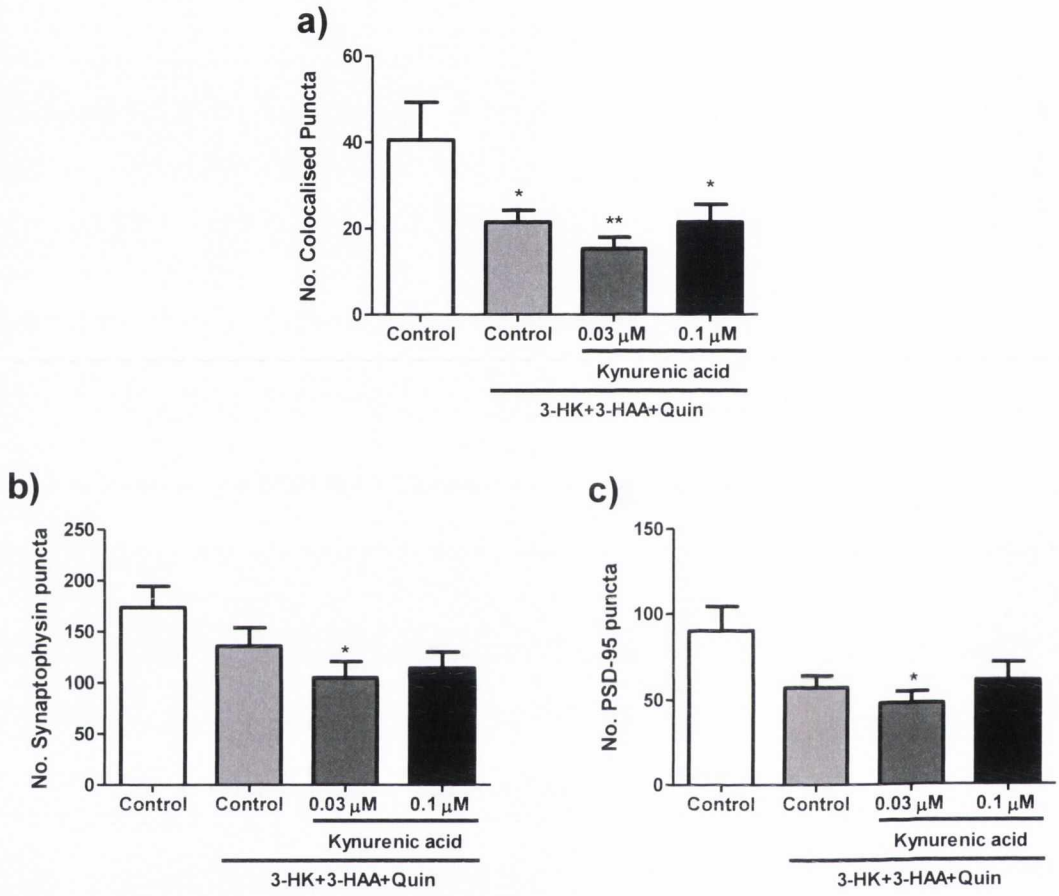

Figure 4.3.5.4: Concentration-related effects of kynurenic acid on the 3-hydroxykynurenine + 3-hydroxyanthranillic acid + quinolinic acid combination-induced reductions in the expression of synaptic markers

Primary cortical neurons (DIV 18-21) were treated with kynurenic acid (0.03 or 0.1 μM) and/or the 3-hydroxykynurenine (3-HK; 0.03 μM) + 3-hydroxyanthranillic acid (3-HAA; 0.03 μM) + quinolinic acid (Quin; 0.1μM) combination for 24 hr. Data expressed as mean ± SEM (n= 41-58 coverslips from 3 independent experiments). The neurons were examined to determine (a) the co-localised expression of pre- and post-synaptic markers synaptophysin and PSD-95, (b) the number of synaptophysin puncta, and (c) the number of PSD-95 puncta in isolation using ImageJ software. *P<0.05, **P<0.01 vs. control (One-way ANOVA followed by Newman Keuls *post hoc* test).

4.4 Discussion

Results from the current investigation demonstrated that IFNγ activates the kynurenine pathway to varying extents in primary microglia, astrocytes, mixed glia and neurons. Of these cultures, only CM from primary mixed glia was capable of inducing neuronal atrophy. In addition, treatment of mature neurons with IFNγ-stimulated mixed glial CM culminated in synapse loss, indicating reduced formation of connections between neurons. Prior treatment of mixed glial cells with the IDO inhibitor, 1-MT (L), was found to attenuate the atrophic effect of the IFNγ-stimulated mixed glial CM. Furthermore, direct treatment of primary cortical neurons with kynurenine pathway metabolites enabled the identification of those metabolites which possess atrophic properties. Of the metabolites examined, 3-hydroxykynurenine, 3-hydroxyanthranillic acid, quinolinic acid and kynurenic acid were found to reduce neuronal complexity. Furthermore, at concentrations that previously demonstrated no effect, a combination of 3-hydroxykynurenine, 3-hydroxyanthranillic acid, and quinolinic acid exhibited a synergistic atrophic effect resulting in reduced neuronal complexity in tandem with synapse loss in mature neurons. Finally, the potential for kynurenic acid to protect against oxidative and excitotoxic agent-related neuronal atrophy is demonstrated.

4.4.1 IFNγ activates the kynurenine pathway in primary cortical cells, of which IFNγ-stimulated mixed glial CM reduces neuronal complexity and synaptogenesis

IFNγ is the most widely used activator of the kynurenine pathway due to its ability to potently induce both IDO gene expression and enzyme activity (Yasui et al., 1986). As such, it was chosen as the stimulus for examination of kynurenine pathway activation in various primary brain cells. Similar to chapter 3 and findings reported in the literature which demonstrate that IFNγ increases IDO and KYNU expression in human foetal microglia and murine microglia (Chen et al., 2011, Guillemin et al., 2005b), IFNγ induced the mRNA expression of IDO and KYNU in primary rat microglial cells. Furthermore, IFNγ reduced the mRNA expression of KAT II, while having no effect on KMO or TDO mRNA expression in these cells. In comparison with previous findings in BV-2 microglia, the ΔΔCt values of vehicle-treated primary microglia were higher for IDO, and KYNU and lower for KAT II mRNA expression (see supplementary **Table S1**). Interestingly, inspite of the lower fold change in vehicle-treated BV-2 microglial cells, they contain higher baseline levels of IDO and KYNU mRNA - enzymes associated with the neurotoxic arm of the kynurenine pathway - and lower baseline levels of KAT II mRNA - the enzyme associated with the neuroprotective arm of the pathway. The concentrations of both tryptophan and kynurenine were increased in the CM of IFNγ-stimulated primary microglia, however there was no change in the concentration of 3-hydroxykynurenine or the

kynurenine over tryptophan ratio. Similar to the previously reported findings in BV-2 microglia, this may be due to the release of tryptophan from reactive microglia, with a lack of neuronal and astroglial cells present for uptake of this amino acid. In all instances, the concentrations of metabolites in the vehicle-treated microglial CM are higher than those reported in vehicle-treated BV-2 microglia CM highlighting the higher level of baseline kynurenine pathway activation in BV-2 microglia. In any case, the increase in primary microglial IDO gene expression alongside the elevation in kynurenine in the CM implies kynurenine pathway activation in response to IFNγ. 3-hydroxykynurenine remaining unchanged may be as a consequence of a lack of induction of KMO expression in IFNγ-stimulated primary microglia. In order to determine the effect of this IFNγ CM on neuronal viability and complexity, primary cortical neurons were treated with CM at either 24 hr or 48 hr. Unlike in chapter 3 where IFNγ-stimulated BV-2 CM was found to reduce both measures at 48 hr, the IFNγ-stimulated microglial CM exhibited no neurotoxic or atrophic properties at either time point.

Consequently kynurenine pathway activation was examined in mixed glia which consist of 70% astrocytes and 30% microglia (McNamee et al., 2010b). Mixed glial cultures were employed based on the knowledge that primary microglia isolated from mixed glia are in an immune-activated state (Ju et al., 2015) which may account for the lack of effect observed in the previously described microglial experiments. As such, in this instance, microglia in an astrocytic environment may be a more effective tool as unstimulated cells would be in a more quiescent state. IFNγ stimulation of mixed glia led to an increase in the mRNA expression of IDO, but had no effect on TDO, KMO or KYNU expression and concurrently reduced KAT II mRNA expression. Regarding the effect on the concentrations of the metabolites, IFNγ reduced both tryptophan and kynurenine, and had no effect on 3-hydroxykynurenine or the kynurenine over tryptophan ratio. These reductions in tryptophan concentrations are contrary to the primary microglial findings, suggesting that the presence of astrocytes may account for uptake of microglia-associsted tryptophan. Furthermore, reductions in kynurenine concentrations may indicate substrate metabolism down the pathway by kynurenine pathway enzymes that although not induced are still present and active. Greater clarity on the extent of pathway activation would be attainable if all metabolites were measured, however concentrations of 3-hydroxyanthranillic acid, quinolinic acid and kynurenic acid were not within our realms to measure.

Following on from this, the effect of IFNγ-stimulated mixed glial CM on neuronal viability and complexity was assessed. IFNγ CM had no effect on the viability of primary cortical neurons, however it reduced the number of neuritic branches, neurite length, the number of primary neurites, and branching at 10, 20, 30, 40 and 50 μm. In order to confirm a role for kynurenine pathway activation in mediating IFNγ-stimulated mixed glial CM-induced atrophy, the protective effect of the IDO

inhibitor, 1-MT (L) was assessed. Considering IDO is the rate limiting enzyme of this pathway, and is present in both astrocytes and microglia, inhibition of IDO prevents activation of both arms of the kynurenine pathway in mixed glial cultures. Prior treatment of mixed glia with 1-MT (L) prevented IFNγ CM-induced reductions in all measures of neuronal complexity, supporting the hypothesis that IFNγ-mediated kynurenine pathway activation in reactive primary microglia drives these atrophic effects.

To confirm that the astrocytic arm of the kynurenine pathway was not involved in the IFNγ-stimulated mixed glial CM-induced reductions in neuronal complexity, the expression of the kynurenine pathway enzymes, and the effect of the CM on neuronal viability and complexity were examined. IFNγ increased the expression of IDO and KMO, reduced the expression of TDO and KYNU, and had no effect on the expression of KAT II in primary cortical astrocytes. This is in accordance with the literature whereby IFNγ (100 IU/ml) has been shown to increase IDO protein expression in human foetal astrocytes (Guillemin et al., 2005b, Guillemin et al., 2001). In addition, IFNγ had no effect on the concentrations of tryptophan and kynurenine pathway metabolites in the CM of astrocytes, with IFNγ CM from astrocytes failing to reduce neuronal viability or complexity. Of potential interest is a role for kynurenic acid in the supportive nature of unstimulated astrocytic CM, which has previously been found by our laboratory to have trophic effects on primary cortical neurons [unpublished data (O'Toole, 2015)]. Treatment of astrocytes with either an IDO or KAT II inhibitor followed by assessment of the effects of this CM on neuronal complexity would provide insight into a role for basal activation of the neuroprotective arm of the kynurenine pathway in driving neuronal complexity.

Considering that IFNγ is present in the IFNγ CM which is applied to neurons, the effect of this inflammatory cytokine on the expression of kynurenine pathway enzymes was assessed. Despite this dose of IFNγ having been shown to have no effect on viability or outgrowth, its presence in the CM could potentially lead to activation of the kynurenine pathway in these neurons. Indeed, IFNγ increased the expression of IDO, but had no effect on the mRNA expression of TDO, KMO, KYNU, KAT II, or on the concentrations of tryptophan and kynurenine pathway metabolites in the neuronal CM. This is in agreement with findings by Guillemin et al. (2005b), who demonstrated increases in IDO protein expression in human foetal neurons. This induction of the rate limiting enzyme could potentially contribute to the reductions in neuronal complexity seen with the IFNγ-stimulated mixed glial CM, however, the fact that the reductions were absent in the presence of either microglial or IFNγ-stimulated astrocytic CM supports the hypothesis that the reductions are glial mediated.

In addition to neurite outgrowth, the potential of IFNγ-stimulated mixed glial CM to induce synapse loss was examined. Synapse loss is a pathological hallmark of neurological disease (Koffie et al., 2011). In this instance, to allow for the measurement of pre- and post-synaptic proteins mature

neurons were incorporated into the experimental design. Mature neurons are more developed in terms of both enzyme and protein expression, thus they are more sensitive to external stimuli (Lesuisse and Martin, 2002). As such, the effect of both IFNγ and IFNγ CM on the viability of these neurons was re-assessed. In both instances there was no reduction in neuronal viability. Regarding the co-localised expression of the synaptic markers, synaptophysin and PSD-95, as a measure of synaptogenesis, the IFNγ-stimulated mixed glial CM was found to reduce this, primarily through reduced expression of PSD-95. The effect of reactive glial CM on the co-localised expression of synaptic markers has not previously been reported, however reactive glial-associated soluble facots have been found to reduce these synaptic markers. Previous work by our lab has demonstrated that TNFα reduced the expression of both synaptophysin and PSD-95 [unpublished data O'Neill (2015)], while another group reported that in mice IL-1β reduced the expression of the post-synaptic marker, PSD-95, through ubiquitintion (Mir et al., 2014). The IFNγ CM-induced reductions in the co-localised expression of synaptic markers was attenuated by prior treatment of the mixed glia with 1-MT (L) implicating mixed glial kynurenine pathway activation and subsequent metabolite release in driving synapse loss. To further clarify a role for microglia as opposed to astrocytes in mediating the deleterious atrophic mixed glia IFNγ CM effects, microglial and astrocytic function could be independently targeted with minocycline or L-alpha aminoadipic acid (L-AAA) respectively. Alternative examining whether the atrophic effects of microglia are present following stimulation of isolated microglial cultures with IFNγ and simulateous supplementation with kynurenine may resolve this issue.

4.4.2 Kynurenine pathway metabolites alter measures of neuronal integrity

In light of the finding that inhibiting the kynurenine pathway in IFNγ stimulated mixed glia was capable of preventing IFNγ CM-induced reductions in neuronal complexity and synapse loss, direct application of kynurenine pathway metabolites onto primary cortical neurons was carried out to investigate their direct atrophic effects. Under normal circumstances the kynurenine pathway is involved in producing NAD^+, however the catabolic system responsible for converting quinolinic acid to NAD^+ is quickly saturated resulting in the accumulation of quinolinic acid (Chen & Guillemin 2009). In times of infection or under pathological conditions the excessive build-up of quinolinic acid and its preceding metabolites could contribute to neuronal damage. This is due to the fact that inflammation favours activation of the neurotoxic arm of the pathway (Connor et al. 2008). These neurotoxic metabolites have the potential to disrupt normal neuronal functioning through oxidative and/or excitotoxic mechanisms which can contribute to inflammation-induced neuronal atrophy (Stadelmann et al. 2011).

The concentration of tryptophan in the plasma of humans is between 40-90 μM (Forrest et al., 2006, Amirkhani et al., 2002) or 39.1-40.6 μM in rat plasma (Pawlak et al., 2003, Topczewska-Bruns et al., 2002), with levels in the brain reliant on the concentrations of free circulating tryptophan (Fernstrom et al. 1976). In line with the literature, whereby tryptophan at 0.1-1000 μM does not affect neuronal viability of human primary neurons as measured by LDH release (Braidy et al. 2009), no effect on viability was observed following treatment of immature and mature neurons with tryptophan (1-100 μM). In addition, no reductions in neuronal complexity were observed following treatment with tryptophan (1-100 μM).

Kynurenine which has a physiological concentration of 1.5 μM in the plasma of humans (Amirkhani et al., 2002) or 1.6-1.83 μM in rat plasma (Pawlak et al., 2003, Topczewska-Bruns et al., 2002) affects NAD^+ synthesis and neuronal viability when concentrations greater than 1 μM were applied to human primary neurons (Braidy et al. 2009). In this instance, treatment of neurons with kynurenine (1 μM) reduced neuronal viability of mature neurons, however no other effects on viability or complexity were observed. This is in contrast to the work done by Braidy and colleagues, however they suggest that the increase in NAD^+ observed indicates an increase in the production of quinolinic acid which may be triggering the reductions in cell viability rather than kynurenine itself (Braidy et al. 2009).

In general there is rapid uptake of kynurenine into both astrocytic and microglial cells (Braidy et al. 2009), which is readily converted to 3-hydroxykynurenine in microglia (Agudelo et al. 2014). Both kynurenine and 3-hydroxykynurenine, which has serum concentrations of 383 nM in humans (Heyes 1994) or 0.05-0.059 μM rat plasma (Pawlak et al., 2003, Topczewska-Bruns et al., 2002) contribute to central pools by crossing the BBB via a saturable transport system. In contrast, 3-hydroxyanthranillic acid - with serum concentrations of 24 nM in humans (Myint et al. 2007) and <100 nM in rat plasma (Brunelli et al., 2013) - quinolinic acid and kynurenic acid passively diffuse across the BBB at a very low rate giving them poor access to the brain. Consequently, peripheral levels of these metabolites do not significantly contribute to the central pool (Fukui et al. 1991).

Treatment of neurons with either 3-hydroxykynurenine or 3-hydroxyanthranillic acid at 0.01-0.1 μM had no effect on neuronal viability of either immature or mature neurons which is supported by the literature whereby only concentrations of 1 μM or above of either metabolite reduce viability (Braidy et al. 2009). Both 3-hydroxykynurenine and 3-hydroxyanthranillic acid at 0.1 μM caused reductions in neurite length and the number of primary neurites. In addition, 3-hydroxyanthranillic acid (0.1 μM) reduced branching at 10 and 20 μm from the soma, and 3-hydroxyanthranillic acid (0.01, 0.03 μM) reduced branching at 20 μm from the soma.

The concentrations of quinolinic in the human brain are usually less than 100 nM (Guillemin & Brew 2002) or 0.3564 µM in rat plasma (Pawlak et al., 2003) but can increase in an inflammatory environment (Guillemin & Brew 2002). As peripheral quinolinic acid crosses the BBB poorly, centrally produced quinolinic acid is more implicated in affecting neuronal integrity. In contrast to Braidy et al. (2009b) who demonstrated that quinolinic acid at concentrations of 0.5 µM or greater reduces viability, this investigation found no such reductions in viability at the concentrations of quinolinic acid tested (0.1-100 µM) in either immature or mature neurons. Reductions in the number of neuritic branches occurred following treatment with quinolinic acid (1 µM). Additionally, reduced neurite length was observed following treatment with quinolinic acid (1, 10, 25, 100 µM), while reductions in the number of primary neurites were observed with quinolinic acid (1, 25, 100 µM), whereas reductions in branching were seen with quinolinic acid (0.1-100 µM).

Similar to the findings described here, Pierozan et al. (2015) have reported that quinolinic acid at concentrations between 10-100 µM with exposure times ranging from 24 to 72 hr failed to affect the viability of rat primary neurons. Moreover, exposure of primary striatal neurons to quinolinic acid at 10, 25 and 100 µM has been reported to result in hyperphosphorylation of neurofilament subunits which is believed to be mediated by NMDA receptor-driven increases in intracellular Ca^{2+}. In addition, this group demonstrated that these same concentrations of quinolinic acid reduced neurite length.

Kynurenic acid, which is found in the human brain at concentrations 150 pmol/g wet weight (Moroni et al. 1988) or 0.0453 µM in rat plasma (Pawlak et al., 2003) is often described as being neuroprotective due to its ability to antagonise the glycine binding site of the NMDA receptor at low concentrations, and the glutamate/quinolinic acid binding site of the NMDA receptor at micromolar concentrations (Sas et al. 2007). The study described here, demonstrates that kynurenic acid at 0.03 µM increases neuronal viability, while no effect on the viability of either immature or mature neurons is observed at any other concentration. This is in agreement with findings presented by Braidy et al. (2009b) who demonstrate no effect of kynurenic acid on neuronal viability at concentrations ranging from 0.1-1000 µM. Additionally, 0.1, 1, and 10 µM kynurenic acid reduced neurite length, the number of primary neurites and branching at 10 and 20 µm from the soma. Excess antagonism of the NMDA receptor may be responsible for this reduction in outgrowth as activation of the NMDA receptor has been shown to have neurotrophic effects (Burgoyne et al. 1993). Kynurenic acid may therefore implement its neuroprotective properties at lower concentrations, or when it is in the presence of other NMDA receptor agonists.

Considering that under physiological conditions these metabolites would not be present in isolation of each other, various combinations of metabolites were applied to both immature and mature neurons to examine if there was a synergistic reduction in measures of neuronal integrity. In all instances, no combination affected the viability of immature or mature neurons. However of the

different combinations, the one that contained all three neurotoxic metabolites reduced neurite length, the number of primary neurites, and branching at 10, 30, 40, and 50 μm from the cell soma. In addition, the 3-hydroxykynurenine + 3-hydroxyanthranillic acid combination reduced the number of primary neurites, and branching at 10 and 20 μm from the cell soma. In the case of synapse loss, 3-hydroxykynurenine, 3-hydroxyanthranillic acid, quinolinic acid and kynurenic acid led to non-significant reductions in the co-localised expression of synaptic markers. All combinations of metabolites reduced the co-localised expression of synaptic markers - primarily through reduced PSD-95 expression - demonstrating a negative synergistic effect on synaptogenesis.

Variations in the literature regarding the effects that kynurenine pathway metabolites have on neuronal complexity may be as a consequence of variations between experimental parameters. These may include differences in the treatment duration and concentration, variations in protocols for the preparation of primary cultures and also the specific type of neuron utilised. In particular the age at which the neuronal cultures are treated may greatly influence the outcomes and cellular resilience or lack thereof to exposure to the various metabolites.

4.4.3 Characterisation of the atrophic effects of glutamate

Previous work carried out by our laboratory has strongly implicated the NMDA receptor in neuronal complexity, with NMDA dose-dependently reducing complexity in the presence of glycine, while glutamate decreased complexity at high concentrations (500 μM) only in the presence of glycine. In spite of glutamate at concentrations of 100 μM or greater saturating all glutamate receptors in neuronal cultures (Metzger et al., 1998), the observed glutamate-induced effects were reported to be NMDA receptor mediated as blockade of the AMPA receptor did not attenuate the reductions (Doucet et al., 2015). Furthermore, noradrenaline-stimulated mixed glial CM protected against glutamate and glycine-induced reductions in the number of neuritic branches and neurite length [unpublished data O'Neill (2015)]. As such, it was of interest to examine the potential role of kynurenic acid in mediating these noradrenergic-related CM protective effects based on recent findings that adrenergic agents increase the levels of kynurenic acid in rat mixed glial cultures and brain slices (Luchowska et al., 2009). Under normal circumstances, glutamate is present in the extracellular matrix of the brain at micromolar concentrations, with these concentrations increasing 100-fold in excitotoxic situations (Gras et al., 2012). Consequently, the first of these experiments outlined in this chapter verified that at the concentration of glutamate and glycine used, no effect on viability was observed. Additionally, the effect on neuronal complexity was assessed and elicited reductions in the number of neuritic branches, neurite length, the number of primary neurites and branching at 10, 20, and 30 μm from the cell soma.

A role for glutamate in the regulation of neurite outgrowth, synaptogenesis and neuronal survival is now well appreciated [see, Mattson (2008) for review]. To further examine the atrophic nature of glutamate, its effect on synapse loss in mature neurons was investigated. Previously our lab has demonstrated that NMDA and glycine induce synapse loss in primary cortical mature neurons neurons [unpublished data (O'Toole, 2015)]. Initially our findings demonstrated a pronounced sensitivity of these neurons to glutamate, with the high concentration (500 μM) used previously in this chapter and also 100 μM and 500 μM used by Doucet et al. (2015) in combination with glycine 1 μM or 10 μM substantially reducing the viability of mature neurons. As such, the concentrations of glutamate were reduced with 0.1-50 μM reducing viability in the presence of glycine 10 μM, but having no effect in combination with glycine 1 μM. As such glutamate 50 μM and glycine 1 μM were chosen to examine the effect on the expression of synaptic markers. In this instance, both glutamate alone and in combination with glycine reduced the co-localised expression of synaptic markers, chiefly through reduced expression of the post-synaptic marker, PSD-95. This is complementary to the mechanism by which the kynurenine pathway combination reduces the co-localised expression of synaptic markers, suggesting that NMDA receptor over-activation and/or oxidative stress negatively regulates PSD-95 expression or recruitment to the synapse. Indeed, other inflammatory-related action at the PSD, reduced the expression of PSD-95 through E3 ligase-mediated ubiquitination in mice (Mir et al., 2014). Furthermore, NMDA has been reported to reduce PSD-95 protein expression in rat primary hippocampal neurons which was dependent on the presence of extracellular Ca^{2+}. This reduction was demonstrated to be as a consequence of NMDA receptor activation and downstream ubiquitnation of PSD-95 (Colledge et al., 2003). In addition, oxidative stress, - generated directly or indirectly as consequence of the action of glutamate or kynurenine pathway metabolites - has been demonstrated to reduce PSD-95 in a rat model of traumatic brain injury (Ansari et al., 2008).

4.4.4 Kynurenic acid as a potential candidate for attenuating the atrophic effects of glutamate

Kynurenic acid is a tryptophan derivative produced as a consequence of tryptophan metabolism down the neuroprotective arm of the kynurenine pathway - so called as a consequence of kynurenic acids broad spectrum antagonism of ionotropic glutamate receptors in rodents (Perkins and Stone, 1982) and primates (Stone and Perkins, 1984). Within the brain, kynurenic acid is primarily produced by astrocytes which express the rate limiting enzymes of the pathway, IDO and TDO (Miller et al., 2004), which metabolise tryptophan to kynurenine, along with KAT enzymes (I and II) which are responsible for the production of kynurenic acid from kynurenine (Guillemin et al., 2001). Of these KAT enzymes, KAT II is responsible for 75% of the production of central kynurenic acid due to its

optimum pH being neutral (Guidetti et al., 1997). The renowned neuroprotective capacity of kynurenic acid became apparent following the discovery of its ability to block the action of excitatory amino acids including, quinolinic acid, NMDA and kainic acid [see, Stone (1993) for review]. Further support for the neuroprotective properties of this metabolite arose after it prevented excitotoxic-driven neuronal loss and seizures in rodents (Stone, 2000).

Considering the aforementioned atrophic effects of glutamate and glycine, the ability of kynurenic acid to attenuate glutamate-related atrophy was investigated. In this instance, 1 and 10 μM kynurenic acid protected against the reductions in the number of neuritic branches, 0.03-10 μM kynurenic acid prevented the reductions in neurite length, 0.03 and 1 μM kynurenic acid attenuated the reductions in the number of primary neurites, and 1 μM kynurenic acid preventing reductions in branching at 20 and 30 μm form the cell soma. However, regarding glutamate-induced synapse loss, no attenuating effect of kynurenic acid at either concentration was effective. In this instance, a higher concentration of kynurenic acid although potentially deleterious in isolation may be protective in the presence of NMDA receptor agonists.

Following on from this, a role for kynurenic acid in protecting against the previously observed atrophy induced by the combination of 3-hydroxykynurenine + 3-hydroxyanthranillic acid + quinolinic acid was examined. The concentrations of kynurenic acid used started at a subthreshold concentration in isolation and increased to atrophic concentrations in order to examine if the atrophic effects of kynurenic acid seen are abolished in the presence of the other competing metabolites. Indeed, all concentrations used protected against the 3-hydroxykynurenine + 3-hydroxyanthranillic acid + quinolinic acid combination-induced reductions in the number of neuritic branches, neurite length, the number of primary neurites, and branching at 10, 20, 30 and 40 μm from the cell soma. In contrast, concentrations of kynurenic acid which had no effect on the co-localised expression of synaptic markers, failed to attenuate the 3-hydroxykynurenine + 3-hydroxyanthranillic acid + quinolinic acid combination-induced reductions as previously proposed, a higher concentration of kynurenic acid may be more successful at blocking these reductions.

4.4.5 Conclusion

The experiments outlined in this chapter support a role for kynurenine pathway activation, and subsequent metabolite release and action on neurons in driving reactive microglial-induced neurite atrophy and synapse loss. Although much work has been carried out with regard to how kynurenine pathway metabolites alter neuronal viability, these findings are the first to demonstrate the properties of kynurenine pathway metabolites with regard to altering neuronal complexity and

synaptogenesis. In addition, the effects of combinations of metabolites at physiological concentrations have not previously been examined on either neuronal viability, complexity or synaptogenesis. Considering that neurite atrophy and synapse loss precede cell death (Knight and Verkhratsky, 2010), intervening in atrophic processes is a more attractive and potentially effective mechanism for ameliorating neurodegeneration. As such, these data propose targeting the kynurenine pathway as a novel route by which these atrophic processes may be hindered, potentially restoring neuronal functioning in neurological disease.

Chapter 5

Noradrenergic-mediated regulation of the kynurenine pathway in primary cortical glia and neurons

5.1 Introduction

Neuroinflammation is common to many, if not all, neurodegenerative disorders (Glass et al., 2010), of which inflammation-driven astrocytic and microglial activation is thought to contribute to neuronal dysfunction and subsequent death (Floyd, 1999). The brain is considered an 'immunologically privileged' organ primarily as a consequence of its segregation from the peripheral immune system by the BBB. It is now recognised that the brain has its own intrinsic immune system, tightly coordinated by both microglia and astrocytes (Rock et al., 2005). Manipulation of inflammatory systems in these cells could potentially attenuate inflammation-associated neuronal atrophy and toxicity.

Noradrenaline is a catecholaminergic neurotransmitter involved in a host of CNS functions, with deficits in this system commonly implicated in the pathophysiology of neurodegenerative diseases (Zarow et al., 2003). As such, understanding the neuroprotective properties of noradrenaline are of interest in determining potential mechanisms of ameliorating or attenuating neurodegenerative processes. The anti-inflammatory capacity of noradrenaline is considered to be one of its most important roles in the CNS, with the β_2-adrenoceptor/cAMP/PKA pathway exhibiting the most potent anti-inflammatory effects of the adrenoceptor signalling cascades (Carnevale et al., 2007). Activation of this pathway results in the increased expression of the NFκB inhibitor, IκBα, which reduces NFκB-mediated induction of inflammatory factors (Gavrilyuk et al., 2002). Under normal conditions noradrenaline can induce the expression of chemokines and other inflammatory factors. However it has been demonstrated *in vivo* that the opposite occurs in the presence of LPS, suggesting that the anti-inflammatory properties of noradrenaline are an adaptive response to neuroinflammation (Hinojosa et al., 2013).

In addition, noradrenaline is renowned for its neuroprotective potential, with β_2-adrenoceptor stimulation culminating in increased expression of neurotrophic factors in both neurons and glia (Day et al., 2014, Counts and Mufson, 2010). Furthermore, noradrenergic agents have protected neurons against toxic insults both *in vitro* and *in vivo* in rodents (Counts and Mufson, 2010, Gleeson et al., 2010, Junker et al., 2002). Likewise, noradrenaline has attenuated the Alzheimer's disease toxin, $A\beta_{1-42}$-induced increases in intracellular ROS, mitochondrial membrane depolarisation and caspase activation in the human neuronal cell line, hNT (Counts and Mufson, 2010). Additionally, the trophic effects of noradrenergic stimulation of astrocytes on rat primary cortical neurons have recently been demonstrated by Day et al. (2014), with noradrenaline-stimulated astrocytic CM increasing neurite outgrowth and complexity as a result of increased release of IL-6 and growth factors. Considering the diverse intracellular responses that occur as a consequence of adrenoceptor activation, understanding the factors involved in driving neuroprotection is imperative. In light of the poor BBB

permeability and pharmacokinetic properties of neurotrophins (Longo and Massa, 2013), their potential therapeutic use is limited. As such, other compounds implicated in the neuroprotective effects of noradrenaline are of interest.

Until recently, little was known about the intracellular mechanisms that regulate kynurenic acid production in the brain. The noradrenergic system is now regarded as having an influential role in the regulation of the activity of KAT enzymes and subsequent kynurenic acid production via a cAMP/PKA-dependent signalling pathway in the rodent brain (Luchowska et al., 2009, Luchowska et al., 2008). Adrenoceptors are expressed on glia and neurons, where they are coupled to G proteins some of which positively or negatively regulate adenylate cyclase and cAMP levels (Rang and Dale, 2012). Of the adrenoceptors (α_1, α_2, β_1, β_2, β_3), α_2, β_1 and β_2 are primarily involved in the regulation of cytokines through the modulation of cAMP levels. α_2- and β-adrenoceptor stimulation exert opposing effects on intracellular cAMP levels, with the former reducing and the latter increasing cAMP levels in these cells [see, Szelényi (2001) for review].

This chapter aims to examine the mechanism by which the noradrenergic system regulates the kynurenine pathway in rat primary cortical astrocytes. Furthermore the ability of noradrenergic agents to activate the pathway in microglia and neurons is assessed. Considering the anti-inflammatory effects of β-adrenoceptor stimulation, the IFNγ-induced changes in the mRNA expression of kynurenine pathway enzymes in primary cortical glia and neurons observed in chapter 4 are re-assessed in the presence of the β_2-adrenoceptor agonist, formoterol. In order to establish a potential role for the kynurenine pathway in mediating the neuroprotective effects of β_2-adrenoceptor stimulation, the effect of CM from mixed glial cultures stimulated with both IFNγ and formoterol with or without the selective TDO inhibitor, 680C91, on neuronal complexity and synaptogenesis is examined. Furthermore, in light of the finding that 3-hydrokynurenine, 3-hydroxyanthranillic acid, and quinolinic acid in combination induce neurite atrophy and synapse loss, the potential for formoterol-stimulated astrocytic CM to protect against these reductions is investigated.

5.2 Study design

5.2.1 Effect of noradrenaline on the mRNA expression of kynurenine pathway enzymes in primary cortical astrocytes

Noradrenergic agents have been reported to increase the production of kynurenic acid in mixed glial cultures (Luchowska et al., 2009). The following experiment was carried out to assess the effect that noradrenaline has on the expression of kynurenine pathway enzymes and determine the role that the various α- and β-adrenoceptors have in mediating these changes. Noradrenaline was chosen on the basis that it is an endogenous ligand of all subtypes of adrenoceptors. The concentrations chosen were shown to increase neuronal outgrowth and complexity through action on glial adrenoceptors as opposed to on neurons directly, with the higher concentration of 10 μM increasing the mRNA and protein expression of IL-6 and various trophic factors (Day et al., 2014)

Primary cortical astrocytes (DIV 12-13) were treated with noradrenaline (1, 10 μM), for 6 hr. Cells were harvested for RNA extraction followed by quantitative PCR to measure the mRNA expression of kynurenine pathway enzymes, including the rate limiting enzymes, IDO and TDO, and the downstream enzymes, KMO, KYNU and KAT II/Aadat.

Primary cortical astrocytes were subsequently pre-treated with the non-selective α-adrenoceptor antagonist, phentolamine (10 μM; 30 min), the α_1-adrenoceptor antagonist, prazosin (10 μM; 30 min), the α_2-adrenoceptor antagonist yohimbine (10 μM; 30 min), or the non-selective β-adrenoceptor antagonist, propranolol (10 μM; 30 min). Cells were harvested for RNA extraction followed by quantitative PCR to measure the mRNA expression of the kynurenine pathway enzymes.

Phentolamine was chosen on the basis that it is a reversible non-selective α-adrenoceptor antagonist as opposed to phenoxybenzamine which is irreversible (Fagbemi and Salako, 1982). Prazosin is reported as the most potent α_1- and least potent α_2-adrenoceptor antagonist (Perrone et al., 1990), and thus was chosen as the α_1-adrenoceptor antagonist. The rank order of potency for the α_2-adrenoceptor is phentolamine> idazoxan> yohimbine> piperoxan= napamezole> mianserin>> prazosin. Yohimbine was chosen on the basis that it is more selective than phentolamine and unlike idazoxan it does not interact with other receptors such as imadizoline receptors (Bousquet et al., 1999). Propranolol was chosen as the non-selective β-adrenoceptor antagonist as it is more pure and potent than the original compound, dichloroisoproterenol and other partial agonists such as oxprenolol or alprenolol (Rang and Dale, 2012).

5.2.2 Effect of isoproterenol on the mRNA expression of kynurenine pathway enzymes in primary cortical astrocytes

In order to further elucidate the role of the β-adrenoceptors in mediating noradrenergic-related changes in kynurenine pathway enzyme expression, primary cortical astrocytes (DIV 12-13) were treated with the non-selective β-adrenoceptor agonist, isoproterenol (1, 10 μM). Cells were harvested for RNA extraction followed by quantitative PCR to measure the mRNA expression of kynurenine pathway enzymes.

Isoproterenol, also known as isoprenaline, is a β_1 and β_2-adrenoceptor agonist exhibiting greater potency at all β-adrenoceptor subtypes than either noradrenaline or adrenaline (Rang and Dale, 2012).

Primary cortical astrocytes were subsequently pre-treated with the non-selective β-adrenoceptor antagonist, propranolol (10 μM; 30 min), the β_1-adrenoceptor antagonist, atenolol (10 μM; 30 min) or the β_2-adrenoceptor antagonist, ICI 118, 551 (10 μM, 30 min) followed by treatment with isoproterenol (1, 10 μM). Cells were harvested for RNA extraction followed by quantitative PCR to measure the mRNA expression of the kynurenine pathway enzymes. Both adrenoceptor antagonists were ineffective in the presence of isoproterenol 10 μM, a higher concentration of the antagonists appears to be needed to compete with this dose of β-agonist, as such, only the effects of the antagonists on isoproterenol 1 μM-induced changes in mRNA expression have been presented in this thesis.

Atenolol was chosen as a β_1-adrenoceptor antagonist due to its widespread use in the treatment of hypertension (Smith and Teitler, 1999). ICI 118, 551 was chosen as a β_2-adrenoceptor antagonist on the basis that it is 543-fold and 661-fold more selective for the β_2-adrenoceptor over either β_1 or β_3-adrenoceptors respectively (Baker, 2005).

To validate a role for the β_2-adrenoceptor in driving activation of the kynurenine pathway in astrocytes, primary cortical astrocytes (DIV 12-13) were treated with the selective β_2-adrenoceptor agonist, formoterol (1, 10 μM), for 6 hr with or without pre-treatment with propranolol (10 μM; 30 min) or ICI 118, 551 (10 μM; 30 min). Cells were harvested for RNA extraction followed by quantitative PCR to measure the mRNA expression of the kynurenine pathway enzymes.

Formoterol was chosen as a β_2-adrenoceptor agonist as a consequence of its high affinity, selectivity and potency for this receptor, alongside its rapid onset of action and long half-life (Anderson, 1993).

Finally to determine a role for cAMP in mediating this β_2-adrenoceptor change in kynurenine pathway enzyme gene expression, primary cortical astrocytes (DIV 12-13) were treated with the cAMP analogue dibutyryl cAMP (dbcAMP) (1, 10 μM) for 6 hr. Cells were harvested for RNA

extraction followed by quantitative PCR to measure the mRNA expression of the kynurenine pathway enzymes.

5.2.3 Characterisation of noradrenaline- and formoterol-induced changes in kynurenine pathway enzyme gene expression in primary cortical microglia and neurons

Primary cortical microglia (DIV 12-13) or neurons (DIV 3) were treated with either noradrenaline (10 μM) or formoterol (10 μM) for 6 hr. Cells were harvested for RNA extraction followed by quantitative PCR to measure the mRNA expression of the kynurenine pathway enzymes.

5.2.4 Effect of formoterol on the IFNγ-induced changes in kynurenine pathway enzyme gene expression in primary cortical microglia, astrocytes, neurons and mixed glia

Chapter 4 demonstrated increases in IDO mRNA expression in IFNγ-stimulated primary cortical microglia, astrocytes, neurons and mixed glia. As such, the ability of formoterol to attenuate this induction is investigated here.

Primary cortical microglia (DIV 12-13), astrocytes (DIV 12-13), neurons (DIV 3), and mixed glia (DIV 12-13) were treated with either formoterol (10 μM), IFNγ (10 ng/ml), or a combination of formoterol (10 μM) and IFNγ (10 ng/ml) for 6 hr. Cells were harvested for RNA extraction followed by quantitative PCR to measure the mRNA expression of the kynurenine pathway enzymes.

5.2.5 Effect of formoterol on the IFNγ-induced changes in the concentrations of tryptophan and kynurenine pathway metabolites in the CM of primary mixed glia

Chapter 4 demonstrated reductions in the concentrations of tryptophan and kynurenine in the CM of IFNγ-stimulated mixed glial, as such the ability of formoterol to attenuate these reductions in tryptophan and kynurenine is investigated here.

Primary cortical mixed glia (DIV 12-13) were treated with either formoterol (10 μM), IFNγ (10 ng/ml), or a combination of formoterol (10 μM) and IFNγ (10 ng/ml) for 24 hr. CM was harvested for HPLC analysis of tryptophan and the kynurenine pathway metabolites, kynurenine and 3-hydroxykynurenine.

5.2.6 Effect of formoterol on the IFNγ-stimulated mixed glial CM-induced changes in neuronal complexity and the expression of synaptic markers

Chapter 4 demonstrated the IFNγ-stimulated mixed glial CM-induced atrophy and synapse loss. As such, the ability of formoterol to attenuate these reductions in neuronal complexity and synaptogenesis is investigated here. Considering that noradrenaline has been reported to increase neuronal complexity (Day et al., 2014), a concentration of formoterol was chosen which had no effect on neuronal viability (DIV 3/ 18-21), complexity, or the co-localised expression of synaptic markers (see supplementary **figure S4**).

Primary cortical mixed glia (DIV 12-13) were treated with either formoterol (10 μM), IFNγ (10 ng/ml), or a combination of formoterol (10 μM) and IFNγ (10 ng/ml) for 24 hr. CM was collected, sterile-filtered and placed on primary cortical neurons (DIV 3/ 18-21) for 24 hr. Fixation and fluorescent immunocytochemistry were performed on neurons for Sholl analysis or analysis of the synaptic markers, synaptophysin and PSD-95, as a measure of synaptogeneis as previously described.

To determine a role for TDO in mediating the protective effects of formoterol, primary cortical mixed glia (DIV 12-13) were pre-treated with the TDO inhibitor, 680C91 (20 μM; 30 min) followed by treatment with either formoterol (10 μM), IFNγ (10 ng/ml), or a combination of formoterol (10 μM) and IFNγ (10 ng/ml) for 24 hr. The resultant CM was collected, sterile-filtered and placed on primary cortical neurons (DIV 3/ 18-21) for 24 hr. Fixation and fluorescent immunocytochemistry were performed on neurons for Sholl analysis or analysis of the synaptic markers, synaptophysin and PSD-95.

680C91 was chosen as a TDO inhibitor due to its potent (Ki= 51 nM) and selective inhibitory activity, exhibiting no effect on IDO activity, demonstrating efficacy both *in vitro* and *in vivo* (Salter et al., 1995). Other *in vitro* studies have identified several compounds that inhibit TDO, however, they have been found to either not influence tryptophan levels in humans or rats (Young, 1986), or else indirectly inhibit the activity of TDO (Green et al., 1976).

5.2.7 Effect of formoterol-stimulated astrocytic CM on 3-hydroxykynurenine + 3-hydroxyanthranillic acid + quinolinic acid-induced reductions in neuronal complexity and expression of synaptic markers

Chapter 4 demonstrated that the combination of 3-hydroxykynurenine + 3-hydroxyanthranillic acid + quinolinic acid caused neuronal atrophy and synapse loss. As such, the ability of formoterol-induced activation of the kynurenine pathway to protect against these reductions is examined.

Primary cortical astrocytes (DIV 12-13) were treated with formoterol (10 μM) for 24 hr. The resultant CM was collected, sterile-filtered and placed on primary cortical neurons (DIV 3/ 18-21) for 2 hr followed by addition of the combination of 3-hydroxykynureine (0.03 μM), 3-hydroxyanthranillic acid (0.03 μM), and quinolinic acid (0.1 μM) for 24 hr. Fixation and fluorescent immunocytochemistry were performed on neurons for Sholl analysis or analysis of the synaptic markers, synaptophysin and PSD-95.

Furthermore, primary cortical astrocytes (DIV 12-13) were pre-treated with the TDO inhibitor, 680C91 (20 μM; 30 min), followed by stimulation with formoterol (10 μM) for 24 hr. The resultant CM was collected, sterile-filtered and placed on primary cortical neurons (18-21) for 2 hr followed by addition of a combination of 3-hydroxykynureine (0.03 μM), 3-hydroxyanthranillic acid (0.03 μM), and quinolinic acid (0.1 μM) for 24 hr. Fixation and fluorescent immunocytochemistry were performed on neurons for analysis of the synaptic markers, synaptophysin and PSD-95.

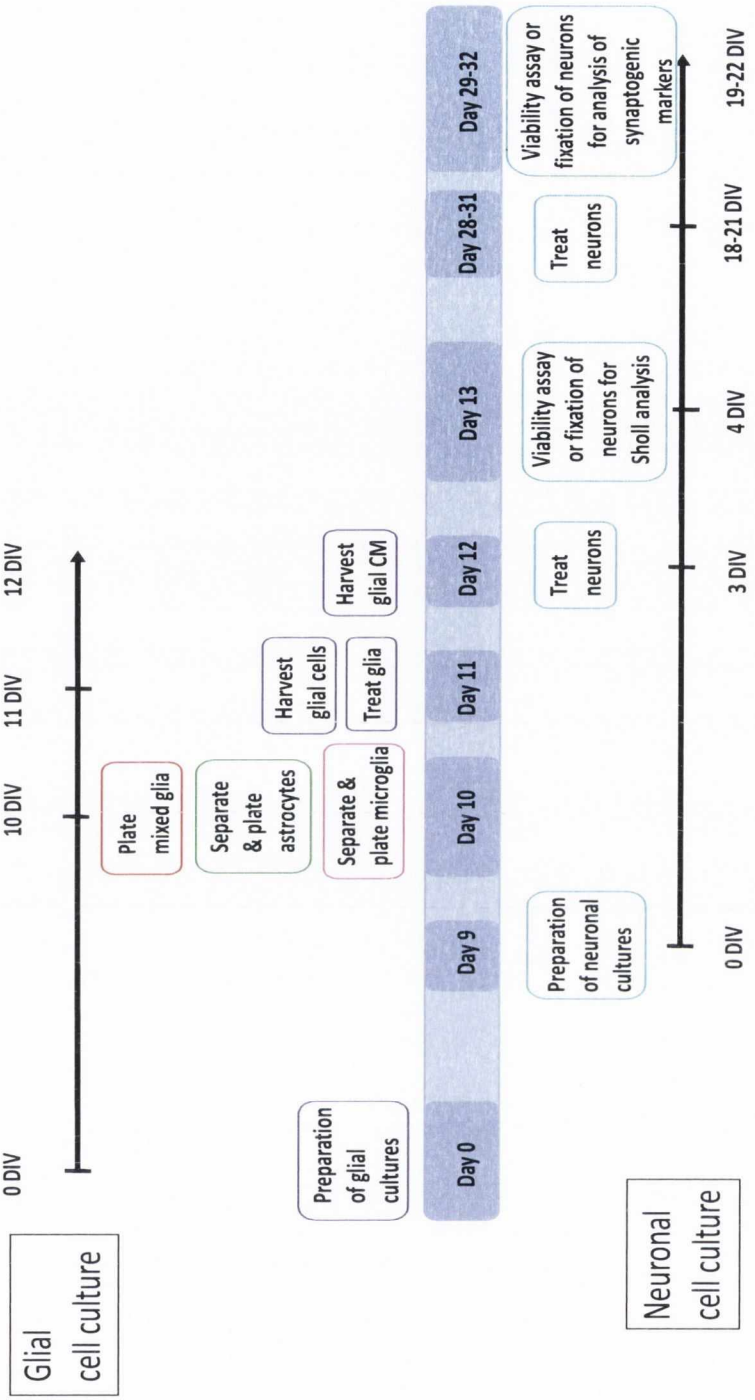

Figure 5.2.1: Diagram showing the timeline of a typical experiment

Glial cells are cultured and grown for 10-12 days upon which they are plated for a minimum of 24 hr prior to treatment. Glial cells are harvested 6 hr post treatment for gene expression analysis, CM is harvested 24 hr post treatment for analysis or treatment of neurons. Neuronal cells are cultured and grown for 3 days upon which they are treated for 24 hr with CM (+/- kynurenine pathway metabolites or glutamate +/- glycine). On day 13 one set of neurons are either assessed for neuronal viability, or they are fixed to allow for assessment of neuronal complexity by Sholl analysis. On day 28-31 the other set of neurons are either assessed for neuronal viability, or they are fixed to allow for assessment of the expression of synaptic markers by Image J analysis.

Table 5.2.1: Table of compounds and concentrations used

To ensure maximal inhibition, all inhibitors/antagonists were incubated on cells for 30 min before additional manipulation with adrenoceptor agonists. Concentrations of agents used were chosen based on those reported in the literature as indicated in the reference column of the table below.

Compound name	***Final concentration***	***In vitro experimental details***	***Reference***
3-Hydroxyanthranillic acid	0.03, 0.1 µM	No effect on viability, neuronal complexity or the expression of synaptic markers in rat primary cortical neurons.	Dose based on dose response studies carried out previously in chapter 4.
3-Hydroxykynurenine	0.03, 0.1 µM	No effect on viability, neuronal complexity or the expression of synaptic markers in rat primary cortical neurons.	Dose based on dose response studies carried out previously in chapter 4.
680C91	20 µM	Inhibited TDO activity in human and murine tumour cell lines.	(Pilotte et al., 2012)
Atenolol	10 µM	Attenuates β-agonist-induced relaxation of pre-contracted muscularis mucosa from rat oesophagus.	(Bahl et al., 1996)
dbcAMP	1, 10 µM	Stimulates proliferation of primary rat Schwann cells.	(Madrigal et al., 2009)
Formoterol	1, 10 µM	Increased the production of kynurenic acid in rat mixed glial cultures.	(Luchowska et al., 2009)
ICI 118, 551	10 µM	Reduces noradrenaline-induced increases in ATP synthesis in rat primary astrocytes. Attenuates β-agonist-induced relaxation of pre-contracted muscularis mucosa from the rat oesophagus.	(Madrigal et al., 2009, Bahl et al., 1996)
Isoproterenol	1, 10 µM	Increases ATP synthesis in rat primary astrocytes; increases cAMP accumulation in rat primary astrocytes.	(Madrigal et al., 2009, Northam et al., 1989)
Noradrenaline	1, 10 µM	10 µM increased mRNA and protein expression of glia growth factors, with this glial CM increasing neuronal outgrowth and complexity but having no effect on outgrowth directly. 1, 10 µM increased IL-6 mRNA expression in primary rat hepatocytes	(Day et al., 2014) (Jung et al., 2000)
Phentolamine	10 µM	Attenuated noradrenaline-stimulated mixed glial CM-induced increases in neuritic length in rat primary cortical neurons.	(Day et al., 2014)
Prazosin	10 µM	Attenuates noradrenaline-induced increases in IL-6 mRNA expression in rat	(Jung et al., 2000)

		primary hepatocytes.	
Propranolol	10 µM	Attenuated noradrenaline-stimulated mixed glial CM-induced increases in neuronal outgrowth and complexity rat primary cortical neurons and increases in glial IL-6 mRNA expression.	(Day et al., 2014)
Quinolinic acid	0.1, 1 µM	No effect on viability at either concentration, no effect of 0.1 µM on neuronal complexity, no effect of 1 µM on the expression of synaptic markers in rat primary cortical neurons.	Dose based on dose response studies carried out previously in chapter 4.
Recombinant rat IFNγ	10 ng/ml	IFNγ increased IDO mRNA expression in glia, and had no effect on neuronal viability, complexity or the expression of synaptic markers in rat primary cortical neurons.	Dose based on previous studies carried out previously in chapter 4.
Yohimbine	10 µM	Attenuates noradrenaline-induced increases in IL-6 mRNA expression in rat primary hepatocytes.	(Jung et al., 2000)

5.3 Results

5.3.1 The noradrenergic system modulates the kynurenine pathway in primary cortical astrocytes.

5.3.1.1 Effect of noradrenaline on the mRNA expression of kynurenine pathway enzymes in primary cortical astrocytes

One-way ANOVA of **TDO** mRNA expression showed an effect of noradrenaline [$F_{(2, 14)} = 4.088$, P= 0.0443]. *Post hoc* analysis revealed increases in TDO mRNA expression following treatment with noradrenaline (10 μM) (P<0.05) compared to control (a).

One-way ANOVA of **KAT II** mRNA expression showed an effect of noradrenaline [$F_{(2, 14)} = 81.43$, P<0.0001]. *Post hoc* analysis revealed reductions in KAT II mRNA expression following treatment with noradrenaline (1, 10 μM) (P<0.001) compared to control (b).

One-way ANOVA of **IDO** mRNA expression showed an effect of noradrenaline [$F_{(2, 15)} = 4.992$, P= 0.0246]. *Post hoc* analysis revealed reductions in IDO mRNA expression following treatment with noradrenaline (10 μM) (P<0.05) compared to control (c).

One-way ANOVA of **KMO** mRNA expression showed an effect of noradrenaline [$F_{(2, 17)} = 6.209$, P= 0.0108]. *Post hoc* analysis revealed reductions in the KMO mRNA expression following treatment with noradrenaline (1, 10 μM) (P<0.05) compared to control (d).

One-way ANOVA of **KYNU** mRNA expression showed no effect of noradrenaline [$F_{(2, 15)} = 2.496$, P= 0.1209] (e) (**figure 5.3.1.1**).

5.3.1.2 Effect of the non-selective α-adrenoceptor antagonist, phentolamine, on the noradrenergic-related changes in kynurenine pathway enzyme mRNA expression in primary cortical astrocytes.

Two-way ANOVA of **TDO** mRNA expression showed an effect of phentolamine [$F_{(1, 42)} = 40.135$, P<0.0001], and noradrenaline [$F_{(2, 42)} = 29.243$, P<0.0001], and an interaction [$F_{(2, 42)} = 5.657$, P= 0.007]. *Post hoc* analysis revealed increases in TDO mRNA expression following treatment with noradrenaline 10μM (P<0.01). Treatment with phentolamine enhanced the noradrenaline-induced increase (P<0.001) (a).

Two-way ANOVA of **KAT II** mRNA expression showed an effect of phentolamine [$F_{(1, 25)} = 113.1$, P< 0.0001], noradrenaline [$F_{(2, 25)} = 53.77$, P<0.0001], and an interaction [$F_{(2, 25)} = 12.5$, P= 0.0002]. *Post hoc* analysis revealed reductions in KAT II mRNA expression following treatment with noradrenaline (1, 10 μM) compared to control (P<0.001). Treatment with phentolamine prevented noradrenergic-induced reductions at both 1 μM (P<0.001) and 10 μM (P<0.001) (b) (**figure 5.3.1.2**).

5.3.1.3 Effect of a selective α_1-adrenoceptor antagonist, prazosin, and the selective α_2-adrenoceptor antagonist, yohimbine, on the noradrenergic-related changes in kynurenine pathway enzyme mRNA expression in primary cortical astrocytes.

Two-way ANOVA of **TDO** mRNA expression showed an effect of noradrenaline [$F_{(1, 30)} = 47.957$, $P<0.0001$], no effect of antagonist [$F_{(2, 30)} = 1.092$, $P= 0.349$], and no interaction [$F_{(2, 30)} = 1.187$, $P= 0.319$]. *Post hoc* analysis revealed increases in TDO mRNA expression with treatment with noradrenaline compared to control ($P<0.01$) (a).

Two-way ANOVA of **KAT II** mRNA expression showed an effect of antagonist [$F_{(2, 29)} = 17.151$, $P< 0.0001$], noradrenaline [$F_{(1, 29)} = 24.676$, $P<0.0001$], and an interaction [$F_{(2, 29)} = 8.181$, $P= 0.002$]. *Post hoc* analysis revealed reductions in KAT II mRNA expression with treatment with noradrenaline (10 µM) ($P<0.001$) compared to control. Pre-treatment with prazosin prevented the noradrenaline-induced reductions in KAT II mRNA expression ($P<0.001$), whereas yohimbine had no effect on the noradrenaline-induced reductions ($P>0.05$) (b) (**figure 5.3.1.3**).

5.3.1.4 Effect of the non-selective β-adrenoceptor antagonist, propranolol, on noradrenergic-related changes in kynurenine pathway enzymes mRNA expression in primary cortical astrocytes.

Two-way ANOVA of **TDO** mRNA expression showed an effect of propranolol [$F_{(1, 27)} = 12.3$, $P= 0.0016$], no effect of noradrenaline [$F_{(2, 27)} = 2.450$, $P= 0.1052$], but an interaction [$F_{(2, 27)} = 5.609$, $P= 0.0092$]. *Post hoc* analysis revealed increases TDO mRNA expression following treatment with noradrenaline (10 µM) ($P<0.05$) compared to control, with pre-treatment with propranolol preventing these noradrenaline-induced increases (a).

Two-way ANOVA of **KAT II** mRNA expression showed an effect of propranolol [$F_{(1, 30)} = 5.814$, $P= 0.0222$], noradrenaline [$F_{(2, 30)} = 183.5$, $P<0.0001$], but no interaction [$F_{(2, 30)} = 2.711$, $P= 0.0827$]. *Post hoc* analysis revealed reductions in KAT II mRNA expression following treatment with noradrenaline (1, 10 µM) ($P<0.001$) compared to control (b) (**figure 5.3.1.4**).

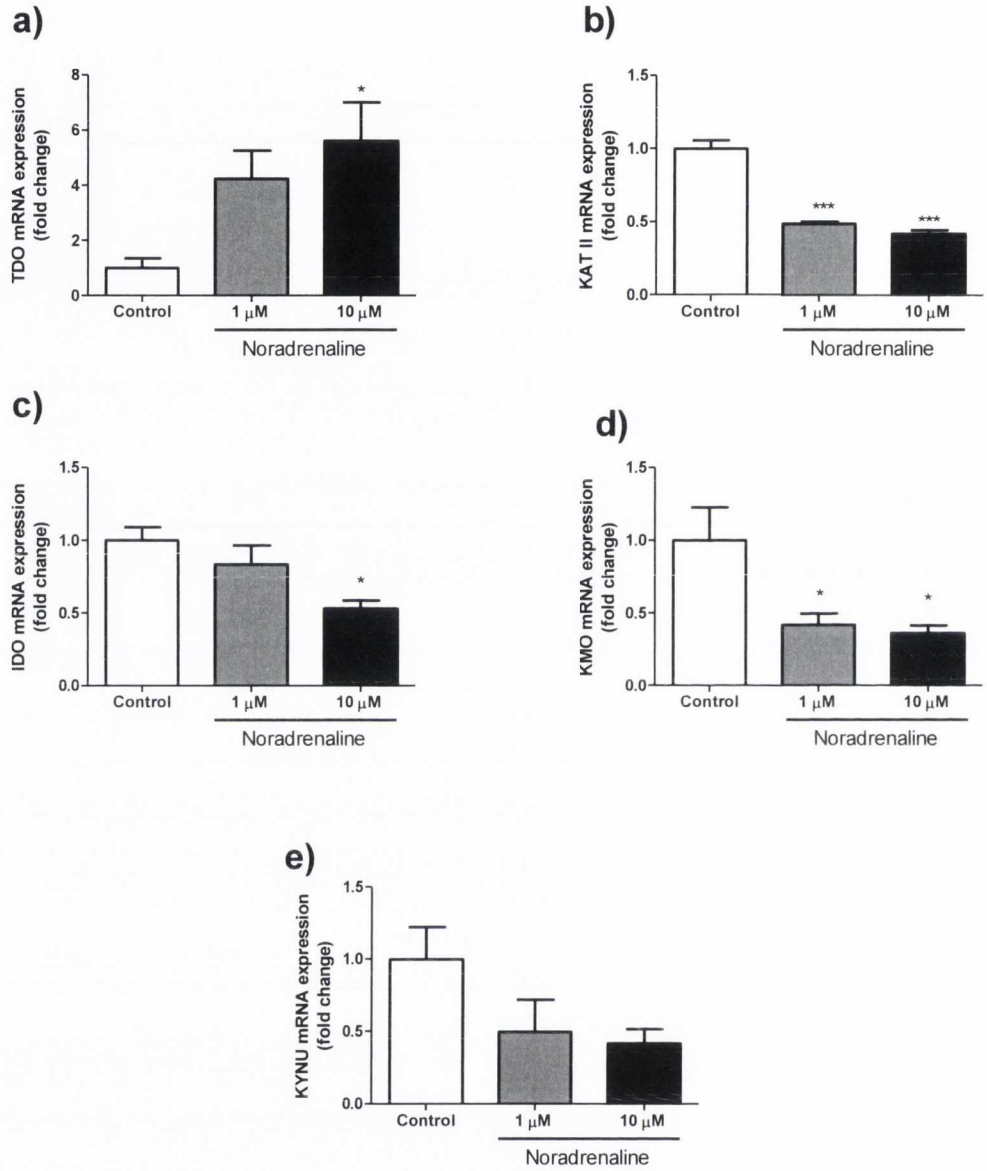

Figure 5.3.1.1 Effect of noradrenaline on the mRNA expression of kynurenine pathway enzymes in primary cortical astrocytes

Primary cortical astrocytes (DIV 12-13) were stimulated with noradrenaline (1, 10 μM) for 6 hr. Cells were harvested for mRNA extraction followed by quantitative PCR to analyse the expression of TDO (a), KAT II (b), IDO (c), KMO (d), and KYNU (e). Data expressed as mean ± SEM (n= 4-6). *P<0.05, ***P<0.001, vs. control. (One-way ANOVA followed by Dunnett's *post hoc* test).

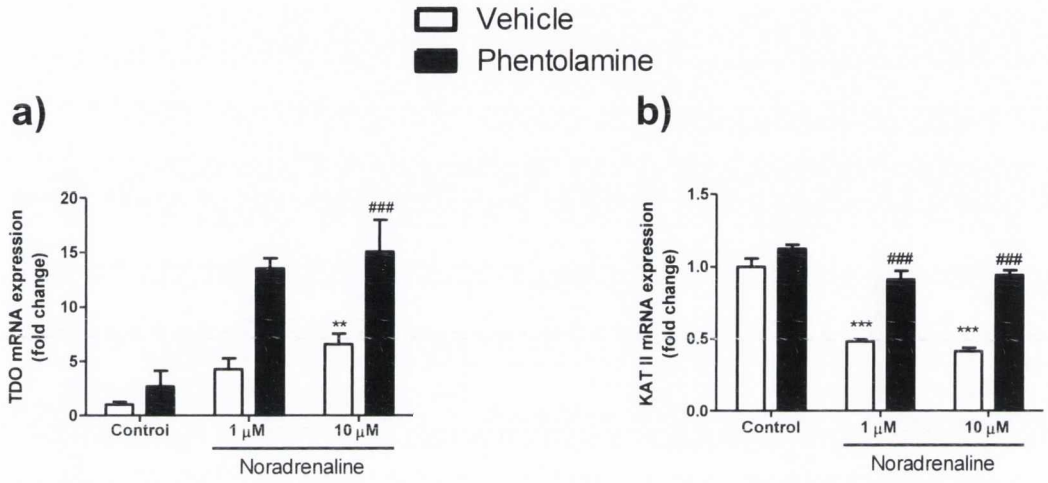

Figure 5.3.1.2: Effect of the non-selective α-adrenoceptor antagonist, phentolamine, on the noradrenergic-related changes in kynurenine pathway enzymes mRNA expression in primary cortical astrocytes

Primary cortical astrocytes (DIV 12-13) were pre-treated with vehicle or phentolamine (10 μM; 30 min) followed by stimulation with noradrenaline (1, 10 μM) for 6 hr. Cells were harvested for mRNA extraction followed by quantitative PCR to analyse the expression of TDO (a) and KAT II (b). Data expressed as mean ± SEM (n= 5-12). **P<0.05, vs. control, ###P<0.001, vs. respective control (Two-way ANOVA followed by Newman-Keuls *post hoc* test).

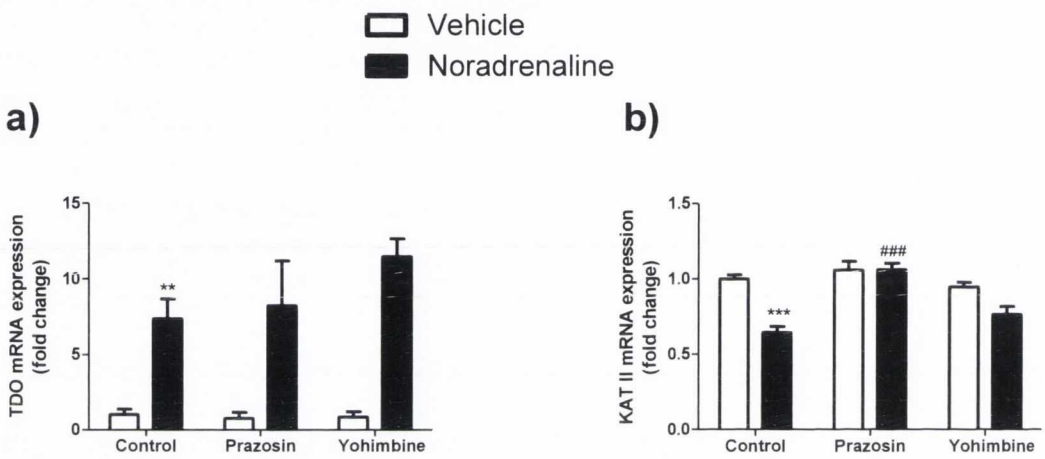

Figure 5.3.1.3: Effect of the selective α_1-adrenoceptor antagonist, prazosin, and the selective α_2-adrenoceptor antagonist, yohimbine, on the noradrenergic-related changes in kynurenine pathway enzyme mRNA expression in primary cortical astrocytes

Primary cortical astrocytes (DIV 12-13) were pre-treated with either vehicle, prazosin (10 μM; 30 min) or yohimbine (10 μM; 30 min) followed by stimulation with noradrenaline (10 μM) for 6 hr. Cells were harvested for mRNA extraction followed by quantitative PCR to analyse the expression of TDO (a) and KAT II (b). Data expressed as mean ± SEM (n= 4-6). **P<0.01, ***P<0.001, vs. control, ###P<0.001, vs. noradrenaline (Two-way ANOVA followed by Newman-Keuls *post hoc* test).

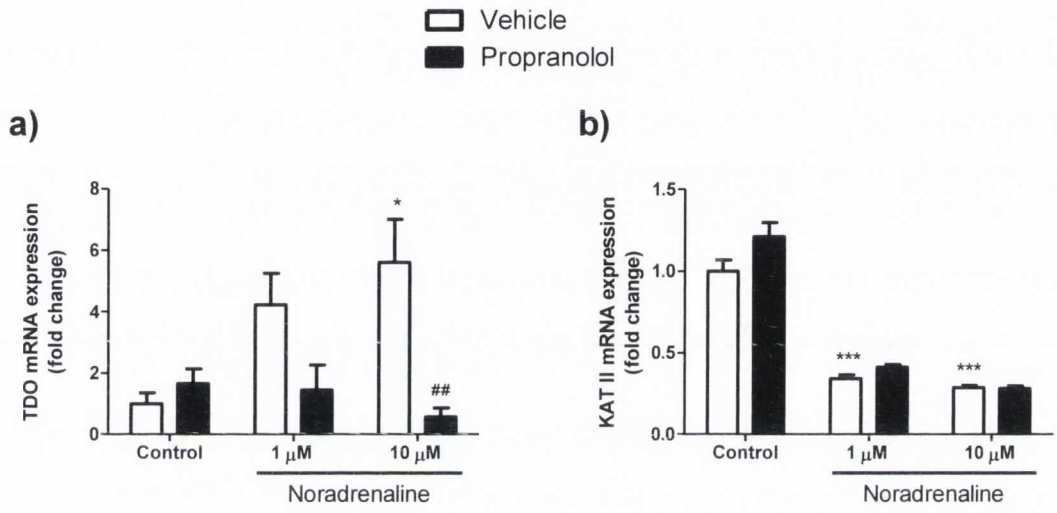

Figure 5.3.1.4: Effect of the non-selective β-adrenoceptor antagonist, propranolol, on the noradrenergic-related changes in kynurenine pathway enzymes mRNA expression in primary cortical astrocytes

Primary cortical astrocytes (DIV 12-13) were pre-treated with either vehicle or propranolol (10 μM; 30 min) followed by stimulation with noradrenaline (1, 10 μM) for 6 hr. Cells were harvested for mRNA extractions followed by quantitative PCR to analyse the expression of TDO (a) and KAT II (b). Data expressed as mean ± SEM (n= 4-6). *P<0.05, ***P<0.001, vs. control, ##P<0.01, vs. respective control. (Two-way ANOVA followed by Newman-Keuls *post hoc* test).

5.3.2 β-adrenoceptor activation induces the kynurenine pathway in primary cortical astrocytes.

5.3.2.1 Effect of isoproterenol on the mRNA expression of kynurenine pathway enzymes in primary cortical astrocytes

One-way ANOVA of **TDO** mRNA expression showed an effect of isoproterenol [$F_{(2, 16)} = 15.11$, P= 0.0003]. *Post hoc* analysis revealed increases in TDO mRNA expression following treatment with isoproterenol (1, 10 μM) (P<0.05) compared to control (a).

One-way ANOVA of **KAT II** mRNA expression showed an effect of isoproterenol [$F_{(2, 17)} = 35.66$, P< 0.0001]. *Post hoc* analysis revealed increases in KAT II mRNA expression following treatment with isoproterenol (1, 10 μM) (P<0.001) compared to control (b).

One-way ANOVA of **IDO** mRNA expression [$F_{(2, 16)} = 1.267$, P= 0.3121] (c), **KMO** mRNA expression [$F_{(2, 17)} = 1.027$, P= 0.382] (d), or **KYNU** mRNA expression [$F_{(2, 17)} = 2.263$, P= 0.1384] (e) showed no effect of isoproterenol (**figure 5.3.2.1**).

5.3.2.2 Effects of selective β-adrenoceptor antagonists on isoproterenol-related changes in kynurenine pathway enzyme mRNA expression in primary cortical astrocytes

Two-way ANOVA of **TDO** mRNA expression showed an effect of antagonist [$F_{(2, 29)} = 12.12$, P<0.0001], isoproterenol [$F_{(1, 29)} = 25.65$, P<0.0001], and an interaction [$F_{(2, 29)} = 16.31$, P<0.0001]. *Post hoc* analysis revealed increases in TDO mRNA expression following treatment with isoproterenol (P<0.001) compared to control, with pre-treatment with atenolol or ICI 118, 551 reducing TDO mRNA expression (P<0.001) compared to isoproterenol (a).

Two-way ANOVA of **KAT II** mRNA expression showed an effect of isoproterenol [$F_{(1, 30)} = 76.018$, P<0.0001], no effect of antagonist [$F_{(2, 30)} = 1.534$, P= 0.232], and no interaction [$F_{(2, 30)} = 1.00$, P= 0.38]. *Post hoc* analysis revealed increases in KAT II mRNA expression following treatment with isoproterenol (P<0.001) compared to control (b).

5.3.2.3 Effect of formoterol on the mRNA expression of kynurenine pathway enzymes in primary cortical astrocytes

One-way ANOVA of **TDO** mRNA expression showed an effect of formoterol [$F_{(2, 16)} = 4.113$, P= 0.0393]. *Post hoc* analysis revealed increases in TDO mRNA expression following treatment with formoterol (1, 10 μM) (P<0.05) compared to control (a).

One-way ANOVA of **KAT II** mRNA expression showed an effect of formoterol [$F_{(2, 17)} = 102.1$, $P< 0.0001$]. *Post hoc* analysis revealed increases in KAT II mRNA expression following treatment with formoterol (10 μM) ($P<0.001$) compared to control (b).

One-way ANOVA of **IDO** mRNA expression showed an effect of formoterol [$F_{(2, 17)} = 5.858$, $P= 0.0132$]. *Post hoc* analysis revealed increases in IDO mRNA expression following treatment with formoterol (1, 10 μM) ($P<0.05$) compared to control (c).

One-way ANOVA on **KMO** mRNA expression showed an effect of formoterol [$F_{(2, 16)} = 4.637$, $P= 0.0285$]. *Post hoc* analysis revealed increases in KMO mRNA expression following treatment with formoterol (1 μM) ($P<0.05$) compared to control (d).

One-way ANOVA of **KYNU** mRNA expression showed no effect of formoterol [$F_{(2, 16)} = 2.27$, $P= 0.14$] (e) (**figure 5.3.2.3**).

5.3.2.4 Effect of a non-selective β-adrenoceptor antagonist on formoterol-related changes in kynurenine pathway enzyme mRNA expression in primary cortical astrocytes

Two-way ANOVA of **TDO** mRNA expression showed an effect of formoterol [$F_{(1, 17)} = 4.805$, $P= 0.043$], no effect of propranolol [$F_{(1, 17)} = 3.669$, $P= 0.072$], and no interaction [$F_{(1, 17)} = 4.172$, $P= 0.057$]. *Post hoc* analysis revealed increases in TDO mRNA expression following treatment with formoterol ($P<0.05$) compared to control with pre-treatment with propranolol reducing the formoterol-induced increases ($P<0.05$) (a).

Two-way ANOVA of **KAT II** mRNA expression showed an effect of formoterol [$F_{(1, 20)} = 43.163$, $P<0.0001$], no effect of propranolol [$F_{(1, 20)} = 3.337$, $P= 0.083$], and no interaction [$F_{(1, 20)} = 1.514$, $P= 0.223$]. *Post hoc* analysis revealed increases in KAT II mRNA expression following treatment with formoterol ($P<0.001$) compared to control (b).

Two-way ANOVA of **IDO** mRNA expression showed no effect of propranolol [$F_{(1, 20)} = 0.364$, $P= 0.533$], formoterol [$F_{(1, 20)} = 0.036$, $P= 0.851$], and no interaction [$F_{(1, 20)} = 4.187$, $P= 0.055$] (c) (**figure 5.3.2.4**).

5.3.2.5 Effect of a β_2-adrenoceptor antagonist on formoterol-related changes in kynurenine pathway enzyme mRNA expression in primary cortical astrocytes

Two-way ANOVA of **TDO** mRNA expression showed an effect of formoterol [$F_{(1, 23)} = 17.521$, $P<0.0001$], no effect of ICI 118, 551 [$F_{(1, 23)} = 0.103$, $P= 0.752$], and no interaction [$F_{(1, 23)} = 0.321$, $P= 0.577$]. *Post hoc* analysis revealed increases in TDO mRNA expression following treatment with

formoterol (P<0.01) compared to control, with pre-treatment with ICI 118, 551 attenuating the formoterol-induced increases (P<0.05) (a).

Two-way ANOVA of **KAT II** mRNA expression showed an effect of formoterol [$F_{(1, 23)}$ = 0.763, P= 0.017], no effect of ICI 118, 551 [$F_{(1, 23)}$ = 3.332, P= 0.083], and no interaction [$F_{(1, 23)}$ = 0.061, P= 0.807]. *Post hoc* analysis revealed no changes in KAT II mRNA expression following treatment with any factor alone compared to control (b).

Two-way ANOVA on **IDO** mRNA expression showed an effect of formoterol [$F_{(1, 22)}$ = 9.447, P= 0.006], no effect of ICI 118, 551 [$F_{(1, 22)}$ = 0.434, P= 0.518], and no interaction [$F_{(1, 22)}$ = 0.608, P= 0.445]. *Post hoc* analysis revealed no changes in IDO mRNA expression following treatment with either factor alone compared to control (c) (**figure 5.3.2.5**).

5.3.2.6 Effect of the cAMP analogue, dbcAMP on the mRNA expression of kynurenine pathway enzymes in primary cortical astrocytes

One-way ANOVA of **TDO** mRNA expression showed an effect of dbcAMP [$F_{(2, 16)}$ = 6.501, P= 0.0101]. *Post hoc* analysis revealed increases in TDO mRNA expression following treatment with dbcAMP (10 μM) (P<0.05) compared to control (a).

One-way ANOVA of **KAT II** mRNA expression showed an effect of dbcAMP [$F_{(2, 17)}$ = 7.72, P= 0.005]. *Post hoc* analysis revealed increases in KAT II mRNA expression following treatment with dbcAMP (10 μM) (P<0.01) compared to control (b).

One-way ANOVA of **IDO** mRNA expression [$F_{(2, 15)}$ = 0.7813, P= 0.9253] (c), **KMO** mRNA expression [$F_{(2, 17)}$ = 0.236, P= 0.7926] (d), or **KYNU** mRNA expression [$F_{(2, 16)}$ = 2.448, P= 0.1225] (e) showed no effect of dbcAMP (**figure 5.3.2.6**).

5.3.2.7 Effect of formoterol on the concentrations of tryptophan, kynurenine, 3-hydroxykynurenine and the tryptophan/kynurenine ratio in the CM of primary astrocytic cultures

Stimulation of primary astrocytes with IFNγ decreased the concentration of **tryptophan** (t= 2.976, P= 0.007, d.f. = 22) (a), **kynurenine** (t= 3.045, P= 0.0061, d.f. = 21) (b), **3-hydroxykynurenine** (t= 6.733, P<0.0001, d.f. = 22) (c) and had no effect on the **kynurenine over tryptophan ratio** (t= 0.3692, P= 0.7157, d.f. = 21) in the CM (**figure 5.3.2.7**).

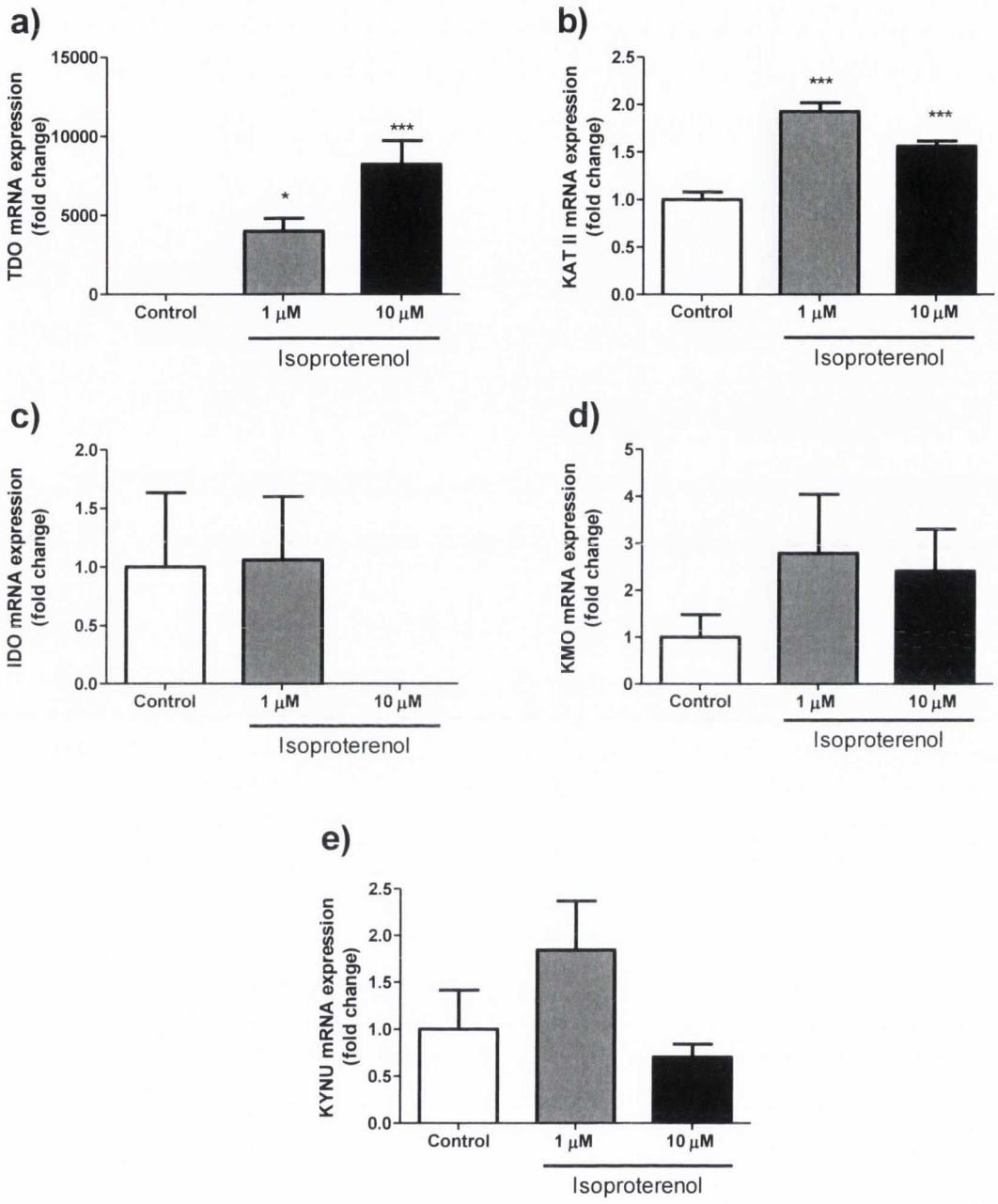

Figure 5.3.2.1: Effect of isoproterenol on the mRNA expression of kynurenine pathway enzymes in primary cortical astrocytes

Primary cortical astrocytes (DIV 12-13) were stimulated with isoproterenol (1, 10 μM) for 6 hr. Cells were harvested for mRNA extraction followed by quantitative PCR to analyse the expression of TDO (a), KAT II (b), IDO (c), KMO (d), and KYNU (e). Data expressed as mean ± SEM (n= 5-6). *P<0.05, ***P<0.001, vs. control, #P<0.05, vs. isoproterenol 1 μM. (One-way ANOVA followed by Dunnett's *post hoc* test).

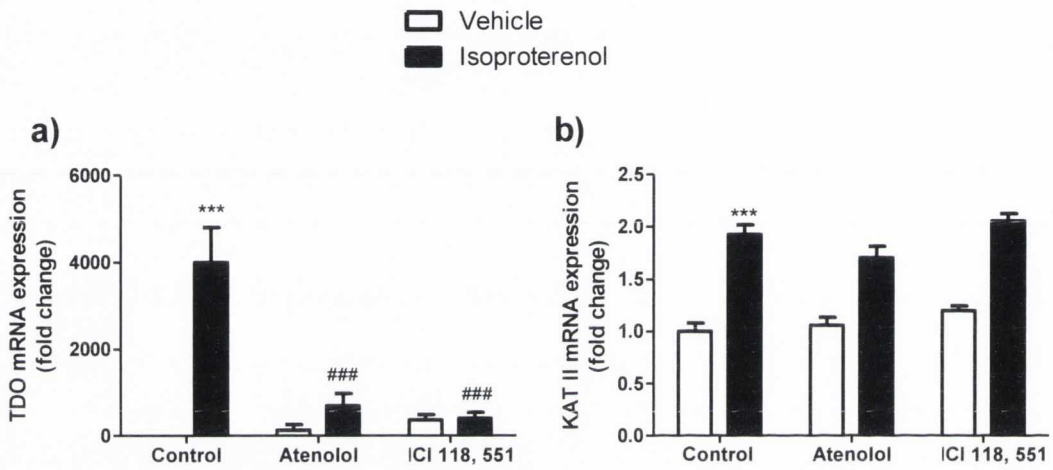

Figure 5.3.2.2: Effects of selective β-adrenoceptor antagonists on isoproterenol-related changes in kynurenine pathway enzyme mRNA expression in primary cortical astrocytes

Primary cortical astrocytes (DIV 12-13) were pre-treated with vehicle, atenolol (10 μM; 30 min) or ICI 118, 551 (10 μM; 30 min) followed by stimulation with isoproterenol (1 μM) for 6 hr. Cells were harvested for mRNA extractions followed by quantitative PCR to analyse the expression of TDO (a) and KAT II (b). Data expressed as mean ± SEM (n= 5-6). ***P<0.001, vs. control, ###P<0.001, vs. isoproterenol (1 μM). (Two-way ANOVA followed by Newman-Keuls *post hoc* test).

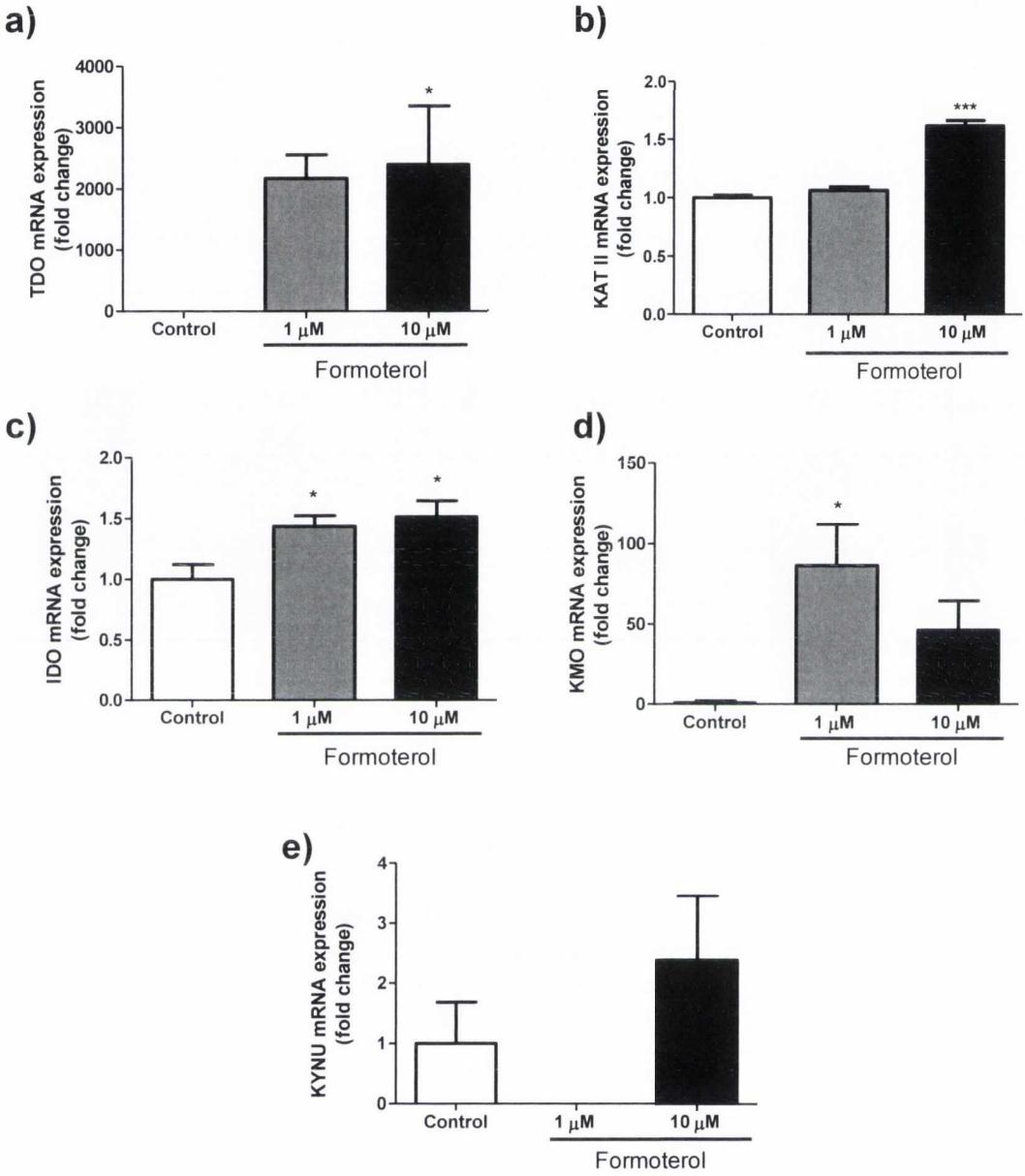

Figure 5.3.2.3: Effect of formoterol on the mRNA expression of kynurenine pathway enzymes in primary cortical astrocytes

Primary cortical astrocytes (DIV 12-13) were stimulated with formoterol (1, 10 μM) for 6 hr. Cells were harvested for mRNA extraction followed by quantitative PCR to analyse the expression of TDO (a), KAT II (b), IDO (c), KMO (d), and KYNU (e). Data expressed as mean ± SEM (n= 5-6). *P<0.05, ***P<0.001, vs. control. (One-way ANOVA followed by Dunnett's *post hoc* test).

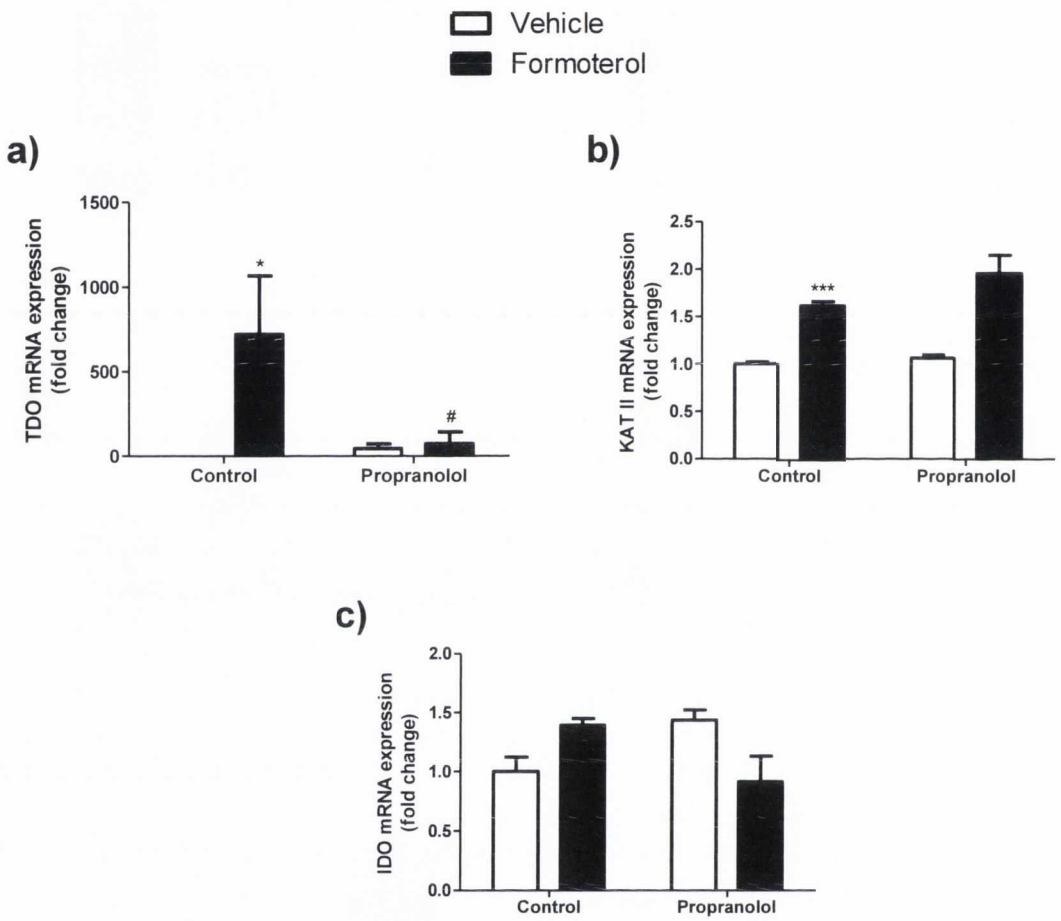

Figure 5.3.2.4: Effect of a non-selective β-adrenoceptor antagonist on the formoterol-related changes in kynurenine pathway enzyme mRNA expression in primary cortical astrocytes

Primary cortical astrocytes (DIV 12-13) were pre-treated with propranolol (10 μM; 30 min) followed by stimulation with formoterol (10 μM) for 6 hr. Cells were harvested for mRNA extractions followed by quantitative PCR to analyse the expression of TDO (a), KAT II (b) and IDO (c). Data expressed as mean ± SEM (n= 4-6). *P<0.05, ***P<0.001, vs. control, #P<0.05 vs formoterol (Two-way ANOVA followed by Newman-Keuls *post hoc* test).

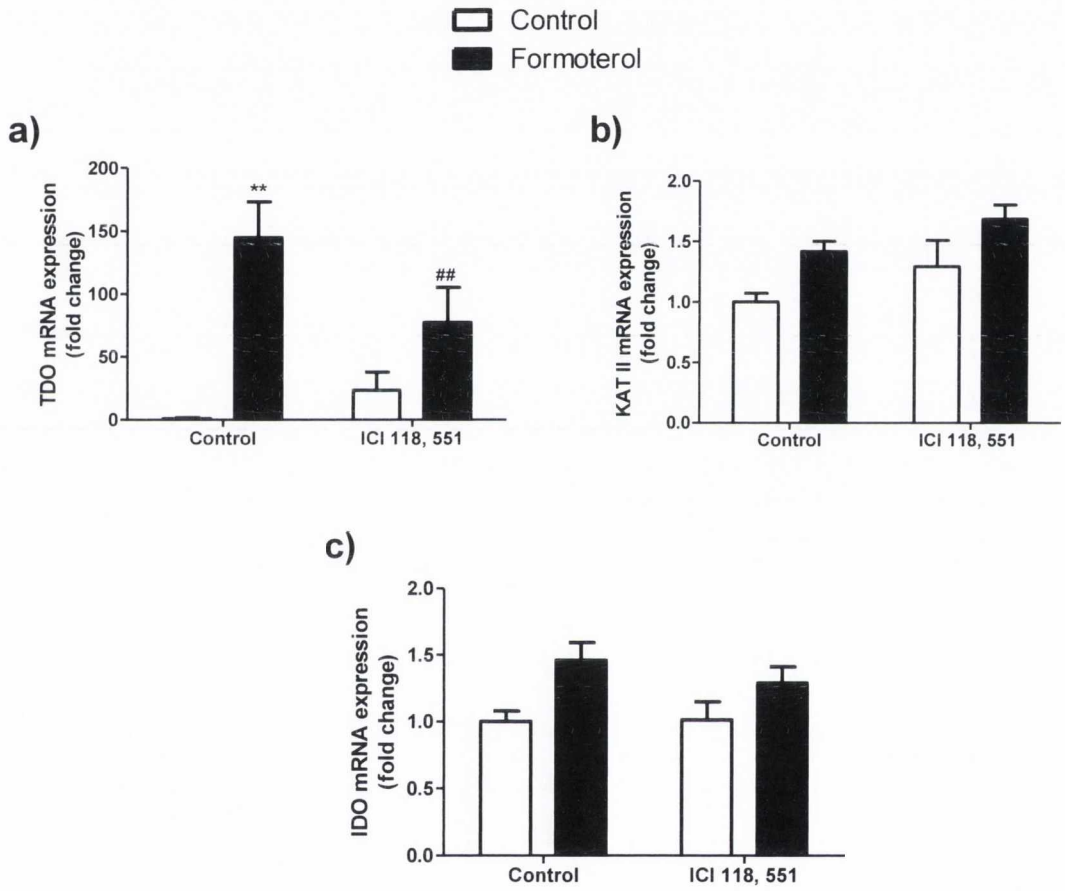

Figure 5.3.2.5: Effect of a β2-adrenoceptor antagonist on the formoterol-related changes in kynurenine pathway enzyme mRNA expression in primary cortical astrocytes

Primary cortical astrocytes (DIV 12-13) were pre-treated with vehicle or ICI 118, 551 (10 μM; 30 min) followed by stimulation with formoterol (10 μM) for 6 hr. Cells were harvested for mRNA extractions followed by quantitative PCR to analyse the expression of TDO (a), KAT II (b) and IDO (c). Data expressed as mean ± SEM (n= 4-6). **P<0.01, vs. control, ##P<0.01, vs. formoterol (Two-way ANOVA followed by Newman-Keuls *post hoc* test).

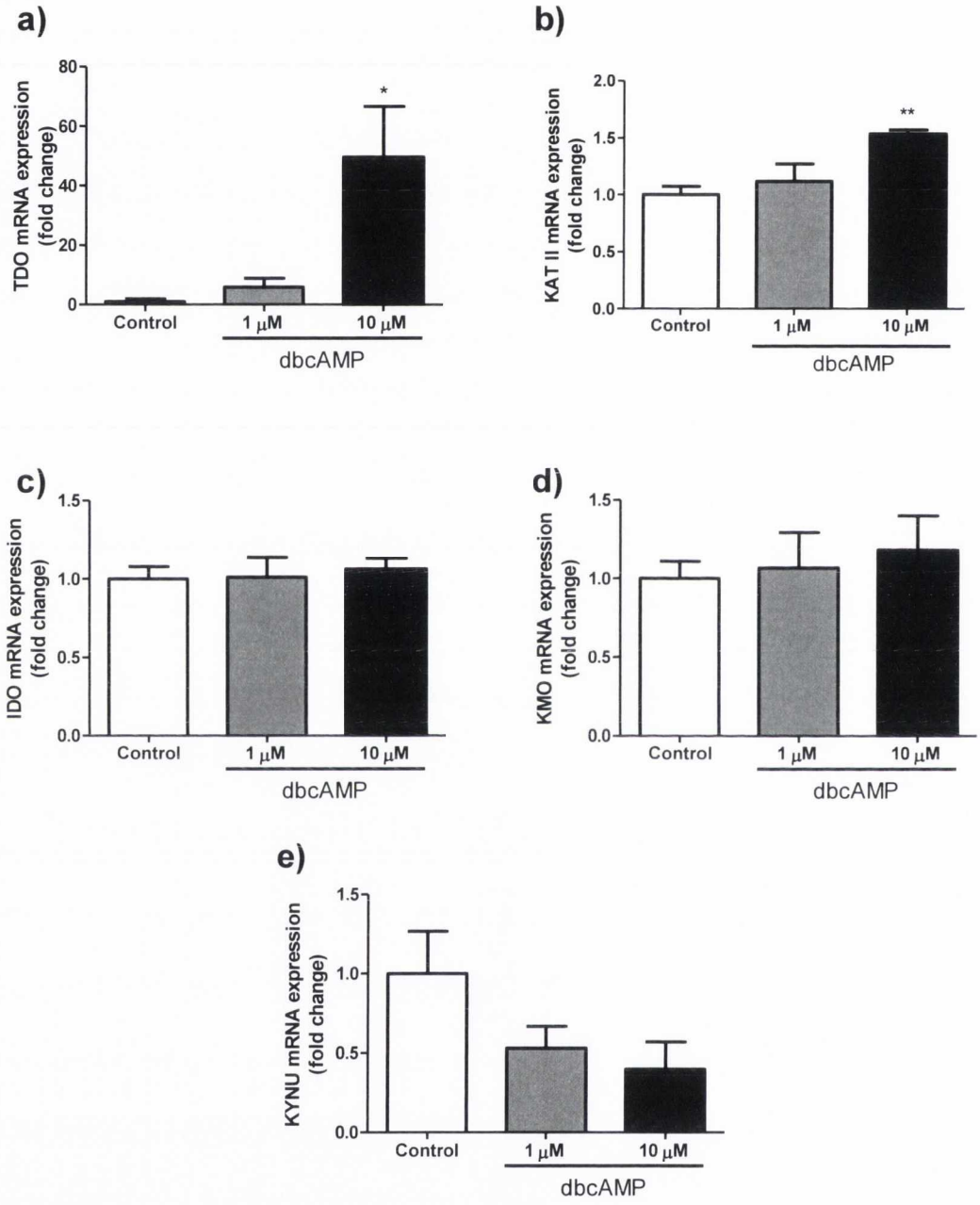

Figure 5.3.2.6: Effect of the cAMP analogue, dbcAMP on the mRNA expression of kynurenine pathway enzymes in primary cortical astrocytes

Primary cortical astrocytes (DIV 12-13) were treated with dbcAMP (1, 10 μM) for 6 hr. Cells were harvested for mRNA extractions followed by quantitative PCR to analyse the expression of TDO (a), KAT II (b), IDO (c), KMO (d), and KYNU (e). Data expressed as mean ± SEM (n= 5-6). *P<0.05, **P<0.01, vs. control (One-way ANOVA followed by Dunnett's *post hoc* test).

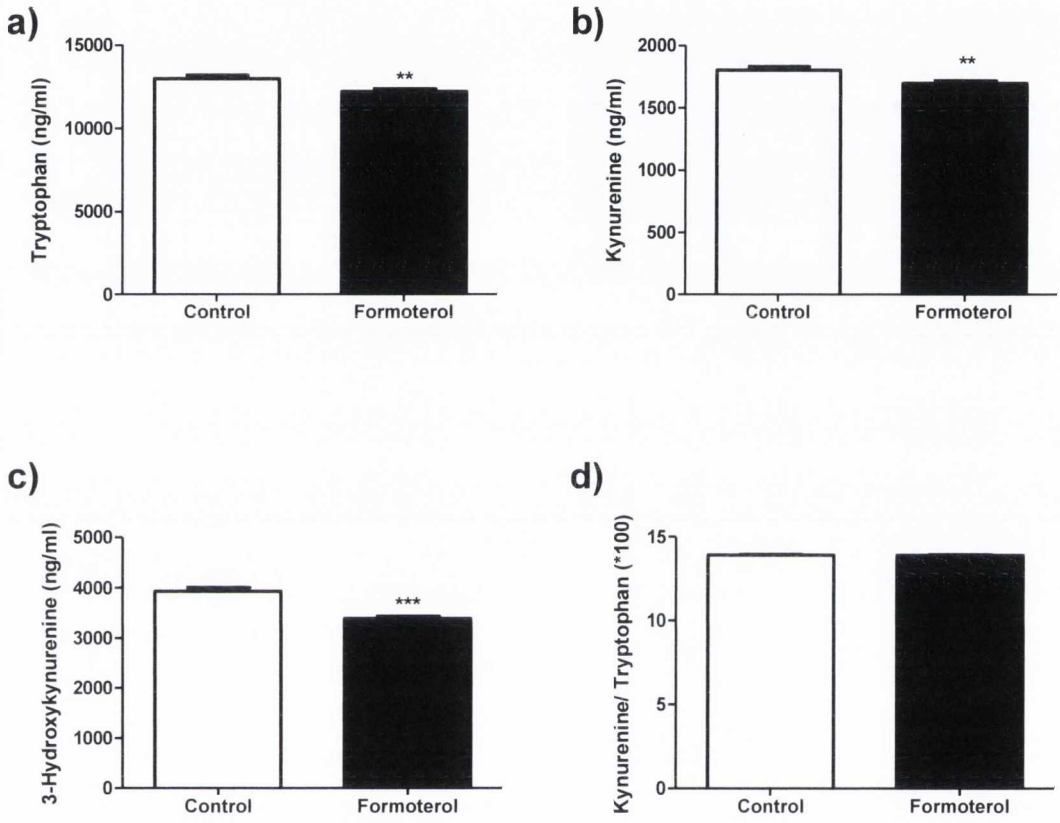

Figure 5.3.2.7: Effect of formoterol on the concentrations of tryptophan, kynurenine, 3-hydroxykynurenine and the kynurenine/tryptophan ratio in the CM of primary astrocytic cultures
Primary cortical astrocytes (DIV 12-13) were stimulated with formoterol (10 μM) for 24 hr. CM was harvested for analysis of the concentrations of (a) tryptophan, (b) kynurenine, (c) 3-hydroxykynurenine, and (d) kynurenine over tryptophan ratio. Data expressed as mean ± SEM (n= 12 wells, from 2 independent experiments). **P<0.01, ***P<0.001, vs. control (Student's *t*-test).

5.3.3 Characterisation of the effect of β_2-adrenoceptor stimulation on inflammation associated changes in kynurenine pathway enzyme mRNA expression in primary microglia and neurons

5.3.3.1 Effect of noradrenaline and formoterol on the mRNA expression of kynurenine pathway enzymes in primary cortical microglia

One-way ANOVA of **TDO** mRNA [$F_{(2, 17)} = 2.234$, P= 0.1415] (a), **KAT II** mRNA expression [$F_{(2, 16)} = 0.6528$, P= 0.5348] (b), **IDO** mRNA expression [$F_{(2, 15)} = 1.621$, P= 2.353] (c), **KMO** mRNA expression [$F_{(2, 17)} = 0.1302$, P= 0.8788] (d), or **KYNU** mRNA expression [$F_{(2, 16)} = 1.564$, P= 0.2438] (e) showed no effect of treatment (**figure 5.3.3.1**).

5.3.3.2 Effect of noradrenaline and formoterol on the mRNA expression of kynurenine pathway enzymes in primary cortical neurons

One-way ANOVA of **TDO** mRNA expression [$F_{(2, 16)} = 1.908$, P= 0.1850], **KAT II** mRNA expression [$F_{(2, 16)} = 1.199$, P= 0.3306] (b), **IDO** mRNA expression [$F_{(2, 16)} = 2.094$, P= 1.601] (c), **KMO** mRNA expression [$F_{(2, 17)} = 0.1374$, P= 0.8727] (d) showed no effect of treatment.

One-way ANOVA of **KYNU** mRNA expression showed an effect of treatment [$F_{(2, 16)} = 4.037$, P= 0.0413] (e). *Post hoc* analysis revealed reductions in KYNU mRNA expression following treatment with formoterol ($P<0.05$) (**figure 5.3.3.2**).

5.3.3.3 Effect of formoterol on IFNγ-induced changes in the mRNA expression of kynurenine pathway enzymes in primary cortical microglia

Two-way ANOVA of **TDO** mRNA expression showed an effect of formoterol [$F_{(1, 34)} = 12.999$, P= 0.001], no effect of IFNγ [$F_{(1, 34)} = 4.34$, P= 0.515], and no interaction [$F_{(1, 34)} = 0.564$, P= 0.458]. *Post hoc* analysis revealed increases in TDO mRNA expression following treatment with formoterol + IFNγ increased ($P<0.05$) compared to control (a).

Two-way ANOVA on **KAT II** mRNA expression showed an effect of IFNγ [$F_{(1, 34)} = 14.726$, P= 0.001], no effect of formoterol [$F_{(1, 34)} = 0.089$, P= 0.767], and no interaction [$F_{(1, 34)} = 0.459$, P= 0.503]. *Post hoc* analysis revealed reductions in KAT II mRNA expression following treatment with IFNγ ($P<0.05$) compared to control (b).

Two-way ANOVA on **IDO** mRNA expression showed no effect of formoterol [$F_{(1, 32)} = 2.766$, P= 0.107], IFNγ [$F_{(1, 32)} = 2.8$, P= 0.105], and no interaction [$F_{(1, 32)} = 2.75$, P= 0.108] (c) (**figure 5.3.3.3**).

5.3.3.4 Effect of formoterol on IFNγ-induced changes in the mRNA expression of kynurenine pathway enzymes in primary cortical astrocytes

Two-way ANOVA of **TDO** mRNA expression showed an effect of formoterol [$F_{(1, 33)} = 149.806$, $P<0.0001$], no effect of IFNγ [$F_{(1, 33)} = 3.393$, $P= 0.075$], and an interaction [$F_{(1, 33)} = 5$, $P= 0.033$]. *Post hoc* analysis revealed increases in TDO mRNA expression of following treatment with formoterol ($P<0.001$) compared to control (a).

Two-way ANOVA of **KAT II** mRNA expression showed an effect of formoterol [$F_{(1, 44)} = 4.832$, $P= 0.034$], IFNγ [$F_{(1, 44)} = 17.426$, $P<0.0001$], and no interaction [$F_{(1, 44)} = 1.616$, $P= 0.202$]. *Post hoc* analysis revealed increases in KAT II mRNA expression following treatment with formoterol ($P<0.01$) compared to control, with treatment with IFNγ preventing these formoterol-induced increases ($P<0.01$) (b).

Two-way ANOVA of **IDO** mRNA expression showed an effect of IFNγ [$F_{(1, 22)} = 52.567$, $P<0.0001$], no effect of formoterol [$F_{(1, 22)} = 0.025$, $P= 0.876$], and no interaction [$F_{(1, 22)} = 0.025$, $P= 0.876$]. *Post hoc* analysis revealed increases in IDO mRNA expression following treatment with IFNγ ($P<0.001$) (c) (**figure 5.3.3.4**).

5.3.3.5 Effect of formoterol on IFNγ-induced changes in the mRNA expression of kynurenine pathway enzymes in primary cortical neurons

Two-way ANOVA of **TDO** mRNA expression showed an effect of formoterol [$F_{(1, 22)} = 8.562$, $P= 0.009$], no effect of IFNγ [$F_{(1, 22)} = 0.077$, $P= 0.785$], and no interaction [$F_{(1, 22)} = 0.075$, $P= 0.778$]. *Post hoc* analysis revealed no changes with any treatments (a).

Two-way ANOVA of **KAT II** mRNA expression showed an effect of IFNγ [$F_{(1, 22)} = 16.408$, $P= 0.001$], no effect of formoterol [$F_{(1, 22)} = 1.048$, $P= 0.319$] and no interaction [$F_{(1, 22)} = 3.408$, $P= 0.081$]. *Post hoc* analysis revealed reductions in KAT II mRNA expression following treatment with formoterol + IFNγ ($P<0.01$) compared to formoterol (b).

Two-way ANOVA of **IDO** mRNA expression showed an effect of IFNγ [$F_{(1, 22)} = 13.63$, $P= 0.002$], no effect of formoterol [$F_{(1, 22)} = 0.006$, $P= 0.941$], and no interaction [$F_{(1, 22)} = 0.005$, $P= 0.943$]. *Post hoc* analysis revealed increases in IDO mRNA expression following treatment with IFNγ ($P<0.05$) compared to control (c) (**figure 5.3.3.5**).

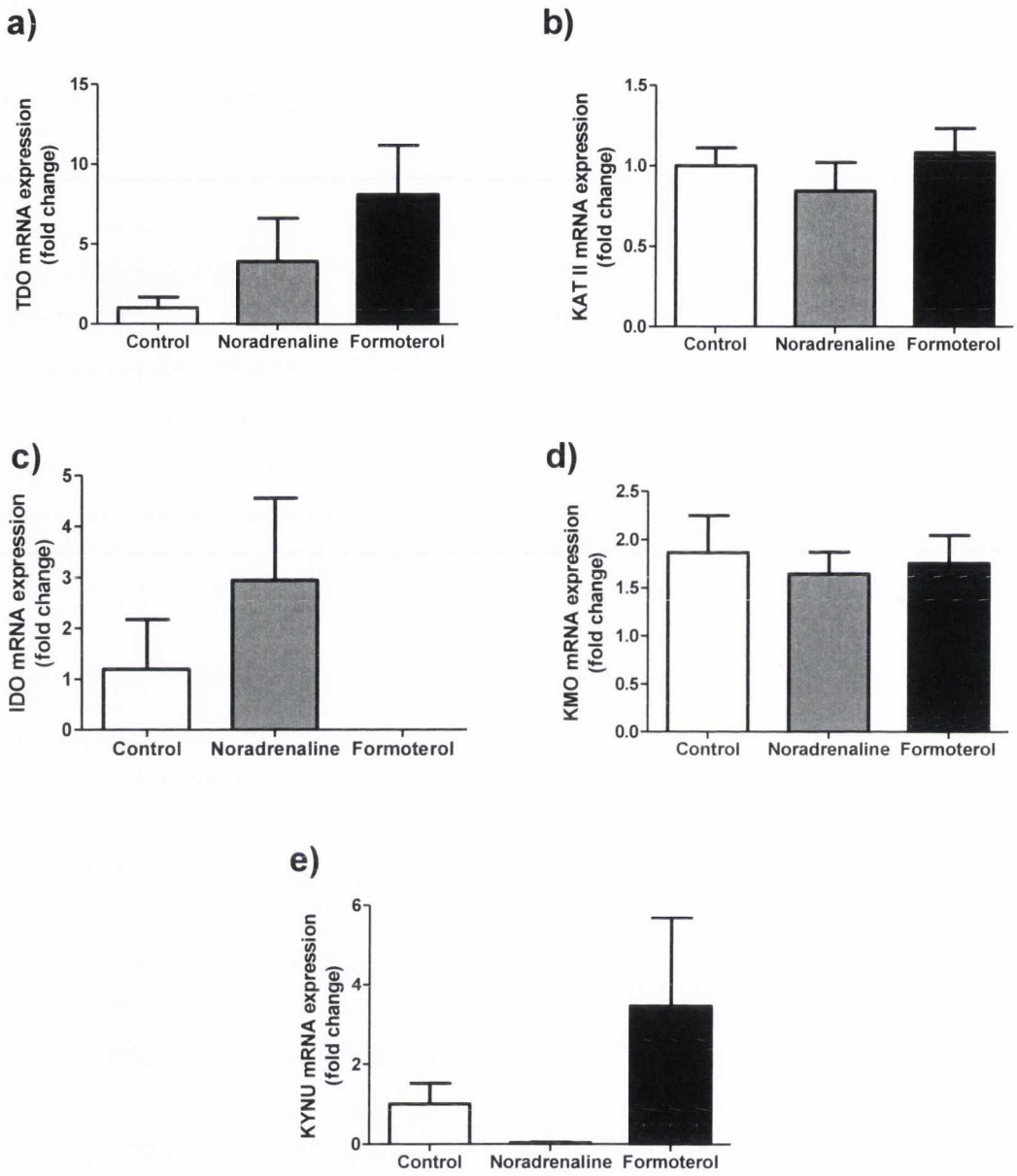

Figure 5.3.3.1: Effect of noradrenaline and formoterol on the mRNA expression of kynurenine pathway enzymes in primary cortical microglia

Primary cortical microglia (DIV 12-13) were treated with vehicle, noradrenaline (10 μM) or formoterol (10 μM) for 6 hr. Cells were harvested for mRNA extractions followed by quantitative PCR to analyse the expression of TDO (a), KAT II (b), IDO (c), KMO (d) and KYNU (e). Data expressed as mean ± SEM (n= 5-6) (One-way ANOVA).

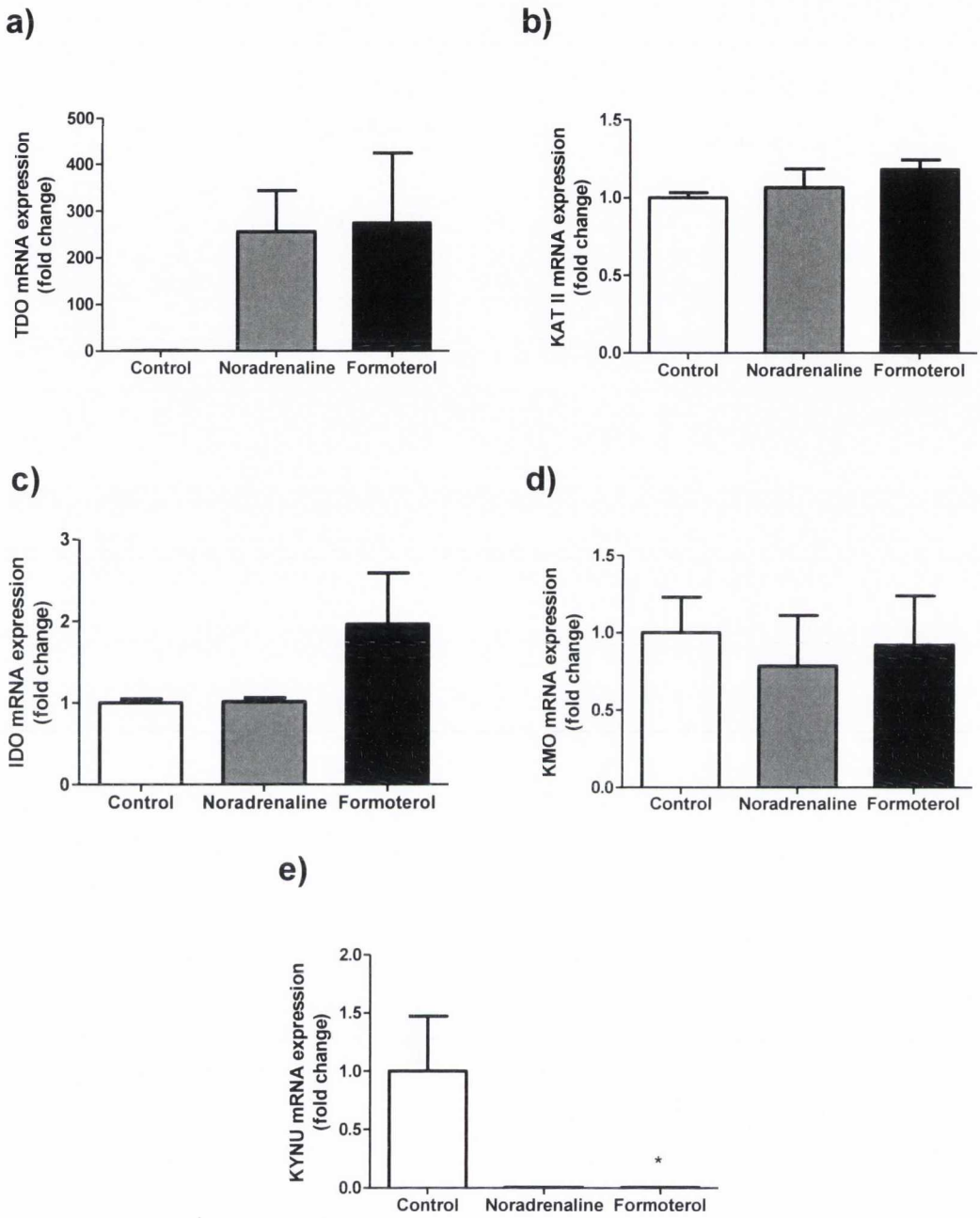

Figure 5.3.3.2: Effect of noradrenaline and formoterol on the mRNA expression of kynurenine pathway enzymes in primary cortical neurons

Primary cortical neurons (DIV 3) were treated with vehicle, noradrenaline (10 μM) or formoterol (10 μM) for 6 hr. Cells were harvested for mRNA extractions followed by quantitative PCR to analyse the expression of TDO (a), KAT II (b), IDO (c), KMO (d) and KYNU (e). Data expressed as mean ± SEM (n= 5-6). *P<0.05, vs. control (One-way ANOVA followed by Dunnett's *post hoc* test).

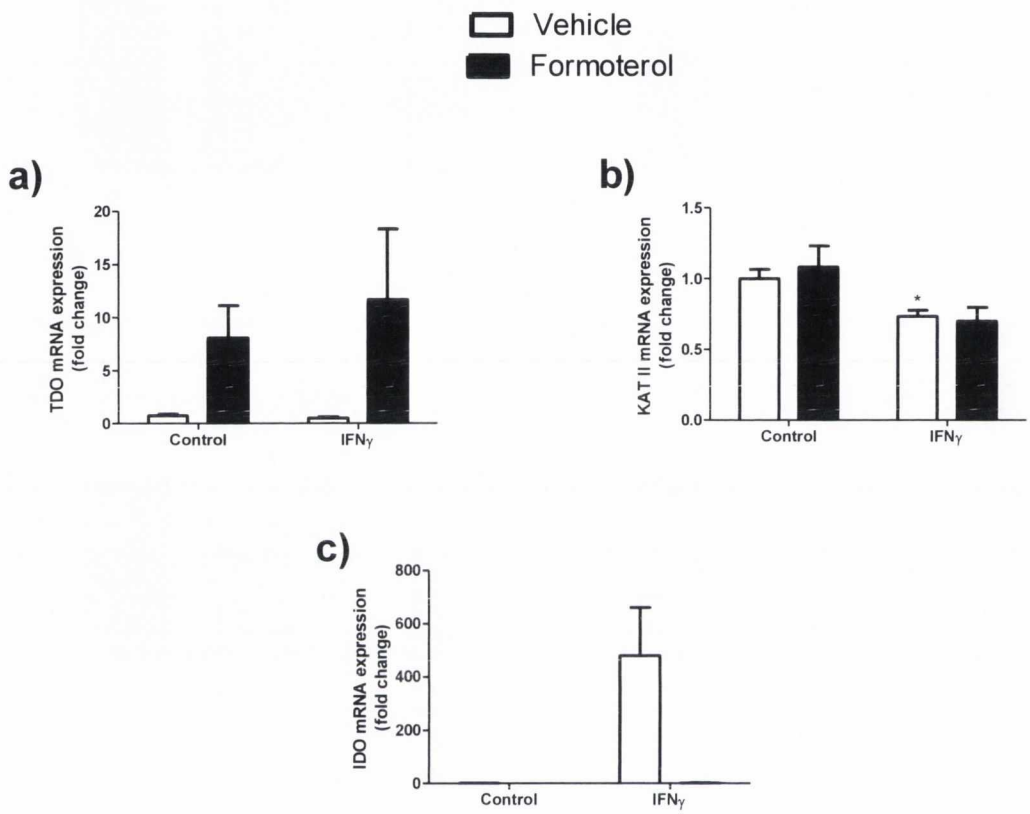

Figure 5.3.3.3: Effect of formoterol on IFNγ-induced changes in the mRNA expression of kynurenine pathway enzymes in primary cortical microglia

Primary cortical microglia (DIV 12-13) were treated with vehicle, formoterol (10 μM), IFNγ (10 ng/ml), or both formoterol + IFNγ for 6 hr. Cells were harvested for mRNA extractions followed by quantitative PCR to analyse the expression of TDO (a), KAT II (b) and IDO (c). Data expressed as mean ± SEM (n= 5-12). *P<0.05, vs. control (Two-way ANOVA followed by Newman-Keuls *post hoc* test).

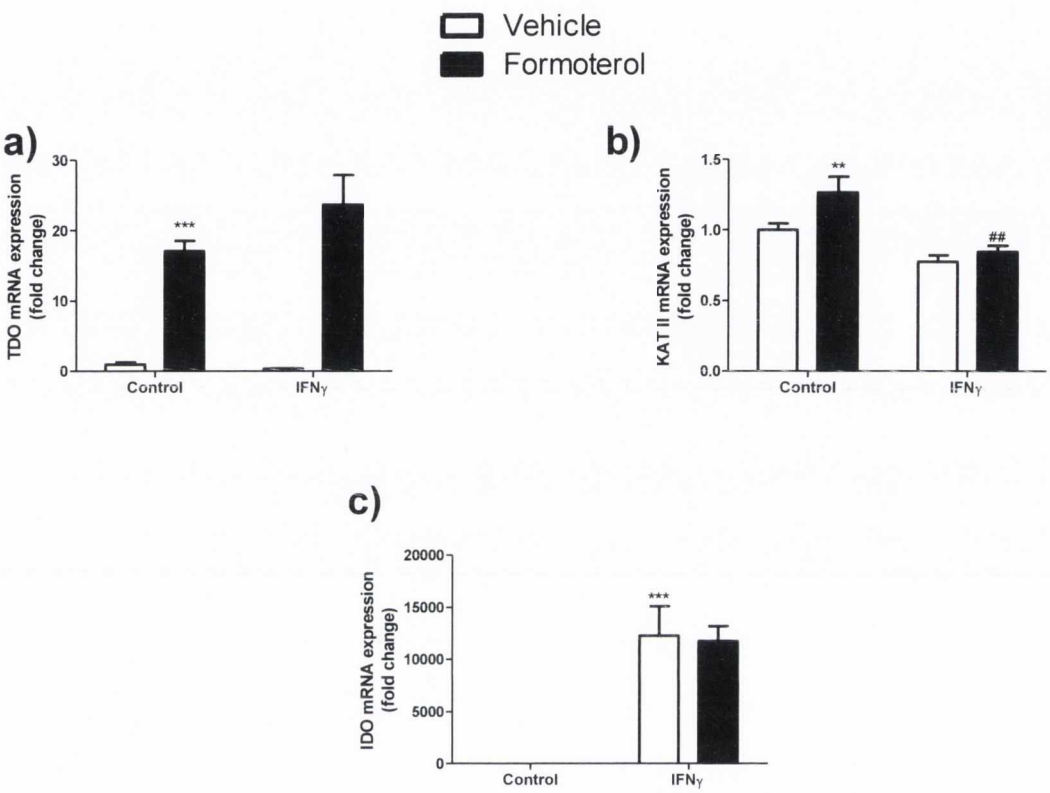

Figure 5.3.3.4: Effect of formoterol on IFNγ-induced changes in the mRNA expression of kynurenine pathway enzymes in primary cortical astrocytes

Primary cortical astrocytes (DIV 12-13) were treated with vehicle. formoterol (10 μM), IFNγ (10 ng/ml), or both formoterol + IFNγ for 6 hr. Cells were harvested for mRNA extractions followed by quantitative PCR to analyse the expression of TDO (a), KAT II (b) and IDO (c). Data expressed as mean ± SEM (n= 6-18). **P<0.01, ***P<0.001, vs. control, ##P<0.01, vs formoterol (Two-way ANOVA followed by Newman-Keuls *post hoc* test).

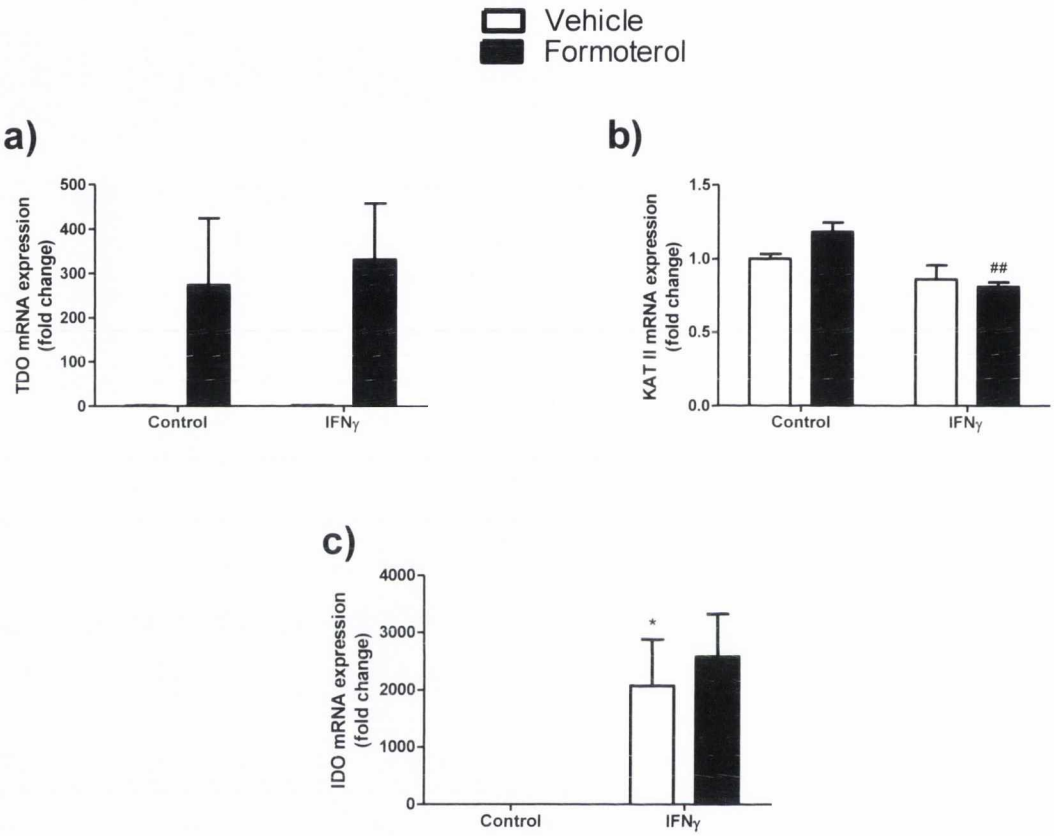

Figure 5.3.3.5: Effect of formoterol on IFNγ-induced changes in the mRNA expression of kynurenine pathway enzymes in primary cortical neurons

Primary cortical neurons (DIV 3) were treated with vehicle, formoterol (10 μM), IFNγ (10 ng/ml), or both formoterol + IFNγ for 6 hr. Cells were harvested for mRNA extractions followed by quantitative PCR to analyse the expression of TDO (a), KAT II (b) and IDO (c). Data expressed as mean ± SEM (n= 4-6). *P<0.05, vs. control, ##P<0.01, vs. formoterol (Two-way ANOVA followed by Newman-Keuls *post hoc* test).

5.3.3.6 Effect of formoterol and IFNγ in combination on the mRNA expression of kynurenine pathway enzymes in primary cortical mixed glia

Two-way ANOVA of **TDO** mRNA expression showed an effect of formoterol [$F_{(1, 22)} = 134.23$, $P<0.0001$], but not of IFNγ [$F_{(1, 22)} = 0.069$, $P= 0.796$], and no interaction [$F_{(1, 22)} = 0.017$, $P= 0.898$]. *Post hoc* analysis revealed increases in TDO mRNA expression following treatment with formoterol ($P<0.001$) compared to control (a).

Two-way ANOVA of **KAT II** mRNA expression showed an effect of IFNγ [$F_{(1, 22)} = 11.827$, $P= 0.003$], no effect of formoterol [$F_{(1, 22)} = 1.848$, $P= 0.19$], and no interaction [$F_{(1, 22)} = 0.424$, $P= 0.523$]. *Post hoc* analysis revealed reductions in KAT II mRNA expression following treatment with IFNγ ($P<0.05$) compared to control (b).

Two-way ANOVA of **IDO** mRNA expression showed an effect of IFNγ [$F_{(1, 22)} = 91.2$, $P<0.0001$], no effect of formoterol [$F_{(1, 22)} = 2.793$, $P= 0.111$], and no interaction [$F_{(1, 22)} = 2.793$, $P= 0.111$]. *Post hoc* analysis revealed increases in IDO mRNA expression following treatment with IFNγ ($P<0.001$) compared to control, with formoterol reducing the increase ($P<0.05$) (c) (**figure 5.3.3.6**).

5.3.3.7 Effect of formoterol and IFNγ in combination on the concentrations of tryptophan, kynurenine, 3-hydroxykynurenine and the tryptophan/kynurenine ratio in the CM of primary mixed glial cultures

Two-way ANOVA of the concentration of **tryptophan** showed an effect of formoterol [$F_{(1, 47)} = 25.87$, $P<0.0001$], no effect of IFNγ [$F_{(1, 47)} = 0$, $P= 0.987$], and an interaction [$F_{(1, 47)} = 15.235$, $P<0.0001$], in the CM of primary mixed glial cultures. *Post hoc* analysis revealed reductions in the concentrations of tryptophan following treatment with formoterol ($P<0.001$) and IFNγ ($P<0.01$) compared to control (a).

Two-way ANOVA of the concentration of **kynurenine** showed an effect of formoterol [$F_{(1, 47)} = 38.638$, $P<0.0001$], no effect of IFNγ [$F_{(1, 47)} = 0.019$, $P= 0.891$], and an interaction [$F_{(1, 47)} = 29.317$, $P<0.0001$], in the CM of primary mixed glial cultures. *Post hoc* analysis revealed reductions in the concentrations of kynurenine following treatment with formoterol ($P<0.001$) and IFNγ ($P<0.001$) compared to control (b).

Two-way ANOVA of the concentration of **3-hydroxykynurenine** showed an effect of formoterol [$F_{(1, 44)} = 18.567$, $P<0.0001$], no effect of IFNγ [$F_{(1, 44)} = 0.357$, $P= 0.553$] and an interaction [$F_{(1, 44)} = 4.445$, $P= 0.041$], in the CM of primary mixed glial cultures. *Post hoc* analysis revealed reductions in the concentrations of 3-hydroxykynurenine following treatment with formoterol ($P<0.001$) compared to control (c).

Two-way ANOVA of the **kynurenine over tryptophan ratio** showed no effect of formoterol [$F_{(1, 47)}$ = 0.171, P= 0.681], IFNγ [$F_{(1, 47)}$ = 0.06, P= 0.801], and no interaction [$F_{(1, 47)}$ = 0.268, P= 0.607] in the CM of primary mixed glial cultures (**figure 5.3.3.7**).

5.3.3.8 Effect of formoterol on the IFNγ-stimulated mixed glia CM-induced reductions in neurite outgrowth and the expression of synaptic markers

Two-way ANOVA of the number of **neuritic branches** showed an effect of formoterol CM [$F_{(1, 67)}$ = 3.399, P= 0.07], IFNγ CM [$F_{(1, 67)}$ = 5.893 P= 0.018], and an interaction [$F_{(1, 67)}$ = 5.822, P= 0.019]. *Post hoc* analysis revealed reductions in the number of neuritic branches following treatment with IFNγ CM (P<0.01) compared to control CM, with formoterol preventing the IFNγ CM-induced reductions (P<0.01) (a).

Two-way ANOVA of **neurite length** showed an effect of formoterol CM [$F_{(1, 67)}$ = 9.596, P= 0.003], IFNγ CM [$F_{(1, 67)}$ = 25.223, P<0.0001], and an interaction [$F_{(1, 67)}$ = 24.345 P<0.0001]. *Post hoc* analysis revealed reductions in neurite length following treatment with IFNγ CM (P<0.001) compared to control, with pre-treatment with formoterol preventing the IFNγ CM-induced reductions (P<0.001) (b).

Two-way ANOVA of the number of **primary neurites** showed no effect of formoterol CM [$F_{(1, 67)}$ = 3.526, P= 0.065], an effect of IFNγ CM [$F_{(1, 67)}$ = 7.112, P= 0.01], and an interaction [$F_{(1, 67)}$ = 10.382 P= 0.002]. *Post hoc* analysis revealed reductions in the number of primary neurites following treatment with IFNγ CM (P<0.001) compared to control, with treatment with formoterol preventing the IFNγ CM-induced reductions (P<0.01) (c).

Three-way repeated measures ANOVA of the number of **neuritic branches at specific distances from the neuronal cell soma** showed an effect of distance ($F_{(25, 1625)}$= 2.053, P=0.002), formoterol CM ($F_{(1, 65)}$= 0.742, P= 0.011), IFNγ CM ($F_{(1, 65)}$= 0.926, P= 0.014), formoterol x IFNγ CM ($F_{(1, 65)}$= 0.923, P= 0.014), but no effect of IFNγ CM x distance ($F_{(25, 1625)}$= 0.923, P= 0.573), formoterol CM x distance ($F_{(25, 1625)}$= 0.785, P= 0.765), formoterol x IFNγ CM x distance ($F_{(25, 1625)}$= 0.785, P= 0.765). *Post hoc* analysis revealed reductions in the number of branches at 10, 20, 30 and 40 μm from the cell soma following treatment with IFNγ CM (P<0.001) compared to control, with pre-treatment with formoterol preventing these IFNγ CM-induced reductions at 10, 20, 30 μm (P<0.001) and 40 μm (P<0.05) (d).

Two-way ANOVA of the **co-localised expression of synaptic markers** showed an effect of formoterol CM [$F_{(1, 176)}$ = 12.774, P<0.0001], IFNγ CM [$F_{(1, 176)}$ = 8.794, P= 0.003], but no interaction [$F_{(1, 176)}$ = 1.579, P= 0.211]. *Post hoc* analysis revealed reductions in the co-localised expression of synaptic

markers following treatment with IFNγ CM ($P<0.001$) compared to control CM, with treatment with formoterol preventing these reductions ($P<0.01$) (e).

Two-way ANOVA of the number of the expression of **synaptophysin** showed no effect of formoterol CM [$F_{(1, 176)} = 0.188$, $P= 0.665$], IFNγ CM [$F_{(1, 176)} = 0.376$, $P= 0.54$], and no interaction [$F_{(1, 176)} = 0.426$, $P= 0.515$] (f).

Two-way ANOVA of the number of the expression of **PSD-95 puncta** showed an effect of IFNγ CM [$F_{(1, 176)} = 15.513$, $P<0.0001$], no effect of formoterol CM [$F_{(1, 176)} = 2.37$, $P= 0.125$], and no interaction [$F_{(1, 176)} = 1.007$, $P= 0.317$]. *Post hoc* analysis revealed reductions in the expression of PSD-95 following treatment with IFNγ CM ($P<0.01$) compared to control (g) (**figure 5.3.3.8**).

5.3.3.9 Effect of TDO inhibition on the ability of formoterol to protect against the mixed glia IFNγ CM-induced reductions in neurite outgrowth and the expression of synaptic markers

Three-way ANOVA of the number of **neuritic branches** showed an effect of IFNγ CM [$F_{(3, 127)} = 9.58$, $P= 0.002$], no effect of 680C91 CM [$F_{(3, 127)} = 2.977$, $P= 0.087$], formoterol CM [$F_{(3, 127)} = 0.095$, $P= 0.759$], formoterol + IFNγ CM [$F_{(3, 127)} = 0.182$, $P= 0.67$], and no 680C91 x IFNγ interaction [$F_{(3, 127)} = 1.322$, $P= 0.253$], 680C91 x formoterol interaction [$F_{(3, 127)} = 0.037$, $P= 0.848$], 680C91 x formoterol + IFNγ interaction [$F_{(3, 127)} = 0.007$, $P= 0.933$]. *Post hoc* analysis revealed reductions in the number of neuritic branches following treatment with IFNγ CM ($P<0.05$) compared to control, with treatment with formoterol preventing the IFNγ CM-induced reductions ($P<0.05$) (a).

Three-way ANOVA of **neurite length** showed an effect of IFNγ CM [$F_{(3, 127)} = 55.209$, $P<0.0001$], 680C91 x IFNγ interaction [$F_{(3, 127)} = 6.172$, $P= 0.011$], no effect of 680C91 CM [$F_{(3, 127)} = 0.501$, $P= 0.481$], formoterol CM [$F_{(3, 127)} = 2.987$, $P= 0.086$], formoterol + IFNγ CM [$F_{(3, 127)} = 3.537$, $P= 0.062$], and no 680C91 x formoterol interaction [$F_{(3, 127)} = 0.010$, $P= 0.911$], 680C91 x formoterol + IFNγ interaction [$F_{(3, 127)} = 0.001$, $P= 0.972$]. *Post hoc* analysis revealed reductions in neurite length following treatment with IFNγ CM ($P<0.001$) compared to control, with formoterol preventing these IFNγ CM-induced reductions ($P<0.001$) (b).

Three-way ANOVA of the number of **primary neurites** showed an effect of IFNγ CM [$F_{(3, 127)} = 6.179$, $P= 0.014$], 680C91 x IFNγ interaction [$F_{(3, 127)} = 5.783$, $P= 0.018$], no effect of 680C91 CM [$F_{(3, 127)} = 2.194$, $P= 0.14$], formoterol CM [$F_{(3, 127)} = 1.002$, $P= 0.319$], formoterol + IFNγ CM [$F_{(3, 127)} = 1.040$, $P= 0.31$], and no 680C91 x formoterol interaction [$F_{(3, 127)} = 0.14$, $P= 0.907$], 680C91 x formoterol + IFNγ interaction [$F_{(3, 127)} = 0.133$, $P= 0.716$]. *Post hoc* analysis revealed reductions in the number of primary neurites following treatment with IFNγ CM ($P<0.01$) compared to control, with formoterol preventing these IFNγ CM-induced reductions ($P<0.05$) (c).

Three-way ANOVA of the **co-localised expression of synaptic markers** showed an effect of 680C91 CM [$F_{(1, 310)} = 25.445$, $P<0.0001$], IFNγ CM [$F_{(3, 310)} = 6.201$, $P= 0.013$], a 680C91 x formoterol interaction [$F_{(3, 310)} = 14.5$, $P<0.0001$], no effect of formoterol CM [$F_{(3, 310)} = 0.184$, $P= 0.668$], formoterol + IFNγ CM [$F_{(3, 310)} = 0.118$, $P= 0.731$], a 680C91 x IFNγ interaction [$F_{(3, 310)} = 3.393$, $P= 0.066$], or a 680C91 x formoterol + IFNγ interaction [$F_{(3, 310)} = 0.545$, $P= 0.461$]. *Post hoc* analysis revealed reductions in the co-localised expression of synaptic markers following treatment with IFNγ CM ($P<0.05$) compared to control, with formoterol preventing the IFNγ CM-induced reductions ($P<0.05$) (e).

Three-way ANOVA of the number of the expression of **synaptophysin** showed an effect of 680C91 CM [$F_{(1, 310)} = 6.696$, $P= 0.01$], but no effect of IFNγ CM [$F_{(3, 310)} = 0.084$, $P= 0.772$], formoterol CM [$F_{(3, 310)} = 0.781$, $P= 0.378$], formoterol + IFNγ CM [$F_{(3, 310)} = 1.591$ $P= 0.208$], a 680C91 x IFNγ interaction [$F_{(3, 310)} = 0.235$, $P= 0.208$], a 680C91 x formoterol interaction [$F_{(3, 310)} = 0.592$, $P= 0.442$], or a 680C91 x formoterol + IFNγ interaction [$F_{(3, 310)} = 0.002$, $P= 0.961$]. *Post hoc* analysis revealed no reductions in the expression of synaptophysin (f).

Three-way ANOVA of the number of the expression of **PSD-95** showed an effect of an effect of 680C91 CM [$F_{(1, 310)} = 17.066$, $P<0.0001$], a 680C91 x formoterol interaction [$F_{(3, 310)} = 13.805$, $P<0.0001$], a 680C91 x IFNγ interaction [$F_{(3, 310)} = 3.393$, $P= 0.048$], no effect of IFNγ CM [$F_{(3, 310)} = 3.816$, $P= 0.052$], formoterol CM [$F_{(3, 310)} = 0.007$, $P= 0.932$], formoterol + IFNγ CM [$F_{(3, 310)} = 0.369$, $P= 0.544$], or a 680C91 x formoterol + IFNγ interaction [$F_{(3, 310)} = 0.738$, $P= 0.391$]. *Post hoc* analysis revealed reductions in the expression of PSD-95 following treatment with IFNγ CM ($P<0.05$) compared to control (g) (**figure 5.3.3.9**).

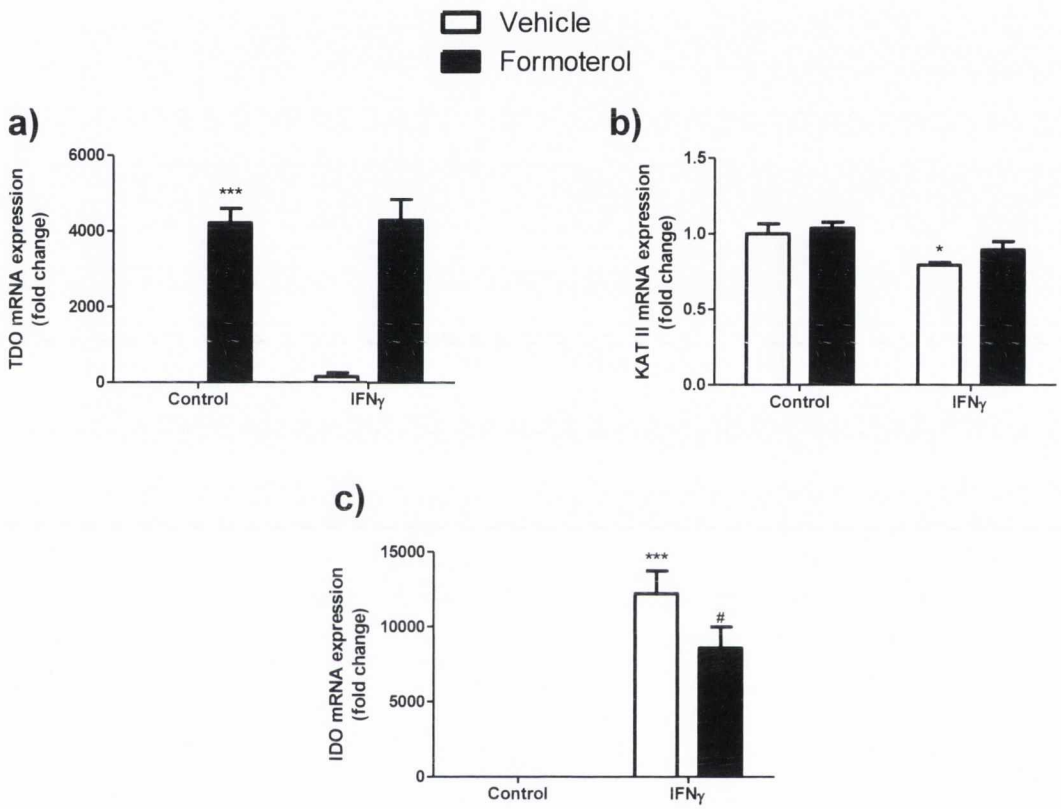

Figure 5.3.3.6: Effect of formoterol and IFNγ in combination on the mRNA expression of kynurenine pathway enzymes in primary cortical mixed glia

Primary cortical mixed glia (DIV 12-13) were treated with either formoterol (10 μM), IFNγ (10 ng/ml) or both formoterol + IFNγ for 6 hr. Cells were harvested for mRNA extractions followed by quantitative PCR to analyse the expression of TDO (a), KAT II (b), IDO (c). Data expressed as mean ± SEM (n= 5-6). *P<0.05, ***P<0.001, vs. control, #P<0.05, vs. IFNγ (Two-way ANOVA followed by Newman-Keuls *post hoc* test).

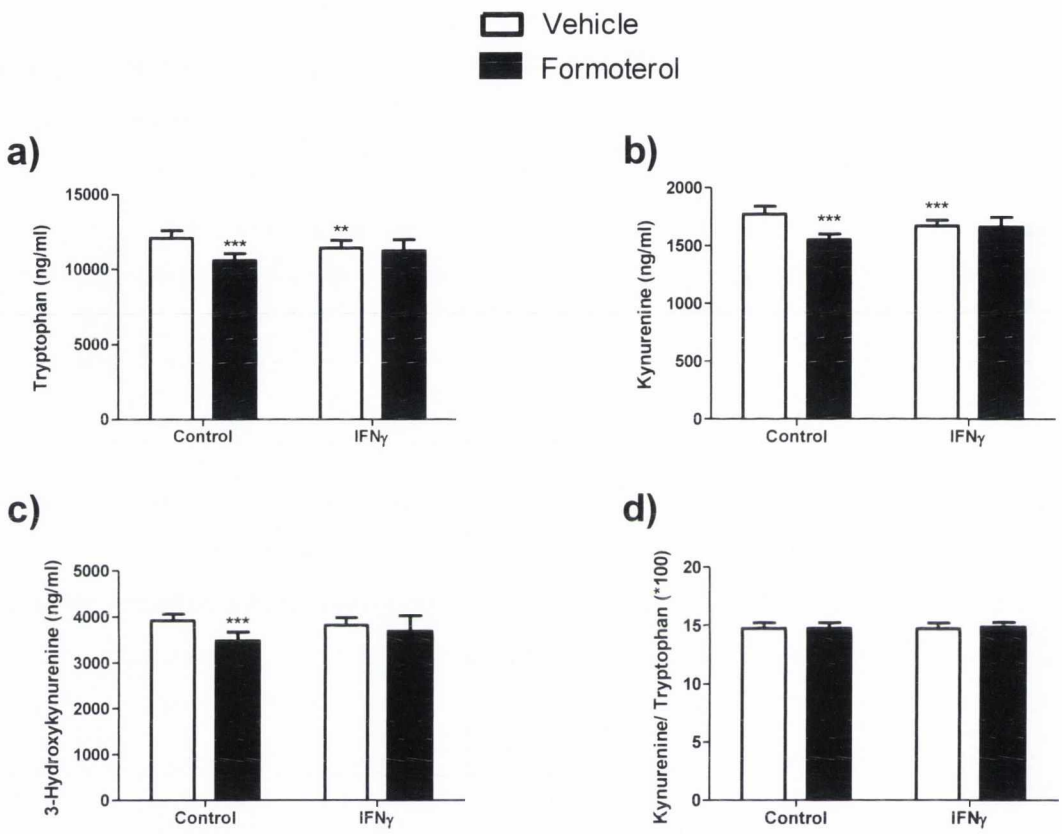

Figure 5.3.3.7: Effect of formoterol on the IFNγ-induced changes in the concentrations of tryptophan, kynurenine, 3-hydroxykynurenine and the tryptophan/kynurenine ratio in the CM of primary mixed glial cultures

Primary cortical mixed glia (DIV 12-13) were treated with either formoterol (10 μM), IFNγ (10 ng/ml) or both formoterol + IFNγ for 24 hr. CM was harvested for analysis of the concentrations of (a) tryptophan, (b) kynurenine, (c) 3-hydroxykynurenine, and (d) kynurenine over tryptophan ratio. Data expressed as mean ± SEM (n= 12 wells, from 2 independent experiments). **P<0.01, ***P<0.001, vs. control (Two-way ANOVA followed by Newman-Keuls *post hoc* test).

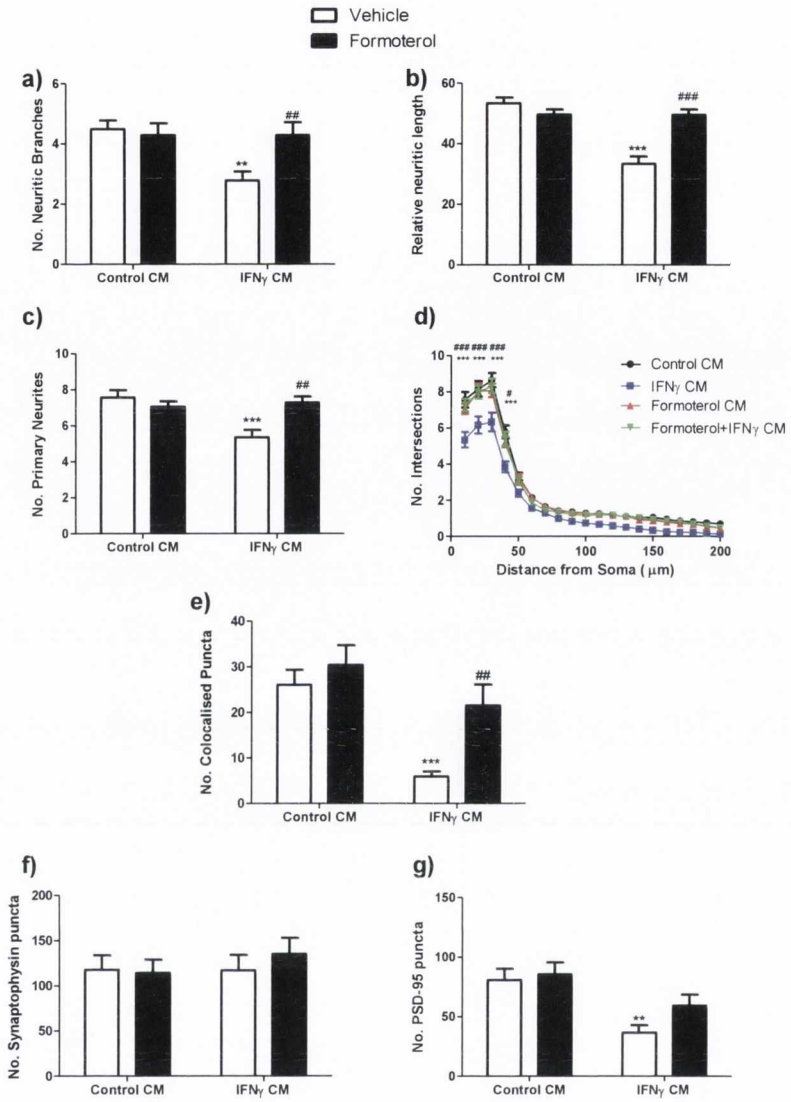

Figure 5.3.3.8: Effect of formoterol of the IFNγ-stimulated mixed glial CM-induced changes in neuronal complexity and the expression of synaptic markers

CM from primary mixed glia treated with vehicle, formoterol (10 μM), IFNγ (10 ng/ml) or both formoterol + IFNγ for 24 hr was placed on primary cortical neurons (DIV 3) for 24 hr. Sholl analysis was performed on one set of neurons to examine the number of neuritic branches (a), neurite length (b), the number of primary neurites (c) or the number of branches at specific distances from the soma (d). Data expressed as mean ± SEM (n= 16-18 coverslips from 3 independent experiments) [Two-way ANOVA followed Newman-Keuls *post hoc* test (a-c)]; Sholl profile, ***P<0.001, IFNγ CM vs. control CM, #P<0.05, ###P<0.001, IFNγ CM vs. formoterol + IFNγ CM [three-way repeated measures ANOVA followed by Bonferroni *post hoc* test (d)]. Another set of neurons were examined to determine the co-localised expression of pre- and post-synaptic markers synaptophysin and PSD-95 (e), and the number of synaptophysin puncta (f), and PSD-95 puncta (g) in isolation using ImageJ software. Data expressed as mean ± SEM (n= 41-50 neurons from 3 independent experiments). *P<0.05, ***P<0.001, vs. control CM, ##P<0.01, vs. IFNγ CM (Two-way ANOVA followed by Newman-Keuls *post hoc* test).

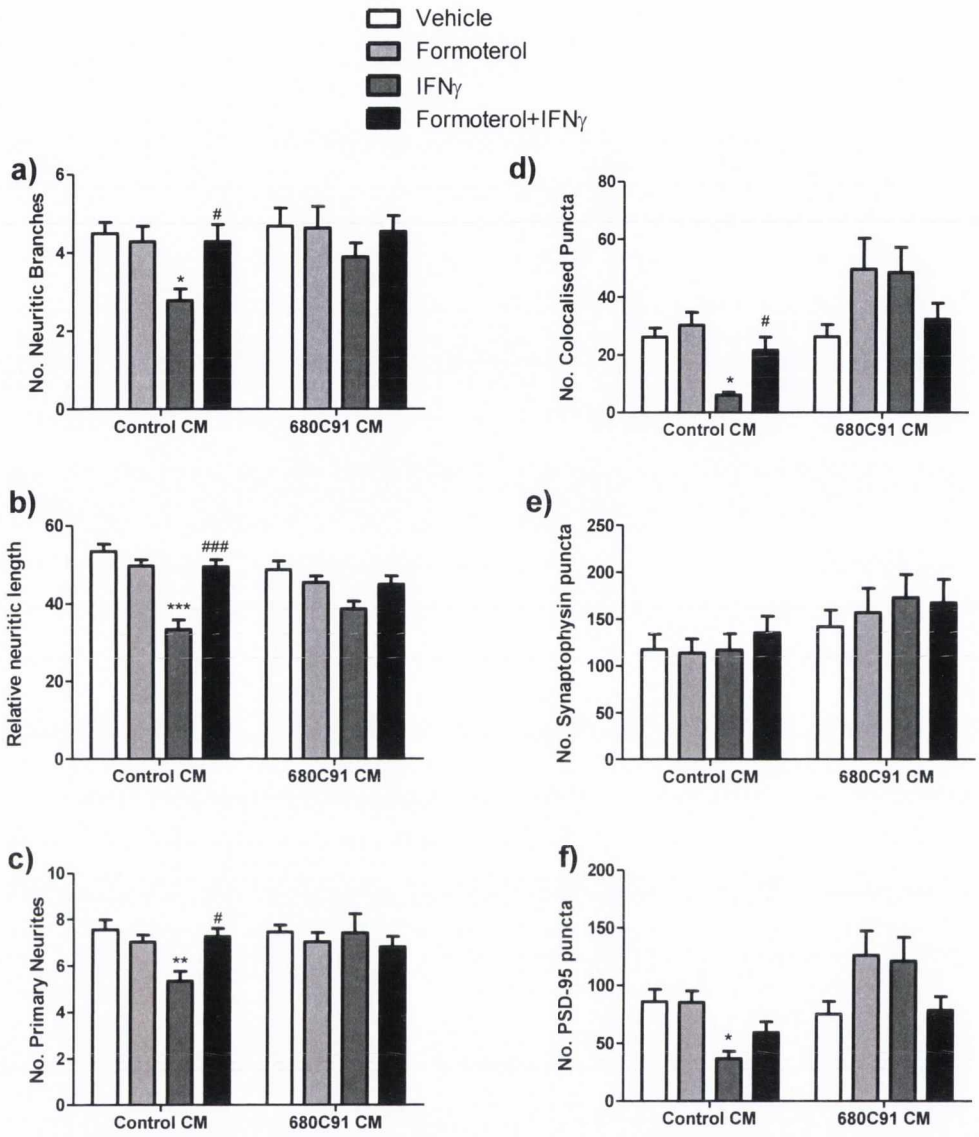

Figure 5.3.3.9: Effect of TDO inhibition on the ability of formoterol to protect against the mixed glia IFNγ CM-induced reductions in neurite outgrowth and the co-localised expression of synaptic markers

CM from primary mixed glia pre-treated with either vehicle or 680C91 (20 μM; 30 min) followed by treatment with either vehicle, formoterol (10 μM), IFNγ (10 ng/ml) or both formoterol + IFNγ for 24 hr was placed on primary cortical neurons (DIV 3) for 24 hr. Sholl analysis was performed on one set of neurons to examine the number of neuritic branches (a), neurite length (b), and the number of primary neurites (c). Data expressed as mean ± SEM (n= 14-18 coverslips from 3 independent experiments). *P<0.05, **P<0.01, ***P<0.001, vs. control CM, #P<0.05, ###P<0.001, vs IFNγ CM [Three-way ANOVA followed by Newman-Keuls *post hoc* test (a-c)] Another set of neurons were examined to determine the co-localised expression of pre- and post-synaptic markers synaptophysin and PSD-95 (d), and the number of synaptophysin puncta (e), and PSD-95 puncta (f) in isolation using ImageJ software. Data expressed as mean ± SEM (n= 34-50 neurons from 3 independent experiments) (Three-way ANOVA followed by Newman-Keuls *post hoc* test).

5.3.4 Determination of the ability of the neuroprotective arm of the kynurenine pathway in astrocytes to protect against the neurotoxic, atrophic kynurenine pathway metabolites

5.3.4.1 Effect of formoterol-stimulated astrocytic CM on kynurenine pathway metabolite-induced changes in neuronal complexity

Two-way ANOVA of the number of **neuritic branches** showed no effect of formoterol [$F_{(1, 71)} = 2.565$, P= 0.114], the 3-hydroxykynurenine + 3-hydroxyanthranillic acid + quinolinic acid combination [$F_{(1, 71)} = 0.753$, P= 0.389], or an interaction [$F_{(1, 71)} = 2.794$ P= 0.009] (a).

Two-way ANOVA of **neurite length** showed an effect of formoterol [$F_{(1, 71)} = 6.218$, P= 0.015], the 3-hydroxykynurenine + 3-hydroxyanthranillic acid + quinolinic acid combination [$F_{(1, 71)} = 12.232$, P= 0.001], and an interaction [$F_{(1, 71)} = 8.95$ P= 0.004]. *Post hoc* analysis revealed reductions in neurite length with treatment with the 3-hydroxykynurenine + 3-hydroxyanthranillic acid + quinolinic acid combination (P<0.01) (b).

Two-way ANOVA of the number of **primary neurites** showed an effect of the 3-hydroxykynurenine + 3-hydroxyanthranillic acid + quinolinic acid combination [$F_{(1, 71)} = 4.638$, P= 0.035], no effect of formoterol [$F_{(1, 71)} = 0.02$, P= 0.888], or an interaction [$F_{(1, 71)} = 1.894$ P= 0.173]. *Post hoc* analysis revealed no changes in the number of primary neurites with any treatment (c).

Three-way repeated measures ANOVA of the number of **neuritic branches at specific distances from the neuronal cell soma** showed an effect of distance [$F_{(25, 1675)} = 989.46$, P<0.0001], formoterol [$F_{(1, 67)} = 5.993$, P= 0.017), 3-hydroxykynurenine + 3-hydroxyanthranillic acid + quinolinic acid combination [$F_{(1, 67)} = 11.815$, P= 0.001], an interaction [$F_{(1, 67)} = 8.637$, P= 0.005], 3-hydroxykynurenine + 3-hydroxyanthranillic acid + quinolinic acid combination x distance [$F_{(25, 1675)} = 3.18$, P<0.0001], formoterol x 3-hydroxykynurenine + 3-hydroxyanthranillic acid + quinolinic acid combination x distance ($F_{(25, 1675)} = 9.616$, P= 0.028], but no effect of formoterol x distance [$F_{(25, 1675)} = 0.341$, P= 0.999]. *Post hoc* analysis revealed reductions in the number of branches at 30 µm from the cell soma with treatment with the 3-hydroxykynurenine + 3-hydroxyanthranillic acid + quinolinic acid combination (P<0.01) compared to control (d) (**figure 5.3.4.1**).

5.3.4.2. Effect of formoterol-stimulated astrocytic CM on kynurenine pathway metabolite-induced changes in the expression of synaptic markers

Two-way ANOVA of the **co-localised expression of synaptic markers** showed an effect of formoterol [$F_{(1, 173)} = 4.59$, P= 0.034], the 3-hydroxykynurenine + 3-hydroxyanthranillic acid + quinolinic acid combination [$F_{(1, 173)} = 4.655$, P= 0.032], and an interaction [$F_{(1, 173)} = 5.751$, P= 0.018]. *Post hoc* analysis revealed reductions in the co-localised expression of synaptic markers with treatment with the 3-hydroxykynurenine + 3-hydroxyanthranillic acid + quinolinic acid combination (P<0.01)

compared to control, with formoterol preventing the 3-hydroxykynurenine + 3-hydroxyanthranillic acid + quinolinic acid-induced reductions ($P<0.01$) (a).

Two-way ANOVA of the number of **synaptophysin puncta** showed no effect of formoterol [$F_{(1, 173)} = 0.776$, $P= 0.38$], the 3-hydroxykynurenine + 3-hydroxyanthranillic acid + quinolinic acid combination [$F_{(1, 173)} = 0.125$, $P= 0.724$], and no interaction [$F_{(1, 173)} = 0.027$, $P= 0.87$] (b).

Two-way ANOVA of the number of **PSD-95 puncta** showed an effect of formoterol [$F_{(1, 173)} = 14.736$, $P<0.0001$], no effect of the 3-hydroxykynurenine + 3-hydroxyanthranillic acid + quinolinic acid combination [$F_{(1, 173)} = 0.113$, $P= 0.738$], and no interaction [$F_{(1, 173)} = 0.606$, $P= 0.437$]. *Post hoc* analysis revealed increases in the number of PSD-95 puncta with treatment with formoterol ($P<0.01$) compared to control (c).

Three-way ANOVA of the **co-localised expression of synaptic markers** showed an effect of IFNγ CM [$F_{(1, 348)} = 12.929$, $P<0.0001$], no effect of 680C91 CM [$F_{(1, 348)} = 0.334$, $P= 0.564$], formoterol CM [$F_{(1, 348)} = 1.117$, $P= 0.291$], formoterol + IFNγ CM [$F_{(1, 348)} = 0.083$, $P= 0.774$], and no 680C91 x IFNγ interaction [$F_{(1, 348)} = 3.213$, $P= 0.074$], 680C91 x formoterol interaction [$F_{(1, 348)} = 0.631$, $P= 0.428$], 680C91 x formoterol + IFNγ interaction [$F_{(1, 348)} = 0.092$, $P= 0.0761$]. *Post hoc* analysis revealed reductions in the co-localised expression of synaptic markers with treatment with the 3-hydroxykynurenine + 3-hydroxyanthranillic acid + quinolinic acid combination ($P<0.01$) compared to control, with formoterol preventing the 3-hydroxykynurenine + 3-hydroxyanthranillic acid + quinolinic acid-induced reductions ($P<0.01$) (d).

Three-way ANOVA of the number of **synaptophysin puncta** showed no effect of 680C91 CM [$F_{(1, 348)} = 0.334$, $P= 0.564$], IFNγ CM [$F_{(1, 348)} = 12.929$, $P<0.0001$], formoterol CM [$F_{(1, 348)} = 1.117$, $P= 0.291$], formoterol + IFNγ CM [$F_{(1, 348)} = 0.083$, $P= 0.774$], and no 680C91 x IFNγ interaction [$F_{(1, 348)} = 3.213$, $P= 0.074$], 680C91 x formoterol interaction [$F_{(1, 348)} = 0.631$, $P= 0.428$], 680C91 x formoterol + IFNγ interaction [$F_{(1, 348)} = 0.092$, $P= 0.0761$] (e).

Three-way ANOVA of the number of **PSD-95 puncta** showed effect of IFNγ CM [$F_{(1, 348)} = 5.942$, $P= 0.015$], no effect of 680C91 CM [$F_{(1, 348)} = 2.082$, $P= 0.15$], formoterol CM [$F_{(1, 348)} = 0.02$, $P= 0.889$], formoterol + IFNγ CM [$F_{(1, 348)} = 0.172$, $P= 0.079$, and no 680C91 x IFNγ interaction [$F_{(1, 348)} = 1.546$, $P= 0.215$], 680C91 x formoterol interaction [$F_{(1, 348)} = 0.408$, $P= 0.523$], 680C91 x formoterol + IFNγ interaction [$F_{(1, 348)} = 1.186$, $P= 0.277$]. *Post hoc* analysis revealed increases in the number of PSD-95 puncta with treatment with formoterol + 3-hydroxykynurenine + 3-hydroxyanthranillic acid + quinolinic acid combination ($P<0.05$) compared the 3-hydroxykynurenine + 3-hydroxyanthranillic acid + quinolinic acid combination alone (e) (**figure 5.3.4.2**).

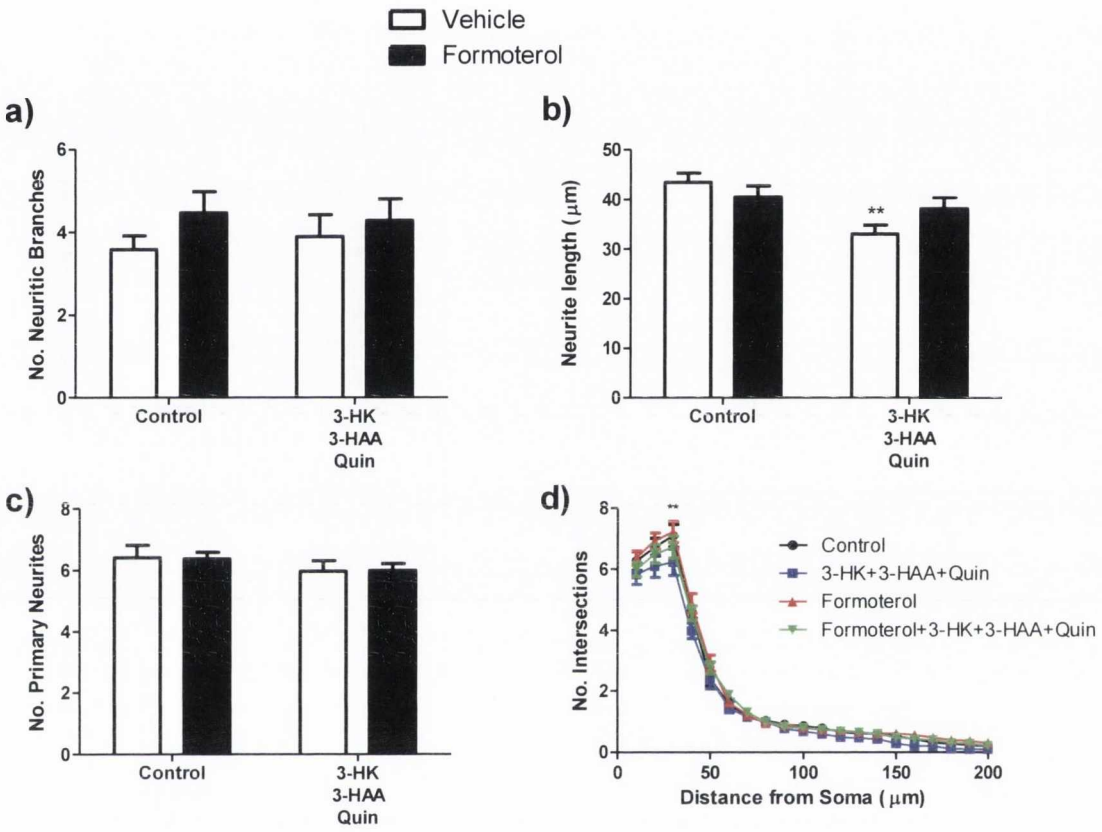

Figure 5.3.4.1 Effect of formoterol-stimulated astrocytic CM on kynurenine pathway metabolite-induced changes in neuronal complexity

Primary cortical neurons (DIV 3) were pre-treated with CM from primary astrocytes treated with vehicle or formoterol (10 μM) for 2 hr, followed by treatment with the 3-hydroxykynurenine (3-HK; 0.03 μM) + 3-hydroxyanthranillic acid (3-HAA; 0.03 μM) + quinolinic acid (Quin; 0.1μM) combination for 24 hr. Sholl analysis was performed on neurons to examine the number of neuritic branches (a), neurite length (b), the number of primary neurites (c) or the number of branches at specific distances from the soma (d). Data expressed as mean ± SEM (n= 14-18 coverslips from 3 independent experiments) **P<0.05, vs. control CM [Two-way ANOVA followed Newman-Keuls *post hoc* test (a-c)]; Sholl profile, **P<0.01, 3-HK+3-HAA+Quin vs. control CM [three-way repeated measures ANOVA followed by Bonferroni *post hoc* test (d)].

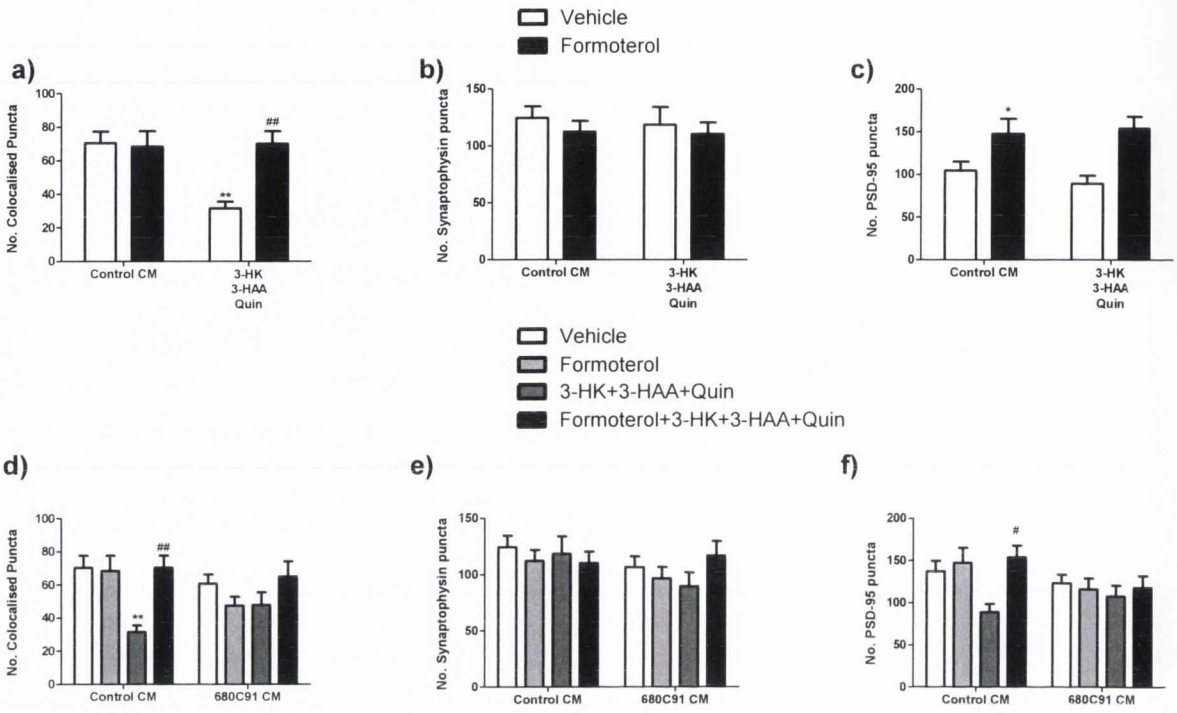

Figure 5.3.4.2 Effect of formoterol-stimulated astrocytic CM on kynurenine pathway metabolite-induced changes in the expression of synaptic markers

Primary cortical neurons (DIV 18-21) were pre-treated with CM from primary astrocytes pre-treated with vehicle or 680C91 (20 μM; 30 min) followed by treatment with formoterol (10 μM; 24 hr) for 2 hr, followed by treatment with the 3-hydroxykynurenine (3-HK; 0.03 μM) + 3-hydroxyanthranillic acid (3-HAA; 0.03 μM) + quinolinic acid (Quin; 0.1μM) combination for 24 hr. Neurons were examined to determine the co-localised expression of pre- and post-synaptic markers synaptophysin and PSD-95 (a, d), and the number of synaptophysin puncta (b, e), and PSD-95 puncta (c, f) in isolation using ImageJ software. Data expressed as mean ± SEM (n= 39-49 neurons from 3 independent experiments). **P<0.01, vs control CM, #P<0.05, ##P<0.01, vs. 3-HK+3-HAA+Quin (Two-way ANOVA followed (a-c) or three-way ANOVA (d-f) by Newman-Keuls *post hoc* test).

5.4 Discussion

The above data lend support to the findings in the literature whereby regulation of kynurenic acid production is mediated by adrenoceptor stimulation and subsequent cAMP/PKA-dependent signalling (Luchowska et al., 2009). Overall these data highlight a novel role for TDO as the rate-limiting enzyme driving the initial step of the neuroprotective arm of this pathway in the presence of both the anti-inflammatory agent, formoterol, and the inflammatory stimulus, IFNγ. Furthermore, the dominant effect of β_2-adrenoceptor stimulation over IFNγ-mediated effects in terms of kynurenine pathway-associated gene expression in primary cortical cells is now apparent. Additionally, the potential for β_2-adrenoceptor stimulation to protect against IFNγ-driven mixed glial CM-induced reductions in neuronal complexity and synaptogenesis is demonstrated

5.4.1 Divergent effects of adrenoceptor subtype stimulation on the activation of the kynurenine pathway in primary cortical astrocytes

The results of this investigation highlight the dynamic effect that noradrenaline has on regulating kynurenine pathway enzyme mRNA expression in primary cortical astrocytes. The combined stimulation of both α- and β-adrenoceptors with noradrenaline resulted in increased TDO and decreased KAT II, IDO, and KMO mRNA expression, suggesting a lack of induction of the neurotoxic arm of the kynurenine pathway and incomplete induction of the neuroprotective arm. Interestingly however, Luchowska et al. (2009) reported increased kynurenic acid production in primary rat mixed glial cultures in response to treatment with the broad spectrum adrenoceptor agonist, adrenaline. Consequently, although KAT II mRNA expression is reduced, there may be sufficient levels of the enzyme to allow for kynurenic acid production.

Blockade of both α_1- and α_2-adrenoceptors with phentolamine, enhanced the noradrenaline-induced increase in TDO mRNA expression, and reverses the noradrenaline-induced decreases in KAT II mRNA expression. Furthermore selective blockade of the α_1-adrenoceptor with prazosin restores the noradrenaline-induced reductions in KAT II mRNA expression. Furthermore non-selective antagonism of the β-adrenoceptor with propranolol, prevents noradrenaline-induced increases in TDO mRNA expression, while having no effect on the reductions in KAT II mRNA expression. In order to remove the negative effects of noradrenaline on KAT II induction to ensure full activation of the neuroprotective arm of the kynurenine pathway, astrocytes were treated with the broad spectrum β-adrenoceptor agonist, isoproterenol. Isoproterenol led to a substantial increase in TDO mRNA expression and a subtle increase in KAT II mRNA expression, with the expression of all other kynurenine pathway enzymes remaining unchanged. Furthermore, blockade of both β_1- and β_2-

adrenoceptors reduced the isoproterenol-induced increases in TDO mRNA expression, however no effect was seen with regard to KAT II mRNA expression.

Considering that both β_1- and β_2-adrenoceptor stimulation activate the neuroprotective arm, the ability of the long-acting (12 hr) β_2-adrenoceptor agonist, formoterol, to mimic the isoprotereno-related findings were assessed. A β_2-adrenoceptor agonist was chosen based on findings by Junker et al. (2002) who demonstrated that astrocyte-associated neuroprotection is achieved by stimulation of either β_1- or β_2- adrenoceptor *in vitro*, whereas *in vivo* this protection is achieved preferentially through stimulation of the β_2-adrenoceptor. In this instance, formoterol demonstrated a positive effect on TDO, KAT II, and IDO mRNA expression, of which increases in TDO mRNA expression was blocked by the non-selective β-adrenoceptor antagonist propranolol, and by the β_2-adrenoceptor antagonist ICI 118,551. In support of these findings, Luchowska et al. (2009) demonstrated that formoterol, and the short-acting (2-6 hr) β_2-adrenoceptor agonist, salbutamol, increased kynurenic acid production in mixed glial cultures and rat brain cortical slices. Similarly, this group demonstrated that the long-acting β_2-adrenoceptor agonist, clenbuterol, with a half-life of approximately 37 hours, increased kynurenic acid production in mixed glial cultures and rat brain cortical slices. Furthermore, of the adrenoceptor agonists examined only formoterol was capable of increasing the activity of KAT I and II in mixed glial cultures (Luchowska et al., 2008).

Although β-adrenoceptor stimulation increased KAT II mRNA expression, blockade of this receptor did not attenuate this increase. Considering that α_1-adrenoceptor activation negatively regulates KAT II mRNA expression, it may be that stimulation of the α_1-adrenoceptor alone or in combination with a β-adrenoceptor antagonist is required for effective downregulation. Indeed, Luchowska et al. (2009) demonstrated that increased kynurenic acid production is PKA-dependent and furthermore PKA pathway activation increases KAT activity. However inhibition of PKA did not reduce KAT I or II activity. This group propose that KATs are constitutively expressed, and PKA inhibition does not affect their levels due to the presence of existing pools of functional KAT enzymes. Recently, Agudelo et al. (2014) reported increases in KAT gene expression in response to exercise-associated PGC-1α1-PPARα/δ intracellular signalling. PGC-1α is involved in mitochondrial biogenesis, and is induced by β-adrenoceptor stimulation directly (Chinsomboon et al., 2009) or indirectly via PKA activation (Gerhart-Hines et al., 2011). PGC-1α is predominantly located in skeletal muscle, however it has also been reported in rodent neurons (Wareski et al., 2009) and astrocytes (Chen et al., 2012). Consequently it could be by this β-adrenoceptor PGC-1α pathway that KAT II mRNA expression is regulated in addition to PKA signalling. Additionally, it may be by this mechanism that IFNγ reduces KAT II mRNA expression, as it has been demonstrated that PGC-1α exhibits a reciprocal relationship with NFκB signalling, with TNFα reducing the expression of PGC-1α both *in vitro* and *in vivo* in the murine skeletal muscle cell line, C2C12, and C57/BL6 mice respectively (Remels et al., 2013).

Additionally, these changes in kynurenine pathway enzyme mRNA expression in primary cortical astrocytes were shown to be cAMP-mediated, with the cAMP analogue, dbcAMP, mimicking the formoterol- and isoproterenol-induced changes in TDO and KAT II mRNA expression although to a lesser extent. Similarly, Luchowska et al. (2009) demonstrated an increase in kynurenic acid production using the cAMP analogues, 8pCPT-cAMP and 8-Br-cAMP in mixed glial cultures and rat brain cortical slices, with both cAMP analogues increasing KAT activity in mixed glial cultures.

In addition, we found that stimulation of astrocytes with formoterol at a concentration that induced TDO, IDO and KAT II mRNA expression, resulted in decreased concentrations of tryptophan, kynurenine, and 3-hydorxykynurenine in the CM, indicating a shift in tryptophan metabolism away from the neurotoxic arm of the pathway.

5.4.2 Characterisation of the effect of mixed glial β_2-adrenoceptor stimulation on inflammation-associated reductions in neuronal complexity and the expression of synaptic markers

Previously in chapter 4 it was shown that IFNγ-stimulated mixed glial CM reduces neuronal complexity and causes synapse loss through activation of the kynurenine pathway, with no atrophic effect seen with IFNγ-stimulated astrocytic or microglial CM. Subsequently, the following experiments aimed to determine whether simultaneous activation of both the neurotoxic and neuroprotective arms of the pathway in these mixed glial cultures could afford protection against kynurenine pathway-driven neuronal atrophy. Considering that both neurons and microglia express functional adrenoceptors (Rang and Dale, 2012), the effect of noradrenaline and formoterol on the mRNA expression of kynurenine pathway enzymes in microglia and neurons were assessed and found to be primarily unaffected by adrenoceptor stimulation.

Consequently, the effect of formoterol on the IFNγ-induced changes in the mRNA expression of the kynurenine pathway enzymes seen in chapter 4 were investigated. In the presence of both stimuli, in all three isolated cortical cells, the formoterol-related induction of TDO was maintained, while a failure of formoterol to induce KAT II mRNA expression was observed. In the case of both neurons and astrocytes, but not microglia, formoterol had no effect on the IFNγ-induced increases in IDO mRNA expression. This upregulation of both rate limiting enzymes in astrocytes alongside a down regulation of IDO in microglia suggests that in the presence of an inflammatory stimulus formoterol favours the neuroprotective arm over the neurotoxic arm.

Regarding mixed glial cultures, formoterol blocked the IFNγ-induced increase in IDO to an extent, while in the presence of both stimuli there remained a strong induction of TDO and no reduction in KAT II mRNA expression. The reduced effect of formoterol on IFNγ-induced increases in IDO mRNA

expression in mixed glial may occur as consequence of increased IDO expression being attenuated in microglia but not astrocytes. Increased mRNA expression in astrocytes is favourable as it, in addition to TDO, is a rate-limiting enzyme of the neuroprotective arm of the kynurenine pathway. Moreover, in the presence of both stimuli, the concentrations of tryptophan, kynurenine and 3-hydroxykynurenine remain reduced. As such, the ability of formoterol to protect against IFNγ-stimulated mixed glial CM-induced atrophy and synapse loss was investigated. In all instances, formoterol protected against the IFNγ CM-induced reductions in the number of neuritic branches, neurite length, the number of primary neurites and branching at 10, 20, 30 and 40 μm from the cell soma. Furthermore, formoterol attenuated IFNγ CM-induced reductions in the co-localised expression of synaptic markers.

Considering the novel finding of a robust increase in TDO mRNA expression in primary cortical mixed glia in response to formoterol, a role for TDO-driven activation of the neuroprotective arm of the kynurenine pathway in mediating the protective effects was examined. Prior treatment of mixed glial cells with the TDO inhibitor, 680C91, failed to block formoterol-mediated protective effects suggesting that in place of TDO-driven kynurenine pathway activation other factors such as growth factors, neurotrophins and cytokines may be involved. Indeed these factors have been implicated in driving noradrenaline-stimulated astrocytic CM-induced increases in neuronal complexity (Day et al., 2014). Additionally, a role for IDO-driven pathway activation cannot be discounted and perhaps the combined inhibition of both rate limiting enzymes would be effective at blocking the formoterol-induced protection. Considering the large increase in TDO mRNA expression elicited by formoterol stimulation of mixed glial cultures, a higher concentration of 680C91 may be required to sufficiently attenuate the TDO-mediated protective effects of this CM. However, it is of interest note that 680C91 prevents the IFNγ-induced atrophy which may indicate that basal levels of astrocytic TDO-mediated kynurenine production contribute to the microglial mediated-atrophy. This also may account for the lack of neuronal atrophy observed following treatment with formoterol + IFNγ-stimulated mixed glial CM with pre-treatment with 680C91. Although 680C91 may be inhibiting TDO-mediated kynurenic acid production, it may also be reducing the availability of kynurenine, diminishing the extent of metabolism down the neurotoxic arm of the pathway in microglia.

In order to more directly assess a role for TDO in this formoterol-induced neuroprotection, the effect of CM from isolated astrocytic cultures - which demonstrated induction of TDO and KAT II, but not IDO mRNA expression in response to formoterol - was assessed in the presence of the atrophic combination of 3-hydroxykynurenine + 3-hydroxyanthranillic acid + quinolinic acid. In this instance however, the potent atrophic effects seen in chapter 4 were not observed, except to a limited extent with reductions in neurite length and branching at 30 μm form the cell soma. This may be as a consequence of the neurotrophic nature of unstimulated astrocytic CM which may itself afford

protection to neurons against atrophic agents (Yoshida et al., 1995). In contrast, the negative effect of the 3-hydroxykynurenine + 3-hydroxyanthranillic acid + quinolinic acid combination on synaptogenesis observed in chapter 4 was maintained, with prior treatment with formoterol-stimulated astrocytic CM protecting against these reductions. Again however, prior treatment of astrocytes with the TDO inhibitor, 680C91, failed to block this formoterol-stimulated astrocytic protection. Previous work carried out by our laboratory has demonstrated that noradrenaline as well as the long-acting β_2-adrenoceptor agonist, salmeterol, increased the co-localised expression of synaptic markers as a consequence of NGF enhancement of synaptic marker expression [unpublished data O'Neill (2015)].

Determining a role for TDO in mediating the neurotrophic effects of unstimulated astrocytic CM previously reported by our lab [unpublished data O'Toole (2015)] would be of interest to assess the basal contribution of kynurenic acid to astrocyte-related neurotropism. Additionally, a more discreet neurotoxic insult might provide further insight into a role for TDO-driven kynurenine pathway activation in mediating the formoterol-related neuroprotective effects. Considering that chapter 4 demonstrated that glutamate and glycine caused robust atrophy and synapse loss which was attenuated by kynurenic acid, the potential of TDO-driven kynurenine pathway activation to protect against these atrophic effects would provide greater clarity.

5.4.3 Conclusion

Overall, these findings highlight the reciprocal control of adrenoceptors on kynurenine pathway enzyme gene induction. Furthermore these findings in conjunction with those made by Luchowska et al. (2009) support a role for β-adrenoceptor agonists as positive regulators of the neuroprotective arm of the kynurenine pathway via the cAMP intracellular signalling pathway in primary cortical astrocytes. Moreover, Luchowska et al. (2009) identified that increased production of kynurenic acid is not necessarily reliant on increased KAT activity, but more so on PKA-related signalling. As such, we propose a robust induction in TDO as a novel mechanism for kynurenine production in formoterol-stimulated astrocytes. Subsequently kynurenic acid production mediated by either KAT II or another unknown PKA-related mechanism can contribute in part to the protective properties of β_2-adrenoceptor stimulated astrocytic CM.

A role for TDO in driving kynurenine pathway activation in the brain has become of interest as a consequence of its mRNA expression being upregulated in cortical astrocytes of schizophrenic patients, in the absence of increased IDO mRNA expression (Miller et al., 2004). Considering that gene expression of both rate-limiting enzymes of the kynurenine pathway are discretely regulated, a role for TDO in pathway activation may be relevant in times of stress due to the known propensity of

stress related-glucocorticoids to induce TDO mRNA expression (Schutz et al., 1975). The identification that noradrenaline - a neurotransmitter but also produced as a consequence of stress-induced activation of the SAM axis - can also induce TDO indicates that kynurenine pathway activation can be regulated by two independent stress axes. Considering that β-agonists are commonly used clinically for the alleviation of asthma attacks (Anderson, 2000), the potential to modulate this pathway in disease circumstances via this mechanism is promising and accessible.

Chapter 6

General discussion

6.1 Summary of main findings

The results obtained from carrying out the experiments described in this thesis have provided important insights into the role that kynurenine pathway activation in glial cells has in mediating changes in neuronal integrity. Considering that the kynurenine pathway is implicated in various CNS disorders which exhibit altered neuronal morphology these findings lend support to a contributing role for kynurenine pathway activation in driving morphological changes in these disorders (Tan et al., 2012). To date, work has been described that profiles the kynurenine pathway in various brain cells (Lim et al., 2013a, Chen et al., 2011, Guillemin et al., 2007, Lim et al., 2007, Guillemin et al., 2003, Guillemin et al., 2001, Espey et al., 1997). However, most of this work has been carried out on human primary cells or rodent cell lines. Similarly, most of the work investigating the effect of kynurenine pathway activation on neuronal function and integrity, is based on the assessment of neuronal viability following treatment with individual kynurenine pathway metabolites directly (Braidy et al., 2011, Braidy et al., 2009b, Okuda et al., 1998, Okuda et al., 1996). There is a need to establish the presence of the kynurenine pathway in various rodent brain cell populations on the basis that they are the species primarily used to investigate the kynurenine pathway *in vivo*. Alongside this, greater clarity as to how kynurenine pathway activation contributes to neurodegeneration is paramount as attenuating synapse loss and/or neurite atrophy interferes in the neurodegenerative processes prior to the initiation of irreversible apoptotic or necrotic damage (Xie et al., 2013, Knight and Verkhratsky, 2010).

The experimental design utilised in this thesis provides a novel approach enabling these elements to be addressed. The initial use of a microglial cell line enabled us to establish and test our hypothesis. Following on from this, the use of isolated and mixed primary glial cells allowed for the investigation of the effect of kynurenine pathway activation in discreet glial cell populations. Furthermore, a more diverse range of measures of neuronal integrity than is currently reported in the literature, were assessed including viability, complexity and the co-localised expression of synaptic markers. In parallel the direct effect of the kynurenine pathway metabolites on neuronal integrity was determined.

The main findings of the current research demonstrated that inhibition of the kynurenine pathway protects against reactive BV-2 microglial-induced reductions in neuronal complexity. Having established this effect in a cell line, we progressed to primary cultures which demonstrated that in isolation, microglia do not share the same propensity as BV-2 microglia to reduce neuronal viability and complexity, however reactive mixed glia induced atrophy, which was attenuated by inhibition of kynurenine pathway activation. We also demonstrated for the first time the dynamic regulation that adrenoceptor subtypes have on enzymes of the kynurenine pathway in primary cortical astrocytes,

with a robust increase in TDO mRNA expression induced by β-adrenoceptor stimulation emerging as a novel regulator of the pathway in the brain. Collectively these findings highlight the important role for kynurenine pathway activation in mediating inflammation-associated neuronal atrophy and synapse loss, with the potential for modulation of the pathway by noradrenergic agents as a novel therapeutic avenue to be explored.

6.2 Activation of the kynurenine pathway in reactive BV-2 microglia induces cytotoxicity and neurite atrophy

The identification of the presence of over-activated microglia in various neurodegenerative disorders has prompted investigations as to whether they are a cause, consequence, or amplifier of the pathophysiology of such disorders [see, Lynch (2009) for review]. The nature of reactive microglia-induced neurotoxicity is also confirmed in so much as they produce pro-inflammatory cytokines, prostaglandins and ROS which are subsequently toxic to neurons (Block et al., 2007a, Block and Hong, 2005). Other potential mechanisms of reactive microglial-mediated neurotoxicity remain under-explored despite their complex and dynamic states of activation in conjunction with the wide range of other factors they are capable of producing. In this thesis we demonstrate an additional mechanism, kynurenine pathway activation, by which reactive microglia induce neurotoxicity and neuronal atrophy. A role for the kynurenine pathway in neurological disease is well established both clinically and pre-clinically (O'Farrell and Harkin, 2015), with reports implicating pathway metabolites in altering normal neurodevelopmental processes (Notarangelo and Pocivavsek, 2016). The extent to which these metabolites interfere with neuronal integrity is unestablished, with the main focus of research in this area on their effect on cellular viability as opposed to atrophic processes (Chen et al., 2011, Braidy et al., 2009b, Okuda et al., 1998). In the last few years, insights into how the predominant neurotoxic metabolite, quinolinic acid, interferes with neuronal complexity was reported *in vitro* (Pierozan et al., 2015). This emerged following the *in vivo* discovery that intrastriatal administration of this metabolite interacts with the phosphorylating system associated with cytoskeletal proteins (Pierozan et al., 2010). Such findings warrant further investigation to fully elucidate and substantiate a role for kynurenine pathway activation in contributing to neuronal atrophy.

The work carried out in this thesis provides greater clarity with regard to the extent to which this pathway can mediate microglial-associated reductions in neuronal atrophy. Furthermore, it lends support to other findings in the literature highlighting a role for pathway activation in microglial-mediated neurotoxicity (Chen et al., 2011). Targeting the pathway at various pivotal points allowed

for the identification of the most efficacious manner to ameliorate kynurenine pathway-induced neurotoxicity and atrophy. Indeed, a failure of IDO inhibition to rescue IFNγ-stimulated BV-2 CM-induced cytotoxicity highlights the important role that IDO has at a basal level of cell viability in an inflammatory setting. Inhibition of KMO with Ro 61-8048, and blockade of the NMDA receptor with MK-801, exhibited a protective effect against both IFNγ-stimulated BV-2 CM-induced neurotoxicity and atrophy implicating downstream of IDO as a more effective target.

Another novel feature of this aspect of work was the examination of a combination of kynurenine pathway metabolites on neuronal complexity. To the best of my knowledge, all other *in vitro* work investigating the neuroactive properties of these metabolites has involved the use of metabolites in isolation (Pierozan et al., 2015, Braidy et al., 2009a, Braidy et al., 2009b, Okuda et al., 1998). The advantage of the work reported in this thesis over other findings in the literature is that where we demonstrate that the effects of the metabolites alone are ineffective, in combination we report synergy.

Considering the classical mechanisms by which over-activated microglia are primarily reported to drive neurotoxicity, we assessed whether inhibiting such a mechanism is protective against IFNγ-stimulated BV-2 CM-induced atrophy. Unsurprisingly, we show that inhibition of nitric oxide production with 1400W, ROS generation with DPI chloride, and induction of other inflammatory processes with dexamethasone, is capable of attenuating CM-induced neuronal atrophy. Collectively, this emphasises the various ways by which over-activated microglia can be manipulated *in vitro* to afford protection against inflammation-driven reductions in neuronal complexity. The identification that the kynurenine pathway is an additional independent mechanism to target in this instance holds great promise therapeutically as a consequence of a large interest in developing BBB permeable compounds which discretely interfere with pathway activation (Breda et al., 2016, Parrott and O'Connor, 2015)

6.3 Activation of the kynurenine pathway in reactive primary cortical mixed glia induces neuronal atrophy and synapse loss

The use of cell lines are extremely advantageous in terms of investigating the strength of a hypothesis prior to examining it *in vitro* in primary cells or *in vivo*. Despite cell lines being a powerful tool for investigating biological mechanisms, the results they yield must be interpreted with caution based on the knowledge that they do not adequately represent primary cells or *in vivo* mechanisms. Indeed, as a consequence of being genetically modified and subjected to serial passaging, these cells are vulnerable to genetic and phenotypic variation, with genetic drift potentially leading to

heterogeneity in cultures (Kaur and Dufour, 2012). Consequently, we aimed to verify the previously described findings in BV-2 microglia by examining a role for kynurenine pathway activation in primary microglia in driving neuronal atrophy. Based on the knowledge that cell death is often an irreversible later stage of neurodegeneration (Elmore, 2007), we aimed to establish a model which exhibited atrophy in the absence of reduced viability.

Initially we demonstrated that isolated primary microglia exhibit a similar, yet diminished kynurenine pathway-related gene and metabolism profile in comparison to BV-2 microglia with a lack of induction of KMO and failure to increase 3-hydroxykynurenine concentrations in the CM following IFNγ stimulation. Consequently, the lack of effect of primary IFNγ-stimulated microglial CM on neuronal complexity was unsurprising. Due to the potential limitations of using isolated microglial cultures such as exhibiting a heightened immune activated state (Ju et al., 2015), we proposed that in a mixed glial environment an atrophic effect might be observed. In this instance a large induction of IDO was achieved in response to IFNγ stimulation, with a reduction in tryptophan and kynurenine in the IFNγ-stimulated mixed glial CM. Upon examining the effect of the IFNγ-stimulated mixed glial CM on neuronal complexity, we found a reduction in all parameters measured. Considering our limited capacity to measure downstream kynurenine pathway metabolites and to further clarify a role for kynurenine pathway activation in mediating this atrophy, we examined the potential of the IDO inhibitor, 1-MT (L), to attenuate these effects. As demonstrated with the BV-2 microglia, 1-MT (L) was capable of mitigating the IFNγ-stimulated mixed glial CM-induced atrophy.

Considering the dominant presence of astrocytes in mixed glial cultures, their role in mediating the IFNγ CM-induced reductions could not be discounted. Indeed, Lee et al. (2013) demonstrated that CM from IFNγ-stimulated human astrocytes reduced the viability of differentiated human neuroblastoma SH-SY5Y cells following treatment for between 6-72 hr. Upon further examination, they determined various factors including IL-6, proteases, NADPH oxidase, prostaglandins and glutamate that contribute to this toxicity with an encompassing blockade of these agents reducing the CM-induced toxicity by 91%. As such, we examined the effect of isolated IFNγ-stimulated astrocytic CM on neuronal complexity and found no effect. As with the isolated microglia, this lack of effect may be as a consequence of the astrocytes being in an immune activated state prior to treatment with IFNγ. In order to further ascertain the role of each cell type in mediating the effects seen in a mixed glial setting, individually knocking down the function of each cell type with compounds such as L-AAA and minocycline that specifically target astrocytes or microglia respectively would provide greater clarity on this issue.

A final component that warranted investigation was the potential for IFNγ to activate the kynurenine pathway in primary neurons, with the metabolites possibly acting in an autocrine manner to induce

atrophy. Considering that in the case of both isolated microglia and astrocytes no effect on neuronal complexity was observed, the potential for this seemed unlikely. In any case, the kynurenine pathway-related gene and metabolic profile of these cells was examined in response to IFNγ stimulation. Indeed an increase in IDO mRNA expression was observed, while no changes in metabolite concentrations in the CM were identified. Collectively, these findings point towards microglia in a mixed glial setting as the driver of IFNγ CM-associated reductions in neuronal complexity on the basis that of all the isolated cultures, only microglial cells exhibited changes in tryptophan and kynurenine pathway metabolites in the CM.

In addition to the effect of IFNγ-stimulated mixed glial CM on neuronal morphology, we examined the extent to which the expression of synaptic markers - indicative of synapse formation - were altered in mature neurons. In this instance we found a reduction in the co-localised expression of synaptic markers following treatment with IFNγ-stimulated mixed glial CM, with inhibition of IDO with 1-MT (L) preventing these reductions. These reductions were primarily as a consequence of a reduction in the number of PSD-95 puncta, which has been shown to be affected by NMDA receptor activation and oxidative stress, alongside other inflammatory cytokines (Mir et al., 2014, Ansari et al., 2008, Colledge et al., 2003). Mature neurons were required due to the delay in the formation of synapses following plating of neurons *in vitro*. The use of mature neurons adds another dimension to this investigation as they are more representative of neurons in the adult brain and subsequently allow for investigation into mechanisms of synapse loss which is a common feature of multiple neurological disorders (Bokde et al., 2009, Balu and Coyle, 2011, Duman and Aghajanian, 2012). In contrast, younger neurons are useful for the investigation of factors which may influence neurodevelopment. Altered neurodevelopment is recognised as a predisposition to the emergence of psychiatric disorders in later life (Holtzman et al., 2013). Thus, the use of neurons at both early and later stages of development *in vitro* enables examination of how factors affect morphology and functionality, with relevance to the pathogenesis of neurodevelopmental, neuropsychiatric and neurodegenerative disorders.

It is now established that glia play a role in the formation and removal of synapses, in addition to influencing synaptic plasticity through direct contact or the release of soluble factors (Chung et al., 2015, Kettenmann et al., 2013). Disrupted glial-neuronal communication may contribute to synapse dysfunction observed in CNS disorders. Indeed, transfer of either unstimulated primary rat microglia or microglial CM onto rat cortical slice cultures enhances NMDA-mediated synaptic responses (Moriguchi et al., 2003). Traditionally, astrocytes have been positively associated with synapse formation, with reactive microglia being held accountable for synapse dysfunction [see, Lynch et al. (2010) for review]. Considering the large repertoire of toxic factors released by astrocytes in

response to IFNγ (Lee et al., 2013), their role in mediating synapse loss in an inflammatory setting requires clarification and cannot be discounted.

6.4 The impact of kynurenine pathway metabolites on neuronal integrity

The development and maturation of neurons is a dynamic process which is vulnerable to disruptions in homeostasis (Gogtay et al., 2004). Excessive production of kynurenine pathway metabolites may be a mechanism by which neurodevelopment is perturbed. Indeed increased levels of kynurenic acid in rodents prenatally, achieved through administration of kynurenine, decreases dendritic spine formation (Pershing et al., 2015), while exogenous administration of kynurenine to rodents during adolescence and adulthood altered contextual memory, spatial working memory, and cognitive flexibility in adults (Pershing et al., 2015, Pocivavsek et al., 2014, Alexander et al., 2013, Pocivavsek et al., 2012). Additionally, inhibition of KMO with Ro 61-8048 in pregnant rodents in a late gestation period increased the levels of kynurenic acid in the embryo, with an increase in NMDA receptor subunits and PSD-95 by adolescence (Forrest et al., 2013a). Additionally, adults exhibit changes in neuronal excitability and reduced dendritic complexity (Khalil et al., 2014a, Pisar et al., 2014, Forrest et al., 2013a, Forrest et al., 2013b). Overall this thesis demonstrates a negative effect of 3-hydroxykynurenine, 3-hydroxyanthranillic acid, quinolinic acid, and kynurenic acid on neuronal complexity, with no effect at any dose tested on the viability of neurons in early or later stages of development. This is contrary to findings reported in the literature whereby the previously listed metabolites except kynurenic acid increased the cytotoxicity of human neurons and astrocytes as well as rat neurons (Braidy et al., 2009b, Okuda et al., 1998). Similar to our findings, Pierozan et al. (2015) reported no effect of quinolinic acid on the viability of rat neurons at doses which were reported by Braidy et al. (2009b) to cause toxicity. Inter-species differences, variations in viability assays and the age of neurons at which treatment occurs, may be responsible for these discrepancies. In fact Okuda et al. (1998) treated primary rat neurons at DIV 2 and examined viability using nuclear stains, Pierozan et al. (2015) treated primary rat neurons at DIV 8 and examined viability with Annexin V-FITC labelling, LDH and MTT assays, while the primary rat neurons in this thesis were treated at DIV 3 or 18-21 and viability was assessed using the Alamar Blue assay.

Surprisingly, very little work has been done investigating the effect of kynurenine pathway metabolites on complexity or synaptogenesis. Pierozan et al. (2015) have recently demonstrated the ability of quinolinic acid to interact with the neuronal cytoskeleton through hyperphosphorylation of neurofilaments resulting in altered neurite: neuron ratio and reduced neurite length in the absence of cell death. Considering the variety of metabolites produced as a consequence of kynurenine

pathway activation, the combined effect of metabolites was of interest. Again, the various combinations of metabolites had no effect on neuronal viability at either stage of development, with the complexity of DIV 3 neurons being reduced by the combined presence of 3-hydroxykynurenine, 3-hydroxyanthranillic acid and quinolinic acid. In contrast, the DIV 18-21 neurons exhibited marked reductions in the co-localised expression of synaptic markers in the presence of all combinations of metabolites demonstrating an increased sensitivity of neurons to these metabolites with age. This reduction in the co-localised expression of synaptic markers, was primarily driven through a reduction in the post-synaptic marker, PSD-95. As previously discussed, Forrest et al. (2013a) reported that prenatal inhibition of KMO, increases the levels of PSD-95 in the offspring at adolescence indicating a potential mechanism by which kynurenine pathway activation may disrupt synaptic connections.

Having explored the effect of kynurenine pathway metabolites on all three measures of neuronal integrity both in isolation of each other and in combination, we aimed to investigate another potential candidate, glutamate - produced and released by reactive microglia and often referred to as a co-factor of quinolinic acid (Dantzer and Walker, 2014b). Previously our lab has reported on the role of glutamate and NMDA receptor activation in driving neuronal atrophy, identifying that inhibition downstream of the neuronal NMDA receptor is a potential mechanism of attenuating neurite shrinkage in the presence of excessive glutamatergic signalling (Doucet et al., 2015). Another potential mechanism of dissipating over-activated NMDA receptor-mediated reductions in neuronal complexity, could be through the increased production and release of kynurenic acid which competes with both glutamate and quinolinic acid at the NMDA receptor. Further to the work carried out by Doucet et al. (2015) we identified a role for glutamate in mediating synapse loss in mature neurons while having no effect on viability. In adittion to reducing the co-localised expression of synaptic markers, glutamate targetted the pre- and post-synaptic terminals, reducing both synaptophysin and PSD-95. Our laboratory has previously identified other agents which interfere with both synaptic markers, $A\beta_{1\text{-}42}$ and TNFα were found to reduce the co-localised expression of synaptic markers through reduced expression of both synaptophysin and PSD-95 [unpublished data O'Neill (2015)]. Similar to findings reported in the literature, more developed neurons exhibited a greater sensitivity to glutamate toxicity. Gupta et al. (2013) demonstrated that neurons cultured from human embryonic stem cells exhibit a gradual increase in responsiveness to glutamate-induced Ca^{2+} influx which was attenuated by NMDA receptor antagonists. Having established the atrophic effects of glutamate on both immature and mature neurons, the potential for kynurenic acid to protect against these deleterious effects was examined. In all instances of reduced complexity kynurenic acid was protective in spite of it being atrophic at such concentrations in isolation. Regarding the glutamate-induced synapse loss, a no-effect dose of kynurenic acid in isolation and a

dose at which kynurenic acid rescued glutamate-induced reductions in complexity failed to rescue the synapse loss. In this instance, a higher concentration of KYNA may be effective.

In the context of kynurenine pathway activation, similar findings were observed with kynurenic acid protecting against the metabolite combination-induced reductions in neuronal complexity and synapse loss. Such findings highlight that blockade of the NMDA receptor is a promising target in disease circumstances where these metabolites or glutamatergic signalling is over-impacting on this receptor. Furthermore, the identification that an endogenous metabolite can compete with excitotoxic levels of glutamate and physiological levels of kynurenine pathway metabolites to attenuate neuronal atrophy encourages manipulation of the neuroprotective arm of this pathway in astrocytes as a novel neuroprotective strategy.

6.5 A role for the noradrenergic system in regulating the kynurenine pathway in primary cortical glial and neuronal cells

Upon identification that kynurenic acid is capable of protecting against neuronal atrophy induced by soluble factors released by reactive glia, the ability to manipulate the astrocytic arm of the kynurenine pathway responsible for the production of this metabolite was examined *in vitro*. Having established that IFNγ has a negative effect on the mRNA expression of KAT II in both microglia and mixed glia, an independent mechanism of stimulating this arm of the pathway warranted investigation. Recent findings by Luchowska et al. (2009) demonstrated the ability of adrenaline and selective β_1- or β_2-adrenoceptor agonists to increase kynurenic acid production in primary rat mixed glial cultures and rat brain cortical slices in a PKA/cAMP-dependent manner. An independent mechanism of KAT induction and kynurenic acid production was reported to be mediated by exercise-induced activation of the PGC-1α1-PPARα/δ axis in the skeletal muscle of mice, with an increase in the mRNA expression of KAT I-IV in percutaneous biopsied skeletal muscle of healthy human volunteers subjected to exercise training (Agudelo et al., 2014). A potential mechanism linking both pathways of kynurenic acid production is through β-adrenoceptor activation and binding of transcription factors to the cAMP response element in the PGC-1α promoter (Kim et al., 2013b). Indeed the β_2-adrenoceptor agonist clenbuterol, increased the mRNA expression of PGC-1α in the skeletal muscle of mice which was attenuated by non-selective blockade of the β-adrenoceptors with propranolol (Miura et al., 2008, Miura et al., 2007). Furthermore, exercise-induced increases in PGC-1α gene expression in the skeletal muscle of mice were prevented by pre-treatment with either propranolol or the β_2-adrenoceptor antagonist ICI-118, 551, with clenbuterol having no effect on PGC-1α mRNA expression in $\beta_{1,2,3}$-adrenoceptor knockout mice (Miura et al., 2008, Miura et al., 2007). Collectively, this provides strong evidence to suggest a role for noradrenaline as regulator of

the neuroprotective arm of the pathway. To fully elucidate the effect of the noradrenergic system on this pathway in astrocytes we investigated the influence that all adrenoceptors individualy and collectively have on the mRNA expression of kynurenine pathway enzymes, with a focus on the enzymes implicated in driving the neuroprotective arm.

Initially we demonstrated that non-selective stimulation of the adrenoceptors with noradrenaline induced TDO, while reducing KAT II, IDO, and KMO. To a certain extent, this gene expression profile is in line with the anti-inflammatory nature of noradrenaline, however an induction in TDO and reduction in KAT II mRNA expression was unexpected. Considering previous reports on adrenoceptor-mediated increases in KAT activity in glial cultures (Luchowska et al., 2009), we hypothesised that noradrenaline would induce KAT II mRNA expression. The effect of noradrenaline on TDO expression has not previously been reported, however, considering stress-related glucocorticoids are the predominant factor which induce TDO expression, it is of interest that noradrenaline is capable of inducing it independently. Upon further investigation into the divergent effects that adrenoceptors have on the mRNA expression of these enzymes we identified the α_1-adrenoceptor as a negative regulator of both TDO and KAT II mRNA expression. Moreover β-adrenoceptors were found to be inducers of the mRNA expression of both enzymes as a consequence of cAMP signalling (**figure 6.1**). Additionally, stimulation of the β_2-adrenoceptor resulted in reduced concentrations of 3-hydroxykynurenine in the astrocytic CM.

This β-adrenoceptor-mediated robust induction of TDO is a relevant and novel finding as for the most part the onus of kynurenine pathway activation lies with stress-related corticosterone-mediated TDO induction (Gibney et al., 2014, Walker et al., 2009). The potential for stress-induced increases in circulating levels of noradrenaline to activate the kynurenine pathway is an important alternative to glucocorticoid signalling due to the strong negative feedback inhibition associated with steroid signalling. Although this feedback inhibition is reported to be disrupted in several psychiatric disorders (Cattaneo and Riva, 2015), the independent or adjunctive role of noradrenaline in kynurenine pathway activation in a stressful setting warrants investigation. Although centrally we propose it to be predominantly involved in driving the astrocytic neuroprotective arm of the pathway, peripherally this compartmentalisation does not occur and its action may subsequently be involved in the generation of the neurotoxic metabolite precursor, kynurenine.

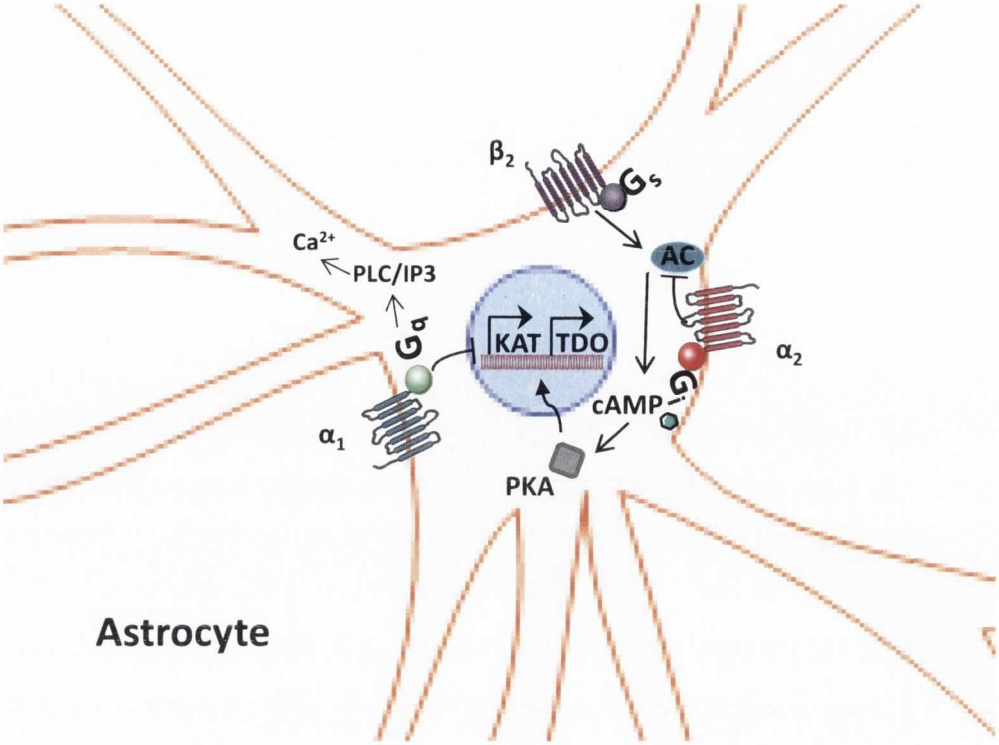

Figure 6.1: Differential effects of adrenoceptor subtypes on KAT II and TDO gene induction
Stimulation of the α_1-adrenoceptor and β_2-adrenoceptor negatively and positively regulate KAT II and TDO gene expression respectively, while α_2-adrenoceptor activation indirectly dampens down this expression through its opposing action on adenylate cyclase activation.

Having established a method of activation of the neuroprotective arm of the kynurenine pathway, we reverted back to a mixed glial culture to examine the interaction between an inflammatory and an anti-inflammatory agent on kynurenine pathway gene expression and metabolic profiles of these cells. In the presence of both IFNγ and the β_2-adrenoceptor agonist, formoterol, the extensive increase in TDO mRNA expression was maintained, the induction in KAT II was lost, while a partial reduction in IFNγ-driven increases in IDO mRNA expression was observed. Additionally, the levels of the neurotoxic metabolite, 3-hydroxykynurenine in the CM were reduced, indicating a shift towards metabolism along the neuroprotective arm of the pathway. The potential for formoterol to prevent the previously reported IFNγ-stimulated mixed glial CM-induced reductions in neuronal atrophy was deemed worthy of investigating to examine if manipulation of this pathway protects against reactive glial-associated neuronal insults. Indeed, we demonstrated an attenuation of IFNγ CM-induced reductions in both neuronal complexity and synapse loss following simultaneous glial β_2-adrenoceptor stimulation; however upon inhibiting TDO this effect was maintained. This may potentially be as a consequence of attenuation of astrocytic TDO-mediated kynurenine production thereby reducing the presence of the precursor from which microglial IDO-driven neurotoxic metabolites can be produced. Furthermore the protective nature of formoterol-stimulated astrocytic

CM against kynurenine pathway metabolite-induced synapse loss was reported, with initial reductions in complexity not being achieved by this combination of neurotoxic metabolites in the presence of unstimulated astrocytic CM. Our lab has previously demonstrated the trophic nature of unstimulated astrocytic CM which may account for this lack of reduction in complexity. Moreover, noradrenaline-stimulated astrocytic CM has previously been shown to be neurotrophic as a consequence of β_1-adrenoceptor-related induction of growth factors and neurotrophins (Day et al., 2014). In this instance, inhibition of TDO was not sufficient to deplete the CM of its protective effect. TDO-mediated production and release of kynurenic acid from astrocytes may be only one of multiple β_2-adrenoceptor-driven trophic components. Here we demonstrate that the induction of TDO mRNA expression is not restricted to the action of corticosteroids produced by stress-related HPA axis activation but additionally by factors produced by activation of the SAM axis, an independent axis of the stress response. As such, TDO-driven kynurenic acid as a beneficial component of astrocytic CM, with the propensity to impart neuroprotection in excitotoxic and inflammatory circumstances cannot be discounted.

IFNγ-mediated kynurenine pathway activation in mixed glia induces neuronal atrophy and synapse loss

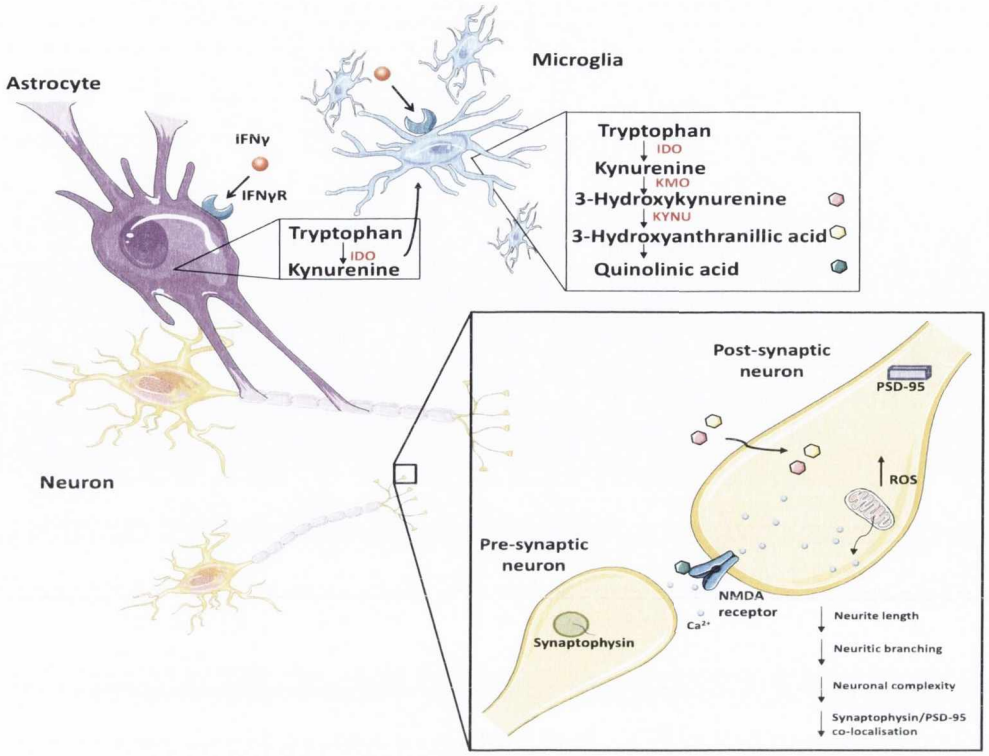

β_2-adrenoceptor stimulation protects against IFNγ-stimulated mixed glial CM-induced neuronal atrophy and synapse loss

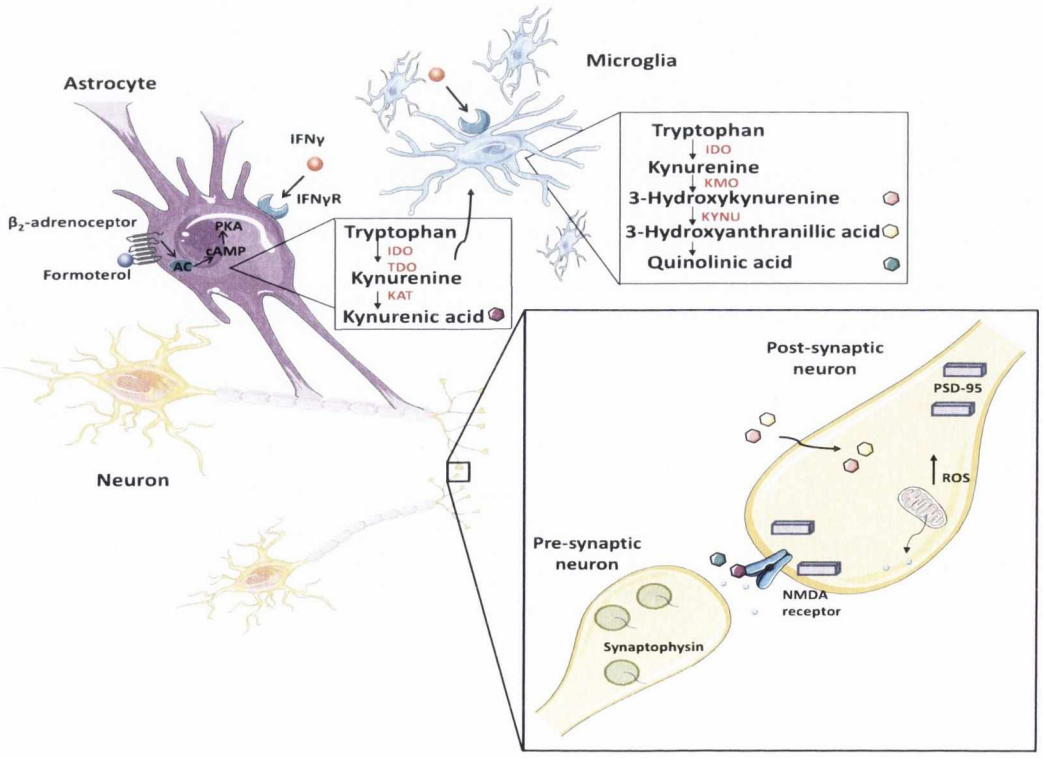

Figure 6.2: The combined effect of simultaneous activation of the neurotoxic and neuroprotective arms of the kynurenine pathway on neuronal complexity and the co-localisation of synaptic markers

Upper panel: Under inflammatory conditions such as in the presence of IFNγ, stimulation of microglia results in activation of the neurotoxic arm of the kynurenine pathway and the release of 3-hydroxykynurenine, 3-hydroxyanthranillic acid, and quinolinic acid resulting in neuronal NMDA receptor over-activation, increased levels of intracellular Ca^{2+} and oxidative stress. IFNγ stimulation of astrocytes leads to the production and release of surplus kynurenine which can feed into the microglial neurotoxic arm of the pathway. The action of the 3-hydroxykynurenine, 3-hydroxyanthranillic acid, and quinolinic acid on the neuron reduces neurite outgrowth and complexity alongside reduced co-localised expression of synaptic markers. ***Lower panel:*** Simultaneous activation of the neuroprotective arm of the kynurenine pathway through stimulation of the astrocytic β_2-adrenoceptor results in TDO and KAT II induction and the production and release of the NMDA receptor antagonist, kynurenic acid. Kynurenic acid has the potential to ameliorate the reactive mixed glial-associated reductions in atrophy through its inhibitory action at the NMDA receptor.

6.6 Clinical relevance

Considering the consistent findings of dysregulated kynurenine pathway activation in both neurodegenerative and neuropsychiatric disorders, manipulation of this pathway represents a clinically relevant avenue of investigation. In light of the implication of this pathway in multiple CNS disorders, research is being carried out in order to identify selective BBB permeable agents with the hope that they will be in addition to useful research tools, potentially useful in a clinical setting (Yu et al., 2016, Dounay et al., 2015b, Rohrig et al., 2015). This thesis demonstrates the potential for pathway activation and downstream metabolites to contribute to neuronal atrophy and synapse loss in the absence of neuronal loss. The potential for specific kynurenine pathway metabolites to interfere with normal neuronal functioning through reversible atrophic mechanisms is now apparent, with the ability to attenuate these effects achieved through manipulation of this pathway with clinically relevant compounds. We have identified β-agonists, specifically formoterol, which through the activation of the neuroprotective arm of the kynurenine pathway is capable of counteracting the effects of activation of the neurotoxic arm. β-agonists are currently used in the treatment of asthma (Ställberg et al., 2015) suggesting that pathway manipulation as opposed to inhibition may be a more achievable mechanism of restoring the dysregulated kynurenine pathway to a point at which the metabolites can carry out their physiological functions in the absence of toxicity.

6.7 Limitations and future directions

Cell culture systems are commonly used for the investigation of biological mechanisms at a cellular and molecular level. These *in vitro* systems are extremely informative and fundamental to pre-clinical research, however potential limitations arise as consequence of a possible failure to respond to stimuli in an identical manner to that observed *in vivo*. Nevertheless, as a consequence of the ability to discreetly manipulate cells, *in vitro* research, particularly that which is described in this thesis, enables the identification of potential candidates which may contribute to disrupted homeostasis and subsequent disease. To more fully understand a role for kynurenine pathway activation in neurodegenerative processes, *in vivo* work should be carried out in conjunction to verify *in vitro* findings. Indeed, work carried out by our lab has demonstrated an increase in the mRNA expression of KAT II in the LPS rodent model of Parkinson's disease following additional treatment with formoterol. In addition to this, formoterol protected against the LPS-induced dopaminergic cell death in the nigra [unpublished data Yssel (2015)]. This finding hints at the potential of formoterol to shift kynurenine pathway activation along the neuroprotective arm in the presence of an inflammatory stimulus which may afford protection *in vivo*. Other avenues of investigation include identifying the potential of formoterol to protect against inflammation/stress-induced kynurenine pathway activation which have previously been reported (Gibney et al., 2014, Gibney et al., 2013, O'Connor et al., 2009).

The benefit of the Sholl analytical technique used for analysis of neuronal outgrowth and complexity in this thesis, is the comprehensive measurement of different parameters of neuritic morphology. Limitations of this technique include the requirement of neurons to be in isolation of each other which is not fully representative of an *in vivo* system in addition to a failure to discriminate between axons and dendrites. Examining the effect of kynurenine pathway activation on neuronal complexity *in vivo* by Fluoro-Jade staining would identify degenerating neurons (Schmued et al., 1997), while other methods such as Golgi-Cox staining or the use of transgenic mice selectively expressing yellow fluorescent protein in neurons could be used for the examination of dendritic spines and the visualisation of individual neurons in brain slices respectively (Risher et al., 2014, Feng et al., 2000). Moreover, advances in technology and software such as three-dimensional imaging now allows for the systematic identification of neurons possessing rich morphological detail along with dense neurite arborisation (Ross et al., 2015).

Furthermore, the assay method developed by Ippolito and Eroglu (2010) and used in this thesis for the quantification of synapses could also be applied *in vivo*. However, this method is an indirect measure and does not necessarily identify the formation of a functional synapse. The identification of synapses would be confirmed by the use of an electron microscope for the identification of synaptic

vesicles and PSDs. Additionally, electrophysiology would provide confirmation that structural observations are correlated to functionality (Kelsch et al., 2010).

Another avenue worthy of investigation is identifying potential mechanisms by which kynurenine pathway metabolites alter neuronal complexity and synaptogenesis. To date, limited work has examined if the metabolites directly interfere with the cytoskeleton, with quinolinic acid having been reported to induce hyprerphosphorylation of neurofilament subunits (Pierozan et al., 2015). It would be of interest to examine the effect of these metabolites on intracellular signalling pathways involved in regulating outgrowth and synapse formation. This could be achieved by investigating the gene and protein expression of enzymes involved outgrowth signalling cascades, alongside specific cytoskeletal and synaptic proteins using quantitative PCR and Western Blot analysis respectively. Considering the oxidative nature of these metabolites, their effect on the oxidative state and functional metabolism of the neuron could be examined using the 'Seahorse' technique. Collectively, these findings would provide greater insight into the mechanism(s) by which kynurenine pathway activation can disrupt neuronal intgrity.

Overall additional complimentary *in vitro* techniques discussed previously would further verify a role for the kynurenine pathway in inducing neurite atrophy and synapse loss. In conjunction, clarification of a role for activation of the neuroprotective arm of the kynurenine pathway in mediating basal levels of astrocytic CM-induced neuroprotection is of interest. Considering our laboratory has previously identified the trophic nature of unstimulated astrocytic CM [unpublished data O'Toole (2015)], examining if inhibition of IDO and TDO alone and in combination attenuate this trophic effect is intriguing. Considering that TDO inhibition is not successful at attenuating formoterol-stimulated mixed glial CM protection against IFNγ-stimulated mixed glial atrophy, the contribution of formoterol-induced IDO driven pathway activation in this instance is worthwhile investigating. As previously mentioned, the effect of simultaneously inhibiting both rate-limiting enzymes prior to formoterol stimulation of mixed glia may result in a lack of neuronal protection against the IFNγ-stimulated mixed glial CM. It is of interest to note that although TDO inhibition did not attenuate the formoterol-stimulated mixed glial CM protection against IFNγ-stimulated mixed glial CM-induced atrophy, TDO inhibition did protect against IFNγ-stimulated mixed glial CM-induced atropy and synapse loss. This may be as a consequence of reduced basal TDO-mediated kynurenine production in addition to IDO-mediated kynurenine production which can feed into the microglial kynurenine pathway. Indeed, this may explain why an atrophic effect is achieved with IFNγ-stimulated mixed glial CM but not with isolated microglial or astrocytic CM. This interaction between both glial cell types may also account for why TDO inhibition did protect against IFNγ-stimulated mixed glial CM-induced atropy and synapse loss due to potentially reduced levels of astrocyte-derived kynurenine available as a substrate for microglial kynurenine pathway metabolism. Verification of the need for the

presence of astrocytes in this instance could be achieved by inhibiting astrocytic function with the astrocytic toxin, L-AAA and subsequently examining if IFNγ-stimulated mixed glial CM loses its atrophic properties. Subsequent supplementation of IFNγ-stimulated mixed glia with kynurenine may then restore this atrophic property. Consequently investigating a role for TDO and subsequently kynurenic acid in protecting against the atrophy induced as a consequence of activation of the neurotoxic arm, could be achieved using isolated astrocytic cultures treated with formoterol with or without prior treatment with the TDO inhibitor, 680C91. The astrocytic CM would subsequently be placed on neuronal cultures followed by the addition of IFNγ-stimulated mixed glial CM. This would allow for inhibition of the neuroprotective arm of the kynurenine pathway without interfering with the contributing role that astrocytes may have in mediating the IFNγ-stimulated mixed glial CM-induced atrophy. The functional relevance of this could subsequently be assessed *in vivo* using the aforementioned techniques, with the aim of affirming potential compounds for therapeutic consideration. For instance, assessment of neuronal complexity in cortical brain slices from rats subjected to exogenous administration of IFNγ, or neurotoxic kynurenine pathway metabolites would determine the atrophic capacity of this pathway *in vivo*. Moreover, examination of the potential of adrenoceptor agonists, such as noradrenaline, or more specifically, formoterol, to attenuate atrophy would be stimulating. Supplementary to this, the propensity for such compounds to ameliorate physiological and behavioural disturbances in animal models which display altered kynurenine pathway activation would be compelling.

Appendix

Publications

O'FARRELL, K. & HARKIN, A. 2015. Stress-related regulation of the kynurenine pathway: Relevance to neuropsychiatric and degenerative disorders. *Neuropharmacology*.

Presentations

O'FARRELL, K., LIM, E., GILLES, G., HARKIN, A. A role for glial-associated kynurenine pathway activation in modulating neuronal outgrowth and complexity. *Poster presentation at the European College of Neuropsychopharmacology (ECNP) Congress, Amsterdam, The Netherlands, August/September 2015.*

O'FARRELL, K., O'NEILL, E., O'TOOLE, E., Lim, E., Gilles, G., HARKIN, A. Inhibitors of the kynurenine pathway protect against microglial-induced neuronal atrophy. *Poster presentation at the International College of Neuropsychopharmacology (CINP), Trinity College Dublin, June 2015.*

O'FARRELL, K., LIM, E., GILLES, G., HARKIN, A. Inflammation-induced activation of the kynurenine pathway leads to reductions in neuronal outgrowth and complexity. *Poster presentation at the European College of Neuropsychopharmacology (ECNP) Workshop for Young Scientists, Nice, France, March 2015* ***(Poster prize)***.

O'FARRELL, K., FAGAN, EM., CONNOR, TJ., HARKIN, A. IFNγ reduces neuronal viability via kynurenine pathway activation in BV-2 microglia. *Poster presentation at the All Ireland Schools of Pharmacy Conference, Trinity College Dublin, April 2014.*

Supplementary figures

Table S1: Average control **ΔΔCt values** for the gene expression of kynurenine pathway enzymes in BV-2 microglia and primary glia and neurons.

Average control *ΔΔCt values	**BV-2 microglia**	**Primary microglia**	**Primary astrocytes**	**Primary mixed glia**	**Primary neurons**
IDO	22.49497954	31.59297	30.14087	30.81521	27.65011
TDO	25.28640429	31.25725	30.01268	30.86435	26.85575
KMO	12.36031834	11.01162	15.03194	30.77812	16.28376
KYNU	18.77923139	25.69114	19.49269	30.15975	22.30352
KAT II	28.9089152	11.27086	9.12251	14.05229	11.35916

* ΔΔCt= Cycle difference corrected for endogenous control

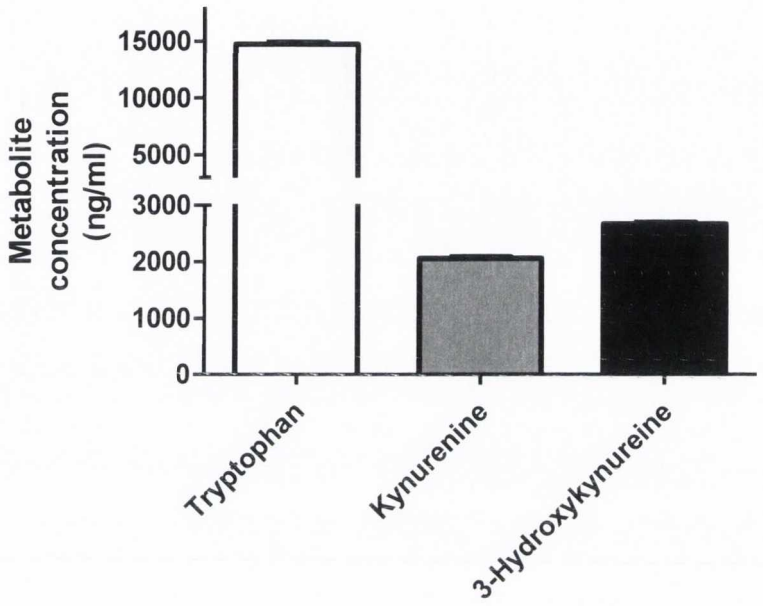

Figure S1: Baseline concentrations of tryptophan, kynurenine, and 3-hydroxykynurenine in cell-free cNBM

cNBM incubated for 24 hr before being harvested for analysis of the concentrations of tryptophan and kynurenine pathway metabolites. Data expressed as mean ± SEM (n= 6).

S2 Effect of 1-MT (L) on the basal concentrations of tryptophan, kynurenine, 3-hydroxykynurenine and the kynurenine/tryptophan ratio in the CM of primary cortical mixed glia

Treatment of primary cortical mixed glia with 1-MT (L) increased the concentration of **tryptophan** (t= 8.394, P<0.0001 d.f.= 22) (a), decreased the concentrations of **3-hydroxykynurenine** (t= 3.814, P= 0.0009, d.f.= 22) (c) and the **kynurenine over tryptophan ratio** (t= 15.55, P<0.0001, d.f.= 21) but had no effect on the concentrations of **kynurenine** (t= 1.600, P= 0.124, d.f.= 22) (b), in the CM of primary mixed glia (**figure S2**).

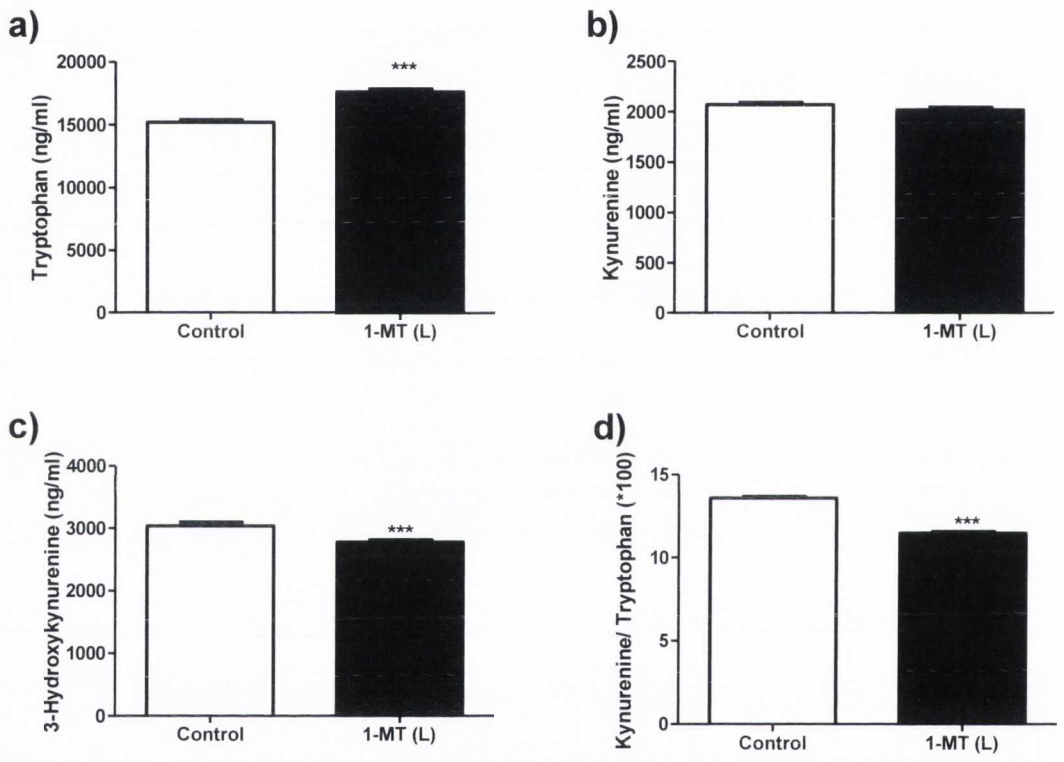

Figure S2: Effect of 1-MT (L) on the basal concentrations of tryptophan, kynurenine, 3-hydroxykynurenine and the kynurenine/tryptophan ratio in the CM of primary cortical mixed glia
Primary cortical mixed glial (DIV 12-13) were treated with vehicle or 1-MT (L) (0.5 mM) for 24 hr. CM was harvested for analysis of the concentrations of (a) tryptophan, (b) kynurenine, (c) 3-hydroxykynurenine, and (d) kynurenine over tryptophan ratio. Data expressed as mean ± SEM (n= 12, from 2 independent experiments). ***P<0.001, vs. control (Student's *t*-test).

S3 Concentration related effects of formoterol on neuronal viability and complexity

One-way ANOVA showed an effect of formoterol [$F_{(2, 91)} = 5.008$, $P = 0.0087$] on neuronal viability. *Post hoc* analysis revealed significant reductions in neuronal viability with treatment with formoterol 1 μM ($P<0.05$) compared to control (a). One-way ANOVA showed no effect of formoterol on the number of neuritic branches [$F_{(2, 31)} = 1.432$, $P = 0.2552$] (b), neurite length [$F_{(2, 31)} = 1.528$, $P = 2.339$] (c), nor on the number of primary neurites [$F_{(2, 31)} = 1.445$, $P = 0.2521$] (d). Two-way repeated measures ANOVA showed an effect of distance [$F_{(25, 75)} = 459.4$, $P<0.0001$], but no effect of formoterol [$F_{(50, 725)} = 0.7319$, $P = 0.9164$], nor a formoterol x distance interaction effect [$F_{(2, 725)} = 1.528$, $P = 0.2339$] on the number of branches at specific distances from the soma (e) (**figure S3**).

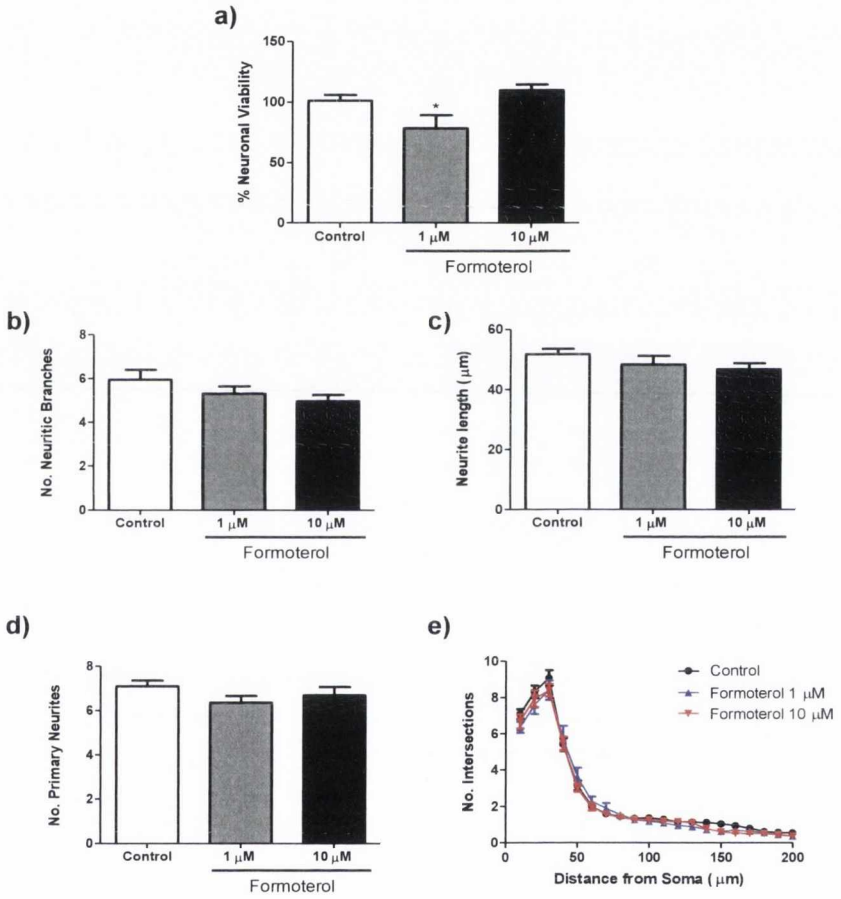

Figure S3: Concentration related effects of formoterol on neuronal viability and complexity

Primary cortical neurons (DIV 3) were treated with formoterol (1, 10 μM) for 24 hr. Neuronal viability was assessed using the alamarBlue® cell proliferation assay (a). Sholl analysis was performed on neurons to examine the number of neuritic branches (b), neurite length (c), the number of primary neurites (d) or the number of branches at specific distances from the soma (e). Data expressed as mean ± SEM (n= 8-16 wells/coverslips from 2 independent experiments). *P<0.05, ***P<0.001, vs. control [One-way ANOVA followed by Newman-Keuls *post hoc* test (a-d), two-way repeated measures ANOVA followed by Bonferroni post hoc test (e)].

S4 Effect of formoterol on neuronal viability and the expression of synaptic markers in mature neurons

Direct treatment with formoterol had no effect on **neuronal viability** of mature neurons (t= 0.4209, P= 0.6795, d.f. = 16) (a).

Direct treatment with formoterol had no effect on the **co-localised expression of synaptic markers** (t= 0.2999, P= 0.7649, d.f. = 95) (b). CM from IFNγ-stimulated primary mixed glia had no effect on the number of **synaptophysin puncta** (t= 1.149, P= 0.2535, d.f. = 99) (c). CM from IFNγ-stimulated primary mixed glia reduced the number of **PSD-95 puncta** (t= 0.2934, P= 0.7699, d.f. = 99) (d) (**figure S4**).

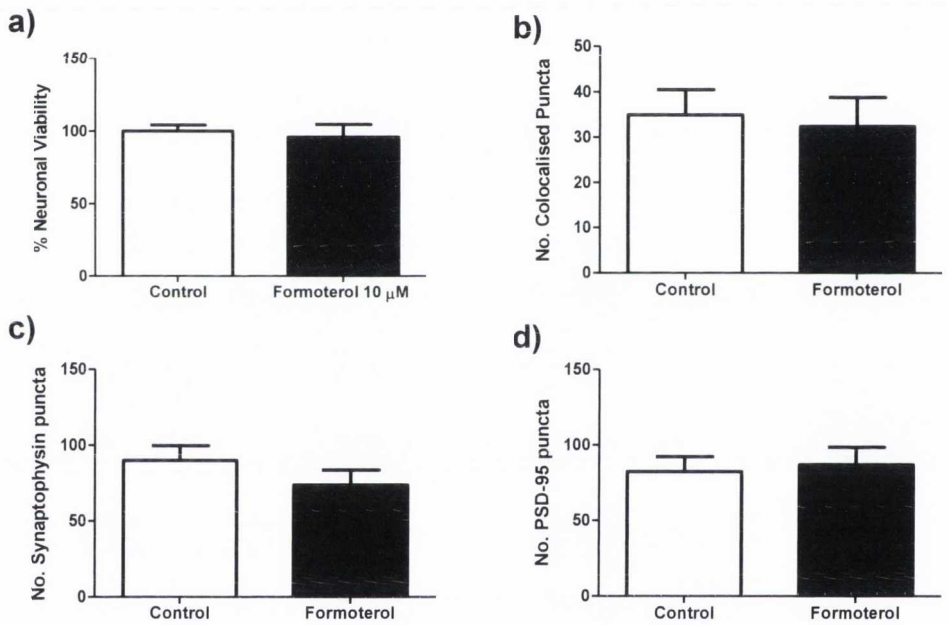

Figure S4: Effect of formoterol on neuronal viability and the expression of synaptic markers in mature neurons

Primary cortical neurons (DIV 18-21) were treated with formoterol (10 μM) for 24 hr. Neuronal viability of one set of neurons was assessed using the alamarBlue® cell proliferation assay (a). Data expressed as mean ± SEM (n= 9 wells from 2 independent experiments). Another set of neurons were examined to determine the co-localised expression of pre- and post-synaptic markers synaptophysin and PSD-95 (b), and the number of synaptophysin puncta (c), and PSD-95 puncta (d) in isolation using ImageJ software. Data expressed as mean ± SEM (n= 44-53 neurons from 3 independent experiments) (Student's *t* test).

References

AARUM, J., SANDBERG, K., HAEBERLEIN, S. L. & PERSSON, M. A. 2003. Migration and differentiation of neural precursor cells can be directed by microglia. *Proc Natl Acad Sci U S A,* 100**,** 15983-8.

ABBOTT, N. J., RONNBACK, L. & HANSSON, E. 2006. Astrocyte-endothelial interactions at the blood-brain barrier. *Nat Rev Neurosci,* 7**,** 41-53.

AGUDELO, L. Z., FEMENIA, T., ORHAN, F., PORSMYR-PALMERTZ, M., GOINY, M., MARTINEZ-REDONDO, V., CORREIA, J. C., IZADI, M., BHAT, M., SCHUPPE-KOISTINEN, I., PETTERSSON, A. T., FERREIRA, D. M., KROOK, A., BARRES, R., ZIERATH, J. R., ERHARDT, S., LINDSKOG, M. & RUAS, J. L. 2014. Skeletal muscle PGC-1alpha1 modulates kynurenine metabolism and mediates resilience to stress-induced depression. *Cell,* 159**,** 33-45.

AHLES, A. & ENGELHARDT, S. 2014. Polymorphic variants of adrenoceptors: pharmacology, physiology, and role in disease. *Pharmacol Rev,* 66**,** 598-637.

AHMARI, S. E., BUCHANAN, J. & SMITH, S. J. 2000. Assembly of presynaptic active zones from cytoplasmic transport packets. *Nat Neurosci,* 3**,** 445-51.

ALBERATI-GIANI, D., CESURA, A. M., BROGER, C., WARREN, W. D., RÖVER, S. & MALHERBE, P. 1997. Cloning and functional expression of human kynurenine 3-monooxygenase. *FEBS Letters,* 410**,** 407-412.

ALBERATI-GIANI, D., RICCIARDI-CASTAGNOLI, P., KOHLER, C. & CESURA, A. M. 1996. Regulation of the kynurenine metabolic pathway by interferon-gamma in murine cloned macrophages and microglial cells. *J Neurochem,* 66**,** 996-1004.

ALEXANDER, K. S., POCIVAVSEK, A., WU, H. Q., PERSHING, M. L., SCHWARCZ, R. & BRUNO, J. P. 2013. Early developmental elevations of brain kynurenic acid impair cognitive flexibility in adults: reversal with galantamine. *Neuroscience,* 238**,** 19-28.

ALOISI, F. 2001. Immune function of microglia. *Glia,* 36**,** 165-179.

AMARAL, M., LEVY, C., HEYES, D. J., LAFITE, P., OUTEIRO, T. F., GIORGINI, F., LEYS, D. & SCRUTTON, N. S. 2013. Structural basis of kynurenine 3-monooxygenase inhibition. *Nature,* 496**,** 382-5.

AMIRKHANI, A., HELDIN, E., MARKIDES, K. E. & BERGQUIST, J. 2002. Quantitation of tryptophan, kynurenine and kynurenic acid in human plasma by capillary liquid chromatography-electrospray ionization tandem mass spectrometry. *J Chromatogr B Analyt Technol Biomed Life Sci,* 780**,** 381-7.

ANDERSON, G. & RODRIGUEZ, M. 2011. Multiple sclerosis, seizures, and antiepileptics: role of IL-18, IDO, and melatonin. *Eur J Neurol,* 18**,** 680-5.

ANDERSON, G. P. 1993. Formoterol: pharmacology, molecular basis of agonism, and mechanism of long duration of a highly potent and selective beta 2-adrenoceptor agonist bronchodilator. *Life Sci,* 52**,** 2145-60.

ANDERSON, G. P. 2000. Interactions between corticosteroids and beta-adrenergic agonists in asthma disease induction, progression, and exacerbation. *Am J Respir Crit Care Med,* 161**,** S188-96.

ANSARI, M. A., ROBERTS, K. N. & SCHEFF, S. W. 2008. Oxidative stress and modification of synaptic proteins in hippocampus after traumatic brain injury. *Free radical biology & medicine,* 45**,** 443-452.

AOKI, C. 1992. Beta-adrenergic receptors: astrocytic localization in the adult visual cortex and their relation to catecholamine axon terminals as revealed by electron microscopic immunocytochemistry. *J Neurosci,* 12**,** 781-92.

ARAQUE, A., PARPURA, V., SANZGIRI, R. P. & HAYDON, P. G. 1999. Tripartite synapses: glia, the unacknowledged partner. *Trends Neurosci,* 22**,** 208-15.

ARDITE, E., PANES, J., MIRANDA, M., SALAS, A., ELIZALDE, J. I., SANS, M., ARCE, Y., BORDAS, J. M., FERNANDEZ-CHECA, J. C. & PIQUE, J. M. 1998. Effects of steroid treatment on activation of nuclear factor kappaB in patients with inflammatory bowel disease. *Br J Pharmacol,* 124**,** 431-3.

BACH, E. A., AGUET, M. & SCHREIBER, R. D. 1997. The IFN gamma receptor: a paradigm for cytokine receptor signaling. *Annu Rev Immunol,* 15**,** 563-91.

BAHL, A. K., CLAYTON, N. M., COATES, J., MARTIN, D. P., OAKLEY, I. G., STRONG, P. & TREVETHICK, M. A. 1996. Comparison of the profiles of agonists as stimulants of the beta 3-adrenoceptor in vitro with their gastroprotective effects in the conscious rat. *Br J Pharmacol,* 117**,** 580-586.

BAKER, J. G. 2005. The selectivity of β-adrenoceptor antagonists at the human β1, β2 and β3 adrenoceptors. *British Journal of Pharmacology,* 144, 317-322.

BAKER, K. G., TORK, I., HORNUNG, J. P. & HALASZ, P. 1989. The human locus coeruleus complex: an immunohistochemical and three dimensional reconstruction study. *Exp Brain Res,* 77, 257-70.

BAL-PRICE, A., MONEER, Z. & BROWN, G. C. 2002. Nitric oxide induces rapid, calcium-dependent release of vesicular glutamate and ATP from cultured rat astrocytes. *Glia,* 40, 312-23.

BALL, H. J., JUSOF, F. F., BAKMIWEWA, S. M., HUNT, N. H. & YUASA, H. J. 2014. Tryptophan-catabolizing enzymes - party of three. *Front Immunol,* 5, 485.

BALL, H. J., SANCHEZ-PEREZ, A., WEISER, S., AUSTIN, C. J., ASTELBAUER, F., MIU, J., MCQUILLAN, J. A., STOCKER, R., JERMIIN, L. S. & HUNT, N. H. 2007. Characterization of an indoleamine 2,3-dioxygenase-like protein found in humans and mice. *Gene,* 396, 203-13.

BALU, D. T. & COYLE, J. T. 2011. Neuroplasticity signaling pathways linked to the pathophysiology of schizophrenia. *Neuroscience & Biobehavioral Reviews,* 35, 848-870.

BANATI, R. B. 2003. Neuropathological imaging: in vivo detection of glial activation as a measure of disease and adaptive change in the brain. *Br Med Bull,* 65, 121-31.

BEAUDET, A. & DESCARRIES, L. 1978. The monoamine innervation of rat cerebral cortex: synaptic and nonsynaptic axon terminals. *Neuroscience,* 3, 851-60.

BEDARD, K. & KRAUSE, K. H. 2007. The NOX family of ROS-generating NADPH oxidases: physiology and pathophysiology. *Physiol Rev,* 87, 245-313.

BEHAN, W. M., MCDONALD, M., DARLINGTON, L. G. & STONE, T. W. 1999. Oxidative stress as a mechanism for quinolinic acid-induced hippocampal damage: protection by melatonin and deprenyl. *Br J Pharmacol,* 128, 1754-60.

BEN-ARI, Y. 2002. Excitatory actions of gaba during development: the nature of the nurture. *Nat Rev Neurosci,* 3, 728-39.

BERGER, F., RAMIREZ-HERNANDEZ, M. H. & ZIEGLER, M. 2004. The new life of a centenarian: signalling functions of NAD(P). *Trends Biochem Sci,* 29, 111-8.

BERGER, S. J., SUDAR, D. C. & BERGER, N. A. 1986. Metabolic consequences of DNA damage: DNA damage induces alterations in glucose metabolism by activation of poly (ADP-ribose) polymerase. *Biochem Biophys Res Commun,* 134, 227-32.

BIRCH, P. J., GROSSMAN, C. J. & HAYES, A. G. 1988a. Kynurenate and FG9041 have both competitive and non-competitive antagonist actions at excitatory amino acid receptors. *Eur J Pharmacol,* 151, 313-5.

BIRCH, P. J., GROSSMAN, C. J. & HAYES, A. G. 1988b. Kynurenic acid antagonises responses to NMDA via an action at the strychnine-insensitive glycine receptor. *Eur J Pharmacol,* 154, 85-7.

BLOCK, M. L. & HONG, J. S. 2005. Microglia and inflammation-mediated neurodegeneration: multiple triggers with a common mechanism. *Prog Neurobiol,* 76, 77-98.

BLOCK, M. L., ZECCA, L. & HONG, J.-S. 2007a. Microglia-mediated neurotoxicity: uncovering the molecular mechanisms. *Nat Rev Neurosci,* 8, 57-69.

BLOCK, M. L., ZECCA, L. & HONG, J. S. 2007b. Microglia-mediated neurotoxicity: uncovering the molecular mechanisms. *Nat Rev Neurosci,* 8, 57-69.

BOCCHINI, V., MAZZOLLA, R., BARLUZZI, R., BLASI, E., SICK, P., KETTENMAN, H. 1992. An immortalised cell line expresses properties of activated microglial cells. *J. Neurosci Res, 31 (4), 616-21.*

BOHAR, Z., TOLDI, J., FULOP, F. & VECSEI, L. 2015. Changing the face of kynurenines and neurotoxicity: therapeutic considerations. *Int J Mol Sci,* 16, 9772-93.

BOKDE, A. L., EWERS, M. & HAMPEL, H. 2009. Assessing neuronal networks: understanding Alzheimer's disease. *Prog Neurobiol,* 89, 125-33.

BOUSQUET, P., BRUBAN, V., SCHANN, S., GRENEY, H., EHRHARDT, J. D., DONTENWILL, M. & FELDMAN, J. 1999. Participation of Imidazoline Receptors and Alpha2--Adrenoceptors in the Central Hypotensive Effects of Imidazoline-Like Drugs. *Annals of the New York Academy of Sciences,* 881, 272-278.

BOZZA, S., FALLARINO, F., PITZURRA, L., ZELANTE, T., MONTAGNOLI, C., BELLOCCHIO, S., MOSCI, P., VACCA, C., PUCCETTI, P. & ROMANI, L. 2005. A Crucial Role for Tryptophan Catabolism at the Host/Candida albicans Interface. *The Journal of Immunology,* 174**,** 2910-2918.

BRAIDY, N., GRANT, R., ADAMS, S., BREW, B. J. & GUILLEMIN, G. J. 2009a. Mechanism for quinolinic acid cytotoxicity in human astrocytes and neurons. *Neurotox Res,* 16**,** 77-86.

BRAIDY, N., GRANT, R., BREW, B. J., ADAMS, S., JAYASENA, T. & GUILLEMIN, G. J. 2009b. Effects of Kynurenine Pathway Metabolites on Intracellular NAD Synthesis and Cell Death in Human Primary Astrocytes and Neurons. *Int J Tryptophan Res,* 2**,** 61-9.

BRAIDY, N., GUILLEMIN, G. J. & GRANT, R. 2011. Effects of Kynurenine Pathway Inhibition on NAD Metabolism and Cell Viability in Human Primary Astrocytes and Neurons. *Int J Tryptophan Res,* 4**,** 29-37.

BREDA, C., SATHYASAIKUMAR, K. V., SOGRATE IDRISSI, S., NOTARANGELO, F. M., ESTRANERO, J. G., MOORE, G. G., GREEN, E. W., KYRIACOU, C. P., SCHWARCZ, R. & GIORGINI, F. 2016. Tryptophan-2,3-dioxygenase (TDO) inhibition ameliorates neurodegeneration by modulation of kynurenine pathway metabolites. *Proc Natl Acad Sci U S A,* 113**,** 5435-40.

BRONTE, V. & PITTET, M. J. 2013. The spleen in local and systemic regulation of immunity. *Immunity,* 39**,** 806-18.

BROWN, G. C. & BAL-PRICE, A. 2003. Inflammatory neurodegeneration mediated by nitric oxide, glutamate, and mitochondria. *Mol Neurobiol,* 27**,** 325-55.

BRUNELLI, L., RISTAGNO, G., BAGNATI, R., FUMAGALLI, F., LATINI, R., FANELLI, R. & PASTORELLI, R. 2013. A combination of untargeted and targeted metabolomics approaches unveils changes in the kynurenine pathway following cardiopulmonary resuscitation. *Metabolomics,* 9**,** 839-852.

BUTOVSKY, O., JEDRYCHOWSKI, M. P., MOORE, C. S., CIALIC, R., LANSER, A. J., GABRIELY, G., KOEGLSPERGER, T., DAKE, B., WU, P. M., DOYKAN, C. E., FANEK, Z., LIU, L., CHEN, Z., ROTHSTEIN, J. D., RANSOHOFF, R. M., GYGI, S. P., ANTEL, J. P. & WEINER, H. L. 2014. Identification of a unique TGF-[beta]-dependent molecular and functional signature in microglia. *Nat Neurosci,* 17**,** 131-143.

CARNEVALE, D., DE SIMONE, R. & MINGHETTI, L. 2007. Microglia-neuron interaction in inflammatory and degenerative diseases: role of cholinergic and noradrenergic systems. *CNS Neurol Disord Drug Targets,* 6**,** 388-97.

CARPENEDO, R., PITTALUGA, A., COZZI, A., ATTUCCI, S., GALLI, A., RAITERI, M. & MORONI, F. 2001. Presynaptic kynurenate-sensitive receptors inhibit glutamate release. *Eur J Neurosci,* 13**,** 2141-7.

CASTANO, A., HERRERA, A. J., CANO, J. & MACHADO, A. 2002. The degenerative effect of a single intranigral injection of LPS on the dopaminergic system is prevented by dexamethasone, and not mimicked by rh-TNF-alpha, IL-1beta and IFN-gamma. *J Neurochem,* 81**,** 150-7.

CATTANEO, A. & RIVA, M. A. 2015. Stress-induced mechanisms in mental illness: A role for glucocorticoid signalling. *J Steroid Biochem Mol Biol.*

CHAO, C. C., HU, S., EHRLICH, L. & PETERSON, P. K. 1995. Interleukin-1 and tumor necrosis factor-alpha synergistically mediate neurotoxicity: involvement of nitric oxide and of N-methyl-D-aspartate receptors. *Brain Behav Immun,* 9**,** 355-65.

CHEN, L. W., HORNG, L. Y., WU, C. L., SUNG, H. C. & WU, R. T. 2012. Activating mitochondrial regulator PGC-1alpha expression by astrocytic NGF is a therapeutic strategy for Huntington's disease. *Neuropharmacology,* 63**,** 719-32.

CHEN, Y., BREW, B. J. & GUILLEMIN, G. J. 2011. Characterization of the kynurenine pathway in NSC-34 cell line: implications for amyotrophic lateral sclerosis. *J Neurochem,* 118**,** 816-25.

CHEN, Y., STANKOVIC, R., CULLEN, K. M., MEININGER, V., GARNER, B., COGGAN, S., GRANT, R., BREW, B. J. & GUILLEMIN, G. J. 2010. The kynurenine pathway and inflammation in amyotrophic lateral sclerosis. *Neurotox Res,* 18**,** 132-42.

CHEN, Y. & SWANSON, R. A. 2003. Astrocytes and brain injury. *J Cereb Blood Flow Metab,* 23**,** 137-49.

CHIARUGI, A., DELLO SBARBA, P., PACCAGNINI, A., DONNINI, S., FILIPPI, S. & MORONI, F. 2000. Combined inhibition of indoleamine 2,3-dioxygenase and nitric oxide synthase modulates neurotoxin release by interferon-gamma-activated macrophages. *J Leukoc Biol,* 68**,** 260-6.

CHIARUGI, A. & MORONI, F. 1999. Quinolinic acid formation in immune-activated mice: studies with (m-nitrobenzoyl)-alanine (mNBA) and 3,4-dimethoxy-[-N-4-(-3-nitrophenyl)thiazol-2yl]-benzenesul fonamide (Ro 61-8048), two potent and selective inhibitors of kynurenine hydroxylase. *Neuropharmacology,* 38**,** 1225-33.

CHINSOMBOON, J., RUAS, J., GUPTA, R. K., THOM, R., SHOAG, J., ROWE, G. C., SAWADA, N., RAGHURAM, S. & ARANY, Z. 2009. The transcriptional coactivator PGC-1alpha mediates exercise-induced angiogenesis in skeletal muscle. *Proc Natl Acad Sci U S A,* 106**,** 21401-6.

CHUNG, W.-S., WELSH, C. A., BARRES, B. A. & STEVENS, B. 2015. Do glia drive synaptic and cognitive impairment in disease? *Nat Neurosci,* 18**,** 1539-1545.

CITRI, A. & MALENKA, R. C. 2007. Synaptic Plasticity: Multiple Forms, Functions, and Mechanisms. *Neuropsychopharmacology,* 33**,** 18-41.

COHEN-CORY, S. 2002. The developing synapse: construction and modulation of synaptic structures and circuits. *Science,* 298**,** 770-6.

COHEN, Z., MOLINATTI, G. & HAMEL, E. 1997. Astroglial and vascular interactions of noradrenaline terminals in the rat cerebral cortex. *J Cereb Blood Flow Metab,* 17**,** 894-904.

COLLEDGE, M., SNYDER, E. M., CROZIER, R. A., SODERLING, J. A., JIN, Y., LANGEBERG, L. K., LU, H., BEAR, M. F. & SCOTT, J. D. 2003. Ubiquitination Regulates PSD-95 Degradation and AMPA Receptor Surface Expression. *Neuron,* 40**,** 595-607.

COLTON, C. A. & GILBERT, D. L. 1987. Production of superoxide anions by a CNS macrophage, the microglia. *FEBS Lett,* 223**,** 284-8.

CONNOR, T. J. & LEONARD, B. E. 1998. Depression, stress and immunological activation: the role of cytokines in depressive disorders. *Life Sci,* 62**,** 583-606.

CONNOR, T. J., STARR, N., O'SULLIVAN, J. B. & HARKIN, A. 2008. Induction of indolamine 2,3-dioxygenase and kynurenine 3-monooxygenase in rat brain following a systemic inflammatory challenge: a role for IFN-gamma? *Neurosci Lett,* 441**,** 29-34.

CONRAD, M. & SATO, H. 2012. The oxidative stress-inducible cystine/glutamate antiporter, system x (c) (-) : cystine supplier and beyond. *Amino Acids,* 42**,** 231-46.

COUNTS, S. E. & MUFSON, E. J. 2010. Noradrenaline activation of neurotrophic pathways protects against neuronal amyloid toxicity. *J Neurochem,* 113**,** 649-60.

CUARTERO, M. I., BALLESTEROS, I., DE LA PARRA, J., HARKIN, A. L., ABAUTRET-DALY, A., SHERWIN, E., FERNANDEZ-SALGUERO, P., CORBI, A. L., LIZASOAIN, I. & MORO, M. A. 2014. L-kynurenine/aryl hydrocarbon receptor pathway mediates brain damage after experimental stroke. *Circulation,* 130**,** 2040-51.

CURZON, G. & GREEN, A. R. 1969. Effects of immobilization on rat liver tryptophan pyrrolase and brain 5-hydroxytryptamine metabolism. *Br J Pharmacol,* 37**,** 689-97.

CZEH, M., GRESSENS, P. & KAINDL, A. M. 2011. The yin and yang of microglia. *Dev Neurosci,* 33**,** 199-209.

DA CUNHA, A. A., NUNES, F. B., LUNARDELLI, A., PAULI, V., AMARAL, R. H., DE OLIVEIRA, L. M., SACIURA, V. C., DA SILVA, G. L., PIRES, M. G., DONADIO, M. V., MELO, D. A., DAL-PIZZOL, F., MOREIRA, J. C., BEHR, G. A., REICHEL, C. L., ROSA, J. L. & DE OLIVEIRA, J. R. 2011. Treatment with N-methyl-D-aspartate receptor antagonist (MK-801) protects against oxidative stress in lipopolysaccharide-induced acute lung injury in the rat. *Int Immunopharmacol,* 11**,** 706-11.

DALMAU, I., FINSEN, B., ZIMMER, J., GONZALEZ, B. & CASTELLANO, B. 1998. Development of microglia in the postnatal rat hippocampus. *Hippocampus,* 8**,** 458-74.

DANTZER, R. & WALKER, A. K. 2014a. Is there a role for glutamate-mediated excitotoxicity in inflammation-induced depression? *J Neural Transm (Vienna),* 121**,** 925-32.

DANTZER, R. & WALKER, A. K. 2014b. Is there a role for glutamate-mediated excitotoxicity in inflammation-induced depression? *J Neural Transm,* 121**,** 925-32.

DARLINGTON, L. G., MACKAY, G. M., FORREST, C. M., STOY, N., GEORGE, C. & STONE, T. W. 2007. Altered kynurenine metabolism correlates with infarct volume in stroke. *Eur J Neurosci,* 26**,** 2211-21.

DAY, J. S., O'NEILL, E., CAWLEY, C., ARETZ, N. K., KILROY, D., GIBNEY, S. M., HARKIN, A. & CONNOR, T. J. 2014. Noradrenaline acting on astrocytic beta(2)-adrenoceptors induces neurite outgrowth in primary cortical neurons. *Neuropharmacology,* 77**,** 234-48.

DELLO RUSSO, C., BOULLERNE, A. I., GAVRILYUK, V. & FEINSTEIN, D. L. 2004. Inhibition of microglial inflammatory responses by norepinephrine: effects on nitric oxide and interleukin-1beta production. *J Neuroinflammation,* 1**,** 9.

DENT, E. W. & GERTLER, F. B. 2003. Cytoskeletal Dynamics and Transport in Growth Cone Motility and Axon Guidance. *Neuron,* 40**,** 209-227.

DINGLEDINE, R., BORGES, K., BOWIE, D. & TRAYNELIS, S. F. 1999. The glutamate receptor ion channels. *Pharmacol Rev,* 51**,** 7-61.

DIVORTY, N., MACKENZIE, A. E., NICKLIN, S. A. & MILLIGAN, G. 2015. G protein-coupled receptor 35: an emerging target in inflammatory and cardiovascular disease. *Front Pharmacol,* 6**,** 41.

DOLPHIN, A. C. 1982. Noradrenergic modulation of glutamate release in the cerebellum. *Brain Research,* 252**,** 111-116.

DOLUSIC, E., LARRIEU, P., MOINEAUX, L., STROOBANT, V., PILOTTE, L., COLAU, D., POCHET, L., VAN DEN EYNDE, B., MASEREEL, B., WOUTERS, J. & FREDERICK, R. 2011. Tryptophan 2,3-dioxygenase (TDO) inhibitors. 3-(2-(pyridyl)ethenyl)indoles as potential anticancer immunomodulators. *J Med Chem,* 54**,** 5320-34.

DONG-RYUL, L., KONDO, H., FURUKAWA, S. & NAKANO, K. 1997. Stimulation of NGF production by tryptophan and its metabolites in cultured mouse astroglial cells. *Brain Res,* 777**,** 228-30.

DOTTI, C. G., SULLIVAN, C. A. & BANKER, G. A. 1988. The establishment of polarity by hippocampal neurons in culture. *J Neurosci,* 8**,** 1454-68.

DOUCET, M. V., LEVINE, H., DEV, K. K. & HARKIN, A. 2013. Small-molecule inhibitors at the PSD-95/nNOS interface have antidepressant-like properties in mice. *Neuropsychopharmacology,* 38**,** 1575-84.

DOUCET, M. V., O'TOOLE, E., CONNOR, T. & HARKIN, A. 2015. Small-molecule inhibitors at the PSD-95/nNOS interface protect against glutamate-induced neuronal atrophy in primary cortical neurons. *Neuroscience,* 301**,** 421-38.

DOUNAY, A. B., ANDERSON, M., BECHLE, B. M., CAMPBELL, B. M., CLAFFEY, M. M., EVDOKIMOV, A., EVRARD, E., FONSECA, K. R., GAN, X., GHOSH, S., HAYWARD, M. M., HORNER, W., KIM, J. Y., MCALLISTER, L. A., PANDIT, J., PARADIS, V., PARIKH, V. D., REESE, M. R., RONG, S., SALAFIA, M. A., SCHUYTEN, K., STRICK, C. A., TUTTLE, J. B., VALENTINE, J., WANG, H., ZAWADZKE, L. E. & VERHOEST, P. R. 2012. Discovery of Brain-Penetrant, Irreversible Kynurenine Aminotransferase II Inhibitors for Schizophrenia. *ACS Med Chem Lett,* 3**,** 187-92.

DOUNAY, A. B., TUTTLE, J. B. & VERHOEST, P. R. 2015a. Challenges and Opportunities in the Discovery of New Therapeutics Targeting the Kynurenine Pathway. *J Med Chem.*

DOUNAY, A. B., TUTTLE, J. B. & VERHOEST, P. R. 2015b. Challenges and Opportunities in the Discovery of New Therapeutics Targeting the Kynurenine Pathway. *J Med Chem,* 58**,** 8762-82.

DUMAN, R. S. & AGHAJANIAN, G. K. 2012. Synaptic dysfunction in depression: potential therapeutic targets. *Science,* 338**,** 68-72.

ELENKOV, I. J., WILDER, R. L., CHROUSOS, G. P. & VIZI, E. S. 2000. The sympathetic nerve--an integrative interface between two supersystems: the brain and the immune system. *Pharmacol Rev,* 52**,** 595-638.

ELMORE, S. 2007. Apoptosis: A Review of Programmed Cell Death. *Toxicologic pathology,* 35**,** 495-516.

EMSLEY, J. G. & MACKLIS, J. D. 2006. Astroglial heterogeneity closely reflects the neuronal-defined anatomy of the adult murine CNS. *Neuron Glia Biol,* 2**,** 175-86.

ERICKSON, J. B., FLANAGAN, E. M., RUSSO, S. & REINHARD, J. F., JR. 1992. A radiometric assay for kynurenine 3-hydroxylase based on the release of 3H2O during hydroxylation of L-[3,5-3H]kynurenine. *Anal Biochem,* 205**,** 257-62.

ESCH, T., STEFANO, G. B., FRICCHIONE, G. L. & BENSON, H. 2002. The role of stress in neurodegenerative diseases and mental disorders. *Neuro Endocrinol Lett,* 23**,** 199-208.

ESPEY, M. G., CHERNYSHEV, O. N., REINHARD, J. F., JR., NAMBOODIRI, M. A. & COLTON, C. A. 1997. Activated human microglia produce the excitotoxin quinolinic acid. *Neuroreport,* 8**,** 431-4.

EUGENIN, E. A., ECKARDT, D., THEIS, M., WILLECKE, K., BENNETT, M. V. & SAEZ, J. C. 2001. Microglia at brain stab wounds express connexin 43 and in vitro form functional gap junctions after treatment with interferon-gamma and tumor necrosis factor-alpha. *Proc Natl Acad Sci U S A,* 98**,** 4190-5.

FAGBEMI, S. O. & SALAKO, L. A. 1982. The effects of prazosin, phentolamine and phenoxybenzamine on inhibitory alpha-adrenoceptors in the guniea-pig isolated ileum. *Br J Pharmacol,* 76**,** 235-43.

FALLARINO, F., GROHMANN, U., VACCA, C., BIANCHI, R., ORABONA, C., SPRECA, A., FIORETTI, M. C. & PUCCETTI, P. 2002. T cell apoptosis by tryptophan catabolism. *Cell Death Differ,* 9**,** 1069-77.

FARAVELLI, C., LO SAURO, C., GODINI, L., LELLI, L., BENNI, L., PIETRINI, F., LAZZERETTI, L., TALAMBA, G. A., FIORAVANTI, G. & RICCA, V. 2012. Childhood stressful events, HPA axis and anxiety disorders. *World J Psychiatry,* 2**,** 13-25.

FARINA, C., ALOISI, F. & MEINL, E. 2007. Astrocytes are active players in cerebral innate immunity. *Trends Immunol,* 28**,** 138-45.

FATOKUN, A. A., HUNT, N. H. & BALL, H. J. 2013. Indoleamine 2,3-dioxygenase 2 (IDO2) and the kynurenine pathway: characteristics and potential roles in health and disease. *Amino Acids,* 45**,** 1319-29.

FEDERICO, A., CARDAIOLI, E., DA POZZO, P., FORMICHI, P., GALLUS, G. N. & RADI, E. 2012. Mitochondria, oxidative stress and neurodegeneration. *J Neurol Sci,* 322**,** 254-62.

FENG, G., MELLOR, R. H., BERNSTEIN, M., KELLER-PECK, C., NGUYEN, Q. T., WALLACE, M., NERBONNE, J. M., LICHTMAN, J. W. & SANES, J. R. 2000. Imaging neuronal subsets in transgenic mice expressing multiple spectral variants of GFP. *Neuron,* 28**,** 41-51.

FERRANTE, M., MIGLIORE, M. & ASCOLI, G. A. 2013. Functional impact of dendritic branch-point morphology. *J Neurosci,* 33**,** 2156-65.

FETLER, L. & AMIGORENA, S. 2005. Neuroscience. Brain under surveillance: the microglia patrol. *Science,* 309**,** 392-3.

FLAVIN, M. P., HO, L. T. & COUGHLIN, K. 1997. Neurotoxicity of Soluble Macrophage Productsin Vitro—Influence of Dexamethasone. *Experimental Neurology,* 145**,** 462-470.

FLOYD, R. A. 1999. Antioxidants, oxidative stress, and degenerative neurological disorders. *Proc Soc Exp Biol Med,* 222**,** 236-45.

FLYNN, K. C. 2013. The cytoskeleton and neurite initiation. *Bioarchitecture,* 3**,** 86-109.

FORREST, C. M., KHALIL, O. S., PISAR, M., DARLINGTON, L. G. & STONE, T. W. 2013a. Prenatal inhibition of the tryptophan-kynurenine pathway alters synaptic plasticity and protein expression in the rat hippocampus. *Brain Res,* 1504**,** 1-15.

FORREST, C. M., KHALIL, O. S., PISAR, M., MCNAIR, K., KORNISIUK, E., SNITCOFSKY, M., GONZALEZ, N., JERUSALINSKY, D., DARLINGTON, L. G. & STONE, T. W. 2013b. Changes in synaptic transmission and protein expression in the brains of adult offspring after prenatal inhibition of the kynurenine pathway. *Neuroscience,* 254**,** 241-59.

FORREST, C. M., MACKAY, G. M., OXFORD, L., STOY, N., STONE, T. W. & DARLINGTON, L. G. 2006. Kynurenine pathway metabolism in patients with osteoporosis after 2 years of drug treatment. *Clin Exp Pharmacol Physiol,* 33**,** 1078-87.

FORREST, C. M., MACKAY, G. M., STOY, N., EGERTON, M., CHRISTOFIDES, J., STONE, T. W. & DARLINGTON, L. G. 2004. Tryptophan loading induces oxidative stress. *Free Radic Res,* 38**,** 1167-71.

FOSTER, A. C. & WONG, E. H. 1987. The novel anticonvulsant MK-801 binds to the activated state of the N-methyl-D-aspartate receptor in rat brain. *Br J Pharmacol,* 91**,** 403-9.

FREEMAN, J. K. & GOLDBERG, M. P. 1994. Confocal microscopic visualization of MK-801-induced cytoplasmic vacuoles in vitro. *Psychopharmacol Bull,* 30**,** 541-7.

FRIEDMAN, H. V., BRESLER, T., GARNER, C. C. & ZIV, N. E. 2000. Assembly of new individual excitatory synapses: time course and temporal order of synaptic molecule recruitment. *Neuron,* 27**,** 57-69.

FUKUI, S., SCHWARCZ, R., RAPOPORT, S. I., TAKADA, Y. & SMITH, Q. R. 1991. Blood-brain barrier transport of kynurenines: implications for brain synthesis and metabolism. *J Neurochem,* 56**,** 2007-17.

FUKUNAGA, M., YAMAMOTO, Y., KAWASOE, M., ARIOKA, Y., MURAKAMI, Y., HOSHI, M. & SAITO, K. 2012. Studies on tissue and cellular distribution of indoleamine 2,3-dioxygenase 2: the absence of IDO1 upregulates IDO2 expression in the epididymis. *J Histochem Cytochem,* 60**,** 854-60.

FUNAKOSHI, MASAAKI, K. & TOSHIKAZU, N. 2011. Modulation of Tryptophan Metabolism, Promotion of Neurogenesis and Alteration of Anxiety-Related Behavior in Tryptophan 2,3-Dioxygenase-Deficient Mice. *International Journal of Tryptophan Research***,** 7.

GALLO, G. 2011. The cytoskeletal and signaling mechanisms of axon collateral branching. *Dev Neurobiol,* 71**,** 201-20.

GALLOWITSCH-PUERTA, M. & TRACEY, K. J. 2005. Immunologic role of the cholinergic anti-inflammatory pathway and the nicotinic acetylcholine alpha 7 receptor. *Ann N Y Acad Sci,* 1062**,** 209-19.

GAO, H.-M., LIU, B., ZHANG, W. & HONG, J.-S. 2003. Critical role of microglial NADPH oxidase-derived free radicals in the in vitro MPTP model of Parkinson's disease. *The FASEB Journal,* 17**,** 1954-1956.

GAO, H. M., JIANG, J., WILSON, B., ZHANG, W., HONG, J. S. & LIU, B. 2002. Microglial activation-mediated delayed and progressive degeneration of rat nigral dopaminergic neurons: relevance to Parkinson's disease. *J Neurochem,* 81**,** 1285-97.

GARTHWAITE, J. & BOULTON, C. L. 1995. Nitric oxide signaling in the central nervous system. *Annu Rev Physiol,* 57**,** 683-706.

GARVEY, E. P., OPLINGER, J. A., FURFINE, E. S., KIFF, R. J., LASZLO, F., WHITTLE, B. J. & KNOWLES, R. G. 1997. 1400W is a slow, tight binding, and highly selective inhibitor of inducible nitric-oxide synthase in vitro and in vivo. *J Biol Chem,* 272**,** 4959-63.

GATE, D., REZAI-ZADEH, K., JODRY, D., RENTSENDORJ, A. & TOWN, T. 2010. Macrophages in Alzheimer's disease: the blood-borne identity. *J Neural Transm (Vienna),* 117**,** 961-70.

GAVRILYUK, V., DELLO RUSSO, C., HENEKA, M. T., PELLIGRINO, D., WEINBERG, G. & FEINSTEIN, D. L. 2002. Norepinephrine increases I kappa B alpha expression in astrocytes. *J Biol Chem,* 277**,** 29662-8.

GERHART-HINES, Z., DOMINY, J. E., JR., BLATTLER, S. M., JEDRYCHOWSKI, M. P., BANKS, A. S., LIM, J. H., CHIM, H., GYGI, S. P. & PUIGSERVER, P. 2011. The cAMP/PKA pathway rapidly activates SIRT1 to promote fatty acid oxidation independently of changes in NAD(+). *Mol Cell,* 44**,** 851-63.

GERMAN, D. C., WALKER, B. S., MANAYE, K., SMITH, W. K., WOODWARD, D. J. & NORTH, A. J. 1988. The human locus coeruleus: computer reconstruction of cellular distribution. *J Neurosci,* 8**,** 1776-88.

GIBNEY, S. M., FAGAN, E. M., WALDRON, A. M., O'BYRNE, J., CONNOR, T. J. & HARKIN, A. 2014. Inhibition of stress-induced hepatic tryptophan 2,3-dioxygenase exhibits antidepressant activity in an animal model of depressive behaviour. *Int J Neuropsychopharmacol,* 17**,** 917-28.

GIBNEY, S. M., MCGUINNESS, B., PRENDERGAST, C., HARKIN, A. & CONNOR, T. J. 2013. Poly I:C-induced activation of the immune response is accompanied by depression and anxiety-like behaviours, kynurenine pathway activation and reduced BDNF expression. *Brain Behav Immun,* 28**,** 170-81.

GINHOUX, F., LIM, S., HOEFFEL, G., LOW, D. & HUBER, T. 2013. Origin and differentiation of microglia. *Frontiers in Cellular Neuroscience,* 7**,** 45.

GIRARD, S., BROUGH, D., LOPEZ-CASTEJON, G., GILES, J., ROTHWELL, N. J. & ALLAN, S. M. 2013. Microglia and Macrophages Differentially Modulate Cell Death After Brain Injury Caused by Oxygen-Glucose Deprivation in Organotypic Brain Slices. *Glia,* 61**,** 813-824.

GIULIAN, D. & BAKER, T. J. 1986. Characterization of ameboid microglia isolated from developing mammalian brain. *J Neurosci,* 6**,** 2163-78.

GLASS, C. K., SAIJO, K., WINNER, B., MARCHETTO, M. C. & GAGE, F. H. 2010. Mechanisms underlying inflammation in neurodegeneration. *Cell,* 140**,** 918-34.

GLEESON, L. C., RYAN, K. J., GRIFFIN, E. W., CONNOR, T. J. & HARKIN, A. 2010. The beta2-adrenoceptor agonist clenbuterol elicits neuroprotective, anti-inflammatory and neurotrophic actions in the kainic acid model of excitotoxicity. *Brain Behav Immun,* 24**,** 1354-61.

GLEZER, I., SIMARD, A. R. & RIVEST, S. 2007. Neuroprotective role of the innate immune system by microglia. *Neuroscience,* 147**,** 867-83.

GOGTAY, N., GIEDD, J. N., LUSK, L., HAYASHI, K. M., GREENSTEIN, D., VAITUZIS, A. C., NUGENT, T. F., HERMAN, D. H., CLASEN, L. S., TOGA, A. W., RAPOPORT, J. L. & THOMPSON, P. M. 2004. Dynamic mapping of human cortical development during childhood through early adulthood. *Proceedings of the National Academy of Sciences of the United States of America,* 101**,** 8174-8179.

GOLDBERG, J. D. & BURMEISTER, W. D. 1986. Stages in axon formation: observations of growth of Aplysia axons in culture using video-enhanced contrast-differential interference contrast microscopy. *The Journal of Cell Biology,* 103**,** 1921-1931.

GOLDBERG, J. L. 2003. How does an axon grow? *Genes Dev,* 17**,** 941-58.

GRAS, G., SAMAH, B., HUBERT, A., LEONE, C., PORCHERAY, F. & RIMANIOL, A. C. 2012. EAAT expression by macrophages and microglia: still more questions than answers. *Amino Acids,* 42**,** 221-9.

GREEN, A. R., WOODS, H. F. & JOSEPH, M. H. 1976. Tryptophan metabolism in the isolated perfused liver of the rat: effects of tryptophan concentration, hydrocortisone and allopurinol on tryptophan pyrrolase activity and kynurenine formation. *Br J Pharmacol,* 57**,** 103-14.

GUIDETTI, P., LUTHI-CARTER, R. E., AUGOOD, S. J. & SCHWARCZ, R. 2004. Neostriatal and cortical quinolinate levels are increased in early grade Huntington's disease. *Neurobiol Dis,* 17**,** 455-61.

GUIDETTI, P., OKUNO, E. & SCHWARCZ, R. 1997. Characterization of rat brain kynurenine aminotransferases I and II. *J Neurosci Res,* 50**,** 457-65.

GUIDETTI, P. & SCHWARCZ, R. 2003. 3-Hydroxykynurenine and quinolinate: pathogenic synergism in early grade Huntington's disease? *Adv Exp Med Biol,* 527**,** 137-45.

GUILLEMIN, G. J. 2012. Quinolinic acid, the inescapable neurotoxin. *FEBS J,* 279**,** 1356-65.

GUILLEMIN, G. J. & BREW, B. J. 2002. Implications of the kynurenine pathway and quinolinic acid in Alzheimer's disease. *Redox Rep,* 7**,** 199-206.

GUILLEMIN, G. J., CULLEN, K. M., LIM, C. K., SMYTHE, G. A., GARNER, B., KAPOOR, V., TAKIKAWA, O. & BREW, B. J. 2007. Characterization of the kynurenine pathway in human neurons. *J Neurosci,* 27**,** 12884-92.

GUILLEMIN, G. J., KERR, S. J. & BREW, B. J. 2005a. Involvement of quinolinic acid in AIDS dementia complex. *Neurotox Res,* 7**,** 103-23.

GUILLEMIN, G. J., KERR, S. J., SMYTHE, G. A., SMITH, D. G., KAPOOR, V., ARMATI, P. J., CROITORU, J. & BREW, B. J. 2001. Kynurenine pathway metabolism in human astrocytes: a paradox for neuronal protection. *J Neurochem,* 78**,** 842-53.

GUILLEMIN, G. J., SMITH, D. G., SMYTHE, G. A., ARMATI, P. J. & BREW, B. J. 2003. Expression of the kynurenine pathway enzymes in human microglia and macrophages. *Adv Exp Med Biol,* 527**,** 105-12.

GUILLEMIN, G. J., SMYTHE, G., TAKIKAWA, O. & BREW, B. J. 2005b. Expression of indoleamine 2,3-dioxygenase and production of quinolinic acid by human microglia, astrocytes, and neurons. *Glia,* 49**,** 15-23.

GUPTA, K., HARDINGHAM, G. E. & CHANDRAN, S. 2013. NMDA receptor-dependent glutamate excitotoxicity in human embryonic stem cell-derived neurons. *Neurosci Lett,* 543**,** 95-100.

HANSSON, E. 1984. Cellular composition of a cerebral hemisphere primary culture. *Neurochem Res,* 9**,** 153-72.

HAROON, E., RAISON, C. L. & MILLER, A. H. 2012. Psychoneuroimmunology meets neuropsychopharmacology: translational implications of the impact of inflammation on behavior. *Neuropsychopharmacology,* 37**,** 137-62.

HARTAI, Z., JUHASZ, A., RIMANOCZY, A., JANAKY, T., DONKO, T., DUX, L., PENKE, B., TOTH, G. K., JANKA, Z. & KALMAN, J. 2007. Decreased serum and red blood cell kynurenic acid levels in Alzheimer's disease. *Neurochem Int,* 50**,** 308-13.

HENDRIE, H. C. 1998. Epidemiology of dementia and Alzheimer's disease. *Am J Geriatr Psychiatry,* 6**,** S3-18.

HENN, A., LUND, S., HEDTJARN, M., SCHRATTENHOLZ, A., PORZGEN, P. & LEIST, M. 2009. The suitability of BV2 cells as alternative model system for primary microglia cultures or for animal experiments examining brain inflammation. *Altex,* 26**,** 83-94.

HERTZ, L., CHEN, Y., GIBBS, M. E., ZANG, P. & PENG, L. 2004. Astrocytic adrenoceptors: a major drug target in neurological and psychiatric disorders? *Curr Drug Targets CNS Neurol Disord,* 3**,** 239-67.

HILL, M., TANGUY-ROYER, S., ROYER, P., CHAUVEAU, C., ASGHAR, K., TESSON, L., LAVAINNE, F., REMY, S., BRION, R., HUBERT, F. X., HESLAN, M., RIMBERT, M., BERTHELOT, L., MOFFETT, J. R., JOSIEN, R., GREGOIRE, M. & ANEGON, I. 2007. IDO expands human CD4+CD25high regulatory T cells by promoting maturation of LPS-treated dendritic cells. *Eur J Immunol,* 37**,** 3054-62.

HILMAS, C., PEREIRA, E. F., ALKONDON, M., RASSOULPOUR, A., SCHWARCZ, R. & ALBUQUERQUE, E. X. 2001. The brain metabolite kynurenic acid inhibits alpha7 nicotinic receptor activity and increases non-alpha7 nicotinic receptor expression: physiopathological implications. *J Neurosci,* 21**,** 7463-73.

HINOJOSA, A. E., CASO, J. R., GARCÍA-BUENO, B., LEZA, J. C. & MADRIGAL, J. L. 2013. Dual effects of noradrenaline on astroglial production of chemokines and pro-inflammatory mediators. *Journal of Neuroinflammation,* 10**,** 1-10.

HOLTZMAN, C. W., TROTMAN, H. D., GOULDING, S. M., RYAN, A. T., MACDONALD, A. N., SHAPIRO, D. I., BRASFIELD, J. L. & WALKER, E. F. 2013. Stress and neurodevelopmental processes in the emergence of psychosis. *Neuroscience,* 249**,** 172-91.

HORNIK, T. C., VILALTA, A. & BROWN, G. C. 2016. Activated microglia cause reversible apoptosis of pheochromocytoma cells, inducing their cell death by phagocytosis. *J Cell Sci,* 129**,** 65-79.

HORVATH, R. J., NUTILE-MCMENEMY, N., ALKAITIS, M. S. & DE LEO, J. A. 2008. Differential migration, LPS-induced cytokine, chemokine and NO expression in immortalized BV-2 and HAPI cell lines and primary microglial cultures. *Journal of neurochemistry,* 107**,** 557-569.

HOU, D. Y., MULLER, A. J., SHARMA, M. D., DUHADAWAY, J., BANERJEE, T., JOHNSON, M., MELLOR, A. L., PRENDERGAST, G. C. & MUNN, D. H. 2007. Inhibition of indoleamine 2,3-dioxygenase in dendritic cells by stereoisomers of 1-methyl-tryptophan correlates with antitumor responses. *Cancer Res,* 67**,** 792-801.

HU, X. & IVASHKIV, L. B. 2009. Cross-regulation of Signaling and Immune Responses by IFN-γ and STAT1. *Immunity,* 31**,** 539-550.

HUANG, Z. J. & SCHEIFFELE, P. 2008. GABA and neuroligin signaling: linking synaptic activity and adhesion in inhibitory synapse development. *Curr Opin Neurobiol,* 18**,** 77-83.

HWU, P., DU, M. X., LAPOINTE, R., DO, M., TAYLOR, M. W. & YOUNG, H. A. 2000. Indoleamine 2,3-dioxygenase production by human dendritic cells results in the inhibition of T cell proliferation. *J Immunol,* 164**,** 3596-9.

IGARASHI, K., GAROTTA, G., OZMEN, L., ZIEMIECKI, A., WILKS, A. F., HARPUR, A. G., LARNER, A. C. & FINBLOOM, D. S. 1994. Interferon-gamma induces tyrosine phosphorylation of interferon-gamma receptor and regulated association of protein tyrosine kinases, Jak1 and Jak2, with its receptor. *J Biol Chem,* 269**,** 14333-6.

IPPOLITO, D. M. & EROGLU, C. 2010. Quantifying synapses: an immunocytochemistry-based assay to quantify synapse number. *J Vis Exp*.

JACK, C. S., ARBOUR, N., MANUSOW, J., MONTGRAIN, V., BLAIN, M., MCCREA, E., SHAPIRO, A. & ANTEL, J. P. 2005. TLR signaling tailors innate immune responses in human microglia and astrocytes. *J Immunol,* 175**,** 4320-30.

JENKINS, L., ALVAREZ-CURTO, E., CAMPBELL, K., DE MUNNIK, S., CANALS, M., SCHLYER, S. & MILLIGAN, G. 2011. Agonist activation of the G protein-coupled receptor GPR35 involves transmembrane domain III and is transduced via Galpha(1)(3) and beta-arrestin-2. *Br J Pharmacol,* 162**,** 733-48.

JOHNSON, M. A., WEICK, J. P., PEARCE, R. A. & ZHANG, S. C. 2007. Functional neural development from human embryonic stem cells: accelerated synaptic activity via astrocyte coculture. *J Neurosci,* 27**,** 3069-77.

JONES, S. P., FRANCO, N. F., VARNEY, B., SUNDARAM, G., BROWN, D. A., DE BIE, J., LIM, C. K., GUILLEMIN, G. J. & BREW, B. J. 2015. Expression of the Kynurenine Pathway in Human Peripheral Blood Mononuclear Cells: Implications for Inflammatory and Neurodegenerative Disease. *PLoS One,* 10**,** e0131389.

JU, L., ZENG, H., CHEN, Y., WU, Y., WANG, B. & XU, Q. 2015. Dual polarization of microglia isolated from mixed glial cell cultures. *J Neurosci Res,* 93**,** 1345-52.

JUNG, B. D., KIMURA, K., KITAMURA, H., MAKONDO, K., OKITA, K., KAWASAKI, M. & SAITO, M. 2000. Norepinephrine stimulates interleukin-6 mRNA expression in primary cultured rat hepatocytes. *J Biochem,* 127**,** 205-9.

JUNKER, V., BECKER, A., HUHNE, R., ZEMBATOV, M., RAVATI, A., CULMSEE, C. & KRIEGLSTEIN, J. 2002. Stimulation of beta-adrenoceptors activates astrocytes and provides neuroprotection. *Eur J Pharmacol,* 446**,** 25-36.

KANAI, M., FUNAKOSHI, H. & NAKAMURA, T. 2010. Implication of Tryptophan 2,3-Dioxygenase and its Novel Variants in the Hippocampus and Cerebellum During the Developing and Adult Brain. *International Journal of Tryptophan Research : IJTR,* 3**,** 141-149.

KANAI, M., NAKAMURA, T. & FUNAKOSHI, H. 2009. Identification and characterization of novel variants of the tryptophan 2,3-dioxygenase gene: differential regulation in the mouse nervous system during development. *Neurosci Res,* 64**,** 111-7.

KARAKUŁA-JUCHNOWICZ, H., FLIS, M., SZYMONA, K., KUCZYŃSKA, M., STELMACH, E. & KOWAL-POPCZAK, A. 2015. New prospects for antipsychotic treatment – the role of the kynurenine pathway. *Psychiatry Pol. ,* 48**,** 1167-1177.

KAUR, G. & DUFOUR, J. M. 2012. Cell lines: Valuable tools or useless artifacts. *Spermatogenesis,* 2**,** 1-5.

KAUR, J., DHAUNSI, G. S. & TURNER, R. B. 2004. Interleukin-1 and nitric oxide increase NADPH oxidase activity in human coronary artery smooth muscle cells. *Med Princ Pract,* 13**,** 26-9.

KELSCH, W., SIM, S. & LOIS, C. 2010. Watching synaptogenesis in the adult brain. *Annu Rev Neurosci,* 33**,** 131-49.

KERR, S. J., ARMATI, P. J., GUILLEMIN, G. J. & BREW, B. J. 1998. Chronic exposure of human neurons to quinolinic acid results in neuronal changes consistent with AIDS dementia complex. *Aids,* 12**,** 355-63.

KETTENMANN, H., KIRCHHOFF, F. & VERKHRATSKY, A. 2013. Microglia: New Roles for the Synaptic Stripper. *Neuron,* 77**,** 10-18.

KHALIL, O. S., PISAR, M., FORREST, C. M., VINCENTEN, M. C., DARLINGTON, L. G. & STONE, T. W. 2014a. Prenatal inhibition of the kynurenine pathway leads to structural changes in the hippocampus of adult rat offspring. *Eur J Neurosci,* 39**,** 1558-71.

KHALIL, O. S., PISAR, M., FORREST, C. M., VINCENTEN, M. C. J., DARLINGTON, L. G. & STONE, T. W. 2014b. Prenatal inhibition of the kynurenine pathway leads to structural changes in the hippocampus of adult rat offspring. *The European Journal of Neuroscience,* 39**,** 1558-1571.

KILBOURN, M. R., SHERMAN, P. & ABBOTT, L. C. 1998. Reduced MPTP neurotoxicity in striatum of the mutant mouse tottering. *Synapse,* 30**,** 205-10.

KIM, J., HONG, H., HEO, A. & PARK, W. 2013a. Indole toxicity involves the inhibition of adenosine triphosphate production and protein folding in Pseudomonas putida. *FEMS Microbiol Lett,* 343**,** 89-99.

KIM, J. A., MITSUKAWA, K., YAMADA, M. K., NISHIYAMA, N., MATSUKI, N. & IKEGAYA, Y. 2002. Cytoskeleton disruption causes apoptotic degeneration of dentate granule cells in hippocampal slice cultures. *Neuropharmacology,* 42**,** 1109-18.

KIM, S., OCK, J., KIM, A. K., LEE, H. W., CHO, J. Y., KIM, D. R., PARK, J. Y. & SUK, K. 2007. Neurotoxicity of microglial cathepsin D revealed by secretome analysis. *J Neurochem,* 103**,** 2640-50.

KIM, S. H., ASAKA, M., HIGASHIDA, K., TAKAHASHI, Y., HOLLOSZY, J. O. & HAN, D. H. 2013b. beta-Adrenergic stimulation does not activate p38 MAP kinase or induce PGC-1alpha in skeletal muscle. *Am J Physiol Endocrinol Metab,* 304**,** E844-52.

KIM, Y. K., MYINT, A. M., VERKERK, R., SCHARPE, S., STEINBUSCH, H. & LEONARD, B. 2009. Cytokine changes and tryptophan metabolites in medication-naive and medication-free schizophrenic patients. *Neuropsychobiology,* 59**,** 123-9.

KLOTZ, L., SASTRE, M., KREUTZ, A., GAVRILYUK, V., KLOCKGETHER, T., FEINSTEIN, D. L. & HENEKA, M. T. 2003. Noradrenaline induces expression of peroxisome proliferator activated receptor gamma (PPARgamma) in murine primary astrocytes and neurons. *J Neurochem,* 86**,** 907-16.

KNIGHT, R. A. & VERKHRATSKY, A. 2010. Neurodegenerative diseases: failures in brain connectivity? *Cell Death Differ,* 17**,** 1069-70.

KNOBLOCH, M. & MANSUY, I. M. 2008. Dendritic spine loss and synaptic alterations in Alzheimer's disease. *Mol Neurobiol,* 37**,** 73-82.

KOCKI, T., LUCHOWSKI, P., LUCHOWSKA, E., WIELOSZ, M., TURSKI, W. A. & URBANSKA, E. M. 2003a. L-cysteine sulphinate, endogenous sulphur-containing amino acid, inhibits rat brain kynurenic acid production via selective interference with kynurenine aminotransferase II. *Neurosci Lett,* 346**,** 97-100.

KOENIG, J. I., KIRKPATRICK, B. & LEE, P. 2002. Glucocorticoid hormones and early brain development in schizophrenia. *Neuropsychopharmacology,* 27**,** 309-18.

KOFFIE, R. M., HYMAN, B. T. & SPIRES-JONES, T. L. 2011. Alzheimer's disease: synapses gone cold. *Mol Neurodegener,* 6**,** 63.

KREUTZBERG, G. W. 1996. Microglia: a sensor for pathological events in the CNS. *Trends Neurosci,* 19**,** 312-8.

KUCUKKAYA, B., AKER, R., YUKSEL, M., ONAT, F. & YALCIN, A. S. 1998. Low dose MK-801 protects against iron-induced oxidative changes in a rat model of focal epilepsy. *Brain Res,* 788**,** 133-6.

KUDO, Y. & BOYD, C. A. 2001. The role of L-tryptophan transport in L-tryptophan degradation by indoleamine 2,3-dioxygenase in human placental explants. *J Physiol,* 531**,** 417-23.

KURKOWSKA-JASTRZEBSKA, I., WRONSKA, A., KOHUTNICKA, M., CZLONKOWSKI, A. & CZLONKOWSKA, A. 1999. The inflammatory reaction following 1-methyl-4-phenyl-1,2,3, 6-tetrahydropyridine intoxication in mouse. *Exp Neurol,* 156**,** 50-61.

KWIDZINSKI, E. & BECHMANN, I. 2007. IDO expression in the brain: a double-edged sword. *J Mol Med (Berl),* 85**,** 1351-9.

LAUDER, J. M. 1990. Ontogeny of the serotonergic system in the rat: serotonin as a developmental signal. *Ann N Y Acad Sci,* 600**,** 297-313; discussion 314.

LAWSON, L. J., PERRY, V. H., DRI, P. & GORDON, S. 1990. Heterogeneity in the distribution and morphology of microglia in the normal adult mouse brain. *Neuroscience,* 39**,** 151-70.

LEE, M., MCGEER, E. & MCGEER, P. L. 2013. Neurotoxins released from interferon-gamma-stimulated human astrocytes. *Neuroscience,* 229**,** 164-75.

LEIBOWITZ, A., BOYKO, M., SHAPIRA, Y. & ZLOTNIK, A. 2012. Blood glutamate scavenging: insight into neuroprotection. *Int J Mol Sci,* 13**,** 10041-66.

LESUISSE, C. & MARTIN, L. J. 2002. Immature and mature cortical neurons engage different apoptotic mechanisms involving caspase-3 and the mitogen-activated protein kinase pathway. *J Cereb Blood Flow Metab,* 22**,** 935-50.

LIBERTO, C. M., ALBRECHT, P. J., HERX, L. M., YONG, V. W. & LEVISON, S. W. 2004. Pro-regenerative properties of cytokine-activated astrocytes. *J Neurochem,* 89**,** 1092-100.

LIM, C. K., BREW, B. J., SUNDARAM, G. & GUILLEMIN, G. J. 2010. Understanding the roles of the kynurenine pathway in multiple sclerosis progression. *Int J Tryptophan Res,* 3**,** 157-67.

LIM, C. K., SMYTHE, G. A., STOCKER, R., BREW, B. J. & GUILLEMIN, G. J. 2007. Characterization of the kynurenine pathway in human oligodendrocytes. *International Congress Series,* 1304**,** 213-217.

LIM, C. K., YAP, M. M., KENT, S. J., GRAS, G., SAMAH, B., BATTEN, J. C., DE ROSE, R., HENG, B., BREW, B. J. & GUILLEMIN, G. J. 2013a. Characterization of the kynurenine pathway and quinolinic Acid production in macaque macrophages. *Int J Tryptophan Res,* 6**,** 7-19.

LIM, S. H., PARK, E., YOU, B., JUNG, Y., PARK, A. R., PARK, S. G. & LEE, J. R. 2013b. Neuronal synapse formation induced by microglia and interleukin 10. *PLoS One,* 8**,** e81218.

LING, Z., ZHU, Y., TONG, C. W., SNYDER, J. A., LIPTON, J. W. & CARVEY, P. M. 2006. Progressive dopamine neuron loss following supra-nigral lipopolysaccharide (LPS) infusion into rats exposed to LPS prenatally. *Experimental Neurology,* 199**,** 499-512.

LOANE, D. J. & BYRNES, K. R. 2010. Role of Microglia in Neurotrauma. *Neurotherapeutics : the journal of the American Society for Experimental NeuroTherapeutics,* 7**,** 366-377.

LOB, S., KONIGSRAINER, A., SCHAFER, R., RAMMENSEE, H. G., OPELZ, G. & TERNESS, P. 2008. Levo- but not dextro-1-methyl tryptophan abrogates the IDO activity of human dendritic cells. *Blood,* 111**,** 2152-4.

LODISH, H. F. 2000. *Molecular cell biology*, New York : W.H. Freeman and Co., c2000.4th ed.

LONGO, F. M. & MASSA, S. M. 2013. Small-molecule modulation of neurotrophin receptors: a strategy for the treatment of neurological disease. *Nat Rev Drug Discov,* 12**,** 507-525.

LONZE, B. E. & GINTY, D. D. 2002. Function and Regulation of CREB Family Transcription Factors in the Nervous System. *Neuron,* 35**,** 605-623.

LOWERY, L. A. & VAN VACTOR, D. 2009. The trip of the tip: understanding the growth cone machinery. *Nat Rev Mol Cell Biol,* 10**,** 332-43.

LUCASSEN, P. J., NANINCK, E. F., VAN GOUDOEVER, J. B., FITZSIMONS, C., JOELS, M. & KOROSI, A. 2013. Perinatal programming of adult hippocampal structure and function; emerging roles of stress, nutrition and epigenetics. *Trends Neurosci,* 36**,** 621-31.

LUCCINI, E., MUSANTE, V., NERI, E., RAITERI, M. & PITTALUGA, A. 2007. N-methyl-D-aspartate autoreceptors respond to low and high agonist concentrations by facilitating, respectively, exocytosis and carrier-mediated release of glutamate in rat hippocampus. *J Neurosci Res,* 85**,** 3657-65.

LUCHOWSKA, E., KLOC, R., OLAJOSSY, B., WNUK, S., WIELOSZ, M., OWE-LARSSON, B. & URBANSKA, E. M. 2009. beta-adrenergic enhancement of brain kynurenic acid production mediated via cAMP-related protein kinase A signaling. *Prog Neuropsychopharmacol Biol Psychiatry,* 33**,** 519-29.

LUCHOWSKA, E., KLOC, R., WNUK, S., OLAJOSSY, B., WIELOSZ, M. & URBANSKA, E. M. 2008. Clenbuterol enhances the production of kynurenic acid in brain cortical slices and glial cultures. *Pharmacol Rep,* 60**,** 574-7.

LUGO-HUITRON, R., UGALDE MUNIZ, P., PINEDA, B., PEDRAZA-CHAVERRI, J., RIOS, C. & PEREZ-DE LA CRUZ, V. 2013. Quinolinic acid: an endogenous neurotoxin with multiple targets. *Oxid Med Cell Longev,* 2013**,** 104024.

LUO, L. 2002. Actin cytoskeleton regulation in neuronal morphogenesis and structural plasticity. *Annu Rev Cell Dev Biol,* 18**,** 601-35.

LYNCH, A. M., MURPHY, K. J., DEIGHAN, B. F., O'REILLY, J.-A., GUN'KO, Y. K., COWLEY, T. R., GONZALEZ-REYES, R. E. & LYNCH, M. A. 2010. The Impact of Glial Activation in the Aging Brain. *Aging and Disease,* 1**,** 262-278.

LYNCH, M. A. 2009. The multifaceted profile of activated microglia. *Mol Neurobiol,* 40**,** 139-56.

MADDISON, D. C. & GIORGINI, F. 2015. The kynurenine pathway and neurodegenerative disease. *Semin Cell Dev Biol,* 40**,** 134-141.

MADGE, D., HAZELWOOD, R., IYER, R., JONES, H. & SALTER, M. 1996. Novel tryptophan dioxygenase inhibitors and combined tryptophan dioxygenase/5-HT reuptake inhibitors. *Bioorganic & Medicinal Chemistry Letters,* 6**,** 857-860.

MADRIGAL, J. L., LEZA, J. C., POLAK, P., KALININ, S. & FEINSTEIN, D. L. 2009. Astrocyte-derived MCP-1 mediates neuroprotective effects of noradrenaline. *J Neurosci,* 29**,** 263-7.

MAES, M. 2011. Depression is an inflammatory disease, but cell-mediated immune activation is the key component of depression. *Prog Neuropsychopharmacol Biol Psychiatry,* 35**,** 664-75.

MAES, M., LEONARD, B. E., MYINT, A. M., KUBERA, M. & VERKERK, R. 2011. The new '5-HT' hypothesis of depression: cell-mediated immune activation induces indoleamine 2,3-dioxygenase, which leads to lower plasma tryptophan and an increased synthesis of detrimental tryptophan catabolites (TRYCATs), both of which contribute to the onset of depression. *Prog Neuropsychopharmacol Biol Psychiatry,* 35**,** 702-21.

MAES, M., VERKERK, R., BONACCORSO, S., OMBELET, W., BOSMANS, E. & SCHARPE, S. 2002. Depressive and anxiety symptoms in the early puerperium are related to increased degradation of tryptophan into kynurenine, a phenomenon which is related to immune activation. *Life Sci,* 71**,** 1837-48.

MAISEL, A. S., FOWLER, P., REARDEN, A., MOTULSKY, H. J. & MICHEL, M. C. 1989. A new method for isolation of human lymphocyte subsets reveals differential regulation of beta-adrenergic receptors by terbutaline treatment. *Clin Pharmacol Ther,* 46**,** 429-39.

MANN, D. M. 1983. The locus coeruleus and its possible role in ageing and degenerative disease of the human central nervous system. *Mech Ageing Dev,* 23**,** 73-94.

MANTYH, P. W., ROGERS, S. D., ALLEN, C. J., CATTON, M. D., GHILARDI, J. R., LEVIN, L. A., MAGGIO, J. E. & VIGNA, S. R. 1995. Beta 2-adrenergic receptors are expressed by glia in vivo in the normal and injured central nervous system in the rat, rabbit, and human. *J Neurosci,* 15**,** 152-64.

MAO, X., REN, Z., PARKER, G. N., SONDERMANN, H., PASTORELLO, M. A., WANG, W., MCMURRAY, J. S., DEMELER, B., DARNELL, J. E., JR. & CHEN, X. 2005. Structural bases of unphosphorylated STAT1 association and receptor binding. *Mol Cell,* 17**,** 761-71.

MARCHI, M., RISSO, F., VIOLA, C., CAVAZZANI, P. & RAITERI, M. 2002. Direct evidence that release-stimulating alpha7* nicotinic cholinergic receptors are localized on human and rat brain glutamatergic axon terminals. *J Neurochem,* 80**,** 1071-8.

MARIEN, M. R., COLPAERT, F. C. & ROSENQUIST, A. C. 2004. Noradrenergic mechanisms in neurodegenerative diseases: a theory. *Brain Research Reviews,* 45**,** 38-78.

MARSTERS, S. A., PENNICA, D., BACH, E., SCHREIBER, R. D. & ASHKENAZI, A. 1995. Interferon gamma signals via a high-affinity multisubunit receptor complex that contains two types of polypeptide chain. *Proceedings of the National Academy of Sciences of the United States of America,* 92**,** 5401-5405.

MATTSON, M. P. 2008. Glutamate and Neurotrophic Factors in Neuronal Plasticity and Disease. *Annals of the New York Academy of Sciences,* 1144**,** 97-112.

MATYASH, V. & KETTENMANN, H. 2010. Heterogeneity in astrocyte morphology and physiology. *Brain Res Rev,* 63**,** 2-10.

MCEWEN, B. S. 2008. Understanding the potency of stressful early life experiences on brain and body function. *Metabolism: clinical and experimental,* 57**,** S11-S15.

MCGEER, P. L. & MCGEER, E. G. 1995. The inflammatory response system of brain: implications for therapy of Alzheimer and other neurodegenerative diseases. *Brain Res Brain Res Rev,* 21**,** 195-218.

MCNAMEE, E. N., GRIFFIN, E. W., RYAN, K. M., RYAN, K. J., HEFFERNAN, S., HARKIN, A. & CONNOR, T. J. 2010a. Noradrenaline acting at beta-adrenoceptors induces expression of IL-1beta and its negative regulators IL-1ra and IL-1RII, and drives an overall anti-inflammatory phenotype in rat cortex. *Neuropharmacology,* 59**,** 37-48.

MCNAMEE, E. N., RYAN, K. M., KILROY, D. & CONNOR, T. J. 2010b. Noradrenaline induces IL-1ra and IL-1 type II receptor expression in primary glial cells and protects against IL-1beta-induced neurotoxicity. *Eur J Pharmacol,* 626**,** 219-28.

METZGER, F., WIESE, S. & SENDTNER, M. 1998. Effect of glutamate on dendritic growth in embryonic rat motoneurons. *J Neurosci,* 18**,** 1735-42.

MILLER, C. L., LLENOS, I. C., DULAY, J. R., BARILLO, M. M., YOLKEN, R. H. & WEIS, S. 2004. Expression of the kynurenine pathway enzyme tryptophan 2,3-dioxygenase is increased in the frontal cortex of individuals with schizophrenia. *Neurobiol Dis,* 15**,** 618-29.

MIR, S., SEN, T. & SEN, N. 2014. Cytokine-induced GAPDH sulfhydration affects PSD95 degradation and memory. *Mol Cell,* 56**,** 786-95.

MIURA, S., KAI, Y., KAMEI, Y. & EZAKI, O. 2008. Isoform-specific increases in murine skeletal muscle peroxisome proliferator-activated receptor-gamma coactivator-1alpha (PGC-1alpha) mRNA in response to beta2-adrenergic receptor activation and exercise. *Endocrinology,* 149**,** 4527-33.

MIURA, S., KAWANAKA, K., KAI, Y., TAMURA, M., GOTO, M., SHIUCHI, T., MINOKOSHI, Y. & EZAKI, O. 2007. An increase in murine skeletal muscle peroxisome proliferator-activated receptor-gamma coactivator-1alpha (PGC-1alpha) mRNA in response to exercise is mediated by beta-adrenergic receptor activation. *Endocrinology,* 148**,** 3441-8.

MIZUNO, T., ZHANG, G., TAKEUCHI, H., KAWANOKUCHI, J., WANG, J., SONOBE, Y., JIN, S., TAKADA, N., KOMATSU, Y. & SUZUMURA, A. 2008. Interferon-gamma directly induces neurotoxicity through a neuron specific, calcium-permeable complex of IFN-gamma receptor and AMPA GluR1 receptor. *FASEB J,* 22**,** 1797-806.

MONIER, A., ADLE-BIASSETTE, H., DELEZOIDE, A. L., EVRARD, P., GRESSENS, P. & VERNEY, C. 2007. Entry and distribution of microglial cells in human embryonic and fetal cerebral cortex. *J Neuropathol Exp Neurol,* 66**,** 372-82.

MONNERIE, H., SHASHIDHARA, S. & LE ROUX, P. D. 2003. Effect of excess extracellular glutamate on dendrite growth from cerebral cortical neurons at 3 days in vitro: Involvement of NMDA receptors. *J Neurosci Res,* 74**,** 688-700.

MORIGUCHI, S., MIZOGUCHI, Y., TOMIMATSU, Y., HAYASHI, Y., KADOWAKI, T., KAGAMIISHI, Y., KATSUBE, N., YAMAMOTO, K., INOUE, K., WATANABE, S., NABEKURA, J. & NAKANISHI, H. 2003. Potentiation of NMDA receptor-mediated synaptic responses by microglia. *Molecular Brain Research,* 119**,** 160-169.

MORONI, F., RUSSI, P., LOMBARDI, G., BENI, M. & CARLA, V. 1988. Presence of kynurenic acid in the mammalian brain. *J Neurochem,* 51**,** 177-80.

MULLER, N. 2013. The role of anti-inflammatory treatment in psychiatric disorders. *Psychiatr Danub,* 25**,** 292-8.

MULLER, N., KRAUSE, D., DEHNING, S., MUSIL, R., SCHENNACH-WOLFF, R., OBERMEIER, M., MOLLER, H. J., KLAUSS, V., SCHWARZ, M. J. & RIEDEL, M. 2010. Celecoxib treatment in an early stage of schizophrenia: results of a randomized, double-blind, placebo-controlled trial of celecoxib augmentation of amisulpride treatment. *Schizophr Res,* 121**,** 118-24.

MUNCH, G., GASIC-MILENKOVIC, J., DUKIC-STEFANOVIC, S., KUHLA, B., HEINRICH, K., RIEDERER, P., HUTTUNEN, H. J., FOUNDS, H. & SAJITHLAL, G. 2003. Microglial activation induces cell death, inhibits neurite outgrowth and causes neurite retraction of differentiated neuroblastoma cells. *Exp Brain Res,* 150**,** 1-8.

MUNN, D. H. 2011. Indoleamine 2,3-dioxygenase, Tregs and cancer. *Curr Med Chem,* 18**,** 2240-6.

MUNNAMALAI, V. & SUTER, D. M. 2009. Reactive oxygen species regulate F-actin dynamics in neuronal growth cones and neurite outgrowth. *J Neurochem,* 108**,** 644-61.

MURAI, K. K. & VAN MEYEL, D. J. 2007. Neuron glial communication at synapses: insights from vertebrates and invertebrates. *Neuroscientist,* 13**,** 657-66.

MYERS, J. P., SANTIAGO-MEDINA, M. & GOMEZ, T. M. 2011. Regulation of axonal outgrowth and pathfinding by integrin-ECM interactions. *Dev Neurobiol,* 71**,** 901-23.

MYINT, A. M. & KIM, Y. K. 2003. Cytokine–serotonin interaction through IDO: a neurodegeneration hypothesis of depression. *Medical Hypotheses,* 61**,** 519-525.

MYINT, A. M. & KIM, Y. K. 2014. Network beyond IDO in psychiatric disorders: revisiting neurodegeneration hypothesis. *Prog Neuropsychopharmacol Biol Psychiatry,* 48**,** 304-13.

MYINT, A. M., KIM, Y. K., VERKERK, R., SCHARPE, S., STEINBUSCH, H. & LEONARD, B. 2007. Kynurenine pathway in major depression: evidence of impaired neuroprotection. *J Affect Disord,* 98**,** 143-51.

MYINT, A. M., SCHWARZ, M. J., VERKERK, R., MUELLER, H. H., ZACH, J., SCHARPE, S., STEINBUSCH, H. W., LEONARD, B. E. & KIM, Y. K. 2011. Reversal of imbalance between kynurenic acid and 3-hydroxykynurenine by antipsychotics in medication-naive and medication-free schizophrenic patients. *Brain Behav Immun,* 25**,** 1576-81.

NAJJAR, S., PEARLMAN, D. M., ALPER, K., NAJJAR, A. & DEVINSKY, O. 2013. Neuroinflammation and psychiatric illness. *J Neuroinflammation,* 10**,** 43.

NAKAGAMI, Y., SAITO, H. & KATSUKI, H. 1996. 3-Hydroxykynurenine toxicity on the rat striatum in vivo. *Jpn J Pharmacol,* 71**,** 183-6.

NIMMERJAHN, A., KIRCHHOFF, F. & HELMCHEN, F. 2005. Resting microglial cells are highly dynamic surveillants of brain parenchyma in vivo. *Science,* 308**,** 1314-8.

NORTHAM, W. J., BEDOY, C. A. & MOBLEY, P. L. 1989. Pharmacological identification of the alpha-adrenergic receptor type which inhibits the beta-adrenergic activated adenylate cyclase system in cultured astrocytes. *Glia,* 2**,** 129-33.

NOTARANGELO, F. M. & POCIVAVSEK, A. 2016. Elevated kynurenine pathway metabolism during neurodevelopment: Implications for brain and behavior. *Neuropharmacology*.

O'CONNOR, J. C., LAWSON, M. A., ANDRE, C., MOREAU, M., LESTAGE, J., CASTANON, N., KELLEY, K. W. & DANTZER, R. 2009. Lipopolysaccharide-induced depressive-like behavior is mediated by indoleamine 2,3-dioxygenase activation in mice. *Mol Psychiatry,* 14**,** 511-22.

O'DONNELL, M., CHANCE, R. K. & BASHAW, G. J. 2009. Axon growth and guidance: receptor regulation and signal transduction. *Annu Rev Neurosci,* 32**,** 383-412.

O'FARRELL, K. & HARKIN, A. 2015. Stress-related regulation of the kynurenine pathway: Relevance to neuropsychiatric and degenerative disorders. *Neuropharmacology*.

O'NEILL, E. 2015. *Protective effects of noradrenergic and neurotrophic signalling on neuronal complexity in vitro.* PhD Thesis, Trinity College Dublin.

O'NEILL, E., KWOK, B., DAY, J. S., CONNOR, T. J. & HARKIN, A. 2016. Amitriptyline protects against TNF-α-induced atrophy and reduction in synaptic markers via a Trk-dependent mechanism. *Pharmacology Research & Perspectives,* 4**,** n/a-n/a.

O'TOOLE, E. 2015. *The impact of pharmacological modulation of the NMDA-R/NO signalling pathway on neuronal complexity in vitro.* PhD Thesis, Trinity College Dublin.

OGAWA, T., MATSON, W. R., BEAL, M. F., MYERS, R. H., BIRD, E. D., MILBURY, P. & SASO, S. 1992. Kynurenine pathway abnormalities in Parkinson's disease. *Neurology,* 42**,** 1702-6.

OKABE, S., MIWA, A. & OKADO, H. 2001. Spine formation and correlated assembly of presynaptic and postsynaptic molecules. *J Neurosci,* 21**,** 6105-14.

OKUDA, S., NISHIYAMA, N., SAITO, H. & KATSUKI, H. 1996. Hydrogen peroxide-mediated neuronal cell death induced by an endogenous neurotoxin, 3-hydroxykynurenine. *Proc Natl Acad Sci U S A,* 93**,** 12553-8.

OKUDA, S., NISHIYAMA, N., SAITO, H. & KATSUKI, H. 1998. 3-Hydroxykynurenine, an endogenous oxidative stress generator, causes neuronal cell death with apoptotic features and region selectivity. *J Neurochem,* 70**,** 299-307.

PACHER, P., NIVOROZHKIN, A. & SZABO, C. 2006. Therapeutic effects of xanthine oxidase inhibitors: renaissance half a century after the discovery of allopurinol. *Pharmacol Rev,* 58**,** 87-114.

PALLOTTA, M. T., ORABONA, C., VOLPI, C., VACCA, C., BELLADONNA, M. L., BIANCHI, R., SERVILLO, G., BRUNACCI, C., CALVITTI, M., BICCIATO, S., MAZZA, E. M., BOON, L., GRASSI, F., FIORETTI, M. C., FALLARINO, F., PUCCETTI, P. & GROHMANN, U. 2011. Indoleamine 2,3-dioxygenase is a signaling protein in long-term tolerance by dendritic cells. *Nat Immunol,* 12**,** 870-8.

PANTOURIS, G., SERYS, M., YUASA, H. J., BALL, H. J. & MOWAT, C. G. 2014. Human indoleamine 2,3-dioxygenase-2 has substrate specificity and inhibition characteristics distinct from those of indoleamine 2,3-dioxygenase-1. *Amino Acids,* 46**,** 2155-63.

PARIANTE, C. M., PEARCE, B. D., PISELL, T. L., OWENS, M. J. & MILLER, A. H. 1997. Steroid-independent translocation of the glucocorticoid receptor by the antidepressant desipramine. *Mol Pharmacol,* 52**,** 571-81.

PARPURA, V., BASARSKY, T. A., LIU, F., JEFTINIJA, K., JEFTINIJA, S. & HAYDON, P. G. 1994. Glutamate-mediated astrocyte-neuron signalling. *Nature,* 369**,** 744-747.

PARROTT, J. M. & O'CONNOR, J. C. 2015. Kynurenine 3-Monooxygenase: An Influential Mediator of Neuropathology. *Front Psychiatry,* 6**,** 116.

PAWLAK, D., TANKIEWICZ, A., MATYS, T. & BUCZKO, W. 2003. Peripheral distribution of kynurenine metabolites and activity of kynurenine pathway enzymes in renal failure. *J Physiol Pharmacol,* 54**,** 175-89.

PELLICCIARI, R., AMORI, L., COSTANTINO, G., GIORDANI, A., MACCHIARULO, A., MATTOLI, L., PEVARELLO, P., SPECIALE, C. & VARASI, M. 2003. Modulation of the kynurine pathway of tryptophan metabolism in search for neuroprotective agents. Focus on kynurenine-3-hydroxylase. *Adv Exp Med Biol,* 527**,** 621-8.

PEMBERTON, L. A., KERR, S. J., SMYTHE, G. & BREW, B. J. 1997. Quinolinic acid production by macrophages stimulated with IFN-gamma, TNF-alpha, and IFN-alpha. *J Interferon Cytokine Res,* 17**,** 589-95.

PERKINS, M. N. & STONE, T. W. 1982. An iontophoretic investigation of the actions of convulsant kynurenines and their interaction with the endogenous excitant quinolinic acid. *Brain Res,* 247**,** 184-7.

PERRONE, M. H., HAMEL, L. T., FERRARI, R. A. & HAUBRICH, D. R. 1990. Napamezole, an alpha-2 adrenergic receptor antagonist and monoamine uptake inhibitor in vitro. *J Pharmacol Exp Ther,* 254**,** 471-5.

PERSHING, M. L., BORTZ, D. M., POCIVAVSEK, A., FREDERICKS, P. J., JØRGENSEN, C. V., VUNCK, S. A., LEUNER, B., SCHWARCZ, R. & BRUNO, J. P. 2015. Elevated levels of kynurenic acid during gestation produce neurochemical, morphological, and cognitive deficits in adulthood: Implications for schizophrenia. *Neuropharmacology,* 90**,** 33-41.

PERSHING, M. L., PHENIS, D., VALENTINI, V., POCIVAVSEK, A., LINDQUIST, D. H., SCHWARCZ, R. & BRUNO, J. P. 2016. Prenatal kynurenine exposure in rats: age-dependent changes in NMDA receptor expression and conditioned fear responding. *Psychopharmacology (Berl).*

PFRIEGER, F. W. & BARRES, B. A. 1996. New views on synapse-glia interactions. *Curr Opin Neurobiol,* 6**,** 615-21.

PIANI, D., SPRANGER, M., FREI, K., SCHAFFNER, A. & FONTANA, A. 1992. Macrophage-induced cytotoxicity of N-methyl-D-aspartate receptor positive neurons involves excitatory amino acids rather than reactive oxygen intermediates and cytokines. *Eur J Immunol,* 22**,** 2429-36.

PIEROZAN, P., FERREIRA, F., DE LIMA, B. O. & PESSOA-PUREUR, R. 2015. Quinolinic acid induces disrupts cytoskeletal homeostasis in striatal neurons. Protective role of astrocyte-neuron interaction. *J Neurosci Res,* 93**,** 268-84.

PIEROZAN, P., ZAMONER, A., SOSKA, A. K., SILVESTRIN, R. B., LOUREIRO, S. O., HEIMFARTH, L., MELLO E SOUZA, T., WAJNER, M. & PESSOA-PUREUR, R. 2010. Acute intrastriatal administration of quinolinic acid provokes hyperphosphorylation of cytoskeletal intermediate filament proteins in astrocytes and neurons of rats. *Exp Neurol,* 224**,** 188-96.

PILOTTE, L., LARRIEU, P., STROOBANT, V., COLAU, D., DOLUSIC, E., FREDERICK, R., DE PLAEN, E., UYTTENHOVE, C., WOUTERS, J., MASEREEL, B. & VAN DEN EYNDE, B. J. 2012. Reversal of tumoral immune resistance by inhibition of tryptophan 2,3-dioxygenase. *Proc Natl Acad Sci U S A,* 109**,** 2497-502.

PISAR, M., FORREST, C. M., KHALIL, O. S., MCNAIR, K., VINCENTEN, M. C., QASEM, S., DARLINGTON, L. G. & STONE, T. W. 2014. Modified neocortical and cerebellar protein expression and morphology in adult rats following prenatal inhibition of the kynurenine pathway. *Brain Res,* 1576**,** 1-17.

POCIVAVSEK, A., THOMAS, M. A., ELMER, G. I., BRUNO, J. P. & SCHWARCZ, R. 2014. Continuous kynurenine administration during the prenatal period, but not during adolescence, causes learning and memory deficits in adult rats. *Psychopharmacology (Berl),* 231**,** 2799-809.

POCIVAVSEK, A., WU, H. Q., ELMER, G. I., BRUNO, J. P. & SCHWARCZ, R. 2012. Pre- and postnatal exposure to kynurenine causes cognitive deficits in adulthood. *Eur J Neurosci,* 35**,** 1605-12.

PONT-LEZICA, L., BECHADE, C., BELARIF-CANTAUT, Y., PASCUAL, O. & BESSIS, A. 2011. Physiological roles of microglia during development. *J Neurochem,* 119**,** 901-8.

PRESCOTT, C., WEEKS, A. M., STALEY, K. J. & PARTIN, K. M. 2006. Kynurenic acid has a dual action on AMPA receptor responses. *Neurosci Lett,* 402**,** 108-12.

QIAN, F., VILLELLA, J., WALLACE, P. K., MHAWECH-FAUCEGLIA, P., TARIO, J. D., JR., ANDREWS, C., MATSUZAKI, J., VALMORI, D., AYYOUB, M., FREDERICK, P. J., BECK, A., LIAO, J., CHENEY, R., MOYSICH, K., LELE, S., SHRIKANT, P., OLD, L. J. & ODUNSI, K. 2009. Efficacy of levo-1-methyl tryptophan and dextro-1-methyl tryptophan in reversing indoleamine-2,3-dioxygenase-mediated arrest of T-cell proliferation in human epithelial ovarian cancer. *Cancer Res,* 69**,** 5498-504.

QIAN, L., GAO, X., PEI, Z., WU, X., BLOCK, M., WILSON, B., HONG, J.-S. & FLOOD, P. M. 2007. NADPH oxidase inhibitor DPI is neuroprotective at femtomolar concentrations through inhibition of microglia over-activation. *Parkinsonism & Related Disorders,* 13**,** S316-S320.

RAISON, C. L., DANTZER, R., KELLEY, K. W., LAWSON, M. A., WOOLWINE, B. J., VOGT, G., SPIVEY, J. R., SAITO, K. & MILLER, A. H. 2010. CSF concentrations of brain tryptophan and kynurenines during immune stimulation with IFN-alpha: relationship to CNS immune responses and depression. *Mol Psychiatry,* 15**,** 393-403.

RAISON, C. L., RUTHERFORD, R. E., WOOLWINE, B. J., SHUO, C., SCHETTLER, P., DRAKE, D. F., HAROON, E. & MILLER, A. H. 2013. A randomized controlled trial of the tumor necrosis factor antagonist infliximab for treatment-resistant depression: the role of baseline inflammatory biomarkers. *JAMA Psychiatry,* 70**,** 31-41.

RANG, H. P. & DALE, M. M. 2012. *Rang and Dale's pharmacology,* Edinburgh; New York, Elsevier/Churchill Livingstone.

REJDAK, K., BARTOSIK-PSUJEK, H., DOBOSZ, B., KOCKI, T., GRIEB, P., GIOVANNONI, G., TURSKI, W. A. & STELMASIAK, Z. 2002. Decreased level of kynurenic acid in cerebrospinal fluid of relapsing-onset multiple sclerosis patients. *Neurosci Lett,* 331**,** 63-5.

REJDAK, K., PETZOLD, A., KOCKI, T., KURZEPA, J., GRIEB, P., TURSKI, W. A. & STELMASIAK, Z. 2007. Astrocytic activation in relation to inflammatory markers during clinical exacerbation of relapsing-remitting multiple sclerosis. *J Neural Transm,* 114**,** 1011-5.

REMELS, A. H. V., GOSKER, H. R., BAKKER, J., GUTTRIDGE, D. C., SCHOLS, A. M. W. J. & LANGEN, R. C. J. 2013. Regulation of skeletal muscle oxidative phenotype by classical NF-κB signalling. *Biochimica et Biophysica Acta (BBA) - Molecular Basis of Disease,* 1832**,** 1313-1325.

REUS, G. Z., JANSEN, K., TITUS, S., CARVALHO, A. F., GABBAY, V. & QUEVEDO, J. 2015. Kynurenine pathway dysfunction in the pathophysiology and treatment of depression: Evidences from animal and human studies. *J Psychiatr Res*.

RISHER, W. C., USTUNKAYA, T., SINGH ALVARADO, J. & EROGLU, C. 2014. Rapid Golgi Analysis Method for Efficient and Unbiased Classification of Dendritic Spines. *PLoS ONE,* 9**,** e107591.

ROCK, R. B., GEKKER, G., HU, S., SHENG, W. S., CHEERAN, M., LOKENSGARD, J. R. & PETERSON, P. K. 2004. Role of microglia in central nervous system infections. *Clin Microbiol Rev,* 17**,** 942-64, table of contents.

ROCK, R. B., HU, S., DESHPANDE, A., MUNIR, S., MAY, B. J., BAKER, C. A., PETERSON, P. K. & KAPUR, V. 2005. Transcriptional response of human microglial cells to interferon-gamma. *Genes Immun,* 6**,** 712-9.

ROHRIG, U. F., MAJJIGAPU, S. R., VOGEL, P., ZOETE, V. & MICHIELIN, O. 2015. Challenges in the Discovery of Indoleamine 2,3-Dioxygenase 1 (IDO1) Inhibitors. *J Med Chem*.

ROSS, J. D., CULLEN, D. K., HARRIS, J. P., LAPLACA, M. C. & DEWEERTH, S. P. 2015. A three-dimensional image processing program for accurate, rapid, and semi-automated segmentation of neuronal somata with dense neurite outgrowth. *Frontiers in Neuroanatomy,* 9**,** 87.

ROSSI, F., VALENTINA, C., GARAVAGLIA, S., SATHYASAIKUMAR, K. V., SCHWARCZ, R., KOJIMA, S., OKUWAKI, K., ONO, S., KAJII, Y. & RIZZI, M. 2010. Crystal structure-based selective targeting of the pyridoxal 5'-phosphate dependent enzyme kynurenine aminotransferase II for cognitive enhancement. *J Med Chem,* 53**,** 5684-9.

SAITO, K., CROWLEY, J. S., MARKEY, S. P. & HEYES, M. P. 1993. A mechanism for increased quinolinic acid formation following acute systemic immune stimulation. *J Biol Chem,* 268**,** 15496-503.

SALTER, M., HAZELWOOD, R., POGSON, C. I., IYER, R., MADGE, D. J., JONES, H. T., COOPER, B. R., COX, R. F., WANG, C. M. & WIARD, R. P. 1995. The effects of an inhibitor of tryptophan 2,3-dioxygenase and a combined inhibitor of tryptophan 2,3-dioxygenase and 5-HT reuptake in the rat. *Neuropharmacology,* 34**,** 217-27.

SASAKI, A., HIRATO, J. & NAKAZATO, Y. 1993. Immunohistochemical study of microglia in the Creutzfeldt-Jakob diseased brain. *Acta Neuropathologica,* 86**,** 337-344.

SAUVE, A. A., WOLBERGER, C., SCHRAMM, V. L. & BOEKE, J. D. 2006. The biochemistry of sirtuins. *Annu Rev Biochem,* 75**,** 435-65.

SAWADA, M., KONDO, N., SUZUMURA, A. & MARUNOUCHI, T. 1989. Production of tumor necrosis factor-alpha by microglia and astrocytes in culture. *Brain Res,* 491**,** 394-7.

SCHEIBLICH, H. & BICKER, G. 2016. Nitric oxide regulates antagonistically phagocytic and neurite outgrowth inhibiting capacities of microglia. *Dev Neurobiol,* 76**,** 566-84.

SCHLEGELMILCH, T., HENKE, K. & PERI, F. 2011. Microglia in the developing brain: from immunity to behaviour. *Curr Opin Neurobiol,* 21**,** 5-10.

SCHMUED, L. C., ALBERTSON, C. & SLIKKER JR, W. 1997. Fluoro-Jade: a novel fluorochrome for the sensitive and reliable histochemical localization of neuronal degeneration. *Brain Research,* 751**,** 37-46.

SCHUCK, P. F., TONIN, A., DA COSTA FERREIRA, G., VIEGAS, C. M., LATINI, A., DUVAL WANNMACHER, C. M., DE SOUZA WYSE, A. T., DUTRA-FILHO, C. S. & WAJNER, M. 2007. Kynurenines impair energy metabolism in rat cerebral cortex. *Cell Mol Neurobiol,* 27**,** 147-60.

SCHUTZ, G., KILLEWICH, L., CHEN, G. & FEIGELSON, P. 1975. Control of the mRNA for hepatic tryptophan oxygenase during hormonal and substrate induction. *Proc Natl Acad Sci U S A,* 72**,** 1017-20.

SCHWARCZ, R., BRUNO, J. P., MUCHOWSKI, P. J. & WU, H. Q. 2012. Kynurenines in the mammalian brain: when physiology meets pathology. *Nat Rev Neurosci,* 13**,** 465-77.

SCHWARZ, M. J., GUILLEMIN, G. J., TEIPEL, S. J., BUERGER, K. & HAMPEL, H. 2013. Increased 3-Hydroxykynurenine serum concentrations differentiate Alzheimer's disease patients from controls. *European Archives of Psychiatry and Clinical Neuroscience,* 263**,** 345-352.

SCHWIELER, L., ERHARDT, S., ERHARDT, C. & ENGBERG, G. 2005. Prostaglandin-mediated control of rat brain kynurenic acid synthesis--opposite actions by COX-1 and COX-2 isoforms. *J Neural Transm (Vienna),* 112**,** 863-72.

SCHWIELER, L., LARSSON, M. K., SKOGH, E., KEGEL, M. E., ORHAN, F., ABDELMOATY, S., FINN, A., BHAT, M., SAMUELSSON, M., LUNDBERG, K., DAHL, M. L., SELLGREN, C., SCHUPPE-KOISTINEN, I., SVENSSON, C., ERHARDT, S. & ENGBERG, G. 2015. Increased levels of IL-6 in the cerebrospinal fluid of patients with chronic schizophrenia--significance for activation of the kynurenine pathway. *J Psychiatry Neurosci,* 40**,** 126-33.

SCOTT, E. K. & LUO, L. 2001. How do dendrites take their shape? *Nat Neurosci,* 4**,** 359-65.

SMITH, C. & TEITLER, M. 1999. Beta-blocker selectivity at cloned human beta 1- and beta 2-adrenergic receptors. *Cardiovasc Drugs Ther,* 13**,** 123-6.

SMITH, M. E., VAN DER MAESEN, K. & SOMERA, F. P. 1998. Macrophage and microglial responses to cytokines in vitro: phagocytic activity, proteolytic enzyme release, and free radical production. *J Neurosci Res,* 54**,** 68-78.

SOFRONIEW, M. V. & VINTERS, H. V. 2010. Astrocytes: biology and pathology. *Acta Neuropathologica,* 119**,** 7-35.

ST'ASTNY, F., HINOI, E., OGITA, K. & YONEDA, Y. 1999. Ferrous iron modulates quinolinate-mediated [3H]MK-801 binding to rat brain synaptic membranes in the presence of glycine and spermidine. *Neurosci Lett,* 262**,** 105-8.

STÄLLBERG, B., NAYA, I., EKELUND, J. & ECKERWALL, G. 2015. Real-life use of budesonide/formoterol in clinical practice: a 12-month follow-up assessment in a multi-national study of asthma patients established on single-inhaler maintenance and reliever therapy. *International Journal of Clinical Pharmacology and Therapeutics,* 53**,** 447-455.

STARK, G. R. 2007. How cells respond to interferons revisited: from early history to current complexity. *Cytokine Growth Factor Rev,* 18**,** 419-23.

STONE, T. W. 1993. Neuropharmacology of quinolinic and kynurenic acids. *Pharmacol Rev,* 45, 309-79.

STONE, T. W. 2000. Development and therapeutic potential of kynurenic acid and kynurenine derivatives for neuroprotection. *Trends Pharmacol Sci,* 21, 149-54.

STONE, T. W., FORREST, C. M. & DARLINGTON, L. G. 2012. Kynurenine pathway inhibition as a therapeutic strategy for neuroprotection. *FEBS J,* 279, 1386-97.

STONE, T. W. & PERKINS, M. N. 1984. Actions of excitatory amino acids and kynurenic acid in the primate hippocampus: a preliminary study. *Neurosci Lett,* 52, 335-40.

STREIT, W. J., GRAEBER, M. B. & KREUTZBERG, G. W. 1989. Expression of Ia antigen on perivascular and microglial cells after sublethal and lethal motor neuron injury. *Experimental Neurology,* 105, 115-126.

SWANSON, L. W. 1976. The locus coeruleus: a cytoarchitectonic, Golgi and immunohistochemical study in the albino rat. *Brain Res,* 110, 39-56.

SZALARDY, L., ZADORI, D., TOLDI, J., FULOP, F., KLIVENYI, P. & VECSEI, L. 2012. Manipulating kynurenic acid levels in the brain - on the edge between neuroprotection and cognitive dysfunction. *Curr Top Med Chem,* 12, 1797-806.

SZELÉNYI, J. 2001. Cytokines and the central nervous system. *Brain Research Bulletin,* 54, 329-338.

TAKAKI, J., FUJIMORI, K., MIURA, M., SUZUKI, T., SEKINO, Y. & SATO, K. 2012. L-glutamate released from activated microglia downregulates astrocytic L-glutamate transporter expression in neuroinflammation: the 'collusion' hypothesis for increased extracellular L-glutamate concentration in neuroinflammation. *J Neuroinflammation,* 9, 275.

TAKEUCHI, H., JIN, S., WANG, J., ZHANG, G., KAWANOKUCHI, J., KUNO, R., SONOBE, Y., MIZUNO, T. & SUZUMURA, A. 2006. Tumor necrosis factor-alpha induces neurotoxicity via glutamate release from hemichannels of activated microglia in an autocrine manner. *J Biol Chem,* 281, 21362-8.

TAN, L., YU, J. T. & TAN, L. 2012. The kynurenine pathway in neurodegenerative diseases: mechanistic and therapeutic considerations. *J Neurol Sci,* 323, 1-8.

TAVARES, R. G., TASCA, C. I., SANTOS, C. E., ALVES, L. B., PORCIUNCULA, L. O., EMANUELLI, T. & SOUZA, D. O. 2002. Quinolinic acid stimulates synaptosomal glutamate release and inhibits glutamate uptake into astrocytes. *Neurochem Int,* 40, 621-7.

THOMAS, S. R., MOHR, D. & STOCKER, R. 1994. Nitric oxide inhibits indoleamine 2,3-dioxygenase activity in interferon-gamma primed mononuclear phagocytes. *J Biol Chem,* 269, 14457-64.

TOJIMA, T., HINES, J. H., HENLEY, J. R. & KAMIGUCHI, H. 2011. Second messengers and membrane trafficking direct and organize growth cone steering. *Nat Rev Neurosci,* 12, 191-203.

TOPCZEWSKA-BRUNS, J., PAWLAK, D., CHABIELSKA, E., TANKIEWICZ, A. & BUCZKO, W. 2002. Increased levels of 3-hydroxykynurenine in different brain regions of rats with chronic renal insufficiency. *Brain Res Bull,* 58, 423-8.

TREMBLAY, M. E. & MAJEWSKA, A. K. 2011. A role for microglia in synaptic plasticity? *Commun Integr Biol,* 4, 220-2.

TREMBLAY, M. E., STEVENS, B., SIERRA, A., WAKE, H., BESSIS, A. & NIMMERJAHN, A. 2011. The role of microglia in the healthy brain. *J Neurosci,* 31, 16064-9.

ULLIAN, E. M., SAPPERSTEIN, S. K., CHRISTOPHERSON, K. S. & BARRES, B. A. 2001. Control of synapse number by glia. *Science,* 291, 657-61.

VAIDYA, V. A., MAREK, G. J., AGHAJANIAN, G. K. & DUMAN, R. S. 1997. 5-HT2A receptor-mediated regulation of brain-derived neurotrophic factor mRNA in the hippocampus and the neocortex. *J Neurosci,* 17, 2785-95.

VECSEI, L., SZALARDY, L., FULOP, F. & TOLDI, J. 2013. Kynurenines in the CNS: recent advances and new questions. *Nat Rev Drug Discov,* 12, 64-82.

VENSTROM, K. A. & REICHARDT, L. F. 1993. Extracellular matrix. 2: Role of extracellular matrix molecules and their receptors in the nervous system. *The FASEB Journal,* 7, 996-1003.

VERKHRATSKY, A. & KETTENMANN, H. 1996. Calcium signalling in glial cells. *Trends in Neurosciences,* 19, 346-352.

VERSTRAELEN, P., PINTELON, I., NUYDENS, R., CORNELISSEN, F., MEERT, T. & TIMMERMANS, J. P. 2014. Pharmacological characterization of cultivated neuronal networks: relevance to synaptogenesis and synaptic connectivity. *Cell Mol Neurobiol,* 34**,** 757-76.

WALKER, A. K., NAKAMURA, T., BYRNE, R. J., NAICKER, S., TYNAN, R. J., HUNTER, M. & HODGSON, D. M. 2009. Neonatal lipopolysaccharide and adult stress exposure predisposes rats to anxiety-like behaviour and blunted corticosterone responses: implications for the double-hit hypothesis. *Psychoneuroendocrinology,* 34**,** 1515-25.

WALTON, N. M., SUTTER, B. M., LAYWELL, E. D., LEVKOFF, L. H., KEARNS, S. M., MARSHALL, G. P., 2ND, SCHEFFLER, B. & STEINDLER, D. A. 2006. Microglia instruct subventricular zone neurogenesis. *Glia,* 54**,** 815-25.

WANG, J., SIMONAVICIUS, N., WU, X., SWAMINATH, G., REAGAN, J., TIAN, H. & LING, L. 2006. Kynurenic acid as a ligand for orphan G protein-coupled receptor GPR35. *J Biol Chem,* 281**,** 22021-8.

WARESKI, P., VAARMANN, A., CHOUBEY, V., SAFIULINA, D., LIIV, J., KUUM, M. & KAASIK, A. 2009. PGC-1{alpha} and PGC-1{beta} regulate mitochondrial density in neurons. *J Biol Chem,* 284**,** 21379-85.

WEBSTER, M. J., KNABLE, M. B., O'GRADY, J., ORTHMANN, J. & WEICKERT, C. S. 2002. Regional specificity of brain glucocorticoid receptor mRNA alterations in subjects with schizophrenia and mood disorders. *Mol Psychiatry,* 7**,** 985-94, 924.

WELCH, A. N. & BADAWY, A. A. 1980. Tryptophan pyrrolase in haem regulation. Experiments with administered haematin and the relationship between the haem saturation of tryptophan pyrrolase and the activity of 5-aminolaevulinate synthase in rat liver. *Biochem J,* 192**,** 403-10.

WONG, E. H., KEMP, J. A., PRIESTLEY, T., KNIGHT, A. R., WOODRUFF, G. N. & IVERSEN, L. L. 1986. The anticonvulsant MK-801 is a potent N-methyl-D-aspartate antagonist. *Proc Natl Acad Sci U S A,* 83**,** 7104-8.

WSZELAKI, N. & MELZIG, M. F. 2011. Research on an in vitro cell system for testing the neurotoxicity of kynurenine pathway metabolites. *Pharmazie,* 66**,** 899-903.

XIE, H., HOU, S., JIANG, J., SEKUTOWICZ, M., KELLY, J. & BACSKAI, B. J. 2013. Rapid cell death is preceded by amyloid plaque-mediated oxidative stress. *Proceedings of the National Academy of Sciences of the United States of America,* 110**,** 7904-7909.

YANG, D., ELNER, S. G., BIAN, Z.-M., TILL, G. O., PETTY, H. R. & ELNER, V. M. 2007. Pro-inflammatory Cytokines Increase Reactive Oxygen Species through Mitochondria and NADPH Oxidase in Cultured RPE Cells. *Experimental eye research,* 85**,** 462-472.

YASUI, H., TAKAI, K., YOSHIDA, R. & HAYAISHI, O. 1986. Interferon enhances tryptophan metabolism by inducing pulmonary indoleamine 2,3-dioxygenase: its possible occurrence in cancer patients. *Proc Natl Acad Sci U S A,* 83**,** 6622-6.

YING, W. 2006. NAD+ and NADH in cellular functions and cell death. *Front Biosci,* 11**,** 3129-48.

YOSHIDA, M., SAITO, H. & KATSUKI, H. 1995. Neurotrophic effects of conditioned media of astrocytes isolated from different brain regions on hippocampal and cortical neurons. *Experientia,* 51**,** 133-6.

YSSEL, J. 2015. *Targeting the noradrenergic system for antiinflammatory and neuroprotective actions in an animal model of Parkinson's disease.* PhD Thesis, Trinity College Dublin.

YU, C. P., PAN, Z. Z. & LUO, D. Y. 2016. TDO as a therapeutic target in brain diseases. *Metab Brain Dis,* 31**,** 737-47.

ZAMANIAN, J. L., XU, L., FOO, L. C., NOURI, N., ZHOU, L., GIFFARD, R. G. & BARRES, B. A. 2012. Genomic Analysis of Reactive Astrogliosis. *The Journal of Neuroscience,* 32**,** 6391-6410.

ZAROW, C., LYNESS, S. A., MORTIMER, J. A. & CHUI, H. C. 2003. Neuronal loss is greater in the locus coeruleus than nucleus basalis and substantia nigra in Alzheimer and Parkinson diseases. *Arch Neurol,* 60**,** 337-41.

ZHANG, L., GUADARRAMA, L., CORONA-MORALES, A. A., VEGA-GONZALEZ, A., ROCHA, L. & ESCOBAR, A. 2006. Rats Subjected to Extended L-Tryptophan Restriction During Early Postnatal Stage Exhibit Anxious-Depressive Features and Structural Changes. *Journal of Neuropathology and Experimental Neurology,* 65**,** 562-570.

ZHUMADILOV, A., BOYKO, M., GRUENBAUM, S. E., BROTFAIN, E., BILOTTA, F. & ZLOTNIK, A. 2015. Extracorporeal methods of blood glutamate scavenging: a novel therapeutic modality. *Expert review of neurotherapeutics,* 15**,** 501-508.

ZINGER, A., BARCIA, C., HERRERO, M. T. & GUILLEMIN, G. J. 2011. The involvement of neuroinflammation and kynurenine pathway in Parkinson's disease. *Parkinsons Dis,* 2011**,** 716859.

ZWILLING, D., HUANG, S. Y., SATHYASAIKUMAR, K. V., NOTARANGELO, F. M., GUIDETTI, P., WU, H. Q., LEE, J., TRUONG, J., ANDREWS-ZWILLING, Y., HSIEH, E. W., LOUIE, J. Y., WU, T., SCEARCE-LEVIE, K., PATRICK, C., ADAME, A., GIORGINI, F., MOUSSAOUI, S., LAUE, G., RASSOULPOUR, A., FLIK, G., HUANG, Y., MUCHOWSKI, J. M., MASLIAH, E., SCHWARCZ, R. & MUCHOWSKI, P. J. 2011. Kynurenine 3-monooxygenase inhibition in blood ameliorates neurodegeneration. *Cell,* 145**,** 863-74.